NATIONAL ELECTRICAL ENGINEERING RESEARCH INSTITUTE

NEERI/E/65/2

The Registrar,
The University of Cape Town,
University Private Bag,
RONDEBOSCH,
Cape Town.

5th October 1972

Dear Sir,

Submission of Thesis - The Lightning Discharge

I have the honour and priviledge of submitting the enclosed thesis entitled "The Lightning Discharge" for consideration as fulfilling the requirements for the degree of Doctor of Philosophy.

The thesis is divided into two parts which may be briefly summa= rised as follows:-

Part I : Experimental Observations on Lightning

This part describes the experimental work carried out over a three year period from 1961 to 1964, during which 2780 oscillograms were obtained of the electric field changes which occurred during flashes of lightning.

The objectives were to ascertain some parameters of lightning occurring in the sub-tropics, in particular the frequency distribution of the magnitudes of the field changes from intra-cloud and cloud-ground strokes and the time intervals between strokes and total dura= tion; secondly it was desired to know the polarity of the discharges and the ratio of the number of intra-cloud to cloud-ground strokes together with information as to the frequency of occurrency of contin= uing currents.

During the course of the analysis of this data, the methods of measurement were critically examined in order to determine the capa= bilities and shortcomings of the system and to ascertain the degree of accuracy attained.

It is thought that these objectives were broadly achieved as judged by the comparisons which were made with observations carried out in South Africa and in Europe by other investigators.

However in so doing it was necessary to consider most carefully the meaning to be attached to the statistical data presented, and in this regard it is thought that a novel approach to the adjustment of truncated distributions was evolved which shows promise of application

in /.....

in many measurements of this kind where the threshold level of mea= surement cannot be made too sensitive for practical reasons.

Secondly it was necessary to consider carefully the fundamental theory of the electrostatic capacitance of aerial systems which were virtually connected to earth and exposed to electric field changes. The reward for this study was an improved understanding of the basic fundamentals as to the factors which determine the charge distribu= tion in earthed conductors - in particular the vertical aerial and this has led to an explanation of the behaviour of tall structures when exposed to thunderstorm electric fields and lightning. Whilst the fundamentals involved in this study are of course not new, their application to this problem has perhaps not been publicised too freely in the literature as judged by the difficulties expressed by various authors regarding the mechanism of discharges from or to conductors protruding from the earths's surface.

Finally the analysis of the data presented in this part of the thesis revealed some interesting differences compared with previously recorded data on lightning. For example the time taken to the crest of the so-called fast "R" elements of the return stroke field change appears to have been much longer than previously reported and this has an important significance. Secondly the ratio of the number of intra-cloud to ground flashes was found to be of the same order in the sub-tropics as measured in temperate areas, namely about 2:1 and a reason is given why values of about 5:1 may have been erroneous= ly measured for tropical conditions in the past. It is also confirmed that sub-tropical lightning tends to be even more negative than posi= tive and to comprise many more multiple stroke flashes than in more temperate climates. Possible reasons for these differences are advanced in Part II of the thesis.

Part II : The Mechanism of the Lightning Discharge

The dissertation contained in this part of the thesis is the result of a determined attempt over many years to try to clarify the physical factors involved in the lightning discharge. The literature on the subject has been so voluminous and in many cases contradictory that it has been difficult to formulate any kind of straightforward funda= mental and unified hypothesis which might reasonably account for some of the anomalies which were apparent either in theories or observations concerning lightning.

Whilst it cannot be claimed that these efforts have been entirely successful, at least it can be said that as a consequence of what is hoped was unbiased and objective probing, some concepts of the light= ning discharge mechanism have been clarified.

In order to arrive at some conclusion it has been necessary not only to take account of the results of the experimental data presented in Part I, but also to draw freely upon the observations of many other investigators whose work is greatly appreciated and acknowledged. It is also admitted that some of the concepts now presented have been discussed with prominent experts in this field, and note has

been/.....

been duly taken whenever constructive criticism has been expressed. This consultation has, it is thought, resulted in a more carefully formulated hypothesis than would otherwise have eventuated, without detracting from the originality of the concepts.

The following is a very broad summary of those areas in which it is believed advances in the knowledge of the lightning discharge mechanism have been hopefully achieved.

1. In an endeavour to explain how a lightning discharge to ground can occur as opposed to intra-cloud discharges, the conventional model of spherical charges was abandoned in favour of a cylindrical model which appeared to be more closely related to known meteorological and aerodynamic processes in thunderstorm cells - at least of the convection type. This indeed established mathematical criteria for the initiation of discharges from the lower extremity of cylindrical cloud charges in preference to discharges within the cylinder which would correspond to intra-cloud flashes.

2. Present hypotheses regarding the lightning stroke mechanism assume that negative charge is lowered by the leader and deposited en route along its length and that upon contact with the earth this charge is neutralised by positive charge available from the earth during the return stroke thereafter leaving the channel positively charged.

   Whilst no basic change to this final outcome is contemplated in this thesis, the detailed mechanism whereby it may be accomplished has been clarified. This proposes that charges of both signs are induced in the conducting leader channel by the action of the main electric field, and that this effect will intensify with increasing leader length. This mechanism provides that an ionising field intensity is available at both extremities of the leader channel to ensure propagation of the positive tipped streamers into the negative bound charge of the cloud as well as the tip of the negatively charged leader.

3. The potential of the negative tip of the leader, and the potential gradient along the leader have been the subject of some controversy. Electrostatically the leader tip potential must tend to zero as the leader approaches ground, and yet the potential gradient along the leader being determined by the properties of an arc is reputedly very low. The hypothesis of the induced positive charge at the top end of the leader provides a solution to this anomaly since by depressing the potential in that area (numerically) a low value of potential gradient is permissible despite the lowering of the potential of the tip.

4. It has been possible to simulate the above described mechanism by means of a computer program which determines the dimensions of the leader which will satisfy specified conditions of field intensity at the cloud end and at the lower tip, taking into account possible variations in the velocity of propagation both of this tip and the mean velocity of penetration of the positive

tips /....

tips of streamers in the cloud. The amount of induced charge needed to maintain the propagation can be ascertained as well as the potential gradient. Numerical computations indicate values of the parameters of the leader which are not seriously at variance with present concepts with the possible exception that the potential gradient needs to be an order of magnitude greater than that of a well established arc, and that the corona radius of the leader is much larger than the observed luminous radius.

5. The charge distribution pattern along the leader has been quoted in the literature as being uniform alternatively exponential and there is evidence in favour of both viewpoints. If however, the leader can discharge more electrons than initially deposited thereon thereby leaving the channel positively charged after the return stroke proper, this matter can be resolved provided there is more positive charge left at the top end compared with the lower end. The latter proviso is an electro-geometrical fact whilst the former requires further consideration regarding the physical structure of the leader channel.

6. The hypothesis has been advanced that the leader consists of a conducting channel in a state of intense corona with negative charge lodged in the outer perimeter approximately bounded by the corona radius where the field intensity equals that of the ionisation level for air. Since the field intensity within the corona radius cannot exceed this ionisation level either, a secondary separation of charge is assumed to occur which deposits still more negative charge in the form of electrons in the outer shell leaving the centre or core of the channel consisting primarily of positive ions. This hypothesis assists in the ex= planation for the retention of charge along the leader length as well as providing a reservoir of electrons to satisfy the conditions imposed by the consideration under point (5) above. This structure of the leader channel is not without precedence since it closely resembles that of a metalic conductor with negative corona.

7. Reasons are given why the step-dart of a stepped leader is more readily explained by assuming that the advance of positive stream= ers into the cloud charge occurs in "bursts" of ionisation which result in surges of electrons down the channel. Since the bursts themselves are a consequence of an increase in induced charge resulting from the extension of the channel, their frequency is dependent upon the leader tip velocity.

8. As a consequence of the above-mentioned hypotheses, the final phase of the discharge of a single stroke consist in the slower neutralisation from above of the positive charge left on the top section of the leader during which period the conductivity of the lower portion decreases substantially. Confirmation both of the existence of the positive charge and its slow rate of neutralisation has very recently been obtained by Berger.

9. Reasons are given which throw some doubt on the supposition that the subsequent strokes of a multiple flash are the conse= quence of tapping new pockets of negative charge in the cloud.

The /....

The proposal of Malan and Schonland that the source of this charge is contiguous at higher levels, is thought to be acceptable. The reason for subsequent strokes is therefore considered to be due to influences external to the mechanism of the discharge. It depends upon the rate at which the ionisation level in the cloud is restored and this is aided by a number of factors which include the rate of charge separation, the rate of dissi= pation of positive charge at the cloud top, and the rate of attraction of fast negative ions from the upper atmosphere and positive ions from the air space between the cloud and the earth which is aided by point discharge. If the combined effect of these influences is sufficiently high, the first discharge may be prevented from stopping thereby giving rise to continuing current following the main discharge.

10. The dart leader of subsequent strokes is thought to be of a similar origin to that occurring in the stepped leader except that it will be continuous as a consequence of the generally higher conductivity of the whole channel. This is supported by the fact that the charge build up in the channel for subsequent strokes takes place more slowly than does the dart leader as proven from field change measurements.

11. When the proposed mechanism of the discharge is applied to posi= tive leaders it becomes quite clear why this discharge is much more severe than its negative counterpart, and why multiple dis= charges are not frequent. Unlike the negative discharge, the positive channel has a copious source of supply of mobile elec= trons from the earth and from its core.

12. If the field intensity required for ionisation of the air at the earth's surface is equal to that of air in free space, the return stroke mechanism proper will commence when the corona envelope of the leader reaches the earth. An upward streamer equal in length to the corona radius will appear. If however the ionisation level at the earth's surface is less, the upward streamer will occur before the corona envelope reaches earth. In the case of a tall earthed structure however, the field in= tensity at the top of the structure is intensified by the charge of opposing polarity raised in the structure. The amount of this charge in relation to the charge on the leader can be calculated by equating the numerical value of the potential on the structure due to its own charge to that due to the charge on the leader, since the resultant potential of the structure must of course be zero. The diversion of the leader to the struc= ture will depend upon whether an upward streamer from the struc= ture can reach the leader channel before it contacts an upward streamer from the earth. It is shown that these calculations depend, however, upon the charge distribution pattern assumed for the structure and the lightning leader, and upon the field intensities required for ionisation and breakdown at the respec= tive points of interest.

13. Finally the classic Le Jay statement for the electric field due to a discharging dipole has been amplified to enable the approximate field change to be calculated for the electrostatic and electromagnetic field changes respectively, firstly ignoring

the/.....

the propagation time resulting from wave velocity in space. This does however, require a detailed knowledge of the discharge mechanism and of the charge distributions involved. A new term is found to exist in the expression for the radiation field indicating an addition to the di/dt dependance which is proportional to i^2/q. This means that if a high rate of rise of current occurs almost coincidental with the peak value of the lightning current, the radiation field intensity will be enhanced accordingly. This may account for the observation that the electromagnetic field intensity appears to exceed that of the electrostatic field at lesser distances than theoretically predicted. The effect of the retarded time to allow for wave propagation can be accounted for by means of an incremental type of computer program, and examples are given of the resulting field change for three assumed charge distributions along the leader.

I sincerely trust that the thesis will be found to be acceptable.

Yours faithfully,

Signed by candidate

R.B. Anderson
Head: Power Electrical Engineering Division
NATIONAL ELECTRICAL ENGINEERING RESEARCH INSTITUTE

ISBN 0 7988 0037 2

SPECIAL REPORT

ELEK 12

ANDERSON, R.B. The Lightning Discharge

The measurement of lightning field changes and the mechanism of the lightning discharge.

NATIONAL ELECTRICAL ENGINEERING RESEARCH INSTITUTE

COUNCIL FOR SCIENTIFIC AND INDUSTRIAL RESEARCH

P.O. Box 395, Pretoria, Republic of South Africa, October 1971.

NATIONAL ELECTRICAL ENGINEERING RESEARCH INSTITUTE

The Lightning Discharge,
by R.B. Anderson

Part I Experimental Observations on Lightning

Summary of contents

1. General

The classic Le Jay statement of the total electrical field intensity at a distance D from an electric dipole is amplified and restated and the objectives of the experimental research are outlined. These are briefly to obtain as much information about lightning field changes as possible in order to be able to effect a statistical analysis which would take account of the many variables encountered, then to examine present hypothesis with a view to explaining any apparent inconsistencies.

2. Description of Equipment

Measurement of lightning field changes was undertaken using four differing aerial systems, two at a time, in order to compare the response using R.C. circuits having different time constants. The aerial circuits were connected to a double beam oscilloscope with manually operated camera. An external trigger was employed for most recordings and the distance of flashes was measured by means of the time interval between the received electrical impulse which produced an audible signal, to that of the following thunder.

3. Frequency Response

The oscilloscope had a frequency response bandwidth from DC to the 300 kHz, but when used with input R.C. circuits having time constants of less than one millisecond, the lower frequency limit was 100 Hz. By comparing the signal magnitudes obtained on two circuits with differing time constants it was considered possible to obtain

(ii)/...

a correction factor for the cases of signals which were outside the response band width.

4. The comparative response of different aerials

A comparison of the deflections produced by the signals received from two aerials confirmed that in fact the frequency response of the system was not adequate and that a method would have to be devised whereby the correct magnitude of the signals could be obtained. It was decided to ignore the very slow field changes pro= duced by intra-cloud flashes.

5. Determination of Magnitude of Field Changes

The parameters of the four aerials circuits were deter= mined and also the theoretical ratios of deflection of the oscilloscope and these were compared with actual results which indicated that in the majority of measure= ments the time constants of the measuring circuits were small compared with those of the field changes.

A calculation is given which shows that if the field change has an inverted exponential wave form, the time constant of the measuring circuit should be at least 100 times that of the field change for linearity of measurement. However the ratio of deflections of two circuits could be used to derive the equivalent time constant of the field change and hence a correction factor could be obtained. The derivation of this factor is explained and the errors of measurement discussed, the conclusion being that an error better than 10% is unlikely to be attained.

6. Extent of Records

Field change records were undertaken in Salisbury, Rhodesia, over two full lightning seasons and one half season, resulting in 2780 oscillograms from 74 thunder= storms. The maximum number of records obtained from one storm was 185 and the average 37 per storm. Since the recordings were made indoors, few of the actual lightning flashes could be observed and the identification of the type of flash was therefore undertaken by examin= ing the wave form of the field change record.

(iii)/...

7. Analysis of oscillograms

The criteria for identification of types of flashes from field change waveforms are outlined, based mainly upon communicated experience of the late Prof. D.J. Malan together with some published data, and confirmed by visual observation. By far the majority of field change records could be readily classified according to this criteria.

8. The distribution of the durations of fast field changes

On the assumption that fast field changes had an inverted exponential wave form the equivalent time constant of the fast components of intra-cloud and cloud-ground flashes could be obtained from comparative measurements with two aerials. The result of the analysis of 481 components of 145 flashes showed that the fast compo= nents of both cloud and ground flashes were remarkably similar in that they could both be classified into four distinct categories of equivalent time constants - namely less than 0,01 ms; 0,10 ms; 1 ms and greater than 10 ms. Intra-cloud flash components had a greater tendency to= wards the latter group than did ground flashes. This analysis excluded the very slow components of from 20 to more than 100 ms which usually characterised intra-cloud flashes. The median time constant for both cloud and ground flash components was between 0,2 and 0,3 ms, which meant that the median duration for 95% of the field change magnitude was 0,6 to 0,9 ms which is much longer than has been reported in previous investigations. An example of a 25 component ground flash with long duration field changes is cited.

9. Field changes due to lightning

The magnitudes of the fast component field changes of the 145 flashes were calculated and divided into range groups showing a comparison between intra-cloud and ground flashes. It was clear that the fall-off with range did not conform to a D^{-3} relationship as expected, and this was at first thought to be due to the discrimi= nation introduced by the trigger threshold level which

(iv)/...

tended to exclude more and more low values of field change as the range increased. In addition flashes occuring beyond about 25 km were thought to be affected by the electromagnetic field change which attenuated at a lesser rate.

A graphical method was therefore devised to correct a normal or lognormal Gaussian distribution for the loss (or truncation) of the lower values. Hence if the measured distribution of field change magnitudes can be identified as either one or the other, similar correc= tions can be effected and this in fact was found to be possible.

Using a mean value of 10 V/m per division for the scale factor for field changes measured on a standard vertical aerial, the positive field changes for the fast components of 479 intra-cloud and 351 ground flashes were determined and grouped in one kilometer and 10 V/m steps. The numbers of records were too few to determine the distribution of magnitudes in such small range steps so they were then grouped into 10 km range steps and they were then more ammendable to statistical treat= ment. The distributions were then corrected for the truncation of low values to normal distributions, and this resulted in a reduction of the median values by factors of the order of from 5 to 15%.

Despite the addition of missing low values, the median values of field change for intra-cloud strokes was higher than that for ground strokes in the range 0-10 km but was lower in the next range of 10-30 km. Very few positive field changes occured for intra-cloud strokes beyond 30 km, and this was assumed to be on account of the change in polarity of field changes beyond the so-called "reversal" distance which was calculated to be at about 12 km.

The most surprising aspect however was that the median value of the field change was not as low for the 10-20 km range compared to the 0-10 km range as would

(v)/...

have been expected for a D^{-3} relationship and this may be due to the intrusion of high magnitude electromagnetic field changes at closer distances than has previously been measured. This would be possible if either the lightning current magnitudes or the rate of change of current were to be unusually high in the type of dis= charge occurring.

10. The proportion of intra-cloud compared with cloud-ground lightning flashes

A general observation from the results of individual storms shows quite definitely that whilst one storm may produce all intra-cloud flashes, another will produce a majority of ground flashes, and this phenomenon is therefore seen to be a function of the type of thunder= storm. Also it would obviously therefore require a large number of observations to determine the mean ratio of the numbers of the two types.

Secondly when the results were analysed on the basis of the number of observations accumulating as the range was increased, the ratio of cloud-to-ground numbers decreased steadily from a very high value to a value below 2,0 up to about 20 km, indicating that the trigger of the measuring circuit was discriminating against intra-cloud flashes with increasing range.

However, when the total number of records obtained over the three years were grouped in three 3,3 km range steps up to 10 km, the best estimate found for the cloud-ground ratio was 2,24. This value is less than half the value of 5,0 usually quoted for tropical countries and is about the same order as measured for temperate zones such as in Europe and the U.K.

11. Number of component strokes in a lightning flash to ground

More confirmation is given regarding the means of identification of ground flashes from field change records, and all oscillograms of observed ground flashes are indicated for this purpose. As a consequence 1430 records of ground flashes were identified and were

(vi)/...

analysed to determine the proportion which had 1, 2, 3 or more components, the maximum recorded being 28 despite a restricted time sweep of about 0,6 seconds.

The analysis showed that 36% of all flashes were single stroke flashes compared with 13% found by Malan, whilst 21% had 6 or more strokes compared with 18% from Malan's observations. The median number of components was three which is one stroke less than that determined by Malan.

Berger in Switzerland had observed that 65% of all flashes were single stroke, of which 36 were positive - there being no case of a positive multiple stroke flash. In this investigation approximately 50% of the 62 positive flashes observed were single stroke flashes but 4 flashes or 3,2% had 10 or more component strokes.

It is confirmed therefore that positive flashes have a lower probability of multiple strokes than do negative flashes which are however in the majority.

12. Time Intervals between component strokes of a lightning flash

An analysis was carried out on the duration of the time interval between the components of multiple flashes sub= divided into the categories of the first, second, third time interval and finally all time intervals. The first three intervals on average decreased with each succession the mean values being 75, 62 and 53 ms respectively com= pared with a mean of 57 ms for all time intervals. Similarly the median values were 45, 37 and 36 ms res= pectively compared with 35 ms for all time intervals. These time intervals were generally in accordance with other observances except Pierce who recorded longer times.

The frequency distributions were however log-normal Gaussian and as a consequence the standard deviation was large, there being a large number of time intervals which were considerably in excess of the mean or median values.

(vii)/...

13. Total duration of lightning flashes to ground

The limit of 0,6 ms time sweep used in the investigation would according to Malan, result in the loss of about 5% of all records which exceeded this duration. Within this limitation, and excluding single stroke flashes which virtually had a zero time duration, the mean value found for the overall duration of flashes was 219 ms, and the median 177 ms and the latter value compares with 200 ms for Malan's observations and 180 ms for both Pierce and Berger.

When single stroke flashes are included the mean value is reduced to 148 ms and the median 67 ms and these are the figures of more interest to the appli= cation of auto-reclosing switchgear on transmission lines.

The duration of a flash was affected by the occasional intrusion of one or more long time interval with a majority of short time intervals, alternatively all time intervals were either all short or all long duration.

14. Slow component field changes

About 4% of all flashes contained one component which was followed by a slow field change having a mean dura= tion of 142 ms and a median duration of 115 ms. One record out of the sixty obtained, contained two slow components.

In about 20% of the cases, the slow component followed the first component whilst 55% succeeded the last and the remainder were distributed among intermediate component strokes of a flash.

These slow components are thought to be identified with "continuing" currents of a few hundred amperes which follow immediately on an impulse current of a few thousand amperes.

15. The polarity of field changes of ground flashes

The majority of ground flashes are designated negative that is they derive from a negative charge in the cloud,

(viii)/...

and the corresponding field change produced is positive - that is the field intensity becomes more positive when a discharge occurs to ground.

In the analysis of 1430 ground flashes 82,6% were purely negative flashes and 8,5% positive whilst the balance ammounting to 8,9% had components of both polarities.

The ratio of purely negative to positive flashes was therefore 9,6:1 which is less than the ratio of between 14 and 17:1 previously recorded in Southern Africa. However in Europe and the U.K. ratios of the order of between 1 and 5:1 have been recorded and this is thought to be due to the differences in the type of thunderstorm.

Some ground flashes definitely produce field changes of both polarity and the reason for such occurrences is not clear.

17. The relative magnitude of field changes in successive strokes of a flash

An analysis was undertaken of 905 ground flash records which continued two or more component strokes, to determine the relative magnitudes between the first, second and third component. This showed that there was a high probability that the field change during the first stroke will be greater than that of subsequent strokes, but there was a significant probability that the reverse was true.

The ratio of the mean and median values of the amplitude of the 2nd component to that of the first was about 0,6, and the third component tended to have the same value as the second. Also comparing the magnitude of each component with that of the mean amplitude for all components in the same flash, the first was between 1,4 and 1,5 times this mean, whereas the second and third were from 0,8 to 0,9 times the mean value.

Appendix I The capacitance of aerial systems

This appendix gives details of the method of calculation of the electrostatic capacitance of various aerial systems

(ix)/...

The National Electrical Engineering Research Institute

The Lightning Discharge,
by R.B. Anderson

Part I Experimental Observations on Lightning

Contents

(xi)/...

(xii)/...

(xiii)/...

List of Figures

1/...

PART I EXPERIMENTAL OBSERVATIONS ON LIGHTNING

1. General

The total electric field intensity at a distance D from a charge dipole can be stated by the well known LeJay[1] relationship:

$$E = \left(\frac{1}{4\pi\epsilon_o\epsilon_r}\right)\left\{\frac{M}{D^3} + \frac{dM}{dt}\frac{1}{cD^2} + \frac{d^2M}{dt^2}\frac{1}{c^2D}\right\} \text{ V/m} \quad \ldots\ldots \quad (1.0)$$

Where M is the electric moment of a charge "Q" situated at a height of "H" above ground, whence M = 2QH; and c is the velocity of light. In this relationship D>>H.

In the static case, namely when the charge Q is stationary and unchanged in value, the second two derivative terms are zero, and the expression merely indicates the electrostatic field intensity. As soon as a discharge occurs however, the value of Q changes - in fact reduces - with time, and in this case of course the total electric field changes with time. The second and third terms are then operative and have become known collectively as referring to the electromagnetic field having two terms namely, the induction or "near field" being proportional to D^{-2}, and secondly the radiation or "distant field" being proportional to D^{-1}.

If these fields are denoted by Es, Ei and Er, respectively, and are all functions of time, the total electric field intensity E(t) may be re-stated as follows:

$$E(t) = Es(t) + Ei(t) + Er(t)$$

and referring to the LeJay equation (1.0)

$$Ei(t) = D/c.d/dt\cdot[Es(t)] \text{ and}$$

$$Er(t) = D/c\cdot d/dt\cdot[Ei(t)]$$

Now since $Es(t) = 2Q(t)H\cdot(4\pi\epsilon_o\epsilon_r D^3)^{-1}$

$$d/dt[Es(t)] = H\cdot dQ/dt\cdot(2\pi\epsilon_o\epsilon_r D^3)^{-1}$$
$$= H\cdot I(t)\cdot(2\pi\epsilon_o\epsilon_r D^3)^{-1}$$

Where I(t) is the lightning current variation with time.

2/...

Where I(t) is the lightning current variation with time.

Hence $Ei(t) = H \cdot I(t) \cdot (2\pi\varepsilon_o\varepsilon_r cD^2)^{-1}$

And $Er(t) = H \cdot dI/dt \cdot (2\pi\varepsilon_o\varepsilon_r c^2 D)^{-1}$

Hence equation (1.0) may then be re-stated generally as

$$E(t) = H(2\pi\varepsilon_o\varepsilon_r)^{-1} \cdot [Q(t) \cdot D^{-3} + I(t) \cdot (cD^2)^{-1} + dI/dt \cdot (c^2 D)^{-1}] \text{ V/m } \ldots \quad (1.1)$$

In the above equations, the time "t" refers to that occurring at the position of the discharge, whereas at any point of observation distant D from the discharge, the electric field will change only after a time $(t - D/C)$ to allow for propagation at the velocity of light. When D>>H, the propagation time from all parts of the discharge path can be regarded as being approximately constant. If however, the distance D is small, or comparable with H, not only is the expression for the electrostatic field itself altered, but also the propagation time changes according to whether the radiation proceeds from the discharge path at ground level, or from the uppermost extremities. These complications are examined later.

Suffice to say at this stage that it is obvious that the electric field intensity as a function of time will vary according to the magnitude of the charge involved and also the time function of the charge variation. In addition it is affected directly by any variations of the height H or distance D.

All the basic parameters which make up equation (1.1) are known to vary, some over a wide range even in the same thunderstorm, and therefore the application of this relationship could be open to considerable error unless these parameters can be statistically determined.

On the other hand statistical data as to the frequency distribution of the resultant lightning field change amplitudes could be obtained more readily and if the number of

3/...

observations is sufficiently large the resulting distribution could be reliable, and whilst there would undoubtedly be variation from storm to storm, or season to season, the deviation of the errors would be known and probably acceptable for most practical considerations.

The object of the research herein described therefore, was to make as large a number of measurements as possible on the characteristics of lightning discharges with a view to determine if possible, statistical relationships which could be applied with confidence. For example, whilst it is known that the electric field intensity at different distances from a given lightning discharge diminishes according to the fundamental laws already described, the lightning discharge itself is also a variable in the sense that the charge, current and waveforms are by no means constant. Consequently there is a need to combine all these variables into a single relationship say of the distribution of field change magnitudes which could be expected at given distances.

Admittedly such measurements would have to be made over a long period so that many values may be obtained at each range, but at worst the data could be analysed on the basis of the distributions which occur when the range is progressively larger, thereby increasing the sample size to suit the number of observations.

Furthermore, there is the question of the difference between the characteristics of intra-cloud lightning flashes compared with those to ground to be taken into account; the former cannot be ignored when applying the information obtained when counting lightning flashes with instruments based on the response to electric field changes. It is vital to consider these factors in view of the fact that relatively little information is available regarding the characteristics of intra-cloud flashes.

Finally this research would not be complete unless an attempt was made te relate the results to existing knowledge and hypotheses of the mechanism of the lightning discharge, and to discuss any aspects which might need further amplification.

4/...

2. Description of Equipment

The equipment consisted basically of a COSSOR Double Beam Oscilloscope having two amplifiers A1 and A2 of differing gains and equipped for external triggering; to it were coupled various arrangements of aerials, which comprised the following and which are pictorially illustrated in Figs. 1 and 2.

(i) A vertical tubular aerial approximately 8 ft. (2,4 m) long mounted on top of a steel pole 6 ft (1,8m) in height. The aerial was connected to the oscilloscope by means of 35 ft (10,5m) of co-axial cable having a capacitance of 900 pf and its screen was earthed to an earth mat buried at the base of the steel supporting pole - this being the only earth for the complete installation. This particular aerial was regarded as the standard, and was used throughout the investigation permanently connected to the A2 amplifier input terminals of the oscilloscope.

(ii) A horizontal aerial consisting of two No. 10 s.w.g. wires at right angles, each 10ft. (3,1m) in length and radiating from the base of the above described aerial at a height of 6 ft. (1,8m) from the ground. The wires were used either eingly, or in parallel and they were connected to the oscilloscope A1 amplifier also by means of co-axial cable the capacitance of which was 770 pf. The capacitance of each arm of the aerial itself was approximately 30pf and this gave rise to a capacitance divider ratio which could be varied by a factor of two according to whether one or two arms were connected.

(iii) The third aerial which was used in the comparison consisted of six horizontal parallel wires 45 ft. (13,6m) in length erected at a height of nearly 16 ft. (4,8m) above ground, and lead directly to the oscilloscope by an insulated down lead, no co-axial cable being employed. This aerial is termed the ERA aerial and is as recommended for use with electrostatic counters designed by

5/...

General View Measuring Equipment

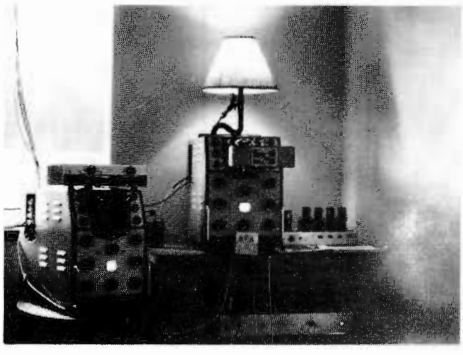

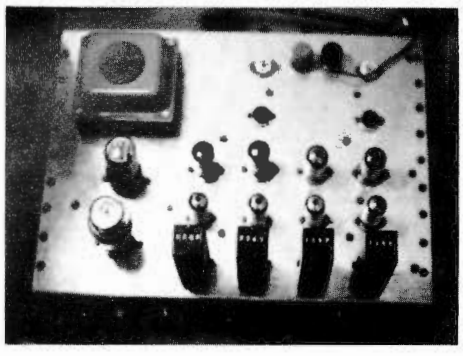

Wood Counter

ERA Counter

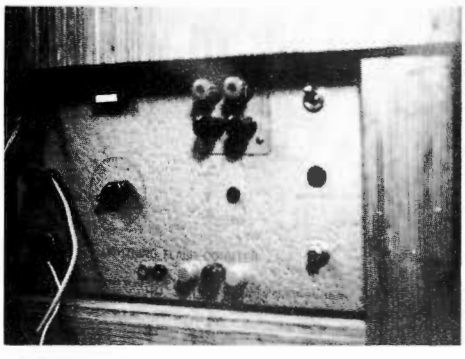

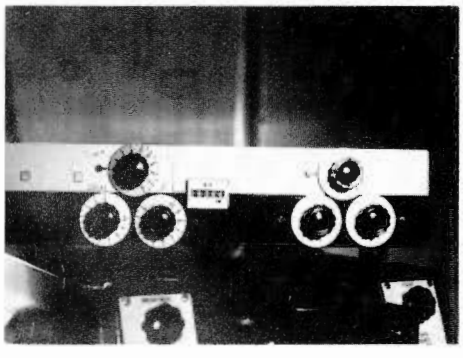

Malan Counter

FIGURE 1

Equipment used in Salisbury

Standard vertical aerial

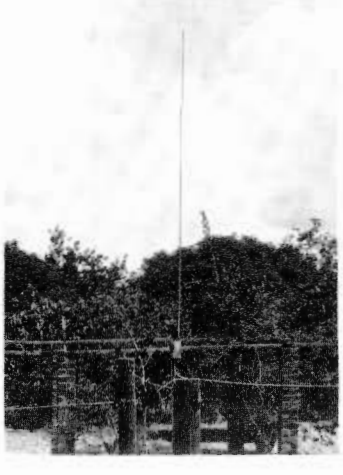

ERA Aerial (N.E.End.)

Single Horizontal aerial.

ERA Aerial (S.W.End.)

FIGURE 2

Measuring Aerial Systems

Pearce[2] and modified by Golde[3] of the Electrical Research Association. (U.K.) and has now been adopted for the standard aerials to be used with lightning flash counters recommended by the International Conference on Large Electric Systems (CIGRE)

The procedure consisted of connecting one of the latter two aerial arrangements at a time, to the A1 amplifier, and to compare the deflections with the so-called standard vertical aerial by photographing the output of the oscilloscope on the occurrence of a stroke of lightning.

To do this effectively, a sensitive counter, the circuit of which is indicated schematically in figure 3 was permanently connected between the standard aerial and the oscilloscope, and the sound of the counter operating gave the signal to close the camera lense and for the film to be moved to the next position. The time from this signal to thunder was also measured by stop watch before proceeding to the next photograph. The complete arrangement is as shown in figure 4.

In the initial stages of the investigation, the object was mainly to obtain as many records as possible of the resultant oscillographic deflections, using the standard aerial.

A time sweep of 150 ms was employed, the A1 beam being connected to produce a 50 Herz timing wave.
Under these conditions, the camera shutter was left open for a period not exceeding 60 seconds, and masks were applied to reduce film fogging. This resulted in oscillograms which could not be resolved in respect of the order of occurrence of the components of field change, but there was no difficulty in measuring the number and the magnitude of the changes. The possibility of obtaining records showing more than one stroke was remote, excepting for field changes of small magnitude which did not operate the audible counter.

Later comparisons were made between the responses from the various aerial arrangements, and a time sweep of the order of 600 ms was then used without a timing wave, and the oscilloscope beam was triggered externally. The control

6/...

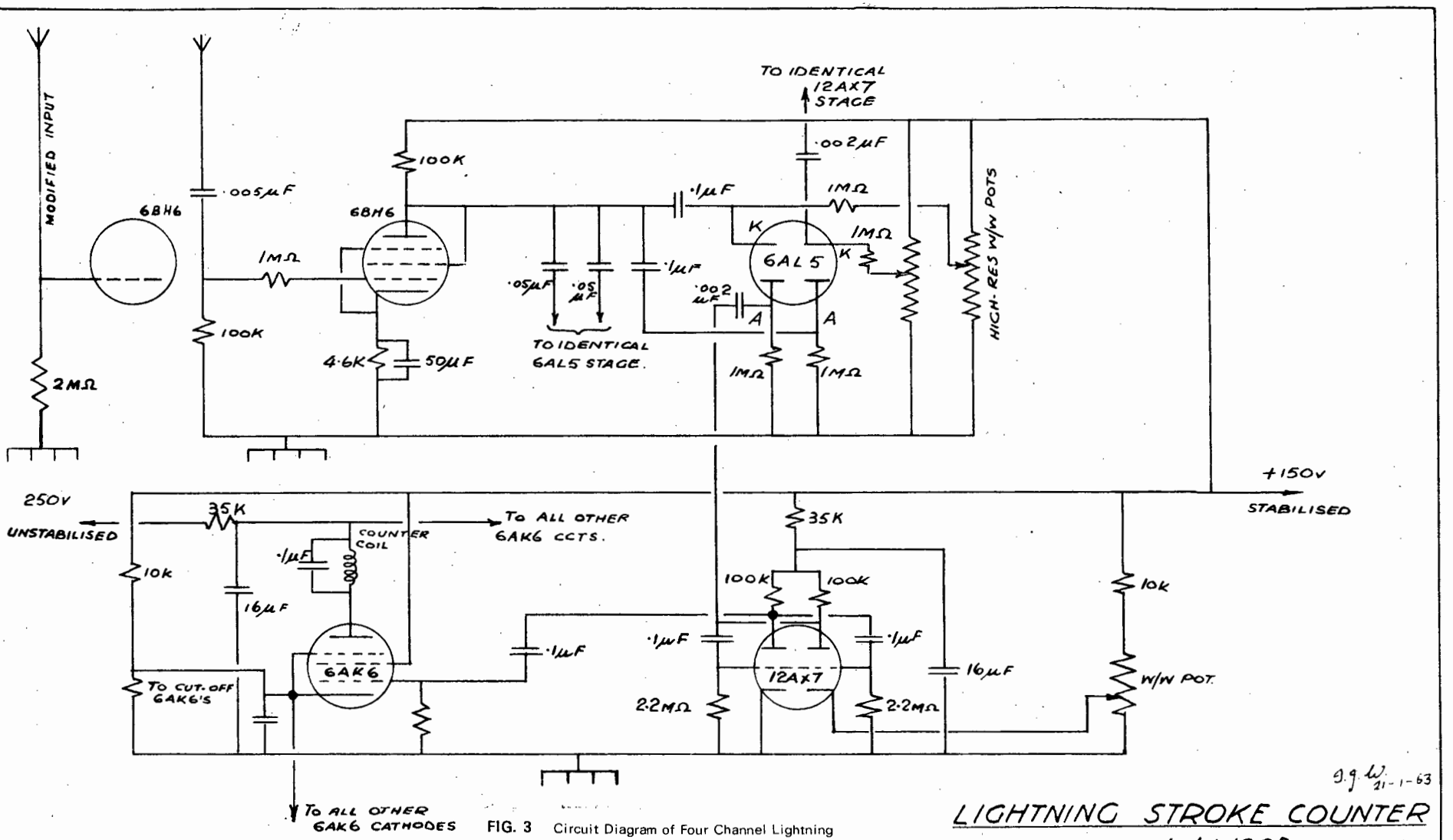

FIG. 3 Circuit Diagram of Four Channel Lightning Stroke Counter

J.J.W. 21-1-63

LIGHTNING STROKE COUNTER

DEVISED BY I. J. WOOD. D.568/4.

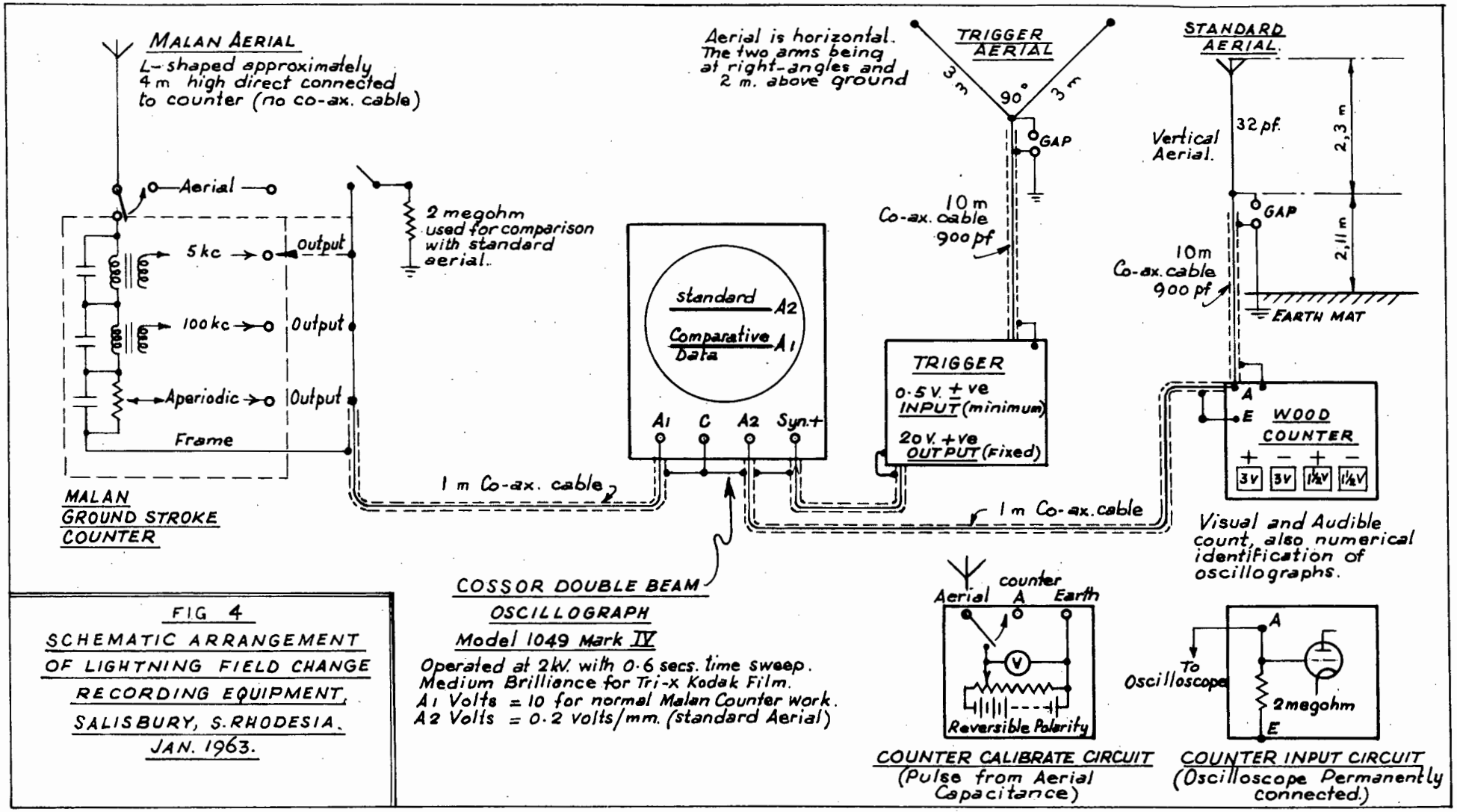

FIG 4

SCHEMATIC ARRANGEMENT OF LIGHTNING FIELD CHANGE RECORDING EQUIPMENT, SALISBURY, S. RHODESIA. JAN. 1963.

on the time sweep was maintained by direct calibration at frequent intervals and this was found to be reasonably constant over the period of a thunderstorm. The length of the traverse was adjusted to come within the photographed area and a good time resolution of the oscillogram was possible.

Occasionally the beam was triggered internally from the A2 amplifier, and the standard aerial, but since this circuit had a relatively slow input time constant of 0.6 ms, an external aerial having no co-axial cable lead-in was later employed. Both arrangements however suffered initially from the disadvantage that the oscilloscope could only be triggered by one polarity at a time, and it was necessary to switch the control whenever there was a change in the predominant polarity of the field changes. A triggering circuit (figure 5) was therefore designed by a colleague which was capable of triggering on either incoming polarity and with a delay not exceeding two microseconds, and this proved very satisfactory.

Other equipment used consisted of separately operated counters of the ERA design and also a prototype of the Malan[4] ground stroke counter, and at one stage the operation of these counters was superimposed on the oscillograph recordings, to indicate whether one or both counters registered during the particular stroke. Oscillograms were also obtained of the comparative outputs of the various channels of the Malan counter for initial testing purposes.

3. Frequency Response

The frequency response of the oscilloscope amplifiers alone as given by the manufacturers was DC to 300 kHz; however the connection of the co-axial cable capacitance used, and a resistence to earth parallel to the input resistence of the oscilloscope amplifier circuit, altered conditions to the extent indicated in figure 6.

In the case of the so-called standard vertical aerial connected to the A2 amplifier, the co-axial cable capacitance was 900 pF and the parallel resistor, mounted in the Wood

7/...

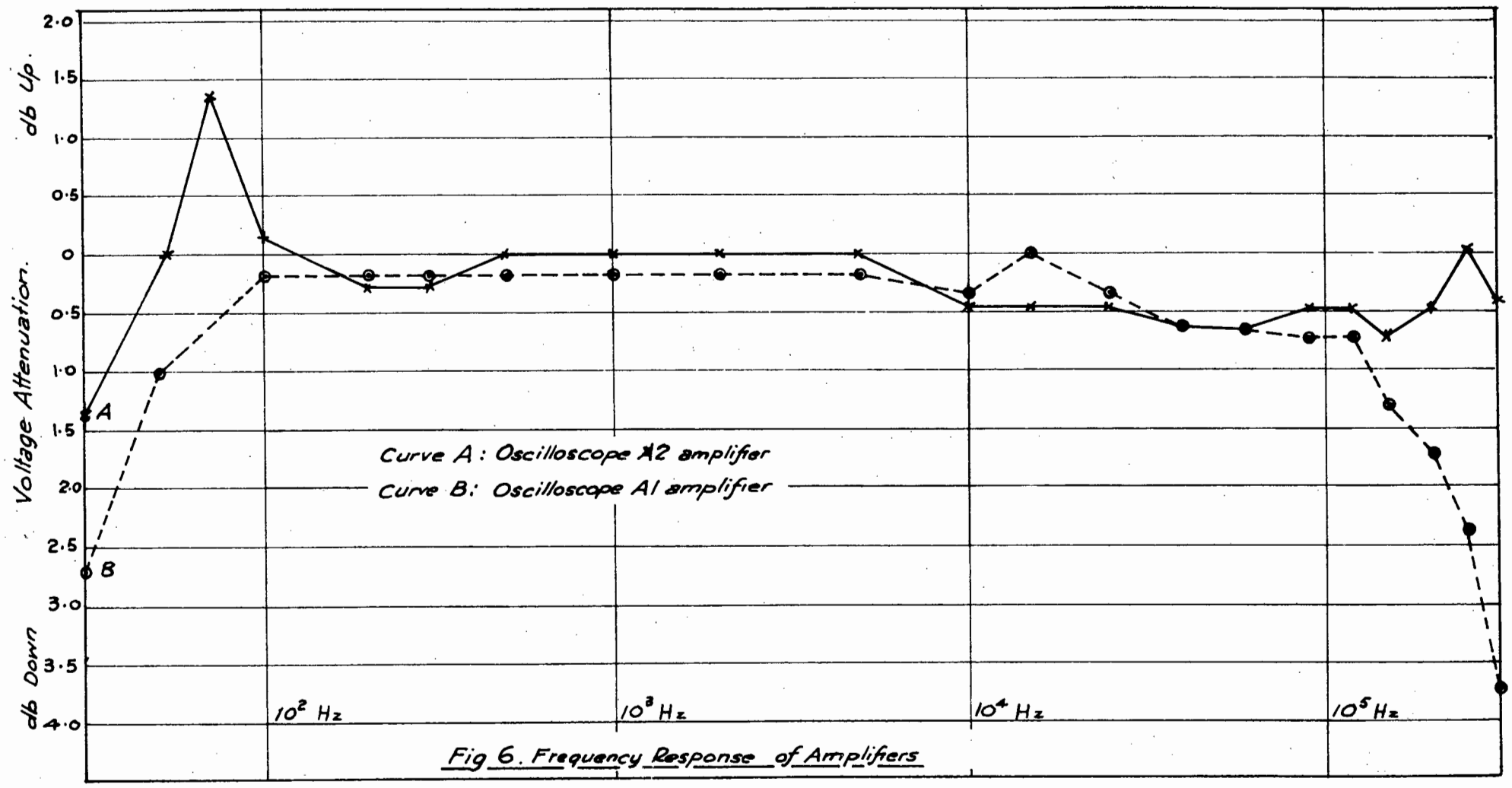

Fig 6. Frequency Response of Amplifiers

counter, was 2 Megohms, whence the circuit time constant was approximately 0,6 ms. The effect of this is illustrated in figure 6, curve A. The attenuation was however constant over the range of 100 Hz to 300 kHz.

In the case of the A1 amplifier and using a co-axial cable having capacitance of 770 pF, an RC time constant of 0,3 ms was maintained, and in this instance the 3 dB limits were only slightly less as indicated in figure 6 curve B.

In view of the above it would be expected that the relative deflections due to field changes would maintain a constant proportion to each other provided that the frequency range of the input signals did not exceed the above limits. If however the rise times of the field changes encountered in practice were longer in duration than the respective time constants of the measuring circuit their magnitudes would be attenuated by differing amounts determined by the R.C. circuit response; conversely if they were of very short duration; they would be attenuated by the amplifier circuit itself and again would not be identical.

Hence in order to determine the approximate frequency range of the field change signals, the actual ratio of the deflections produced on two of the aerial circuits were examined, and analysed, and information regarding this frequency range could then be obtained.

4. <u>The comparative response of different aerials</u>

The first comparison made was between the magnitude of oscillograph deflections produced by the effect of lightning field changes on the standard vertical aerial and on the horizontal aerials respectively - both being fed to the oscilloscope through co-axial cable. The time constant of the former was 0,6 ms, as previously stated, and of the latter 0,3 ms for the particular amplifier range switch position. The oscillograms indicated field changes of both the slow and fast variety and were all taken with the 600 ms time sweep. It was ascertained from an examination of the records that the maximum value of field change was almost invariably associated with a fast change - that is a change which appeared as a vertical line or

8/...

wave front on the oscillogram - even though with intra-cloud discharges a slow field change may also be, and was usually present. The resolution was such that these fast field changes would be defined as taking place in less than say 10 ms on the slow time sweep scale.

In view of this observation the slow field changes were ignored and only fast field changes were measured using the zerovolts base line as zero if no slow field change was present, or the level of the instantaneous value of the slow field change, if the fast change to be measured happened to be superimposed there on. Each oscillogram showing a comparison of two aerials, resulted in a number of readings being obtained according to the number of components present, and as a result of which 96 recordings were obtained from 41 flashes for the single wire horizontal aerial, and 210 from 63 flashes for the twin horizontal array. The ratios of the oscillograph deflections from the standard aerial to the simultaneous deflections from the other aerials were calculated, and these indicated a considerable dispersion. Instead of maintaining a constant value as expected, the ratios varied between 1,0 and 2,6 in the case of the standard versus the single norizontal aerial deflections, and between 0,5 and 1,4 when using the double horizontal aerial (of twice the capacitance). This in fact means that the frequency range for these observations exceeded the limits of the response of the circuits. In view of the dispersion of values, the results were plotted cumulatively on probability paper as shown in figures 7 A and B respectively and the frequency distributions proved to conform closely to a log-normal Gaussian distribution. The median value of the ratios due to the single wire aerial was approximately twice that for two wires, and this confirmed that the outputs of the two aerials were approximately in the inverse ratio of their capacitances to earth.

The frequency distribution of the ratios of the standard aerial deflection to that of the high ERA aerial was determined from 164 readings from 41 flashes. This distribution was also log-normal and is illustrated in figure 8. This

9/...

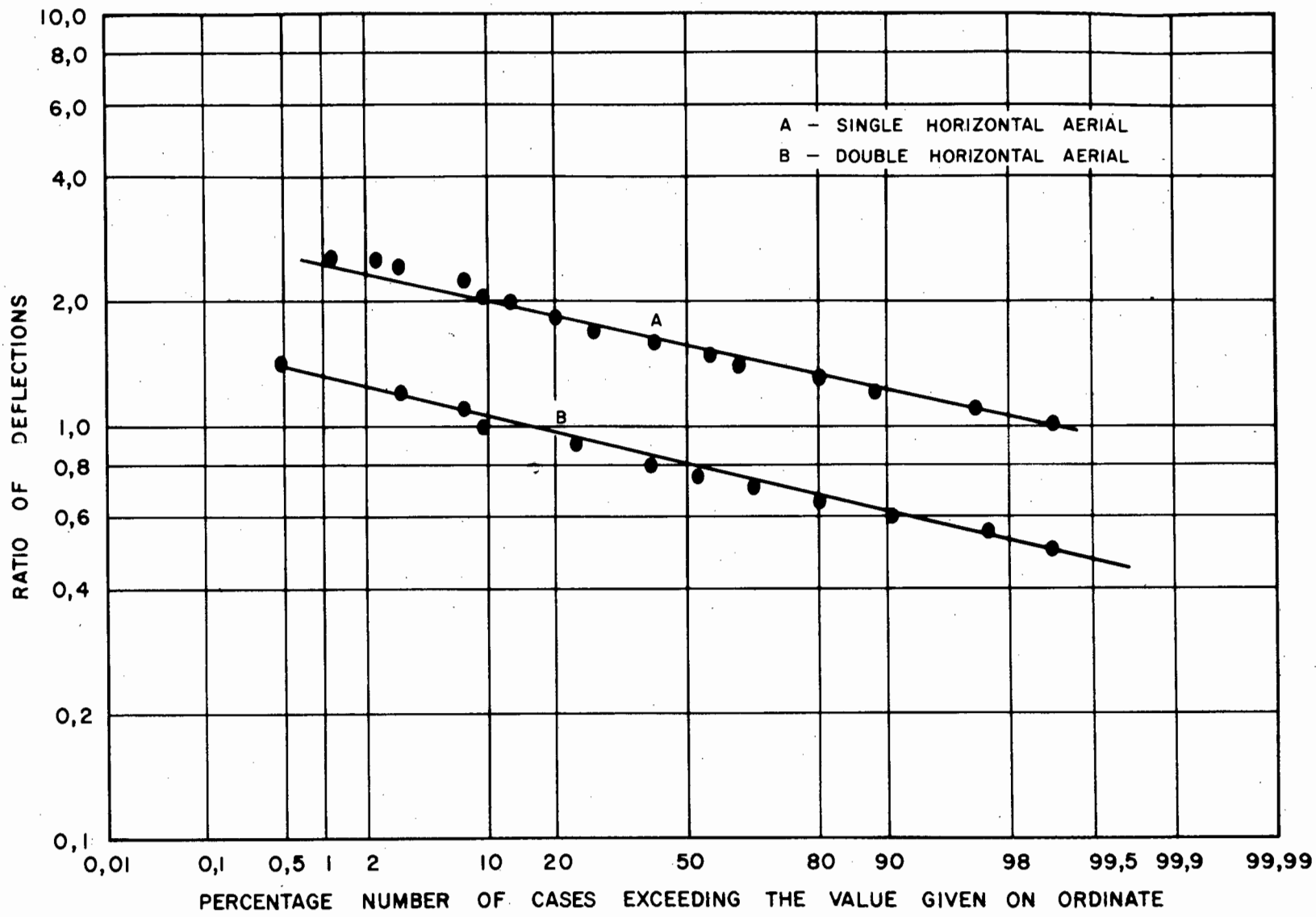

FIGURE 7

DISTRIBUTION OF RATIOS OF DEFLECTIONS OF STANDARD VERTICAL AERIAL TO HORIZONTAL AERIALS

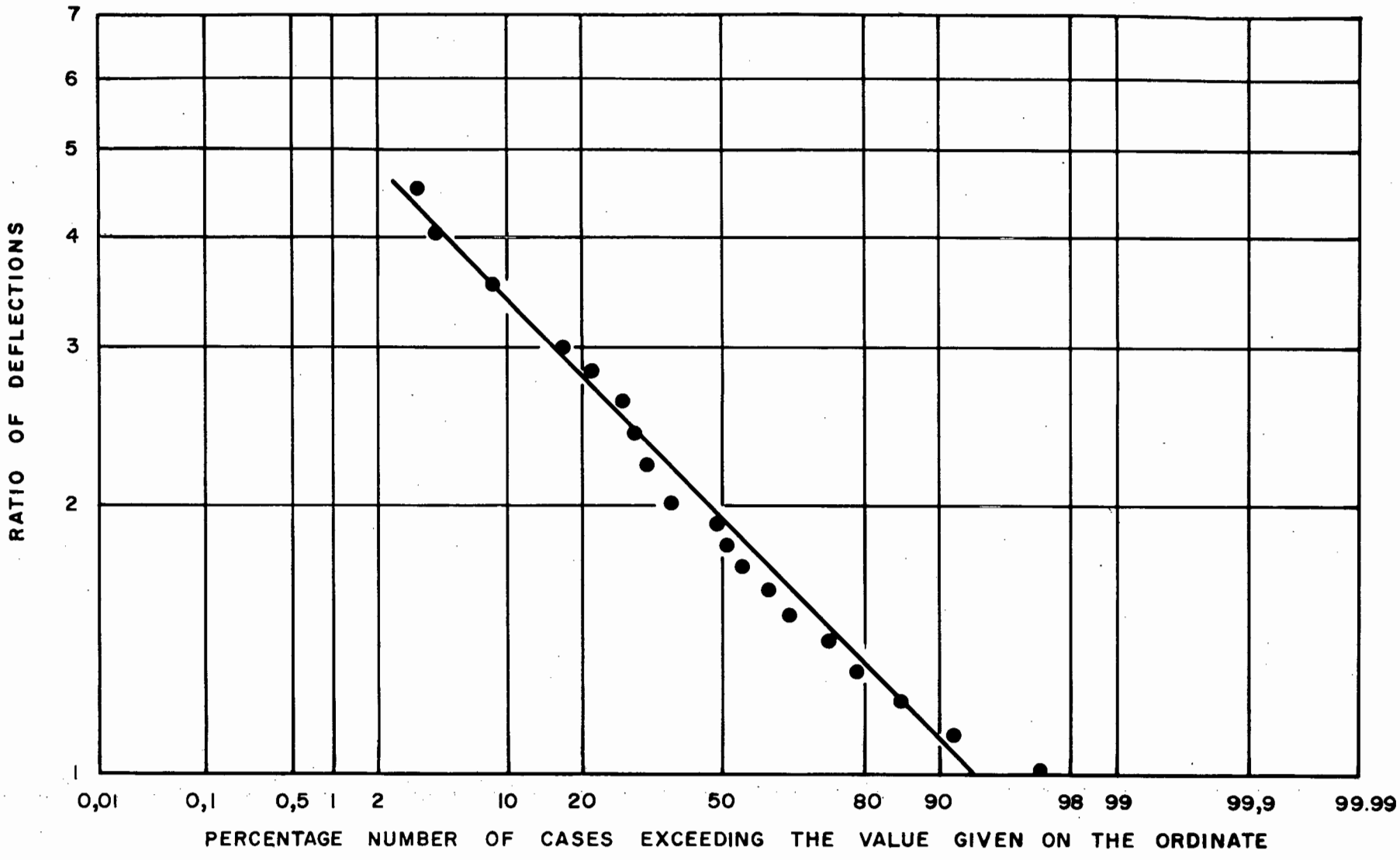

FIGURE 8

DISTRIBUTION OF RATIOS OF DEFLECTIONS OF STANDARD VERTICAL AERIAL TO THAT OF ERA AERIAL

lognormality would be expected in this comparison, since the time constant of the ERA aerial which was not provided with a co-axial cable lead-in, was less than 0.1 ms, namely one sixth of that of the standard vertical aerial.

5. Determination of Magnitude of Field Change

Considering the input system to act purely as a capacitor divider, as a first approximation, the magnitude of the absolute field change in units of volts per metre may be expressed in the general form:-

$$\text{Field Change } Ec = (Ca+Co)/Ca \;.\; df/h \qquad (2.0)$$

Co = the capacitance to earth of the lead-in co-axial cable (if any) including the oscilloscope input capacitance.

Ca = the capacitance of the aerial.

d = the deflection of oscilloscope beam in arbitrary linear divisions.

f = the scale multiplier factor for the amplifier used, in volts per division.

h = the effective height of the aerial in metres.

The capacitances of each of the aerial systems was measured accurately using a 1000 Hz capacitance bridge. Similarly the capacitances of the co_axial cables and of other capacitances connected to make up the value of the circuit capacitance Co were determined; the corresponding value of the capacitance voltage ratio could then be calculated.

10/...

The capacitances of the various aerial systems, however, were also checked by calculations, as indicated in Appendix I and in each case the results were compared with the measured value.

The effective heights of the horizontally mounted aerials were taken as that of the height of the horizontal portion of the aerial above ground. In the case of the so-called standard vertical aerial however, the effective height was 3,26m as determined in Appendix I. This was the midpoint of that portion of the aerial which was above the steel support upon which it was mounted, as illustrated in figure 9.

The scale multiplier factors for each of the amplifiers and their sensitivities were of course available and were checked. The A1 amplifier was graduated in terms of the voltage required to produce full scale deflection which in the case of this oscilloscope was 87,5 mm. Hence a scale multiplier of 10 volts corresponded to a sensitivity of 0,1275 V/mm. The A2 amplifier was calibrated directly in terms of volts/mm. All values obtained are indicated in Table I.

Accordingly, with all measured parameters known, it was possible to evaluate equation (2.0) and to determine the ratios of the deflection assuming a constant value for the magnitude of the field change.

11/...

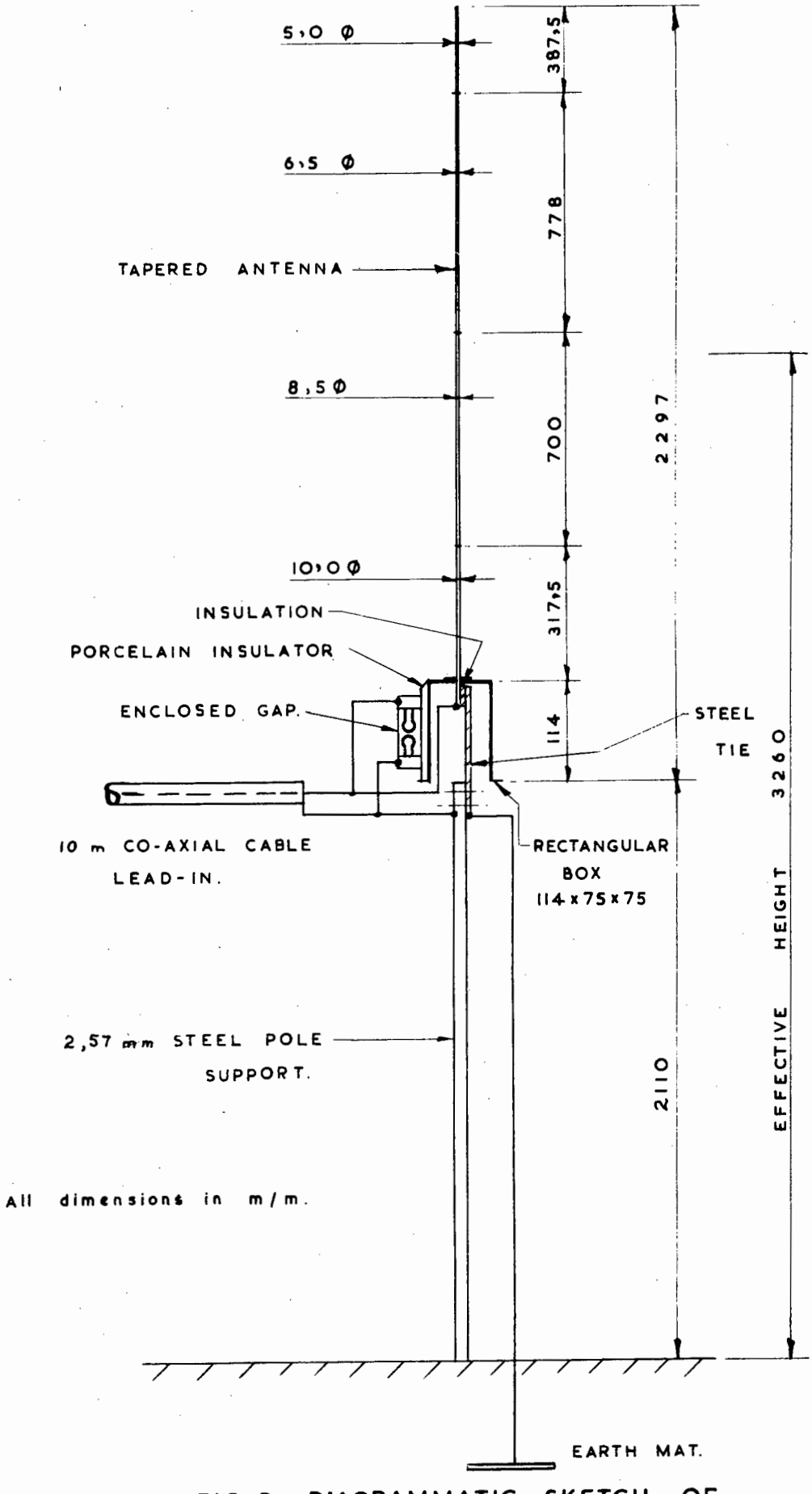

FIG. 9. DIAGRAMMATIC SKETCH OF VERTICAL ANTENNA

Table I Parameters of the various aerial systems

Item	Parameter		Standard Vertical Aerial	Horizontal Aerials		
				Single	Double	ERA
1	Overall Height above ground	metre	4,41	1,84	1,88	4,85
2	Effective Height	metre	3,26	1,84	1,88	4,85
3	Capacitance of Aerial (Ca)	pF	32	28	61	276
4	Capacitance of input-co-axial cable	pF	900	770	770	-
5	Additional connected cir=cuit capacitance	pF	45	9	9	-
6	Value of circuit capacitan=ce (Co+Ca)	pF	977	807	840	276
7	Value of Circuit Resistance	M/ohm	0,64	0,372	0,372	0,366
8	Capacitor Voltage Ratio (Co+Ca)/Ca	-	30,6	28,8	13,8	1,0
9	Oscilloscope scale Multi=plier Full scale deflection	-	0,2V	10V	10V	1000V
10	Equivalent Scale multiplier factor f.	V/mm	0,2	0,1275	0,1275	12,75
11	Calibrated Scale multiplier	V/div	0,560	0,3575	0,3575	35,75
12	Oscilloscope deflection per unit V/m Field change-d/Ec	mm/v	0,533	0,500	1,070	0,380
13	Minimum Ratio of Deflec=tions: Standard Aerial/ others	-	1	1,07	0,500	1,400
14	Time constant Measuring Circuit	ms	0,625	0,300	0,313	0,101

Now referring to the experimental results of the distri=bution of ratios depicted in figures 7 and 8 it is clear that most values of these ratios are in excess of the values given in Table 1 Item 13, as illustrated by the following table.

12/...

Ratio of Deflections	Calculated Minimum	Measured Values		
		98% Exceed	50% Exceed	2% Exceed
Standard Aerial/Single Horizontal	1,07	1,05	1,55	2,50
Standard Aerial/Double Horizontal	0,50	0,52	0,76	1,2
Standard Aerial/ ERA Aerial	1,40	1,0	1,9	4,7

This indicates that some correlation exists between calculated anc actual measurements; but the fact that most measured values exceed the calculated values, suggests that the waveform of the field change is outside the limits of the frequency response of the circuits.

Hence the accuracy with which the peak value of the field change can be measured depends upon the response characteristics of the measuring circuit to the waveform. The approximation of equation (2.0) assumes that this waveform has a comparatively steep front with a duration which is short compared to the time constant of the measuring circuit. On the other hand if it is too short, it will be attenuated by the H.F. response of the amplifiers which have a 3 db limit of about 250 kHz. (or a rise time to peak of 1μs). Considering that the return stroke of a lightning discharge has a duration of the order of magnitude of 100μs it is unlikely that the duration of the accompanying field change would be much less than this. Hence there is a greater probability that the duration may be larger and this should be examined in relation to the R.C. measuring circuit, which is depicted schematically below:

13/...

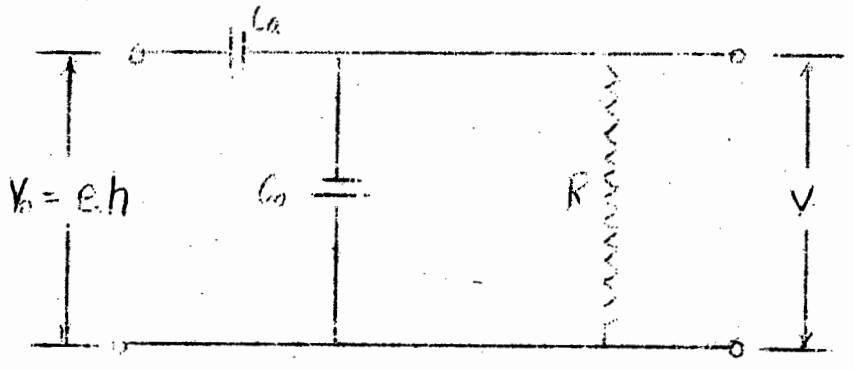

The differential equation which describes the output voltage "V" in terms of the field change "e" at an effective height of h is given by the following expression

$$dV/dt+V/CR = Cah/C \cdot de/dt \qquad (3.0)$$

Where $C = Ca+Co$

If it is now assumed that the field change has the following exponential form:

$$e = Ec[1-\exp(-t/T)]v/m \qquad (3.1)$$

Where Ec is the overall field change and T is its de= cay time constant. If To = RC, the time constant of the measuring circuit, then the solution of equation (3.0) is:-

$$V = Ca/C \cdot hEc[\exp(-t/To)-\exp(-t/T](1-T/To)^{-1} \qquad (3.2)$$

The output voltage V is a maximum when dv/dt = 0 whence the value of t_m when this occurs is as follows:-

$$t_m = T \cdot Ln[(T/To)/(1-T/To)] \qquad (3.3)$$

Putting T/To = Tr and $Ln[Tr/(1-Tr)]=\alpha$

14/...

and substituting "t_m" for "t" in equation (3.2) the maximum output voltage Vm is then:-

$$Vm = Ca/C \cdot hEc[\exp(\alpha Tr) - \exp(\alpha)](1-Tr)^{-1} \text{ volts} \qquad (3.4)$$

Now Equation (2.0) can be written as follows:-

$$Ec = C/Ca \cdot Vm/h \qquad (3.5)$$

Where Vm = deflection of oscilloscope (d) times the scale multiplier factor (f)

= maximum voltage measured at the oscilloscope.

and inverting (3.4) accordingly the following equation results:-

$$Ec = C/Ca \cdot Vm/h \cdot (1-Tr)[\exp(\alpha Tr) - \exp(\alpha)]^{-1} \text{ V/m} \qquad (3.6)$$

Hence it is clear that the bracket terms on the right hand side of equation (3.6) represent a multiplying factor for equation (3.5) which is dependent only on the value of Tr=T/To, which in turn is the ratio of the time constant (or a measure of the duration) of the field change to that of the measuring circuit.

Calculated values of the bracket terms are given below:--

Tr=T/To	Equation (3.6) Bracket Terms
0,01	1,05
0,10	1,29
1,00	2,72
2,70	4,85
10,00	12,90

The above indicates that if the field change waveform is exponential as defined, the duration time constant T must be less than one hundredth of the time constant of the measuring circuit if the bracket term is to approximate unity; conversely, if it is not, then the appropriate correction has to be applied to obtain the correct value of the field change. For example, with a circuit time constant To as used of 0,6 ms, the field

15/...

change time constant should not exceed 6μs, that is a nominal duration of 18μs, otherwise the measured voltage would have to be multiplied by some factor greater than unity, to obtain the absolute value of the field change magnitude.

Hence unless tha time constant of the measuring circuit is large compared with that of the field change duration it would not be possible to calculate the absolute value of the field change without any knowledge of the waveform. This difficulty may be partly resolved, however, if a measurement is made simultaneously with circuits having different time constants, since the ratio of the deflections must then be a function of the duration, if the waveform of the field change is not an infinite step function.

Bruce and Golde[5] discuss the waveform of field changes and conclude from their examination of all available records that initially the field intensity during the return stroke of lightning increases abruptly, corresponding to what they term the "b" portion, or the first "R" element described by Malan. This is followed by a slowly tailing off "c" portion, often much larger in magnitude. This description is approximated by the inverse exponential form of equation (3.1) and it is proposed to use it in order to deduce the duration of the return stroke and hence the factor by which measurements must by multiplied in order to calculate the magnitude of the field change.

Equation (3.6) may be also written as the magnitude of the field change per volt namely:-

$$Ec/Vm = C/C_a h \cdot (1-Tr)[\exp(\alpha Tr)-\exp(\alpha)]^{-1} \text{ V/m/V} \qquad (3.7)$$

Where Vm is the minimum output voltage measured at the oscilloscope, C/C_a is the ratio of the total existing circuit equivalent capacitance to that of the aerial - i.e. the inverse of the capacitor divider ratio.

h is the effective height of the aerial

16/...

Tr = T/To is the ratio of the time constant of the assumed exponential field change to that of the measuring circuit.

α = Ln[Tr/(1-Tr)]

Then if equation (3,7) is multiplied by the scale factor f = V/unit deflection or V/d for the oscilloscope, the field change per unit deflection Ec/d is obtained.

Hence choosing a range of values for T, the corres= ponding values of Ec/d may be calculated for the circuits depicted on Table I, and the ratio of the deflection of the standard vertical aerial circuit to that of the others may thus be determined. The calculated results are given in Table II below and these are further depicted in figures 10 and 11.

T	Ratio of Deflections			Field Change Ec/d -"V/m/division			
ms	Std/1H	Std/2H	Std/ERA	Std	1H	2H	ERA
0,00	1,07	0,50	1,40	5,3	5,6	2,6	7,4
0,01	1,12	0,52	1,69	5,6	6,3	2,9	9,5
0,05	1,22	0,57	2,24	6,5	8,0	3,7	14,7
0,1	1,30	0,60	2,68	7,5	9,7	4,5	19,9
0,2	1,40	0,65	3,26	9,0	12,6	5,8	29,3
0,3	1,47	0,68	3,68	10,3	15,2	7,0	38,0
0,5	1,57	0,72	4,26	12,8	20,1	9,2	54,7
0,7	1,63	0,75	4,68	15,1	24,7	11,3	70,7
1,0	1,70	0,78	5,13	18,4	31,2	14,3	94,3
2,0	1,83	0,83	5,99	28,5	52,1	23,7	170,9
3,0	1,90	0,86	6,45	38,1	72,3	32,8	246,2
5,0	1,97	0,89	6,99	56,6	111,6	50,5	395,1
10,0	2,06	0,93	7,56	101,1	207,9	93,9	764,2

Table II. Calculated Values of Ratios of Deflection and Field Change for Aerial Systems.

T = Time constant of assumed inverse exponential field change waveform.
Std=Standard Vertical Aerial
1H & 2H = Single and Double Horizontal Aerials, respectively,
ERA= Six wire horizontal aerial to E.R.A. Specification.

17/...

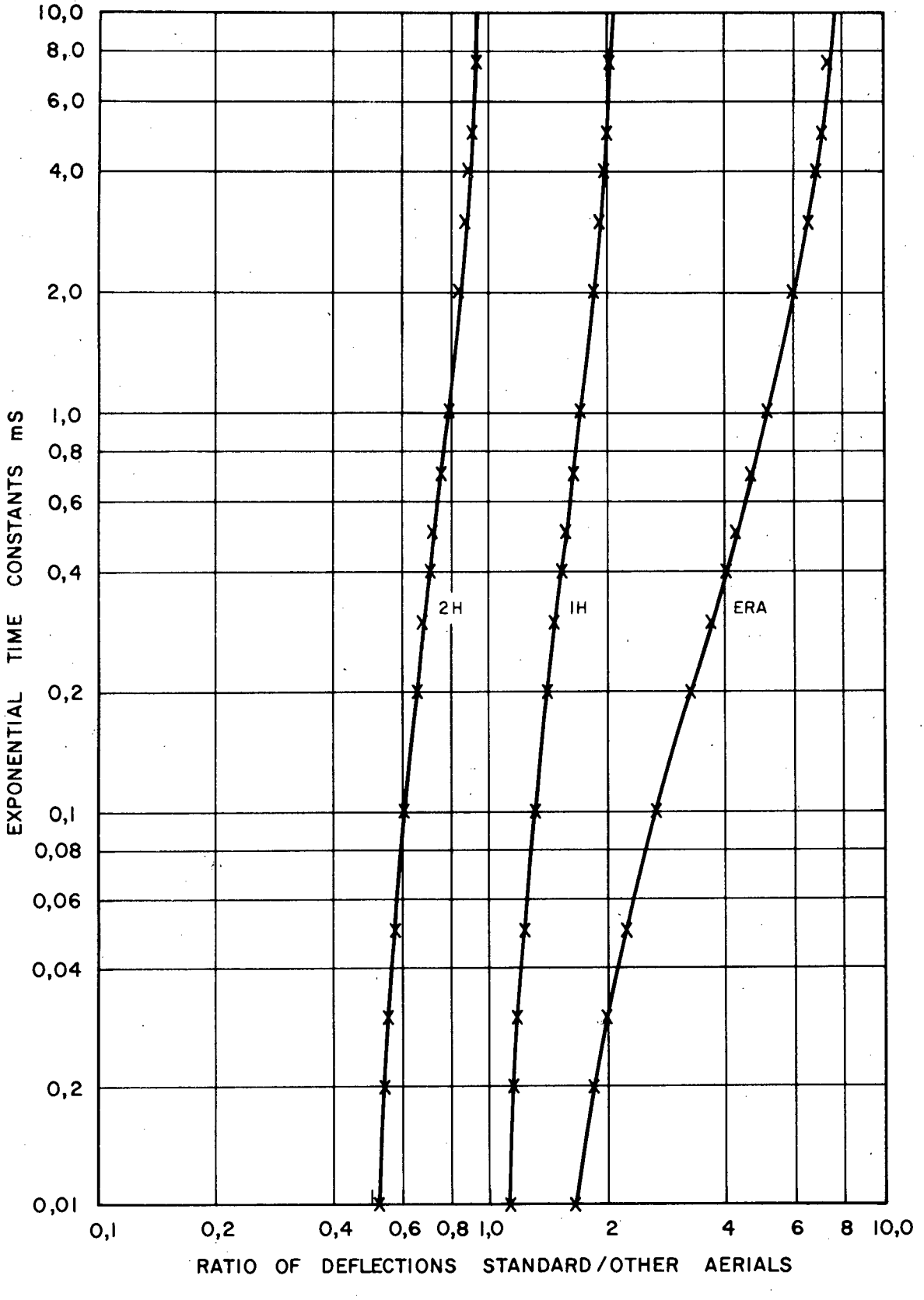

FIGURE 10

CALIBRATION OF AERIAL SYSTEMS

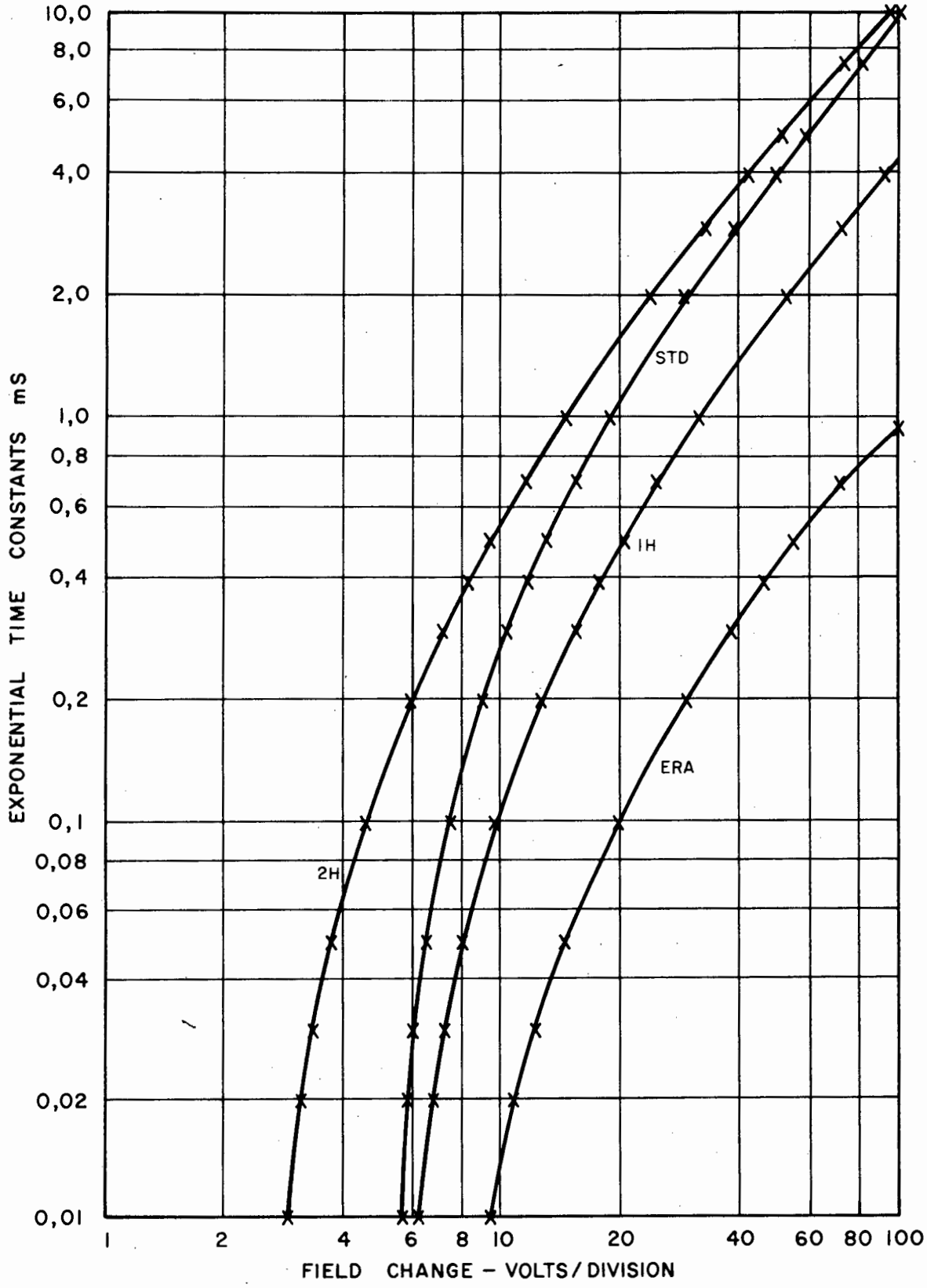

FIGURE 11

CALIBRATION OF AERIAL SYSTEMS

It will be clear from the above that if the ratio is obtained from the deflections observed of field change measurement with two circuits of differing time constants it is possible to obtain a time T representing the duration of the field change in terms of the time constant of the inverse exponential waveform assumed. The fact that the range of observed values generally falls within that of the calculated values indicates that the assumption as to the waveform is a fair approximation.

In so far as accuracy is concerned, the results obtained from recordings using the single or double horizontal aerials can be expected to be more critical than those from the ERA aerial since the differences in ratio are correspondingly smaller. This would mean that the time constants in these cases would be less accurate. On the other hand the values of the resulting field change magnitudes are not so critical since the variation is relatively small for comparitively large variations in time constant.

By way of example, if the error in the measurement of the ratio of deflections was of the order of 10%, the time constant could be in error by a factor of two when calculated from the results from the two horizontal aerials (1H and 2H). The following Table III therefore shows the errors that would arise on this basis over the range of times indicated in Table II.

Time Error ms	Percentage Ratio Error			Percentage Field Change Error			
	Std/1H	Std/2H	Std/ERA	Std	1H	2H	ERA
0,05-0,1	6,5	5,5	20,0	15,5	21,2	21,5	35,2
0,1 -0,2	7,8	8,5	21,2	20,0	30,0	29,0	47,2
0,5 -1,0	8,2	8,3	20,5	42,8	48,0	58,5	72,5
1,0 -2,0	7,8	6,5	16,8	55,0	67,0	66,0	80,0
5,0-10,0	4,5	4,5	8,1	77,0	86,5	86,0	93,5

Table III Errors in Ratio measurements and Field Change Magnitude for a factor of two error in time constant.

18/...

In order to undertake accurate measurements of the deflection ratios, the oscillograms were carefully enlarged by an expert photographer to maintain an exact magnification which amounted to a 5,32 times increase in dimensions. One scale division was exactly 15 mm, and deflections were read to the nearest one tenth of a division. Hence it is expected that the measurement accuracy was better than 5 percent, and a ratio of two measurements in which the errors were fortunately additive, would not be more than 10% in error. Consequently it may be confidently claimed that mean errors of ratio measurement were of the order of 5%, and the corresponding errors likely to arise in the calculation of the time constant of the field change would depend upon which aerial circuits were used and at which end of the time scale the results occured. Taking account, however, of other sources of error such as in the measurement of circuit parameters, in particular the capacitance of the aerials, it is doubtful if an overall accuracy of better than 10% could be obtained. Nevertheless, by depicting the resulting data in the form of cumulative distribution curves derived from histograms, it can be confidently expected that the information thereby gained indicates an order of magnitude which is within a reasonable degree of accuracy since this method of presentation tends to minimise the effect of inaccuracies of individual results. The most reliable results however can be expected from the comparisons between the standard vertical Aerial measured with those of the ERA aerial.

6. Extent of Records

Salisbury, S. Rhodesia has a mean isokeraunic level of 80 thunderstorm days, and preliminary work was started in October 1961, but the first useful recordings were not obtained until early February 1962, with over half the lightning season gone. Fortunately there were a number of late thunderstorms and 305 oscillograms based on a 150 ms time sweep were obtained from eight thunderstorms, which included 121 records from one storm. This lightning season was notable for its sporadic storms and

19/...

only 61 thunderstorm days occured by comparison with a mean of 80 days. However, preparations for the 1962/63 season were started early with the intent of catching the early storms which are notoriously severe, and believed to deliver the largest proportion of ground strokes.

The first records in the new season were obtained in early November 1962, but the storm season did not develop rapidly. Storms were scattered and unproductive, and over six storms the maximum number of records obtained per storm was 22 and the minimum three. However from late November onwards better results were obtained and in all, 742 records were obtained from 30 thunderstorms which however, amounted to an average of only 25 records per storm the best being 94 in one storm. The season ended early by comparison with the previous year, and 61 thunderstorms days occured to the 30th April, 1963, indicating that the season's lightning activity was, like the previous year, well below normal.

The 1963/64 season was a bumper year by comparison with the previous two years. Thirty six storms were recorded yielding 1 693 recordings which was over 56 percent more than the previous two seasons put together. The maximum number of flashes recorded on one day was 185 on February 19th, 1964 over a period of 5 hours 12 minutes amounting to an average of approximately one flash every two minutes.

The month to month recordings and totals over the three years are shown in Table IV indicating that 74 thunderstorms were monitored yielding a total of 2780 oscillograms or an average of over 37 per storm.

Most records were obtained after 1700 hours each day although several thunderstorms occurred before this. Consequently the number of possible records could have been greater, the results obtained are neverthless considered to be representative.

20/...

Year	Months	Number of Thunder= storms Recorded	Records Taken per day			Total Records	Seasonal Total
			Min	Max	Average		
1962	February	4	3	121	52	210	
"	March	1	24	24	24	24	
"	April	3	5	89	37	111	*345
"	November	10	3	94	30	304	
"	December	5	4	29	19	95	
1963	January	5	2	51	30	148	
"	February	4	4	45	28	111	
"	March	5	2	19	12	59	
"	April	1	25	22	25	25	742
"	October	5	10	72	33	168	
"	November	3	25	38	32	95	
"	December	10	2	71	32	318	
1964	January	9	7	105	61	551	
"	February	6	2	185	86	517	
"	March	3	11	18	15	44	1693
Total	15	74	2	185	37	2780	2780

Table IV Number of Thunderstorms recorded each month and number of oscillographic records obtained

*Half Season only.

7. Analysis of Oscillograms

It should be appreciated at once that all records were obtained indoors where storms could not be adequately observed, and it was not usually possible to observe whether lightning strokes were to ground or were between clouds. However all readable records were carefully enlarged and printed maintaining a constant linear scale and data was read off the positives with the aid of a transparent graticule.

Later records were made into slides and projected onto a screen mounted at a fixed diatance from the projector when values of the deflections could be more easily determined with even greater accuracy than the previous method.

21/...

Since it was necessary to decide first of all whether the field changes were due to cloud-cloud discharges or ground discharges, recourse was made to information privately communicated by Malan in respect of extensive observations carried out in South Africa by him and his associates, lead by Schonland.

This information was basically as follows:-

(a) Intra-cloud flashes

The field changes from intra-cloud flashes normally consisted of a "slow" component lasting anything from 20 to 500 ms or more up to about one second total duration. This field change may however contain "fast" elements (or "K" field changes) superimposed as "spikes" (usually of small magnitude) on the slow field change.

A second type of field change consisting of many "fast" field changes sometimes occurs and is characterised by time intervals between spikes of usually much less than 15 ms.

(b) Ground flashes

The most usual type of field change associated with ground flashes is a large and very fast (R-element) field change with a duration of less than a millisecond. One only may occur, but usually more than one, up to as many as fourteen with a median number of about three. These "R" elements may be spaced in time between 30 and 500 milliseconds apart, with a median value of about 40 ms, and a complete multi-stroke flash may last again up to about one second. On some occasions one of the "R" field changes, usually the last, may be followed by a long duration slow field change due to "continuing" currents.

Confirmation of the above categories of field change forms was also published bo D. Muller-Hillebrand[6] and by Brook and Kitagawa[7].

22/...

These general types were readily recognisable in the 600 ms time sweep records, where a resolution down to 10 ms was possible, and typical oscillograms are reproduced as figure 12. However some difficulty was inevitable with the earlier records taken with the 150 ms sweep, since the time sweep was free running and the actual intervals between individual component field changes could not be ascertained; what may have been a ground discharge, might therefore appear as a cloud discharge having many closely spaced fast elements, but these cases were found to be rare in later records.

However, only if more than two intervals between components in excess of about 15 ms occured, the record was classified as a ground discharge, and possibly this classification therefore erred in favour of a larger number of cloud strokes. On the other hand there were many records indicating a single component field change which could have been produced by either a cloud or a ground discharge and these were classified as ground strokes since they never contained slow components. A few records indicated that both types of discharge had occured, the one following the other, and both were counted for the purpose of the analysis.

Subsequently it was possible to arrange to observe some of the ground flashes which occured simultaneously with the taking of the oscillographic record, and these confirmed the above classification of these cases. Furthermore by far the majority of positive field changes classified as cloud flashes were found upon analysis to have occured within 10 km range; this is to be expected on account of the fact that beyond this range, which coincides approximately with the so-called "reversal" distance for the polarity of the electric field, intra-cloud flashes produce negative field changes of small magnitude.

8. <u>The distribution of the durations of fast field changes</u>

As a result of the division of records into intra-cloud (to be referred to frequently as "cloud" discharges) and ground dis= charges the following records as shown in Table V were obtained

23/...

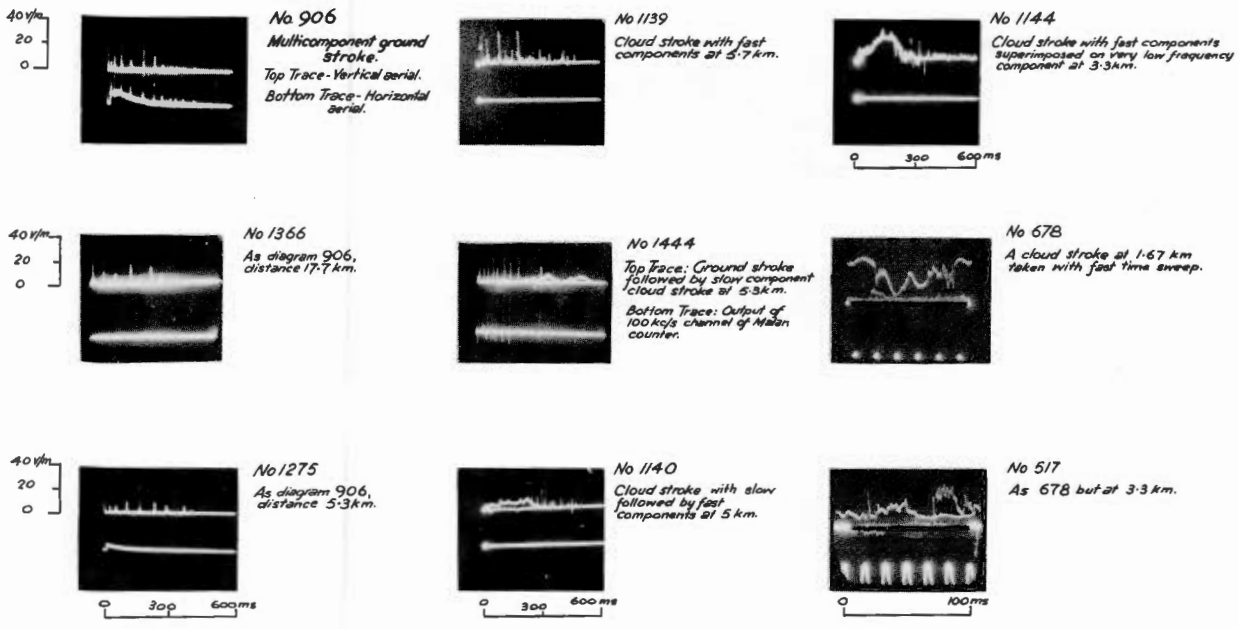

FIGURE 12

Typical example of field change due to cloud and ground lightning strokes

in the initial comparisons between the output of the standard vertical aerial (Std) and the three horizontal aerials designated 1H, 2H and ERA respectively.

Item	Description	Std/1H	Std/2H	Std/ERA	Total
1	Number of Cloud Flashes	37	23	15	75
2	Number of Ground Flashes	4	40	26	70
3	Total Number of Flashes	41	63	41	145
4	Number of Cloud Fast Components	89	77	82	248
5	Number of Ground Fast Components	7	133	82	222
6	Total number of Components	96	210	164	481

Table V Number of Cloud and Ground Flashes and Number of Components Measured.

The ratios of the deflection of the standard aerial to that of the others were then determined for each component and based upon the assumption that all field changes were of the inverted exponential form described in section 5, the equivalent time constant of this exponential was determined for each component. The times so calculated ranged from less than 0,01 ms to greater than 10 ms and figure 13 shows the resulting histogram for cloud and ground flashes respectively. In each case the first group shows the percentage of all records in which the calculated time constant was less than 0,02 ms whilst in the last group the times exceed 10 ms.

The similarity between the two histograms is remarkable, to say the least, and quite unexpected in view of the current belief that the duration of ground stroke field changes is generally of the order of 100 micro-seconds. If the actual waveform is close to the exponential form there are four categories of field change duration for the fast components of both cloud and ground flashes namely

24/...

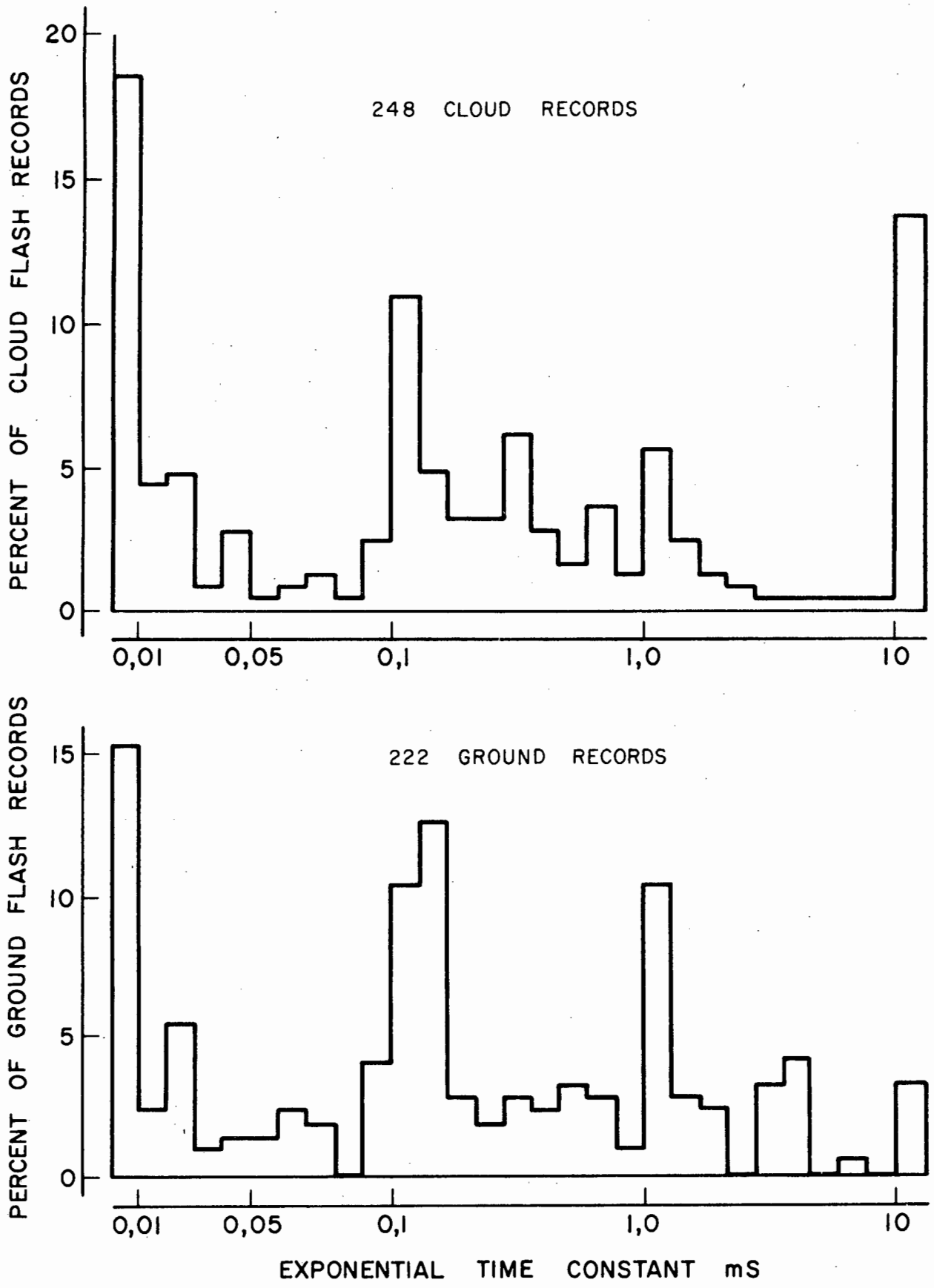

FIGURE 13

PROPORTION OF RECORDS HAVING THE TIME CONSTANTS INDICATED

(i) Those having very short times, less than 0,01 ms exponential time constant, which may be further defined as being less than 0,03 ms duration for 95% of the magnitude of the field change.

(ii) Those having a time constant in the region of 0,1 ms (or equivalent to 0,3 ms in duration)

(iii) Those having a time constant of 1,0 ms (3 ms duration) and

(iv) Those having very long durations exceeding 10 ms (30 ms) which is much more prevalent for cloud flashes than for ground flashes.

In the case of cloud flashes the components of group (iv) are additional to the very slow field changes lasting tens to hundreds of milliseconds which have been ignored in this analysis. Also with cloud flashes the division between group (ii) and (iii) that is between 0,1 and 1,0 ms time constant, is not so clearly in evidence as with ground flashes.

Figure 14 indicates the respective cumulative distribution of exponential time constants and shows that the median values for both cloud and ground flashes is in the range of from 0,2 to 0,3 ms; this means to say that the median duration of the field changes is in the range of 0,6 to 0,9 ms which in the case of ground flashes is much higher than presently reported values.

It is of interest to note that the durations for ground flashes have prominent peaks at 0,1 and again at 1,0 ms time constants, and this order of magnitude of change is not readily explicable. The duration of the field change is most probably linked with the time taken by the return stroke to neutralise charge deposited on the leader and this would be a function of the velocity of the return stroke and the length of the lightning channel. If the return stroke is associated with the shortest length of channel and highest return stroke velocity, then with subsequent strokes, the length of path should be longer due to the charge being situated at a greater height and/or further away and also the velocity of the return stroke may be less due to the lower field intensity. In this way discrete steps in

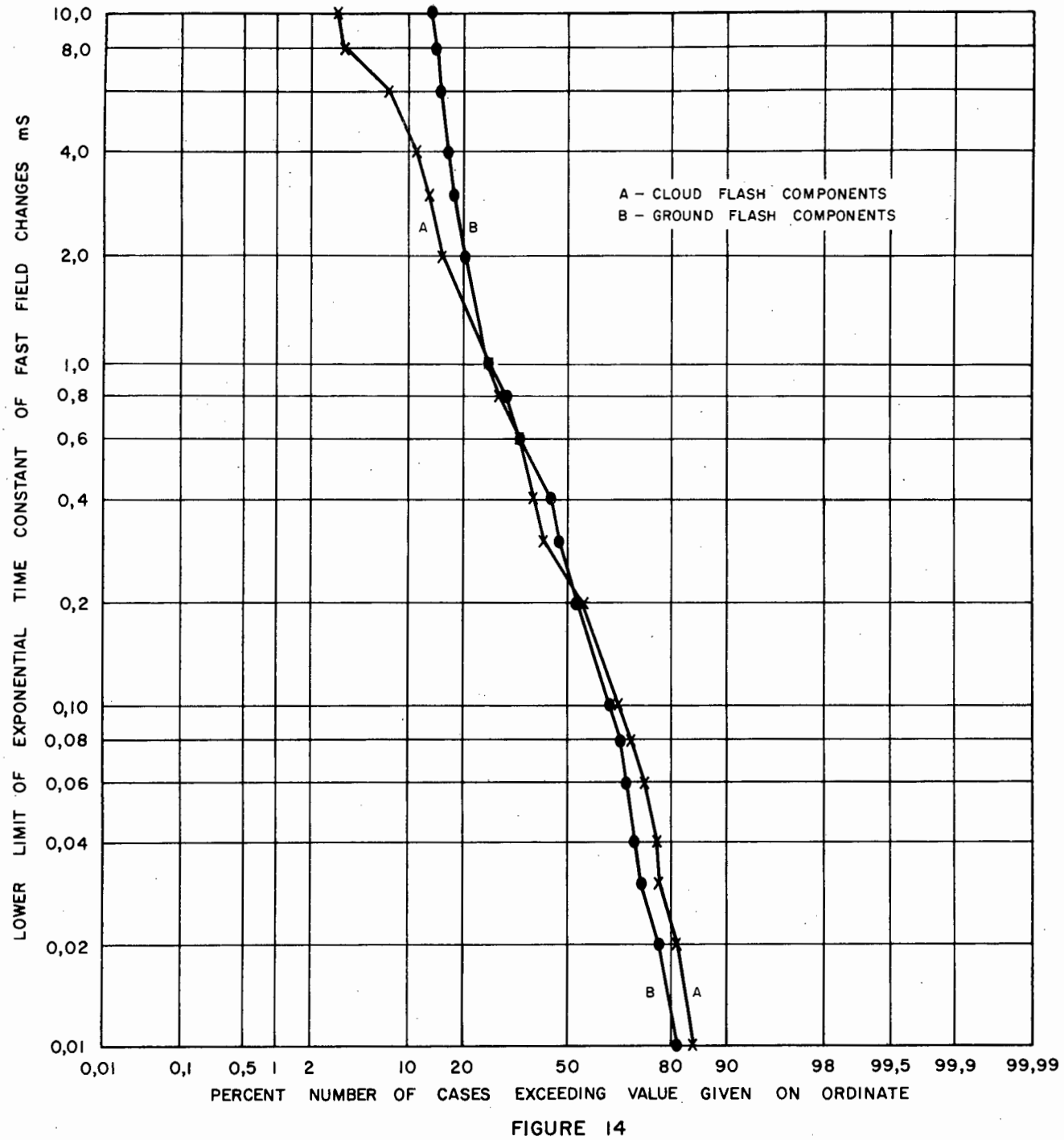

FIGURE 14

FREQUENCY DISTRIBUTION OF EXPONENTIAL TIME CONSTANTS FOR CLOUD AND GROUND COMPONENT FIELD CHANGES

field change duration would be possible. However this would mean that the field change duration should get progres= sively larger for each subsequent component and this is cer= tainly not in evidence in the analyses reported above. In fact the time duration changes appear to be distributed purely at random. Further evidence that the duration of ground flash compcnents can and does on ocassion reach the above order of magnitude is given in Appendix II which describes in more detail a magnetic tape recording of a multiple flash obtained in Pretoria.

This also provides a good example of the random distri= bution of duration times and Table VI taken from this record illustrates the effect. This was a 25 component flash recorded on a high fidelity tape and the time constant of the RC measuring circuit was about 1 ms; hence whilst the peak values of the field change are therefore not significant without correction, the duration times to the peak value are on the other hand unaffected by the circuit parameters, and may be regarded as accurate. The shortest measurable rise time was 0,1 ms, the mean was 0,41 ms, but duration to peak of 1,0 ms or greater have been recorded on three occasions. The time intervals between strokes are also given and conform to the expected distribution.

26/...

Component No.	Rise time ms	Time from Start ms	Time Intervals ms
1	$<$0,1	0	
2	0,4	69	69
3	0,2	127	58
4	1,0	178	51
5	0,7	214	36
6	0,15	273	59
7	0,2	321	48
8	0,4	417	96
9	0,2	430	13
10	0,48	472	42
11	0,2	499	27
12	0,3	509	10
13	1,2	519	10
14	0,6	532	13
15	1,0	538	6
16	0,6	556	18
17	$<$0,1	596	40
18	0,4	612	16
19	0,3	624	12
20	0,1	633	9
21	0,4	648	15
22	0,5	668	20
23	0,1	726	58
24	0,55	802	76
25	$<$0,1	830	28
Mean	$<$0,41 ms		33 ms

Table VI Rise Times of Field Change, Time Intervals and total duration of a 25 component Multiple flash of lightning.

In terms of frequency, if the inverted exponential waveform may be regarded as representing a quarter herz then the frequency equivalent of the exponential time constant T is f = 1/12T. Hence a value of 0,1 ms for the time constant T would be equivalent to a frequency of less than 10 kHz. If the field change is assumed to have a duration of five times the time constant, instead of three times, the equivalent frequency reduces to 5 kHz. Both these values of frequency are in the range observed most frequently for ground flashes thereby lending evidence in support of at least this particular time constant value.

27/...

In concluding this section it is apparent that much more information is required concerning the actual waveform of the field change during a return stroke. The investi=gation so far reveals a number of interesting though as yet unexplained features of cloud and ground fast field changes, but the questions arising may only be treated in general terms in view of the assumptions which have had to be made regarding the waveforms. The question is studied in more detail in Part II of this thesis in relation to calculations of the field change waveform.

It is necessary to try to explain why the field change duration of components varies over a wide range even in the same flash and also whether this is in some way dependent upon the equally variable time interval between the components.

9. Field Changes due to lightning

In the case of the 145 lightning flashes examined in detail where the exponential time constants have been calculated, the magnitude of the field change for the particular component can also be calculated by means of the multiplier constants given in Table II. For all other data it would be possible to obtain approximate values for the field change magnitudes by using the multiplier constant applicable to say the median value of the duration. For the standard vertical aerial, a multiplier constant of about 10 V/m per unit deflection could be used, corresponding to a time constant of 0,3 ms, bearing in mind, however, that in the case of field changes having shorter or longer time constants the error could be of the order of a factor of two.

Furthermore, field change magnitudes must be reviewed in conjunction with the range of the flashes, in view of the high rate of attenuation particularly in the case of the electrostatic field.

The results for the 145 lightning flashes were therefore subjected to more detailed analysis in that a histogram of field change magnitudes was determined separately for cloud

28/...

and ground flashes and using intervals of 10 seconds for the time to thunder from zero to 40 seconds; the equivalent range intervals at 3 seconds per kilometer, were therefore 3,3; 6,7; 10 and 13,3 km respectively.

A significant number of results was obtained only for the range equivalent to 10-20, and 20-30 secs time to thunder for cloud strokes, and 20-30 seconds for ground strokes, and the cumulative frequency for these three cases is shown in Table Table VII.

Field Change V/m	Cloud Fast Components		Ground Strokes
	Time to Thunder 10-20 secs	Time to Thunder 20-30 secs	Time to Thunder 20-30 secs
	Range 3,3 to 6,7 km	Range 6,7 to 10,4 km	Range 6,7 to 10 km
10	93,2	83,5	85,5
20	80,7	62,3	58,5
30	67,3	49,5	42,7
40	52,8	32,8	31,7
50	45,1	27,5	26,2
60	39,4	25,7	22,0
70	36,7	22,9	21,4
80	33,6	20,9	19,3
90	31,7	19,2	16,6
100	30,8	18,3	16,6
200	25,0	11,0	6,9
300	20,2	7,3	3,5
400	17,2	3,7	2,1
500	13,5	2,8	1,4
600	7,7		
700	3,8		
800	2,9		
900	1,0		
1000	1,0		
Number of Cases	104	109	145

Table VII Percentage Number of Cases in each distance group in which the field change magnitude shown in the first column was exceeded.

29/...

Comparing the two ranges for cloud strokes, there is a significant fall out in higher values in the 20-30 sec range, but certainly not on the basis of D^{-3} as anticipated. This may be partly affected by the fact that very large values are excluded from the distribution either because they were off-scale or because, since there was no off-set of the vertical deflection of the two traces, the deflections coincided when the magnitude were large enough to cause overlapping, and these cases could not be used to determine the ratio of the deflections of the two traces. The comparison between cloud and ground components in the 20-30 second bracket show close similarity which leads to indicate that the fast components of cloud flashes have similar characteristics to those of ground flashes at least within 10 km range.

A much more likely explanation of the discrepancy observed when comparing data from different ranges, lies in the fact that all recordings of field changes are undertaken above a threshold level set by the trigerring level for the recording equipment. In this case a minimum level of approximately 5 V/m was maintained and hence if the range is doubled for example, the electrostatic field change is reduced by a factor of eight according to the D^{-3} relationship. This means in effect that at twice the range, only field changes in excess of 40 V/m at that range will trigger the equipment and so on as the range increases, and the sampling procedure controlled by the trigger therefore tends to exclude and more low values with increasing distance. This is further complicated by the effect of the electromagnetic field change. In the case of the induction field, attenuating at D^{-2}, the recording level is not so surely cut-off - for example for twice the range, the limit is 20 V/m; for the radiation field on the other hand it is even less at 10 V/m.

This unavoidable, but nevertheless important consideration means in effect that the frequency distributions of any data compiled at differing ranges will be more and more truncated by the omission of data at the lower end of the scale. Unfortunately, also, it is not possible to decide

30/...

where the level of truncation is, because of the variable effect of the electromagnetic field which according to Malan[8] for example is more prominent than the electrostatic field at ranges exceeding about 25 km.

The data can be adjusted by graphical means however, in the following manner, if some basic assumptions are made. Provided that the minimum level of recording set by the trigger is sufficiently low, it can be confidently expected that all flashes will be recorded up to a given range which must also be chosen sufficiently close to the point of measurement - say 3,3 km (or 10 seconds for time to thunder). Since there were no cases when flashes occured within this range which did not operate the trigger, this preliminary assumption is justified; in other words it is assumed that all flashes within 3,3 km given rise to field changes in excess of the trigger threshold level, in this case, of 5 V/m.

If now the distribution of the magnitudes of the field changes within this range is found, and it closely approximates to say a log-normal guassian distribution, it may be assumed, with some justification, that the distributions for other ranges should likewise be log-normal. The justification is however presumptive in that is is based on the fact that much of the data connected with lightning seems to conform to either a normal or log-normal form of distribution, for example lightning current magnitudes.[9] However the application of the method itself also proves the point since no adjustment would be possible if the premise does not hold, as will be later shown.

The first four columns of the following Table VIII illustrate an example of a hypothetical log-normal distribution of 1000 records of field changes.

31/...

The cumulative distribution set out in the fourth column is plotted as curve A on figure 15. If it is then assumed that the 198 values below 1,5 V/m were omitted from the distribution due say to the limitation by the threshold level of the trigger circuit, the remaining 802 values would appear to follow the cumulative distribution of column 5, and when expressed as a percentage, of column 6. These values are plotted as curve B on figure 15 and it is seen that whilst the upper values follow a reasonable straight line, the lower values indicate a severe departure from the log-normal form. If therefore a straight line is drawn at a tangent to the upper position of curve B to give curve C, a first approximation of a new log-normal distribution is obtained which is observed to be closer to the real values which are as yet unknown. These are shown in column 7 of Table VIII.

New information is however now available to the effect that 86 percent of the number of records were apparently in excess of 1,5 V/m, alternatively 14 percent or 111 records may be added to the truncated distribution below 1,5 V/m. Hence a new distribution may now be constructed with the addition of these values making the new total 802+111 = 913 records.

Obviously this distribution will lie closer to the distribution sought, but will also display a curved portion at the lower value end indicating that a final solution has not yet been reached. A second process of approximation done exactly as the first will however add another but smaller number of values below 1,5 V/m to get even closer to the final solution. The process converges very repidly - nearly 60 percent of the missing values having been added with the first approximation alone, so that in this case two operations will already come close to the final solution.

It is seen also that the method should fail if the solution sought is not a log-normal distribution in the first place; such as distribution would not have higher values which lie close to a straight line, and therefore they should first

33/...

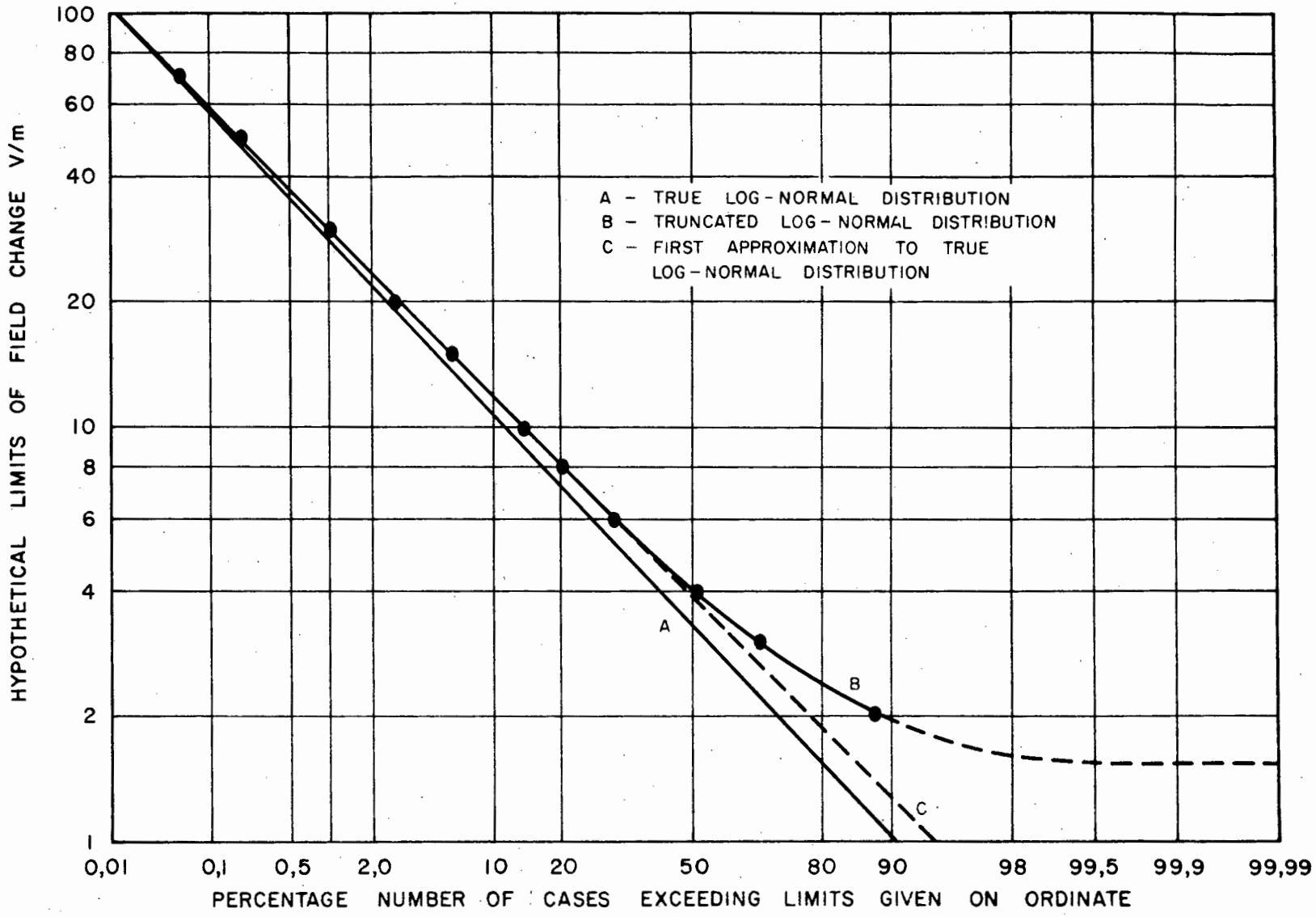

FIGURE 15

HYPOTHETICAL DISTRIBUTING FIELD CHANGES

be arranged in another form such as an expected normal distribution and if the upper values now lie reasonably, on a straight line, the identical procedure may then be carried out.

Since truncated distributions arise frequently in practice the above method was first reported to a CIGRE Study Committee Meeting in Trondheim in 1963[10] and later reproduced in an unpublished ERA report by Chan[11]. More recently, at the writers request, some further work was done by Markham which is reproduced herein as Appendix III.

In order to obtain an indication of the overall distribution of field changes at different ranges, more results were needed, and in order to obtain these it was assumed that a mean equavalent time constant of 0,2 to 0,3 ms could be assumed for measurements undertaken with the standard vertical aerial; this value is close to the median value found in section 8 and results in a convenient multiplier factor of 10 V/m per division according to Table II of that section. The effect of this approximation would be that the magnitude of field changes which were of shorter duration than the value assumed would be over estimated, whilst those having longer durations would be assigned magnitudes which would be too small. If the number of observations is sufficiently large however, and the distribution of durations purely random as observed it can be expected that the distribution of field change magnitudes would be reasonably correct.

In this analysis it is necessary to define the polarity of field changes. In the case of a ground flash, the field change is considered positive when the electrostatic field at the earth's surface becomes more positive as a consequence of the discharge. This is equivalent to negative charge being located in the cloud and being discharged to earth, and by far the most commonly observed field changes due to ground flashes are in fact positive. The position is somewhat different with cloud flashes since for vertical discharges between the upper positive charge and a negative

34/...

charge at a lower attitude, the resultant field change is positive at close range, but is negative beyond a critical distance commonly referred to as the "reversal" distance. This reversal distance is purely a function of the geometric position of the charges and their magnitudes, and in the case of equal positive and negative charges situated vertically one above the other at height of H1 and H2 respectively it is given by the relationship

$$Do = H_2\left\{(H1/H2)^{2/3}[1+(H1/H2)^{2/3}]\right\}^{\frac{1}{2}} m \qquad (4.0)$$

The theoretical minimum value of the reversal distance is obtained by putting H1 = H2, whence $Do = \sqrt{2}\ H_2$. More realistically perhaps H1/H2 would normally exceed 2, whence if H1 is say 4 Km, Do is then approximately 8 km.

At the reversal distance itself the field intensity at ground level is zero and in the case of an intra-cloud discharge for the idealised case of vertically disposed charges) there would be no field change during the discharge. This would mean that the magnitude of field changes in the case of cloud discharges would appear to attenuate at a more rapid rate than would be indicated by the D^{-3} relationship.

A total of 377 field change records classified as depicting ground flashes and 555 records of cloud flashes were examined.

After neglecting purely negative field changes there remained 351 records classified as ground discharges of which the range had been determined for 244 by the method of the time to thunder. Correspondingly there remained 479 records of cloud discharges with the range determined for 373. Of these records there was a fair proportion in which either the magnitude was off-scale, or the time to thunder was in excess of 60 seconds, and they were recorded at the limits for which the information was known. This method of treatment though not strictly accurate, does not however affect the distribution in the region of the smaller field changes and lesser distances which are in the area which is of main interest.

35/...

The maximum field change magnitudes were tabulated for ranges in steps of one kilometre medians up to 20 km and for field changes in steps of 10 V/m resulting in the distribu= tion of magnitudes shown in Tables IX and X. The numbers of records available for each kilometre of range are seen to be too few to even attempt to determine the statistical fre= quency distribution in small steps, especially as they would require to be more numerous still if the deviation of results due to the effect of waveform time constants referred to above is to be nullified. The number of records for steps of 10 km however appear more reasonable as indicated on these tables, and the distribution then conforms approximately to a normal form excepting for the values of field change in the range 0-10 V/m.

It is pertinent here to again consider the question of the minimum values of field change, which must obviously either derive from lightning discharges of small total charge at close range, or, in the majority of cases, should be due to more severe discharges occuring at greater distances from the point of measurement. If a frequency distribution of field changes is therefore to be of any value it must take into account the total number of discharges down to the minimum value, since these small values would constitute a large pro= portion of the total number of strokes, particularly as the range increases.

However, the distribution must be limited in range, otherwise it would admit of a very large number of low value field changes due to discharges emanating from distant light= ning strokes, and thereby complicate the interpretation of the results.

The audible counters which were used to indicate that a flash had occured, were set by means of a capacitance dis= charged pulse, to a minimum response of $1\frac{1}{2}$ volts positive or negative, and the counter was in parallel with the input from the standard vertical aerial. At the median value of the response of this aerial, the minimum field change recorded

36/...

Table IX Distribution of Magnitude of Positive Field Changes of intra-cloud lightning discharges.

Time to Thunder Seconds	Range km	Number of Records of Field Change:Volts/Metre in Groups shown below											
		0-10	10-20	20-30	30-40	40-50	50-60	60-70	70-80	80-90	90-100	>100	Total
1.5- 4.5	1	-	-	-	1	1	-	-	7	-	2	-	11
4.5- 7.5	2	-	1	1	-	2	5	7	5	6	1	1	29
7.5-10.5	3	1	1	1	-	5	9	5	8	2	1	1	34
10.5-13.5	4	2	2	1	5	2	10	10	2	3	1	1	39
+13.5-16.5	5	1	8	22	11	12	13	10	8	2	4	5	96+
16.5-19.5	6	1	4	3	1	9	11	-	2	1	-	-	32
19.5-22.5	7	3	7	7	7	6	3	1	1	2	1	-	38
22.5-25.5	8	5	1	8	-	2	2	2	1	1	1	-	23
25.5-28.5	9	5	1	3	-	2	1	1	-	--	-	-	13
28.5-31.5	10	1	5	-	4	-	-	1	2	-	-	-	13
Total 0- 10km		19	30	46	29	41	54	37	36	17	11	8	328
31.5-34.5	11	1	-	1	1	2	1	-	-	-	-	-	6
34.5-37.5	12	-	2	2	-	2	-	1	-	1	-	-	8
37.5-40.5	13	1	2	1	2	-	1	-	-	-	-	-	7
40.5-43.5	14	-	1	-	2	-	-	1	-	-	-	-	4
43.5-46.5	15	- -	4	1	-	-	-	-	-	-	-	-	5
46.5-49.5	16	-	1	-	-	-	-	-	-	-	-	-	1
49.5-52.5	17	1	-	1	1	-	-	-	-	-	-	-	3
52.5-55.5	18	-	-	1	-	2	-	-	-	-	-	-	3
55.5-58.5	19	-	-	-	-	-	-	-	-	-	-	-	0
58.5-61.5	20	1	1	1	1	-	-	-	-	-	-	-	4
Total 11 - 20km		4	11	8	7	6	2	2	-	1	-	-	41
>61.5	>20	1	1	-	1	-	1	-	-	-	-	-	4
Not Timed		7	20	28	14	11	14	7	3	1	1	-	106
Total All		31	62	82	51	58	71	46	39	19	12	8	479

+ Includes a number of observations for which the range was determined as between 4 and 6 km.

37/...

Table X Distribution of Magnitudes of Positive Field Changes of Lightning discharges to Ground

Time to Thunder	Range	Number of Records of Field Change in Volts per Metre Groups shown below											
Seconds	km	0-10	10-20	20-30	30-40	40-50	50-60	60-70	70-80	80-90	90-100	>100	Total
1.5- 4.5	1	-	-	-	-	-	-	-	-	-	-	-	0
4.5- 7.5	2	-	-	-	-	-	1	-	-	-	-	-	1
7.5-10.5	3	-	1	-	-	1	2	-	-	-	-	-	4
10.5-13.5	4	-	3	-	3	-	2	-	1	-	-	-	9
+13.5-16.5	5	3	5	2	3	1	5	2	2	-	-	-	23+
16.5-19.5	6	1	1	1	3	1	2	2	-	-	-	-	11
19.5-22.5	7	1	3	3	3	2	2	2	1	-	1	-	18
22.5-25.5	8	-	2	4	2	5	4	4	2	-	-	-	23
25.5-28.5	9	2	1	2	2	3	2	-	1	-	-	1	14
28.5-31.5	10	2	1	2	1	3	3	1	3	-	-	-	16
Total 0 - 10km		9	17	14	17	16	23	11	10	-	1	1	119
31.5-34.5	11	-	2	5	3	3	-	1	1	-	-	-	15
34.5-37.5	12	-	2	2	1	3	1	-	-	-	-	-	9
37.5-40.5	13	2	2	2	2	1	4	1	-	-	-	-	14
40.5-43.5	14	-	1	1	-	-	-	-	-	-	-	-	2
43.5-46.5	15	-	2	-	4	-	-	1	-	-	-	-	7
46.5-49.5	16	-	1	1	1	4	-	-	1	-	-	-	8
49.5-52.5	17	1	2	1	2	2	4	2	1	-	-	-	15
52.5-55.5	18	-	1	2	1	4	2	-	-	-	-	-	10
55.5-58.5	19	-	-	-	2	-	1	-	-	-	-	-	3
58.5-61.5	20	1	3	5	3	1	1	-	2	1	-	-	17
Total 11 - 20km		4	16	19	19	18	13	5	5	1	-	-	100
>61.5	>20	2	12	4	2	4	1	-	-	-	-	-	25
Not Timed	-	13	38	21	10	11	5	2	2	1	3	1	107
Total All		28	83	58	48	49	42	18	17	2	4	2	351

+ Includes a number of observations for which the range was determined as between 4 and 6 km.

should therefore have been about 10 V/m, but the oscillographic records show that in fact the counter responded to a level of 5 5 V/m and frequently below. The grid of the first valve of the counter was however directly connected to the aerial, and the sensitivity of the counter would therefore have been affected by small values of dc voltage such as would be present during slow field changes. Secondly if the rise times of the field change vary over a large range, as has been indicated, the threshold level for the response of the equipment would also vary accordingly. These factors would affect the minimum registration, but judged from the evident departure from a normal distribution, the total number of records at the zero end of the scale was below the expected value.

As outlined above however, the records may be corrected on the assumption that the distribution of field changes should have been normal, by adding to them that proportion of records below 10 V/m indicated by the magnitude of the departure from normality. For example figure 16 indicates the cumulative frequency distribution of the actual records of table X for all lightning strokes to ground, plotted on normal arithmetic probability paper; from this it is evident that whilst the actual records indicate that 92,2% of them exceeded 10 V/m, a first approximation to a normal distribution would require 81% to exceed this value. Hence the number of readings below 10 V/m should be increased from 7,8% of the total readings to 19% of the total and the frequency distribution readjusted accordingly. The resultant distribution indicated that there was still a slight departure from normality to the extent that 27,8% of records should be less than 10 V/m, instead of the 19% found in the first approximation. However, the adjustments as a first approximation resulted in an increase in the number of low values by a factor of 2,44 and in the second adjustment, this factor was 1,46, the limit being unity, and the proportional adjustments are therefore rapidly converging. For this reason it is assumed that the frequency distribution represented by the second adjustment is suffi-

39/...

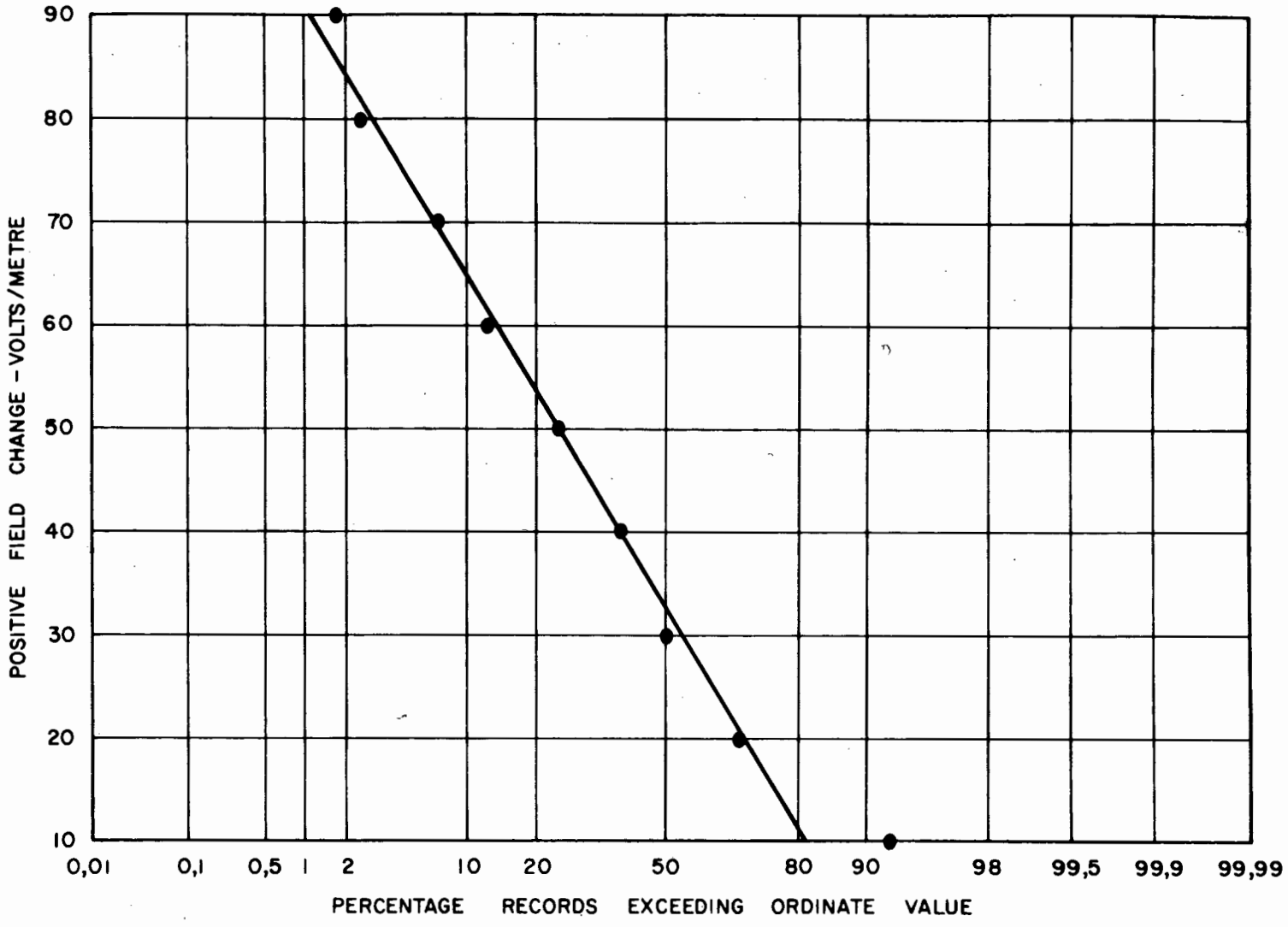

FIGURE 16

UNCORRECTED FREQUENCY DISTRIBUTION OF MAGNITUDE OF FIELD CHANGES FOR LIGHTNING STROKES TO GROUND

ciently accurate for all practical purposes, and the adjustments made in this manner to all the distributions were finally as stated in Table XI.

Table XI Adjustments to the Number of Records of Field Changes less than 10 V/m in Magnitude.

		% Proportion of Total Records less than 10 V/m	
(i)	Ground Strokes	As found	As Adjusted
	Ground strokes 0 - 10 km	7,5%	15,0%
	" " 10 - 20 km	4,0%	11,8%
	" " exceeding 20 km	8,0%	47,0%
	All Ground Strokes	7,8%	27,8%
(ii)	Cloud Strokes		
	Cloud Strokes 0 - 10 km	5,8%	10,8%
	" " 10 - 20 km	9,9%	28,5%
	All Cloud Strokes	6,2%	17,0%

The final frequency distributions for all records after adjustment are plotted in figure 17 and the values obtained are tabulated in Table XII and XIII. The median values both as found, and after the adjustment for low values, is given in Table XIV below. (See pages 40 and 41 for Tables XII and XIII).

Table XIV Median Values of Positive Field Changes due to Lightning

		50% of Records exceed the values shown		
(i)	Ground Strokes	As Found	As Adjusted	% Reduction
	Ground Strokes 0 - 10 km	41,6v/m	38,8v/m	93,2%
	" " 10 - 20 km	36,2 "	34,2 "	94,5%
	" " exceeding 20 km	15,0 "	11,5 "	93,2%
	All Ground Stroked	32,2 "	26,8 "	83,2%

40/...

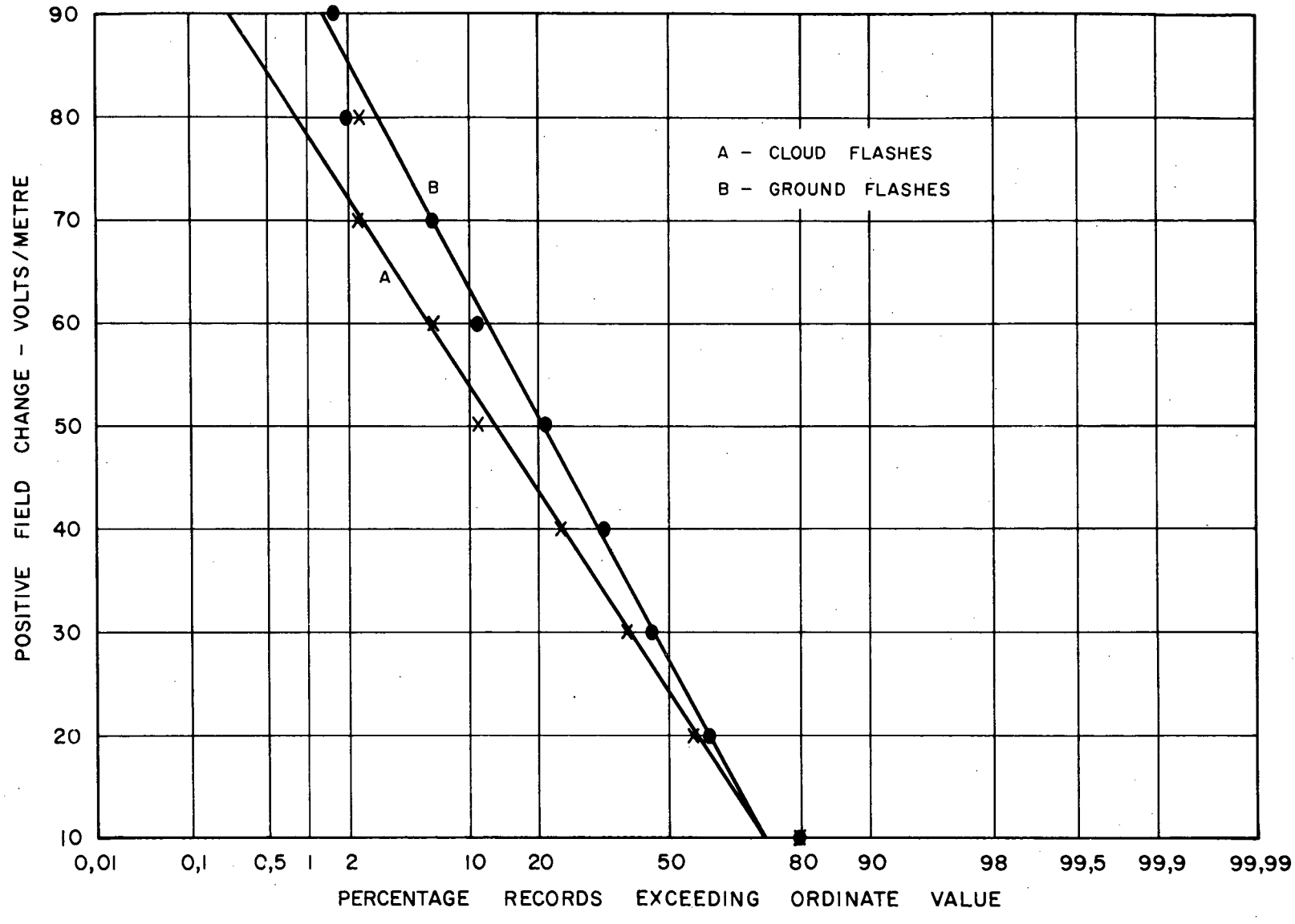

FIGURE 17

CORRECTED FREQUENCY DISTRIBUTION OF MAGNITUDE OF LIGHTNING FIELD CHANGES

Table XII Cumulative Distribution of Field Change Magnitudes for Ground Flashes

Range km	Data	Grouped Limits of Field Change Magnitudes-Volts/Metre												
		0-10	10-20	20-30	30-40	40-50	50-60	60-70	70-80	80-90	90-100	100-110	Total	Med. Value
0-10km	Number of Records	16	17	14	17	16	23	11	10	-	1	1	126	
	Cumulative Number	126	110	93	79	62	46	23	12	2	2	1		
	% Exceeding Limits	100%	87.2	73.8	62.7	48.1	36.5	18.2	9.5	1.59	1.59	0.8		
	Corrected to Normal	100%	85.0	74.8	62.2	48.0	34.8	22.8	13.4	7.2	3.5			38.8 v/m
10-20km	Number of Records	10	16	19	19	18	13	5	5	1			106	
	Cumulative Number	106	96	80	61	42	24	11	6	1				
	% Exceeding Limits	100%	94.2	75.5	57.6	39.6	22.6	10.4	5.7	8.94				
	Corrected to Normal	100%	88.2	75.5	58.5	39.6	22.0	10.4	4.0	1.3	0.35			34.4 v/m
Exceeding 20 km	Number of Records	17	12	4	2	4	1						40	
	Cumulative Number	40	23	11	7	5	1							
	% Exceeding Limits	100%	57.5	27.5	17.5	12.5	2.5							
	Corrected to Normal	100%	53.0	34.5	19.2	9.0	3.5							11.5 v/m
	Distance not Measured	*34	38	21	10	11	5	2	2	1	3	1	128	-
All	Ground Strokes	77	83	58	48	49	42	18	17	2	4	1	400	
	Cumulative Number	400	323	240	182	134	85	43	25	8	6	2		
	% Exceeding Limits	100%	80.7	60.0	45.5	33.5	21.2	10.8	6.25	2.0	1.5	0.5		
	Corrected to Normal	100%	72.2	60.0	45.5	32.0	20.5	11.8	6.2	3.0	1.3			26.8 v/m

*By difference

41/...

Table XIII Cumulative Distribution of Positive Field Change Magnitudes due to Lightning Cloud flashes

Range km	Data	Grouped Limits of Field Change - Volts/Meter 0-10	10-20	20-30	30-40	40-50	50-60	60-70	70-80	80-90	90-100	100-110	Total	Med Value
0-10km	Number of Records	31	30	46	29	41	54	37	36	17	11	8	340	
	Cumulative Number	340	309	279	233	204	163	109	72	36	19	8		
	% Exceeding Limits	100%	91.0	82.2	68.5	60.0	48.0	32.1	21.2	10.3	5.6	2.35		
	Corrected to Normal	100%	89.2	81.8	71.0	58.5	45.0	32.0	21.0	12.4	7.0			46.2 v/m
10-20km	Number of Records	9	11	8	7	6	2	2	-	1	-	-	46	
	Cumulative Number	46	37	26	18	11	5	3	1	1				
	% Exceeding Limits	100%	80.3	56.6	39.2	23.9	10.9	6.5	2.17	2.17				
	Corrected to Normal	100%	71.5	56.0	39.0	24.0	12.5	6.0	2.2	0.58	0.23			23.2 v/m
Exceeding 20km	N Number of Records	* 9 * By difference	1	-	1	-	1						12	-
	Distance not Measured	18	20	28	14	11	14	7	3	1	1		117	-
All	Cloud Strokes	67	62	82	51	58	71	46	39	19	12	8	515	
	Cumulative Number	515	448	386	304	253	195	124	78	39	29	8		
	% Exceeding Limits	100%	87.0	75.0	59.0	49.0	37.8	24.0	15.1	7.55	3.87	1.55		
	Corrected to Normal	100%	83.0	73.2	61.5	48.0	35.0	24.0	14.5	8.5	4.3			38.6 v/m

42/...

(ii) Cloud Strokes		As Found	As Adjusted	% Reduction
Cloud Strokes	0 - 10 km	48,8v/m	46,2 v/m	94,5%
" "	10 - 20 km	27,2 "	23,2 "	85,3%
All Cloud Strokes		41,6 "	38,6 "	92,7%

The figures for total strokes include a large number of records for which the range was not determined, and there is thus no direct relationship between them and the remainder of the data. These additional records were obtained when the lightning frequency was so severe that the camera film had to be moved to the next photograph position before a range determination could be made; furthermore thunderclaps were, on these occasions, following each other so rapidly as not to be easily identifiable with the corresponding field change records. However since no recording was undertaken during periods when storms were outside the audible range for thunder, the frequency distribution for all lightning flashes refers to this restricted range, and is valuable in that the number of records is considerably more than would otherwise have been the case.

Considering first the data in Table XII for ground strokes, it is clear that the median values of field change for strokes occuring between 10 and 20 km distant, was not much less than for strokes in the range of 0 - 10 km, whereas it was expected that values, roughly proportional to the inverse cube of the distance, would be obtained. Furthermore, since the area of country in the range of 10 - 20 km is three times that of the latter, a similar ratio of the observed numbers of readings would have been expected, whereas they were approximately equal.

An increase of range by a factor of two should up to about 20 km, result in a reduction in the magnitude of field changes by one eighth, and since field changes of the order of 80 v/m were exceeded in only about 7% of the records in the range 0 - 10 km, it would be expected that practically all field changes due to strokes in the range of 10 - 20 km

43/...

would be less than 10 v/m, whereas in fact, even after adjustments had been made to allow for low values, over 88% of the records exceeded this value. One possible explanation of this apparent contradiction between theory and observation may be that in spite of what is believed to an adequate adjustment to compensate for low values below 10 v/m, in fact many more were not recorded. This however does not satisfactorily account for the large number of recordings in excess of 10 v/m which were as numerous as the recordings for the 0 - 10 km range. Possibly therefore the number of observations for either or both of the chosen range brackets may not have been adequate.

The same argument however, could not be applied with equal certainty to the total records which were approximately four times the number, and for the purpose of further calculations it is assumed that the margin of error when using all records would not be very great. The range of these records would certainly not exceed 30 km, in view of the fact that not a single observation was obtained when thunder could not be heard in under 90 seconds.

Hence, as already referred to in connection with the previous sample of field changes, there is now further evidence that the inverse cube relationship does not appear to hold in respect of field change magnitude for ground flashes, and the possibility therefore exists that the electromagnetic components of the field change are influencing the measurements at distances of much less than 25 km. According to the extension of the Le Jay statements as defined in Equation (1.1) this possibility could exist if either the lightning currents or their rates of change were unusually high.

With reference to cloud stroke data, table XIII indicates that two thirds of the records of field changes due to cloud strokes were in the range of 0 - 10 km, amounting to 340 readings after adjustment for low values. Hence the frequency distribution of field changes derived therefrom should be at least as accurate as derived from the total records of ground strokes.

44/...

In the range 10 - 20 km however the records amounted to only 46 in number and there is an obvious deficiency when it is considered that the area is three times that of the 0 - 10 km range; furthermore there were negligible recordings in the range exceeding 20 km. This deficiency would be partly due to the fact that, as with the ground stroke records, fewer recordings were made on the more distant storms although there was no conscious effort on the part of the observer to differentiate. However the largest single factor contribu= ting to the deficiency must be the fact that the reversal distance may occur in this region and the polarity of the field changes due to intra-cloud discharges changes and being negative would not be recorded in this data. Unfortunately, although 76 records of negative cloud field changes were ob= tained, the range was determined for so few of these that the total number of strokes in this range could not be estimated, and therefore the proportions which were positive likewise could not be calculated.

However, some reliance may be placed upon the fact that observations were made on thunderstorms without any prior knowledge as to whether lightning strokes were between clouds or to ground, and that any natural inclination on the part of an observer not to record the more distant storms as frequently as close ones, would therefore have applied equally to both types of discharge.

Referring to Table XII only 106 out of a possible 378 ground strokes, equivalent to 28% were recorded in the range 10 - 20 km and it is improbable therefore, that a similar proportion of cloud strokes would have been recorded for that range, had their field changes all been positive. Applying this proportion to the cloud stroke records of Table XIII the possible total number of records in this range was 1020, and 28% or 286 would have been recorded. However, in fact only 46 positive field change records were recorded, which amounts to 16% of the 286 possible and this proportion is

45/...

important to the following calculation.

If only 16% of the cloud field changes in the range 10 - 20 km produce positive field changes, it would not be unreasonable to assume that the range at which reversal of polarity takes place is equivalent to 16% of the total area between 10 and 20 km radius. If R is the radius of the area within which positive cloud field changes occur, then $R = [0,16(20^2-10^2) + 10^2]^{\frac{1}{2}} = 12,2$ km. This value according to equation (4.0) is of the correct order of magnitude for the reversal distance and is equivalent, for example, to the case of two charges of opposite polarity situated at 6 and 11 km height above ground, which are, according to Malan within the range of values observed in South Africa.

In view of the above it may be assumed with confidence that the frequency distribution for all cloud field changes obtained from the total number of record applies to a range not exceeding about 12 km. With regard to the frequency distribution of positive field changes for cloud strokes in the range of 10 - 20 km, it is noted that the median value at 23.2 v/m was approximately half that for the 0 - 10 km range, whereas it would be expected that this should have been of the order of less than one eighth.

Hence as with ground flashes there appears to be a similar apparent discrepancy from the D^{-3} relationship, only with intra-cloud flashes it would be more difficult to trace the reason because electric field changes are so much more complicated than for ground flashes. The inves= tigation in this case refers only to the so-called "fast" components which may well dissipate more energy in the form of electro-magnetic radiation.

It is clear from the above discussion that the question of field change magnitude and waveforms for lightning dis= charges appears to require a more detailed fundamental study if the observed phenomena are to be satisfactorily explained. A study of the mechanism of the discharge should perhaps

46/...

clarify the question of the relative magnitudes of electro= magnetic radiation compared with the attenuation of the elec= trostatic portion of the field change, and this is undertaken in more detail in Part II of this thesis.

10. The proportion of intra-cloud compared with cloud-ground lightning flashes

It has been conceded in literature that the number of intra-cloud flashes throughout the globe, exceeds the number between cloud and ground, and it is generally thought that the ratio varies between about 2:1 in temperate latitudes to values in excess of 5:1 in the tropics. Pierce[12] discusses a correlation with latitude, whilst Popolansky[13] relates the value to the number of thunderstorm days, and as yet there are no reliable statistics on the subject. The reason of course is that observation of this parameter is very difficult in view of the extreme variability of the phenomenon.

In this investigation it was found, for example that the storm which occured on the 15th April 1962 recorded 89 flashes all of which were intra-cloud, whilst the storms which occured in late November to early December of the same year 86 records were obtained of which only 15 were cloud flashes. It follows therefore that the production of one kind or the other depends upon the type of thunderstorm, and a large number of observations would be needed to establish the mean value.

Secondly, as described in the previous section, measure= ment by means of the field change introduces discriminatory sampling, whereby the response of the measuring circuit differs for the two types of flash. For example 369 cloud and 219 ground flashes analysed in Tables IX and X can be grouped in each range and the cloud to ground ratio determined from the cummulative numbers up to the limit of progressively increasing range with the results shown in Table XV.

47/...

Time to Thunder Range Seconds	Range Limits km	Number Observations		Cumulative Numbers		Ratio Cumulative Numbers cloud/ ground
		Cloud	Ground	Cloud	Ground	
1,5- 4,5	1,5	11	0	11	0	Infinity
4,5- 7,5	2,5	29	1	40	1	40
7,5-10,5	3,5	34	4	74	5	14,8
10,5-13,5	4,5	39	9	113	14	8,1
13,5-16,5	5,5	96	23	209	37	5,7
16,5-19,5	6,5	32	11	241	48	5,0
19,5-22,5	7,5	38	18	279	66	4,2
22,5-25,5	8,5	23	23	302	89	3,4
25,5-28,5	9,5	13	14	315	103	3,1
28,5-31,5	10,5	13	16	328	119	2,8
31,5-34,5	11,5	6	15	334	134	2,5
34,5-37,5	12,5	8	9	342	143	2,4
37,5-40,5	13,5	7	14	349	157	2,2
40,5-43,5	14,5	4	2	353	159	2,2
43,5-46,5	15,5	5	7	358	166	2,2
46,5-49,5	16,5	1	8	359	174	2,1
49,5-52,5	17,5	3	15	362	189	1,9
52,5-55,5	18,5	3	10	365	199	1,8
55,5-58,5	19,5	0	3	365	202	1,8
58,5-61,5	20,5	4	17	369	219	1,7

Table XV Analysis of number of cloud and ground flashes recorded in 1962/63 lightning season.

These records apply to the 1962/63 lightning season only and indicate that the ratio of the number of cloud flashes recorded to those of ground flashes decreased steadily as the range of observation increased. Whilst it is appreciated that the number of observations of either of the cases would decrease with range because of the decreasing magnitude of the field change, nevertheless the rate of falling off in numbers must differ. From the previous section it is clear that the field changes due to cloud flashes reduce in magnitude more rapidly than to those for ground flashes and this would account for the observation of Table XV.

48/...

Nevertheless it was suspected that the number of records was too scant upon which to base any definite conclusion since it would be expected that the difference in the rate of falling-off in number of observations would not be large at close range.

All records for the complete three years of observation were therefore analysed, and the records grouped in steps of 3,3 km limits up to 10 km - that is for the ranges of time to thunder of 0-10, 10-20 and 20-30 seconds. The number of records obtained per square kilometer could therefore be calculated for each group and the ratio of these obtained. Table XVI shows the result of this analysis.

Time to Thunder Range (secs)	Distance km	Number of Records		Number per Km^2		Ratio of Numbers
		Cloud	Ground	Cloud	Ground	Cloud/ Ground
0-10	0-3,3	127	40	3,64	1,14	3,20
10-20	3,3-6,7	360	171	3,44	1,63	2,11
20-30	6,7-10	186	199	1,07	1,14	0,94
0-20	0-6,7	Best Estimate		3,64	1,63	2,24

Table XVI Number of Records and Ratio of Cloud and Ground flashes in specified range groups.

This analysis indicates that in the case of the cloud flash records, the tendency to falling off in recording numbers were not very large until after 6,7 km. It also shows that the number of ground flashes recorded in the 0-3,3 km range was in fact low since there is no reason why less should have been recorded in this range than in the next.

Accordingly the ratio of the numbers of cloud and ground flashes for these observations should be less than 3,20 in the first range, and only slightly greater than 2,11 as judged from the second range, and a good compromise would be to use

49/...

the cloud flash density for the first range fo 3,64 aand the ground record density for the second range of 1,63 thus by giving the best estimate of the ratio as 2,24.

This very low value would not have been deduced from the records of the one season set out in Table XV where for observations up to 6,5 km the ratio was 5,0, a figure which has been more generally accepted in the literature for tropical areas. On the other hand, occasional storm clouds have been observed which exhibit a very high intra-cloud flashing rate which appears to occur in the top of the cloud. Such storm clouds are rara but if they were to be included in any observation of cloud and ground discharges they would tend to increase to cloud/ground ratio, temporarily perhaps, to very high values.

11. Number of component strokes in lightning flashes to ground

In carrying out an analysis of the number of component strokes in ground flashes from field change records cognisance had to be taken of the identification of the records bearing in mind that whilst intra-cloud flashes usually include a slow component of long duration, ground flashes nevertheless do contain the occasional slow component following a stroke to ground which has been identified by other investigators as resulting from "continuing" currents.

By far the greater majority of ground flash field change records however are clearly characteristic, and Fig. 18(a) shows a number of these which were visually identified. The identification of intra-cloud flashes has been primarily on the basis of work carried out by Malan, privately communicated, and on published information by Muller Hillebrand[6] and Brook and Kitagawa[7] and there is overwhelming evidence in the oscillographic records obtained in this investigation of a distinct form of field charge differing from that of ground flashes and conforming to the descriptions cited. Examples of these are included in Fig. 18(b). Included are a few

50/...

Osc. No.		
977	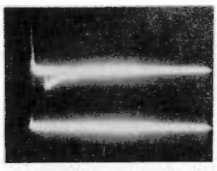	600 ms Time Sweep Std. Aerial with Counter ERA. Aerial 6,7 km Range
1545	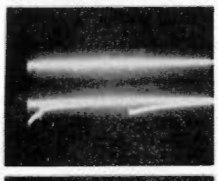	620 ms Std. Malan Counter 15,7 km
1916	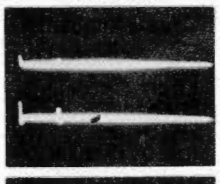	600 ms Std. Counter Grid 9,3 km
1922	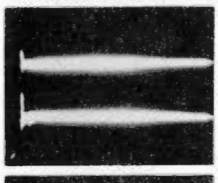	600 ms Std. Counter Grid 15,7 km
1977	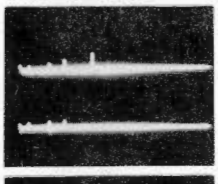	600 ms Std. Counter Grid 11,0 km
2235	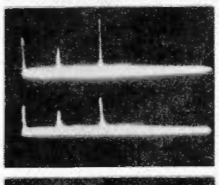	620 ms Std. Counter Input 9,7 km
2237	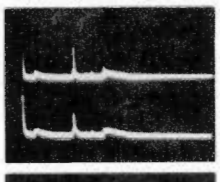	620 ms Std. Counter Input 9,7 km
2488	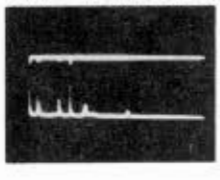	600 ms Std. (Reversed Polarity) Counter Input 11,7 km

Osc. No.		
2667	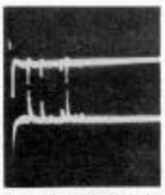	620 ms (part) Counter Grid Counter Input (Reversed Polarity) 7,3 km
2669	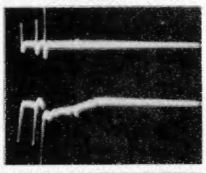	620 ms Counter Grid Counter Input (Reversed Polarity) 9,7 km
2675	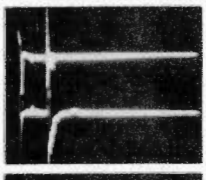	620 ms Counter Grid Counter Input (Reversed Polarity) 3,0 km
3043	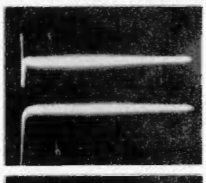	580 ms Counter Grid Counter Input (Reversed Polarity) 16,7 km
3046	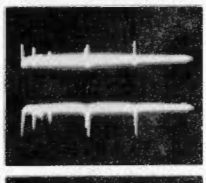	580 ms Counter Grid Counter Input (Reversed Polarity) 21,0 km
3053	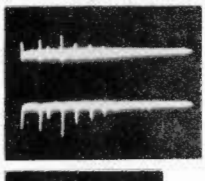	580 ms Counter Grid Counter Input (Reversed Polarity) 16,7 km
3072	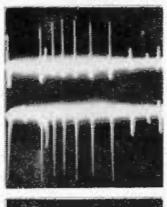	580 ms (part) Counter Grid Counter Input (Reversed Polarity) 9,0 km
3077	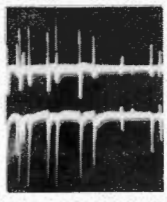	580 ms (part) Counter Grid Counter Input (Reversed Polarity) 8,3 km
3082	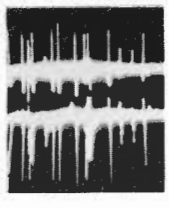	580 ms (part) Counter Grid Counter Input (Reversed Polarity)

-NOTE: The information on the right of oscillograms indicates the time sweep, the connections for each trace in order, and the range if known.

FIG. 18(a) The recorded field change of observed ground flashes.

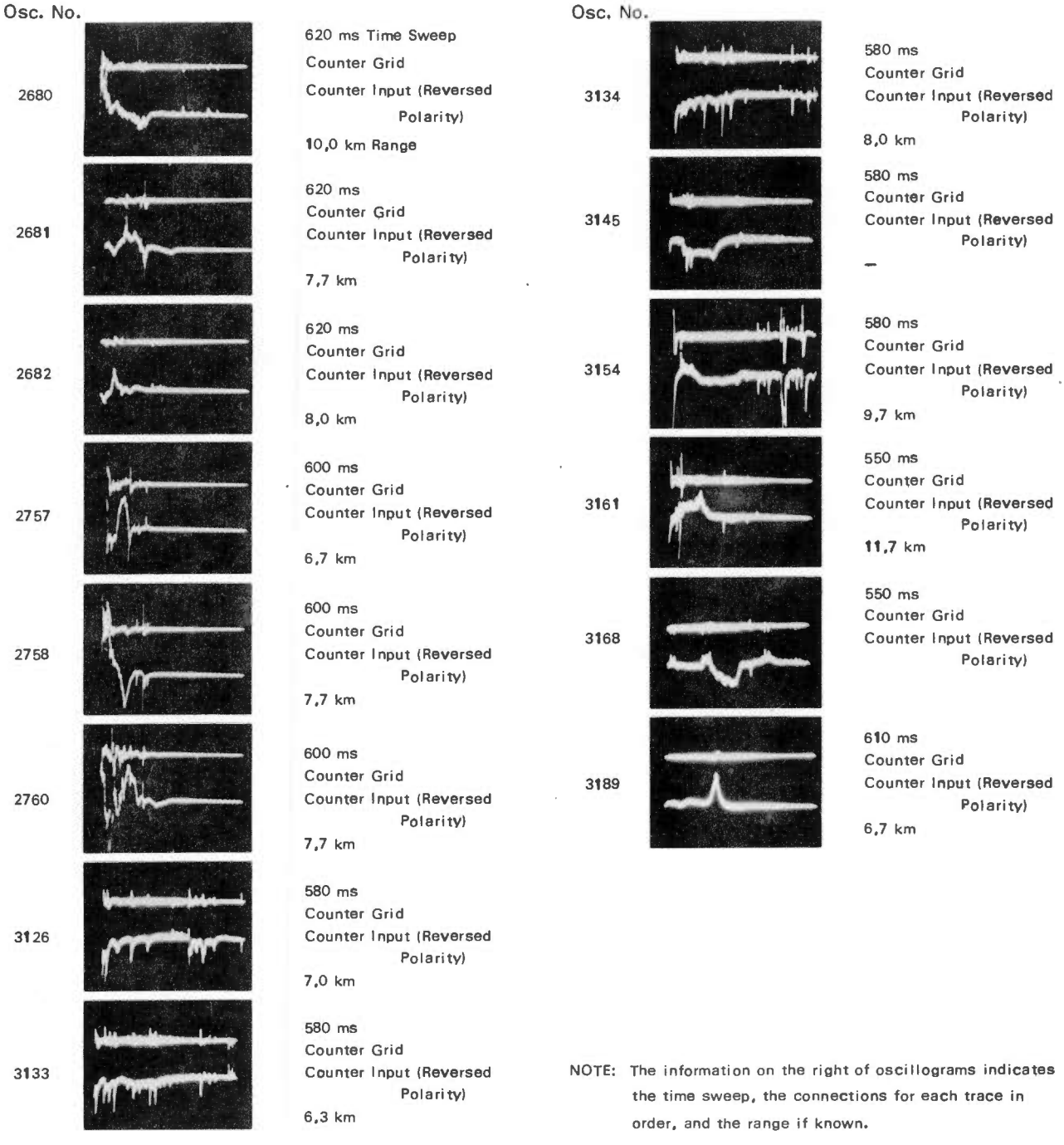

NOTE: The information on the right of oscillograms indicates the time sweep, the connections for each trace in order, and the range if known.

FIG. 18(b) Recorded field changes assumed to be due to intra-cloud flashes.

examples of intra-cloud flash field changes that appear to have very little underlying slow component but in which the time intervals between the fast components are so short, less than 15 ms for example, as to render them suspect, and such cases have been identified by Malan as intra-cloud flashes. It is of course possible for a large magnitude slow com= ponent of field change to occur which would be so severly attenuated by circuits of relatively short time constants as to be unobserved.

Finally many cases occur when the characteristic field changes for both ground and inter-cloud discharges appear consecutively on the same record and these have been classi= fied as two separate discharges for the purpose of counting.

In the early stages the oscillograph was used with a continuous internally triggered time sweep which therefore displayed all field change data but without time resolution. Later a single sweep of about 0,6 seconds was used, operated from the external trigger previously described, and in this instance the information was limited to this period. These aspects are discussed further in connection with the inter= pretation of the results.

All data was abstracted from the oscillograms at the CSIR using a D-MAC pencil follower equipment to digitise the coordinates of magnitude and time from a projection of the oscillogram and to transfer this to punched paper tape. A program was devised for the analysis of the data to render information regarding the number of components, the time intervals and total time together with their magnitude in arbitrary units.

Altogether 1430 flashes were analysed having the number of strokes indicated in Table XVII which also shows the cumulative results and the percentages of the total in regard to each category.

51/...

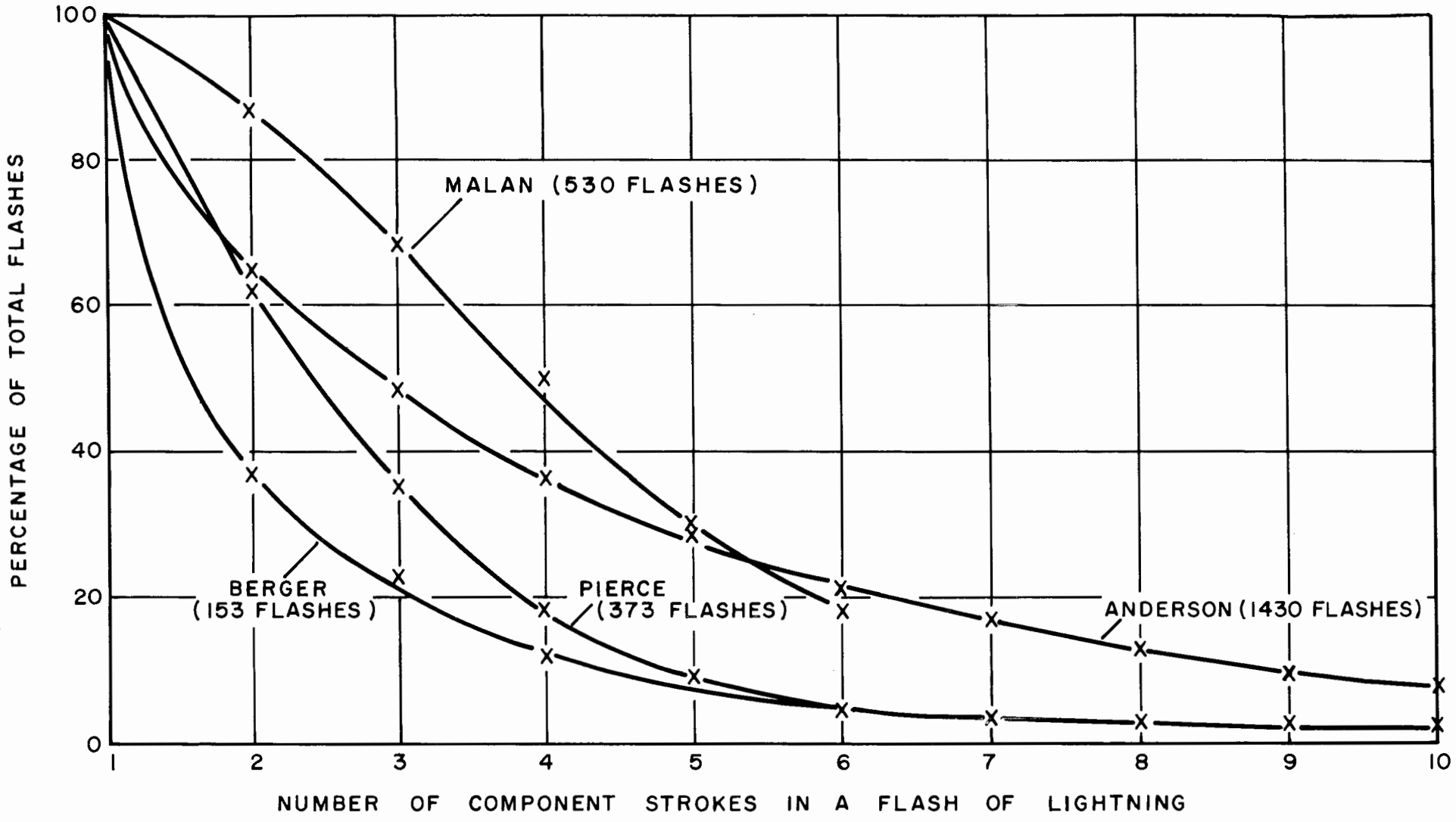

FIGURE 19

PERCENTAGE OF FLASHES HAVING AT LEAST THE NUMBER OF STROKES INDICATED

Reporter	Number of Component Strokes in Flashes of Lightning to Ground					
	1	2	3	4	5	6 or more
Malan[14]	13%	19%	18%	20%	12%	18%
Pierce[15]	38%	27%	17%	9%	4%	5%
Berger[16]	65%	13%	10%	3%	4%	5%
Anderson	36%	16%	12%	8%	7%	21%

Table XVIII Percentage number of Flashes having the indicated number of strokes

The most significant aspect of the data herein presented is the higher tendency to multiple stroke flashes observed for the Transvaal in South Africa and Rhodesia as obtained from the records of Malan and from this report, when compared with Pierce in the U.K. and Berger on Mt. San Salvatore, Switzerland. The latter in particular observed the largest proportion of single stroke flashes and only 5% with 6 or more strokes, whilst in Southern Africa between 13% and 36% were single stroke flashes but approximately 20% exceeded six strokes. Pierce on the other hand observed about the same propertion of single stroke flashes as did the writer but thereafter the distribution dropped rapidly to the 5% level recorded by Berger.

The corresponding thunderstorm day levels are 15 for the United Kingdom, 50 in Switzerland and about 80 in Southern Africa and it can be reasonably postulated that the above differences are associated with the degree of severity of lightning discharges, which therefore must increase with the thunderstorm day level.

It is shown in Appendix II, Part II, that when the charge separation area is large, as would be the case in very active thunderstorms, intra-cloud flashes are the more likely - but if the ground flash regime is finally attained the charges involved are much larger and it would be expected that a high proportion of multiple flashes would result. However further explanations are required as to the discharge mechanism which

53/...

can give rise to multiple stroke flashes and this is discussed in Part II.

An interesting feature reported by Berger[16] was that of the 153 flashes observed, 36 were positive (conveying positive charge to ground) and these were all single stroke flashes. Despite the high probability of 0,65 in favour of single stroke flashes, there should still have been about twelve multiple positive flashes.

This aspect was therefore examined in respect of the present data with the results indicated in Table XIX.

Number of Strokes	Negative Flashes		Positive Flashes	
	Number Flashes	% Total	Number Flashes	% Total
1	444	37,6	62	50,8
2	181	15,3	27	22,1
3	143	12,1	18	14,8
4	99	8,4	4	3,3
5	88	7,5	3	2,5
6	48	4,1	3	2,5
7	45	3,8	1	0,8
8	34	2,9	0	0,0
9	19	1,6	0	0,0
10 and above	80	6,7	4	3,2
Total	1181	100,0	122	100,0

Table XIX Comparison of the number of component strokes of positive and negative flashes

Table XIX shows that 87,7% of all positive flashes had up to three component strokes whereas only 65% of all negative flashes were in the same category, and this indicates a significant tendency for positive flashes to have fewer components. Considering that in the case of Berger's data there was a much lower probability of multiple strokes for even negative flashes, the expectancy of a positive multiple stroke would be even less.

54/...

would be even less.

Nevertheless both results suggest that there is an inhibiting factor present in the case of positivily tipped downward strokes which is not present when the leader is negative, and this factor would need explanation in any detailed propagation mechanism. It may be either that it has to do with the lower velocity of positive streamers compared with negative, or that in the case of positive discharges more charge is neutralised with each stroke, thereby leaving less charge over for subsequent discharges.

12. Time intervals between component strokes of a lightning flash

An analysis was carried out on the time intervals between the first, second, third and fourth component strokes, and between all recorded strokes of lightning flashes without regard however as to the inter-relation which may exist between them. For example the frequency distribution of first and second time intervals was obtained independently for all results where they existed, irrespective of whether they occured within multistroke flashes or were simply two or three stroke flashes. The reason for this mode of treatment lies purely in the practical aspect of wanting to know what the pause times between strokes of a flash are and not the previous or following history - which however would be of considerable interest and could also be extracted from the results in due course - but the number of permutations increases markedly and more results are required if they are to prove meaningful.

The results exclude those in which the oscilloscope beam was free-running of course, and in this case the effect of a restricted sweep time would be negligible if, as was observed, the mean value of time intervals was short by comparison.

The frequency distributions of first, second, third and all time intervals have been plotted in Fig. 20, and some pertinent results are shown in Table XX.

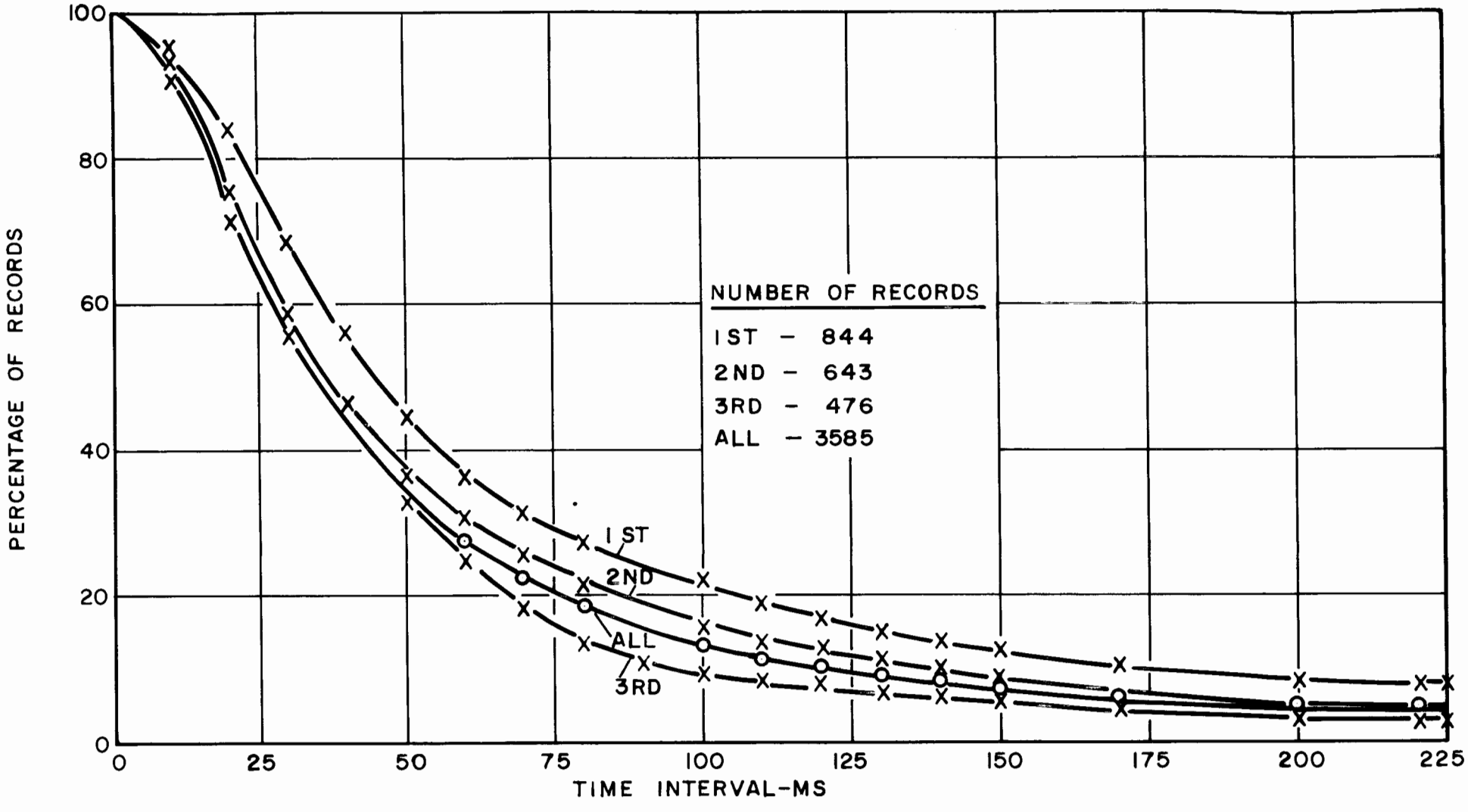

FIGURE 20

PERCENTAGE OF RECORDS IN WHICH INDICATED TIME INTERVAL BETWEEN STROKES IS EXCEEDED

Time Interval ms	Percentage of records exceeding time interval indicated in column 1			
	1st Interval	2nd Interval	3rd Interval	All Intervals
10	95,3	93,8	93,3	91,2
20	84,0	75,1	73,1	71,6
30	68,6	58,8	59,5	56,0
40	56,1	46,7	44,7	44,0
50	44,7	36,2	32,6	34,4
100	22,1	15,9	9,7	13,8
150	12,8	9,0	5,9	7,7
200	8,2	5,1	3,2	4,5
300	3,3	2,0	2,1	2,1
500	0,1	0,5	0,2	0,1
Total Records	844	643	476	3585
Mean Interval ms	74,7	62,1	53,1	56,8
Median Interval ms	44,7	36,6	35,7	34,9
Std. Deviation ms	82,8	75,1	65,9	69,2

Table XX Frequency distribution of 1st, 2nd, 3rd and all time intervals between strokes of multiple flashes

Comparing the order of time intervals, it is evident that not only the duration of the interval but also the deviation from mean values reduces with increasing order from the first to the third time interval, but the extent of this reduction also converges except in the case of the standard deviation of the third interval which falls steadily. It may therefore be said that on average the succeeding time intervals are less than their predecessor, and not so dispersed, but taken all in all the spread is still very considerable.

The first time interval is significantly longer than all time intervals, the mean being 31,5% in excess, the median 28,2% and the standard deviation being 20,0% larger than the values for all time intervals. This result is clearly seen on Fig. 21 which illustrates in addition that the distribution

56/...

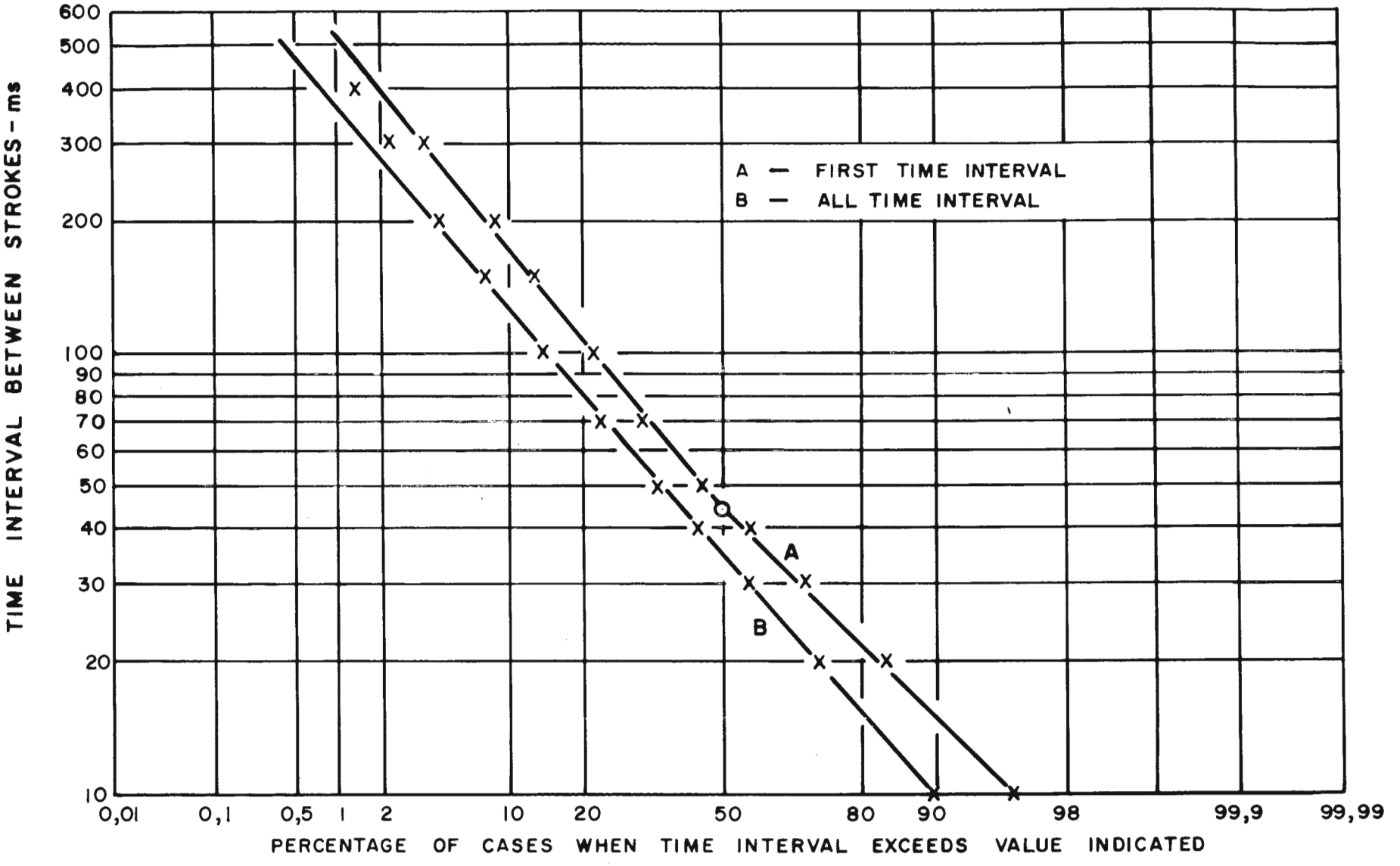

FIGURE 21

DISTRIBUTION OF THE TIME INTERVALS BETWEEN STROKES OF A LIGHTNING FLASH

of all time intervals closely conforms to a Gaussian log-normal distribution, whilst that of first time interval has two log-normal trends before and after the calculated median value.

This type of departure may be due to the truncation of lower values, but it might well also be a fact that there is an absolute limit to the minimum value of time interval.

By way of comparison with other observers the following Table XXI gives some data of interest.

Time Interval ms		Percentage of records exceeding indicated interval			
		Anderson	Pierce	Malan	Berger
50		34,4%	64%		
100		13,8%	26%		
200		4,5%	9%		
Mean	ms	57	93	45-63	
Median	ms	35	65	30-50	40

Table XXI Distribution of Time Intervals with mean and median duration

In connection with the above table the interval durations given by Pierce are notably larger than others and he made the same point when comparing his data with that given by Bruce and Golde[5]. However, considering that the dispersion of time intervals is so large it would not be at all surprising if results taken over relatively small samples differ considerably.

Considered from the standpoint that the time intervals between strokes represent the time ellapsing between the tapping of new sources of charge from the cloud, it appears unlikely that streamers of fixed velocity should traverse to neighbouring charge centres, since these would then range over distances which would be very large or very short and in no strict sequence. It seems necessary therefore to seek an explanation in some other mechanism capable of explaining the very large dispersion in time intervals despite a small median value.

57/...

13. Total duration of lightning flashes to ground

In this case and judging from previous observations by Malan[14] some 5% of all discharges would exceed the 600 ms which was the approximate limiting time sweep used in this investigation. Nevertheless the data was analysed and the results are compared with those of Malan in Table XXII.

Duration of flash	% of records with durations exceeding the Indicated values				
ms	Including Single Strokes	Excluding Single Strokes	Malan	Pierce	Berger
50	53,7%	79,4%	88%		
100	44,8%	66,2%	77%		
150	37,8%	55,9%	62%		
200	30,2%	44,7%	50%		
250	24,5%	36,2%	36%		
300	20,9%	30,9%	25%		
400	13,7%	20,3%	13%		
500	7,2%	10,7%	7%		
Total Number	1430	967	530	373	153
Mean Duration ms	147,7	281,5	-	245	
Median Duration ms	66,9	177,1	200	180	180
Std.Deviation ms	182,0	183,1	-	-	-

Table XXII Distribution of total duration of flashes with mean and median values

The frequency distribution of the duration of flashes can be dipicted in two ways. In the first, all single stroke flashes which have virtually zero time duration may be added, in which case a possibly more correct absolute distribution is obtained if for example one is applying the data for the purpose of determining the probability of success with circuit breaker auto-reclosing cycles. In this case successful operation is measured against all lightning flashes to the system. Secondly of course, for the intensive study of the

multiple stroke discharge, single stroke flashes are ommitted. In the preceeding table Berger's figure of 180 ms median duration definitely excludes single stroke flashes which were by far in the majority, and which if included, would have reduced the figure very considerably. Whether Pierce included 33% of his records of flashes which were single strokes, is not stated, but Malan includes them. In this instance however there were only 13% single stroke records and their omission or addition would not change the distribution radically.

It is evident that the lack of records in excess of 600 ms in the present investigation has tended to lower the duration times when compared with Malan, but it is noteable that despite this, there were more long duration flashes in the range exceeding 400 ms in the present records.

It is of interest to note that both Malan and Pierce found a correlation of the duration of flashes with the order of the number of component strokes. Unfortunately one quotes the median values and the other the mean values which differ significantly as shown in Table XXII, but the comparison is nevertheless indicated in Table XXIII below, showing also an estimate of the median value for Pierce's observations based on 0,73 of the mean.

Number of Strokes in flash	Malan Median Value	Pierce Mean Value	Pierce Estimated Median
2	80 ms	150 ms	110 ms
3	150 ms	200 ms	147 ms
4	200 ms	340 ms	250 ms
5 or more	350 ms	515 ms	380 ms

Table XXIII Mean and Median values of flash duration with increasing order of number of strokes

The correction factof of 0,73 for the ratio of the median to the mean duration was obtained from Table XXII where both values were given by Pierce. In the present investigation this ratio was 0,81 and in both cases indicating

59/...

a departure from a normal Gaussian distribution. Unlike the distribution of time intervals between strokes which followed a log-normal distribution the total durations in this investi=gation do not, neither do the values quoted by Malan. Further investigation confirms that they do not follow a normal dis=tribution either and the reason for this is not very obvious. It is possible however that the erratic manner of the dis=tribution of very long and very short intervals may have some influence. There are many cases where the time intervals are more or less equal within a flash, that is either all long or all short; there are however also many cases where the majority are short intervals but one or two or more are long and vice versa. Examples of these are given below in Table XXIV.

Osc. No.	Time intervals - ms	Total ms
897	8-19-30-14-21	93
907	86-48-67-56-17-15-21-35-9-87	442
1111	51-33-29-13-20-19-25-21-29-29	270
1112	63-46-24-181	313
1117	37-12-29-17-315	410
1124	6-35-8-30-28-41-96-14-55-162-3-17	495
1040	20-31-14-349-350-83-84-20	952
1526	128-257-22-134	541
2114	50-111-71-310	543
2433	168	168
2607	244-165	409
2630	439-112	551
3027	461	461
3175	108-99-396	604

Table XXIV Typical Patterns of time intervals between strokes

Hence it is clear that whilst there is a correlation between the duration of a flash and its number of strokes, there is also a pattern which indicates that a flash having a long duration may consist of a large number of strokes

60/...

with short time intervals between them, or it may comprise a few components with one or two very long time intervals, and this dual form of distribution might well account for the observed irregularity in the frequency distribution pattern for the duration of all flashes.

14. Slow component field changes

In 4,1% of the flashes recorded, or 60 records, a slow field change was observed to follow one of the strokes, and in one case two strokes in the same flash, and examples of the recordings are shown in Fig. 22. Of the 60 records, 12 or about 20% followed the first stroke and in all cases there were succeeding strokes without slow components, 16 or about 27% followed an intermediate stroke whilst 33 or 55% succeeded the last stroke of the flash.

The 60 slow components were distributed in the stroke order as indicated in Table XXV.

Stroke Order	Number of slow Components	Percentage of Total
1	12	20,0
2	9	15,0
3	8	13,3
4	4	6,7
5	7	11,7
6	6	10,0
7	2	3,3
8	4	6,7
9	2	3,3
10	1	1,7
11	2	3,3
12	1	1,7
13	2	3,3
Total	60	100,0

Table XXV Number and percentage of slow components associated with the stroke order indicated

61/...

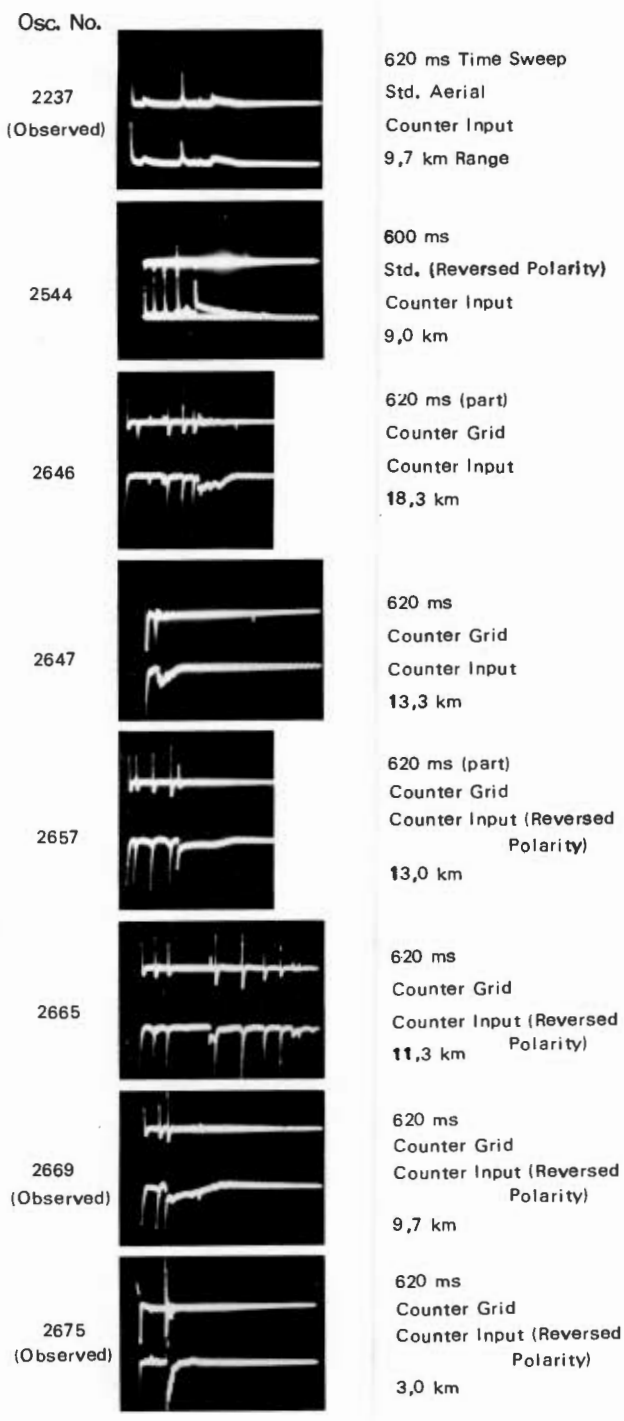

NOTE: The information on the right of oscillograms indicates the time sweep, the connections for each trace in order, and the range if known.

FIG. 22 Examples of slow field changes following component strokes of ground flashes.

It can be inferred from this table that apart from the preference for the last stroke, slow components could thereafter be associated with any other stroke within a flash with a second preference for the first stroke.

The term "slow" is of course relative and in this context it is defined as a field charge which significantly delays the decay time of the measuring R.C. circuit potential beyond that which the time constant of the circuit would otherwise dictate. In this case a time constant of less than 1 ms was used, so that if no slow component field change was present, or if it was very slow by comparison, the decay time would not be observed when using a time sweep of about 600 ms. These field changes are therefore relatively large and their duration can be measured up to the point when the rate of change of field is insignificant in so far as this is determined by the measuring circuit time constant.

Table XXVI gives the frequency distribution of the duration of these field changes.

Duration ms	Percentage of Records exceeding indicated duration	
20	92,3	Mean Duration - 142 ms
40	82,7	Median Duration - 115 ms
60	71,2	Standard Deviation - 104 ms
80	67,3	
100	61,5	
150	40,4	
200	25,0	
300	9,6	
400	1,9	

Table XXVI Distribution of the durations of slow component field changes

Both the mean and the median duration of slow components are about 65% of the values for complete flashes given in Table XXII.

62/...

indicating that they are substantial components of field change which merit a full explanation.

Brook et al[17] in a sample of 200 records found that 90% were ground flashes and of these about 50% contained slow components, which is an exceedingly high proportion compared with the present record and would appear to indicate that they are associated with a particular kind of thunderstorm. Pierce[15] on the other hand does not give the proportion observed but does not say whether they were in significantly large numbers. He did however observe that there appeared to be two types - in the first, which he terms S(α), the field change immediately followed the return stroke (R element) without interruption until a steady field was obtained. In the second, or S(β) type, the field change was interspersed with quiescent intervals often immediately succeeding the R element. With a one millisecond time constant this latter type would have produced a single slow component apparently not associated with the R element, and this has not been observed in the present records. However there is some evidence supporting the view that slow components are associated with certain types of storm in that several are observed to occur in one thunderstorm and thereafter there are large gaps in the chronological record.

As for their explanation, Berger[18] observes from direct lightning current measurement, that downward negative strokes usually produced a number of impulse currents of the order of thousands of amperes and some of these are followed by "continuing" currents of the order of hundreds of amperes lasting for ten to 100 ms and more. The impulse currents are clearly identified with the fast R element field change of the return stroke, and the continuing current would pro= duce the slow component field change observed by other investigators. The possibility of a discharge to ground triggering off an intra-cloud discharge cannot, however, be discounted, and this would also produce a slow field change; also the fact that since these field changes occur in close proximity to the junction (or J.) process between successive

63/...

R elements, there could also be some confusion as to whether they are associated with the return stroke proper or whether they are a separate distinct phenomenon. This matter will be further discussed in Part II of the thesis however.

15. The Polarity of field changes of ground flashes

Reference to Fig. 18(a) will indicate that there was one observed case of a ground flash in which not all component strokes had the same polarity. In view of this, the 1430 records were subdivided according to Table XXVII.

Description of Subdivision	Number of flashes	Percentage
(i) All components positive	1181	82,6
(ii) All but one component positive	40	2,8
(iii) Both polarities	69	4,8
(iv) All but one component negative	18	1,3
(v) All componente negative	122	8,5
Total	1430	100,0

Table XXVII Polarity of field changes of ground flashes

It is seen that positive field changes (negative flashes) certainly predominate but not to the same extent as observed previously for Southern Africa. The ratio of purely one polarity to the other in this case is 9,6:1 in favour of negative flashes whereas Anderson and Jenner[19], from mag= netic link studies of lightning currents to transmission lines in Rhodesia, noted a ratio of 14:1 whilst Schonland[20] and Halliday[21] both recorded a ratio of 17:1 for South Africa.

Observations in Europe on the other hand, are very differ= ent. Berger, for example, in a private communication, records 125 downward negative flashes to 39 positive resulting in a ratio of 3,2:1 for Switzerland whilst Popolansky[22] in Czechoslovakia found a ratio of 5,2:1.

64/...

Pierce[15] gives ratios of positive/negative field changes measured at Cambridge in the U.K. which vary between 4,5 for large field changes at close range to 1,1 for distant field changes of small magntidue. He does not however appear to have differentiated between field changes due to intra-cloud flashes with those toground, and in the case of the field changes due to discharges at large distances, those due to intra-cloud flashes are likely to be so small as to be neg= ligible; hence the ratio of 1,1 recorded should apply mainly to ground flashes.

Mackerras[23] recording in Queensland found ratios for ground flashes which also varied with distance from about 9:1 at close range to 2,5:1 at about nine to twenty kilometers, with a mean value of 4,8:1 in favour of negative flashes. He also observed complex polarities in approximately 18% of his recordings.

The evidence is therefore seen to be substantial that in the predominately heat or convection type of storms prevalent in the Southern African sub-tropics, over 80% of ground flashes are negative in polarity - that is they lower negative charge to ground, whereas in Europe and the U.K. the proportion is very much less, the lower limit being of the order of 50%. In Queensland which is also subtropical but at the coast com= pared to plateau conditions inland for Southern Africa, close range storms produce about the same proportion of negative flashes as in the present investigation, and there appears to be no radical reason why this should change with increasing distance unless there is some sampling mechanism which tends to favour positive flashes when at a distance, for example the current flowing or charge deposited in a stroke.

Whilst Pierce[15] found that the field change variation with distance was the same for both positive and negative field changes, Berger[18] records that downward positive flashes had up to 300 C charge per flash compared with a maximum of 80 C for negative flashes and correspondingly the the values of $\int i^2 dt$ were also longer; furthermore he observed that all positive flashes were single strokes which means that

65/...

the field change would take place in one step. Hence there is the distinct possibility that positive flashes giving rise to negative field changes might intrude in greater numbers when recording at long range simply on account of the higher magnitude field change triggering the recording equipment more frequently.

However, in so far as the different ratios of positive to negative flashes is concerned in Europe compared with Southern Africa, the most plausible explanation seems to be in the different types of thunderstorm which may occur. A high preferance for negative flashes would appear to conform more closely to the classic bi-polar structure of a convection type of thundercloud with virtually always the same polarity orientation with some occasional cases where the positive charge, normally in the higher reaches, either moves downwards at some stage of the thunderstorm or the positive charge itself breaks down and discharges to earth after the negative charge has been depleted by previous ground flashes.

Where positive flashes are more prevalent, it would appear that the charging mechanism may be different and that, as a consequence, positive charges are more frequently found in the lower altitudes. Berger in a communicated statement records the consecutive polarity of charges in clouds passing over Mt. San Salvatore in Lugano and in which positive and negative charge followed each other in about equal proportions. This may also be the situation with respect to frontal type thunder= storms which result from the meeting of two layers or wedges of air masses at differing temperatures and moisture contents and in which it is difficult to envisage the same type of vertical charge seperation process as occurs with the con= vection types of thunderstorm more prevalent in the tropics.

In view of the above comments, which are at this stage somewhat conjecture, it is necessary to state that the con= siderations which follow in Part II are mainly confined to the classical bipolar cloud model, although the principles of the mechanism of a discharge to ground must always be somewhat similar, whatever the manner of charge separation.

66/...

16. The relative magnitude of field changes in successive strokes of a flash

An analysis was undertaken of 905 oscillograms of ground flashes which had at least two component flashes, and on which no component magnitude was off-scale.

First of all a comparison was made of the mean, median and standard deviation of the ratios of the magnitudes of the second component to the first, the third to the first and the third to the second, with the result indicated in Table XXVIII below.

Description of Magnitude Ratio	Mean	Median	Standard Deviation
2nd to 1st (905 values)	1,4	0,6	5,6
3rd to 1st (671 values)	1,3	0,5	8,1
3rd to 2nd (671 values)	1,4	0,9	2,1

Table XXVIII Ratio of Magnitudes of oscilloscope deffections due to field changes of the first, second and third component of a lightning flash

It is observed that the three distributions are far from normal Gaussian, and accordingly the standard deviation and to a lesser extent the mean values are perhaps not significant since a few very large values of ratios would have considerable influence on these parameters. However the median values are in all cases less than unity indicating a 50% probability that the second component for example would have a magnitude 0,6 of the value of the first. Similarly the third component shows a tendency to be lesser in magnitude than the second.

Also whilst there is a high probability that the two components following the first will be less in magnitude, cases do occur when the reverse is true, and these cannot be ignored. This is particularly emphasised by the fact that the mean values of the ratio are all in excess of unity.

In a second analysis the amplitudes of the first, second

67/...

and third components were expressed as ratios to the mean value of all components of the same flash, and the results of this analysis are more consistent and are as indicated in Table XXIX.

Description of Magnitude Ratio	Mean	Median	Standard Deviation
1st component to Mean (905 values)	1,5	1,4	0,7
2nd component to Mean (905 values)	0,9	0,8	0,5
3rd component to Mean (671 values)	0,9	0,8	0,5

Table XXIX Ratio of magnitudes of oscilloscope deflections due to the first, second and third component, to that of the mean value for all components of the same flash

In this case the distributions are closely normal Guassian, and there is now much more conclusive evidence of the larger magnitude of the first component compared with the second or third component. The ratio of the mean and median of the second component to that of the first is 0,6 and 0,57 respectively which agrees closely with the median value for this ratio given in Table XVIII. Table XXIX also shows that the second or third components have identical distributions, and both tend to be less in magnitude than the mean value for the flash.

The above analysis therefore does no more than indicate that the probability that the first component will be larger than all others, is high, but there is still a significant probability that it will be less.

17. Acknowledgements

With respect to the part of this work carried out in Rhodesia the author is indebted to a large number of persons for assis= tance either by way of discussion or through correspondence or papers or more directly by the loan of equipment or time

and the provision of finance. The oscilloscope was provided by the Federal Power Board together with photographic film, and the Southern Rhodesia Electricity Supply Commission paid for developing the printing and supplied the remainder of the ancillary equipment such as the Malan and ERA Counters, and the counter designed by I.J. Wood of that organisation. The oscilloscope trigger was designed and made by V.G. Miles of the Federal Meteorological Department, who also gave of his time to devise and test the electronic equipment in use. Special thanks are due to W.G. Gentles for enlarging most of the oscillographic records with such precision in his limited spare time, and for helpful advice on photographic matters.

I further gratefully acknowledge constructive advice received from the late Prof. D.J. Malan of the Bernard Price Institute of Geophysics of Johannesburg without which the complete analysis of the field change records would not have been possible. Also many papers were referred to, not all being listed in the bibliography.

Thanks are due to the ERA Lightning Investigation Committee for Central Africa for financial support and use of the ERA counter data, and especially to its Honorary Secretary, and my colleague R.D. Jenner also of the S.R. Electricity Supply Commission with whom the author has been associated for many years in this field, and who organised the provision of equipment and counter data. Last and not least I am very grateful to my wife and family who patiently endured the long hours of recording and testing at my home, with its consequent disorganisation.

The work of analysing the data was largely accomplished at the National Electrical Engineering Research Institute of the Council for Scientific and Industrial Research of South Africa, and the author gratefully acknowledges this assistance. Thanks are due to many colleagues who assisted, and to Prof. Jacobsz, Head of the Numerical Analysis Division of the National Research Institute for Mathematical Sciences and his staff, in particular Mrs. L.O. Stander who did the extensive programming for the computer analysis.

69/...

My thanks are also due to Mr. J.D.N. van Wyk, my Director, for permission to undertake and process this work and to Mr. J.H.J. Filter for reading the manuscript and for many helpful suggestions.

18. References

(1) Le Jay P. L'Onde Electrique (1926) 5 p. 493

(2) Pierce E.T., "The influence of individual veriations in the field changes due to Lightning Discharges upon the design and performance of lightning flash counters "Archiv. f. Met. Geophysik und Bioklim Ser. A.9. (1956) p. 78-86.

(3) Golde R.H., "Lightning Flash Counter" Electrical Research Association Report on description installation and op= eration of the modified Pierce Counter. July 1957.

(4) Malan D.J., Lightning Counter for flashes to ground. Gas Discharges and the Electricity Supply Industry Butterworth, London, 1962, p112-116.

(5) Bruce C.E.R. and Golde R.H., The Lightning Discharge J. Inst. Elect. Eng. Vol. 88 Part II No. 6 pp 487-504 Dec. 1941

(6) Muller-Hillebrand D., "Lightning Counters I and II Arkiv for Geofysik Band 4 nr. 10, 11. 1963

(7) Kitagawa N. and Brook M., A comparison of intra-cloud and cloud to ground lightning discharges J. Geophys. Res. 65(4) 1960

(8) Malan D.J., Physics of Lightning The English Uni= versity Press Ltd. London 1963 pp 116

(9) Anderson R.B., A comparison between some lightning parameters measured in Switzerland with those in Southern Africa. CSIR Special Report Elek. 6 May 1971

(10) Anderson R.B., Counting Lightning Strokes. "A statictі= cal approach". Report to CIGRE Study Committee No. 8 Trondheim 1963

(11) Chan Y.H., Design Characteristics of a Lightning Flash Counter Elect. Res. Assn Report No. 5145 Private and Confidential

(12) Pierce E.T., "The Counting of Lightning Flashes" Stanford Research Institute Special Technical Report 49, 1968 Appendix B "Proportion of flashes to earth"

(13) Popolansky F., Correlation between the number of Lightning flashes and thunderstorm days. Report to CIGRE Study Committee No. 8 Working Group "Lightning Flash Counters" Copenhagen June 1967

(14) Malan D.J., "The relation between the number of strokes, stroke interval and the total durations of Lightning Discharges" Geofisica Pura e Applicata - Milano Vol. 34 pp. 224-230 (1956).

70/...

(15) Pierce E.T., Electrostatic field-changes due to lightning discharges Quart. J. Roy. Mateorol. Soc. 81 (348) 1955 pp 211-228

(16) Berger K., Details of Downward negative flashes to Mt. San Salvatore - privately communicated

(17) Brook M., Kitagawa N. and Workman E.J., Quantitative study of strokes and continuing currents in Lightning discharges to ground. Jour. Geophys. Res. 67(2)637-47 1962

(18) Berger K., Novel observations on Lightning Discharges Jour. Frankl. Inst. Vol. 283 No. 6 June 1967

(19) Anderson R.B. & Jenner R.D., A summary of eight years of Lightning investigation in Southern Rhodesia. Trans. S.A. Inst. Elect. Eng. July and Sept. 1954

(20) Schonland B.F.J., Proc. Roy. Soc. Series A. 1928 118 p. 233

(21) Halliday E.C., Proc. Roy. Soc. Series A. 1932, 138 p. 205

(22) Popolansky F., Measurement of Lightning Currents in Czechoslovakia Proc. CIGRE 1970 Biennial Session Paper No. 33-03

(23) Mackerras D., A comparison of Discharge Processes in Cloud and Ground Lightning Flashes Jour. Geophys. Res. Vol. 73 No. 4 Feb. 15, 1968

71/...

THE CAPACITANCE OF AERIAL SYSTEMS

PART I APPENDIX I

Summary Aerial systems are used frequently in experimental work connected with lightning - for example in the measurement of electric field changes or in applications to lightning flash counters. It is important therefore to be able to determine the parameters of these systems, in particular their capacitance and effective height.

The capacitance of aerials is dependant upon the charge distribution in the aerial and this in turn upon the operating conditions, and in most cases it is necessary to arrive at a compromise which best fits the actual electric field conditions with minimum errors.

This appendix describes methods of calculation for a number of cases and discusses some of the errors that arise between calculation and measurement.

Contents

THE CAPACITANCE OF AERIAL SYSTEMS

PART I. APPENDIX I.

1. Capacitance of a charged sphere

The capacitance C of any electrode or charged volume is defined as the quantity which relates the potential V of the electrode or charged volume to that of its total charge q namely:

$$V = q/C \text{ volts} \qquad (1.0)$$

In the case of an isolated charge such as might be lodged on a sphere of radius "r" the potential on the surface of the sphere is calculated by assuming the charge is situated at a point at the centre of the sphere whence:-

$$V = q/4\pi\epsilon_o\epsilon_r \; r \text{ volts} \qquad (1.1)$$

Where ϵ_o is the permitivity of free space and has the approximate value of $10^{-9}/36\Pi$ farad-meters, and ϵ_r is the dielectric constant of the media which is assumed to be unity for air. This potential is that of the surface of the sphere relative to zero potential at infinity and the capacitance by definition is simply:-

$$C = 4\pi \; \epsilon_o\epsilon_r \; r \text{ farads} \qquad (1.2)$$

If however the charged sphere is relatively close to an infinite perfectly conducting plane, such as the earth is usually considered to be when the radius of the sphere is small compared to that of the earth, the potential at the surface of the sphere may be referred to this plane by considering the effect of a like charge of opposite polarity situated as a mirror image below the conducting surface as illustrated in Figure 1.

2/...

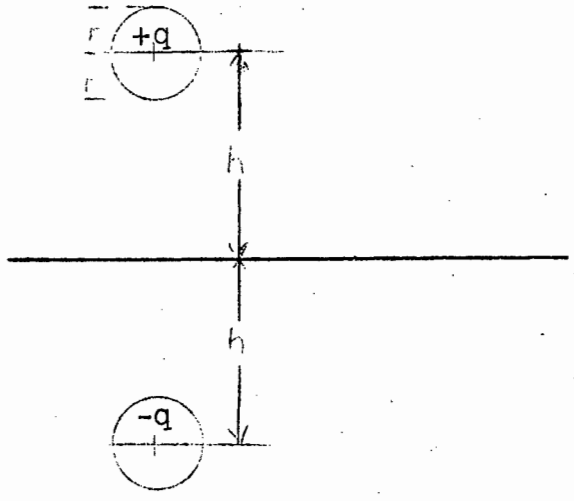

Figure 1. Charge +q on sphere of radius r, at a height h above conducting zero potential plane.

The charge on the sphere now distributes itself such that more charge is situated on the lower portion of the sphere due to the attraction of charge of opposite polarity on its image but if the radius of the sphere is small compared with its height above ground this effect is neglected, or in other words $h \pm r \approx h$. The potential on the surface of the sphere is then given by the following:-

$$V = q/4\Pi\epsilon_o\epsilon_r \cdot (1/r-1/2h)$$

In this case if $2h >> r$ the effect of earth is seen to be negligible. Likewise the capacitance is simply:-

$$C = 4\Pi\epsilon_o\epsilon_r \, (1/r-1/2h)^{-1} \text{ farad} \qquad (1.4)$$

However, the potential of the sphere is reduced and the capacitance increased by the proximity of the earth by an amount proportional to r/2h in both cases

3/ ...

2. Capacitance of a horizontal cylindrical conductor of finite length

The following method of calculation is described by Jordan[1] using identical principles to the above. First of all considering the potential relative to infinity, the potential at a point P on the surface of the conductor is derived assuming that the total charge q is distributed, say uniformly, along the centre line of the conductor, of length "L" and radius "r", as in figure 2.0. This is analogous to the case of a sphere, in that the charge in that case was considered to be located at its centre.

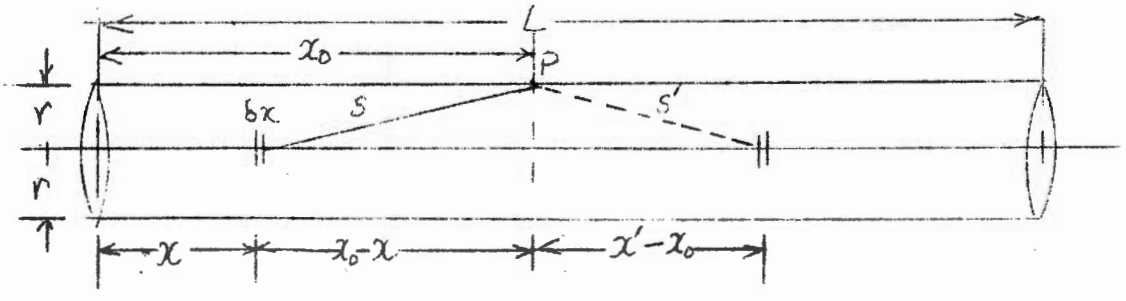

Figure 2.0 Diagram illustrating potential at P due to charge q distributed along centre line of conductor of length L and radius r.

The charge δq on a small element δx situated x from one end of the conductor is given by:-

$$\delta q = q/L \cdot \delta x \qquad (2.0)$$

The increment of potential at the point P (distant x_o from the same end) due to the elemental charge δq is then:-

4/...

$$V = \delta q/4\pi\epsilon_o\epsilon_r s$$

$$\text{when } s = [(x_o-x)^2+r^2)]^{\frac{1}{2}} \qquad (2.1)$$

Substituting for δq and putting $\epsilon_o = \epsilon$ and $\epsilon_r = 1$ (for air) and integrating for "x" between the limits 0 and x_o.

$$V_1 = q/4\pi\epsilon L \cdot \int_0^{X_o} [(x_o-x)^2+r^2]^{-\frac{1}{2}}\, dx \qquad (2.2)$$

Similarly for that portion of the charge q which lies to the right hand of point P when $x' > x_o$ and

$$s' = [(x'-x_o)^2+r^2]^{\frac{1}{2}} \quad \text{whence}$$

$$V_2 = q/4\pi\epsilon L \cdot \int_{x_o}^{L} [(x'-x_o)^2+r^2]^{-\frac{1}{2}}\, dx' \qquad (2.3)$$

The potential at P is therefore given by $Vo=V_1+V_2$ and results in the following expression:-

$$V_o = q/4\pi\epsilon L \cdot \left\{\sinh^{-1}[(L-x_o)/r] + \sinh^{-1}(x_o/r)\right\} \qquad (2.4)$$

The bracket term of equation (2.4) gives rise to a function which is illustrated diagrammatically in figure 2.1 below.

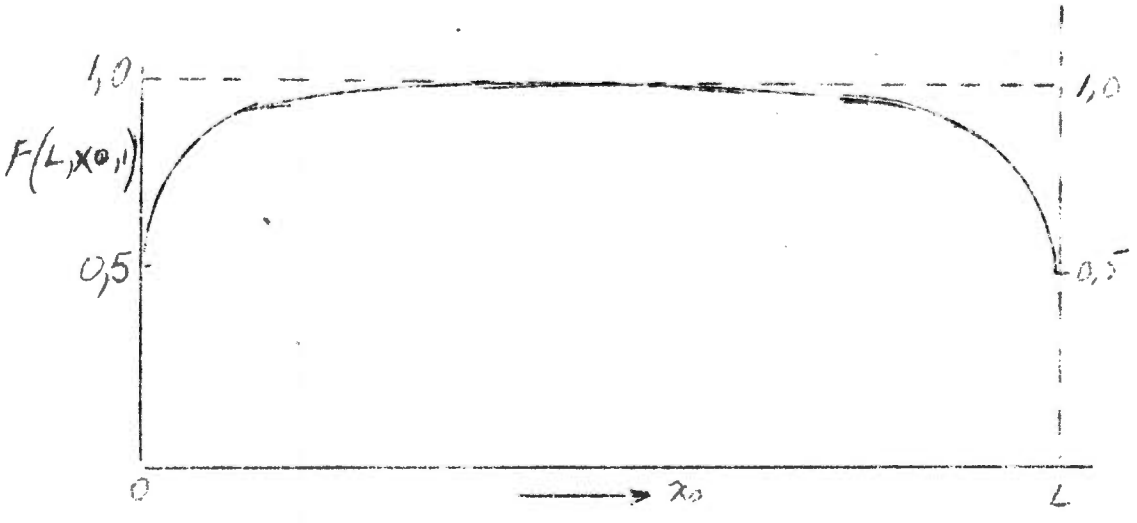

Figure 2.1 Calculated potential along surface of conductor for assumed uniform charge distribution.

5/...

The actual potential at any point along the surface of the conductor should of course be uniform, but merely because of the charge distribution assumed, the potential at the extremities falls off as shown. It can be seen that the charge per unit length would need to be increased sharply as the extremities are approached if a uniform potential is to be achieved. A better approximation to the actual charge distribution has been calculated with the aid of a computer[2], but it is found that it is sufficiently accurate for all practical purposes to find the average potential, since this value is only a few percent less than the potential calculated for the midpoint $x_o = L/2$. In other words, the effect of the fall of potential at the extremities is negligible. The average potential is given by the expression:-

$$V = 1/L \cdot \int_o^L V_o \, dx_o$$

Where V_o is as given in equation (2.4). This integral results in the following expression:-

$$V = q/2\pi\epsilon L \cdot [Ln(2L/r) - 1] \quad (L >> r) \qquad (2.5)$$

So in this case

$$C = 2\pi\epsilon L \, [Ln(2L/r) - 1]^{-1} \qquad (2.6)$$

In order to calculate the effect of the earth, the potential at the point P, Figure (2.0) must be reduced by a term derived from the image charge as illustrated in Figure 2.2.

6/...

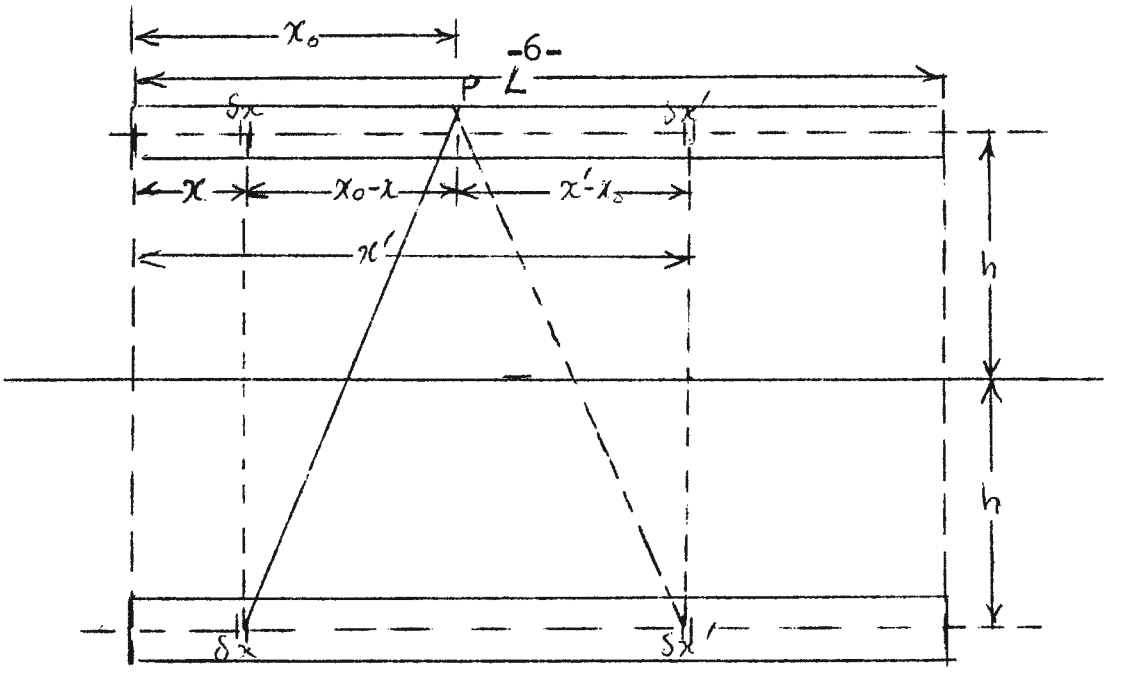

Figure (2.2) Potential at P due to the charge -q in the image.

For the case of $x<x_o$ the additional term is therefore

$$V_{11} = q/4\pi\epsilon L \cdot \int_o^{x_o} [(x_o-x)^2+(2h)^2]^{-\frac{1}{2}} \quad dx \qquad (2.7)$$

and when $x>x_o$

$$V_{12} = q/4\pi\epsilon L \cdot \int_{x_o}^{L} [(x'-x_o)+(2h)^2]^{-\frac{1}{2}} \quad dx \qquad (2.8)$$

The integrals are of course identical to the previous cases with "2h" replacing "r", and possibly 2h cannot be neglected when compared with L in the case of short aerials. Hence the complete expression for the average potential of of the conductor including the effect of earth is:-

$$V = q/2\pi\epsilon L \cdot [\sinh^{-1}(L/r) - \sinh^{-1}(L/2h) + [1+(2h/L)^2]^{\frac{1}{2}} - (1+2h/L)] \qquad (2.9)$$

Where $\sinh^{-1}(L/r) = \text{Ln}\ (2L/r)$ if $L>>r$.

Of special interest perhaps is the case when L is infinitely long or at least $L>>2h$ whence only the two $\sinh^{-1}$ terms remain in the bracket and the expression reduces to the well known form namely that:-

$$V = q/2\pi\epsilon L \cdot \text{Ln}\ (2h/r) \qquad (2.10)$$

7/...

Whence the capacitance per unit length is:-

$$C/L = 2\pi\epsilon \ [Ln(2h/r)]^{-1} \qquad (2.11)$$

When a horizontal conductor is placed at a height h in a uniform say negative electrostatic field of intensity E V/m such as produced by charges in the clouds, the potential due to this field at the height h is of course V = E.h. The conductor would initially have charges induced in it of ± q, the positive value of which being on the upper most side (as E is assumed to be negative) whilst the negative charge would lodge on the lower side.

If the negative charge is allowed to escape say by attaching a radio-active material to the conductor, the conductor will become charged to the value of the potential of the field at that height.

If on the other hand the conductor is earthed, for example by connecting it to an R C circuit for the measurement of field change, the potential of the conductor is reduced to zero and the negative charge escapes to earth leaving a positive charge only on the conductor. This apparent anomaly is explained by the fact that at any point on the surface of the conductor at height h above ground, the potential due to the electrostatic field is E.h which is negative for a negative field whilst the potential at that point due to the induced positive charge on the conductor is positive but the quantity of charge is such that the potential due to it is of equal magnitude to that of the potential of the inducing field, thereby making the potential at the point zero.

The charge on the conductor under these circumstances is given by

$$q = C^{\circ}V^{\circ} = C.h.E$$

8/...

If the field changes by a small increment δE, in a in a time δt, the change in δq will be $q = C.h.\delta E$.
In the limit $dq/dt = C.h.dE/dt$.

Whence the current flowing between the conductor and earth is given by:-

$i = C.h.\ dE/dt$.

The Capacitance of a conductor is not intrinsically dependant upon the value of dE/dt and its equivalent frequency spectra, but when it is measured using frequencies that have a corresponding wavelength which is comparable with the length of the conductor, corrections have to be applied to the measured value to compensate for the distributed nature of the capacitance and inductance.

3. The Capacitance of a vertical conductor

Obviously in the case of a horizontal conductor a vertical lead may be required to connect such conductor to other circuits; alternatively a vertical aerial itself may be employed. Hence it is necessary to calculate the capacitance of such a vertical conductor and to consider it in relation to a possible connection to a horizontal member.

The method of calculation for a vertical aerial is in general similar to that outlined for the horizontal conductor in that a charge distribution is assumed, whereupon the potential at a given point P on the surface of the conductor and distant x_o from the bottom end say is found; finally the average potential is derived and from this the capacitance is found.

By way of experimentation three different charge distributions are assumed, firstly uniform, secondly linear - that is a uniformly increasing charge per unit length from zero at the base to a maximum at the top, and finally a parabolic distribution also assuming zero charge at the base. The effect of earth is taken into account from the outset, since the base end

is assumed to be in contact with it either directly or through a measuring circuit. Figure 3.0 illus= trates the basic method of calculation.

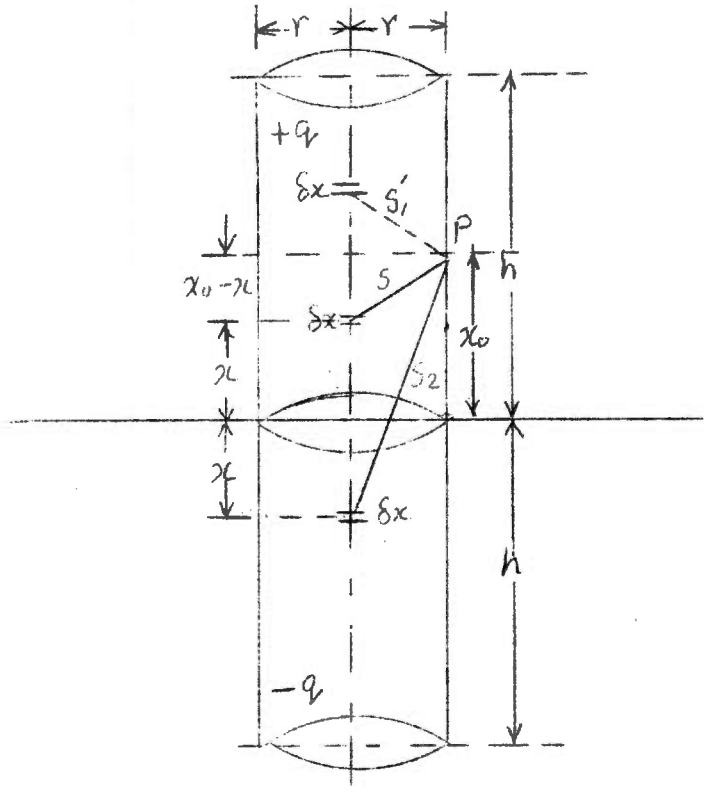

Figure 3.0 Diagram illustrating basic arrangement of a vertical conductor of height "h" and radius "r" in which a charge "q" is distributed along its length in any assumed manner.

Consider the potential at a point P on the surface of the conductor distant x_o from the base, and assume that the charge q is distributed along the centre line of the conductor in a prescribed manner. If the charge distribution is uniform the charge in a small element δx distant x from the base is $\delta q = q/h . \delta x$.

As before, the potential at P must be found for the charge situated below P i.e. when $x < x_o$, and above P when $x > x_o$; in addition the potential is re= duced by the charge in the mirror image. The potential

10/...

equation for this case is as follows:-

$$V_{oo} = q/4\pi\epsilon h \cdot \left[\int_o^{x_o} (S_1)^{-1}\, dx + \int_x^h (S_1')^{-1} dx - \int_o^h (S_2)^{-1} dx\right]$$

Where $S_1 = [(x_o - x)^2 + r^2]^{\frac{1}{2}}$

$S_1 = [(x - x_o)^2 + r^2]^{\frac{1}{2}}$

$S_2 = [(x + x_o)^2 + r^2]^{\frac{1}{2}}$

The integrals are all standard forms and the result is as follows for the case of a uniform distribution of charge:-

A. $$V_{oo} = q/4\pi\epsilon h \cdot \left\{2 \sinh^{-1}(x_o/r) + \sinh^{-1}[(h-x_o)/r] - \sinh^{-1}[(h+x_o)/r]\right\} \qquad (3.1)$$

For the case of a linear distribution of charge $\delta q = 2q/h^2 \cdot x\delta x$. Whence upon integration the potential is:-

B. V

B. $$V_{o1} = 2q/4\pi\epsilon h^2 \left\{x_o \sinh^{-1}[(h-x_o)/r] + x_o \sinh^{-1}[(h+x_o)/r] + [(h-x_o)^2+r^2]^{\frac{1}{2}} - [(h+x_o)^2+r^2]^{\frac{1}{2}}\right. \qquad (3.2)$$

For the parabolic distribution $\delta q = 3Q/h^3 \cdot x^2\delta x$ Whence after the necessary integration the potential equation is likewise:-

C. $$V_{o2} = 3q/4\pi\epsilon^3 \cdot \left\{2 (x_o^2 - r^2/2) \sinh^{-1}(x_o/r) + (x_o^2 + r^2/2)\sinh^{-1}[(h-x_o)/r] - (x_o^2 - r^2/2) \sinh^{-1}[(h+x_o)/r]\right.$$

$$+ 1/2(3x_o+h)[(h-x_o)^2+r^2]^{\frac{1}{2}} 1/2 (3x_o - h) [(h+x_o)^2+r^2]^{\frac{1}{2}}$$

$$\left. - 3x_o [x_o^2 + r^2]^{\frac{1}{2}}\right\} \qquad (3.3)$$

Putting $h = 2m$ and $h/r = 10^3$ the above functions are plotted as Curves A,B and C respectively on figure 3.0 (attached) in terms of the following general equation;

$$V_o = q/\pi\epsilon h \cdot F(h, x_o, r)$$

11/...

CONDUCTOR OF HEIGHT h , RADIUS r (ONE END TOUCHING EARTH) TOTAL CHARGE Q

POTENTIAL $V_{xo} = \frac{Q}{2\pi\epsilon_o h}\{F(h, r, x_o)\}$ VOLTS WHERE $\begin{matrix} h = 2m \\ r = 2mm \end{matrix}$

(A)

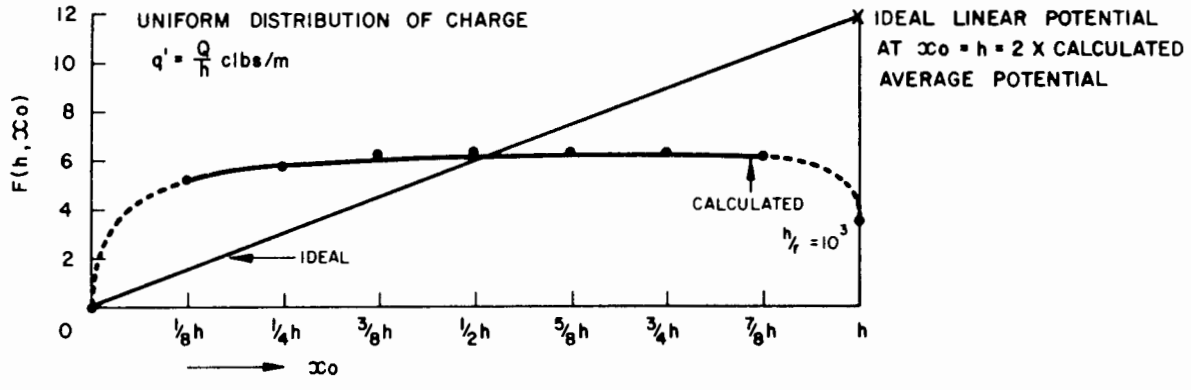

(B)

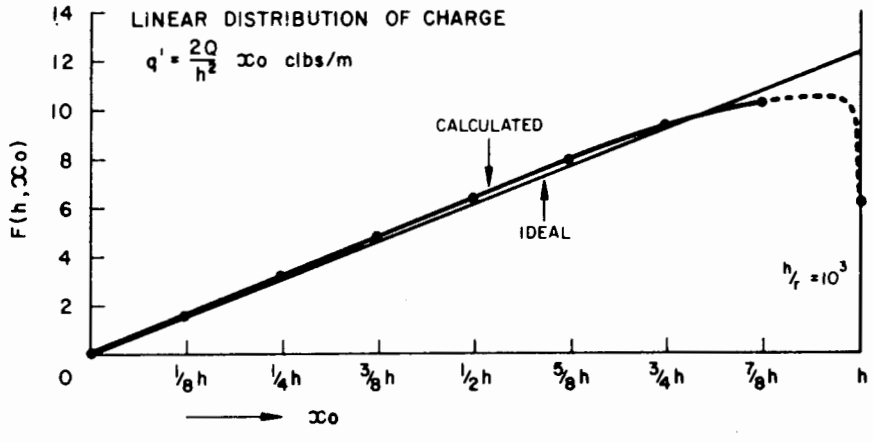

(C)

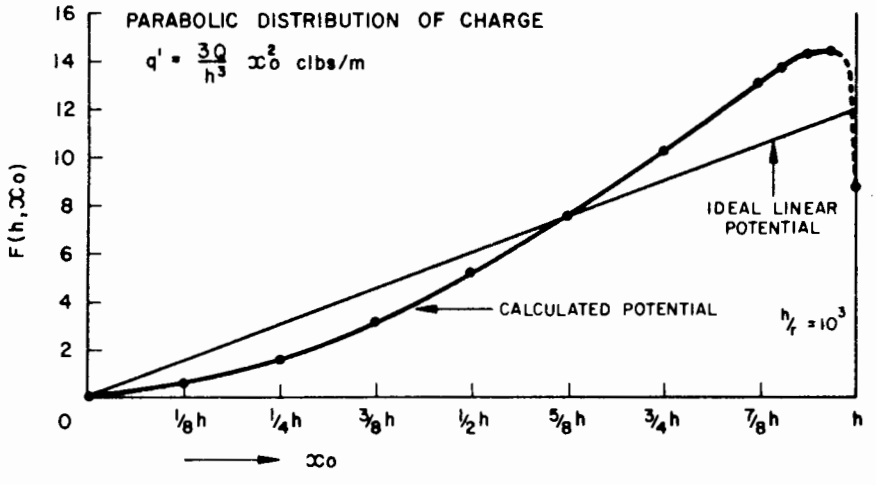

PART I APPENDIX I FIGURE 3.0

POTENTIAL OF VERTICAL CONDUCTOR IN A UNIFORM ELECTRIC FIELD

For the purpose of comparison, an ideal linear potential along the conductor equal to the potential in a uniform field is also plotted in each case such that the potential at $x_o=h$ is twice the calculated average potential of the conductor.

They show that if the charge distribution is assumed to be linear the potential along the vertical conductor closely conforms to the linear potential of the field. As in the case of the horizontal conductor, the potential at the extremity, in this instance the top end, falls away sharply, indicating that the charge distribution should actually be altered at the extremity. But as before, a sufficiently close estimate of the capacitance can be obtained by averaging the potential by integration with respect to x_o and dividing the result by h.

For each of the cases mentioned the resultant average potential is calculated to be as follows:-

(a) For a uniform charge distribution

$$V_o=q/2\pi\epsilon h\cdot [(Ln(h/r)-1)] \qquad (h>>r) \qquad (3.4)$$

(b) For a linear charge distribution

$$V_1=q/2\pi\epsilon h\cdot [(Ln(2h/r)-3/2] \qquad (h>>r) \qquad (3.5)$$

(c) For a parabolic charge distribution

$$V_2=q/2\pi\epsilon h\cdot [Ln(h/r)-5/6)] \qquad (h>>r) \qquad (3.6)$$

The above expressions are significantly close to each other provided Ln(h/r) is sensibly larger than unity, as it usually is. For $h/r=10^3$ for example the values for the capacitances per unit height are 9,402; 9,106; and 9,144 pF/m respectively. Hence insofar as the calculation of capacitance is concerned, any charge distribution would produce a result usually accurate enough for practical purposes; however the case of the linear charge distribution best fits the linear field gradient assumed, and is therefore adopted. The capacitance of a vertical conductor, when in a uniform electrostatic field, is therefore taken to be as follows:-

$$C = 2\pi\epsilon h\cdot [Ln(2h/r) - 3/2]^{-1} \qquad (3.7)$$

12/...

The requirement that when connected to earth, the potential at any point along the conductor surface must be zero is sufficiently satisfied if the calcu= lated average potential of the conductor due to its own charge is made equal in magnitude to the average potential of the inducing electrostatic field E over the height of the conductor. Here in this case

$$V = \tfrac{1}{2} E.h \qquad (3.8)$$

Compared with a horizontal conductor also at a height h above ground, the vertical conductor is seen therefore to have an effective height of h/2.

The capacitance of an aerial is however dependant upon the charge distribution and the conditions of operation. For example a useful method of measurement as described by Scuka[3], is to charge the aerial by means of a battery to a predetermined potential, and then to discharge it through a resistance at the same time measuring the voltage decay versus time on an oscilloscope. This can be done repeatedly by connec= ting and disconnecting the battery supply from the aerial. The capacitance is then calculated from the exponential decay time constant which can be easily determined by plotting the logarithm of the observed voltage against time. This results in a straight line from which the exponent 1/RC can be determined, and since the resistance R used in the circuit is known the value of the capacitance C can be calculated.

In the case of a vertical aerial, however, the charge distribution during such a test can be expected to be such that it is more concentrated at the end closest to earth, or in direct opposition to what is assumed to be the most likely condition when the aerial is under the influence of a uniform electro=

13/...

static field. If, for example, the charge distribu= tion is linear in the inverse sense for such a test condition, the potential equation involved is as follows, neglecting insignificant terms:-

$$V = q/2\Pi\epsilon h \cdot [3 \sinh^{-1}(h/r) - 2 \sinh^{-1}(2h/r) - 1/2] \quad (3.9)$$

The following table illustrates the calculated cppacitances per unit height for three values of h/r and compares the test condition of equation 3.9 with that of the capacitance in a uniform field: equation 3.7.

Parameters	$h/r=10^2$	$h/r=10^3$	$h/r=10^4$
Capacitance in a uni= form field	14,63 pF/m	9,11 pF/m	6,60 pF/m
Capacitance in the test condition	16,35 "	9,75 "	6,90 "
Calculated percen= tage increase	11,8%	7,1%	4,5%

Hence the tendency for charge to concentrate on the portion of the aerial closest to the earth can have a marked effect in the case of small values of the ratio h/r, and in general, the measured capacitance exceeds the capacitance in a uniform field.

By way of comparison with other results Goodlet[4] gave the following expression for the capacitance of a vertical conductor per metre of height:-

$$C/h = 111,0 \cdot \left\{ 2 [\mathrm{Ln}(2h/r) - 1] - 1,09 \right\}^{-1} \text{ pF/m} \quad (3.10)$$

He goes on to support his calculation by a number of measurements which all show very close agreement, but neither the charge distribution assumed, nor the method of measurement, was outlined.

14/...

However, for a value of h/r of 10^3 the capacitance per unit height would therefore be 9,16 pF/m which compares favourably with the value of 9,11 pF/m given in the table above for the capacitance in a uniform field.

Also Anderson and Jenner[5] gave a similar expression for the capacitance of a vertical conductor of height h, and radius r, with its base H above ground (converted to metric units)

$$C/h = 111{,}0 \left\{ 2[\mathrm{Ln}(2h/r)-1]-\mathrm{Ln}(3/2h+H) + \mathrm{Ln}(1/2h+H) \right\} \quad \text{pF/m} \qquad (3.11)$$

When H=0 the two logarithmic terms containing H reduce to Ln 3= 1,0986, in which case the expression is almost identical to that obtained by Goodlet.

The expression derived by the writer differs slightly only in the value of the numerical constant and this value depends upon the form of charge distribution assumed. It is contended, however, that since the linear charge distribution assumed gives rise to a potential along the conductor which closely matches that of the inducing uniform field, the resulting capacitance is the best approximation under the particular conditions of operation.

4. The capacitance of the experimental standard vertical aerial

This aerial consisted of a tapered aluminium rod 2,30 m in length supported on a steel pole of 2,54 cms (1inch) in diameter and 2,11 m high as illustrated in figure 4.0 below.

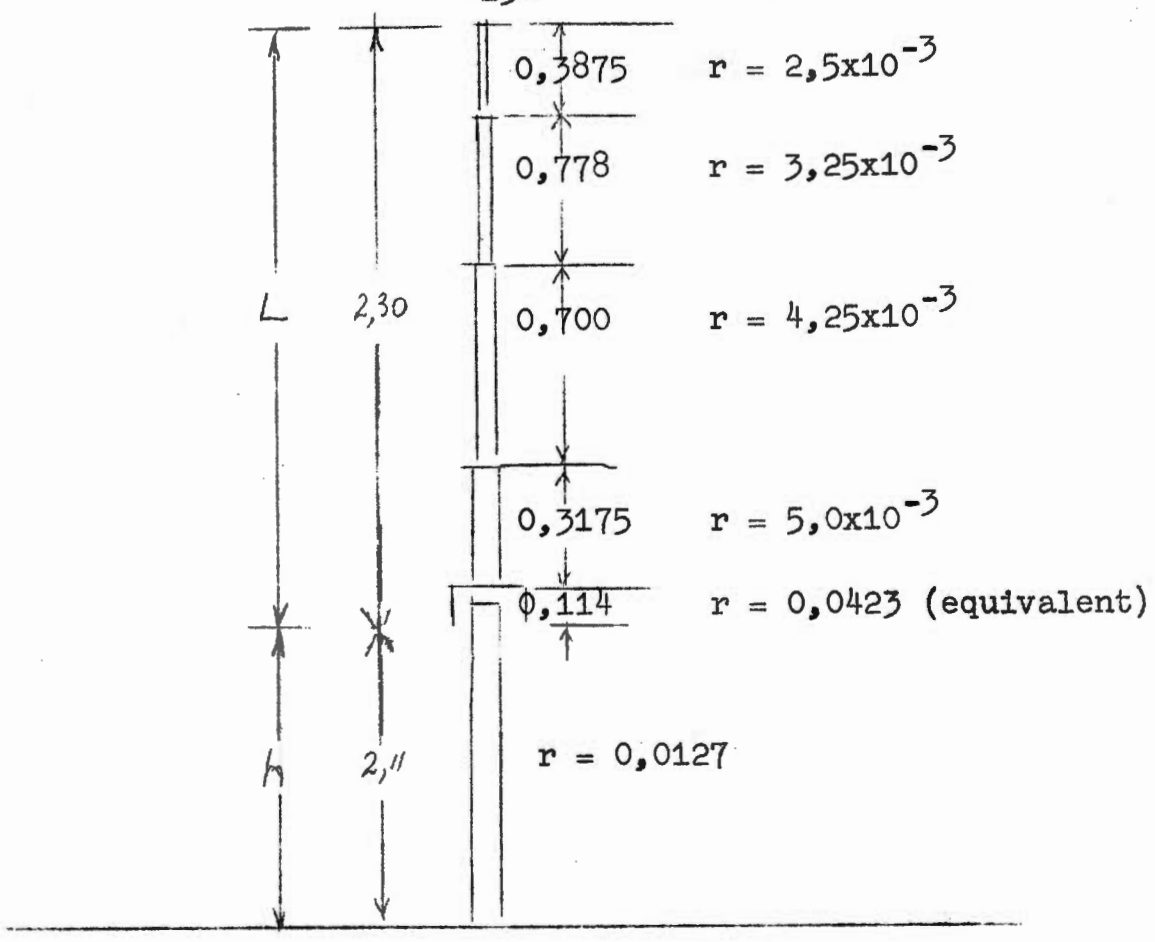

Figure 4.0 Dimensions of standard vertical aerial in metres. (Not to scale)

First considering that the radius of the conductor will enter into the calculation of capacitance within a logarithmic term it is reasonable to assume that a weighted mean radius will result in a sufficiently accurate value of capacitance. The connection box at the base of the aerial was actually a square section, and the equivalent radius was assumed to be that of a circle having the same area. The weighted mean radius for the whole aerial was then obtained by multiplying the length of each section by its radius, adding together the five results and then dividing by the total length. The result obtained was 5,6 mm, and since this value was larger than the radius of any of the sections above the connection box, the weighted mean for these sections alone namely 3,7 mm was also used in calculations to provide an lower limit of capacitance.

16/...

Whilst the manner of the charge distribution to be assumed has been shown to be relatively immaterial, a linear form was used for the aerial including its support as illustrated in figure 4.1

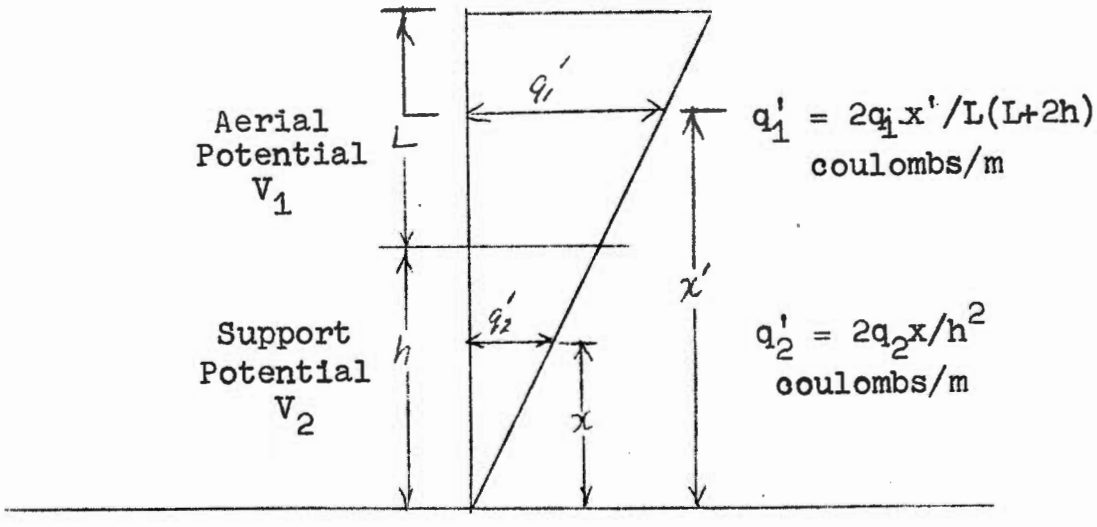

Figure 4.1 Form of charge distribution assumed for vertical aerial and support.

The process to be carried out has been illustrated in the previous case and will not be repeated here in detail except to outline the steps to be taken as follows:

(i) Find the average potential V_{11} of the aerial of length L due to its own charge q_1 distri= buted as q_1' in the prescribed manner in the aerial itself and also in its image.

(ii) Find the average potential V_{12} of the aerial due to the charge q_2 in the support distribu= ted as q_2' in the manner prescribed in the support and also in the image of the support.

(iii) Find the average potential V_{21} of the support due to the charge q_1 in the aerial including the image.

(iv) Find the average potential V_{22} of the support due to its own charge q_2 and that of its image.

Since potential is a scalar quantity and may be added directly then:-

17/...

The average potential of the aerial $V_1 = v_{11} + V_{12}$ (4.3)
and the average potential of the support $V_2 = V_{21} + V_{22}$ (4.4)

These potentials are stated in terms of q_1 and q_2 and the relative value of which may be found by equating these potentials to the average potential in an assumed uniform Field E over the length or height of the respective sections, in order that the resultant potential shall be zero.

The potential of the electric field at the top of the aerial is $E.(L+h)$ and at the base it is $E.h$; hence the mean value is $\frac{1}{2}[E(L+h)+Eh] = \frac{1}{2} E(L+2h)$
The mean potential over the height of the support is simply $\frac{1}{2}E.h$ Hence

$$V_1 = \tfrac{1}{2}E\ (L+2h) \qquad (4.5)$$
$$V_2 = \tfrac{1}{2}\ E.h \qquad (4.6)$$

The potentials V_1 and V_2 calculated from the integration as previously described have the following form of expression:-

$$V_1 = 1/2\pi\epsilon \cdot [Aq_1+Bq_2] = \tfrac{1}{2}\ E\ (L+2h) \qquad (4.7)$$
and $$V_2 = 1/2\pi\epsilon\ [Cq_1+Dq_2] = \tfrac{1}{2}\ E.h \qquad (4.8)$$
Dividing (4.7) by (L+2h) and (4.8) by h and equating the two left hand sides:-

$$[Aq_1+Bq_2](L+2h)^{-1} = [Cq_1+Dq_2]\ h^{-1}$$

Whence $q_1/q_2 = M = [D/h - B/(L+2h)][A/(L+2h) - C/h]^{-1}$

$$M = (D'-B')\ (A'-C')^{-1} \qquad (4.10)$$

Substituting for $q_1 = Mq_2$ or $q_2 = q_1/M$, as the case may be, in equations (4.7) and (4.8) to obtain the average potential of the aerial or the support in terms of the charge on that earial or the support then:-

18/...

Average potential of the aerial $V_1 = q_1/2\Pi\epsilon \cdot [A+B/M]$ (4.11)
and average potential of the support

$$V_2 = q_2/2\pi\epsilon \cdot [CM+D] \quad (4.12)$$

Whence the capacitance of the aerial and the support can be obtained as

$$C_1 = q_1/V_1 = 2\pi\epsilon(A+B/M)^{-1} \quad (4.13)$$

and $$C_2 = q_2/V_2 = 2\pi\epsilon(CM+D)^{-1} \quad (4.14)$$

The expressions for A, B, C and D contain up to eleven terms each, but some are negligible when L or h is large compared with "r" and these terms are neglected in the expressions given below:-

$$V_{11} = q_1 A/2\pi\epsilon$$

Where $A = 1/L(L+2h) \cdot \left\{(L+2h)\ \sinh^{-1}(L/r_1) \cdot \right.$

$\left. - h^2/L - (L+h)^2/L - (L+2h)\right\}$

$$V_{12} = q_2 B/2\pi\epsilon$$

Where $B = 1/h^2 \cdot \left\{1/2(L+2h)\sinh^{-1}[(L+2h)/r_1]\right.$

$- 1/2\ (L+2h)\ \sinh^{-1}(L/r_1) + L(3/4+h/L)$

$\left. + (L+2h)\ (h/2L - 1/4) + h^2/L\right\}$

$$V_{21} = q_1 C/2\pi\epsilon \cdot$$

Where $C = 1/L(L+2h) \cdot \left\{(L+h)^2/h)\sinh^{-1}\ [(L+h)/r_2]\right.$

$-L(L+2h)/2h \cdot \sinh^{-1}(L/r_2) - h\ \sinh^{-1}(h/r_2)$

$-L(L+2h)/2h \cdot \sinh^{-1}[(L+2h)/r_2] + L(1+L/4h)$

$\left. - 1/2\ (L+h)^2/h + h/2 + (L+2h)\ (L/4h - 1/2) + h\right\}$

19/...

$$V_{22} = q_2 D/2\pi\epsilon$$

Where $D = 1/h^2 \; [h \sinh^{-1}(h/r_2) - 3/2h]$

For the standard vertical aerial L = 2,30 m h = 2,11 m $r_1 = 5{,}6 \times 10^{-3}$m or $3{,}7 \times 10^{-3}$m $r_2 = 12{,}7 \times 10^{-3}$m and the numerical values of the above expressions are given in the following Table I:-

	$r_1 = 5{,}6 \times 10^{-3}$m	$r_1 = 3{,}7 \times 10^{-3}$m
Constant A	1,2256	1,4058
Constant B	2,3647	2,0478
Constant C	0,1653	0,1653
Constant D	2,0408	2,0408
" A'	0,1880	0,2156
" B'	0,3627	0,3141
" C'	0,0784	0,0784
" D'	0,9704	0,9704
Radio $q_1/q_2 = M$	5,5431	4,7822
Aerial Capacitance C_1	33,6 pF	30,3 pF
Support Capacitance C_2	18,8 pF	19,6 pF
Aerial Potential V_1	$q_1/2\Pi\epsilon \cdot [1{,}6522]$	-
Support Potential V_2	$q_1/2\Pi\epsilon \cdot [0{,}5335]$	-
Ratio V_1/V_2	3,097	-
Aerial Effective Height for V_1	3,26 m	-
Support Effective Height	1,055m	-
Ratio Effective Heights	3,090	-

Table I Numerical Evaluation of constants for the Standard Vertical Aerial

It is clear from the above, first of all, that the effect of the radius of the aerial on its capaci=

20/...

tance, is small, whereupon the value of 33,6pF is the more acceptable because it applies to the weighted radius of the complete aerial. The measured value was 44 pF but this was found to include 14 pF internal capa= citance measured between the connecting box and the steel support with the aerial portion removed, whence the resultant measured value was therefore 30 pF. Accordingly a value of 32pF was adopted as the capaci= tance for the aerial as being an approximate mean between calculated and measured values.

For field change measurements, the standard ver= tical aerial was connected to the oscilloscope by means of co-axial cable connected to the base of the aerial with its screen connected to the top of the support within the connection box shown on figure 4.0. The base of the support was connected to an earth mat burried beneath it.

The question then arose as to whether the poten= tial applied to the measuring circuit was in fact the difference between that of the aerial and its support, or whether it was the potential of the aerial alone. Firstly in so far as the effect of the electric field is concerned, and in the absence of the measuring circuit, the actual potential of the two parts is zero and no potential difference arises between the two even if the field intensity changes. However the amount of charge on both the aerial and its support changes with any change in the field intensity, but in this case only the current flowing from the vertical aerial flows through the measuring circuit; the current de= livered by the support on the other hand flows directly to earth.

When the aerial is connected to an RC circuit for field change measurement therefore the aerial potential will vary with respect to the support, and its magnitude

21/...

will depend entirely upon the values of the resistence and capacitance of the measuring circuit as if the aerial was on its own.

Secondly when comparing the response of the vertical aerial with that of others, the theoretical ratios of the oscillographic deflections due to the response from this aerial compared with that of the others was quite outside the range of actual ratios measured if the input potentials were based upon the difference in effective heights of the aerial and its support. When on the other hand the vertical aerial response was based upon its own effective height alone, the theoretical and actual ratios then coincided.

5. The capacitance of an inverted L- or T-shaped aerial

In this case there is a direct connection between a horizontal section and a vertical section as shown in figure 5.0.

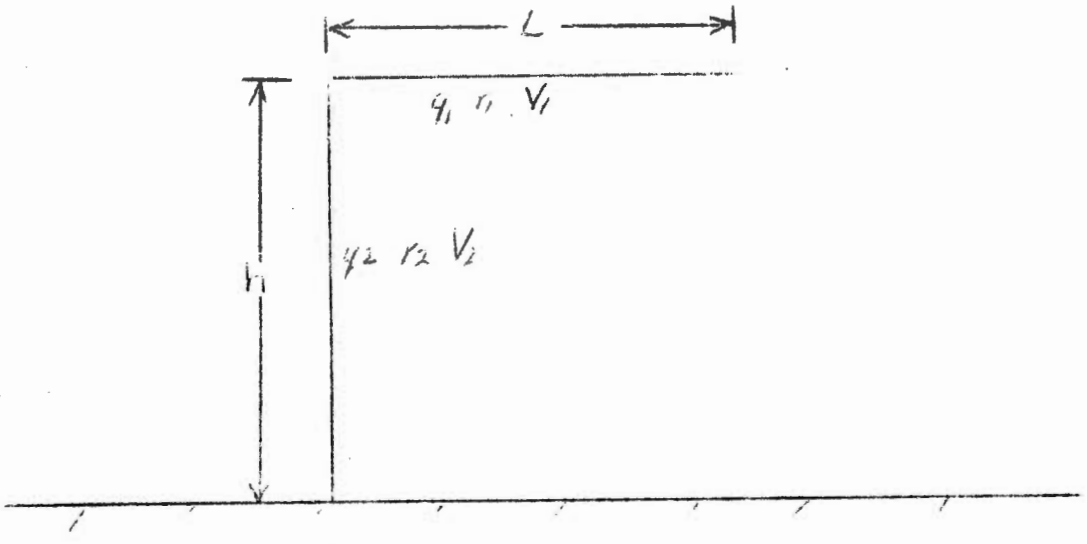

Figure 5.0 Diagram showing an inverted L-shaped aerial.

The average potential of the horizontal part of the aerial has the general form:-

$$V_1 = 1/2\Pi\epsilon \cdot [Aq_1+Bq_2] \qquad (5.1)$$

22/...

Where Aq_1 results from the calculation of the average potential of this port of the aerial due to its own charge q_1, and is given in equation (2.9).

The term Bq_2 however is the average potential of the horizontal portion due to the charge q_2 in the vertical section. This is calculated by the same method already outlined, the charge q_2 being assumed to be distributed in a linear manner as before.

Then also the average potential of the vertical section has the form:-

$$V_2 = 1/2\Pi\epsilon \cdot [Cq_1+Dq_2] \qquad (5.2)$$

In this case the term Cq_1 refers to the average potential of the vertical section due to the charge q_1 in the horizontal section and Dq_2 refers to the average potential due to the charge q_2.

It remains therefore to combine these results on the basis that

$$V_1 = E.h \text{ and } V_2 = 1/2\ E.h. \qquad (5.3)$$

This means, as previously, that in order to make the potential along the surface of either portions of the aerial zero, the average potentials may be equated to the average potential existing in the inducing field over the dimensions of the respective parts.

Hence from (5.3) $V_1 = 2\ V_2$ substituting this in (5.1) and (5.2)

$$Aq_1 + Bq_2 = 2\ Cq_1 + 2\ Dq_2 \qquad (5.4$$

$$\text{Whence } q_1/q_2 = M = (2D-B)(A-2C)^{-1} \qquad (5.5)$$

$$\text{So } q_1 = Mq_2 \text{ or } q_2 = q_1/M \qquad (5.6)$$

And substituting the respective values in (5.1) and (5.2)

23/...

$$V_1 = q_1/2\Pi\epsilon\cdot(A+B/M) \text{ and } V_2 = q_2/2\Pi\epsilon\cdot(CM+D) \qquad (5.7)$$

If C_1 is the capacitance of the horizontal section on its own and C_2 is likewise the capacitance of the vertical section then

$$C_1 = q_1/v_1 = 2\Pi\epsilon(A+B/M)^{-1} \text{ and } C_2 = q_2/V_2 = 2\Pi\epsilon(CM/D)^{-1} \qquad (5.8)$$

Hence if q is the total charge on the complete aerial system

$$q = q_1 + q_2 = C_1V_1+C_2V_2 \qquad (5.10)$$

If now it is assumed that the capacitance Ca of the complete system is to be referred to the effective height of the horizontal portion, that is to the potential V_1, substitute $V_2 = 1/2\ V_1$ in equation (5.10) whence

$$q = V_1\ (C_1 + 1/2\ C_2) = V_1Ca \qquad (5.11)$$

$$\text{Hence } Ca = C_1 + 1/2\ C_2 \qquad (5.12)$$

Where Ca is the capacitance of the complete aerial referred to the effective height of the horizontal member.

Re-substituting for the values of C_1 and C_2 taken from (5.8).

$$Ca = 2\pi\epsilon[(A+B/M)^{-1} + 1/2\ (CM+D)^{-1}] \qquad (5.13)$$

Where $M = (2D-B)(A-2C)^{-1}$ from (5.5)

The values of the constants A, B, C and D are obtained from the integrations to obtain average potentials and the results of a numerical calculation assuming L = 10 m h = 5 m, $r_1 = r_2 = 2 \times 10^{-3}$m. are given in the following Table.

24/...

Description of Parameter	Numerical Result
A. $1/L \left[\sinh^{-1}(L/r_1)-\sinh(L/2h)+[1+(2h/L)^2]^{\frac{1}{2}} -(1+2h/L\right]$	0,7744
B. $1/h \left[\sinh^{-1}(2h/L)- [1+(L/2h)^2]^{\frac{1}{2}}+L/2h\right]$	0,0935
C. $1/L \left[\sinh^{-1}(L/h)+L/h \sinh^{-1}(h/L)- - \sinh^{-1}(L/2h)-L/2h \sinh^{-1} (2h/L)\right]$	0,0643
D. $1/h \left[\sinh^{-1}(h/r_2) - 3/2 \right]$	1,4038
M. $(2D-B)\ (A-2C)^{-1} = q_1/q_2$ = Ratio of charges	4,2046
A + B/M	0,7966
CM + D	1,6738
C_1 = Capacitance of horizontal portion (including effect of vertical portion)	69,76 pF
C_2 = Capacitance of vertical portion (including effect of horizontal portion)	33,19 pF
$Ca = C_1 + 1/2\ C_2$ = Capacitance of L-shaped aerial	86,35 pF

In the case of the T-shaped aerial, the general equations connecting the potential of the two portions with the effective heights are identical to those of the L-shaped aerial. The only difference lies in the constants relating the mutual effect of the charge on one portion to that of the other. Hence the constants A and D are identical whilst B and C differ because of the relative position of the vertical portion, and are given below together with the results of a numerical calculation as before assuming $L = 10m$, $h = 5m$, $r_1 = r_2 = 2 \times 10^{-3}m$.

25/...

Description of Parameter of T-shaped Aerial	Numerical Result
A. As for L-shaped Aerial	0,7744
B. $1/h\ [8h/L\ \sinh^{-1}(L/4h) - 1/hL\ [\ 1+(4h/L)^2\ ]^{\frac{1}{2}}]$	0,3760
C. $1/L[2\ \sinh^{-1}(L/2h) + L/h\ \sinh^{-1}\ (2h/L)$ $-2\ \sinh^{-1}(L/4h) - L/2h\ \sinh^{-1}(4h/L)]$	0,1119
D. As for L-shaped Aerial	1,4038
M. As for L-shaped Aerial	4,416
C_1 = Capacitance of horizontal portion (including effect of vertical section)	64,65 pF
C_2 = Capacitance of vertical section (including effect of horizontal portion)	29,28 pF
$C_a = C_1 + 1/2C_2$	79,29 pF

Hence the capacitance of this T-shaped aerial is approximately 8% less than that of an otherwise identical L-shaped aerial. This percentage would not be the same, however, for another choice of dimensions.

6. The effect of a conducting support

This has been partly dealt with in section 4 which describes the case of a vertical aerial mounted on top of a conducting support. Perhaps a more common occurence, however, is the case of an insulated vertical downlead of an aerial which is stapled to or is close to a vertical support which may be conducting - either because it is metalic or because it is of wood, say, and is saturated with water. Figure 6.0 illustrates the case, diagramatically.

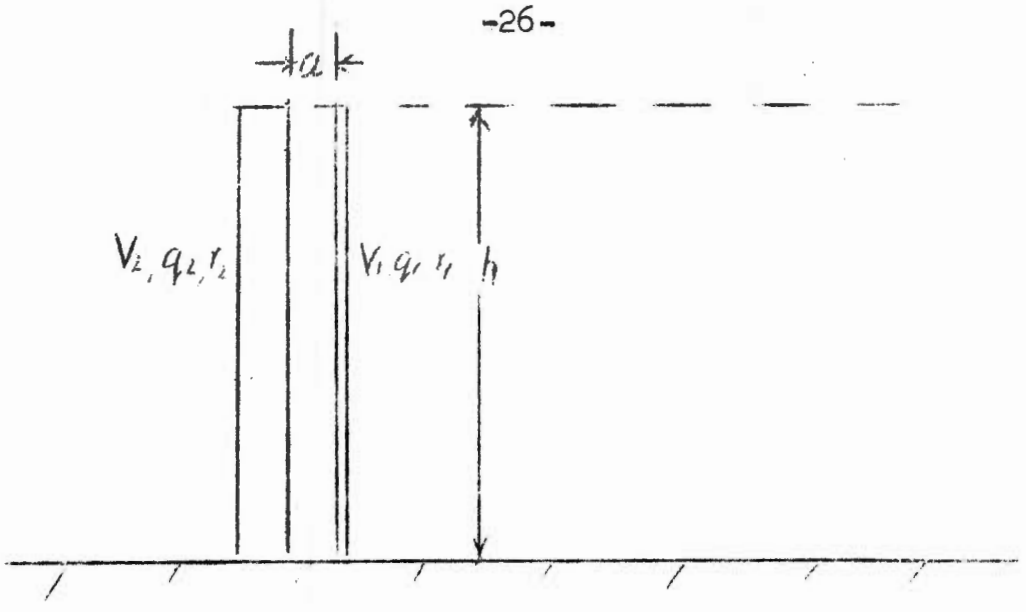

Figure 6.0 Arrangement of vertical donductor and conducting support

As previously, the average potential V_1 of the con= ductor is made up of two terms namely the potential due to its own charge q_1 and that due to the charge in the support and can be stated as follows:-

$$V_1 = 1/2\Pi\epsilon \cdot [Aq_1 + Bq_2] \qquad (6.1)$$

Where $A = 1/h\ [\sinh^{-1}(h/r_1) - 3/2]$ (6.2)

The calculation of B is undertaken in a similar manner as set out in previous examples and results in the following expression:-

$$B = 1/h\Big\{[1+1/2\cdot(d/h)^2]\ \sinh^{-1}(h/d) - 1/4\cdot(d/h)^2\sinh^{-1}(2h/d) - [1+(d/2h)^2]^{\frac{1}{2}} - 1/2\,'[1+(d/h^2]^{\frac{1}{2}}+d/h\Big\} \qquad (6.3)$$

Where $d = a + r_2$

Similarly the potential of the support is due to its own charge q_2 and that of the charge q_1 in the conductor and in this instance the constants are simi= lar. Hence:-

$$V_2 = 1/2\Pi\epsilon \cdot (Cq_1 + Dq_2) \qquad (6.4)$$

27/...

Where C is as B except that $d = a+r_1$, i.e. r_2 is replaced by r_1, and D is as A except r_1 is replaced by r_2.

Under the influence of a field E, $V_1 = V_2$ hence:-

$$Aq_1 + Bq_2 = Cq_1 + Dq_2 \text{ and } q_1/q_2 = M = (D-B)(A-C)^{-1} \qquad (6.5)$$

So that $q_1 = Mq_2$ and $q_2 = q_1/M$
Re-sbustituting the above in (6.1)

$$V_1 = q_1/2\pi\epsilon.(A+B/M) \qquad (6.6)$$

The capacitance of the vertical conductor, including the effect of the support is therefore:-

$$C_1 = 2\pi\epsilon(A+B/M)^{-1} \qquad (6.7)$$

The capacitance of the support (out of interest) is

$$C_2 = 2\pi\epsilon.(CM+D)^{-1} \qquad (6.8)$$

By way of an example, it is assumed that h = 5m $r_1 = 2 \times 10^{-3}$m and $r_2 = 2{,}5 \times 10^{-2}$m. that is a 4 mm thick wire, say, and a 5 cm thick supporting pole. Then it is assumed that the wire is spaced 5 cms from the pole i.e. $a = 5 \times 10^{-2}$m.

The following table then gives the results of the calculations.

28/...

Parameters	Numerical Result
A	1,500
B	0,682
C	0,754
D	0,898
M	0,290
Capacitance of vertical wire alone	37,05 pF
C_1 = Capacitance of vertical wire including effect of support	14,45 pF
Capacitance of support alone	61,80 pF
C_2 = Capacitance of support including effect of vertical wire	50,20 pF

Thus it is clear that the conducting support reduces the capacitance of the wire in this case considerably - by a factor of 2,55 infact - but the effect of course depends upon the distance maintained between the two. A similar effect occurs with vertical supports for a hori= zontal aerial, but the distances are in this case usually quite large so that the capacitance reduction is small.

7. The Capacitance of the ERA Aerial

This aerial consisted of six parallel horizontal wires of length L and radius r spaced d apart and erected between two wooden poles at a height h above ground, together with a down lead of radius r_2. The effect of the possible con= ductivity of the wooden supporting poles when wet has been neglected.

The rigorous calculation of the capacitance of this type of aerial has been undertaken and since it is a very long and tedious process it will not be repeated in detail. The principles of calculation however are exactly as pre= viously enumerated, particularly for the L-shaped aerial of Section 5. The main addition is the calculation of

29/...

the potential of any individual wire due to the charge on the other wires and here it is necessary to assume that the total charge q_1 on the wires is distributed evenly among the six wires. Although this may not in fact be true, experience has shown that reasonable differences in this type of assumption does not affect the final outcome by more than a few percent.

The notation to be used below is exactly as that previously used and the following general statements can be made - where A, B, C and D are the constants of the aerials obtained from the respective integrations to obtain average potentials.

1. Potential of Horizontal portion of Aerial alone = $q_1/2\pi\epsilon \cdot A$
2. Potential of Horizontal portion of Aerial with downlead = $q_1/2\pi\epsilon \cdot (A+BM)$
3. Potential of vertical lead on its own = $q_2/2\pi\epsilon \cdot C$
4. Potential of vertical lead with effect of horizontal portion $q_2/2\pi\epsilon \cdot (C+D/M)$
5. Ratio of charge q_1 in vertical lead to that of horizontal portion = $q_2/q_1 = M = (A-2D)(2C-B)^{-1}$
6. C_1 = Capacitance of Horizontal portion with effect of downlead = $2\pi\epsilon \cdot (A+BM)^{-1}$
7. C_2 = Capacitance of Vertical downlead with effect of horizontal portion = $2\pi\epsilon (C+D/M)^{-1}$
8. Ca = Capacitance of Combined horizontal aerial with down lead = $C_1 + 1/2C_2$

Where $A = 1/L \left\{ \sinh^{-1}(L/d) + 1/6 \sinh^{-1}(d/2r_1) - \sinh^{-1}(L/2h) + [1+(2h/L)^2]^{\frac{1}{2}} - 2h/L - 1{,}561 \right\}$ (7.1)

$B = 1/L \left[\sinh^{-1}(2h/L) - [1+(L/2h)^2]^{\frac{1}{2}} + L/2h \right]$ (7.2)

30/...

$$C = 1/h \left[\sinh^{-1}(h/r_2) - 3/2\right] \qquad (7.3)$$

$$D = i/h\left[\sinh^{-1}(L/h) + L/h \sinh^{-1}(h/L) - \sinh^{-1}(L/2h) - L/2h \sinh^{-1}(2h/L)\right] \qquad (7.4)$$

For the experimental ERA aerial used L = 13,28 m, h = 4,85 m and d = 0,1525 m. The wire used was rectangular in section being 2,147 x 1,416 mm or 3,038 sq. mm. The equivalent radius was taken to be approximately that of a circle of the same cross-sectional area namely 0,9834 mm, so that, 1,0 mm was assumed.

The values of the various constants calculated were as follows:-

$A = 0,288 \quad B = 0,0266 \quad C = 1,585 \quad D = 0,1363$

$M = q_1/q_2 + 0,0608 \quad (A + BM) = 0,287 \quad (C + D/M) = 2,40$

The resultant capacitances are therefore:-

C_h = Capacitance of horizontal portion on its own = 193,2 pF

C_v = Capacitance of vertical downlead on its own = 35,1 pF

Hence C_1 = Capacitance of horizontal portion with effect of downlead = 190,1 pF

And C_2 = Capacitance of vertical downlead with effect of horizontal portion = 23,2 pF

So C_a = Capacitance of complete aerial = $C_1 + 1/2\ C_2$ = 201,7 pF

A single capacitance measurement on the above referred to ERA aerial used in the experimental work, gave a value of approximately 260 pF using a 1 kHz Wayne Kerr bridge and making due allowance for the capacitance of test leads.

Later, at the CSIR Pretoria, measurements were made on a number of these aerials using the discharge technique recommended by Scuka[3], and although the aerials were erected identically, the values varied between 238 and

31/...

288 pF with a mean value of 256 pF.

Yet another set of measurements was undertaken in Pretoria, this time using a 1 kHz capacitor bridge. The capacitances of four aerials were 259, 266, 256 and 261 including their down leads and making due allowance for a 19 pF capacitance of the test leads. On the other hand when the vertical down leads were removed from the supporting pole and connected direct to the bridge termi= nals at ground level, the capacitances of the first three of the four aerials mentioned above were 252, 250 and 246 pF respectively. The above values were all on the high side compared with calculated values, and accordingly further calculations were carried out as described below.

Firstly the capacitance of the horizontal section alone could be calculated from published formulae[5]. This was as follows for a horizontal aerial of length L m, and height h consisting of "n" parallel wires of radius r and spaced "d" apart.

$$C = 111{,}2\ L \cdot \{1/n\left[P11 + (n-1)\ P12\right] - k\}^{-1}\ pF \quad (7.5)$$

Where for $1/4h<1$ and using logarithms to the base 10:-

$$P11 = 4{,}605\left[\log(L/r) - K_2\right]$$

$$P12 = 4{,}605\left[\log(L/d) - K_2\right]$$

$$K_2 = \log\{L/4h + 1 + \left[1 + (L/4h)^2\right]^{\frac{1}{2}}\}$$

and $k = 1{,}18$ for $n = 6$ as obtained from a table given in the reference.

Substituting the values of L, d, r and H given above, the calculated capacitance was 183 pF which is to be compared with 193 pF calculated for the horizontal section on its own by the previous mehtod. The agreement within five percent can be regarded as good, whence the discrepancy between these figures and measured values is still not explained.

A second rigorous calculation of the capacitances of the experimental ERA aerial was carried out this time assuming that the charge in the six wires of the horizontal

32/...

portion was not distributed uniformly between the wires but could be calculated on the basis that the average potential of each of the wires must be equal.

The charge was then found to be distributed such that the two outer wires carried 0,2040q (where q was the total charge) the adjacent index wires 0,1555 q, whereas the innermost wires carried 0,1406 q. The capacitance of the horizontal portion including the effect of a vertical down lead was then C_1 = 191,21 pF, and that of the down lead including the effect of the horizontal portion was C_2 = 22,94 pF, whereas the combined capacitance in a uniform electric field would be $C_a = C_1 + \frac{1}{2}C_2$ = 202,68 pF - that is to say not very much in excess of the previous calculation.

Since it was clear that the charge distribution under test conditions would differ substantially from that in a uniform electric field, calculations were then made assuming that the charge in the vertical downlead would be distributed in an inverse linear manner - namely a uniformly increasing charge density from zero at the top to a maximum at the bottom. Furthermore these calculations were made on both the experimental ERA aerial in which L = 13,28 m H = 4,85 m and r = 1 mm, and the standard CIGRE aerials used in Pretoria in which L = 14 m H = 5 m and r = 1,5 mm. The comparative results were as follows:-

	ERA Aerial	CIGRE
C_1 Capacitance of Horizontal Portion including effect of downlead	191,17	203,17
C_2 Capacitance of downlead	30,55	30,53
$C_a = C_1 + C_2$ = Overall aerial capacitance, under test	221,72	233,69

Whilst the above figures showed improvement towards the test values, they still appeared to be on the low side and hence it was suspected that the wooden pole suports, regarded so far as being good insulators might on the other hand be conducting if moisture was to be present in the wood.

33/...

In order to calculate the effect of conducting supports, it was assumed that they would carry a negative charge (as opposed to a positive charge imposed on the aerial conductors under test conditions). The potential of the supports due to their own charge would be negative but the charge would be of such a value that this potential exactly balanced that induced by the positive charge on the conductors in order to make the potential of the supports zero. As in previous aerial calculations it is assumed that the calculation of average potentials of the conductors and supports would give sufficiently accurate results.

If q_1 = charge on the horizontal portion of the aerial
q_2 = charge on the vertical downlead at one end
q_3 = charge on the support nearest to the downlead
and q_4 = charge on the support farthest from the downlead

Then assuming that the support poles had a radius of 0,075 m and that the downlead was spaced 0,5 m away, the ratio of charges and the resulting capacitances calculated were as follows:

	ERA Aerial	CIGRE Aerial
Ratio q_1/q_2 Assuming no supports	6,26	6,66
Ratio q_1/q_2 Assuming conducting supports	5,52	5,35
Ratio q_3/q_2 Assuming conducting supports	-0,88	-0,85
Ratio q_4/q_2 Assuming conducting supports	-0,45	-0,42
C_1 = Capacitance of Horizontal Section	195,24 pF	207,16 pF
C_2 = Capacitance of Vertical lead	35,39 pF	38,70 pF
$C_a=C_1 + C_2$ = Capacitance under test condition	230,63 pF	245,86 pF

It is now evident that calculated values of capacitance, especially of the standard CIGRE aerial approach to within 20 to 30 pF of the measured values and this margin of error can be regarded as satisfactory in view

34/...

of other practical factors not taken into account - for example sag in the wires of the horizontal portion could influence the effective value of H. Also the downlead was not vertical but at an angle to the support pole and was also insulated whereby the capacitance could be larger than calculated.

Better accuracy was also not necessary on account of the fact that these aerials were connected to circuits having a capacitance C_c of 100 pF of less, and under condition of steep fronted field wave form, the input voltage to the circuit would be Ca/(Ca + Cc). The effect of a variation of aerial capacitance from 230 to 260 pF for example produces a variation of the above ratio from 0,6975 to 0,7225 which is an increase of 3,5%.

However the results of the above calculation show that the wood poles should properly be regarded as being conducting if there is any possibility of moisture in= gression.

8. References

(1) Jordan E.C. Electromagnetic waves and radiating systems Constable Company Ltd., 1953 Page 56 Example 9.

(2) P.G. Stewart. A computer method to determine the charge distribution along a horizontal conductor to secure a uniform potential distribution. Internal CSIR report.

(3) V. Scuka. Measurements of electric fields of thunder= storms; Inst. of High Tension Research Uppsala 1965 Publ. Almquist and Wiksell Manuscript.

(4) Goodlet B.L. "Lightning" Jour. Inst. n. Elect. Eng. Vol. 81 (1937) App. II P. 24.

(5) Anderson R.B. and Jenner R.D. "A summary of eight years of lightning investigation in Southern Rhodesia" Trans. S.A. Inst. Elect. Eng. July 1954, App. I. p. 239.

(6) Handbook of Chemistry and Physics 25th Edition p. 2334.

Part I Appendix II

A recording of a 25 component multiple flash of Lightning

1. Introduction

High speed tape recordings of the input wave forms resulting from lightning flashes were undertaken in Pretoria as part of a research project which included apparatus for direction finding of lightning-flashes. It was important to know the wave forms at the input to a circuit which was being used as a trigger for the direction finding station.

The recorder used was a Precision Instrument Model P.I. 6200 Magnetic Tape Recorder capable of at least four channel operation, and the highest tape speed was 37,5 inches per second (0,95 m/s) at which the frequency response was satisfactory up to 100 kHz.

Simultaneous recordings over a 12 minute interval were undertaken of the light output from lightning flashes, the response of a 10 kHz loop direction finder, the trigger timing operation, and the aperiodic signals received on the output side of the first triode of the input circuit for the trigger as indicated in the circuit diagram given below.

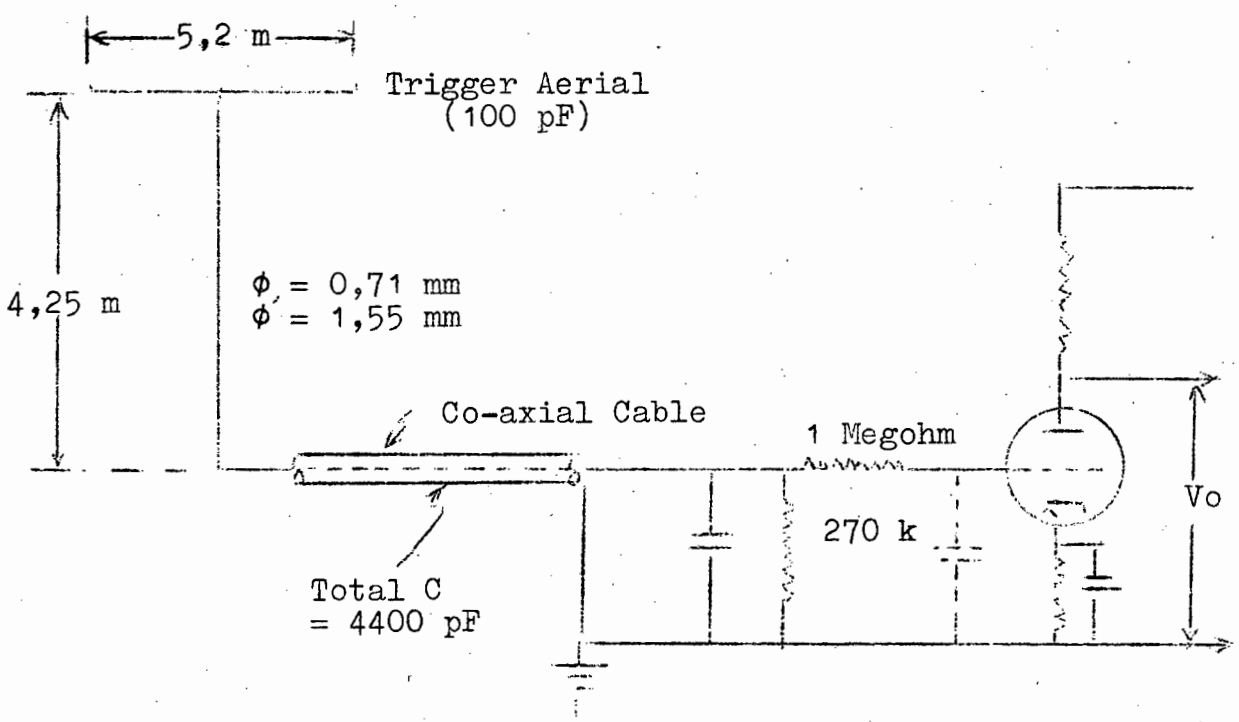

CIRCUIT DIAGRAM OF TRIGGER INPUT

2/...

Part I Appendix II

The T-shaped trigger aerial was insulated to a diameter of 1,55 mm, the conductor diameter being 0,71 mm, and whilst the calculated capacitance was 56 pF, the measured value was 100 pF indicating that the effect of its wooden supporting poles was significant.

The equivalent electrical circuit obtained from the above diagram is as depicted below, taking account of the capacitance of the triode with due regard to its amplifi= cation factor.

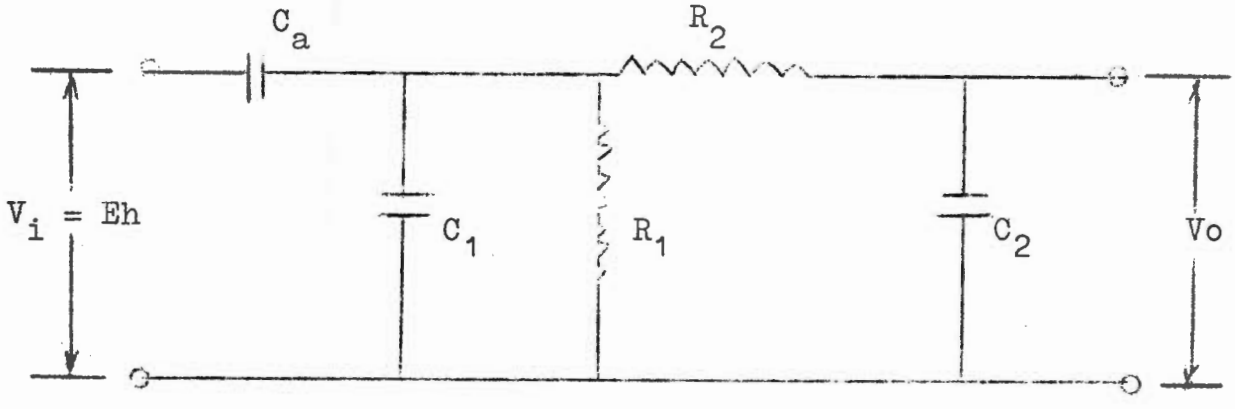

$C_a = 10^{-10}$ F $\qquad R_1 = 2,7 \times 10^5$ ohms

$C_1 = 4,4 \times 10^{-9}$ F $\qquad R_2 = 1 \times 10^6$ ohms

$C_2 = 1,6 \times 10^{-11}$ F

EQUIVALENT CIRCUIT OF TRIGGER INPUT

The 3dB band width of the circuit confirmed by both calculation and measurement was from 140 Hz to 9 kHz, its corresponding rise and fall time constants being 16 μs and 1,2 ms respectively.

2. Recording Data

The recording was undertaken during an active storm when many close ground flashes were taking place and the tape was then played back at one tenth speed to a Siemens Oscillomink recorder having an ink jet paper chart and a response capability of 1 kHz. The paper speed was 50 cms/sec, and when the recording was examined it was found

3/...

to contain a high frequency noise component which may be attributed either to pickup or instability of the particular recorder channel. However, since the noise level was small and of constant amplitude, the general wave form of the traces could still be followed, and measured.

The complete recording contained data on a number of flashes and intra-cloud and ground flashes could be readily distinguished from the display of the aperiodic signal coupled with the other information. For example ground flashes were notable for the regular negative pulsations which occurred some milliseconds apart with relatively quiescent periods during the intervals between pulses. This pattern was followed also by the regular light pulses and ringing of the 10 kHz loop aerial circuit. Intra-cloud flashes on the other hand produced a more or less continuous disturbance in all three channels with frequent bursts of light output and 10 kHz ringing which was however generally of lesser amplitude.

3. Characteristics of the multiple flash

One of the most prominent records obtained was of a 25 component multiple flash which exceeded 830 ms in duration and which was displayed over more than four meters of paper recording. The record was cut up into sections omitting the quiescent periods but otherwise set out exactly as recorded on Fig. 1 attached. In some respects the impressive nature of the recording is lost by this treatment, but it does enable the individual disturbances to be studied more closely.

The circuit could respond to rise times of 16 μs and the first stroke indicated such a fast element. The field was maintained in this case for about 0,8 ms and then fell to zero in about 2 ms which time however is dictated by the time constant of the measuring circuit.

The record is remarkable for the fact that the rise times for all subsequent strokes were more than that for the first- in some cases lasting more than a millisecond.

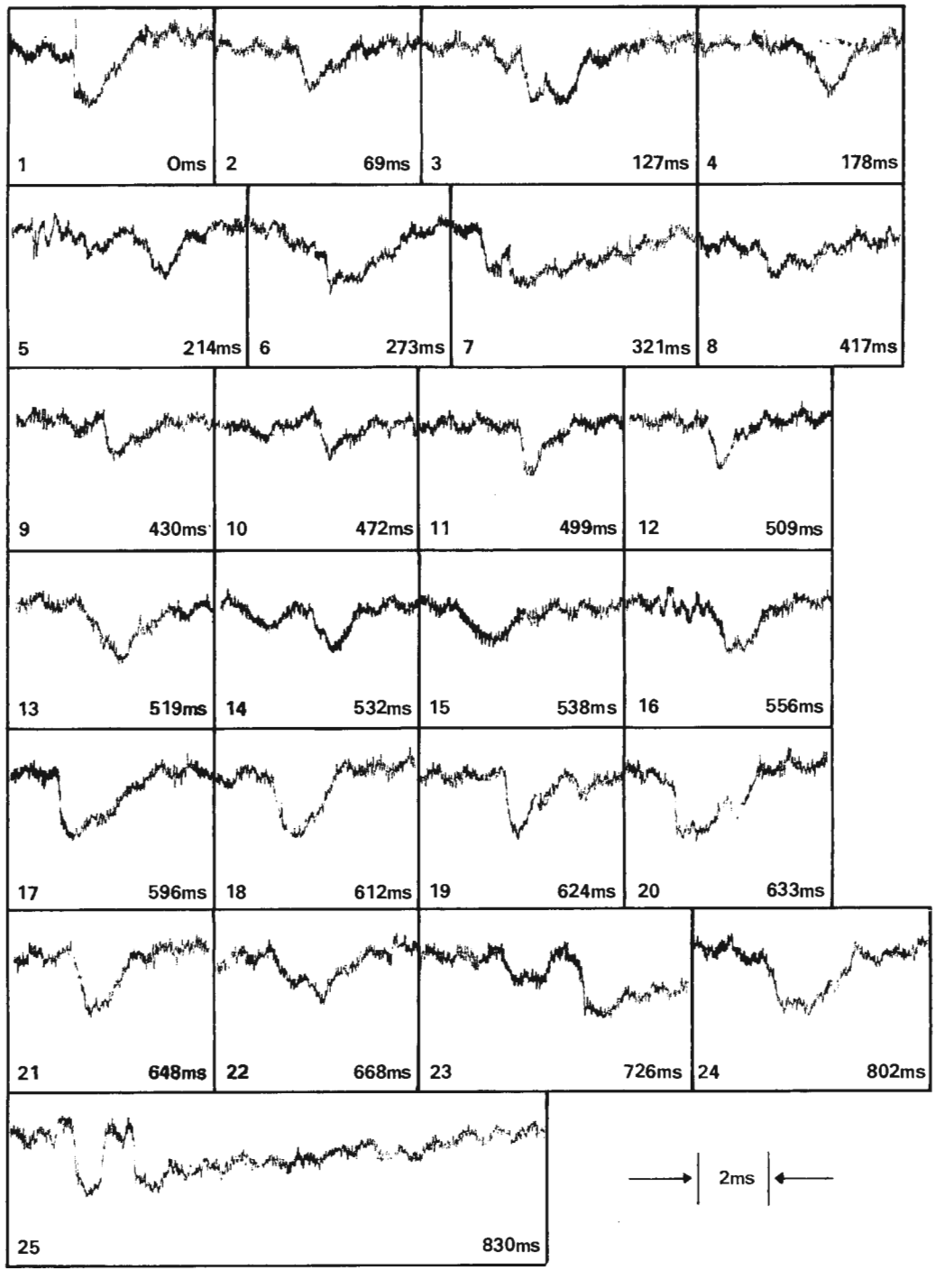

FIGURE 1 (Appendix II)

Segmented diagram of electrostatic field change recorded during a single lightning flash to ground. 25 Different component strokes were identified and the time from start to each stroke in millisec. is indicated

Part I Appendix II

Also there is a distinct irregularity in the distribution of rise times and in fact also the overall wave forms for each component. These characteristics are difficult to explain in terms of classical theory and also they do not conform to previously reported data.

With regard to the wave tails observed there is definite evidence of the occurence of slow field changes immediately following at least some of the strokes. If the potential of the measuring circuit is allowed to decay normally it will do so exponentially with a time constant of about one millisecond. Those components, therefore, which indicate much longer decay times do so on account of a sustained slow field change.

This was particularly the case with stroke number 25, the last, in which the decay time was drawn out to 12 ms approximately.

However stroke numbers 6, 7, 17, 20, 23 and 24 all show similar prolongations but of lesser duration. These cases would appear to be consistent with the notion of continuing currents in strokes which are discussed in the main paper.

Part I Appendix III

Fitting of truncated and censored lognormal distributions to the lightning data of Berger by R. Markham*

The manner in which the problem was solved is outlined below for the case of all flashes. The other two cases, namely positive and negative flashes were treated in an analogous manner. The results only are given.

(a) All flashes

If the variable X follows the lognormal distribution, then the transformed variable Y = ln X follows the normal distribution. The following calculations were carried out on the transformed data.

(i) Determination of goodness of fit of the lognormal distribution

It is known that no values below 2kA were recorded. Thus under the hypothesis that the underlying distribution of the flashes is lognormal the observations form a random sample drawn from an incomplete lognormal distribution. The problem is to determine whether the underlying distribution is lognormal with 2kA as the point of truncation (cf. A. Hald : Maximum Likelihood Estimation of the Parameters of a Normal Distribution which is Truncated at a known point, Skandinavisk Aktuarietidskrift, 1949, 119 - 134).

The data were transformed as mentioned above, and the mean and standard deviation of the underlying normal distribution were estimated

as $\bar{x} = 3,4575$ (ln kA)

and $s = 0,7112$ (ln kA).

*Mr. Markham is with the Statistics Division of the National Research Institute for Mathematical Sciences, Council for Scientific and Industrial Research, Pretoria.

2/...

Part I Appendix III

Maximum current, kA X	Y = ln X	Probability of Occurrence	Ob= served fre= quency	Ex= pected fre= quency
≤2	≤0,6931	0,0000508	0	0,0
2 - 5	0,6931 - 1,6094	0,0046296	2	0,7
5 - 10	1,6094 - 2,3026	0,0475124	11	7,8
10 - 15	2,3026 - 2,7081	0,0937885	12	15,4
15 - 20	2,7081 - 2,9957	0,1120864	8	18,4
20 - 30	2,9957 - 3,4012	0,2103746	35	34,5
30 - 40	3,4012 - 3,6889	0,1590909	38	26,1
40 - 50	3,6889 - 3,9120	0,1110851	17	18,2
50 - 60	3,9120 - 4,0944	0,0761099	12	12,5
60 - 70	4,0944 - 4,2485	0,0522475	9	8,6
70 - 80	4,2485 - 4,3820	0,0362183	8	5,9
80 - 90	4,3820 - 4,4998	0,0254253	3	4,2
90 - 100	4,4998 - 4,6052	0,0180882	2	3,0
100 - 120	4,6052 - 4,7875	0,0225576	3	3,7
120 - 140	4,7875 - 4,9417	0,0122844	2	2,0
140 - 160	4,9417 - 5,0752	0,0069862	0	1,1
160 - 180	5,0752 - 5,1930	0,0041256	0	0,7
180 - 200	5,1930 - 5,2983	0,0025175	1	0,4
≥ 200	≥ 5,2983	0,0048215	1	0,8
		TOTALS	164	164,0

Chi-square Test

For this test it was necessary to group the above data as below.

Maximum Current, kA	Observed Frequency	Expected Frequency
≤10	13	8,5
10 - 15	12	15,4
15 - 20	8	18,4
20 - 30	35	34,5
30 - 40	38	26,1
40 - 50	17	18,2
50 - 60	12	12,5
60 - 70	9	8,6
70 - 80	8	5,9
80 - 100	5	7,2
100 - 120	3	3,7
120 - 140	2	2,0
140 - 180	0	1,8
≥180	2	1,2
TOTALS	164	164,0

3/...

Part I Appendix III

Chi square = 18,5 with 11 degrees of freedom. This means that if the transformed data were drawn from a normal distribution the probability of obtaining a value of chi square as extreme as or more extreme than 18,5 is about 0,07. This value can be considered consistent with the hypothesis of lognormality at the 0,05 level of significance.

(ii) Probability of there being flashes less than 2kA

If one accepts that the observations are from a lognormal distribution, then,

Probability of there being flashes with maximum current less than 2kA = 0,00005

(iii) Estimate of the number of flashes less than 10 kA given the number exceeding 10kA

In order to make this estimate use was made of the information already known concerning the observed strokes, viz. that 13 out of the 164 were less than 10kA. Further the assumption was made that no flashes of less than 2kA occurred. In view of (i) this appeared to be justified.

Here it is known that we have 13 flashes less than 10kA, but we assume that we do not know their actual values. This is an example of a censored sample, and a censored normal distribution was fitted to the transformed data, (cf. Hald (loc. cit.)).

The mean and standard deviation were estimated as

$\bar{x}$ = 3,4638 (ln kA)

s = 0,7009 (ln kA)

Part I Appendix III

Maximum current, kA X	Y = lnX	Probability of Occurence	Ob= served fre= quency	Ex= pected fre= quency
≤10	≤ 2,3026	0,0487720	13	8,0
10 - 15	2,3026 - 2,7081	0,0916666	12	15,0
15 - 20	2,7081 - 2,9957	0,1116666	8	18,3
20 - 30	2,9957 - 3,4012	0,2122956	35	34,8
30 - 40	3,4012 - 3,6889	0,1615392	38	26,5
40 - 50	3,6889 - 3,9120	0,1128131	17	18,5
50 - 60	3,9120 - 4,0944	0,0770927	12	12,6
60 - 70	4,0944 - 4,2485	0,0527103	9	8,6
70 - 80	4,2485 - 4,3820	0,0363658	8	6,0
80 - 90	4,3820 - 4,4998	0,0253973	3	4,2
90 - 100	4,4998 - 4,6052	0,0179717	2	3,0
100 - 120	4,6052 - 4,7075	0,0222393	3	3,7
120 - 140	4,7875 - 4,9417	0,0119797	2	2,0
140 - 160	4,9417 - 5,0752	0,0067408	0	1,1
160 - 180	5,0752 - 5,1930	0,0039399	0	0,6
180 - 200	5,1930 - 5,2983	0,0023804	1	0,4
≥ 200	≥ 5,2983	0,0044288	1	0,7
		TOTALS	164	164,0

Chi-square Test

For this the data were grouped as in the table below.

Maximum Current, kA	Observed Frequency	Expected Frequency
≤10	13	8,0
10 - 15	12	15,0
15 - 20	8	18,3
20 - 30	35	34,8
30 - 40	38	26,5
40 - 50	17	18,5
50 - 60	12	12,6
60 - 70	9	8,6
70 - 80	8	6,0
80 - 100	5	7,2
100 - 120	3	3,7
120 - 140	2	2,0
140 - 180	0	1,7
≥180	2	1,1
TOTALS	164	164,0

5/...

Part I Appendix III

Chi-square = 18,6 with 11 degrees of freedom. As before the exceedance probability is approximately 0,07 and we do not reject the hypothesis of lognormality at the 5% level of significance.

Hence, under this hypothesis and with N strokes exceeding 10kA, the estimated number of flashes less than 10kA is computed as 0,0513 N.

(b) Positive Flashes

(i) Determination of goodness of fit of the lognormal distribution

Chi-square = 1,17 with 4 degrees of freedom.
This is consistent with the hypothesis that the data is drawn from a lognormal distribution. If the hypothesis is true, the probability of obtaining a value of chi-square of 1,17 or larger is approximately 0,88. Hence, we are dealing with a fairly good fit.

(ii) Probability of flashes less than 2kA

Probability of there being flashes in the region less than 2kA = 0,0025.

(iii) Estimate of the number of flashes less than 10kA given the number exceeding 10kA

Chi-square = 1,15 with 4 degrees of freedom. This value is consistent with the hypothesis.

If N flashes are registered with stroke currents exceeding 10kA, then the estimated number of flashes less than 10kA is computed as 0,1315N.

(c) Negative flashes

(i) Determination of goodness of fit of the lognormal distribution

Chi-square = 20,04 with 8 degrees of freedom which indicates that deviations from the hypothesis are significant at the 2% level.

(ii) Probability of flashes less than 2kA

This probability is not estimated since the data are probably not drawn from a lognormal distribution.

(iii) Estimate of the number of flashes less than 10kA given the number exceeding 10kA

Chi-square = 20,8 with 8 degrees of freedom. Deviations

Part I Appendix III

from the hypothesis are significant at the 2% level, and as a result no estimate of the number of flashes less than 10kA can be made.

Note: This is the last page of Part I. Any following script will refer to Part II.

NATIONAL ELECTRICAL ENGINEERING RESEARCH INSTITUTE

The Lightning Discharge

by R.B. Anderson

Part II A proposed new model for the Lightning Discharge

Contents

NATIONAL ELECTRICAL ENGINEERING RESEARCH INSTITUTE

The Lightning Discharge

by R.B. Anderson

Part II A proposed new model for the lightning discharge

Summary of contents

The conventional method representation of the bi-polar thunder cloud cell by means of spherical charges does not lend itself readily to the calculation of critical field intensities within the cloud - nor can the mechanism of intra-cloud versus cloud-ground discharges be explained.

Secondly there is still some need to amplify some aspects of the observed phenomena of the lightning discharge; for example, the reasons for the variation of charge and current magnitudes and of the time intervals between strokes of a multiple flash, need to be further investigated.

Finally the application of the classical Le Jay statement of the total electric field requires further amplification when the magnitude of the charges involved are functions of time.

This thesis therefore sets out to try to clarify existing knowledge of the lightning discharge and to advance alternative hypotheses to explain the phenomena wherever this appears to be required.

The properties of an isolated spherical space charge are enumerated together with the effect of the proximity of the earth. The field intensity is a maximum at the outer boundary of the charge and is not greatly affected by the earth unless it is comparatively close.

The short-comings of the conventional model are demonstrated showing that the field intensity on the centre line between two charges is always in excess of that above or below the charges therefore favouring an intra-cloud discharge particularly in the initial stages when the charges are in close proximity.

It may be assumed that charge separation in a cloud takes place over a horizontal circular area of Radius R, the charge separates vertically upwards a distance L_0 and downwards a distance L_1 to form the approximate shape of a cylinder. The charge density at the position of separation may be regarded as zero increasing

towards the extremities in a linear or other assumed manner. The field intensity along the axis of such a cylindrical charge arrangement may then be calculated, and it is found that this may either be a maximum at the extremities or at or near the charge separation area depending entirely upon the relative dimensions of the cylinder. For example for equal quantities of positive and negative charge, enclosed in respective cylinders of equal length L and radius R, it is found that if $2L/R = 4$, the field intensity at the centre equals that at the extremities when ignoring the effect of earth. Assuming that the field intensity necessary for ionisation in the whole region is the same, breakdown will occur at the extremities of the cylinder rather than at the charge separation area when $2L/R$ exceeds 4. The above model, which is described in more detail in Appendix I is therefore capable of explaining the requirements which will determine whether intra-cloud lightning flashes will occur compared with flashes to ground. The proximity of the earth tends to assist breakdown at the lower extremity of the charged cylinder, but this effect is of secondary importance.

5. The electrical breakdown process within clouds (Page 13)

Intra-cloud breakdown occurs in an area of low charge density but high field intensity and arcs develop which have induced charge at their tips as a consequence of induction from the main field which intensifies the field between these tips and the main charges of opposite polarity. The arc channels grow in each direction simultaneously, neutralising the charge en route in the volumes penetrated. The result is a relatively slow continuous discharge but it is interspersed with pulses which give rise to fast "K" field changes believed to be due to spasmodic extension of the streamers. This is consistent with the notion of pockets of charge being neutralised with each extension, but it is later surmised that the breakdown process itself could be of a spasmodic type if the field intensity required for initial breakdown is higher than that required to maintain it. In other words, when ionisation ahead of the arc tips is initiated, it proceeds over a finite distance until the field intensity falls below a lower critical value when it stops temporarily.

6. The breakdown process at the cloud top (Page 15)

Although observations of electrical breakdown at the top of a cloud are scant, there is definite evidence that this does occur. However it appears likely that dissipation of the positive charge is assisted by the attraction of fast negative ions from the more highly conducting clear air above the cloud and this also assists in the production of ground flashes.

7. The historical background to the mechanism of a lightning discharge to ground (Page 16)

The original hypothesis by Schonland and modified by Bruce and Golde as to the mechanism of the lightning discharge to ground is described in which negative charge is lowered by the leader and followed by upward moving positive charge which may then develop streamers to neighbouring charge centres to produce subsequent strokes of the flash.

iii/ .....

Subsequently Malan and Schonland postulated that the charge for subsequent strokes was abstracted from areas of charge which were contiguous and which were at higher and higher altitudes. This was later confirmed by radar observation of Hewitt and by Brook et al.

The problem still remains however that the charge separation process does not appear to have the capability of generating a sufficient quantity of charge in the time required to sustain a multiple stroke. Furthermore there is as yet no reasonable ex= planation for the observed variability of the time intervals between strokes of between 10 ms up to 500 ms.

8. The initiation of the downward leader stroke (Page 18)

The possible physical conditions which exist at the boundary of negative bound charge when it reaches sufficient concentration to produce an ionising field intensity, are examined, and it is concluded that conducting arc or spark channels will be created which when exposed to the electric field will have positive tips facing the bound negative charge as a consequence of electron migration to the lower end by the electrostatic process of in= duction. This provides a mechanism to explain how the arc channels elongate until finally they comprise the start of the downward leader. The charge on the leader comprises a positive induced charge at the upper end which is exactly balanced by the electrons which migrated to the lower extremities. In addition neutralisation of bound charge in the cloud by the positive tips constitutes a virtual transfer of the charge to the lower end of the leader.

The stepping of the leader is explained by assuming that the positive tips advance in spasmodic bursts each of which sends a pulse of electrons down the channel. The field intensity at the positive tip ends falls mementarily giving rise to a pause until the pilot leader has advanced sufficiently to increase the induced charge thereby raising the field intensity again to ionisation level.

The above hypothesis compares reasonably well with those postulated by other investigators and appears to explain some facets of the observed behaviour of the leader which have not hitherto been too clearly defined in terms of the physical reactions which take place.

9. The charge distribution on the leader channel (Page 28)

Malan and Schonland considered that the charge lowered on the leader channel was distributed uniformly along its length, whilst Bruce and Golde gave reasons why it should be distributed ex= ponentially - that is increasing exponentially from the top to the bottom of the channel.

Calculations show that the ratio of the field change during the leader stroke to that occuring during the return stroke would vary according to each assumption, when the distance D from the point of observation to the lightning stroke is large compared with the height H of the channel, and when the quantity of charge neutralised by the return stroke equals that deposited

originally during the leader stroke. For a uniform charge dis= tribution, this ratio should be unity whereas for a linear dis= tribution - that is uniformly increasing charge from top to bottom of the channel, the ratio should be 2,0. For an expo= nential distribution it should however exceed 3,0.

Pierce found that the observed ratios were most frequently close to unity thereby supporting the case for a uniform charge distribution. However it is shown that if after the return stroke, the channel is left with a positive charge on it, the ratio of leader to return stroke field change could still be unity despite a linear or even exponential charge distribution. This suggests a mechanism for the discharge which would allow more electrons to migrate from the channel to ground than ori= ginally deposited on the channel, and this has been later found to be a feasible proposition.

The only two other explanations of this anomaly would be either that the charge lowered in the leader is less than that neutralised during the return stroke, which is unlikely, or that the method of measurement of field change could be at fault. The leader field change is so much slower than that of the fast "R" element of the return stroke that it is possible that the former could be underestimated unless measurement is undertaken using a circuit having an adequately long time constant. Pierce records having paid specific attention to this point, however.

10. <u>The field intensity surrounding the leader channel (page 35)</u>

The vertical field intensity exerted by the charge in the leader is shown to be greatly influenced by the pattern of charge distribution assumed; since the field intensity is in any case limited by the field strength of the media this in effect means that the radial dimensions of the leader will be affected. The field intensity at the top end opposes that of the main cloud charge field but this effect is lessened if the charge is mostly concentrated at the lower end of the leader.

A uniform charge distribution on the leader would tend to cause the corona radius to be greater at the centre than at the extremities, and this has not been observed. With a linear dis= tribution of charge however, a more uniform corona radius results.

The radial distribution of charge in the leader was also con= sidered, and that in which the negative charge formed a concentric sheath around the core was found to be more appropriate to the mechanism of the discharge. Under high potential conditions the field intensity between the core of the channel and the corona radius boundary would be kept down to the ionisation field in= tensity level by a separation of charge which would tend to drive more electrons into the outer corona shell thereby creating a positive ion core. This core would be capable of sustaining an electron flow at velocities close to that of light, and would be responsible for the luminosity of the leader during the passage of electrons down the core.

It was thereafter possible to envisage a complete conception of the leader channel as comprising a positive core with a negative sheath forming the corona shell. The top end would however consist

v/ .....

predominantly of positive ions whilst the lower end would com= prise mainly negative charge. It was considered that some of the negative charge in the corona shell must also exist in the form of negative ions in order than the charge should not tend to migrate to the lower end of the channel. This would also account for the relatively slow velocity of the return stroke tip when the potential collapses, since time would be needed to extract all the negative charge from the corona shell.

Finally the question of branching was considered, but no new explanation could be evoked except that the large diameter of the corona sheath might contribute to the possibility of avalanches developing simultaneously in more than one direction.

11. The potential of the lightning leader (Page 47)

The simple example of the lowering of a spherical space charge towards the earth indicates that the potential of the charge must also be forced gradually to zero and this must of course apply equally to the lightning leader. If the potential gradient of the leader is confined to that of an arc in the channel and cannot ex= ceed the ionisation level of say 1×10^6 V/m in the cloud and 3×10^6 V/m ahead of the tip, it is clear that as the tip approaches the earth its potential also approaches zero and hence the potential of the top end must also change. This can be accomplished by the intro= duction of an induced positive charge at the top end, as postulated earlier, and it is also assisted by the movement of negative charge away from the cloud area towards the lower end of the channel.

The notion that the potential of the leader tip is maintained at a very high level, not much less than the cloud potential, until it nears the earth causing a sudden breakdown, must be abandoned in favour of the more gradual process envisaged above.

The potential of the top end of the leader channel, due to its own charge is shown to be inversely proportional to the length of the leader and not dependent upon its radius or charge distri= bution. At the bottom end it is likewise more related to the length of the channel than to the radius.

At the top end therefore the potential is mainly determined by the cloud charges whilst at the bottom end it is mainly deter= mined by the charge on the leader channel itself.

12. A model of the lightning leader (Page 52)

In view of the previous qualitative discussions it became necessary to envisage a mathematical model of the leader progression which would enable quantitative calculations to be performed.

This involved first of all the concept of a cylindrical bi= polar cell with the charge distribution arranged say linearly and with the dimensions and charge values chosen such that the field intensity at the lower extremity was -1×10^6 V/m when ionisation and breakdown of the media was assumed to start.

The leader itself was then assumed to form a cylinder, the length of which increased at a velocity V_2, fixed arbitrarily at say 2×10^5 m/s. The upward moving positive tips were assumed to be

vi/ .....

enclosed also in a cylinder of a variable radius but with an upper boundary B_1 which moved into the lower negative bound charge a distance z_1 at a mean velocity v_1 which would be much less than the actual positive tip velocities, and where the ratio of $v_2/v_1 = c$ could be varied over a wide range. Hence the movement of the upper boundary B_1 determined the amount of bound negative charge neutralised and virtually moved into the leader.

The field intensity at the boundary B_1 between the positive tips and the bound charge was assumed to remain constant at -1×10^6 V/m and this determined the amount of charge of both signs which had to be induced on the leader.

The field intensity required for breakdown ahead of the leader was assumed to be 1×10^6 V/m whilst the leader was in the cloud, say for 50% of its traverse, but at the boundary of clear air it was assumed to be increased to 2×10^6 V/m and continue to increase to 3×10^6 V/m at ground level. These values could however be varied at will.

The potential gradient of the leader assumed to start with, was that of an arc, namely 2×10^3 V/m, but it was found later that this had to be varied to allow for higher values.

The computer program, which carried out a dual iterative function, calculated the charge on the leader and its radius and potential for an advance in 5% steps to ground. This program is described in Appendix II.

13. Numerical Results of Computation (Page 62)

A specific numerical case is outlined in some detail. This refers to a charge of $\pm$ 71 C distributed in cylinders of 4 km in length and 0,5 km in radius situated above and below a charge separation area which is assumed to be 8 km above ground. This allows for a leader traverse distance to earth of 4 km which at a velocity of 2×10^5 m/s is accomplished in 20 ms. The field intensity at the charge base is -1×10^6 V/m and its initial potential is $-6{,}4 \times 10^8$ Volts.

Whilst there is no absolute indication as to the relationship between the charge deposited on the leader and the total charge accumulated, an analysis of the variables show that if the arc voltage drop of even 1×10^4 V/m has to be maintained along the leader, the charge deposited would require to be of the order of 35 C and this appeared to be too high taking other criteria into account as well. Values of an order of magnitude higher, namely 1×10^5 V/m were however more realistic.

The potential gradient along the leader is herein defined as the difference in potential between the upper boundary of the positive streamer tips and that of the lower tip of the leader divided by the length of the leader. Since at the upper end, the potential gradient is controlled to a breakdown value of 1×10^6 V/m, it follows that even allowing an arc gradient of 1×10^4 for most of the leader, the overall potential gradient will be higher than this value. Nevertheless it is suggested that despite the high average current values for the leader the mean potential gradients should be higher than that of arcs as determined in the laboratory.

vii/ .....

The analysis of this special case also indicates that the induced charge on the leader should not exceed about 1 to 2 C and that the velocity of the leader tip should be in the order of 20 to 30 times that of the mean velocity of advance of the positive streamer tips in the cloud, but that this relative velocity changes during the progress of the leader.

The potential of the leader tip, tended to maintain a con= stant value until the last 5% of its traverse when it would reduce to zero. This value however was much lower than the cloud poten= tial depending upon the allowable potential gradient assumed.

Very significant changes occured during the last 5% of the leader traverse to ground which are discussed again in a later section.

14. The dart leader (Page 70)

The model of the leader discussed is Section 12 also made provision for the possibility of the fast dart leader of subsequent strokes, and in Section 13 numerical results were obtained on the basis that since the dart leader followed a pre-ionised path, the field intensity for breakdown at the leader tip would be much lower than that of undisturbed air. A figure of 1×10^6 V/m was arbi= trarily chosen and it transpired from the results that in order to deposit the same charge as for the first leader, the velocity of the positive tips would need to be increased by a factor of ten to keep pace with the high velocity dart, and there was no reason= able physical mechanism which would permit this. On the other hand the charge delivered in subsequent strokes was on the average less than that of the first stroke, as proved by the field change observations reported in Part I and a figure of about 1/3 the charge of the first stroke was suggested compared with 1/5 reported by Uman, and this would permit lower positive tip velocities.

Nevertheless speculation as to the mechanism of the dart leader suggested that the step dart during the stepped leader might have an identical mechanism to the dart in subsequent strokes - except of course for the interruptions which occured in the former case.

If it is assumed, as suggested earlier, that ionisation and breakdown in the cloud area occurs in bursts - high velocities of streamer advance would be possible and pockets of charge would be neutralised until the field intensity falls below ionisation level. The velocity of advance thereafter would be very much slower until such time as the field intensity again builds up to the point where another burst occurs. The mean velocity of the positive tips lies therefore between these two extremes and would be the value de= rected on the computed curves.

In the case of the stepped leader the charge involved per burst, or step, would be small, since there are many steps during the leader progression. The dart in subsequent strokes would either need to deliver a much larger charge, or the charge is already available in the channel when the dart occurs.

This matter is considered further after the return stroke mechanism is examined.

viii/ .....

15. Corona Losses (Page 75)

Since the order of magnitude of the potentials of a lightning leader were known, Peek's formula for corona loss on conductors was adapted to fit the conditions for a negative leader stroke as closely as possible, and from which an estimate could be made of the amount of charge which would be needed to satisfy these losses.

The resultant expression for the charge dissipated showed that it was proportional to $r^{\frac{1}{2}}$ where r was the radius of the current carrying core, about which there is only limited information. Assuming that the leader traversed a height of 4 km at a velocity of 2×10^5 m/s the corona loss charge for a one metre radius was found to be about 2 C and negligible if the radius was of the order of 1 mm.

According to Peek the losses on positively charged conductors would be approximately three times that for negative charge, and this should also be reflected in the positive leader.

However the results are derived from conditions on metalic conductors which may not apply in the case of a gaseous discharge, and must therefore be accepted with some reserve.

16. The striking distance of the lightning leader (Page 79)

The numerical data described in Section 13 shows that some significant changes appeared to take place during the last 5% of the leader traverse distance to ground. If the velocity ratio - that is the ratio of the leader tip velocity to that of the mean velocity of the positive tips in the cloud is kept constant, the potential gradient of the leader increases and so does its radius. If however a constant potential gradient is assumed, the velocity ratio must decrease, but the leader radius must also increase even more and this would be accompanied by an increase in the induced charge on the leader. This would mean in effect that breakdown conditions begin to occur before the leader tip actually contacts the earth, and this is due to the effect of the leader image which only begins to assume a significant effect upon the leader tip when it it close to earth.

The field intensity at the surface of the earth, beneath the leader increases by a factor of ten during the first 95% of the leader traverse, and by a further factor of 10 during the last 5%; if however the field intensity for ionisation and breakdown of the air at the ground surface is less than that for air in free space, an upward leader should occur from the ground towards the downward moving lightning leader. There is some uncertainty as to whether upward leaders may be assisted by positive ion discharge from a rough earth surface or by negative ion concentration above the surface such as is believed to occur with short laboratory sparks.

The striking distance of a leader is defined as the distance between the corona shell of the leader tip and earth, at the moment when an upward leader starts out from the earth. It is shown that this will depend on the charge on the leader, its distribution, and upon the relative magnitude of the breakdown value of the air at the leader tip compared with that at the surface of the earth.

ix/ .....

In addition it is shown that during the last 5% of the leader traverse to ground its corona radius increases by a factor of two due to the proximity of its image, and this effectively reduces the striking distance.

17. The effect of a protruding conductor on the striking distance (Page 87)

The first case considered was that of a lightning leader descending directly onto a protruding conductor. The method of attack followed was to calculate the potential and vertical field intensity at the top of the structure due to a charge "q" on the lightning channel distributed say in a linear manner. Since the structure must be at zero potential, it will assume a charge "q_o" distributed such that the potential at the top of the conductor due to that charge is equal in magnitude but opposite in polarity to that induced by the leader - thereby making the resultant potential zero. The field intensity due to this charge could also be calculated, and this field reinforced that due to the leader, and in the limit it could be assigned a value which would cause ionisation and breakdown at the top of the conductor thereby starting an upward streamer.

The resultant equations provided a solution relating the striking distance to the dimensions of the structure and to the charge in the lightning channel in the form of a family of curves. Numerical values of striking distance versus charge could then be obtained for a particular structure height and width (or equivalent radius).

These calculations whilst correct in principle are nevertheless subject to the validity of the assumptions involved as to the manner of charge distribution both in the leader channel and the structure, and also of the values assigned to the limiting field intensity which will cause breakdown at the top of the structure.

Of greater interest perhaps in the case when a lightning leader descends near a tall structure and the possibility exists that as a consequence of a streamer developing from the top, the lightning leader may be diverted to the structure. The method of numerical computation is similar to that for the case of the lightning leader progressing from overhead but consideration has to be given to the starting of upward streamers both from the structure and from the ground. The streamer which reaches the lightning channel first is the one which determines the final discharge path of the descending leader.

18. The return stroke (Page 94)

In this section the physical concept of the return stroke mechanism is critically examined in an endeavour to explain more fully the many and various experimental observations carried out over the years and to ascertain to what extent they can be integrated into an acceptable unified hypothesis.

Firstly the velocity of the luminous tip of the return stroke at approximately 1/10th of that of light is nevertheless still relatively slow if the lightning channel is to be regarded as a highly conducting plasma. Furthermore assuming the same premise, there appears to be no valid reason why once the conducting channel

x/ .....

has been established between cloud charge and ground, the whole of the remaining charge in the cloud should not be discharged as con= tinuing current. Other questions concern the large variability in the distribution of peak current magnitudes, charge in strokes, and time intervals between strokes.

Firstly it is shown by calculation that the velocity of the return stroke can be related to the measured waveform of the current discharged to ground by assuming that this current is derived by neutralising charge distributed along the channel starting from the earth upwards. In other words the electrons deposited in the channel are discharged from a point on the channel coinciding with that of the tip of the luminous upward moving streamer, and it is surmised that this provides an important clue as to the mechanism of the discharge.

Secondly it seems clear that after discharging the negative charge the channel must be left with a nett positive charge, and this means that more electrons drain from the channel than were originally deposited there. This apparent anomaly takes on a physi= cal meaning if it is assumed that these electrons are derived from the corona shell as a consequence of ionisation between the core and the corona radius to keep the field intensity within the corona sheath down to the breakdown level of the air.

When considering how much positive charge is left on the channel, it becomes evident that the concept of a rising zero potential streamer - namely the return stroke proper - cannot exist, other= wise continuing current would always follow. This leads to the proposition that the potential gradient of the return stroke channel has some finite value and is not as low as that of an arc. This gradient might properly be provided by the inductance of the core.

The properties of a number of computed cases of leaders in= volving differing values of cloud charge and dimensions of cylinders are critically examined to try to find a common factor; it was found for example that the value of the accumulated cloud charge itself did not control the charge deposited in the leader, but it had some influence on the relative velocities between leader tip and positive tip advance in the cloud. A longer leader length gave rise to higher values of charge deposit due to the increased induction and the longer time for positive tip penetration.

Finally it was concluded that the controlling factor seemed to be the potential developed in the cloud which could differ over a large range even for the same value of accumulated charge, according to the dimensions of the charge. Thereafter the potential gradient of the leader channel appears to be the limiting factor as regards charge deposition, but this gradient needs to have a mean value of the order of 1×10^5 V/m which may exceed that of an arc.

Typical values of charge on the leader and relative velocity are given in Table 18.1.10 on Page 110. For example a cloud charge of 71 C situated 4 km above and below a charge separation area at 8 km, that is having a 4 km leader length would deposit about 8 C of which about 1 C was induced charge. The velocity of the leader tip when approaching close to the earth would then be

about 20 times that of the mean velocity of the positive tips. The last few percent of the leader traverse to ground is obviously significant in that electrons start to surge out of the leader during that period, the source being the corona charge. Thereafter a progressive discharge of the corona charge occurs as the return stroke tip moves upwards, but as it does so, the channel becomes more positive with the charge density increasing as the tip approaches the top of the channel where in fact it reaches the portion which is already charged positively.

19. Continuing Current and Subsequent Strokes (Page 111)

In Part I of this thesis it was observed that continuing currents appeared to be rare occurrences, whereas other investigators, also using field change observations, observed at least 50% of strokes with slow component field changes immediately following the first R element of the return stroke. Berger's most recent analysis - completed after most of this thesis had been written - confirms that continuing currents are in fact not as frequently observed by him as earlier records tended to show.

As a consequence of the hypothesis put forward herein, this anomaly is now easier to understand. The slow field change following the return stroke is undoubtedly due to the neutralisation of the positive charge left at the top of the leader after the return stroke discharge, and this could easily have been mistaken for continuing currents which would give rise to a similar effect. Nevertheless continuing currents do occur and they depend upon the conductivity of the channel being maintained and also upon the maintenance of ionisation levels in the cloud.

Berger has also provided experimental evidence that the return stroke channel is left with a positive charge on it after the initial high current discharge thereby strengthening the hypothesis herein propounded. Accordingly there can be reniewed confidence in the mechanism proposed.

In general therefore, the return stroke ends with the neutralisation of the positive charge left at the top of the channel since the field intensity must have fallen below ionisation level if the charge generation process is not fast enough to sustain it. The lower end of the channel loses its conductivity rapidly and is incapable of sustaining further current flow to ground.

When a break does finally occur, the upper reaches of the lightning channel are still conducting the charge of both signs can once more be induced thereby tending to recharge the channel. However it is clear that in the main the production of a subsequent stroke requires further assistance from sources external to the mechanism.

These are in effect available in a number of forms namely the discharge of positive charge at the cloud top, which is also in a state close to ionisation according to the theory of the cylindrical charge distribution. Also the attraction of fast negative ions from the upper atmosphere, and of positive ions from below assist to build up the field intensity at the channel top.

In conformity with the notion discussed earlier, the dart leader of a subsequent stroke is not the main phenomena of the

stroke development but is evidently due to a fresh burst of ion= isation once the critical level has again been reached. This is supported by Berger's later field change measurements indicating a much slower initial field change for a subsequent leader, com= pared with the one microsecond rise time of the current. Although not mentioned again in the thesis, this was also the evidence of the 25 component multiple stroke reported in Part I Appendix II. Here the majority of the field changes had slow rise times - the mean value being 0,4 ms which would in any case have suffered severe attenuation due to the small time constant of the measuring circuit.

The resulting stroke sequence is finally indicated on Figures 19.0.1 and 19.0.2.

20. The effect of polarity change (Page 117)

Lightning discharges from positively charged clouds are thought to be associated with isolated positive charge such as would occur if the lower negative charge in a bi-polar structure had been dissi= pated by a previous series of discharges to ground. For this reason the discharge path could be much larger than that of ground flashes and would be consequently associated with higher magnitudes of in= duced charge.

In addition the propagation velocities of the respective tips of the leader channel are likely to be reversed in that the nega= tive tips in the cloud should propagate faster than they did through virgin air. Similarily the positive tipped leader should proceed at a slower rate because there is no charge ahead of it to in= tensify the field. The result of this would be that the charge extracted from the cloud should greatly exceed that of the nega= tive leader case. This is in fact what Berger observed in all 27 of his records. The charge was in the order of 7 to 10 times that of the median value for negative discharges. It was not surprising therefore that not one positive multiple discharge occured for one simple reason that there could not be too much charge available to meet such a high demand.

A second reason arises out of the discharge mechanism itself. In the case of a positive leader, the positive charge is lodged as ions in the corona shell where they are not as freely available as are electrons, or otherwise it is bound on cloud droplets. The negative charge is however in copious supply both in the channel core and in the ground when contact is made. Hence, according to the discharge mechanism proposed, negative charge in the form of electrons may neutralise the corona shell and the bound charge in the cloud with no stopping mechanism. Hence in the case of a positive discharge the process must continue until all positive charge in the cloud is neutralised. In the case of the negative discharge the supply of free electrons was strictly limited to the corona sheath.

In part I multiple positive discharges were reported but their probability of occurrence was much lower than for ground flashes.

21. Field changes due to lightning (Page 119)

The classical expression for the total electric field atributed to Le Jay refers to a single point in time and needs to be amplified

if it is to describe the electric field change when the value of charge varies with time, as occurs during the discharge process. A similar expression developed by Jordan for an oscillating dipole is perhaps more expressive and shows also that the three compo= nents of the electric field namely the electrostatic, induction and radiation fields can be found from a statement for any one of them by differentiation or integration as the case may be. How= ever this is only strictly applicable when the propagation time is taken into account. Nevertheless approximate expressions for the variation of magnitude with time of the respective field changes may be obtained by neglecting the propagation time.

The calculations assume the wave form of the current delivered to ground during the return stroke, and also the charge distribution along the leader at the moment of contact with the earth. Assuming then that the charge on the leader is neutralised progressively from the ground up, the electrostatic field change variation with time can then be evaluated.

The induction field change may likewise be obtained by differ= entiating the previous expression with respect to time and when multiplied by S/c, where S is also a function of time, and c is the velocity of light. The radiation field change is likewise deter= mined.

When the distance D of the point of observation from the lightning stroke is large compared with the height H of the stroke, all three expressions for the respective field changes agree with the Le Jay concept namely the proportionality to D^{-3}, D^{-2} and D^{-1} respectively and Q, i, and di/dt.

The radiation field change however contained a new term pro= portional to i^2/q which has not been previously identified and which adds directly to the di/dt term. In the case of very high rates of rise of current coincident with the peak value therefore, the radiation field change could be much larger than previously thought possible.

The question of the retardation time due to the velocity of propagation of the wave can be resolved by means of an incremental type of computer program. This was used to determine the respective increments of time at the location of the point of observation com= pared with that at the lightning-stroke itself thereby enabling the curve of field variation with real time at the point of observation to be evaluated.

The curves for three cases of charge distribution, namely uniform, linear and exponential, were computed, from which it was evident that the electromagnetic component of the field change assumed a magnitude which exceeded the electrostatic component at some value of D less than 20 km in the case of a uniform or linear charge distribution, and less than 40 km in the case of an ex= ponential charge distribution on the leader. This could be at least partly responsible for the observed departure from the D^{-3} relation reported in Part I of this thesis. It is considered how= ever that another source of error could have been introduced by the omission of some measurements at very close range due to their having been off scale.

xiv/ .....

Finally the over-discharge of electrons from the leader during the return stroke would be equivalent to levelling out say a linear charge distribution to an approximate uniform distribution. Alternatively an initial exponential charge distribution will discharge approximately as a linear distribution. Since no measurements have been made on this aspect it is not possible to be more precise, but at least the approximate form of field change may be deduced from a comparison of the three cases presented.

22. Acknowledgements (Page 130)

The author acknowledges assistance received from a large number of people including his family and members of the National Research Institute for Mathematical Sciences and the National Electrical Engineering Research Institute. Benefit has also been derived through discussion with CIGRE Study Committee 33.01 Working Group of Lightning, and in particular Dr. R.H. Golde, Prof. Dr. K. Berger, Prof. S.A. Prentice and Dr. T.E. Allibone. The ever willing help of the late Prof. Dr. D.J. Malan during the initial years was greatly appreciated.

Finally the author very much appreciates the permission of the Council for Scientific and Industrial Research of South Africa to submit this thesis to the University of Cape Town in compliance with the requirements for a Ph.D. degree and he gratefully acknowledges the help and assistance received from his supervisors, Dr. H.D. Einhorn and Cd. G.H. Webster in this regard.

23. References (Page 132)

Publications directly referred to in this Part II of the thesis are listed, but many other papers have been read over a period of some twenty-five years during which a study of lightning has been undertaken. The hypotheses presented therefore embodies thoughts and ideas which result from some considerations not directly included in the list of references.

Appendix I The cylindrical model of cloud charges

This appendix gives the basis for the concept of the cylindrical cloud model in some detail and this proceeds to the derivation of formulae for the calculation of field intensity and potential at points along the centre line of the cylinder. Numerical results are given and curves drawn for many of the important parameters required for the study of the initiation and progression of lightning discharges within and from charged clouds.

Appendix II Description and Flow Chart of Computer Program for Lightning Discharge Model

By Mrs. L.O. Stander - Computer Science Division, National Institute for Mathematical Sciences

This appendix describes the development of the computer program to simulate the progression of the leader from the base of the charge in the cloud to the ground. Basically it calculates the field intensities and potentials at different positions along the progressing leader which at the same time requires solutions of the radial dimensions of the leader and of the positive charge area at the cloud end of the leader, and this involved a double iteration

in the program. First the leader radius R_2 was found which would satisfy the conditions of a given ionising field intensity at the two extremities of the leader for a fixed value of the radius R_{z1} of the induced positive charge area. This then also gave the potentials and the mean potential gradient of the leader. Then if these values did not comply with controlled requirements as to the desired potential gradient, the value of R_{z1} was varied until it did so, but with each variation a new value of R_2 was computed.

Finally when R_{z1} equalled the radius R_1 of the main negative charge cylinder, the potential gradient for the leader was calculated for each value of R_2 found.

The program was arranged to make calculations for any assumed value of the initial charges and their dimensions, including the possibility of the upper positive charge escaping vertically, and for any assumed value of the ratio of the velocities of the lower leader tip to the mean velocity of penetration of the positive tips into the main negative charge.

The appendix includes a flow chart and an example of the complete computer print-out which shows the incremental values of the many functions used for the computation including the induced and total charge on the leader and the field intensity and potential at all points of interest.

The computer model of the lightning leader discharge was found to be an invaluable tool to determine the conditions attending the breakdown process.

R.B. Anderson,
National Electrical Engineering Research Institute,
Council for Scientific Industrial Research,
P.O. Box 395,
PRETORIA.
Republic of South Africa.

PART II

A PROPOSED NEW MODEL FOR THE LIGHTNING DISCHARGE

1. Introduction

In most previous models of thunderclouds, it has proved to be convenient to represent the cloud charges as contained on or in imaginary spheres, whereupon calculations of the field changes at ground level have been effected assuming various heights and dis= position of the centres of these spheres where the charge can theoretically be assumed to be concentrated. Whilst this method of analysis gives approximate results at ground level which may be realistic, it does not assist in the calculation of the field intensitites likely to be encountered within the cloud itself, nor does it permit a reasonable explanation of the mechanism likely to lead to cloud to ground flashes as opposed to intra-cloud flashes.

Secondly, whilst the mechanism of the downward leader and subsequent return stroke has been postulated, including that of the subsequent strokes of multiple flashes, there is still apparently some need to explain the observed velocity of the return stroke, the variation in the charge delivered per stroke and its relation to variation in current magnitude and wave form, and the reason for continuing current after some strokes.

Finally, for calculations of the field change related to real time, the application of the classical statements attributed to Le Jay (1926) are somewhat obscure, especially when the distance from the lightning channel is not large compared with its height, and this needs further elucidation.

2. The isolated Spherical Space Charge

Consider a positive charge Q distributed uniformly throughout a sphere of radium R, and the conditions at a point P as illustrated in Fig. 2.0.1

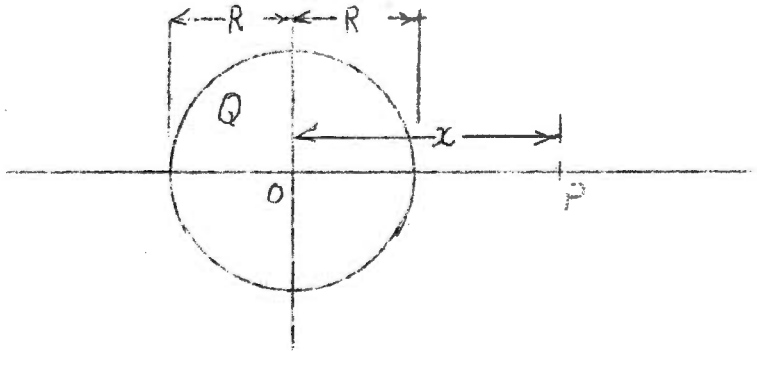

Fig. 2.0.1. The isolated spherical space charge

So long as $x > R$ the potential at the point P, and the potential gradient (which shall be hereinafter equated to the field intensity) are obtained from the well known relationships namely

$V_{(x> R)}$/....

$$V_{(x>R)} = \frac{Q}{4\pi\varepsilon x} \text{ Volts} \quad \ldots\ldots\ldots\ldots\ldots\ldots\ldots\ldots \quad (2.1)$$

$$E(x>R) = -\frac{dv}{dx} = \frac{Q}{4\pi\varepsilon x^2} \text{ V/m} \quad \ldots\ldots\ldots\ldots\ldots\ldots \quad (2.2)$$

Where $\varepsilon = \varepsilon_o \varepsilon_r$ and $\varepsilon_r = 1$ for air.

And $\varepsilon o = 10^{-9}/36\pi$ farad-meter

Normally these considerations are terminated at a point on the surface of the sphere, putting $x = R$, but in the case of a uniformly distributed charged volume it can be shown that when $x < R$

$$V_{(x<R)} = \frac{Q}{8\pi\varepsilon R}\left(3 - x^2/R^2\right) \text{ Volts} \quad \ldots\ldots\ldots\ldots\ldots\ldots \quad (2.3)$$

and $$E_{(x<R)} = \frac{Qx}{4\pi\varepsilon R^3} \text{ V/m} \quad \ldots\ldots\ldots\ldots\ldots\ldots\ldots\ldots\ldots \quad (2.4)$$

Whence at the centre of the sphere $x = 0$ and at the boundary $x = R$

$$Vo = \frac{3Q}{8\pi\varepsilon R} \text{ and } V_r = \frac{2Q}{8\pi\varepsilon R} \quad \ldots\ldots\ldots\ldots\ldots\ldots\ldots \quad (2.5)$$

$$E_o = 0 \text{ and } E_r = \frac{Q}{4\pi E R^2} \quad \ldots\ldots\ldots\ldots\ldots\ldots\ldots \quad (2.6)$$

The above results are illustrated in the following diagram Fig.2.0.2

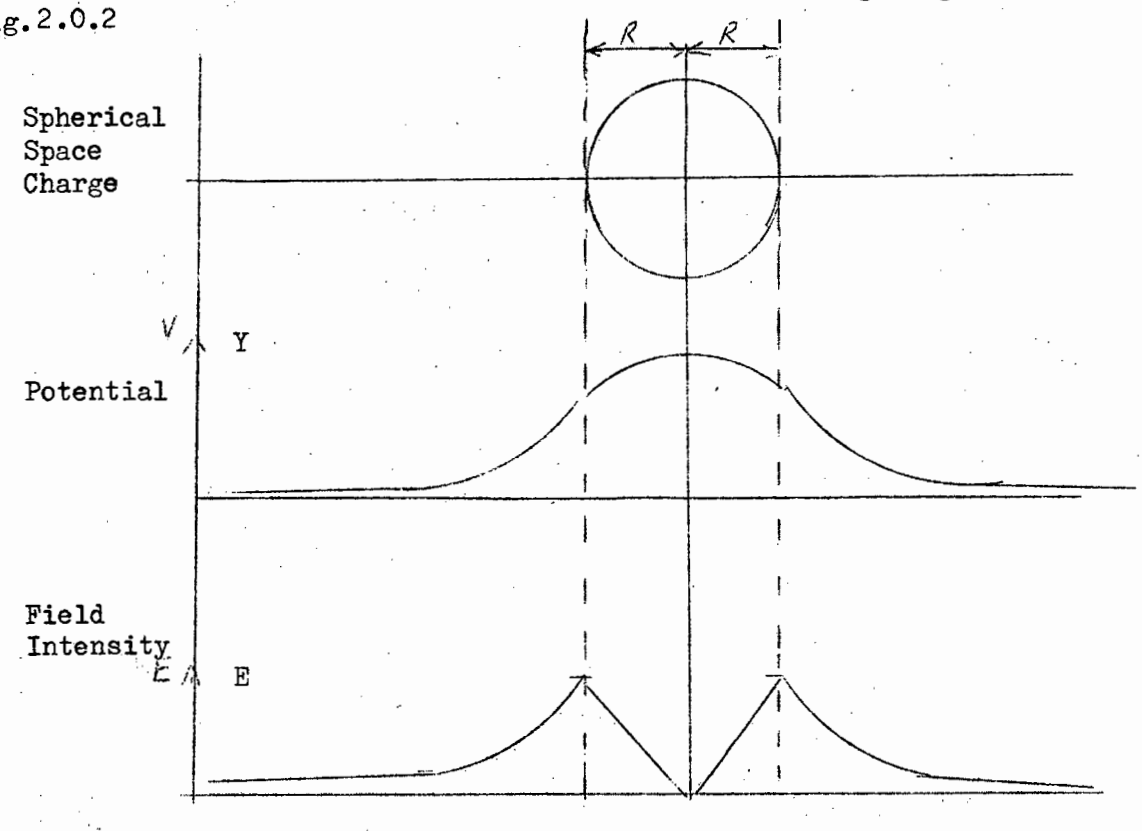

Fig.2.0.2 Illustration of the potential and field intensity associated with a spherical space charge.

The/...

The most pertinent result of the above is the realisation that the field intensity is a maximum at the boundary of the charged spherical charge, and insofar as this affects a cloud, ionisation and breakdown can be expected to occur around the perimeter of the charge in the first instance.

This simple model may be used to give some indication of the probably critical dimensions of R for various values of Q, given a limiting value of Em which would be needed to cause breakdown in the cloud. According to Macky (1931) a value of 1 x 10^6 V/m for the moisture laden lower portions of a thundercloud might well be applicable whence from equation 2.6

$$R_m = 3(Q.10^9/Em)^{\frac{1}{2}}m \quad \ldots\ldots\ldots\ldots\ldots\ldots\ldots\ldots\ldots\ldots\ldots\ldots \quad (2.7)$$

Typical values of R_m together with the resultant values for the charge density and maximum potential are given in the following Table 2.1.1

Q Coulombs	Meters	Charge Density Coulombs/m^3	Maximum Potential Volts
1	95	0,280 x 10^{-6}	0,142 x 10^9
5	212	0,125 x 10^{-6}	0,318 x 10^9
10	300	0,084 x 10^{-6}	0,450 x 10^9
50	671	0,040 x 10^{-6}	1,007 x 10^9
100	956	0,027 x 10^{-6}	1,412 x 10^9
500	2120	0,012 x 10^{-6}	1,185 x 10^9

Table 2.1.1. Typical values of critical radius, charge density and maximum potential of an isolated spherical charged volume for a boundary field intensity of Em = 1 x 10^6 V/m

The above calculations are all related to a zero potential sphere at infinity but the effect of the earth may be simulated by assuming that it consists of a horizontal zero potential plane below which is a mirror image of the charge situated in the cloud as indicated in the following Fig. 2.0.3.

Fig. 2.0.3/...

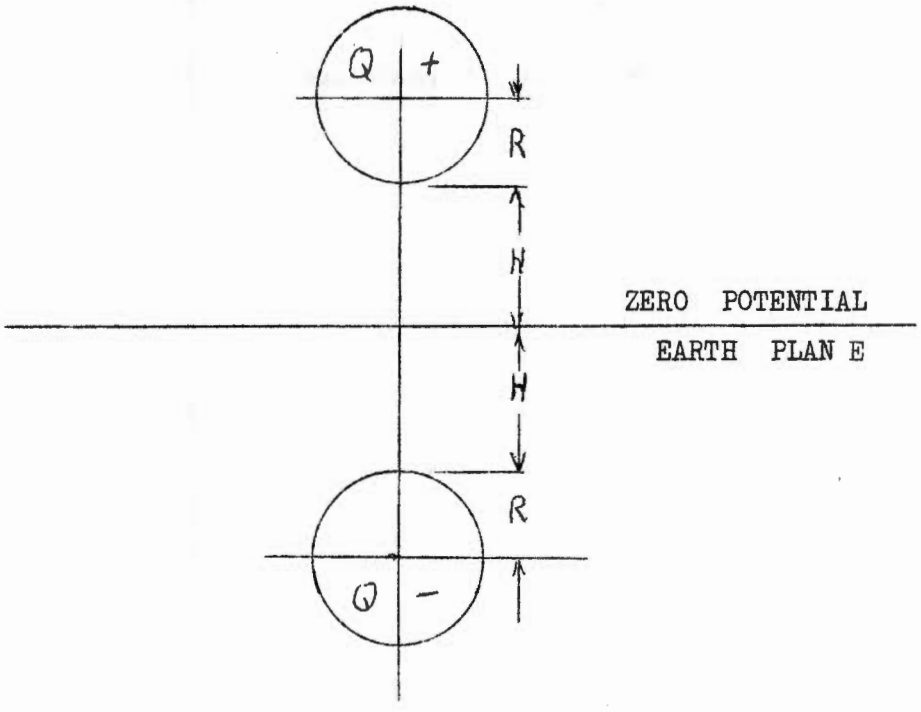

Fig. 2.0.3. Simulation of an isolated positive charge Q situated above a zero potential earth plane.

The potential at the centre of the upper charge is reduced by an amount given by the following from equation 2.1.

$$V = Q/4\pi\varepsilon.2(H+R) \text{ Volts} \quad \ldots\ldots\ldots\ldots\ldots\ldots\ldots \quad (2.8)$$

and expressed as a proportion of the original potential

$$V/V_o = \frac{1}{3} \cdot \frac{R}{H+R} \quad \ldots\ldots\ldots\ldots\ldots\ldots\ldots\ldots\ldots\ldots \quad (2.9)$$

The height of the cloud charge would rarely be less than 2 km, and for a radius of say 1 km, the reduction of potential would be about $\frac{1}{9}$ or not much more than 10%.

Similarly the increase of field intensity at the point P would be given by

$$e = Q/4\pi\varepsilon(2H+R)^2 \text{ V/m} \quad \ldots\ldots\ldots\ldots\ldots\ldots\ldots \quad (2.10)$$

and expressing this as a ratio of the original field intensity at P

$$\frac{e}{E} = \frac{R^2}{(2H+R)^2} \text{ V/m} \quad \ldots\ldots\ldots\ldots\ldots\ldots\ldots \quad (2.11)$$

For the same parameters as the example above, this increase amounts to 4% of the original field intensity, and, in consequence, it is reasonable to suggest that for all practical purposes, the effect of the earth may in those circumstances be neglected. It is also clear that because the field intensities

in/...

in the region of the charges in the cloud are relatively unaffected by the earth plane - with the proviso that it is not too close - the probability of ground flashes occurring compared with intra-cloud flashes is not greatly influenced by the height of the charges above ground.

3. The Conventional Bi-polar Model

Disregarding the earth plane, the potential and field intensities existing within the cloud may at first be examined by means of the conventional model consisting of say two charges of opposite polarity, initially equal in magnitude, and contained in spherical volumes of space charge, as depicted in Fig. 3.0.1.

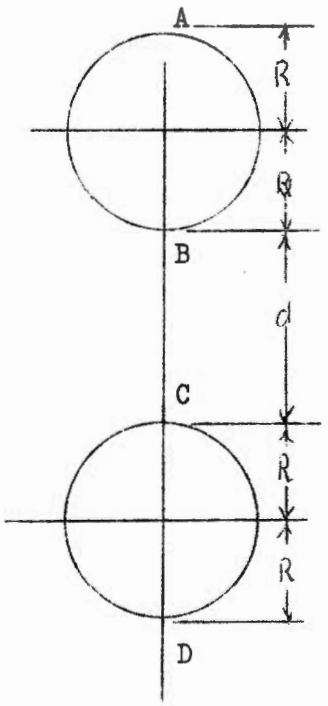

Fig. 3.0.1 Conventional arrangement of bi-polar cloud charges

The points of immediate interest are those labelled A, B, C and D and the field intensity at each of those points is simply the algebraic sum of that due to each of the charges with due regard to the sign of the charge and the direction of the field.

Conventionally the vertical component of field intensity at any point in this system is positive if unit positive charge placed at that point would tend to move downwards. Consequently for equal values of charge Q, the field intensities at B and C and at any point between is positive and is the sum of that due to the two charges whereas the field intensity at A or D is the difference of that due to each of the charges and the resultant field intensity is in this case negative.

The field intensity at A or D is therefore given by the expression:-

Ea = Ed/.....

$$E_a = E_d = \frac{Q}{4\pi\varepsilon}\left[-\frac{1}{R^2} + \frac{1}{(d+3R)^2}\right] \quad V/m \ldots\ldots (3.1)$$

Similarly

$$E_b = E_c = \frac{Q}{4\pi\varepsilon}\left[+\frac{1}{R^2} + \frac{1}{(d+R)^2}\right] \quad V/m \ldots\ldots (3.2)$$

It is clear therefore that the field intensity at B and C between the charges will always exceed that at A or D and would therefore favour the development of intra-cloud discharges rather than ground. This would in particular be accentuated during the initial stages of the charge separation process when the two charges are close together. For example if B and C are coincident i.e. d = o then

$$E_a = E_d = \frac{Q}{4\pi\varepsilon R^2}\left[-\frac{8}{9}\right] \quad V/m \ldots\ldots (3.3)$$

$$E_b = E_c = \frac{Q}{4\pi\varepsilon R^2}\left[+2\right] \quad V/m \ldots\ldots (3.4)$$

Hence the field intensity at the junction of the charges is more than twice that either below or above the charges and clearly an intra-cloud discharge would be the more likely.

In view of the fact that the breakdown strength of the air in the neighbourhood of the charge separation area is not normally in excess of 1.5 times that in the lower reaches of a moist cloud, the model is not a very satisfactory one to explain the incidence of ground flashes in some thunderstorms. ?

4. A New Cloud Charge Model

An approach to a new cloud charge model which is more realistic perhaps, may be based upon the fact that the charge separation process appears to take place in the region above the freezing level of the atmosphere, and charges of opposite polarity are respectively carried upwards or downwards from this region, the exact mechanism being still a somewhat controversial matter. Nevertheless the nett result is usually a concentration of negative charge in the lower regions of a cloud and positive charge towards the top, and it may therefore be postulated that the charge density varies from zero in the immediate vicinity of the charge separation area to a maximum at the extremities of the cloud volume.

The exact manner of the charge distribution is a matter of some conjecture but for the purposes of a model any suitable distribution may be chosen, for example linear, parabolic, cubic of even exponential; and these may differ for the negative and the positive charged volumes respectively.

The next requirement is the physical form containing the charges and the most favoured appears to be generally cylindrical in shape to coincide with a circular vortex or updraft channel suggested by Vonegut (1965). However the choice of shape could be varied such as by employing inverted cones, ellipsoids or

paraboloids/...

paraboloids, but in each case the mathematics could be considerably involved and may not be justified considering the inexactness and variability of thunderstorm cells anyway.

As a starting off point however, it is assumed that charge separation takes place uniformly over a circular area of radius R, and that thereafter the charge separates and is confined to a cylindrical form having any convenient height or depth above and below the separation area. Initially the amount of positive and negative charge separated is assumed equal, and it is convenient also, though not necessary, to assume that the separation distance is the same for both charges say L and the cylinder containing them therefore has a length 2L. The charge distribution per unit volume may as a first approximation be assumed to be linear and to be the same for either polarity of charge it may then be expressed as equation 4.1 namely:-

$$q^1 = \frac{4Q}{\pi R^2 L^2} x \text{ coulombs/m}^3 \quad \ldots\ldots\ldots\ldots\ldots\ldots \quad (4.1)$$

Where x is measured from the centre of the cylinder up to a distance of L as depicted in Fig. 4.0.1.

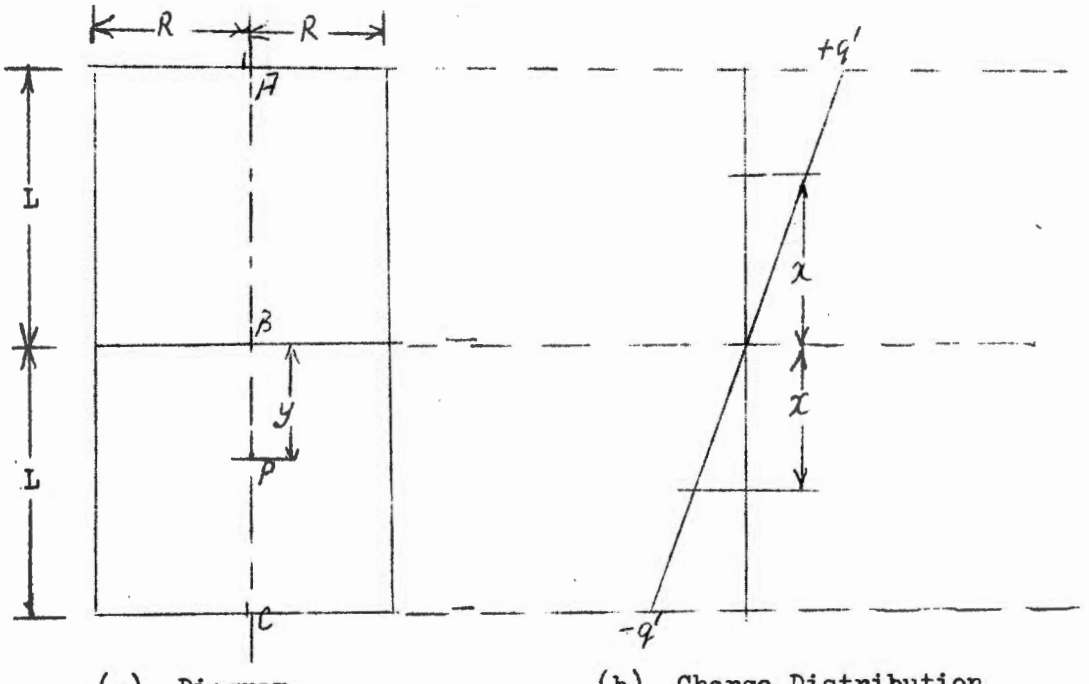

(a) Diagram (b) Charge Distribution

Fig. 4.0.1. Diagram showing cylindrical model of charged cloud with linear charge distribution.

In Fig. 4.0.1 the points of interest are the field intensities at A, B and,Cand that at a Point P which is any distance "y" from B up to y = L. Since the distribution has been assumed to be symmetrical around the point B, the field intensities at the extremities of the cylinder, or any points equidistant from B are equal.

By/...

By means of the normal process of integration the field intensity at the point P may be calculated resulting in the following expression: equation 4.2

$$E_p(y) = \frac{4Q}{\pi\varepsilon R^2 L^2} \left\{ R^2/2 \sinh^{-1} \left(\frac{L-y}{R}\right) + R^2/2 \sinh^{-1} \left(\frac{L+y}{R}\right) - \left(\frac{L+y}{2}\right) \left[(L-y)^2 + R^2\right]^{\frac{1}{2}} - \left(\frac{L-y}{2}\right) \left[(L+y)^2 + R^2\right]^{\frac{1}{2}} + L^2 - y^2 \right\} \text{ V/m} \quad \ldots\ldots\ldots \quad (4.2)$$

Where Q is the magnitude of the total charge of one polarity. The field intensity at A or C is obtained by putting y = L in equation 4.2 namely

$$E_a = E_c = \frac{Q}{2\pi\varepsilon L^2} \left[\frac{L}{2R} - \sinh^{-1} \left(\frac{L}{2R}\right)\right] \text{ V/m} \quad \ldots\ldots\ldots\ldots \quad (4.3)$$

Where Q is always a positive quantity. The field intensity at B is obtained by putting y = 0 in equation 4.2 namely

$$E_b = \frac{Q}{\pi\varepsilon L^2} \left\{ \sinh^{-1} \left(\frac{L}{R}\right) - \frac{L}{R} \left[\left[1+\left(\frac{L}{R}\right)^2\right]^{\frac{1}{2}} + \left(\frac{L}{R}\right)^2\right] \right\} \text{ V/m} \quad \ldots \quad (4.4)$$

In order to investigate the relative values of E_a or E_c compared with E_b, the value of the ratio E_y/E_b has been plotted for values of $y = 2L(\frac{1}{2}-a)$ from a = 0 to a = 0,5, and the result is shown in Fig. 4.0.2 (separately attached).

It is evident first of all that the field intensity is a maximum either at point C or B depending only on the value of L/R and that there is a particular value of L/R for which the two field intensities are equal in magnitude - in this case 2L/R = 4,1.

Secondly for values of 2L/R>4 the field intensities at the extremities of the cylindrical charged volume exceed that at the centre in which case it would be expected that breakdown could occur first in these areas.

The question as to where a discharge will first be initiated depends also, however, upon the actual value of the field intensity required at a given point to cause ionisation and breakdown of the media at this point, and to obtain some information on this Table 4.1.1 has been compiled from the data given by Golde (1970) as to typical physical conditions within a thundercloud.

Table 4.1.1/ .....

Altitute Km	Pressure mb	Temperature °C	*Relative Air Density	+ Critical Field Intensity V/m
0	1 013	+28	0,97	$2,92 \times 10^6$
1	899	+20	0,89	$2,66 \times 10^6$
2	795	+14	0,50	$2,40 \times 10^6$
3	701	+ 8	0,72	$2,16 \times 10^6$
4	616	+ 2	0,65	$1,94 \times 10^6$
5	540	- 3	0,58	$1,73 \times 10^6$
6	472	- 8	0,51	$1,54 \times 10^6$
7	410	-13	0,46	$1,37 \times 10^6$
8	356	-18	0,41	$1,21 \times 10^6$
9	307	-24	0,36	$1,08 \times 10^6$
10	264	-31	0,32	$0,95 \times 10^6$
11	226	-41	0,28	$0,85 \times 10^6$
12	195	-50	0,25	$0,75 \times 10^6$

Table 4.1.1 Typical physical conditions within a thundercloud
* Air density relative to NTP of 1 013 mb and 20°C
+ Breakdown of air at NTP assumed to be 3×10^6 V/m.

At this juncture it is necessary to consider the intrinsic breakdown strength of air and of moisture laden clouds more carefully. In the former case, the widely used breakdown value of 3×10^6 V/m for air at normal temperature and pressure refers to the breakdown of a uniform field between two electrodes spaced one centimeter apart. If the spacing of the electrodes is increased the average breakdown strength tends to a lower value quoted by Alston et al (1968) as $2,4 \times 10^6$ V/m. However the electric stress at the surface of the electrode where ionisation first takes place, is higher than the average value, and would correspond to the actual disruptive stress which is sought, that is the intrinsic breakdown strength which could be independent of the electrode configuration. Peek (1929) showed that the field intensity for ionisation was dependent upon the radius of the electrode, and if this was very small the stress could exceed 3×10^6 V/m - however this is due to the fact that electrons must be accelerated a finite distance to cause avalanches, and if the radius was sufficiently large, ionisation occurred at a stress very close to 3×10^6 V/m. For these reasons it would appear that this is the correct value of stress applicable to air when there is no restriction due to the effect of electrodes, and has been adopted throughout for the conditions at normal temperature and pressure (NTP) below the cloud level. For temperatures and pressures, other than NTP, the intrinsic strength would vary directly as the relative air density as shown in Table 4.1.1.

When/ .....

When considering the conditions within the cloud however, the electric strength is lowered by the pressence of water drops. As mentioned earlier, this was demonstrated in the classic experiments of Macky (1931) whereby the field intensity required to breakdown a column of water drops falling through a vertical electric field was measured under varying conditions of drop size and spacing. The value of 1 x 10^6 V/m has since been accepted as a representative value for clouds containing water drops, and this according to Mason (1961) extends well above the freezing level where water may still exist in a supercooled state. The division between water and ice is not finite however but generally ice only occurs above the - 35°C level and water only below the 0°C level, and the region between is a mixture of the two which tends to more ice particles at the upper and more water at the lower extremeties.

In terms of altitude, and referring to the values set out in Table 4.1.1 the cloud may therefore be considered to be more or less homogeneous electrically from cloud base, which may be at 2 km or even less, up to at least 8 km where the relative air density lowers the intrinsic breakdown strength for air to about 1 x 10^6 V/m in any case. Above this altitude therefore, the electric strength is less than anywhere else in the cloud and the air in this region is the more likely to break down under stress should the field intensity be sufficiently high. At the boundary between air and cloud, and particularly at its base, there is a distinct increase in the electric strength - by a factor of more than two. However the presence of precipitation might alter conditions to some extent; nevertheless it is known that the spacing of water drops in rain is very large compared to that in the interior of clouds and hence the effect on the breakdown strength is likely to be minimal.

Reverting again to the cylindrical model of cloud charge distribution, which is described in some detail in Appendix I, the following tables illustrate some critical values of radius, charge, maximum charge density and potential which would occur when the field intensity is 1 x 10^6 V/m simultaneously at the centre of the charges, and at the extremities of the cylinder, that is to say when the probability of intra-cloud or ground discharge is equal.

Length L of one Cylinder	Critical Radius R		Critical Ratio 2L/R		Critical Charge Q		Maximum Charge Density x 10^{-6}	
	H=4km	H=8km	H=4km	H=8km	H=4km	H=8km	H=4km	H=8km
km	km	km	-	-	Clbs	Clbs	Clbs/m^3	Clbs/m^3
1	0,49	0,48	4,06	4,13	28	27	0,075	0,075
2	1,03	0,98	3,88	4,08	118	113	0,036	0,037
3	2,33	1,49	2,58	4,03	422	257	0,017	0,025
4	-	2,06	-	3,89	-	475	-	0,018
5	-	2,86	-	3,50	-	828	-	0,013
6	-	4,65	-	2,58	-	1 684	-	0,008

Table 4.1.2 Critical Values of Cylindrical Cloud Charge Parameters for equal probability of intracloud or ground flashes $L_o = L_1 = L$ $Q_o = Q_1 = Q$

Table/ .....

As an example of the application of the above table, if the height of the separation area is say 6 km and the length of each charged cylinder L is say 3 km then the following values are obtained:-

$H = 6 \times 10^3 m$

$L = 3 \times 10^3 m$

$2L/H = 1,0$

$R = 0,257 \times H$

$= 1,542 \times 10^3 m$

$2L/R = 3,89$

$Q = 7,398 \times H^2 \times 10^{-6}$

$= 266$ Coulombs

$q/m^3 = 0,142 \times 10^{-3}/H$

$= 0,0237 \times 10^{-6}$ Coulombs/m^3

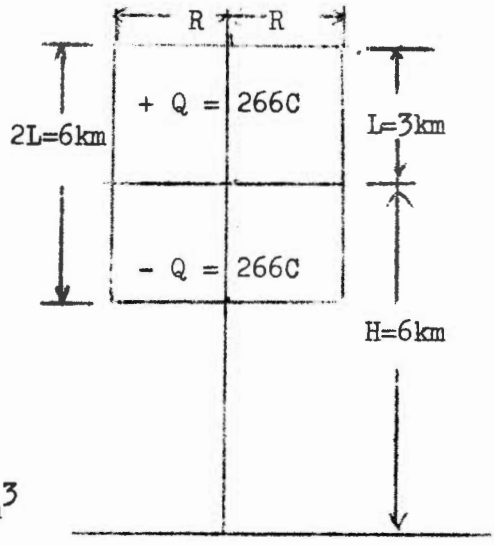

The above means that if a total charge of 532 coulombs of both signs is distributed in a linear manner in a cylinder of radius R symmetrically placed with its centre at 6 km altitude and of the dimensions given, the field intensity at the lower extremity will be equal in magnitude to that at its centre, and will be the critical value of 1×10^6 V/m for ionisation and breakdown. If the cylinder has a larger 2L/R ratio than the above, the field intensity at the lower extremity would exceed that at the centre (or charge separation area) and a breakdown towards earth is more possible.

In the meteorological sense, if charge separation was occuring over a circular area of say 1,54 km radius, at an altitude of 6 km, an intra-cloud flash would be more likely to occur until the charges have separated over an equal distance above and below the centre of at least 3 km. Once the $\pm$ 3 km mark is passed, however, a ground flash from the lower extremity is more than likely.

Exactly at the $\pm$ 3 km distance a charge separation of $\pm$ 266 coulombs would be necessary to produce breakdown in either direction. At separation distances of less than $\pm$ 3 km, that is during the early stages of the separation process, a charge separation of less than $\pm$ 266 coulombs would either produce an intra-cloud flash or no discharge at all; on the other hand, at separation distances greater than 3 km a charge of more than 266 coulombs would be required to initiate a flash but having attained the necessary value, a ground flash would occur.

5. The/ .....

5. The Electrical Breakdown Process Within the Cloud

There is much evidence that the rate of charge accumulation in a thundercloud cell is a relatively slow process, taking minutes to reach the critical values for breakdown (Workman 1967) whereas for discharges to ground up to 10 coulombs may be neutralised in a few milliseconds and 100 coulombs or so in about a second. The break= down process in the cloud therefore must make the charge available quickly and the charge must be able to move rapidly to satisfy this condition.

Taking firstly the case of the intra-cloud breakdown, the amount of charge bound on charge carriers in the high field inten= sity area in the centre is limited, most being accumulated in the extremities of the cell.

When the field intensity reaches a critical value for ionisation, breakdown will occur in this area perhaps considerably remote from the bulk of the charge which is inducing the field intensity, and any theory of breakdown must of course explain how these bound charges become involved.

It/ .....

It is not the purpose of this paper to try to explain in detail the breakdown mechanism, since this is bound to be quite complicated, but certain fundamental observations may not be out of place. Firstly this breakdown occurs in the centre of an extended field and in an area where there is only a sparse charge distribution, and as soon as any of the opposing charges begin to be neutralised, the overall field intensity starts to collapse, and it continues to do so until it is almost zero - despite this, the discharge con= tinues to the end.

It would appear therefore that an actual current carrying arc developes in this region and extends simultaneously in both the upward and downward directions towards the main location of charges of opposing polarity, as illustrated in the following Fig. 5.0.1(a)

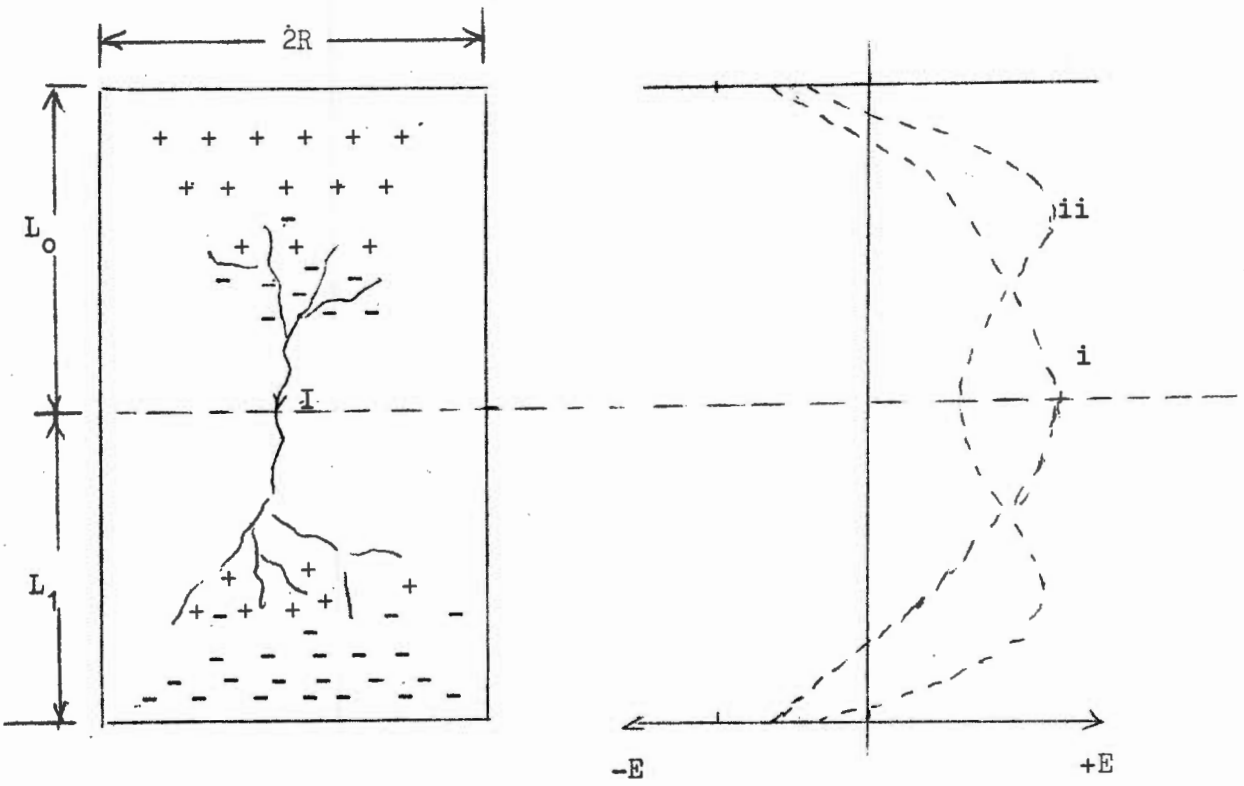

(a) Diagram of Arc Discharge (b) (i) Initial Field Intensity
(ii) Developed Field Intensity

Fig. 5.0.1 Diagram indicating growth of arc column during intra-cloud breakdown.

The/...

The voltage gradient required to maintain this arc is very much less than the value of the field intensity in the neighbour= hood, and hence it should grow rapidly in length, and this it may do by means of streamers which in the case of those uppermost contain negative ions and electrons at the tips which neutralise positive charge in the area, and vice versa at the lower end
During this process the field intensity pattern changes, and looks possibly like that which would be produced by two isolated spherical charges. In this event the field intensity at the extremities of the advancing streamers is accentuated thereby assisting the break= down in this area as illustrated on Fig. 5.0.1(b).

The field change produced by such a discharge is slow and continuous, taking about a second or more, but superimposed thereon are a multiplicity of so called "spikes", named "K" changes which according to Brook and Kitagawa (1960) are dispersed at intervals of about 680μs. These could well be due to spasmodic extension of the streamers in small steps similar to but much slower than the stepped leader of ground strokes. This would be consistent with the notion that both polarity of charges are bound upon carriers which could conceivably form small pockets of charge dispersed generally throughout the charged area.

A further aspect of the above described mechanism, which is however common to all forms of lightning discharge, is the necessity to explain how single arc channels are produced when the charges which are being moved are dispersed over a considerable volume of space. It seems that an arc channel may start at a particular point where the field intensity is highest, and there= after all discharge paths from many directions pass through this point. A means whereby streamers and filaments can be formed in directions other than the prevailing direction of the main field must therefore be found.

6. The Breakdown Process at the Cloud Top

Theoretically a discharge from the concentrated positive charge at the top of a cloud is possible, but in practice it has not been observed very frequently. Mackerras (1968) refers to high-cloud discharges however, and on some occasion a bright spasmodic luminosity is observed to take place in that region, sometimes very actively, but on very few occasions is an actual arc channel visible - indicating that these may in fact be the termination of discharges within the cloud itself. Disregarding the earth, the nextnearest conducting plane is the electrosphere (Malan 1967) some 50 to 60 km in altitude, and this is hardly a likely target for a discharge. More possible perhaps is a discharge directed through or around the charge separation area to the seat of negative charge in the lower reaches of the cloud. Visible arcs around the outside of clouds have certainly been photographed.

However it is perhaps more probable that owing to the greater conductivity of the upper atmosphere, and the ionisation taking place there due to cosmic radiation, positive charge is dispersed quite rapidly by way of ionic conduction or leakage currents. Alternatively the charge is more widely dispersed than indicated by a cylindrical model so that the field intensity in that vicinity rarely reaches ionisation levels before that in the centre between the charges.

It is/...

A recent paper by Brown et al (1971) somewhat supports what has been discussed above. They calculate that the upward directed electric field from the conventional bi-polar thunderstorm cell will concentrate fast negative ions in the vicinity of the cloud top forming a dense screening layer. These negative ions will be drawn from the clear air above the cloud and are able to exert electric fields close to breakdown intensities. However these calculations are based upon the establishment of an electric field deep within the cloud and they do not consider what would happen with the emergence of positive charge carried upwards towards the so-called screening layers. Hence whilst this postulation appears to be sould it also follows that the negative ions entering the channel top would very soon be neutralised by the positive ions raised towards them.

Several investigators have detected radar echoes from the top of cloud turrets. In particular Workman (1967) refers to descending areas of reflectivity which always proceeds a lightning discharge within the cloud. Such echoes might of course be due to descending charge carriers, but it is also possible that they emanate from areas of ionisation or ion-recombination which would also tend to descend as the positive charge on the carriers is neutralised by the descending negative ions forming the screening layers.

Finally it is clear that the neutralisation of the positive charge in the upper cloud or its escape due to ionisation, will create conditions more favourable to the production of ground flashes from the lower negative charge.

7. The historical background to the mechanism of a lightning discharge to ground

One of the earliest explanations of the sequence of events describing a flash of lightning was evolved by Schonland (1938) and this was later modified by Bruce and Golde (1941) and is depicted in Fig. 7.0.1. Schonland considered that negative charge was lowered by the leader stroke from an isolated charge in the cloud and upon contacting earth, this charge was neutralised by an upward moving positively charged column which eventually penetrated the cloud until the channel became neutral. The development of a streamer from a new neighbouring charge to the partly ionised channel served to explain a subsequent stroke of the same flash.

The lowering of negative charge in the first instance appeared to be confirmed by the observed resulting field change, whilst the upward moving neutralisation process coincided with the bright luminous return stroke which traversed the distance at a velocity of about one tenth of that of light. Schonland surmised also that subsequent negative streamer from a neighbouring charge centre having a velocity equal to that of the leader stroke, namely from 1 to 2 x 10^5 ms, would need to transverse from 3 to 6 km to account for the observed pause of about 30 ms between the first and a subsequent stroke of a multiple lightning flash.

Bruce and Golde on the other hand considered that it was more probable that after the neutralisation of the negative charge on the leader, the channel would become positively charged instead of neutral. It was more reasonable to suggest therefore that a positive streamer would develope towards a neighbouring negative charge centre. Upon

contact/ .....

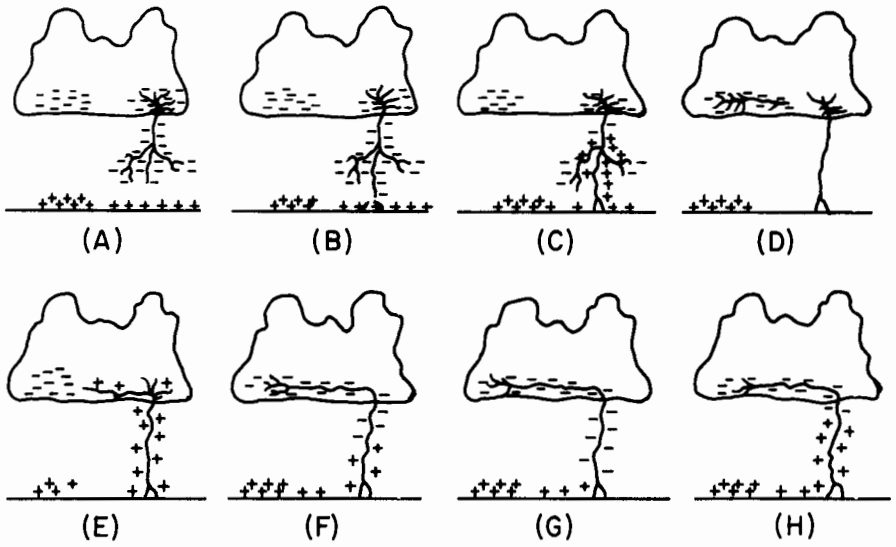

FIGURE 7·0·1

DIAGRAM ILLUSTRATING LEADER AND RETURN STROKES – (A) TO (D) SCHONLAND – (A) TO (C) AND (E) TO (H) BRUCE AND GOLDE (1941)

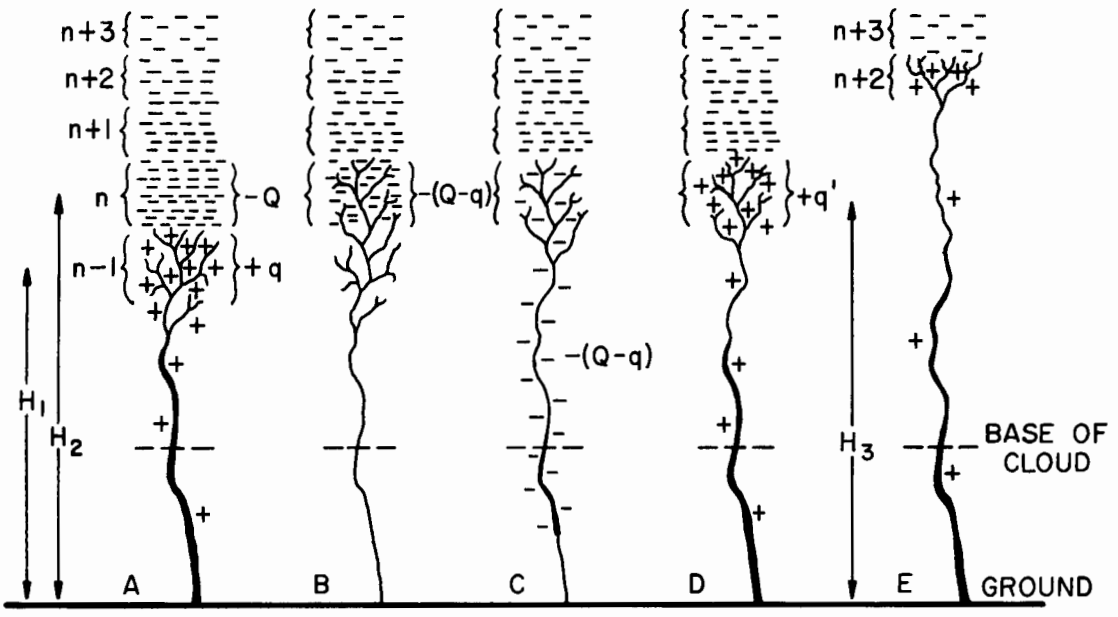

FIGURE 7·0·2

SEQUENCE OF EVENTS FOR GROUND STROKES SCHONLAND AND MALAN (1951)

contact with this centre the negative charge would now decend the leader channel followed by an upward moving positive charge which neutralised it to complete the process.

Both viewpoints assumed therefore that the negative charge in a thundercloud would consist of a number of isolated pockets which would be discharged one after the other, thereby accounting for the multiple subsequent strokes of a flash which according to the photographic observations of Schonland and Malan could be as many as fourteen.

Ten years later Schonland and Malan (1951) postulated a tentative theory based upon their observations of the field changes which occured during the intervals between strokes which they had termed "junction" or J-field charges and which appeared to indicate that the subsequent strokes of a flash tapped negative charge centres which were situated at higher and higher levels and that these charges were in fact contiguous.

A revised sequence of events was therefore proposed as indicated on Fig. 7.0.2. The negative charge in the cloud was envisaged as a vertical column which was tapped by each successive leader by lowering negative charge to earth. After contact with the earth the charge on the leader was neutralised and replaced by positive charge which concentrated mainly in the area in the cloud below the remaining negative charge. The so-called J-process then consisted in the neutralisation of this charge by a relatively slow advance of positive streamers vertically into the negative charge in the cloud. They supported this argument by referring to measurements of the velocity of positive streamers by Malan himself, and by Allibone and Meek (1938) which gave values of the order of 3×10^4 m/s whereupon the distances traversed in 30 ms would be of the order of one kilometre.

Hence not only did this explain the tapping of charge at successive increments of height of about 1 km, but also it accounted for the median delay time of about 30 ms between the successive strokes of a multiple flash.

In further confirmation of this notion Hewitt (1957) showed by means of radar observations that the successive strokes of a flash proceeded from areas in the cloud which were consistently at higher altitude. Finally Brook, ε Kitagawa and Workman (1962) using one of the methods prescribed by Schonland and Malan, confirmed again that the apparent leader height increased with the stroke order.

Whilst this proposal now appears to be well established it is still difficult to envisage how successive strokes may occur for reasons which will be described in the following section.

The amount of charge dissipated per stroke, according to Bruce and Golde (1941) and more recently Berger (1971) is of the order of 8 coulombs whilst the mean time interval between strokes of a flash according to Malan (1956) and confirmed in this investigation was between 50 and 60 ms. Hence the average rate of charge accumulation would require to be about 150 C/s to sustain such a discharge for successive strokes. The mean recovery rate of thunderstorm cells on the other hand is of the order of 10 to 20 seconds (Workman 1967) and hence it appears to be completely outside the realms of possibility

that/ .....

that multiple stroke flashes could be sustained by the normal charge separation process since from 750 to 1500 C would need to be seper= ated to meet this requirement.

However the sequence postulated by Schonland and Malan fits the cylindrical charge model very well, and according to this model, the neutralisation of successive portions of charge would reduce the length of the lower negatively charged cylinder. This would in turn result in a lower field intensity which would tend to be below the initial ionisation level, of say 1 x 10^6 V/m, thereby inhibiting further breakdown. Hence it must be concluded that either the ion= isation level must be maintained by other means, or in fact it must in itself be lower once breakdown conditions have been initiated or both. However, before giving detail consideration to the events subsequent to the completion of the return stroke, the probable process from the start of ionisation in the cloud is first of all examined.

8. The iniation of the downward leader stroke

According to the cylindrical model of cloud charges outlined in Section 4, the cloud charge separation process proceeds to a point whereby its physical dimensions and charge quantity favour the attainment of a vertical field intensity at the lower extremity just equal to the level required for ionisation and breakdown of the media in that region. Assuming that charge separation occurs above the freezing level it is most probable that the altitude of the breakdown area could be from two to three kilometers or so below, namely, where the cloud consists mainly of finely divided water drops at temperatures possible above zero.

The air in this region becomes ionised over a restricted area and this entails orientation of the products of ionisation such that positive ions are created close to or within the negative charged volume thereby tending to neutralise negative charge which is bound on the cloud droplets or other carriers, whilst free elec= trons tend to be expelled downwards in the direction of the field towards the earth. This is illustrated in Fig. 8.0.1 below.

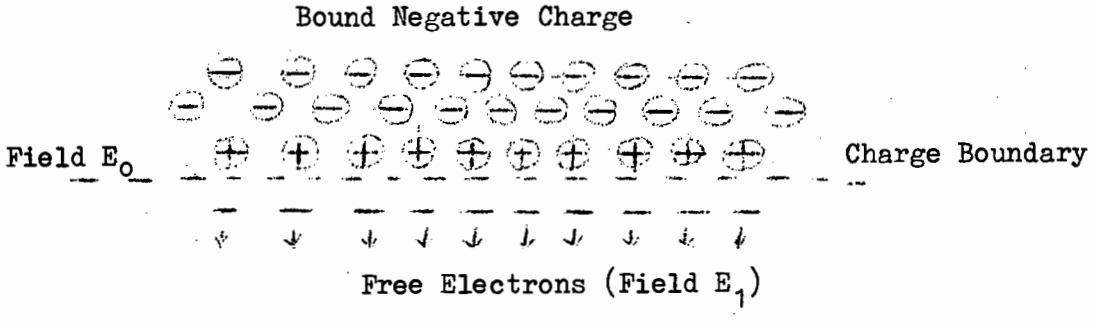

Fig. 8.0.1 Effect of ionisation at negative charge boundary in cloud

It is clear from Fig. 8.0.1 that the possibility exists that the effect of ionisation is merely to separate charge such that the bound negative charge is virtually converted into mobile electrons which move from the boundary in the field direction. The initial ionising field intensity E_o at the boundary is thereby reduced, but

owing/ .....

owing to the virtual elongation of the dimensions of the cylindrical charge, the field intensity below the electron charged volume is increased so that further ionisation takes place and the electrons continue to move downward.

Physically it would be expected that this reaction would take place in a somewhat confined area where the concentration of bound negative charge is greatest, and that it would be accompanied by minute spark channels which would tend to join up forming the first manifestation of an embryo arc or spark channel which eventually becomes the downward leader stroke.

One of the basic properties of such arcs or sparks is that they consist of a conducting plasma of ions which are mobile and in which, by induction from the electric field causes electrons to migrate and concentrate at the lower tips thereby concentrating positive ions at the top end close to the negative bound charge. If the distance between these ions and the negative bound charge is small a high field intensity will be maintained. This is diagramatically illu= strated in Fig. 8.0.2.

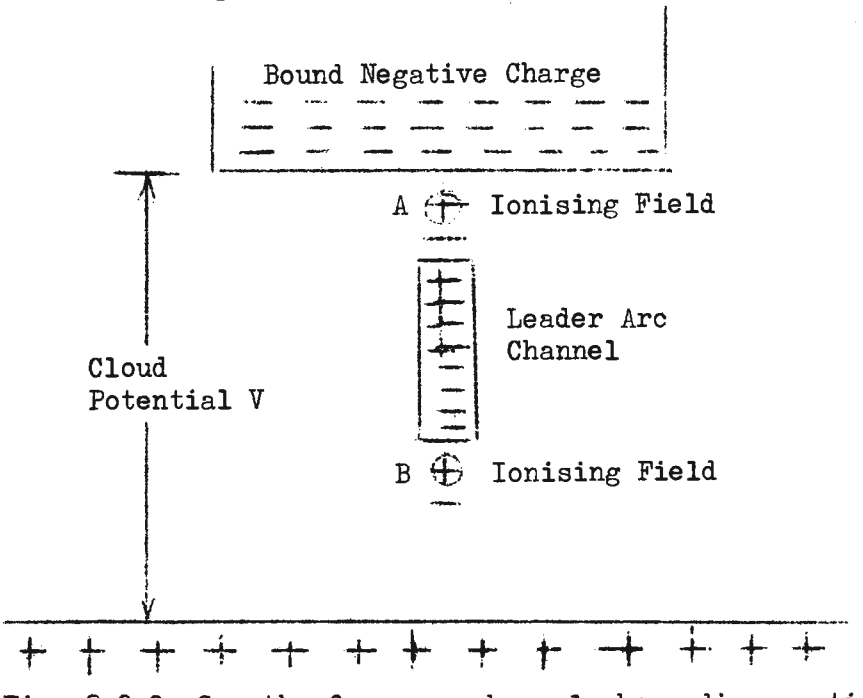

Fig. 8.0.2 Growth of an arc channel shown diagramatically

In the area "A" near the charge boundary the field intensity must be sufficiently high to cause ionisation of the air ahead of the tips of the channel, and this can be ensured if the field created by the bound negative charge when reinforced by the positive charge in the tip of the arc is large enough, and this will be so expecially when the distance between the tip and the bound charge is small. Ionisation of the air will create positive ions ahead of the channel which will advance relatively slowly and this will elon= gate the channel. The released electrons on the other hand migrate rapidly down the channel. The elongation of the positive tip to= gether with the migration of electrons from the vicinity tends to increase the field intensity at the tip temporarily so that the velocity of the positive ions increases until such time as the tip reaches bound negative charge. When this occurs some of the positive ions combine with the bound electrons and field intensity is there= by temporarily reduced.

Meantime/ .....

Meantime at the negative extremity of the channel at "B" - an additional electron is accumulated for each positive ion created at the top end, so that provided that the concentration of electrons is sufficiently large, an ionising field intensity can be created ahead of the negative tip also. In this case, for each ion pair formed ahead of the tip, an electron from the tip combines with the positive ion leaving a free electron, hence the channel extends itself physi= cally from one positive ion to the next.

Regarding the arc channel in isolation, it must contain as many free positive ions at the top end as it has free electrons at the other, and its extension in both directions would depend on the field intensity which each end is capable of producing. This in turn depends upon the amount of charge in the tips and upon the magnitude of the intensity of the main field in which the arc is produced.

However when the one end of the channel, in this case the positive end, is close to the bound negative charge area, the temporary intensification of the field assists to extend the channel more rapidly and eventually it reaches the bound negative charge and neutralises some of it.

When this happens the balance between electrons and positive ions in the arc channel is changed, and there are then more elec= trons at the lower negative end of the channel, the excess being equal to the amount of bound negative charge neutralised at the positive end of the channel. The arc channel therefore acts as a means whereby charge is virtually moved from the bound negative charge volume to the negative tip of the channel. However it is to be noted that in this mechanism current flows in the channel only during the extension of the positive tips; on the other hand charge transfer is effected by virtue of neutralisation of positive ions in those tips and no current flows. Hence if the positive tip channels have to negotiate a path ahead of them where there is no bound charge, they will do so rapidly because of the field intensi= fication which takes place as they advance and during this advance electrons are migrating in increasing quantity thereby tending to cause an increase of current in the arc channel. When the tips encounter bound negative charge however, this advance is temporarily halted owing to the neutralisation process which then takes place and during which no current flows along the arc. It follows also that extensions of the positive end of the channel will produce extensions at the negative end as well because of the intensification of elec= trons which occurs.

It would be expected that the negative charge in the cloud bound as it is on charge carriers such as water drops or other heavy carriers, would tend to be fairly evenly distributed volumetrically and there= fore extensions of positively tipped sparks would be short and interspersed with neutralisation of each droplet; consequently assum= ing that there would be very many of such minute reactions taking place, the nett effect overall would be that the extension of an arc channel would occur virtually simultaneously with the neutrali= sation of bound charge ahead of it.

It has been shown however that when charge is virtually moved from the area around the positive tipped streamers to a position at

the/ .....

the lower end of the channel, the field intensity at this positive end tends to fall and the reaction would therefore tend to stop unless the positive ion concentration could be increased to offset it.

Since as illustrated in Fig. 8.0.2 the plasma channel forming an arc or even a spark is conducting and is situated within the main electric field existing between the cloud and the earth, equal positive and negative charges are induced towards the two extremities respectively, as a result of induction from the main field, and this effect intensifies as the channel lengthens to bridge the gap between the main charges of the electric field. This process is illustrated in Fig. 8.0.3 which follows:-

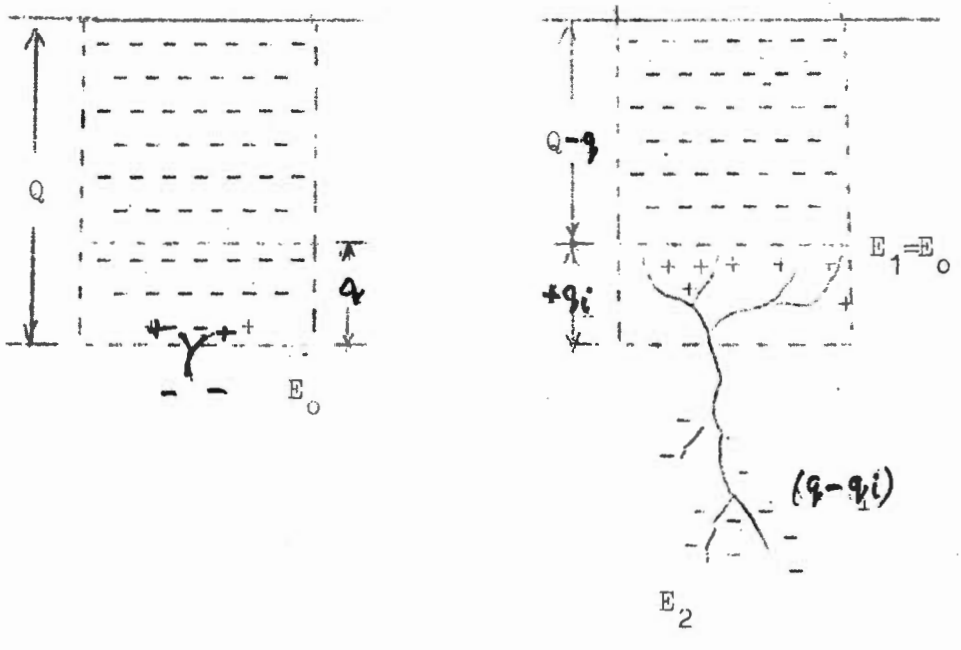

Fig. 8.0.3 Diagram illustrating development of the leader stroke with induced charge to maintain ionisation fields E_o, E_1 and E_2 simultaneously

Fig. 8.0.3 (a) indicates a volume of bound negative charge Q which has just attained an ionisation field intensity Eo at its base; sparking is initiated in this area with ion orientation such that the upper tips contain positive ions, whilst the lower tips contain electrons in sufficient concentration to ionise the air ahead of them.

In Fig. 8.0.3 (b) the spark channels have developed into fully fledged arcs which progress by the mechanism described above until a negative charge "q" has been moved from its original position as part of the bound charge Q to the lower extremities of the leader channel. The field intensity E_1 at the new boundary would have fallen below ionisation level were it not for the charge $\pm$ "q_i" which is induced in the conducting plasma of the leader arc channel merely by the migration of electrons to the lower end, so that the positive ions intensify the field at the upper end. The charge in

the/ .....

the lower extremities is therefore made up of the negative counter part of the induced charge q_i together with the negative charge "q" which was virtually removed from the bound charge in the cloud. The field intensity E_2 at the negative tip of the advancing leader is reinforced by the addition of this induced charge as the tip progresses, but the charge must be concentrated within a sufficiently small volume to ensure that the field intensity is high enough for ionisation to take place otherwise it could not make progress.

Since the induced charge q_i is a function of the length of the leader channel with respect to the main inducing field it is clearly necessary for a balance to be maintained between the rate at which the leader advances and the rate at which bound negative charge in the cloud is neutralised, if the progress is not to be interrupted. For example if the velocity of the tips is very slow, or slows doen the amount of induced charge q_i generated may not be at a sufficiently high rate to maintain the field intensity in the cloud E_1 at ionisa= tion and the process of neutralisation will stop. This could be what happens in the case of the stepped leader.

On the other hand it would seem necessary to assume that the mechanism contains an element of elasticity in order to explain the stepped leader fully, or for that matter, the progression of the leader itself. In the latter case when the field intensity below the cloud charge reaches ionisation level, a small amount of charge neutralisation immediately lowers the field intensity again below the initial level, and according to the mechanism proposed, positive ion reinforcement would be required to start from the first instant if the reaction is to be able to continue without interruption. Similarly with regard to the stepped leader, the lower tip may be capable of self propagation at a lower velocity without the assistance of charge reinforcement due to the advance of the positive streamers at the top but as a consequence of a moderate charge increase induced as a result of the increase in length of the channel. However this may not be capable of continuing indefinitely if the velocity of advance of the leader is not sufficient to ensure that the field intensity ahead of the tip is sufficiently high to maintain ionisation field.

If on the other hand it is postulated that the value of field intensity required for the initial ionisation is higher than that required to maintain it the above difficulties are overcome. This is no new hypothesis in certain related fields - for example corona discharge inception and extinction or even the properties of the arc itself, both as regards the potential required to maintain it together with the photo-emission from the ion colision and recombi= nation processes taking place in the plasma. Certainly in the case of neutralisation of negative space charge by positive ion penetration the emmission of energy resulting from such recombinations may well assist to maintain the ionisation process at a lower breakdown level than initially.

Hence if the field intensity at the positive tipped end of the channel reaches an initial critical value for ionisation, the posi= tive streamers may now advance until the field intensity falls below a lower limit which will not support ionisation and they then cease, or at the least, slow down considerably. This impulsive advance would give rise to a pulse of current down the stroke in order that electrons may be conveyed to the negative tip and the velocity

of/ .....

of this pulse would be expected to be high since the process involves the transfer of electrons through the conducting plasma of the arc. Schonland (1938) indicated that the step darts of a leader are observed to have a velocity in excess of 1×10^7 m/s. This was of the same order as that of the velocity of advance of the luminous tip of the return stroke, and also of the dart leader of subsequent strokes. This phenomenon is consistant with that of a current surge along an ionised path.

The pause time between steps of the leader would, according to the above postulation, be due to the time required for the field intensity at the positive end of the channel to rise again to the higher initial value and this therefore depends upon the velocity of advance of the so-called "pilot" streamer of the leader stroke the existence of which was postulated by Schonland but not actually observed by him. This is also in agreement with Schonlands statement that he found a linear relationship between the pause time "t" and the length of the step "l" such that if the duration "t" increases it was followed by a corresponding increase in length of the step such that l/t was in fact the effective velocity of the tip of the pilot leader which he then surmised must exist.

Schonland rejected the notion of a travelling surge down the leader on the grounds that "such an explanation must always give a pause time which increases with the length of the channel and such an increase is not observed".

This objection does not apply in this case because the pause time is herein defined as the time required for the field intensity at the positive end of the channel in the cloud to build up to ionising level again, and this is related to the velocity of the leader. The longer its length the greater is the amount of induced charge available at both extremities and hence if the velocity of the leader is high enough it could ensure that the field intensity at the positive end does not fall below ionisation and no pause will occur at all. This is in fact the case for the dart leaders of subsequent strokes which are not stepped.

Schonland on the other hand regarded the pause time as the time necessary for the field at the lower negative tip of the channel to approach the critical value for ionisation whereas the present submission is that if the negative tip is to advance at all, the field intensity at the tip must already have attained its critical value. If this were not so it is somewhat difficult to explain not only how the pilot streamer continues to advance but also by what mechanism a signal is transmitted to the top end of the channel to initiate the downward step dart. Furthermore Schonland identifies the minimum velocity observed for the pilot leader of about 1×10^5 m/s with that of the drift velocity of electrons in avalanche in a critical field intensity of about 3×10^6 V/m in front of the tip below which ionisation by electron impact cannot occur. It is obvious however that this does not explain how the velocity can be larger, since the maximum observed for the leader is about 2×10^6 m/s, although the majority do not exceed 5×10^5 m/s.

It is herein submitted that the velocity of the leader tip is not primarily dependent upon the field intensity ahead of the tip since this cannot exceed the minimum level for ionisation which varies over a restricted range. It is however dependent upon the

concentration/ .....

concentration of electrons within the arc channel and this concentration is in turn dependent upon the amount of charge accumulated both as a result of the advance of the positive tipped end and also by induction as the leader channel increases in length within the main electric field. The dimensions of the leader tip will be automatically adjusted to maintain ionisation at the tip and also axially to maintain the potential, and it is the latter which mainly determines the velocity of propogation as will be made clearer in the following section which discusses this aspect.

The remarkable constancy of the observed pause time of between 50 and 90 μs despite leader velocities which vary by more than a factor of five, suggests that no correlation exists between the velocity of the leader and the rate of restoring ionisation in the cloud. The density of bound charge in the cloud can vary however and neutralisation of charge to below ionisation levels may involve larger or smaller volumes of charge with consequently differing lengths of path over which the positive streamers must be developed. If the charge densities are high, these distances over which neutralisation occurs are smaller whereupon pause times for the stepped leader should be shorter for what may be identifal velocities of propagation of the remote leader tip, which is unaffected by small variations in the cloud charge density.

Some support for this notion is evident from the work of Brook and Kitagawa (1960) in which a comparison is drawn between the pulse interval occuring during the leader stage of intra-cloud strokes and ground strokes. They found that for the latter a mean value of 80 μs was obtained which agrees with Schonland's observation. However, for intra-cloud strokes the mean value of the pause was 680 μs or a factor of 8,5 times that for ground strokes. As pointed out in section 4 and 5 herein, intra-cloud flashes occur in regions where the variation of field intensity with distance is small - particularly in the charge separation area where the charge density tends to zero. Consequently if ionisation does occur it is likely to extend over a much larger distance than for ground flashes where the field gradients are high and the corresponding ionisation distances comparatively small especially close to the boundary of the charged volume.

Whilst the minimum velocity of negative streamers has been stated to be 1×10^5 m/s that of positive streamers is much less - of the order of 1×10^3 m/s being that of the drift velocity of positive ions in an avalanche; the distance traversed at this velocity during a pause time of say 100 μs would be only 0,1 m. The extension of the positive tipped streamers however is mainly a function of the rapidity with which ionisation can take place ahead of the channel and the actual velocities are at least an order of nagnitude higher. Velocities of from 1,6 to $3,6 \times 10^4$ m/s have been measured by Malan (1951) and Allibone and Meek (1938) who found values of from 2,1 to $2,6 \times 10^4$ m/s, so that larger traverse distances are indeed possible.

Considering that in the cloud charge region, the charge bound on each individual charge carrier has to be released by a spark, the mean value of the velocity of advance of streamers over a large area is likely to be very much less that that for an individual streamer. For example the leader itself may traverse the distance of say 4 km to ground in 40 ms at minimum velocity whereas in the same interval, the positive streamers could traverse 1,44 km at a velocity of $3,6 \times 10^4$ m/s but much less at the mean value. Such

distances/ .....

distances are commensurate with those indicated by the cylindrical model of the negative cloud charge. As already shown in section 4, the field intensity is zero within a distance of about one fifth of the cylinder length from the lower extremity, and the maximum length for the negative charged cylinder is unlikely to exceed 5 km.

To summarise this section so far, therefore, it is submitted that a positive charge is needed at the junction of the leader arc system and that of the bound negative charge in the cloud in order to maintain the field intensity level of ionisation during the advance of the leader downwards. This positive charge is available as a result of the effect of the main electric field which induces a positive charge at the top of the conducting arc system by means of a corresponding displacement of negative charge or electrons towards the lower extremities of the leader channel.

The charge on the leader channel therefore includes the negative counterpart of the induced charge, in addition to the charge equivalent to that of bound cloud charge neutralised during the process.

The maintainance of ionisation levels at the extremities of the leader channel is cricitally dependent upon the rate of advance of the leader tip since the amount of induced charge increases proportionally with the length of the channel.

Charge is transferred down the channel during the extension of positive streamers, but when these encounter negative charge and neutralise it no current flows. If the velocity of advance of the leader is too slow, the induced charge generated may be insufficient to maintain ionisation field at the extremities of the positive streamers, and the process of neutralisation would tend to stop.

If on the other hand the field intensity required to produce ionisation in the cloud is assumed to be higher than that required to maintain it, ionisation when once started may then proceed over a finite distance, thereby releasing bound charge over this distance. A pulse of current would arise as a consequence of the sudden electron migration to the lower end of the channel. This would afford a comprehensive explanation of the bright step dart which proceeds down the channel at a high velocity until it reaches the tip of the slow moving pilot streamer.

However, since it has been found necessary to assume that there is an increasing accumulation of positive charge in the form of ions at the channel top, the spasmodic ionisation described would result in neutralisation of some of this charge by recombination with bound negative charge without causing a migration of electrons to the lower end and the field intensity will fall temporarily below ionisation. This will result in a pause until such time as the field intensity increases again as a consequence of the advance of the leader which results in an increase in the induced charge.

The bright steps are therefore identified as due to current surges which take place as a result of the spasmatic extensions of the positive tips through the volume or over the distance where no bound negative charge exists, whilst the pauses result from the short periods of neutralisation after which the field intensity has again to be built up, before the positive streamers can restart.

At/ .....

At this juncture it is pertinent to refer to the exposition by Loeb (1966) regarding the initiation of a leader stroke. Firstly he postulates the existence of a small positive charge beneath the negative charged volume; this charge moves upwards towards the main negative charge thereby increasing the field intensity to between 0,7 and 1,0 x 10^6 v/m, as found by Macky (1931). At this value of field intensity water drops will elongate producing positive streamers having velocities from 5 x 10^4 up to 1 x 10^6 m/s, but a value of 2 x 10^5 m/s is taken as being representative. As a result of the observations of other investigators he then states that the positive streamers will direct themselves upwards in the form of an inverted cone, thereby neutralising negative charge and virtually funnelling the area down to a smaller one represented by the apex of the cone which is also propagating downwards forming the start of a leader having a radius of 0,5 to 1,5 m. In this way he explaines how the leader collects charge over a wider area and reduces it to a small area by the conical funnel arrangement postulated.

The funnelling model appears to be very useful and is certainly needed to explain the mechanism in the final analysis. However there are some difficulties in regard to what happens once the initial positive charge has been neutralised since the funnelling process would cease. However it is considered that in view of the mechanism now proposed it is unnecessary to postulate the pre-existence of a small positive charge. It is adequate that streamers with positive tips develop when the field intensity produced by the main cloud charge concentration is sufficiently high, and these streamers must diffuse into the bound charge in a divergent manner as described by Loeb whilst retaining the arc channel at the apex for propogation downwards.

There will later be some quarrel over the maximum diameter stated by Loeb for the leader channel of 1 to 3 m, which however may be resolved when the source of light emission from the channel is considered. The very high positive streamer velocities compared with earlier measurements of the order of 1,5 to 3,5 x 10^5 m/s are also discussed with relation to a model, but it is now clear that the extreme divergence of these streamers both latterly and upwards would give rise to a mean velocity of advance into the main negative charge which is much lower than the tip velocity of individual streamers.

In this dissertation, the reason for the stepping of the leader has been attributed to pauses in positive streamer advance due to intermittent lowering of the field intensity. When the leader has advanced sufficiently to reinforce the positive ion charge in the tips (by induction) they advance again over a short distance and this sends a pulse of electrons down the channel. This would be somewhat similar to what Loeb describes as an "ionising wave of potential gradient". However, his explanation of the stepping process is different and is summarised as follows:

Referring to the leader advancing is small steps of length "ℓ" m - remarkably constant at about 100 m - the field ahead attenuates as a result of dissipation by repulsion forces in the electron cloud, also as a consequence of energy dissipation by ionisation and excitation and the leader nearly ceases to advance after a distance $\ell/2$.

Then/ .....

Then follows a description of upward positive streamers increasing in velocity as they meet the downward moving charge until a lack of continuity of current occurs, whereupon a spacewave of potential gradient accompanied by ionisation sweeps down over the distance "ℓ" to the end of advance of the pilot streamer. Such space waves have been observed and reported.

At the end of the pilot leader advance the space wave of potential gradient restarts the advance downwards, but it is also partially reflected upwards causing reionisation but little luminosity. This gives rise to a series of pulses up the channel at intervals proportioned to the length "ℓ".

Above the cloud base the channel is expanding and the upward waves weaken in intensity. Despite this they still seem to neutralise the cloud charge higher up as the positive water point coronas expand draining more of the charge in the negative cell.

Loeb maintains therefore that the conductivity of the channel is maintained by the drainage resulting from the space waves associated with downward negative and upward positive streamers. This suffices to keep the channel conducting for tens of milliseconds of the streamer movement. It is therefore not essential to invoke an ultra high potential and a constant gradient in excess of $x/p = 3 \times 10^3$ v/m to maintain conductivity.

The similarities between Loebs hypothesis and this dissertation are that the pilot leader can only advance if the field intensity created ahead of it is sufficient to ionise the air, and that the stepping pulses come from above and pass down the channel. Also in both theories there is a stated tendency to a discontinuity of current which must be revived. But whereas Loeb envisages the leader tip as being responsible for the near stoppage and elliciting counter action by means of an upward space wave, this paper suggests that as the pilot progresses - and provided that it does so, more negative charge is induced in it as well as positive ions at the top end, which soon gives rise to a fresh breakdown in the cloud which in turn precipitates a downward surge.

At this point it is pertinent to review the alternative suggestion of Bruce (1944) referring to the discovery of the "glow" as opposed to the "arc" regime of spark channels. A high potential of the spark channel relative to the surrounding media gives rise in the first instance to a corona discharge of low luminosity, namely, a glow discharge, which is sustained by a current of the order of milliamperes. As the channel lengthens however, the current flowing increases steadily till at a value of about one ampere there is a sudden transition to what he calls an arc condition which is accompanied by a still further sudden increase in current to about hundred amperes. Since an arc has a negative resistance characteristic, this glow to arc transition is also accompanied by a reduction in voltage gradient along the channel by a factor of ten or more.

Since from section 4, the negative potential at the start of the leader is likely to be of the order of 10^8 to 10^9 volts according to the charge and height above ground, the potential along the leader rises towards the tip depending upon the current flow. At first this is likely to be small since it has only to supply the

induced/ .....

induced charge, and any losses due to corona which in the first instance will be small because the difference in potential to that of the surrounds will initially also be small. The potential gradient along the leader will be high, so that the rise in potential of the tip would tend to follow that of its surrounds but is probably less and the difference would increase. This would continue until glow to arc transition occurs, and what might then be termed a space wave of potential gradient must occur to readjust the potentials to suit the new condition. This according to the present submission will call for an increase in the induced charge on the leader and hence an electric pulse down the leader - as discussed in a later section.

For the next step to take place in a similar manner, glow conditions must again be reverted to for the whole channel and this is probably not possible because if corona conditions were sufficiently established before the change, they would be even more established after an infusion of more charge, and arc conditions should thereafter prevail. This is even more acentuated when the leader approaches nearer to the earth.

The other perhaps conclusive factor against this theory is that only one coulomb of charge deposited at the rate of one ampere would require one second. Not only is the charge known to be much larger, but also the time is much shorter, hence the current at least at the top end of the channel must be many amperes. If one could visualise a negative streamer emanating from the end of the last step, however, glow conditions might be possible for just this short extension until an arc extends it as the bright step which would also call for a pulse of electrons from the top end.

9. The charge distribution on the leader channel

Malan (1963) and also Schonland were of the opinion that the charge along a leader channel is distributed uniformly along its length and the support for this statement lies primarily in the magnitude of the observed field change. Bruce and Golde (1941) on the other hand considered that the charge is distributed exponentially with more charge situated towards the lower negative tip. Their contention is that if the leader is assumed to be a conductor charged at high potential, the charge will distribute itself according to the capacitance to earth along the leader which is known to decrease as the height above ground increases if the radius of the channel is assumed to be constant. Experimental proof was also obtained for this by means of simulating the conditions in an electrolytic tank.

The evidence in support of a uniform charge distribution is based upon the premise that the field change during the leader progression to earth should equal that of the field change during the return stroke when the distance D of observation from the stroke is large compared with its height H. The calculations are given by Anderson (1969) and these show that provided the amount of charge dissipated during the return stroke is equal to that lowered by the leader then

$$Er/Es = [\,1 + (D/H)^2\,]^{3/2} \left\{ (D/H)^{-1} - [\,1 + (D/H)^2\,]^{-\frac{1}{2}} \right\} \quad .. \quad (9.1)$$

Where Er is the return stroke field change and Es is the total field change. It can be shown that in the limit, when D/H approaches

infinity/ .....

infinity, Er/Es approaches the value of $\frac{1}{2}$ and this is already substantially the case when D/H exceeds 5,0.

The case of an exponential distribution of charge is not readily ammenable to calculation because it results in integrals of the form

$$\int x^n (x^2 + a^2)^{-m} e^{kx} \, dx$$

Where "n" is an integer and "m" is a fraction having value of $\frac{1}{2}$, 3/2, 5/2 etc. and the solution is a slowly converging series in each case. However a linear distribution of charge is considered to be a fair approximation and in this case it has been shown (Anderson 1969 (a)) that:-

$$E_r/E_s = 2 \left[(D/H)^{-1} - \operatorname{csch}^{-1}(D/H) \right] \left[1 + (D/H)^2 \right]^{3/2} \qquad (9.2)$$

In this case E_r/E_s approaches the value of 1/3 when D/H is large.

From these results it would be expected that in the case of an exponential distribution of charge E_r/E_s will be an even smaller fraction, perhaps of the order of 1/4.

Hence the ratio of the leader field change $E\ell$ to that of the return stroke E_r in the three cases mentioned should be 1,0 for a uniform distribution, 2,0 for a linear distribution and probably exceeding 3,0 in the case of an exponential distribution.

Thus by observing the relative magnitudes of the field change which occur during the leader stroke compared to those of the return stroke, or the total, the probable charge distribution may be deduced. However the method of measurement of field change has to take into account both the very slow field changes which occur during the leader stroke as well as the fast so called "R" field changes of the return stroke - consequently the time constant of the measuring circuit must be long enough for the purpose otherwise erroneous results could be obtained.

In the evidence which follows the notation due to Schonland (1938) is used whereby two major types of leader stroke are identified. Firstly Type $L(\alpha)$ leaders which are in the majority, consist of fairly straight forward discharges to ground with a minimum amount of branching and a fairly constant velocity. Type $L(\beta)$ leaders on the other hand consist of a fast moving first portion with excessive branching followed by a second portion to ground where the velocity and illumination is a minimum and in which no branching occurs. These leaders are thought to proceed first of all to an isolated positive space charge below the main negative charge before continuing to earth - hence the high initial velocity. Both the neutralisation of this charge and the profuse branching would tend to enlarge the leader field charge compared with that of the return stroke.

Pierce (1955) obtained many observations of field change in England at distances over 20 km and using a measuring circuit with a time constant low enough to be able to record the very slow field changes associated with leaders. He reports that for discharges containing one stroke, $L(\beta)$ type leaders produced field changes which

were/ .....

Now the effect of an induced charge of both signs appearing on the leader, can be represented on Fig. 9.0.1 by making the point charge q positive and the distributed charge q negative and this would then be an added effect to that of the main charges.

The field intensity due to these charges say q' is therefore obtained from 9.3 and 9.5 with changed sign and may be written as follows for D>>H:-

$$\text{Field Intensity after leader} = E_1 = q'H/2\pi\varepsilon D^3 - q'H/6\pi\varepsilon D^3$$

$$= q'H/3\pi\varepsilon D^3 \quad \ldots\ldots\ldots \quad (9.8)$$

During the return stroke only the negative value of q' is immediately dissipated whence the field intensity after the return stroke is given by

$$E_2 = q'H/2\pi\varepsilon D^3 \quad \ldots\ldots\ldots\ldots\ldots\ldots\ldots\ldots\ldots\ldots \quad (9.9)$$

Hence the field change after the leader is given by (9.8) and this is positive and therefore added to the original field change. The field change after the return stroke is $E_2 - E_1 = q'H/6\pi\varepsilon D^3$ and is therefore also positive and again half the magnitude of that during the leader.

Thus the effect of any value of induced charge "q'" is merely to increase the field change during both the leader and the return stroke by equal proportions, the overall ratio remaining the same.

If it is now considered that the remaining positive portion of the induced charge q' neutralises an equal quantity of bound negative charge in the cloud situated at a higher altitude, the field change can be ascertained from the arrangement shown in Fig. 9.0.2.

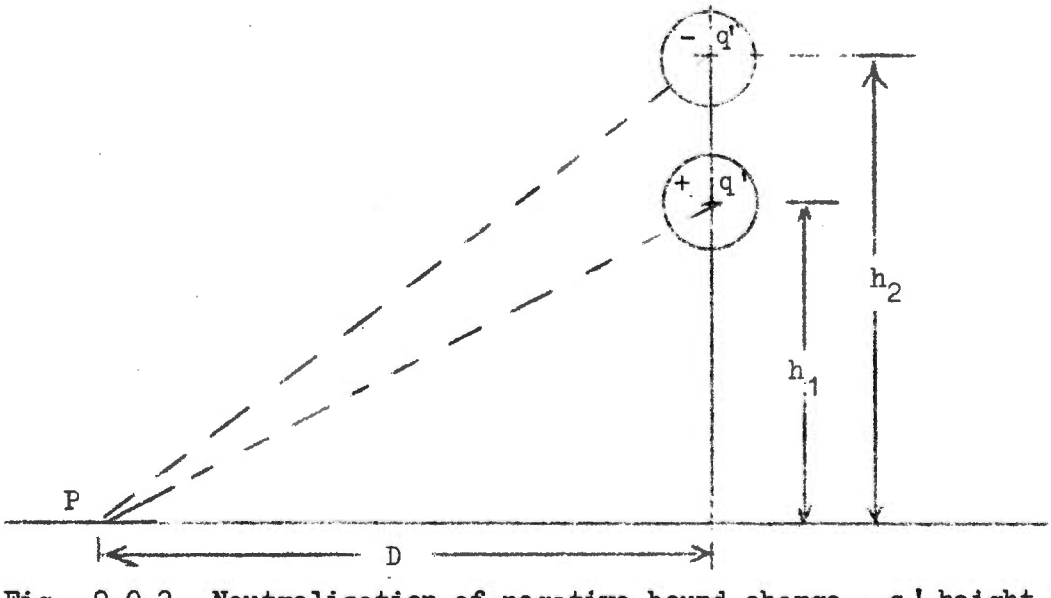

Fig. 9.0.2 Neutralisation of negative bound charge - q' height h_2 by an equal positive charge at height h_1 moving up to h_2.

Assuming/ .....

Assuming D>>H the field intensity at P before neutralisation is given by

$$E_2 = -q'(h_2 - h_1)/2\pi\varepsilon D^3 \qquad (9.10)$$

Since - q' is bound charge +q' must move upwards to the height h_2 to effect neutralisation but the field intensity will then be zero.

Hence the field change is

$$-E_2 = q'(h_2 - h_1)/2\pi\varepsilon D^3 \qquad (9.11)$$

This therefore is a positive field change added to that of the return stroke, and which would tend to reduce the ratio of the leader return stroke field change.

However it is likely to be a slow process and part of the so-called junction (or J) field change which occurs between strokes of a flash, and if the distance $(h_2 - h_1)$ is small it will also be of relatively small magnitude.

If on the other hand the leader channel was left positively charged after it had discharged all negetive charge to earth, a further rapid positive field change would occur during the return stroke as illustrated in Fig. 9.0.3 below:-

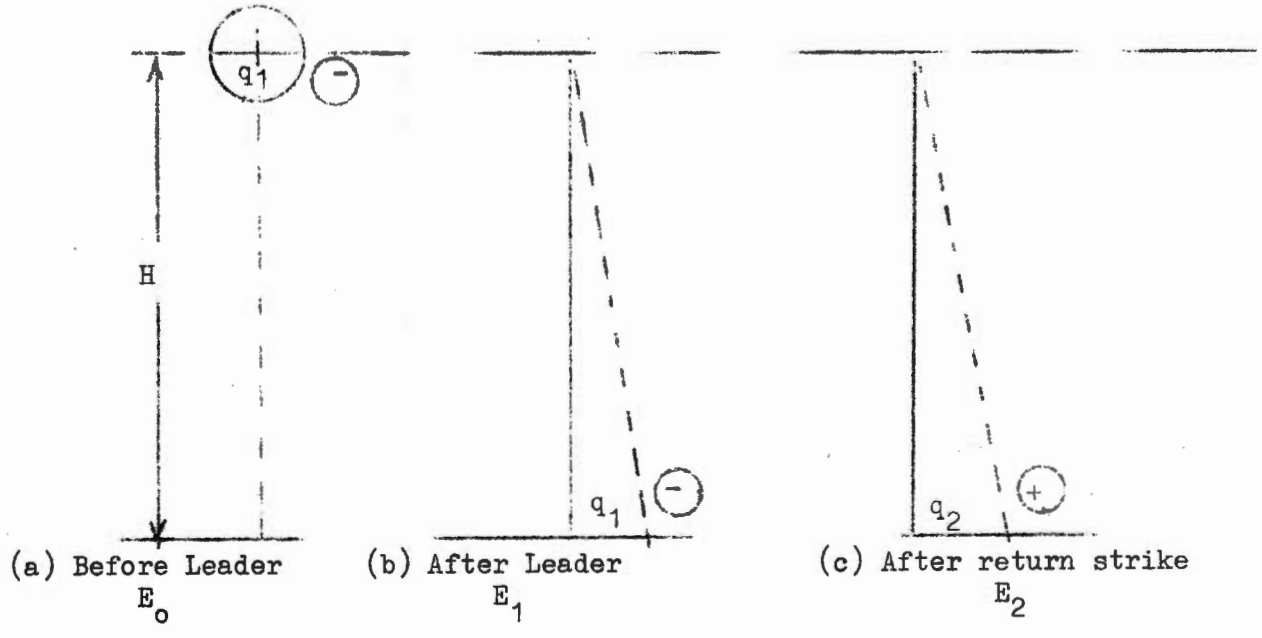

Fig. 9.0.3 Diagram illustrating sequence of charge distributions including a positively charged return stroke

The field change during the leader namely $E_1 - E_0$ has been given above for D>>H as equation (9.6) namely

$$E_\ell = -q_1 H/3\pi\varepsilon D^3 \qquad (9.6)$$

The/ .....

The field intensity E_1 after the leader and before the return stroke has likewise been given before as equation (9.5) namely

$$E_1 = q_1 H/6\pi\varepsilon D^3 \qquad (9.5)$$

Now if for example the negative charge q_1 is suddenly replaced by a positive charge q_2 distributed in like manner, the field intensity after the return stroke will be

$$E_2 = q_2 H/6\pi\varepsilon D^3 \qquad (9.12)$$

The field change during the return stroke would therefore be $E_r = E_2 - E_1$ whence

$$E_r = (q_2 - q_1)\, H/6\pi\varepsilon D^3 \qquad (9.13)$$

Since q_2 is positive and q_1 negative, this field change is positive and is virtually due to the numerical sum of the charges, and if q_2 is made equal in magnitude to q_1 then

$$E_r = -\, q_1 H/3\pi\varepsilon D^3 \qquad (9.14)$$

This is of course now equal to the leader field change $E\ell$, and would therefore afford an explanation as to how the ratio of these field changes could be unity with charge distributions which are not uniform.

In view of what has already been postulated with regard to the existence of positive ions at the top of the channel, it is not difficult to visualise that when the leader contacts the earth, more electrons may migrate to earth that were originally deposited on the channel by the leader thereby leaving excess positive ions in the channel. However it might be expected that if this was to occur under the electric field conditions pertaining the concentration of positive ions would be greater at the top of the channel than at the earth end.

In this case, it can be shown that the field intensity with an inverted linear distribution of charge (uniformly increasing from the ground upwards) is given by the expression, namely

$$E_2 = q_2 H/3\pi\varepsilon D^3 \qquad D \gg H \qquad (9.15)$$

This is twice the value compared with (9.12) and the corresponding field change during the return stroke is then given by the following expression

$$E_r = (2q_2 - q_1)\, H/6\pi\varepsilon D^3 \qquad (9.16)$$

In/ .....

In this case, if q_2 is half the magnitude of q_1 (which is negative) the field change during the return stroke would be equal to that during the leader.

This section may therefore be summarised by saying that the near equality in magnitude of the leader and return stroke field changes observed by Pierce may be the result of a positively charged channel left after the return stroke and this would permit the assumption being made that the original charge distribution in the leader could well be linear or even exponential.

10. The field intensity surrounding the leader channel

Consider first of all a relatively short length of leader channel of length L and radius "r" suspended vertically remote from earth as indicated in Fig. 10.0.1

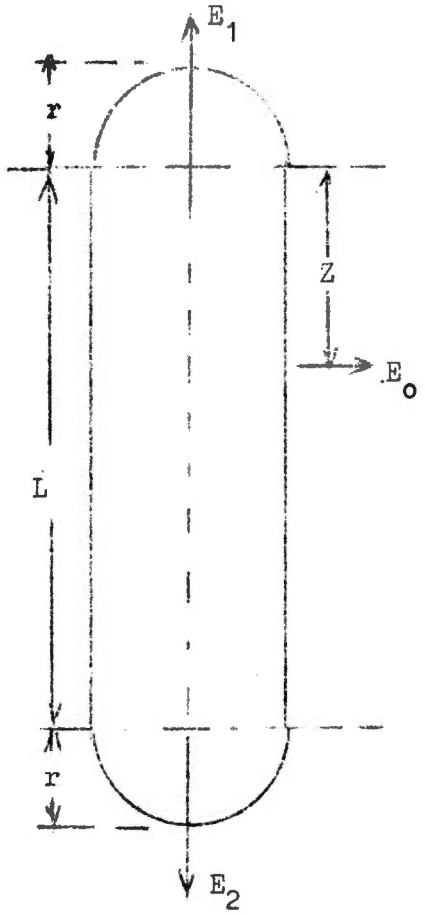

Fig. 10.0.1 Diagramatic view of short leader channel

Assume also that this short leader carries a charge q distributed along the centre line for length L according to the general relationship namely:-

$$q' = (n+1)qz^n(L^{n+1})^{-1} \quad C/m \quad \ldots\ldots\ldots\ldots\ldots \quad (10.1)$$

Where "n" is zero for a uniform distribution, or any positive integer 1, 2 or 3 etc. say, representing a linear, parabolic or cubic distribution of charge etc. increasing towards the lower end. The field is considered positive if unit positive charge placed in the field tends to move downwards, and the vertical field intensity E_1 and E_2 at the top and lower end respectively is given by the relationships indicated in Table 10.1.1 which also shows the ratio of E_2/E_1 when L>>r.

Table 10.1.1/ .....

+ Exponent n	Field intensity E_1 (Top End)	Field intensity E2 (Bottom End)	Ratio E_2/E_1
0	$-q/4\pi\varepsilon Lr$	$q/4\pi\varepsilon Lr$	$\neq$ -1
1	$-2q/4\pi\varepsilon L.\,[\,\ln(L/r) - 1\,]$	$2q/4\pi\varepsilon Lr$	$-L/r.\,[\,\ln(L/r) - 1\,]$
2	$-3q/4\pi\varepsilon L^2$	$3q/4\pi\varepsilon Lr$	$-L/r$
3	$-2q/4\pi\varepsilon L^2$	$4q/4\pi\varepsilon Lr$	$-2L/r$
4	$-5/3q/4\pi\varepsilon L^2$ *	$5q/4\pi\varepsilon Lr$	$-3L/r$
m >1	$-\frac{m+1}{m-1}\,q/4\pi\varepsilon L^2$	$(m+1)q/4\pi\varepsilon Lr$	$-(m-1)L/r$

Table 10.1.1 Vertical Field intensity at the extremities of a short length of leader channel

+ Exponent of equation for charge distribution (see equation 10.1)

* Calculated from the observed progression of the second and third columns

$\neq$ Assuming the values of "r" at the two extremities are equal

The vertical field intensity set up by the leader charge is of course added algebraically to that of the main field produced by the cloud charges, and it is of some importance that at the top end, the main field is reduced by the leader field, whereas at the lower end it is reinforced. Furthermore, as to be expected, the more charge deposited towards the lower end of the channel the less the opposing field is at the top end.

It seems to be important also to realise that q, L and r are all dependent variables which will be mutually adjusted to satisfy some limiting condition. For example the value of "r" at the lower tip of the channel will be such that the resultant value of field intensity to cause ionisation is not exceeded for a particular value of q and L. The value of "r" therefore can be regarded as the corona radius of the channel, and this will vary according to the charge distribution assumed, and the length of the channel.

Since the field intensity at the lower tip is required to be at least equal to the breakdown value for air, whatever charge distribution is assumed for the leader, it follows from Table 10.1.1. that for a linear charge distribution the corona radius of the leader would be twice that required if the charge were to be distributed uniformly, and correspondingly larger if more charge still is distributed towards the lower end as would be the case say for an exponential distribution.

This factor has an important implication at ground level to the effect that the less charge distributed towards the lower end of the leader, the closer will it have to approach the ground before final breakdown between the plasma core of the channel and earth can take place - that is to say that the so-called striking distance of the leader will be less.

The/ .....

The next consideration is the horizontal component of field intensity along the leader channel as indicated by the symbol E_o on Fig. 10.0.1. Again assuming a line distribution of charge along the leader, and for the case when L>>r the horizontal component of field intensity for a uniform distribution is the same of course for z = 0 and z = L and is given by the expression in (10.2).

$$E_o(z = 0) = q/4\pi\varepsilon Lr \quad \ldots\ldots\ldots\ldots\ldots\ldots \quad (10.2)$$

This is identical to the value for the vertical field intensity E_1 and E_2 Table 10.1.1. The field intensity at 45° from the vertical would be the vector sum of the two values and hence higher in magnitude. Alternatively, if the field intensity is constant at the ionisation value for air, the corona radius would change accordingly. Since a factor of $\sqrt{2}$ is involved, this suprisingly suggests that the shape of the base of the corona envelope is cylindrical; this is however dependent upon the assumption as to how the charge is distributed.

For a uniform charge distribution the horizontal field intensity at the centre of the leader channel i.e. when z - L/2, is twice the value at the extremities, alternatively the corona radius is double. This would give rise to a channel which tends to bulge in the centre and no evidence of this, at least optically, has been obtained.

In the case of a linear distribution of charge on the other hand the three corresponding values of the horizontal component of field intensity are as follows.

$$E_o(z = 0) = q/2\pi\varepsilon L^2 \quad \ldots\ldots\ldots\ldots\ldots\ldots \quad (10.3)$$

and $$E_o(z = L/2) = E_o(z = L) = q/2\pi\varepsilon Lr \quad \ldots\ldots \quad (10.4)$$

$$= E_2 \text{ when } L/r >> \ln(L/r) \quad \text{(See Fig. 10.0.1)}$$

In this case it is seen that at least for the lower half of the leader length, the corona radius tends to be uniform assuming the same value of ionising field intensity of the air, and compared with the case of a uniform charge distribution, this is favoured in view of photographic evidence which tends to suggest that the corona radius is in fact approximately uniform.

The above expressions lead to a convenient means to calculate the approximate corona radius for a linear charge distribution namely that

$$r/q = 1/2\pi\varepsilon LE \text{ m/c} \quad \ldots\ldots\ldots\ldots\ldots\ldots \quad (10.5)$$

whence if $E = 3\times10^6$ V/m say and $L = 4\times10^3$

$$r/q = 3/2 \text{ m/c} \quad \ldots\ldots\ldots\ldots\ldots\ldots \quad (10.6)$$

It/ .....

It is clear from the above that, assuming a linear distribution of charge, a leader diameter of the order of 3m could only support a total leader charge of one coulomb and charge deposition of between 5 and 10 C would require much larger leader dimensions than presently thought to be possible. All the evidence on this however is photo= graphic, and as is well known this could be misleading depending as it does upon the intensity of the light source, the optical system used as well as the sensitivity of the photographic emulsion employed. The use of photomultiplier techniques and quartz lenses for the study of laboratory sparks has certainly revealed the very weak luminosity of pre-discharge streamers which are generally invisible to the naked eye let alone less sensitive photographic materials.

Finally it is necessary to determine what the effect on the field intensity would be if the charge is distributed differently across the radial cross section of the channel. If for example the distribution radially is uniform as assumed for the cylindrical case of cloud charges, the field intensity at the lower extremity for a linear dis= tribution of charge axially is given by the expression

$$E_2 = q/2\pi\varepsilon L^2 \cdot [\, 2L/r - \mathrm{Sinh}^{-1}(L/r)\,] \ldots\ldots \quad (10.7)$$

Since $\sinh^{-1}(L/r) = \ln(2L/r)$ when $L \gg R$

and $2L/r \gg \ln(2L/r)$

equation (10.7) can be rewritten as follows, namely:-

$$E_2 = q/\pi\varepsilon Lr \quad \ldots\ldots\ldots\ldots\ldots\ldots\ldots \quad (10.8)$$

For equal values of r this value of field intensity is twice that given in Table 10.1.1 which is also for a linear charge distri= bution but distributed along the centre line. Hence for the same value of E_2 the corona radius in the present case equation (10.8) must be doubled.

Possibly a most realistic case to examine is that in which the charge is assumed to form an annular ring concentrically around the core of the channel - as might be expected of a corona sheath as illustrated in Fig. 10.0.2.

Fig. 10.0.2/ .....

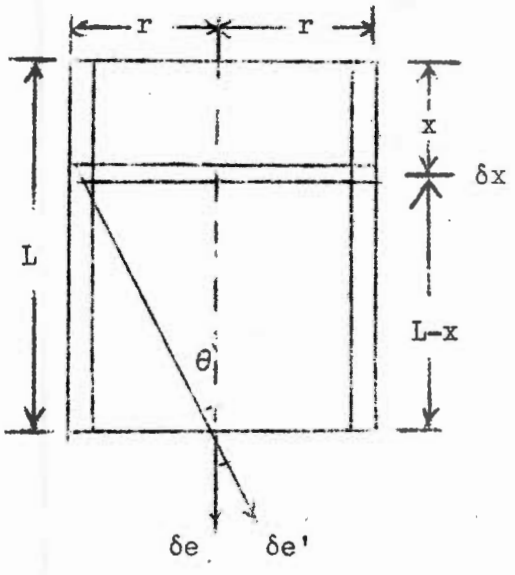

Fig. 10.0.2 Case of a linear charge distribution arranged concentrically

The charge distribution is assumed linear per unit length and is say

$$q' = \frac{2q}{L^2} \times C/m$$

The charge in a small anular ring of thickness δx is then

$$\delta q = \frac{2q}{L^2} \times \delta x$$

The field intensity at the point P on the axis at the base of the channel is then:-

$$\delta e = \frac{\delta q}{4\pi\varepsilon S^2} \cos\theta \text{ where } \cos\theta = \frac{L-x}{S} \text{ and } S = [(L-x)^2 + r^2]^{\frac{1}{2}}$$

Hence the field intensity due to all charge in the cylindrical shell is given by

$$E = \frac{q}{2\pi\varepsilon L^2} \int_0^L \frac{x(L-x)dx}{[(L-x)^2+r^2]^{3/2}}$$

Putting $(L-x) = X, dx = -dX, x =$ L-X we have:-

E/ .....

$$E = \frac{q}{2\pi\varepsilon L^2}\left\{-\int \frac{(L-X)XdX}{[X^2+r^2]^{3/2}}\right\} = \frac{q}{2\pi\varepsilon L^2}\left\{-L\int \frac{XdX}{[X^2+R^2]^{3/2}} + \int \frac{X^2dX}{[X^2+R^2]^{3/2}}\right\}$$

$$= \frac{q}{2\pi\varepsilon L^2}\left[\frac{L-X}{[X^2+r^2]^{\frac{1}{2}}} + \ln\left|X + \sqrt{X^2+r^2}\right|\right]$$

$$= \frac{q}{2\pi\varepsilon L^2}\left[\frac{x}{[(L-x)^2+r^2]^{\frac{1}{2}}} + \ln\left|(L-x) + \sqrt{(L-x)^2+r^2}\right|\right]_0^L$$

$$= \frac{q}{2\pi\varepsilon L^2}\left[\frac{L}{r} + \ln(r) - \ln\left|L + \sqrt{L^2+r^2}\right|\right]$$

Hence $E = \frac{q}{2\pi\varepsilon L^2}\left[\frac{L}{r} - \text{Sinh}^{-1}\left(\frac{L}{r}\right)\right]$

Now when $L>>r$ $L/r>>\sinh^{-1}(L/r)$ whence

$$E = \frac{q}{2\pi\varepsilon Lr} \quad \ldots\ldots\ldots\ldots\ldots\ldots\ldots\ldots \quad (10.9)$$

This/ .....

This case is now identical to that of assuming that the charge is arranged along the centre line of the channel as the case n = 1 of Table 10.1.1.

Hence it has been shown that the mode of charge distribution both axially along the leader channel as well as radially, has a significant effect upon the field intensity around the leader and at its tip. The dimensions of the leader, that is primarily its corona radius, will therefore be dependent upon this distribution and will adjust itself until the field intensity equals that for ionisation of the media through which it is penetrating.

The effect of earth cannot be neglected when the leader tip approaches ground and in the case of a linear distribution of charge along the leader arranged concentrically the field intensity at the tip allowing for the effect of the earth is given by the following expression, namely:

$$E_t = q/2\pi\varepsilon L^2 \cdot \left\{ -\text{Sinh}^{-1}(L/r) + L/r + \text{Sinh}^{-1}\left[(2h-2L)/r\right] - \text{Sinh}^{-1}\left[(2h-L)/r\right] + L\left[(2h-2L)^2 + r^2\right]^{-\frac{1}{2}} \right\} \text{ V/m} \quad \ldots\ldots \quad (10.10)$$

Where L is the length of the leader, and h is the total height of the top of the leader above ground.

Similarly the field intensity at ground level immediately below the leader is given by the expression namely:-

$$E_g = q/\pi\varepsilon L^2 \cdot \left\{ \text{Sinh}^{-1}\left[(h-L)/r\right] - \text{Sinh}^{-1}(h/r) + L\left[(h-L)^2 + r^2\right]^{\frac{1}{2}} \right\}$$

V/m ..... (10.11)

In the special case when the leader reaches ground level L = h whence both the above expressions reduce to the following namely:-

$$E_t = E_g = q/\pi\varepsilon h^2 \cdot \left[h/r - \text{Sinh}^{-1}(h/r)\right] \quad \ldots\ldots \text{ V/m} \quad \ldots\ldots \quad (10.12)$$

And when $h >> r$ $\quad h/r >> \text{sinh}^{-1}(h/r)$

Whence $E \approx q/\pi\varepsilon hr$ ..... (10.13)

Hence/ Page 41(a) .....

Hence if $E = 3 \times 10^6$ V/m and h = 4 km say then r/q = 3 m/C and this is half the value calculated for this case when neglecting the effect of the earth.

Two points are of importance in this regard. Firstly the leader may theoretically approach the earth until contact is made - that is according to the cylindrical model with the charge arranged either uniformly or concentrically. In practise the tip also contains elec= trons and in effect the corona envelope must extend ahead of the tip as it does radially, and this therefore will be the first to make actual contact. The corona radius "r" is therefore identified as the so-called "striking distance" of the leader, since at this juncture the leader process is at an end and the whole system breaks down to form an arc bridging the distance between cloud charge and the earth. This matter will however be referred to again in a later section.

Secondly, the calculations made so far neglect the main field due to the cloud charges, including any induced positive charge at the top end of the leader. These charges according to their polarity will of course add to or subtract from the field produced by the leader, but usually the numerical value will be small compared with that due to the leader charge, the bulk of which is in close proximity to the lower tip.

As mentioned previously, the supposition of a concentric radial distribution of charge on the leader has as its basis the concept of a corona envelope. Firstly a spherical space charge in which the charge may be distributed uniformly within the sphere, may attain a field intensity at its surface sufficiently high for ionisation, whereas the field intensity within the sphere is lower and tends to zero at the centre. Fundamentally, however, the charge may be situ= ated at a point in the centre or distributed uniformly on the sur= face of an imaginary spherical shell, the result would be identical. Similarly with a cylindrically shaped charge such as the leader, its corona radius may be determined by any of the three suppositions mentioned as to the distribution of charge - the definition being that radius from the centre line of the cylinder which gives rise to a field intensity capable of ionisation of the air at that point. Hence the corona radius of the channel may be calculated on the assumption that the charge is distributed along the centre line, but it may as well be distributed in a concentric shell - and this view is favoured because it assists with the explanation as to how charge becomes deposited along the length of the channel as it elongates - instead of all charge being concentrated at the lower end.

Since the cylinder, by virtue of its charge, is also at a high potential for most of its travers towards the earth, it is fully analogous to a conductor charged to a state of corona - and the term corona radius therefore becomes appropriate.

As shown previously the corona radius of a lightning channel is very large compared with normal conductor standards and this poses the question as to what are the conditions existing between it and the core of the channel; furthermore of what does the core itself consist?

Firstly in the case of a metalic conductor, all the charge is initially situated on or in it, but at the high field intensity con= ditions at which is necessary to promote the onset of corona, some charge leaves the surface of the conductor and is deposited in the

surrounding/ .....

surrounding media. This phenomena has been studied by many investi= gators and in particular Loeb (1965) describes the work of many ex= perts in this field. It is not intended therefore to describe these results or theories in detail. Suffice to say that it is regarded as well established that space charges of ions of both signs, and electrons, form up in the media surrounding the conductor thereby modifying the normal electric stress pattern which would have other= wise existed.

In the case of a negatively charged conductor positive ions space charge is to be found in the vicinity of the conductor surface with negative ions and electrons displaced to the vicinity beyond and ex= tending away from the conductor. In the case of short spark or arc discharges, modern theories of the mechanism suggest space charge distributions which are mainly disposed axially along the length of the arc with secondary emissions which tend to be radially disposed.

The very long spark has of course not been investigated in view of practical difficulties, but of course the principles which apply in the laboratory spark should in some measure at least be capable of extra-polation to the case say of the lightning discharge.

The conventional description of the lightning leader channel (Loeb 1966) assumes that it consists of highly conducting plasma core of few millimeters in diameter and a surrounding sheath of not more than 3 or 4 centimetres or so in extent. A plasma core however envisages gas in a high state of ionisation with ions and electrons in about equal proportions in equilibrium. This does not seem to fit the theory of the lightning leader mechanism very well, since, if free electrons for example are in fact present and are mobile in the core, there appears to be no reason why they should not be impelled by the electric field producing them to the lower end of the channel - or even driven radially outwards to the limits of the corona radius until the field gradient becomes too small for ionisation by collision.

In view of the above it would appear to be more valid to invoke the results of the corona investigation referred to by suggesting that in fact the centre portion of the lightning leader consists mainly of positive ions which have become separated as space charge by the prospective high radial electric field - the negative charge consisting of ions and electrons being forced to the perimeter but in quantity in excess of the positive ions to maintain the negative potential of the leader. Such an arrangement is described in Fig. 10.0.3.

Fig. 10.0.3/ .....

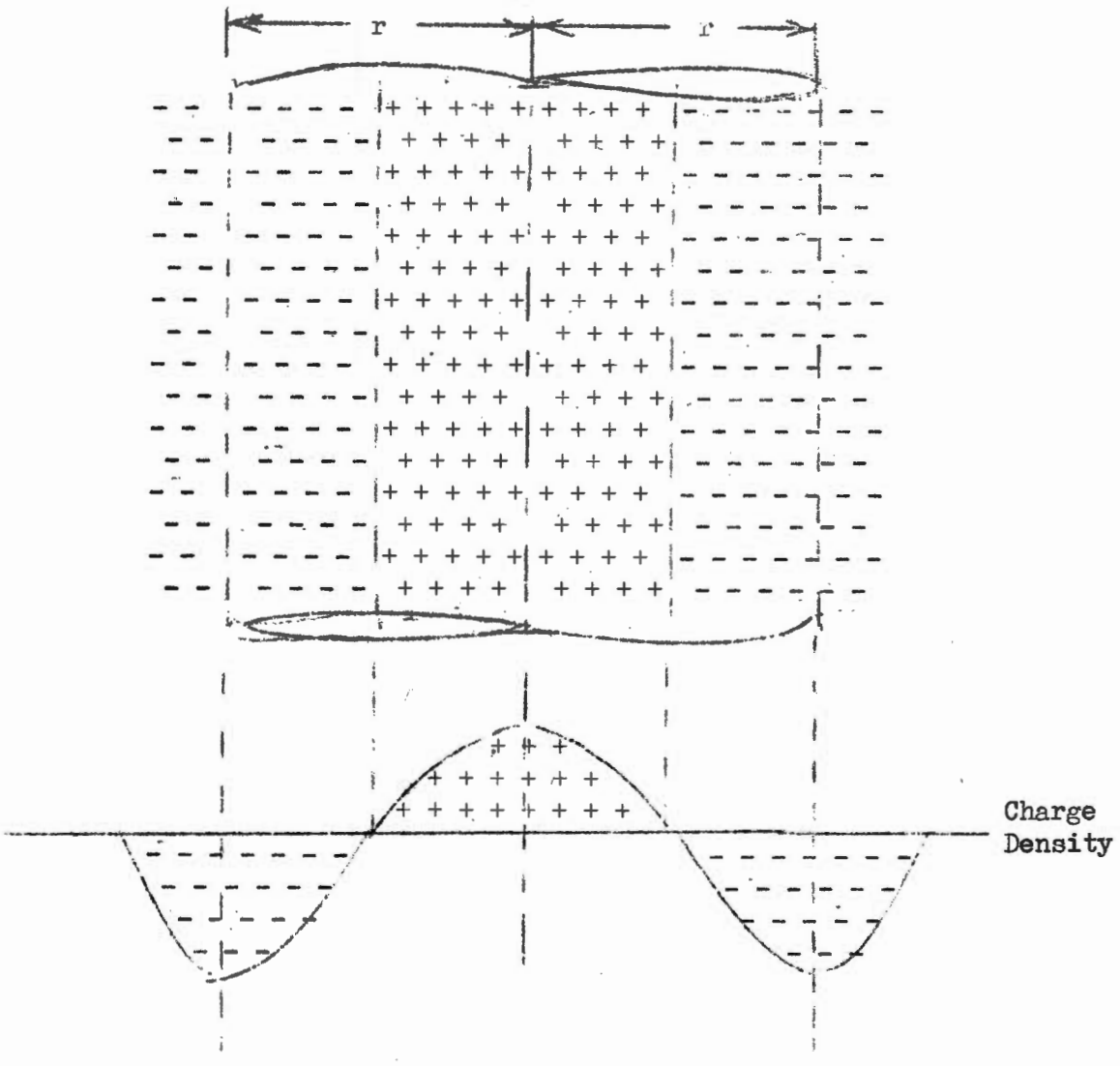

Fig. 10.0.3 Diagrammatic representation of radial charge distribution of leader channel

The charge distribution shown in Fig. 10.0.3 is similar to that shown in Fig. 3.7 of Meek and Craggs (1954) excepting that in the latter no charge is shown to be present in close proximity to the conductor. However in this case the consideration was in connection with the corona regime applicable to a negative point positive plane gap, and it could be expected that if the metallic conductor is replaced by an ionised column or other conducting media, conditions would differ.

An attempt has been made to calculate the field conditions radially from the centre of the lightning-channel, using the above assumptions, and whilst this is possible, the results are not meaningful unless the limits of the various charge zones are known and also the actual form of the distribution. But whatever the field configuration may be, the radial component of field intensity at the centre line would be zero, and in view of this, there still remains the possibility that in fact there is no charge present at that point. There would then be no actual core to the leader channel but rather two concentric cylinders of charge, the innermost being made up of positive ions, and the outermost electrons and negative ions.

The inclusion or omission of the inactive core of the channel does not influence the ultimate corona radius nor the field intensity

exhibited/ .....

exhibited at the perimeter or the tip, and for the purpose of further discussion the charge configuration illustrated in Fig. 10.0.3 is assumed.

It is now therefore possible to build up a proposed physical picture of the leader channel as dipicted in Fig. 10.0.4.

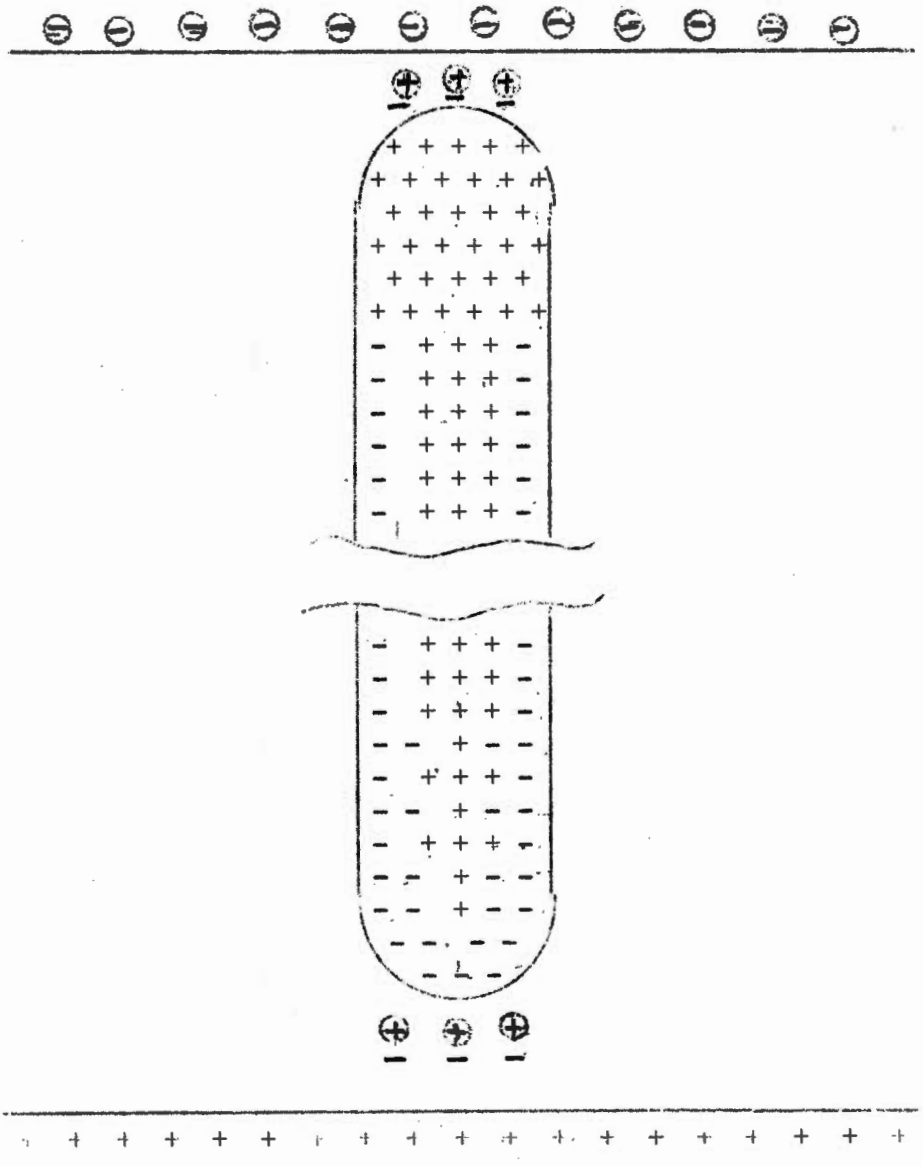

Fig. 10.0.4 Diagramatic representation of charge disposition in a lightning leader

Figure 10.0.4 shows all the features so far discussed with the exception that the core of the leader is now shown to consist of a positive column of ions down which any electrons freed by ionisation at the top may traverse at velocities which can approach that of light. The velocity of the positive ions upwards will probably be of the order of their drift velocity of namely about 1×10^3 m/s, and this will assist the extension of the positive upper tip. However, the velocity of this tip would not be limited to that of the velocity of the positive ions if the field at the head of the tip is sufficiently high for ionisation to take place - for in this case new positive ions are created during the advance. The speed with which this takes place adds to the velocity of the ions themselves andvalues as high as 5×10^6 m/s have been measured by Kritzinger (1962).

Similarly/ .....

Similarly at the lower end of the channel, free electrons, if in sufficient concentration, ionise the air ahead of them and the mechanism of this must follow the Townsend concept. The positive ions thereby created follow into the positive column above them whilst some of the electrons are directed into the negative corona shell, and are left behind by the advancing tip.

Electron passage down the column must follow the concentration of positive ions by the mechanism of jumping from one ion to the next, and this is most likely to be confined towards the central position of the channel. It can be expected that herein lies the region where energy is expended in the form of light and heat accounting for both the axial potential gradient and the high temperature of the core. It is therefore quite probable that photographic impressions of the leader would only record this highly active central core and would exclude the less active region beyond, where the only energy expended is due to the corona losses and the adjustment of charge in the corona sheath when the potential changes. In addition the very high current flowing during the return stroke is likely to be forced to flow within the smallest diameter possible, by the electromagnetic field then surrounding the core.

The conception of Fig. 10.0.4 is of course intended to apply to the leader channel as a whole having a diameter of the order of a few metres and a length of a few kilometers. The breakdown processes which occur at the extremities may quite concievably follow the pattern of the laboratory spark discharge between electrodes, perhaps on a larger scale. For example Reather's cathode directed positive streamers, as outlined by Meek and Craggs (1953), consist of positive ion avalanches in succession with electron tails and assisted by photo emission which in this case are directed from the leader tip upwards into the negative cloud. The only difference is that whereas in the spark discharge, the cathode charge is mainly confined to the surface of the electrode (in the absence of secondary streamers) the positive streamers in the cloud actually move into the charged area. At the lower negative end of the leader however the anode is for the most part remote, and the streamers have to propogate without much assistance from the main directing field. Here electron tipped avalanches from the leader channel proper may also develope in the usual manner. However, in this case the model proposes that ionising field intensities may be atteined purely as a result of the accumulated charge within the confined dimensions of the leader channel, and it does not seem to be necessary to evoke the assistance of photo-emission to assist with the process.

The lightning leader also differs from the conventional spark discharge in regard to the necessity for negative charge being deposited along the channel route and not all accumulated at the lower end. In order to achieve this, the lightning channel must as a whole be raised to a sufficiently high potential relative to its surrounds to induce excessive corona conditions.

It is of interest here to note that the velocity of the negative charge in the outer corona shell cannot be high otherwise this too would migrate towards the advancing tip of the leader, and it must be assumed that in fact it exists mainly in the form of negative ions at this stage. This view is not inconsistent with that of the concept of corona in that the outward ejection of electrons as a consequence of the potential, eventually leads to attachment with molecules of

air/ .....

air at the extreme boundary where the field intensity can no longer support ionisation. This may also be the reason why the velocity of the return stroke is reduced to that of about 1/10th of that of light since on collapse of the potential the negative charge needs time to return to the core.

Finally in this section the question of branching must be discussed. According to Schonland (1938), severe branching is associated with what he terms type β leaders in which the velocity during the initial portion of the stroke is high, whereas for the later progression to ground, the velocity is very much reduced and little branching occurs. He attributes the phenomena to the presence of pockets of positive space charge in the first instance, whence the leader velocity is increased during the approach to this charge and is accompanied by multiple branching. On the other hand there is much photographic evidence showing that branching of the first leader under other circumstances is a common phenomena. For example most flashes selected at random from the records in Pretoria showed branching of one kind or another, and it is therefore necessary to consider other possible reasons for this phenomena.

Firstly as regards the leader tip itself, it has been shown that for the case of the concentric charge distribution, the field intensity in the direction of propagation of a straight channel tends to be twice that of the field intensity at right angles. Since the field intensity cannot exceed that for ionisation in any direction the channel tip tends to elongate such that the corona radius will be greater at the tip than it would be radially and this in itself points towards an extension in the direction of movement rather than laterally. However the effect of the main field produced by the cloud charges, whilst being small compared with that due to the leader charge, is nevertheless directed vertically, and would therefore tend to guide the tip along the field direction since there is no radial component.

The presence of pockets of positive space charge however will, as Schonland suggested, distort the generally vertical direction of the main field, and this no doupt accounts for the tortorous path followed by the leader in any case. Serious departures from the vertical must therefore surely be due to such distortion as a consequence either of large volumes of positive space charge being present in the air or in prominent features on the earth where a concentration of positive charge has taken place. Strokes occuring at 45° across the sky are not uncommon and could be the result of a concentration of positive charge on the earth induced by another large negative charge in the cloud above, which has not as yet reached ionisation - such as in a neighbouring thunderstorm cell.

Branching may however be somewhat unrelated to the above in that the leader, having selected a particular direction of advance, suddenly chooses to advance along another direction simultaneously. Cognisance must also be taken of the fact that Schonland and Malan established that the return stroke followed up each branch in succession, indicating that charge had been previously deposited thereon. In one case cited by Schonland (1938), the branch continued to develop in length until the main channel reached the earth whereupon the branch stopped abruptly; on the other hand some branches are very short and appeared to have stopped advancing at an early stage.

One/ .....

One possibility is suggested as a consequence of the comparatively large diameter of the corona sheath of the leader. This is that whilst the overall field intensity created ahead of the tip results mainly from the total charge on the leader; the breakdown avalanches which develop are on the other hand much smaller in extent, and may be localised at several points around the perimeter of the lower portion of the corona envelope. It would then be possible to envisage that usually one, but sometimes two (or perhaps even more) of these avalanche craters stem from the beginning of the extension of the leader in one or more directions.

An alternative conjecture would be that the leader approaches two separated centres of positive space change in which case streamer development from and to these charges could cause the leader to branch.

Suffice to say, in conclusion, that it would be difficult to make calculations of the leader field intensities and potential taking account of branching, and this has not even been attempted. However the effect of branching could be at least qualitatively assessed.

11. The potential of the lightning leader

In Section 4 it has been shown that the maximum potential within cloud space charges varies between 0,5 and $2{,}5 \times 10^9$ volts according to altitude, and for the case when a field intensity of 1×10^6 V/m has been reached at the extremities of a cylindrically shaped arrangement of charges. The conducting leader channel is connected electrically to the region of high negative potential at its uppermost extremity and thereafter the lower tip traverses the space between the charge and earth where the potential in this space, in the absence of the leader, steadily approaches zero. Mathematically, the potential in the space rises from a high negative value in the cloud to zero at the earth's surface.

Since the lightning channel should exhibit the properties of an arc or spark having comparatively low voltage gradients of the order of several tens to hundreds of volts per metre, it would be expected that the potential of the lower tip would be maintained at a high level compared with the potential to earth in space.

However consider first of all a charge "q" contained in a spherical volume of radius "r" situated "h" above earth. The field intensity at the surface of the sphere is then given by the expression namely:-

$$E = q/4\pi\varepsilon \cdot [\,1/r^2 + 1/(2h-r)^2] \quad - \text{V/m} \quad \ldots\ldots \quad (11.1)$$

Similarly the potential at the perimeter of the spherical charge is given by the expression namely

$$V = q/4\pi\varepsilon \cdot [\,1/r - 1/(2h-r)] \quad \text{Volts} \qquad (11.2)$$

If it is assumed that the field intensity E does not exceed the ionisation breakdown level, say 3×10^6 V/m, the radius of the spherical

charge/ .....

charge is then determined by the value of the charge "q" and the height "h" above ground.

If now the charge is say kept constant and is positive and the sphere is moved close to earth that is "h" is reduced, the field intensity would tend to increase above ionisation level but the radius "r" would increase in order to maintain the field intensity constant.

On the other hand both a reduction in the height "h" and an increase in the value of "r" would reduce the potential of the sphere.

There is therefore no possibility of maintaining both the potential and the field intensity limitations simultaneously and hence the potential must inevitably fall as the charge is lowered towards the earth. For a negative charge the potential will rise towards zero.

The case of the lightning leader is identical to the above. The field intensity at the tip must be maintained at ionisation level and the injection of more charge as the leader progresses is accompanied by a tendency to increase the corona radius and the potential must inevitably fall (numerically).

It follows from the above argument that if the potential of the lower end of the leader tip must rise from a high negative value at the start to zero upon contact with the earth, and if the potential gradient along the leader is less than that of the surrounding space the potential at the top end of the leader must also rise during the progression of the leader.

This is achieved in two ways - firstly as a consequence of the virtual transfer of negative charge from the bound charge area in the cloud towards the lower tips of the lightning channel. Secondly, the introduction of an induced positive charge at the top end, as envisaged for other reasons in the previous section, will also tend to make the potential of that end more positive. This is illustrated diagramatically in the following figure 11.0.1.

Fig. 11.0.1/ .....

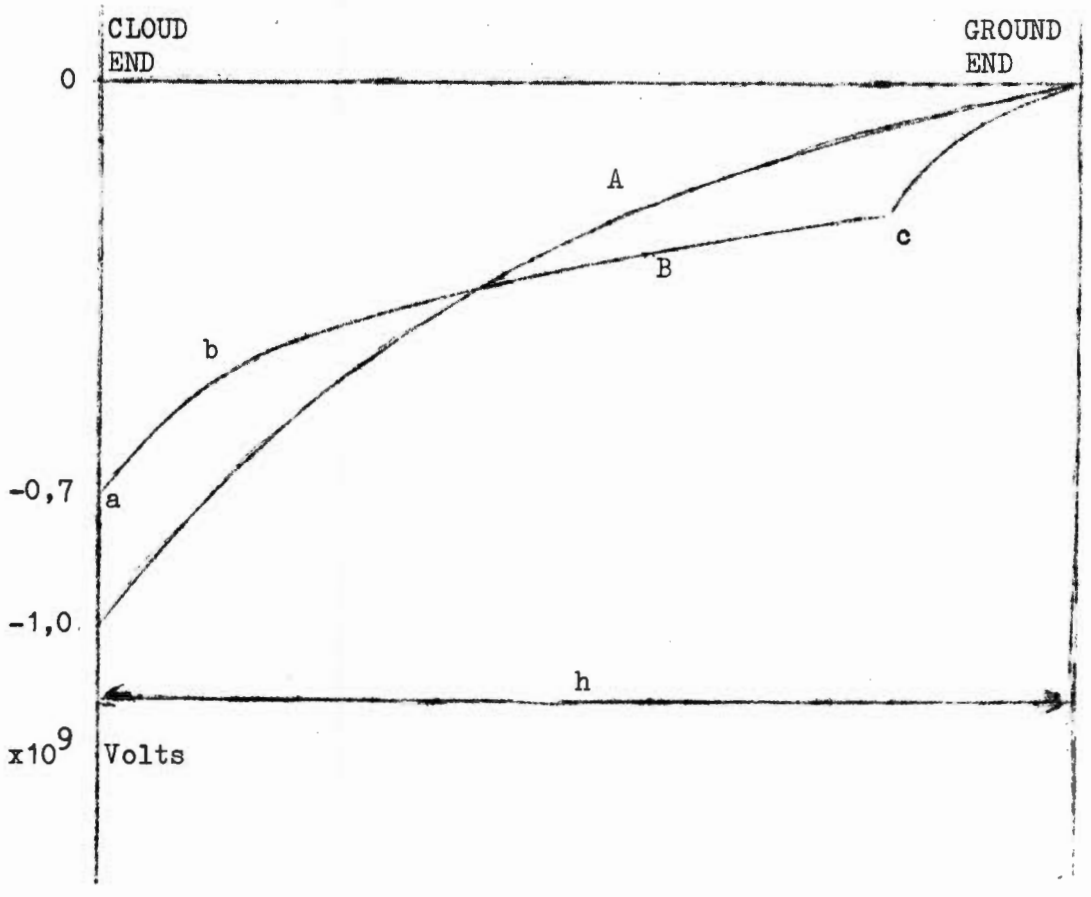

Fig. 11.0.1 Diagram illustrating potential in space between cloud and ground.
A - potential in space in absence of leader
B - potential along leader channel

Curve A illustrates that before the leader starts out, the potential at the cloud is say $-1x10^9$ Volts and it rises steeply at the initial rate of say $1x10^6$ V/m for breakdown until it reaches a more or less constant gradient, until finally the potential approaches zero at the earth's surface.

Curve B illustrates a leader channel which has progressed to the point "c" after which the potential rises rapidly at an initial value of say $3x10^6$ V/m - for ionisation. Then the normal arc voltage gradient of say $1x10^4$ V/m is maintained between b and c whilst between "a" and "b" the voltage gradient cannot exceed say $1x10^6$ V/m. This results in a short fall of potential from the original value of $-1x10^9$ Volts to say $-0,7x10^9$ Volts, and it is this shortfall which must be made up by the lowering of negative charge together with the effect of a positive induced charge at this end of the leader channel.

The potential along the axis of a cylindrical volume of charge having a linear axial charge distribution has been calculated in Appendix I and may be applied to a long cylinder such as the leader channel. At the top end of the channel, the effect of earth may be neglected and for a channel of length L and radius r the potential at the top of the channel is given by the following expression namely:-

V_1/ .....

$$V_1 = qr/3\pi\varepsilon L^2 \cdot \left\{ [1+(L/r)^2]^{3/2} - (L/r)^3 - 1 \right\} \quad \ldots\ldots\ldots \quad (11.3)$$

When L>>r the above expression reduced to the following

$$V_1 = q/2\pi\varepsilon L \quad \ldots\ldots\ldots\ldots\ldots\ldots\ldots\ldots\ldots \quad (11.4)$$

Hence when the length L of the channel becomes large compared with its radius r, the contribution to the potential at its top end due to its own charge is inversely proportional to the length of the channel, and is virtually independent of its radial dimensions.

Similarly for the case when the charge on the leader is arranged concentrically instead of being radially distributed uniformly, the expression for the potential at the top of the channel is then as follows namely:-

$$V_1 = qr/2\pi\varepsilon L^2 \cdot \left\{ [1+(L/r)^2]^{\frac{1}{2}} - 1 \right\} \quad \ldots\ldots\ldots\ldots\ldots \quad (11.5)$$

When L>>r this expression reduces to that of (11.4) indicating that at the top end, the potential contribution of the leader is also unaffected by the manner of the radial distribution of the charge. This contribution is however small compared to that of the charges in situ in the cloud, and it is the latter which will mainly determine the potential existing at the start of the leader channel.

Reverting now to the lower end of the leader and neglecting the effect of earth for the present, the potential due to the charge on the leader alone, which in this case will be larger than the contri= bution of the cloud charges, is given by the following expression namely:-

$$V_2 = qr/2\pi\varepsilon L^2 \cdot \left\{ L/r \sinh^{-1}(L/r) - 2/3 [1 + (L/r)^2]^{3/2} + (L/r)^2 [1 + (L/r)^2]^{\frac{1}{2}} - 1/3 (L/r)^3 + 2/3 \right\} \quad \ldots. \quad (11.6)$$

And when L>>r this expression reduces the following namely

$$V_2 = q/2\pi\varepsilon L \cdot [\sinh^{-1}(L/r) - 1] \quad \ldots\ldots\ldots\ldots\ldots\ldots \quad (11.7)$$

Similarly when the charge is arranged concentrically:-

$$V_2 = qr/2\pi\varepsilon L^2 \left\{ L/r \sinh^{-1}(L/r) - [1 + (L/r)^2]^{\frac{1}{2}} + 1 \right\} \ldots \quad (11.8)$$

And/ .....

And when L>>r this expression also resolves to that of (11.7).

It may therefore be concluded firstly that the potential at both the extremities of the leader channel, due to its own charge, is independent of the manner of radial distribution of charge. Furthermore, even at the lower end, it is more dependent upon the length of the channel than it is on the radius.

The effect of earth on the potential at the lower end will be to lower the potential by an amount inversely proportional to the length of the channel which in the limit, that is when the leader contacts the earth, will render the potential zero. This also applies to the potential due to all charges in the cloud.

This argument implies that in fact, the potential of the leader tip steadily approaches zero as the tip approaches the earth, and that it is not an effect which would give rise to a sudden change when breakdown occurs between the tip and earth.

The notion that the tip of the lightning channel maintains the very high potential of the cloud until it is very close to ground must therefore be abandoned in favour of a more gradual process in a time interval dependent upon the velocity of the leader.

The actual value of the potential gradient along the leader is not well defined. Firstly the lowering of say only 1C of charge in a matter of 20 ms say would give rise to a current of 50 amperes flowing at the top end of the leader, and this is more than sufficient to establish arc conditions as opposed to a spark. Under these conditions the potential gradient should lie between 2×10^3 and say 6×10^3 V/m. On the other hand the current flowing into the lower extremity should be very much less than that flowing at the top end since charge is deposited en route down the leader. Hence the potential gradient may decrease towards the top. In fact Bruce (1944) put forward the proposition that the stepped leader extended first of all as a glow streamer in which the current would initially be very small and the potential gradient correspondingly high, perhaps of the order of 10 to 100 times that of an arc. As the leader extended the current would increase until at a value of about 1 ampere, glow-to-arc transition would take place resulting in a higher current and lower level of potential gradient.

It is however difficult to envisage how this transitory behaviour can occur at the lower tip in isolation, since the potential of the tip has been shown to be influenced by that at the top end. However, it is possible that the induced charge at the top may at first be only just sufficient to maintain a glow discharge on the leader until it extends sufficiently to permit arc conditions.

This leads to a possible explanation of the stepped leader since it suggests that during the progress of the pilot, the potential gradient along the leader is high - following the natural gradient in space to some extent. A transistion from glow-to-arc would then give rise to an increase in current with corresponding lower potential gradient which in turn requires a higher charge transfer which reduces the field intensity at the top end to stop the process.

12. A model of the lightning leader

As a result of the foregoing discussion it is now possible to consider a model for the lightning leader progression starting basically with any two charges, Q_o and Q_1 arranged in the form of cylinders of length L_o and L_1 respectively and having a common radius $R_o = R_1$. It is further assumed that these charges are situated such that the charge separation area is H above ground as depicted in Fig. 12.0.1.

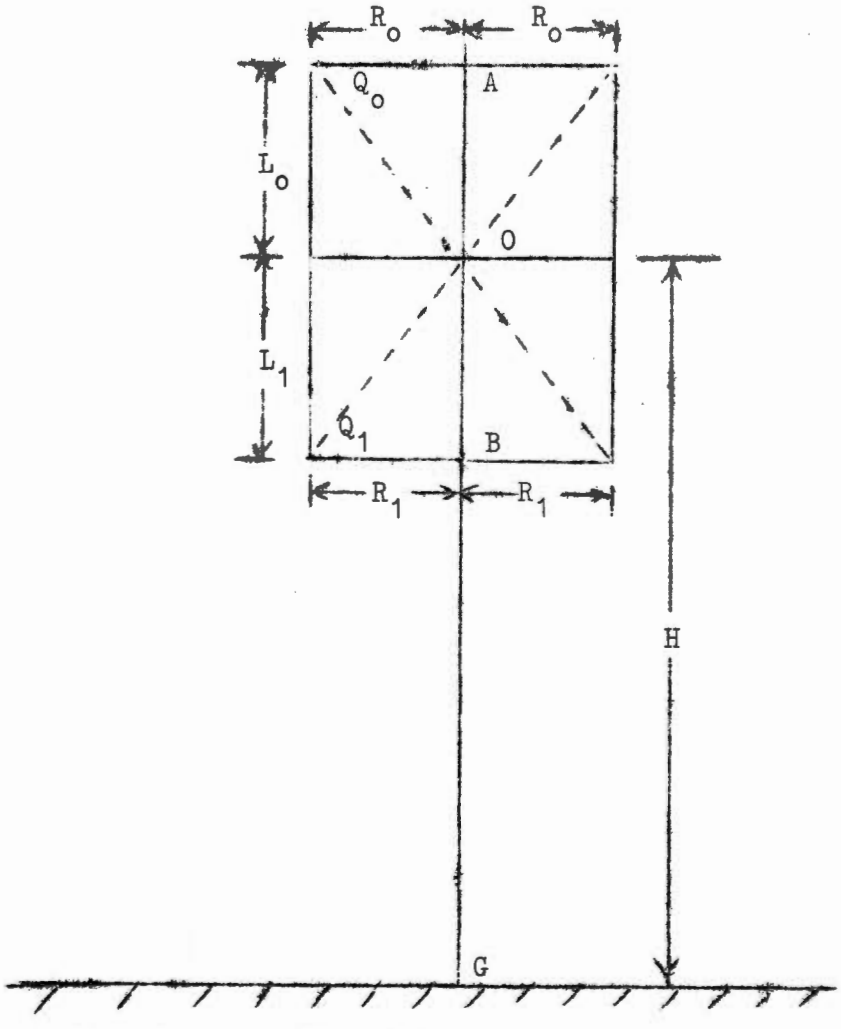

Fig. 12.0.1 Basic configuration of a bi-polar cylindrical charged cell with a linear distribution of charge

If it is assumed for the sake of the model that the charge is distributed in a linear manner from zero at the charge separation area to a maximum at the extremities, the radial charge distribution being uniform, the field intensity at any point along the centre line AOBG may be determined according to the expressions given in Section 4 and Appendix I.

If now $Q_o = + Q$ and $Q_1 = - Q$ the convention for the polarity of the field intensity and its direction is assumed to be such that the vertical component of field intensity at a point is positive if unit positive charge placed at that point would tend to move downwards. The field intensity at A due to charge Q_o therefore is negative as Q_o is positive and this component predominates since the charge Q_o is the closest. The component due to the charge Q_1, is less in magnitude and is positive as Q_1 is negative. The resultant vertical field

at/ .....

at A is therefore negative, the field intensity due to the respective image charges being so small by comparison does not influence the above statement. By the same criteria the field intensity at O is positive whilst that at any point between B and G is negative. In this connection a positive field intensity is regarded as an electric field which is directed downward.

The values of the dimensions L and R, and the charge Q, are then chosen such that the field intensity at B will be equal to or in excess of that at O and wil be say -1×10^6 V/m. This is assumed to be the value required for breakdown of the media at B as derived by Mecky (1931); however the field intensity at A will then also be near this value and this needs to be taken into consideration during the discharge process.

As pointed out in Section 4, any value of Q can be used since the L and R dimensions are adjusted accordingly, but the value chosen should determine the severity of the individual stroke discharges and whether there is a capability of a multiple stroke discharge. According to early investigations, the average discharge involves a dipole moment of 100 C.km which at a height of say 4 km would involve 25 C per flash. Hence at an average of three components per flash approximately 8.C would be dissipated per stroke.

More recently Berger (1970) has communicated data for the charge in downward multiple strokes measured by the integration of current wave forms of direct measurements on the tower on Mt. San Salvatore, Lugano Switzerland. All of the lightning strokes measured were less than 250 C per stroke and 50% were less 6,5 C; these results included strokes with continuing currents however so that the values of charge associated with purely impulse currents would be less - probably much less in view of the large amount of charge delivered as continuing current.

Similarly Berger (1971) reported on the charge in negative downward single stroke flashes only, in which all 47 strokes measured carried less than 126.C. and 50% less than 7,5 C. including continuing current charge. Also the total charge delivered per flash did not exceed 250.C with 50% less than 14.C.

Hence it is not easy to define what is needed in a model, but it would appear that for an average condition for impulse charges alone, that is excluding continuing currents, about 5.C. would be delivered per stroke involving about 20.C. of total charge. However the accumulation of charge in the cloud could be at least 250 C or more to allow for continuing current discharge and for the possibility that not all the negative charge in the cloud would be neutralised during a single flash.

The next step in the model process is to assume that after a short interval of time, the boundary B of the negative cloud charge moves upwards to a position B_1, say at a velocity v_1 m/s covering a vertical distance of Z_1. Similarly and simultaneously the negative charge dissipated in the area Z_1 is virtually moved into the start of the leader of length Z_2, and having a new radius R_2, represented by a new lower boundary B_2 which has advanced from the original point B at a velocity of say v_2 m/s. This step is then shown on Fig. 12.0.2.

Fig. 12.0.2/ .....

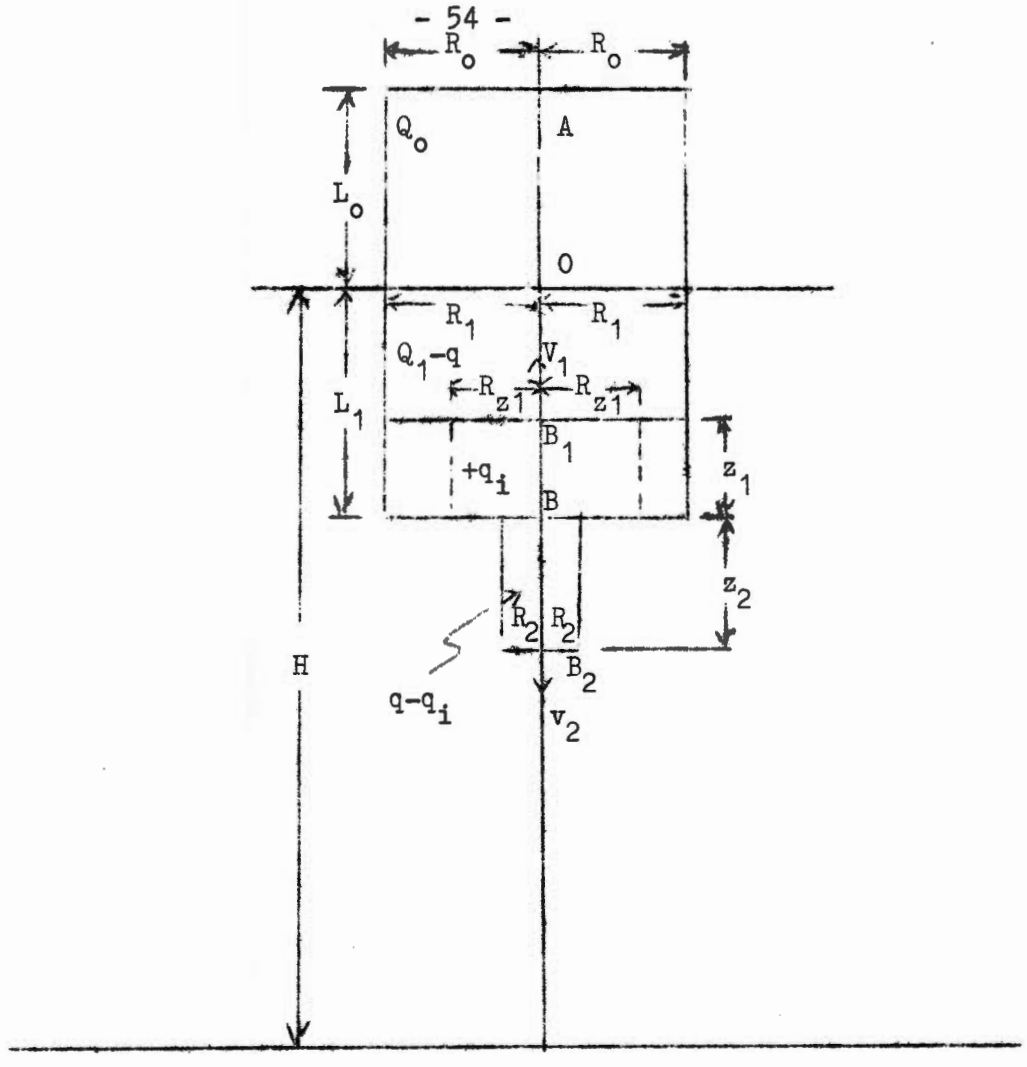

Fig. 12.0.2 Diagrammatic representation of the development of a leader channel

Disregarding for the present the significance of the area z_1 on Fig. 12.0.2, decisions are then required as to the order of magnitude to be assigned to the velocities v_1 and v_2 for upon them depends the amount of charge involved.

First dealing with the velocity v_2, being that of the leader tip, the only information available is due to the measurements of Schonland, Malan and colleagues.

Referring to the first leader Schonland (1938) gives values from a minimum of 1×10^5 m/s for a negative leader (which coincides with the drift velocity) to a maximum of 5×10^5 m/s for type α leaders, the most frequent value being $1{,}5 \times 10^5$ m/s. He also remarks that the velocity was approximately constant. For the first portion of the type β leader however velocities varied between 5×10^5 m/s and 2×10^6 m/s, and for the second portion the velocity fell to values of the order of the minimum. Type β leader however were in a minority.

For the step darts leader superimposed on the stepped leader, and for the uninterrupted dart leaders of subsequent strokes a very high value of velocity of 1×10^7 m/s is quoted.

A comparison with the negative laboratory spark is afforded by the results reported by Raether quoted by Meek and Craggs (1953) as follows:-

Point/ .....

Point-plane gap ..... $2x10^4$ m/s
Sphere-plane gap .... $2,5x10^5$ m/s
Uniform field ..... $7,9x10^5$ m/s

The result for the point-plane gap is perhaps the nearest geometric comparison with the lightning leader, nevertheless it indicates a velocity nearly an order of magnitude less than the drift velocity of electrons in avalanche; the remaining cases however are within the limits observed by Schonland for the leader pilot streamer velocity.

Loeb (1965) reports the results of work by Kritzinger (1962) in which he measured the velocity of negative corona and streamers from a point at 50 kv over 10 cm gaps which varied from $6x10^5$ m/s to $1,5x10^6$ m/s. At 300 kV the velocity was $1x10^6$ m/s for a 30 cm gap and increased to $3,5x10^6$ for a 20 cm gap. These velocities are in the highest range discussed by Schonland and are influenced by the length of the gap and the potential.

The differences in velocity are attributed by these investigators to progression by means of avalanches which are inherently slow and invisible, to that of streamers which are less stable but attain high speeds when the voltage applied to the gaps greatly exceed the minimum required for breakdown. Hence by analogy, the more common type α and the later portion of the type β leaders would conform to an avalanche type of progression whilst the first portion of the type β leader gives rise to streamer propagation.

With regard to positive streamer velocities there are many laboratory measurements varying over a wide field some of the reported results being as follows:-

Schonland (1938) $1,6x10^4$ m/s
Malan (1951) $1,6-3,6x10^4$ m/s
Allibone and Meek (1938) $2,1-2,6x10^4$ m/s

Meek and Craggs (1953) reporting Raether's measurements give the positive streamer velocities corresponding to the same gap arrangements indicated earlier namely:-

Point-plane gap $2,5x10^5$ m/s
Sphere-plane gap $1x10^6$ m/s
Uniform field gap $1,5x10^6$ m/s

These values of velocity were all much larger than those for the negative streamers in the same gap arrangements, whereas previously reported values were about one hundred times lower.

Kritzinger (1962) by comparison measured velocities from $1,5x10^5$ to $5x10^6$ m/s for streamers but in particular he noted that they together with repeated return strokes built up the luminosity of a slower moving leader channel having velocities from $1x10^4$ to $1x10^5$ m/s which he identified as the streamers of Allibone and Meek (1938). Loeb (1965) attributes this phenomenon to ionising space waves of potential which he claims are akin to the return strokes of lightning as Kritzinger noted. In applying this data to the mechanism of the penetration of positive streamers into a negatively charged volume of cloud it is apparent that perhaps the fast moving streamers exist in the breakdown process between the positive tips

and/ .....

and the millions of bound negative charges; however the progress of the ionised channel proper into such volumes is more probably much slower.

In order to involve the negative charge distributed over a very large volume in the cloud considerable lateral movement of streamers would be necessary so that the upwards velocity of the boundary B_1 of the negative charge in Fig. 12.0.2 would be expected to be very much lower.

Hence in the model of the lightning discharge suggested it may be expected that the positive mean velocity v_1 is likely to be very much less than that of the negative leader tip, not so much as a consequence of the prospective velocities of the tips themselves but as a result of the geometry, namely the large area to be covered by the positive streamers compared with the restricted area of the negative leader tip.

With regard to the actual velocity of streamer tips, it would appear that this is not entirely dependent upon the tip field intensity - except that a minimum ionising field must be present - but rather on the rate at which ionisation can be propogated ahead of the tip. This in turn is related to the potential of the tip which is maintained by the potential of the source of charge.

Hence the velocity of the leader is expected to be greatest when the cloud potential is highest and to be affected also by the proximity or otherwise of positive space charge which lies ahead in the path of the leader, which would increase its velocity as it approaches. The potential at the base of negative charged volumes indicated in Appendix I varies with the dimensions of the charges and also significantly with their height above ground. For example, for equal lengths of L_0 and L_1, the lengths of the positive and negative cylindrical charges, the potential does not exceed about 1×10^9 V, nor does it fall below about $0{,}5 \times 10^9$ V when H is 4 km. However if the positive charge reaches a length of say 6 km, the potential can be as high as $1{,}6 \times 10^9$ V.

On the other hand if H = 8 km, the potential varies from about $0{,}5 \times 10^9$ V for the smallest dimensioned cylinders up to in excess of 2×10^9 for the largest.

For the average and most common leader the velocities varied by a factor of five over the minimum, and this is about the same order of magnitude for the variation in potential.

Hence for the model of the discharge a velocity of $V_2 = 2 \times 10^5$ m/s is assumed for first trials for the leader and this is assumed to be related to V_1 by a factor "c" which may vary from 1 to 100 to represent the possible range of velocities of advance of the lower boundary B_1 (Fig. 12.0.2 refers).

From this the following relationships are derived namely that $z_1 = v_1 t$, and $z_2 = V_2 t$ and $V_2 = cV_1$ where "t" is the time ellapsed from the time of start of the leader on its downward path. Assuming constant velocities therefore, the length of the leader z_2 increases until it traverses the full distance between cloud and ground namely $(H-L_1)$ in a time given by $t_{max} = (H-L_1)/V_2$ seconds. At the same time the boundary B_1 moves upwards into the charge Q_1 releasing a portion "q" to be deposited on the leader.

If/ .....

If the charge Q_1 is assumed to be distributed in a linear manner then the amount of charge displaced is then given by the relationship:-

$$q = Q_1 [1-(1-z_1/L_1)^2] \quad \ldots\ldots\ldots\ldots\ldots\ldots\ldots \quad (12.1)$$

where $z_1 = v_1 t = c v_2 t$

It is clear that since the amount of charge deposited on the leader is limited to a few coulombs, the velocity v_1 must be restricted as also the total charge Q_1. For example if Q_1 = - 100 C and say q = - 10 C is moved out in say 20 ms, then $Z_1/L_1 = 0{,}0513$ and for L_1 = 4 km z_1 = 205,2 m, and $V_1 = 1\text{x}10^4$ m/s whence the ratio "c" is 20 - that is $v_2/v_1 = 20$.

The next step in the model assumes that during the advance of the boundary B_1, the field intensity at the central point along the axis, say, must not be allowed to fall below a minimum value.

This assumption does not allow for the possibility that if the field intensity required for ionisation at B was initially say $1\text{x}10^6$ V/m that thereafter a lesser value is needed to maintain ionisation. This however would result in a transient behaviour which, as previously surmised, could result in the stepping of the leader, and it is ignored for the present because the stage must eventually be reached when the initial ionisation level must again be maintained.

In order to maintain a value of field intensity of $1\text{x}10^6$ V/m at B_1 therefore, it is necessary to induce a positive charge q_i in the area z_1 distributed in such a manner and over such dimensions as to give this result. At the same time an equal amount of charge, but of opposite polarity, is deposited in the leader channel z_2 simultaneously.

The process now involves the calculation of the resultant field intensity at B_1 due to all charges and a solution for the value of q_i results from the premise that this field intensity must be equal to say $1\text{x}10^6$ V/m. This is however more easily said than done because many other variables now have to be introduced, and since the formulae for field intensity are relatively complicated, a computer becomes necessary for the calculations.

Assuming a charge Q is enclosed in a cylinder of length L and Radius R and it is distributed linearly in the axial direction - that is uniformly increasing density from zero at one end to a maximum at the other - and assuming further that the charge is situated in a given position relative to the height H above ground as depicted in Fig. 12.0.2, the field intensity at any point along the axis is given by a general expression as follows, namely:-

$$E = K [\pm \text{ Part I} \pm \text{ Part II}] \quad \text{where } K = Q/2\pi\varepsilon L^2 \quad \ldots\ldots \quad (12.2)$$

$$\text{and Part I or Part II} = \Big\{ \sinh^{-1}[(a-b)/R] - \sinh^{-1}[(a-c)/R]$$

$$+/ \ \ldots\ldots$$

$$+ [(a+b)/R] \left[1+ [(a-b)/R]^2\right]^{\frac{1}{2}} - [(a+c)/R] \left[1+ [(a-c)/R]^2\right]^{\frac{1}{2}}$$

$$+ (b/R)^2 - (c/R)^2 \Big\}$$

Part I refers to the real charges and Part II to their images and a, b, c and d, are values in terms of the lengths L, z or H according to the point for which the calculation of field intensity is wanted. In these the values of z_1 and z_2 have been stipulated in terms of the velocities v_1 and v_2 chosen, and the time, but the values of R for each case has to be determined.

Referring to Fig. 12.0.2 the values of $R_o = R_1$ are taken from a particular case involving $Q_o = + Q$ and $Q_1 = - Q$ and $L_o = L_1$ say which are chosen such that the field intensity at B is $1x10^6$ V/m and as fully described in Appendix I. Other cases given of unequal charges and lengths could also be used if desired. Then if the radius Rz_1 of the positive charge area z_1 is assumed constant, the value of the radius of the leader channel R_2 for any z_2 may be calculated on the basis that the field intensity at the point B_2 has to be equal to that of the value for ionisation at that point. The charge distri= bution in the area z_1 and that of the leader z_2 must also be assumed.

The program is an iterative one to find the value of q_i and R_2 which will fit the stipulated conditions and is carried out as follows:-

The total time for the leader to reach ground is calculated and divided into an arbitrary number of steps - for convenience 5% of the total time per step - and a value of ionising field intensity at B_2 - the leader tip, is assigned to each step, say $1x10^6$ V/m during its traverse through the cloud and the higher values varying between say $2x10^6$ and $3x10^6$ V/m in the clear air between cloud base and the ground. This also therefore settles the value of z_2 for each step, and also z_1 if the value of "c" is now chosen.

Choosing a fixed but artitrary value of Rz_1, and a convenient starting value for R_2 the field intensity at the point B_1 is cal= culated for the three known charges namely:

E_{01} due to the positive charge Q_o in L_o and R_o in the upper cloud
E_{11} due to the remaining negative charge (Q_1-q) left in (L_1-z_1) and R_1,
and E_{21} due to the negative charge "q" moved into the leader of dimensions z_2 and R_2

The sum of the three is then Eb_{11} which will fall short of the ionisation level by the difference $Ed = - 1x10^6 - Eb_{11}$

It is this difference Ed which has to be made up by the induced charge $\pm q_i$ placed in the z_1 and z_2 areas respectively.

If/ .....

If $E(+q_i) = q_i F(z_1)$ where $F(z_1)$ is the function depending upon the dimensions of the z_1 area and the form of charge distribution

And $E(-q_i) = - q_i F(z_2)$ Where $F(z_2)$ refers to the charge distribution and dimensions of the leader time step

Then $Ed = E(+q_i) + E(-q_i)$

Whence $q_i = Ed/[F(z_1) - F(z_2)]$

Hence having found the value q_i of induced charge which will satisfy the condition that the field intensity at B_1 equals $-1x10^6$ V/m for an arbitrary value of the ratio Rz_1 and R_2, the field intensity at the leader tip B_{21} namely $Eb2$ is now calculated from the following components field intensities:-

E_{02} due to the positive charge Q_o in L_o and R_o in the upper cloud
E_{12} due to the remaining negative charge (Q_1-q) left in (L_1-z_1) and R_1
Ez_{12} due to the positive charge q_i found and induced in z_1 of radius Rz_1
and Ez_{22} due to the negative charge $(q-q_i)$ now deposited on the leader to z_2 and R_2

The sum of these intensities, namely Eb_2, is unlikely to be equal to, but may be close to the value stipulated for that step. If it is numerically less than the required value, the value of R_2 arbitrarily chosen was too large, and vice versa, whereupon a stipulated reduction in R_2 (or increase) is then tried and the complete calculation repeated until Eb_2 finally falls within say 10% of the stipulated value.

Having then found a solution, using the first chosen value of the radius Rz_1 of the induced charge in the z_1 area, potential considerations must now follow. Here it is assumed that the potential difference along the conducting arc or spark formed in the z_1 and z_2 areas must equal some assumed value which may vary from say $2x10^4$ V/m up to $2x10^5$ V/m or more depending upon whether arc conditions are assumed to be present justifying the lower value perhaps, or spark conditions in which the potential gradient may be high.

The potential at the beginning or top end of the spark, namely at B_1 and that at the lower end, namely B_2 termed Vb_1 and Vb_2 respectively may then be related as follows:-

Let the potential difference $VD_1 = Vb_2 - Vb_1$

And the arc potential gradient $VD_2 = (z_1 + z_2) Vg$

Where Vg is the assumed value of potential gradient for an arc or spark.

Then/ .....

Then the ratio VD_1/VD_2 must be made equal to or at least within 10% of unity. The potentials Vb_1 and Vb_2 may be calculated from the following general formula for cylindrical charges in which the charge distribution is linear namely:-

$$V = K\ [\ \pm \text{Part I} \pm \text{Part II}] \quad \text{Where} \quad K = QR/2\pi\varepsilon L^2 \quad .. \quad (12.3)$$

and Part I or Part II $= \Big\{ a/R \sinh^{-1}[(a-b)/R] - a/R \sinh^{-1}[(a-c)/R]$

$$-2/3\left[1+[(a-b)/R]^2\right]^{3/2} + 2/3\left[1+[(a-c)/R]^2\right]^{3/2}$$

$$+a/R[(a-b)/R]\left[1+[(a-b)/R]^2\right]^{\frac{1}{2}}$$

$$-a/R[(a-c)/R]\left[1+[(a-c)/R]^2\right]^{\frac{1}{2}}$$

$$+a/R(b/R)^2 - 2/3(b/R)^3 - a/R(c/R)^2 + 2/3(c/R)^3 \Big\}$$

As for the field intensity equation (12.2) a, b, c, and d are values representing the dimensions L_1 z_1 or z_2 and H_1 Part I being the expression for the real charges whilst Part II is that for the mirror images.

The potential at the two points is calculated as the sum of the potentials due to the four sets of charges namely Q_o,(Q_1-q), q_i, and $(q-q_i)$ in the respective areas and if the value of VD_1/VD_2 is not close to unity the value of Rz_1 is now adjusted accordingly. However for each new value of Rz_1 chosen, a new value of R_2 must also be found in turn until all conditions are satisfied.

During the trial and error which was inevitable over the ten months which it has so far taken to develop the computer program a number of factors became clear.

In the initial program there was no adjustment of Rz_1 to allow for a constant potential gradient along the leader channel; this caused the potential of the leader tip to rise from a negative value of the order of -10^9 volts to zero as it progressed to earth. This would have been accepted as correct were it not for the fact that it transcended the known properties of an arc or spark which the leader channel must possibly be assumed to be.

There is some doubt over this question however in view of the fact that the measured potential gradient along an arc for example is that occuring when the arc is fully fledged and is not part of the initial breakdown process. The lightning leader on the other hand, whilst it must necessarily convey currents in excess of the maximum of one ampere, is still nevertheless a breakdown streamer

and/ .....

and its potential gradient may therefore be uncertain - particularly in the case of the stepped leader. If on the other hand it becomes as a spark channel, despite its high current, the potential gradient could be greatly in excess of say 1×10^5 V/m and there seems to be no particular cogent reason why it should not assume the natural gradient determined by the electrostatic field conditions which would alter as it progresses to ground.

However the program was altered to allow any chosen value of potential gradient to be entered, and as explained earlier the iterative program adjusted both Rz_1 (which enclosed the positive induced charge) and R_2 that of the leader, to meet the stipulated conditions.

The second factor which became clear was that the assumption of a linear distribution of charge axially for the leader channel (z_2, R_2) which was however distributed uniformly in a radial direction gave values for the leader radius R_2 which appeared to be too large. The criterion for this was however purely intuitive since the trial runs were aimed at keeping the leader radius down as low as possible. This lead to the concept of the concentric charge distribution referred to in Section 10 which allowed for half the radius for the same limiting value of field intensity. It was also found that the potential at B_1 and B_2 tended to be unaffected by the form of radial distribution of charge. In view of the above the program was altered to allow for the field intensity only being calculated on the basis of the concentric charge distribution the general formula for which being as follows, namely:-

$$E = K\,[\pm \text{ Part I} \pm \text{ Part II}] \quad \text{Where } K = Q/2\pi\varepsilon z^2 \quad \ldots\ldots \quad (12.4)$$

$$\text{and Part I or Part II} = \left\{ \sinh^{-1}\,[(a+z)/R] - \sinh^{-1})a/R) \right.$$

$$\left. - z/R \left[[1 + (a+z)/R]^2 \right]^{-\frac{1}{2}} \right\}$$

where "a" is in terms of L_o, L_1, z_1, z_2, and H, and z refers to Z_2.

Also $Q = (q - q_i)$ the charge on the leader.

This/ .....

This concentric form of charge distribution for the leader channel effectively halved the radius of the leader channel compared with a radial distribution which was uniform, and as has been previously discussed it has some basis in the physical model. Its disadvantage is the fact that in practise the leader tip will of course not present the form of an open-ended concentric cylinder described by the model. However it has the advantage that the tip may proceed to ground level without introducing infinite field intensities, and the interpretation to be placed on this is that the distance from the earth to the core of the leader equals the corona radius. This matter is referred to again when discussing the striking distance of the leader.

At one stage during the development of the program, a parabolic form of charge distribution was assumed for the positive charge area z_1 on the grounds that since the charge will then be more concentrated towards the positive tips of the streamers, less charge might be required to maintain a breakdown field intensity in the B_1 region. This proved to make no material difference to the calculations and was therefore abandoned. However this does illustrate that even a substantial change in the assumption as to the form of charge distribution to be used did not affect the final calculations because of other factors which were affected and which had a compensating effect. For example to this case the change in the potential at B_1 would have been less than the change in field intensity hence the radius of the z_1 area would be affected and so on.

Finally the program was arranged to calculate the field intensity at the cloud top at A and also at ground level at G immediately below the leader. In the case of the cloud top field, and in order to study the effect of a rapid movement of charge upwards, the top boundary A was allowed to proceed at a velocity v_o proportional to v_1 such that $v_o = c_o v_1$ whence the proportion c_o could be made any desired value. Thus if c_o was made equal to say 20, this meant that the boundary A at the cloud top would move upwards at a velocity which was 20 times that of the velocity of the boundary B_1 thereby simulating the effect of the upper positive charge dissipating into the upper atmosphere.

The program was written by Mrs. L. Stander of the Numerical Analysis Division of the National Research Institute for Mathematical Sciences and is described in Appendix II.

13. Numerical Results of computations

Referring to Fig. 12.0.2, a first choice of parameters for a computation on the model was as follows:-

$Q_o = 71$ C $L_o = 4$ km $R_o = 0{,}5$ km $H = 8$ km
$Q_1 = -71$ C $L_1 = 4$ km $R_1 = 0{,}5$ km
$v_2 = 2 \times 10^5$ m/s $v_2 = cv_1$ where c is variable
$v_o = c_o v_1$ where c_o was initially kept constant at 2×10^5 in order to keep the boundary A virtually stationary.

Since the velocity of the leader tip v_2 was kept constant for convenience, the traverse of the leader over the 4 km to ground was arranged in 20 equal steps of 200 m (not to be confused with the "stepped" leader) amounting to 5% of the distance at time intervals of 1 ms making a total traverse time of 20 ms.

This/ .....

This particular configuration of charge ensured that the field intensity at both the upper and lower extremities of the cylinder was $-1x10^6$ V/m initially and the program was arranged such that for each step advanced by the leader, sufficient positive charge q_i should be induced into the z_1 area to ensure that the field intensity at the lower extremity B_1 did not fall numberically below this value - in other words an ionising level having once been achieved, it was to be maintained at $-1x10^6$ V/m during the advance of the leader.

Since the ratio 2L/R was 16 and well in excess of 4, there was no question that the field intensity at the centre of the cylinder at O would be at ionisation level - in fact it was $3,6x10^5$ V/m - and intra-cloud breakdown was therefore obviated.

The field intensity Eb_2 at the leader tip was stipulated for each step and for the first stroke of the flash it was assumed that initially for 50% of the traverse to ground - that is for 2 km - the leader penetrated cloud media in which case the ionisation level was assumed to remain constant at $-1x10^6$ V/m.

At the lower cloud boundary however, where clear air conditions may occur, an abrupt increase in the field intensity required for breakdown was assumed, say, from $-2x10^6$ V/m increasing steadily to $-3x10^6$ V/m at ground level.

Assuming a starting value for the leader radius R_2 say equal to the cloud cylinder radius R_1, and for Rz_1 enclosing the induced positive charge, the computer then first of all calculates, by means of an iterative process, the value of induced charge q_i and the corresponding value of R_2 to meet the conditions stipulated above for the first step. Next the potential gradient is tested and if this is not within 10% of that stipulated for the program run, an appropriate adjustment is made to Rz_1 and the process of finding a new value of q_i and R_2 and again the potential gradient is repeated until this criterion is finally also satisfied, and all data is then printed out and the next step is commenced.

At the 50% step where the abrupt charge is field intensity is assumed to take place, a repeat calculation is carried out in order to indicate what adjustment is necessary to the values to start forging the leader through the higher strength air.

In order to simulate the effect of a dart leader of subsequent strokes, it was reasoned that the effect of the pre-ionised channel followed by the dart was a lower breakdown strength, arbitrarily assumed to be $-1x10^6$ V/m, in view of the lack of any known experimental data on the subject.

The value of $-1x10^6$ V/m breakdown strength for a pre-ionised channel may be too low if judged by work of Goodlet Edwards and Perry (Meek & Craggs 1953 pp 295) who showed the breakdown voltage between two co-axial cylinders fell from 88 kV to 64 kV as a result of successive sparking when the gap is enclosed. This amounts to a reduction of approximately 73% on normal breakdown field strengths.

First/ .....

First of all the advance of the boundary B_1 upwards at a velocity v_1 decides the amount of bound charge q finally neutralised and deposited on the leader according to the following Table 13.1.1.

Velocity Ratio "c"	Velocity v_1	Charge q deposited on leader
5	$4,0x10^4$ m/s	-25,6 Coulombs
10	$2,0x10^4$ "	-13,2 "
15	$1,3x10^4$ "	- 9,0 "
20	$1,0x10^4$ "	- 6,9 "
25	$0,5x10^4$ "	- 5,6 "
30	$0,7x10^4$ "	- 4,7 "
50	$0,4x10^4$ "	- 2,8 "
100	$0,2x10^4$ "	- 1,4 "

Table 13.1.1 Charge "q" neutralised in cloud and deposited on leader

$Q_1 = -71C$ $v_2 = 2x10^5$ m/s $v_2 = cv_1$

Whilst there is no absolute criterion as to the amount of charge lowered by the leader as a proportion of the total cloud charge, there is reason to suppose that it should not exceed say 10 C. Bearing in mind that the figures in Table 13.1.1 do not include the induced charge it is therefore evident that values of the ratio "c" in excess of 15 should be used which correspond to velocities of v_1 of less than $1,3x10^4$ m/s.

Low values of the velocity v_1 are perhaps quite realistic in view of the fact that this represents a mean velocity of advance of the positive streamer tips. The actual velocity of individual sparks would however require to be much higher if they are to traverse the whole of the volume represented by the dimension z_1 of radius Rz_1.

In the case of the high velocity dart of the order of $1x10^7$ m/s, that is 50 times the value assumed for the stepped leader, the traverse time is of course reduced by this proportion and for the same ratio "c" the charge moved is the same as in Table 13.1.1. The velocity v_1 on the other hand is also 50 times larger, and whilst this may be possible up to a point it is more than likely that actual values will be less, and the limiting ratio of velocity "c" will therefore be higher than for the stepped leader, and the charge moved correspondingly less.

Dealing first of all with the case of the dart leader, since the control value of the leader tip field intensity is constant at $-1x10^6$ V/m, and choosing a value of c = 20, the computed values of induced charge q_i for various values of potential gradient have been plotted on Fig. 13.0.1 using a percentage time or distance basis for the leader tip traverse. The discontinuities evident in the curves are due to the limits set for the various control values in order to prevent the number of iterations becoming too large.

Fig. 13.0.1/ .....

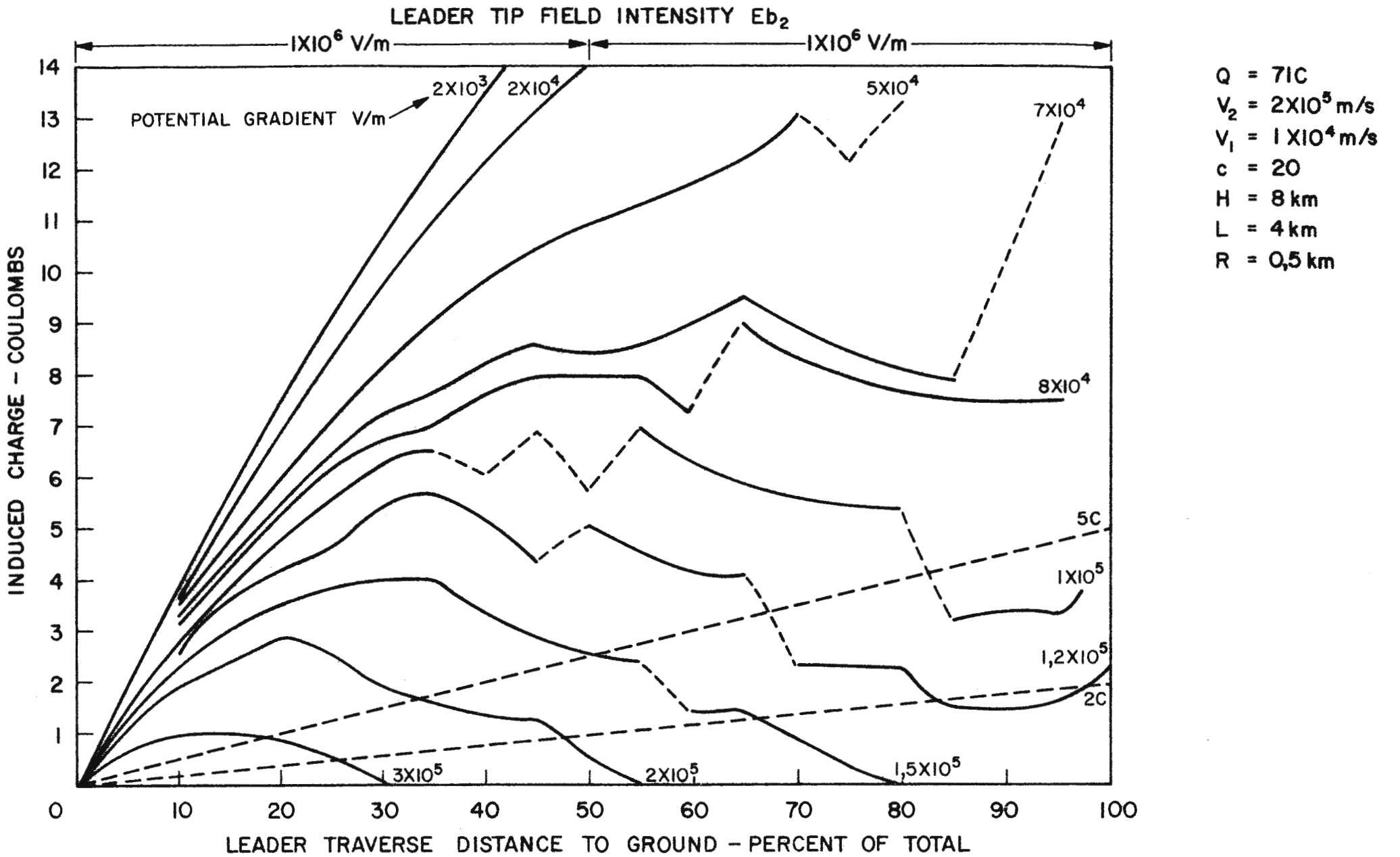

FIGURE 13·0·1

INDUCED CHARGE AT CONSTANT VELOCITY AND VARIABLE POTENTIAL GRADIENT

Fig. 13.0.1 illustrates clearly that for a potential gradient of $2x10^3$ to $2x10^4$ V/m which would be normal for a full bodied arc, the induced charge on the leader would be enormous and quite out of the question - for example 14 C would be needed up to about 50% of the traverse.

However it also shows that for induced charges of the order of 5 C or less indicated by the dotted lines, the potential gradient along the leader should exceed about $1x10^5$ V/m, and that at the start of the leader values of $3x10^5$ V/m would be needed to meet the boundary conditions stipulated.

Again if the value of the radius Rz_1 enclosing the induced positive charge q_i is plotted as Fig. 13.0.2 for various values of the potential gradient along the leader, the corresponding points for a maximum induced charge of 1; 2; or 5 C can be plotted in by noting the intersections of the dotted lines on Fig. 13.0.1 with the distance of traverse.

This now indicates even higher limits for the value of potential gradient along the leader if the value of Rz_1 is not to exceed 0,5 km, which is the radius of the main charge cylinder.

It also shows that for this assumed velocity ratio of 20, an induced charge of between 1 and 2 C will be needed corresponding to a potential gradient greater than $1,2x10^5$ V/m.

It is now necessary to consider the case of variable velocity ratios keeping the potential gradient constant. Here a value of $1,5x10^5$ V/m is suggested by the previous example as being of the right order of magnitude, and the induced charge was then calculated for velocity ratios varying between c = 5 and c = 100 and plotted in Fig. 13.0.3.

This figure shows that for a constant potential gradient, if the induced charge is to increase in linear proportion to the length of the leader, as would be expected, the velocity ratio $c = v_2/v_1$ must increase from a value below 5 to start with, to a value of say 100 to induce 2 C, and 50 to induce 1 C. For a constant value of leader velocity v_2, the velocity of the positive tips represented by v_1 must therefore start off at high value and then slow down as the leader progresses. Alternatively if the positive tip velocity remains constant the velocity of the leader tip must increase substantially as it progresses towards ground. The latter has not been observed by Schonland or by anyone else so far as the writer is aware, and the former, that is a slowing down of the positive tip velocity, is a possibility but the velocity change is very large.

If the variation of Rz_1 is now examined for the same case - that is for a constant leader potential gradient of $1,5x10^5$ V/m with variable velocity, the computed results are indicated on Fig. 13.0.4. This again shows that if the radius of the positive charge volume Rz_1 is not to exceed that of the main charge of 0,5 km, induced charges reaching a maximum of less than 1 C would be permitted and again the relative velocity of the leader to that of the positive tips would need to change by a factor approaching 10.

Considering/ .....

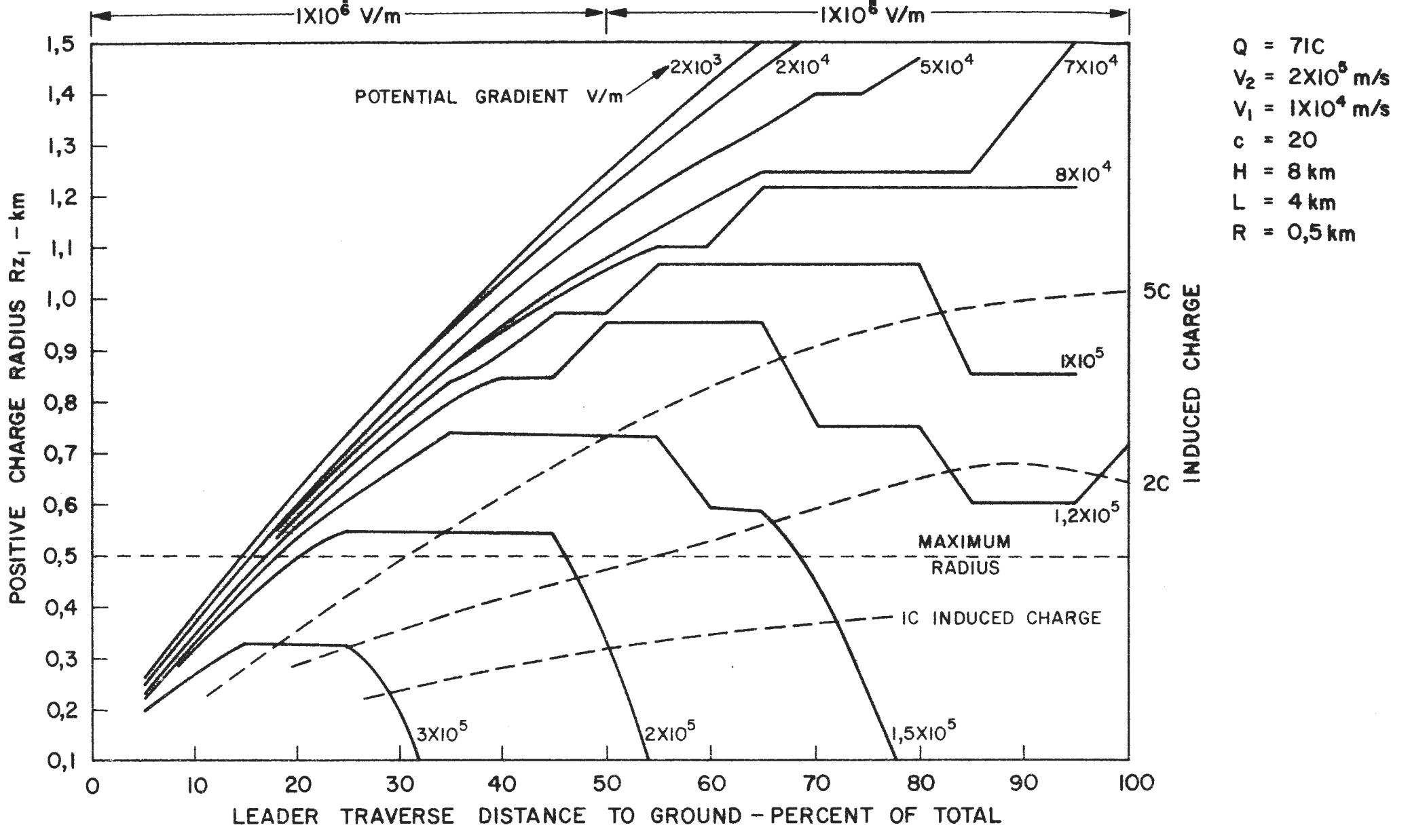

FIGURE 13 · 0 · 2

POSITIVE CHARGE RADIUS AT CONSTANT VELOCITY AND VARIABLE POTENTIAL GRADIENT

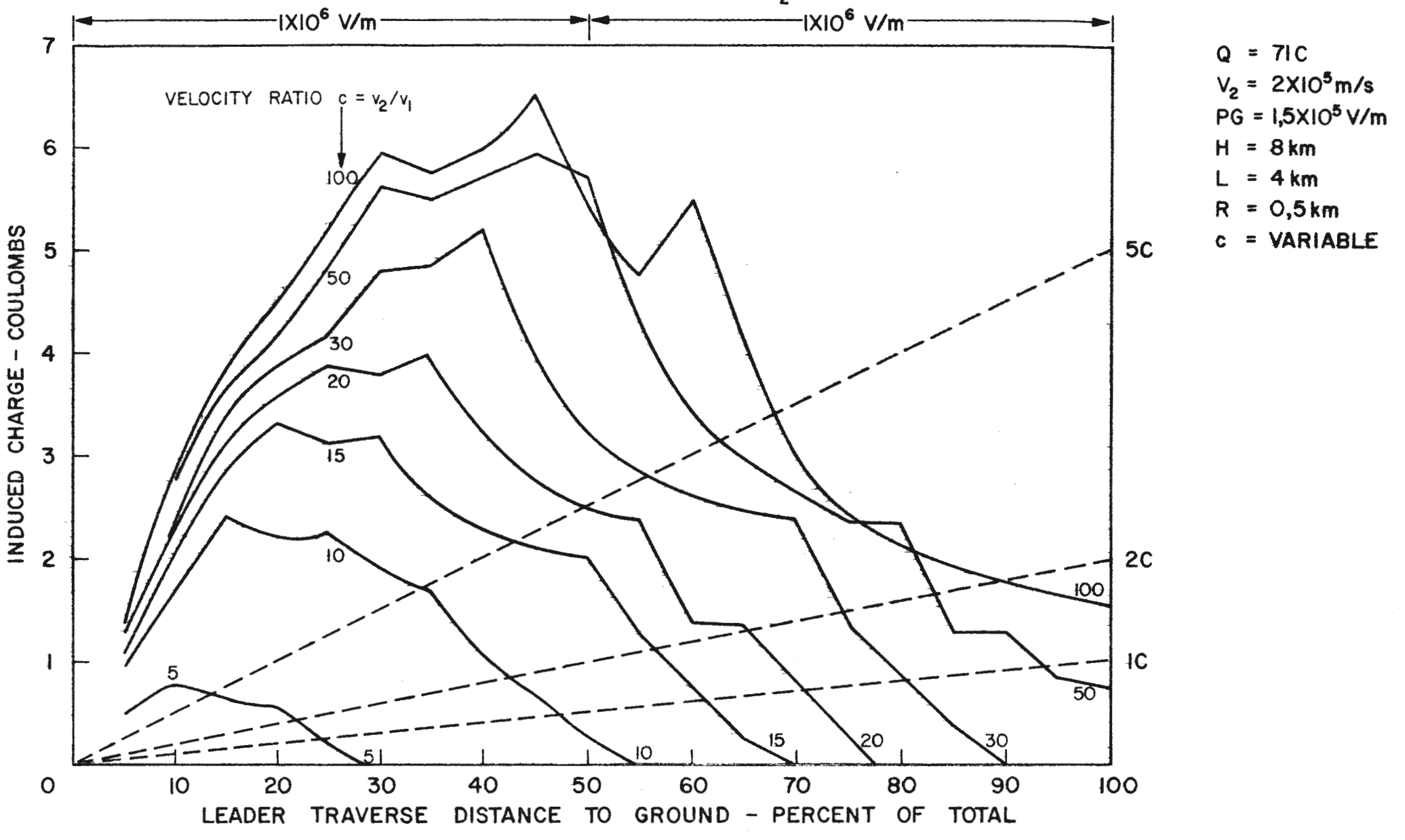

FIGURE 13·0·3

INDUCED CHARGE FOR CONSTANT LEADER POTENTIAL GRADIENT AND VARIABLE VELOCITY RATIO

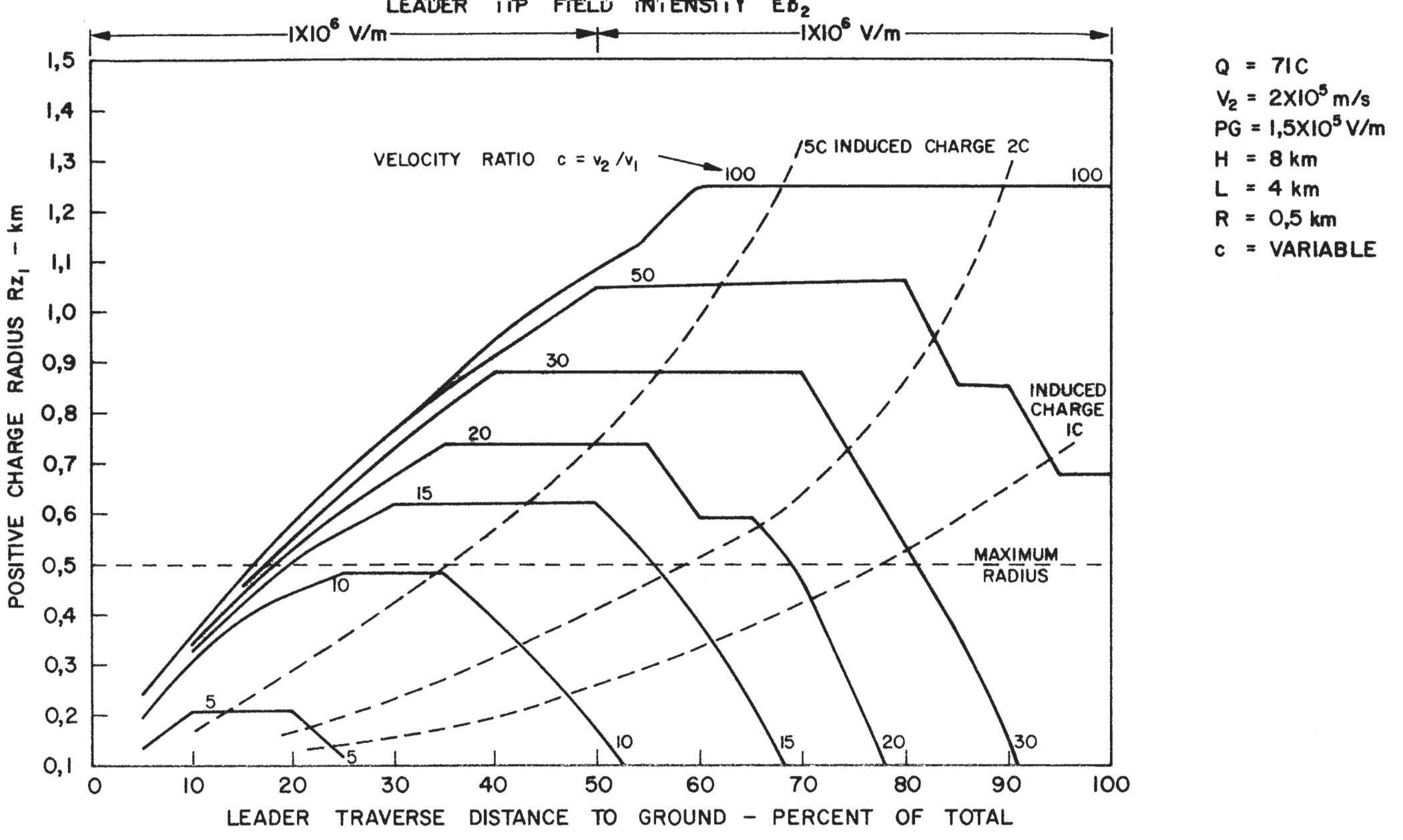

FIGURE 13·0·4

POSITIVE CHARGE RADIUS FOR CONSTANT LEADER POTENTIAL GRADIENT AND VARIABLE VELOCITY

Considering the physical factors involved it would be expected that the volume of positive charge induced at the top of the leader channel will begin with dimensions not much larger than the leader channel radius, but will increase with the propagation of the leader somewhat resembling the funnelling arrangement postulated by Loeb (1966) and referred to earlier. However it is unlikely that the radius enclosing this charge would exceed that of the cylinder enclosing the main negative bound charge which is being neutralised. Regarding the potential gradient of the leader, it is evident that the applicable values greatly exceed that of the laboratory arc, and there is also no particular physical reason why it should remain constant.

It is evident from the numerical results so far that if the velocity ratio remains constant, the potential gradient must vary and vice versa and the limitations placed upon these functions by the dimensions of the positive induced charge suggest that both the velocity ratio and the potential gradient should vary.

The computer program was therefore modified to seek an iterated value for Rz_1 during the initial traverse of the leader until such time as it reached a value equal to R_1, which is the radius of the cylinder enclosing the bound negative charge. In order to do this, an arbitrary starting value for the potential gradient had to be stipulated for the iterative program until $Rz_1 = R_1$, and thereafter the potential gradient could be calculated. The starting value had to be as high as possible, otherwise the initial induced charge tended to be in excess of the final wanted value; on the other hand if too high, the assumed potential gradient would exceed the maximum value which electrostatic considerations would allow, and the program would not function correctly. Hence computer calculations during the initial period when Rz_1 is approaching R_1 must all be regarded as arbitrary.

Fortunately as observed from Fig. 13.0.5 this initial period lasted only during the first 20 to 25% of the leader traverse, and at least the trend of conditions during this period can be seen.

It would appear that irrespective of the field intensity required for breakdown at the leader tip, induced charge on the leader can be achieved with less change in velocity ratio than previously but in the reverse order. Initially the velocity ratio is required to be high and for a given linear increase in induced charge it falls steadily. This means that for a constant leader velocity, the velocity of the positive streamers starts off very slowly and increases steadily as the leader progresses to earth. Alternatively of course for a constant positive tip streamer velocity the leader velocity is initially high, slowing down during the later portion of its traverse.

The computer study shows also that the results are the same whether the leader tip field intensity is say 1×10^6 V/m for the complete traverse, as might be expected of the dart leader, or whether it has to negotiate higher field strengths below the cloud base of from 2 to 3×10^6 V/m.

Regarding the arbitrary area up to about 25% of the leader traverse, all that can be said is that the assumed values of potential gradient were too low and that in fact higher values should be

used/ .....

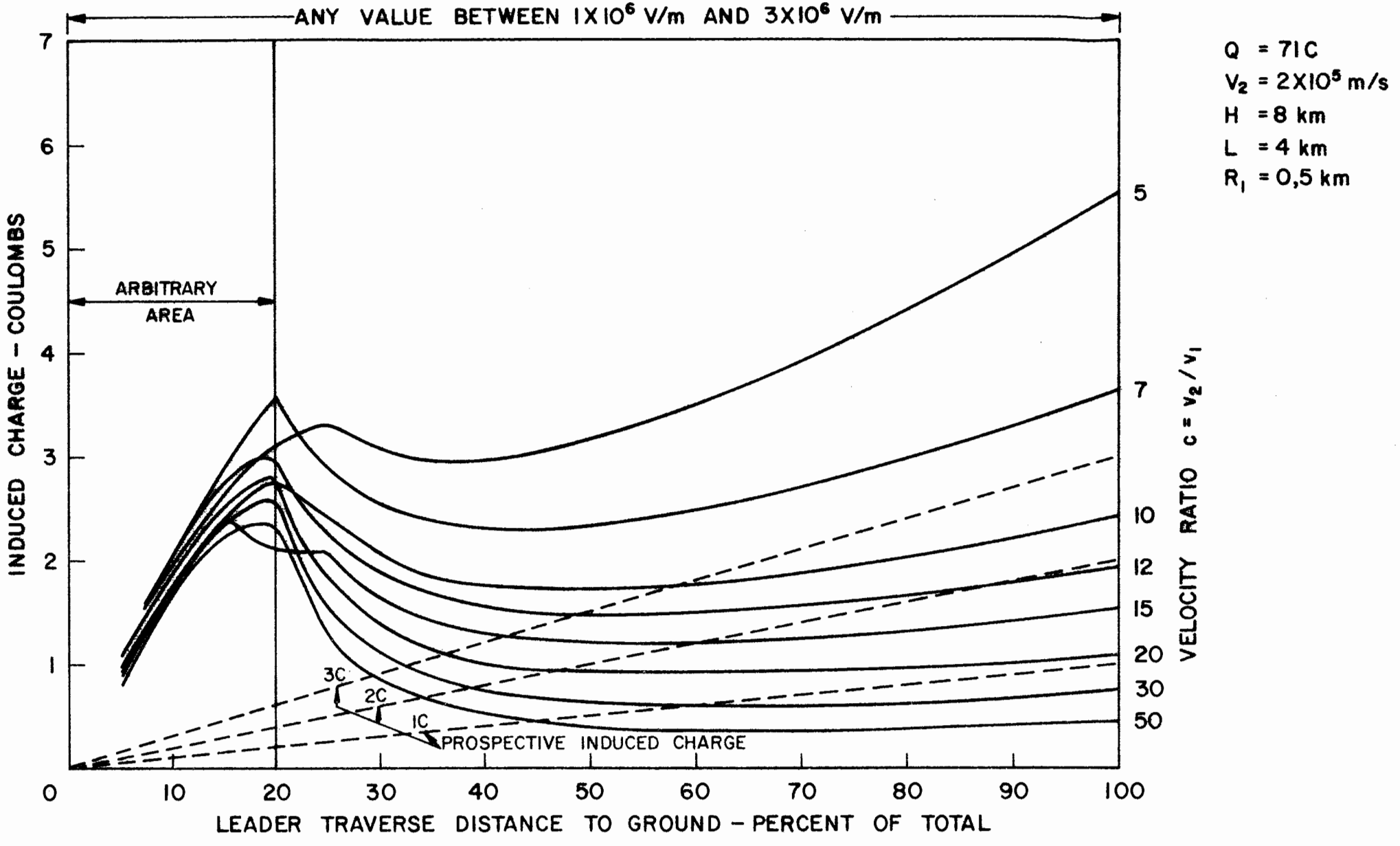

FIGURE 13 · 0 · 5

INDUCED CHARGE FOR VARIABLE VELOCITY RATIO ($Rz_1 = R_1$ FROM 25 %)

used to keep the induced charge down to small values approaching zero. On the other hand the model may concievably give somewhat inadequate results during this stage in view of the fact that the charges are assumed to be enclosed in relatively thin discs with large radii whereas the field intensity is calculated for the centre line of the discs only.

Although there is no exact basis upon which to determine what amount of charge might be lowered from a charge dipole of differing dimensions and charge magnitude, it is seen from Table 13.1.1 that if the velocity ratios "c" are as low as 5 to 10, the charge abstracted by the leader will be from 13 to 26 coulombs to which must still be added the induced charge which could, according to Fig. 13.0.5, vary between 2,5 and 5,5 coulombs. These would mean that the total charge lowered by the leader would be from about 16 C to 31 C which is per= haps possible, but well in excess of the mean values measured by Berger and others of between 5 and 10 coulombs. Furthermore if the stroke was to be followed by continuing current much more charge will usually then be lowered from the cloud, whereas there is, in this case, only a limited amount available.

On the other hand for velocity ratios in the range of from 20 to 50, the charge extracted from the cloud is in this case between 3 and 7 coulombs and the induced charge from Fig. 13.0.5 would not ex= ceed 1 coulomb. These orders of magnitude are much more realistic but nevertheless arbitrary and probably depend finally upon the potentials.

Fig. 13.0.6 and 13.0.7 therefore shows the calculated values of the potential gradient along the leader. Firstly Fig. 13.0.6 is for the case when the field intensity at the leader tip is maintained at $1x10^6$ V/m and it includes the arbitrary area between 0 and 25% of the leader traverse when the gradient was stipulated for the program run until such time as the positive charge radius Rz_1 equalled that of the negative bound charge radius R_1. An interesting point regarding this arbitrary area was that the values of gradient used could not exceed the maximum which in most cases occurred at 25 to 30% of the traverse, there being no solutions of the equations in such cases within the limits of the iteration process allowed in the program.

The starting potential at the cloud in this case was $-6,4x10^8$ Volts and the mean potential gradient over the 4 km to ground is therefore $1,6x10^5$ V/m. The potential gradients during the initial traverse of the leader to ground however vary from about $3x10^5$ V/m when the velocity ratio "c" is 50, down to $3x10^4$ V/m when c = 5.

In every case the potential gradient reduces during the traverse of the leader and between 90 and 95% of its traverse the values of potential gradient have fallen to below $1,5x10^5$ when c = 50 to below $1x10^4$ V/m when c = 5.

It is interesting to note that the very low value achieved in the latter case is of the same order of magnitude of the arc voltage drop which lies between $2x10^3$ and $1x10^4$ V/m, but this case also coincides with the case when the charge on the leader is about 30 coulombs and the current flowing in the leader during its advance is of the order of 1500 amperes.

More realistically, when considering velocity ratios of not less

than/ .....

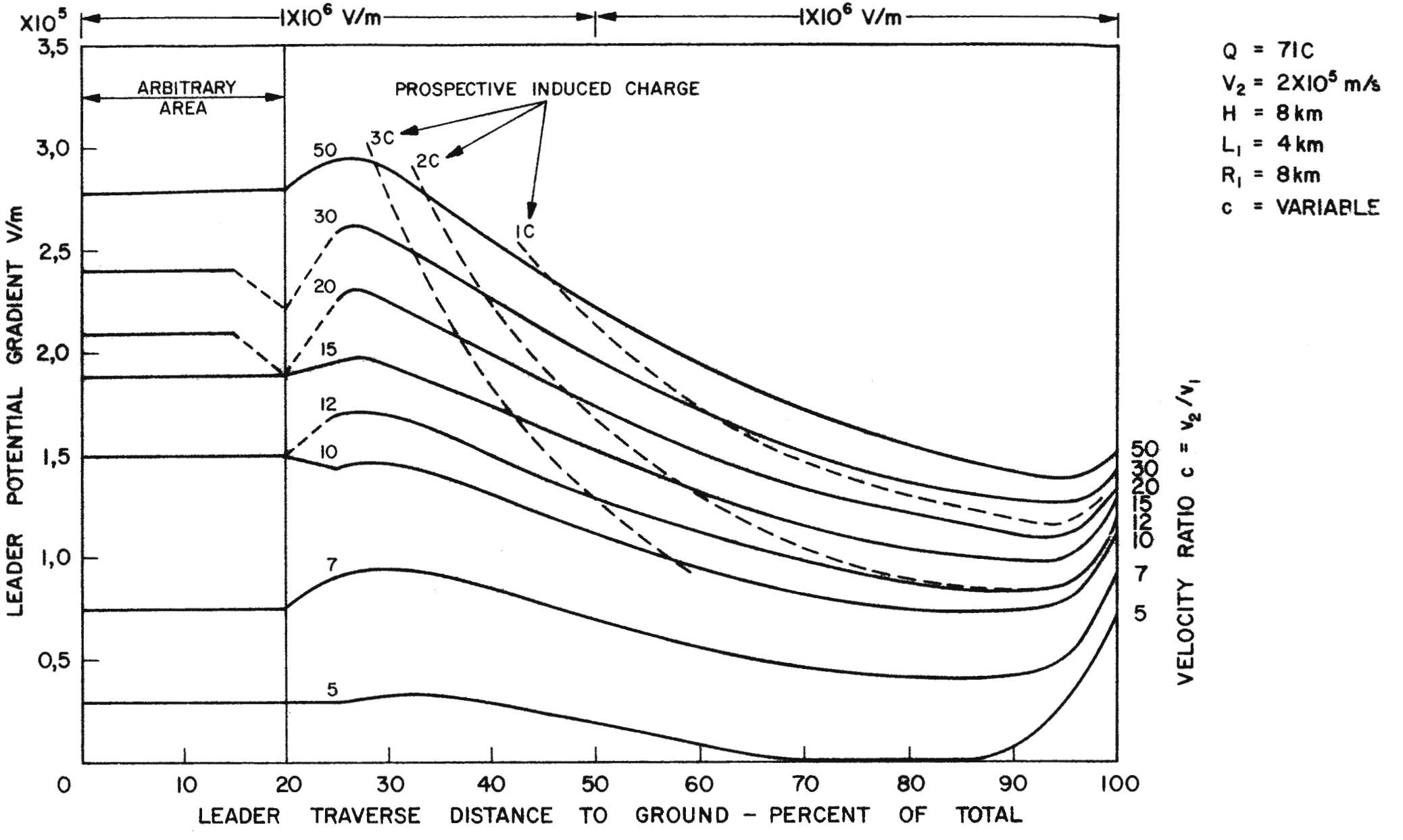

FIGURE 13 · 0 · 6

LEADER POTENTIAL GRADIENT FOR VARIABLE VELOCITY RATIO ($Rz_1 = R_1$ FROM 25%)

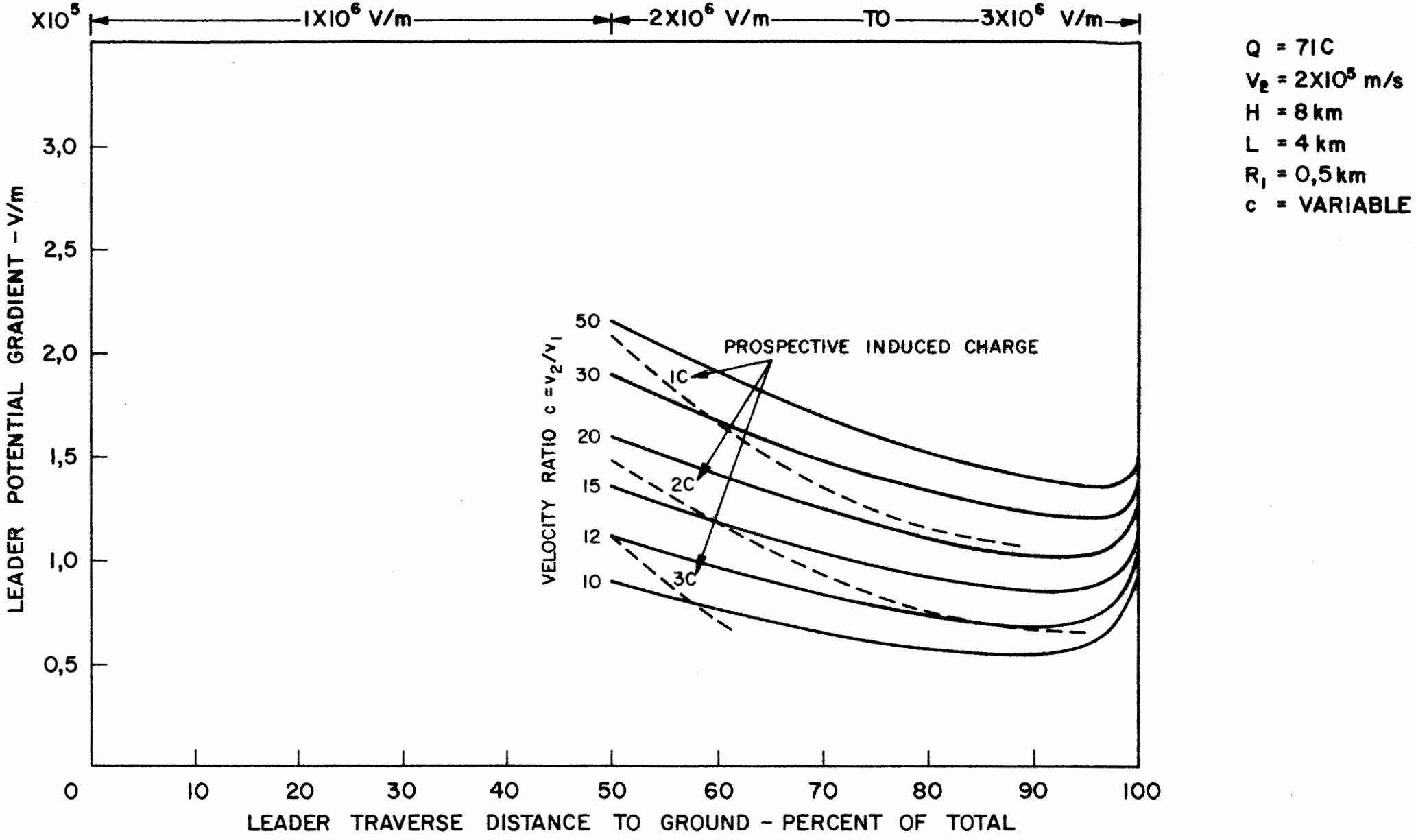

FIGURE 13·0·7

LEADER POTENTIAL GRADIENT FOR VARIABLE VELOCITY RATIO ($Rz_1 = R_1$ FROM 25%)

than c = 15, the lower limit of potential gradient (for the case of a tip field intensity of $1x10^6$ V/m) is $1x10^5$ V/m which is an order of magnitude greater than the accepted value for an arc volt drop. Values in excess of $2x10^5$ up to $3x10^5$ V/m are indicated however during the initial advance in the cloud.

Fig. 13.0.7 on the other hand illustrates the effect of a leader forging its way through air having a breakdown strength varying from $2x10^6$ V/m at cloud base to $3x10^6$ V/m at the earth's surface. At a velocity ratio of c = 50 there is not much difference in the potential gradient compared with the $1x10^6$ V/m limit on ionisation level, but at C = 5 the values of potential gradient became negative and the case does not therefore exist. The minimum value reached at c = 10=however, was $5x10^4$ V/m compared with $7,5x10^4$ V/m when the limiting field in= tensity was $1x10^6$ V/m.

The above quoted figures of potential gradient are in general identified as those applying for streamers as opposed to arcs in short gap breakdown phenomena. This is so despite the higher currents flow= ing into the leader stroke.

Furthermore, and contrary to popular expectation, the potential of the leader tip falls much more rapidly during the advance of the leader as a result of the high potential gradients. As a consequence of this the final breakdown across the relatively short gap as the tip approaches the earth is not so sudden an affair as imagined, since the field intensity at the earth is building up to breakdown values as the leader approaches and when it reaches a height equal to its corona radius above earth, the field intensity at the earth is equal to the field intensity at the tip of the channel.

The increase in potential gradient during the last 5 to 10% of the leader traverse to ground as indicated on Fig. 13.0.6 and 13.0.7 is a feature of the calculation at constant velocity ratio. If one of the prospective induced charge lines (shown dashed) is followed, it will be noted that the velocity ratio must reduce slowly during pro= gression until at the end of the traverse the reduction is rapid. The 2 C line for example indicates a falling velocity ratio from c = 50 to c = 12 during the leader traverse between about 35% and 90%. This, in all probability, is due to an increase in velocity of the positive tips as a consequence of a build up of the positive in= duced charge at the top end of the leader.

Fig. 13.0.5 on the other hand shows that the velocity ratio re= mains close to a value of 12 for the 2 C line whereas Fig. 13.0.6 and 13.0.7 whould therefore indicate an increase in potential gradient during this period.

This change in conditions is obviously due to the effect of earth which begins to manifest itself more substantially when the leader approaches close to ground. It is observed to be much more prominent at the lower values of velocity ratio "c" than at high values, and this in turn relates it to the charge which is highest with low values of "c". In a sense the mathematical conception of the leader may begin to depart from its physical characteristics at this point, and this may therefore be a possible criterion for breakdown. In this regard it should be noted that a 5% traverse is equivalent to 200 metres, and it is of interest to note that a radical change begins to occur at about this distance from earth at value of c between 12 and 20.

The/ .....

The initial potential at the upper end of the channel is deter= mined of course by the magnitude, dimensions and disposition of the positive and negative cloud charges and is shown in Figs. 13.0.8 and 13.0.9 for the two cases of leader tip field intensity.

In these cases, it has an initial value of about $6{,}5 \times 10^8$ Volts, and during the progression of the leader the upper potential varied both as a consequence of the advance of the leader charge downwards and the advance of the positive tips upwards. It is also modified by the induced charge and prospective values of one, two and 3 C are shown as dashed lines on the respective figures.

At the upper end of the channel an increase in the value of in= duced charge raises the potential more positive (or decreases the potential numerically) as would be expected. However the induced charge has the opposite effect upon the potential of the lower tip of the channel - a result which was not predicted from a qualitative consideration. Fig. 13.0.8 and 13.0.9 show that the higher the prospective value of induced charge the higher is the numerical value of potential of the tip above zero. Furthermore, a leader following the course indicated by a linear increase in induced charge - that is following any one of the dashed lines indicating prospective induced charge - the potential of the tip at values of 1 to 2 C tends to remain constant until very late in the traverse when after 95% it must of course revert sharply to zero.

The inverted effect of the induced charge is of course due to the differing potential gradients. The 1 C prospective charge line is associated with velocity ratios of between 50 and 20 which also in turn refers to lower values of charge and therefore leader current, whereupon the potential gradient is correspondingly high. For 2 C prospective induced charge on the other hand the velocity ratios tend to fall to below 10, with higher values of charge and corres= ponding current and with lower potential gradients. This is illus= trated clearly on Figgs. 13.0.6 and 13.0.7.

The total charge lowered by the leader, that is the sum of the in= duced charge neutralised by the upward advance of the positive stream= ers at B_1, is now shown on Fig. 13.0.10 for velocity ratios varying between 10 and 50 and is the same for the two cases whether the leader tip field intensity is held constant at -1×10^6 V/m, or whether it is raised from the 50% transverse onwards from -2×10^6 V/m to -3×10^6 V/m.

The dashed lines shown on this figure are derived from Fig. 13.0.5 and represent the cases of a linear increase in induced charge with length of leader for values of one, two and three coulombs. It will be clear therefore that if the total charge lowered by the leader is not to exceed about 10 C, the induced charge will be between 1 and 2 C and the velocity ratio will decrease from some value in excess of 50 to approximately 15.

The computed values of the Radius R_2 of the leader are shown in Fig. 13.0.11 and 13.0.12. Both sets of data show the characteristic change in radius between 90 and 100% of the leader traverse, and as before this is more pronounced when the velocity ratio is low and also when the field intensity maintained for the leader tip is at the lower values. The computation is based upon a leader of constant radius and

it/ .....

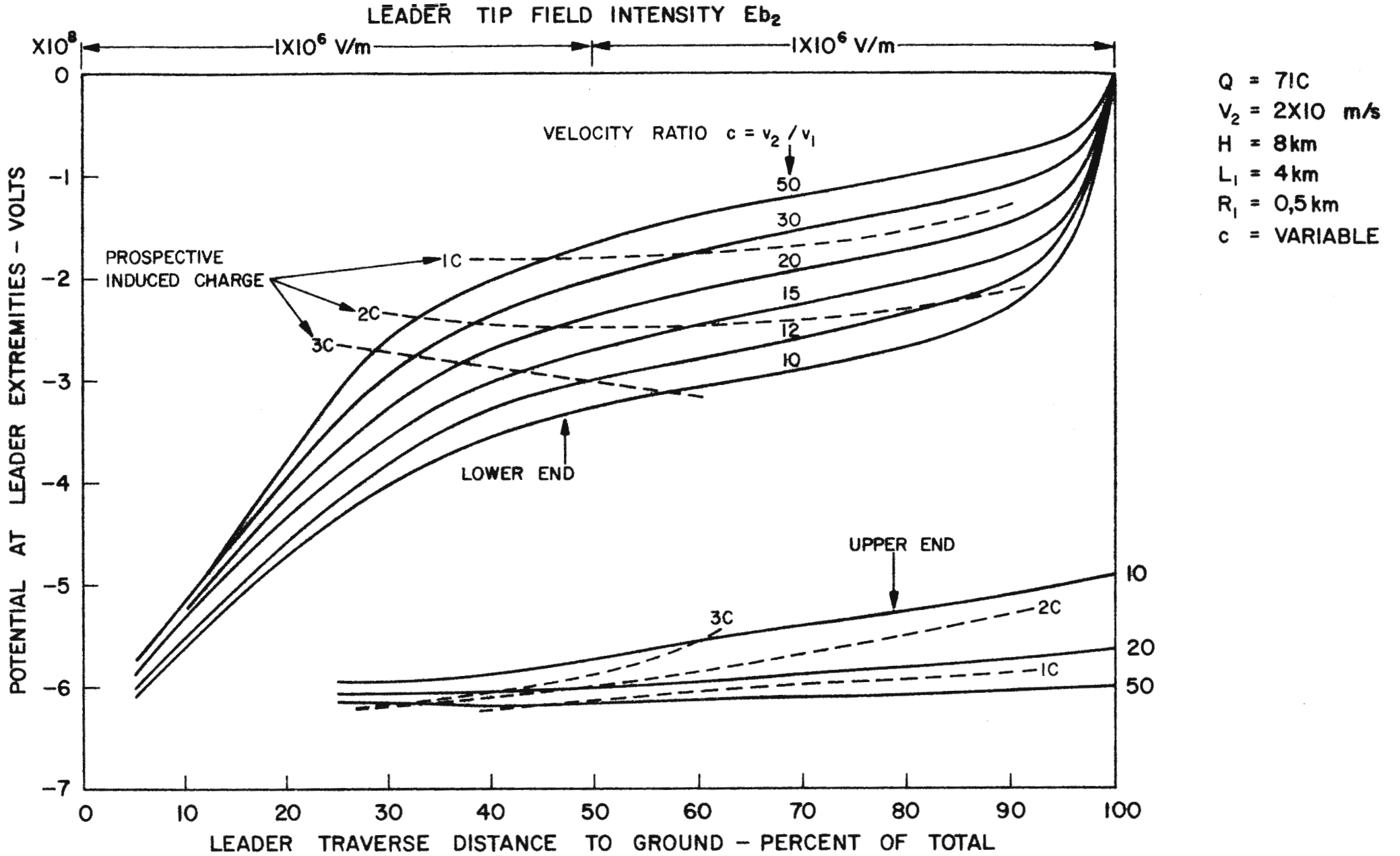

FIGURE 13·0·8

POTENTIAL AT LEADER EXTREMITIES FOR VARIABLE VELOCITY RATIO ($Rz_1 = R_1$ FROM 25 %)

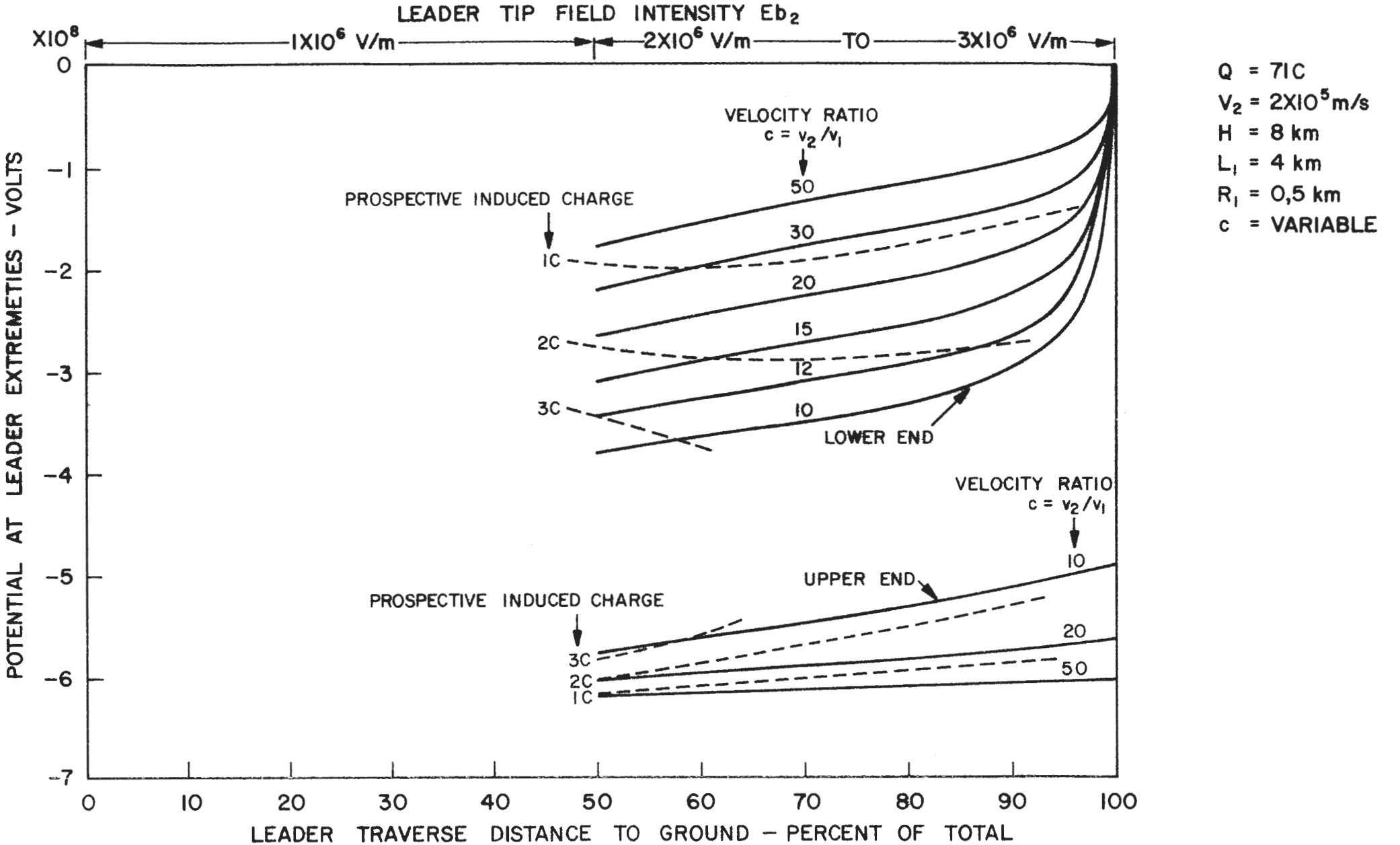

FIGURE 13·0·9

POTENTIAL AT LEADER EXTREMITIES FOR VARIABLE VELOCITY RATIO ($Rz_1 = R_1$ FROM 25%)

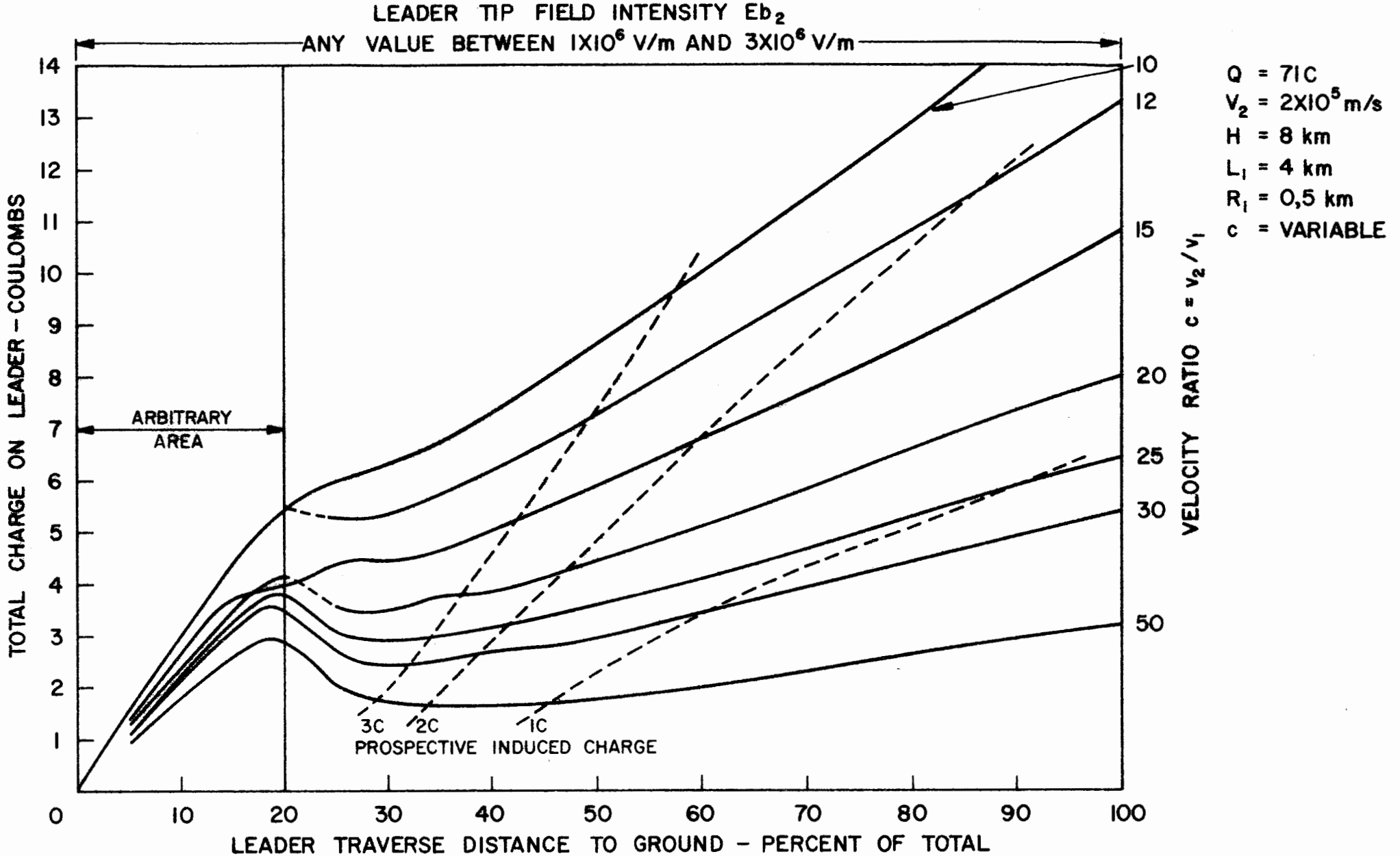

FIGURE 13·0·10

TOTAL LEADER CHARGE FOR VARIABLE VELOCITY RATIO ($Rz_1 = R_1$ FROM 25%)

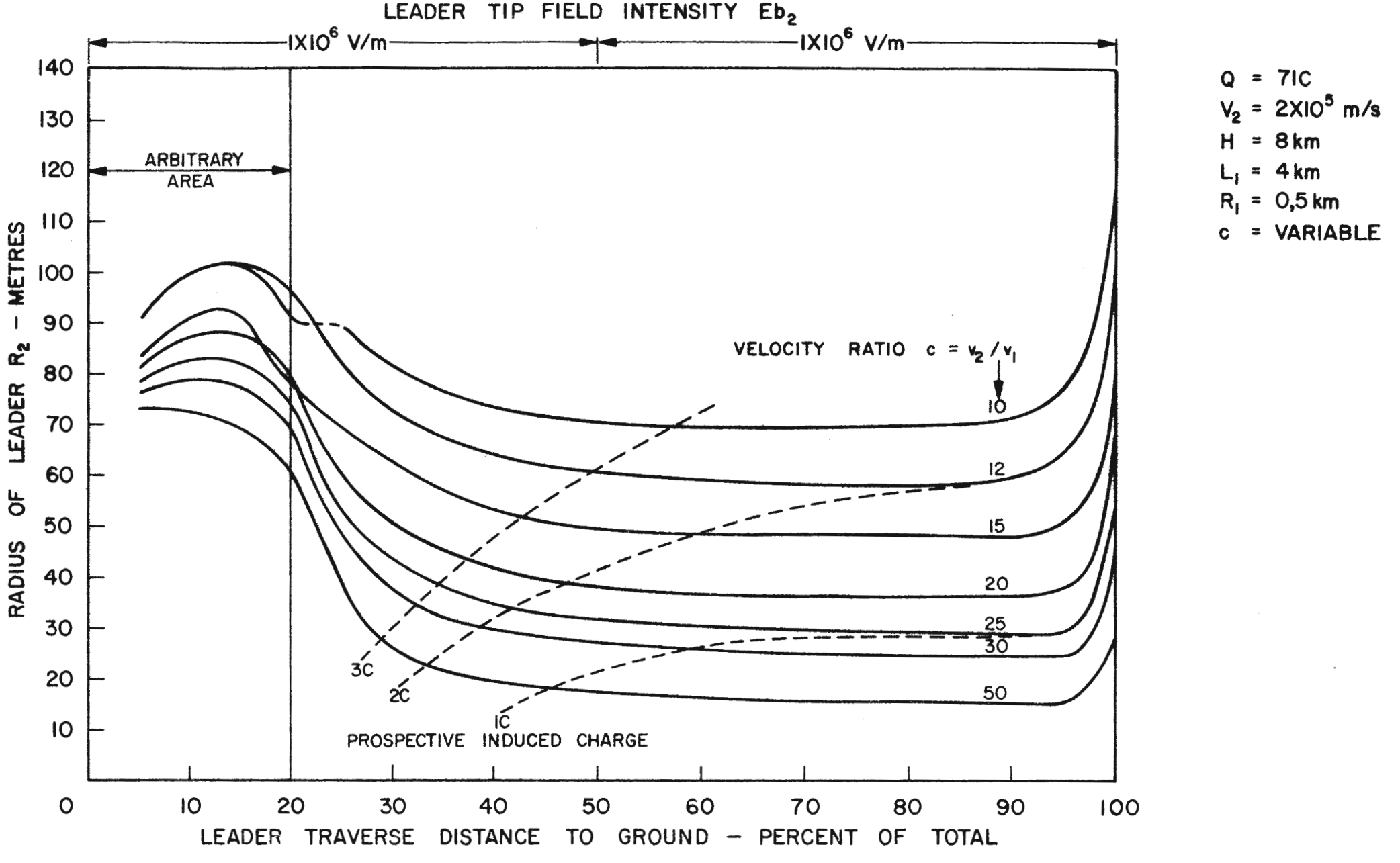

FIGURE 13 · 0 · 11

RADIUS OF LEADER CHANNEL FOR VARIABLE VELOCITY RATIO ($Rz_1 = R_1$ FROM 25 %)

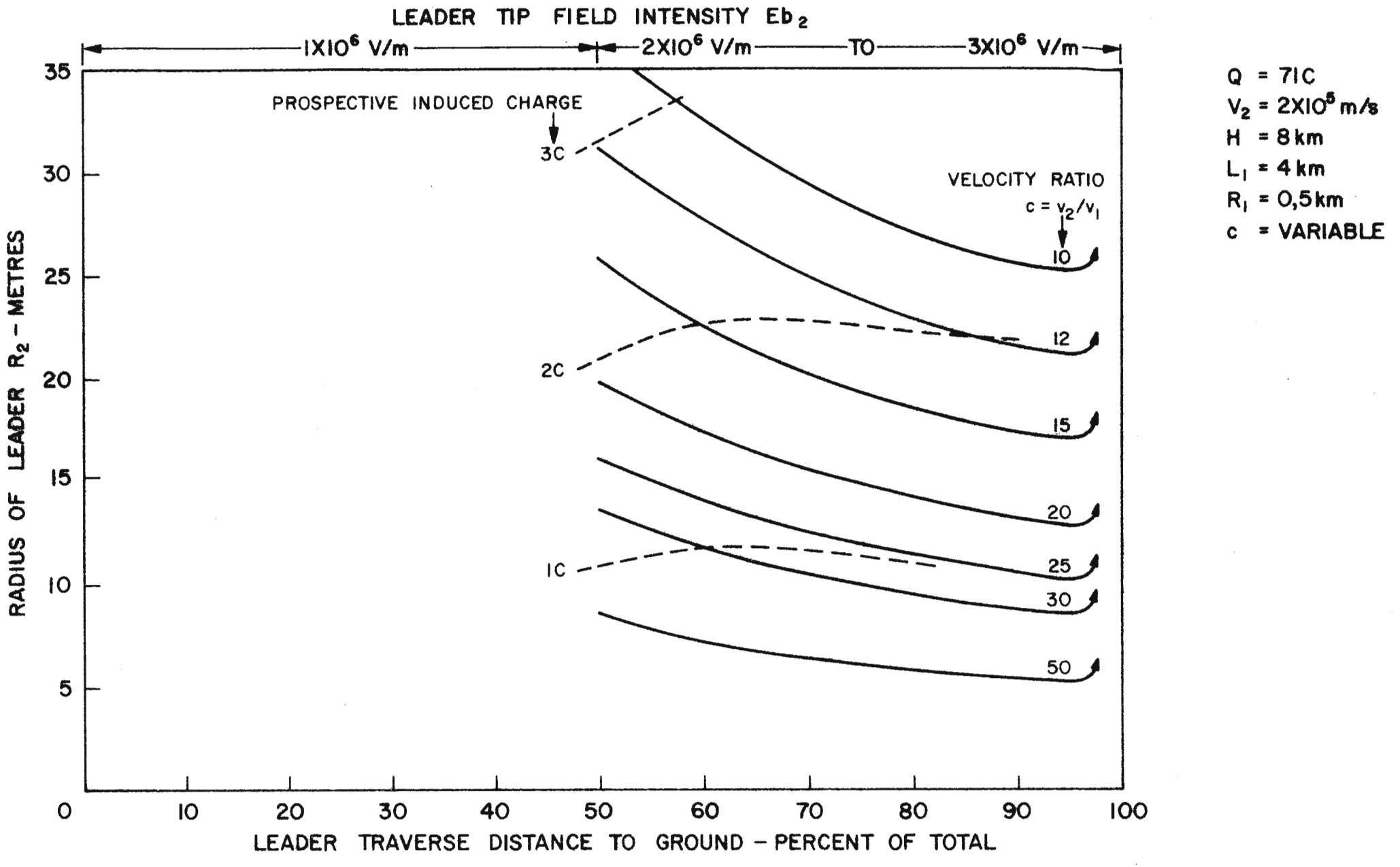

FIGURE 13·0·12

RADIUS OF LEADER CHANNEL FOR VARIABLE VELOCITY RATIO ($Rz_1 = R_1$ FROM 25%)

it is unrealistic to assume that when it reaches near the earth, the whole leader tends to expand. What is far more likely is that the lower end of the leader tends to fan outwards upon sensing the mirror image of the charges in the earth. That the effect is not due to a discontinuity in the functions used for the calculation is proved by the fact that finite values of radii are calculated - these are shown on Fig. 13.0.11 but omitted on Fig. 13.0.12 merely for convenience. Furthermore there is no such discontinuity or even abrupt change indicated in the value of charge on Fig. 13.0.5 or Fig. 13.0.10. This therefore must be accepted as a consequence of the electrostatic conditions surrounding the leader on closely approaching the earth and has a significance with regard to the "striking" distance, or more precisely, the distance when breakdown conditions begin to be effective, and this is discussed further under the question of the striking distance.

The second point regarding the leader radius is that it varies in an inverse ratio to the field intensity maintained for the tip. This is understandable since for the same charge the radius needs to be correspondingly less for the higher field intensity. Referring to Section 10 the approximate expression for the corona radius is given by equation (10.13) which states as follows, namely:-

$$r/q = 1/\pi\varepsilon E \; h \; m/C$$

where E is the tip field intensity and h is the overall height of the leader channel.

Hence for a channel height of 4 km and for $E = 1 \times 10^6$ V/m $r/q =$ 9,0 m/C and for $E = 3 \times 10^6$ the value of 3,0 m/C, and this is as calculated from the charge and radius for all values of velocity ratio of the computed results, for the case of 100% of the leader traverse.

14. The dart leader

An important question now arises regarding the dart leader. The first leader forges an ionised channel through air which has a field strength of say 3×10^6 V/m and in so doing the radius of the channel is small. If the subsequent dart leader lowers the same quantity of charge, its radius will be limited to the dimensions of the now preionised channel, in which case the field intensity at its boundary in the radial direction would still be 3×10^6 V/m, but the field strength of the ionised air in the channel would be less, say 1×10^6 V/m. This may result only in an increased velocity of the tip since the field intensity along the direction of propagation is so much less - and this is in accordance with observation. In other words, given a driving potential such as produced by the cloud charge, the leader will be propagated at a higher velocity the less the resistance to breakdown ahead of the tip.

On the other hand, if only one third of the first leader charge is deposited in the channel, the field intensity both axially and radially would not exceed 1×10^6 V/m. However while there is evidence that, excluding continuing currents which consume very large values of charge after the return stroke, the charge lowered in subsequent strokes is on average less than that for the first stroke, but there

is/ .....

is nevertheless a considerable scatter in the values and some sub= sequent strokes are known to be more severe than the first.

In part I Section 16, the ratio of magnitude of field changes of 905 1st component strokes to that of the mean for each flash was given as 1,5 with a median ratio of 1,4 and a standard deviation of 0,7. This states virtually that there is a 50% probability that the ratio would be 1,4 but there is also a fair probability that the field change of the first stroke could be less than the mean value for the flash.

Regarding the 2nd component, which would comprise the dart leader, the mean value of the ratio was 0,9 and the median value 0,8 with a standard deviation of 0,5. On this basis the ratio of the field change of the 1st stroke to that of the 2nd would be of the order of 1,7. However due to the time constant used for measurement, the slow= er leader field change would be attenuated more than that of the high velocity dart leader whence the ratio of field changes would be some= what greater - perhap of the order of 3. This would therefore suggest that the dart leader charge is about 1/3 of that of the first leader. Uman (1969) reports the results of various investigators concluding that whilst the average charge lowered by the stepped leader is 5 C that of the subsequent dart leader is about 1 C. Berger (1967) gives a few examples of the peak value of lightning currents deliver= ed in the first and subsequent strokes from which it can be ascertained that there is a more or less random distribution of high and low currents, the first not being necessarily the largest. However the peak current delivered may not be directly related to the charge in the stroke depending so much as it does upon the wave from of the current discharge.

Hence whilst the model suggests that the dart leader can deposit a charge equal to the 1st stepped leader, it is more than likely to be less depending upon the state of pre-ionisation of the channel.

Another aspect affecting the dart leader is its very high velocity varying from $1x10^6$ to $2x10^7$ m/s, compared with a range of $1x10^5$ to $3x10^6$ for the stepped leader. If the charge deposited is equal in the two cases this suggests that the rate of extraction of charge from the cloud is increased by a factor of at least ten - and this seems to be improbable because the field intensities at the top of the leader have no special reason to increase - in fact the model holds this constant at a breakdown value of $1x10^6$ V/m.

Referring to Fig. 13.0.12 a leader with a tip field intensity of $3x10^6$ V/m and with a velocity ratio of about 17 would have a radius of 15 m and from Fig. 13.0.10 would deliver about 9 C of charge. On the other hand for a dart leader having a field tip intensity of $1x10^6$ V/m the velocity ratio required for the same radius according to Fig. 13.0.11 is about 50, and again on Fig. 13.0.10 this positive tip velocity in the first case would be $1,18x10^4$ m/s assuming a leader velocity of $2x10^5$ m/s, but the positive tip velocity would be $4x10^4$ m/s in the case of a dart leader having a velocity of $2x10^6$ m/s.

Looked at in another way, if the velocity ratio c remained the same, that is the ratio of the leader tip velocity to that of the upper positive tips, the dart leader would extract the same amount of charge as the slower first stepped leader in about one tenth of the time - but the positive tip velocity would have to be also ten times

higher/ .....

higher. On the other hand, if the charge lowered by the dart was only one tenth of that of the stepped leader, the velocity of the positive tips would remain unchanged. The charge deposited by the dart leader is certainly more than one tenth, but if it is one fifth then the positive tip velocity must increase by a factor of two; if one third the factor increases to $3^1/3$ and so on.

The above figures do not ring true for the reason that there is presently no reasonable mechanism which would explain why the upper positive tips of the dart leader should increase in velocity. If anything, due to the discharge of some of the charge in the cloud the field intensity will tend to fall and the velocity of proga= tion will reduce or stop rather than increase.

Since there is no satisfactory explanation of this to be found in the literature it is permissable to speculate on various possi= bilities which may be followed up.

First there is a marked similarity with the step darts which proceed down the leader channel at regular intervals corresponding to each step. This dart has a high velocity of equal order of mag= nitude to the dart leaders of subsequent strokes and the high velocity is said to be due to the fact that the dart follows a pre-ionised path in both cases. Schonland (1938) derived an expression for the ve= locity of the dart (or wave) as follows:-

$$v_w = n_i^{1/3} v_e d \text{ .. m/s} \quad \ldots\ldots\ldots\ldots\ldots\ldots\ldots \quad (13.1)$$

where n_i is the electron density in front of the wave,

v_e is the electron drift velocity,

and d is the mean distance between electrons, assumed also to be the wave front distance over which a strong electric field extends. Loeb (1966) considers this to be suspect on the basis that there are no physical grounds for the assumption that the time for the wavefront to go a distance "d" is the time for each electron to travel the average distance between electrons. Secondly for initial electron densities greater than $10^{12}/m^3$ the formula predicts dart velocities in excess of the speed of light.

Loeb takes care of these points in the following modified expression, namely:-

$$v_w = \alpha v_e d/\ln(n_f/n_i) \quad \ldots\ldots\ldots\ldots\ldots\ldots\ldots\ldots \quad (13.2)$$

Where α is Townsend's first ionisation coefficient and is the number of new electrons created per centimetre by a drifting elec= tron and where n_f is the final electron density after the wave front has extended a distance d and is given by

n_f/ .....

$$n_f = n_i \exp{\cdot}(\alpha v_e t) \quad \text{and} \quad t = d/v_w \quad \ldots\ldots\ldots\ldots\ldots\ldots \quad (13.3)$$

According to Uman (1969) if the ratio n_f/n_i is chosen say about 10^5 then for an electric field of $7{,}2 \times 10^6$ V/m, d = 0,3 m, $\alpha = 4 \times 10^4$ /m, $v_e = 3 \times 10^5$ m/s then the wave velocity is 3×10^8 m/s or the speed of light. The total potential difference across the wave front is 2×10^6 Volts.

If the electric field chosen is smaller, the value of α, d and v_e will also be smaller, and a reasonable dart leader velocity is found. Also the potential difference across the wave front will be less.

There can therefore be little doubt that this mechanism explains the dart velocity whether it be in the stepped leader or subsequently the dart propagating in the ionised path left by the previous stroke, but it was observed by Schonland that if the interval between strokes becomes large, the dart leader would again proceed in a series of steps. This he attributed to the fact that the degree of ionisation in the channel decays with time until a point would be reached where= by it required a fresh breakdown process as for the first stepped leader.

Hence it is reasonable to suppose that if the precise mechanism for the dart in a stepped leader is evaluated, the same mechanism may be applicable exactly to the dart of subsequent strokes.

The model herein described and evaluated for a particular case indicated the position that occurs when the leader is assumed to progress at a constant velocity of say 2×10^5 m/s and does not account for the steps or darts. However it does show that if the charge in= duced on the leader by the electric field is to increase proportin= ately with the length of the leader the velocity ratio must decrease steadily - and for a constant leader tip velocity this means that the velocity of the positive tips must increase.

Correspondingly the potential gradient along the leader is shown to decrease steadily as the leader advances to ground. (Except during the last 10% of the traverse).

Now these could be regarded as mean values which would be attained if in fact there were no dart leaders or stepping, but it is obvious that the mean velocity of the positive tips for example may also be achieved by a series of bursts at high velocity followed by quiescent periods at low velocity. Similarly the potential gradient of the leader may fluctuate between high and low values as determined by the current flow in the leader. In this regard, if during the pilot lead= er progress the magnitude of the current flowing is small, the poten= tial gradient would tend to be high corresponding with that of a streamer; on the other hand a sudden burst of current would tend to lower the gradient during this transient period. Hence the poten= tial of the tip of the leader would momentarily fluctuate above and below the mean potential for the point in space.

In view of the above considerations the following hypothesis of the possible mechanism may be advanced.

The/ .....

The charge separation process proceeds initially to the point where the field intensity increases to an initial breakdown level of say $-1x10^6$ V/m at a point or small area at the base of a cylindrical charge containing negative charge bound say on water drops.

Immediately ionisation takes place in that area, it spreads rapidly over a restricted volume of negative charge until the field intensity is too low to support further ionisation. This may perhaps be in the region of say $-0,5x10^6$ V/m. The bound negative charge is neutralised by some of the positive ions which were the product of ionisation, leaving a nett negative charge in the form of free electrons which are expelled downwards in the direction of the field thereby creating ionised spark channels which join up to form the nucleous of the start of the downward leader.

These spark channels being conducting and under the influence of the electric field extend in length due to the concentration of electrons and positive ions at their extremities, and in addition they are assisted to do so by the induced charge separation which virtually adds more charge of each sign to the extremities as the channel increases in length. This may be regarded as a relatively slow process occuring as it does when the external field intensity is less than breakdown, but the local field intensity at the respective tips is still sufficient to ionise the air immediately ahead of them.

The space previously occupied by negative bound charge has been neutralised but it does contain the positive induced charge on the channel tips which eventually builds up the field intensity again to reach the level of $-1x10^6$ V/m whereupon another burst of ionisation takes place.

This now causes a surge of electrons down the channel at the high velocity of the stepped dart and in so doing causes the potential of the tip of the leader to change abruptly to a new level determined by the redistribution of charge along the leader.

The leader tip continues to extend and the step dart repeats itself at intervals dependent upon the velocity of the leader. The induced positive charge at the top increases steadily with the increase in leader length so that when ionisation bursts occur, the velocity of the ionisation wave front in the bound charge increases thereby fulfiling the average requirement that for a constant leader tip velocity, the velocity ratio decreases - that is the mean velocity of the positive tips increases as the leader proceeds to ground.

If therefore the step dart lowers charge into the leader with each step over and above what has already been deposited in previous steps, including the charge lowered during the progress of the pilot leader, it follows that the charge lowered per step dart is very small since there are numerious steps of the order of 50 to 100 m in length in one leader of a few kilometres in length. This in turn means that the intermittent breakdown process taking place at the upper extremities is also very confined in volume and suggests therefore that the fall in field intensity below ionisation level is not very large before the process stops.

The/ .....

The single dart leader for subsequent strokes, if it is to re= semble the stepped leader dart at all, must therefore either deliver a very much larger charge - with a corresponding large volume of ionisation taking place in the cloud at as rapid a rate, or some if not all charge must already be available in the pre-ionised channel.

The one outstanding difference between the stepped leader and that of subsequent leaders is the fact of the extensive ionised channel which the dart follows, and if this is suspended so to speak between the cloud charge and the earth without actually main= taining low conductivity contact, the full capacity of induced charge on this channel would be available so long as there is an inducing field present. The possibility therefore exists that if at some interval after the first return stroke has taken place, contact be= tween the channel and earth is lost, electrons must immediately regroup at the lower end of the channel to establish this induced charge and this may in fact constitute the dart leader. Under these circumstances the negative induced charge would at least be discharged to earth, and according to Fig. 13.0.10 this amounts to 1/7th of the total charge that would otherwise have been lowered by the first stepped leader. The dart leader of subsequent strokes does deliver more than this to the earth so that it must be assumed that the dart charges the channel up to full potential by virtue of a burst of ionisation in the cloud capable of the same relative high velocity. This is indeed possible since the induced positive charge can be made available at the positive tipped streamers at the same rate as the dart descends the ionised channel.

This line of reasoning suggests that the leader breaks contact with the earth first. If it did not, the top of the channel would remain highly positive and the discharge would be continuous as it frequently is. In Part I Section 14 is was indicated that only 4% of all flashes produced continuing currents. However the measurements were made with a circuit having other time constants of less than 1 ms and this would be bound to suppress the slow field charges aris= ing from continuing current so that only very large field changes would be detected. This would account for the fact that other in= vestigators have found what has been assumed to be continuing current in about 50% of all flashes.

The argument with regard to the mechanism of the dart leader however cannot be completed before consideration of the return stroke which proceeds it, and this is undertaken in a later section.

15. Corona losses

Now that the potential of the leader channel is clarrified - at least in so far as the particular model is concerned - it is pertinent to consider possible losses sustained by the leader before the advent of the return stroke. Such losses would amount to the reduction of the charge available for neutralisation during the return stroke.

In this connection Bruce and Golde (1941) postulated that of a total of 8 C lowered by the leader only one coulomb was neutralised by the return stroke and this of course would have a very significant effect upon the magnitude of current delivered to ground. Such losses of charge could be accounted for in two ways. First of all electrons expelled into the outer perimeter of the corona sheath

could/ .....

could become attached to heavy air molecules and thereby become immobilised possibly never to be able to return to the active channel. Secondly by means of corona loss which may be defined as leakage loss due to the neutralisation of electrons or negative ions from sources of positive ions external to the leader channel. These ions would be either present in the space between the leader and earth as a con= sequence of its conductivity or they may be supplied from space charge generated by points on the earth under the influence of the electro= static field.

An approximate quantative estimate of the possible loss may be obtained by means of the empirical formula devised by Peek (1929) for corona loss on conductors adapted to suit a vertical channel.

This is as follows for two conductors of radius "r" and spaced "2s" cms apart namely:-

$$P = 241(f+25)\ [(r+6/2s+0,04)/2s]^{\frac{1}{2}}(V-V_d)^2 x10^{-5}\ \text{watts/m} \quad .. \quad (15.1)$$

Where f = frequency
V = Applied potential (r.m.s.) kV
V_d = Disruptive potential (rms) kV

$$\text{And } V_d = E_d r.m.\ln(2s/r)\ \text{kV} \quad ..... \quad (15.2)$$

$$\text{And } E_d = E_o \delta \left[\left(\frac{1+0,3}{\delta r}\right) \cdot \frac{1}{1+230r} \right] \text{kv/cm} \quad ..... \quad (15.3)$$

Where E_o = Field Intensity to cause ionisation kV/cm
δ = relative air density
m = surface smoothness factor for the conductor (taken as unity)

First of all the value of V_d, the disruptive voltage at the con= ductor surface may be disregarded in this case since its magnitude is likely to be very small compared with the applied potential.

For example for a conductor size even as small as 1 mm and for δ = 0,9 say, then E_d = 1,175 E_o and where E_o is say 30 kV/cm ($3x10^6$ V/m), the value of E_d is then only 35 kV/cm.

The value of V_d in equation (15.2) is then largely controlled by the value of the radius chosen, and the value of "s" is equivalent to the height above ground of an element say 1 m in length. To make V_d as large as possible, the first value of r would not exceed say 10 cms whilst the value of r in the logarithmic term would not be less than 1 mm. Under these circumstances, the assuming s = 4 km, V_d works out at $5,55x10^6$ Volts. Even this exagerated value of V_d is still very much less than the potential of the leader channel which from Fig. 13.0.9 is likely to be at least $1x10^8$ Volts.

Reverting now to Eq (15.1), the value of 6/2s can be disregarded compared to the value of r, and if this is at least 1 cm so can the constant 0,04. The frequency f may be taken as unity.

Now/ .....

Now having due regard for the fact that Peek's formula applied to two conductors, the loss on a single lightning channel will be half this value. Furthermore if only one third of the loss occurs when the conductor is negative a further reduction by a factor of 3 is required. The loss due to d.c. potential should be of the same order as an equal rms value of the a.c. potential.

Hence Equation (15.1) may then be simplified to the following in respect of the corona loss of one meter length of a lightning channel of radius r and height s above ground and expressing V in volts instead of k.V.

$$P = V^2(r/2s)^{\frac{1}{2}}x10^{-8} \text{ watts/m} \quad \ldots\ldots\ldots\ldots\ldots\ldots \quad (15.4)$$

According to section 13 it was noted that the potential of the leader extremities remained more or less constant for any given value of induced charge. If therefore V_1 is the potential at the top, V_2 the potential at the bottom of the leader channel and if z is the length of the leader at any instant t. Then the potential of an element δz at distance x from the top would be given by

$$V_{(x)} = V_1 + (\frac{V_2-V_1}{z})x \quad \ldots\ldots\ldots\ldots\ldots\ldots \quad (15.5)$$

The current flowing in the element is $P\delta x/V$ amperes and this may be substituted in equation (15.4) as well as making $s = h-x$ where h is the height of the top of the leader above ground.

$$\text{Whence } i = (r/2)^{\frac{1}{2}}(h-x)^{-\frac{1}{2}}[V_1+(V_2-V_1)x/z] \quad \delta x \times 10^{-8} \quad \ldots \text{ amperes} \quad (15.6)$$

Now if x is first kept constant, current will flow in the element δx during the period when $z = x$ to $z = h$ where $z = \overline{v}t$ and $\overline{v}$ is the velocity of the leader tip. Hence the charge delivered to the element δx can be calculated from $\int idt$ between the limits of $t_m = h/\overline{v}$ and $t_o = x/\overline{v}$ putting $z = \overline{v}t$.

For sake of simplicity substitute the following constants in equation (15.6)

$$a = [r/2]^{\frac{1}{2}}(h-x)^{-\frac{1}{2}}.\delta x.10^{-8}$$

$$b = V_1$$

$$c = (V_2-V_1)x$$

Then $i = a[b+c/\overline{v}t]$ amperes

Whence/ .....

$$\text{Whence } \delta q = ab\int_{t_o}^{t_m} dt + \frac{ac}{\overline{v}}\int_{t_o}^{t_m} 1/t\ dt$$

$$\text{Hence } \delta q = ab(t_m - t_o) + ac/\overline{v}.\ln^{1}(t_m/t_o) \text{ coulombs} \quad \ldots\ldots \quad (15.7)$$

Where $tm = h/\overline{v}$ and $t_o = x/\overline{v}$

In order to obtain the total charge dissipated in corona loss, equation (15.7) may then be integrated with respect to x over the limits x = h to x = o and rewriting, the following integral therefore requires a solution namely

$$q = K_1\int_o^h (h-x)^{\frac{1}{2}}dx + K_2\int_o^h x(h-x)^{-\frac{1}{2}}\ln(h/x)dx \quad \ldots\ldots\ldots \quad (15.5)$$

where $K_1 = (r/2)^{\frac{1}{2}}V_1\ 1/\overline{v}\ x\ 10^{-8}$

And $K_2 = (r/2)^{\frac{1}{2}}\ (V_2-V_1)\ 1/\overline{v}\ x10^{-8}$

The first part of the integral resolves into $2/3\ K_1h^{3/2}$ and the second part resolves finally into $0,374\ K_2h_m^{3/2}$ where the constant term 0,374 is the difference between two infinite but rapidly con= verging logarithmic series.

Hence the solution of equation (15.5) may be restated as follows:-

$$q = (r/2)^{\frac{1}{2}}/\overline{v}.h^{3/2}\ [2/3\ V_1 + 0,374(V_2-V_1)]\ x10^{-8} \text{ coulombs} \quad (15.6)$$

Where r = radius of lightning leader channel
$\overline{v}$ = velocity of leader channel tip
h = height of top of leader channel
V_1 = potential of top of leader channel
V_2 = potential of tip of leader channel

From the example in Section 13, Fig. 13.0.9 for the case where the cloud charge is $\pm$ 71 C and the charge induced in the channel is say 1 C.

$\overline{v} = 2x10^5$ m/s
$h = 4x10^3$ $\qquad h^{3/2} = 2,53x10^5$
$V_1 = -6x10^8$ V $\qquad 2/3\ V_1 = -4x10^8$
$V_2 = -2x10^8$ V $\qquad 0,374(V_2-V_1) = 1,5x10^8$

The/ .....

The value of the radius of the leader core is not known, but from the photographic evidence of Schonland (1953) the luminous radius varied between 0,5 and 5 m but this may include the corona radius which is visible at the extremity of the step dart, and may not be the radius of the current carrying core which should be less than that of a return stroke. Orville (1968) has deduced a value of less than 0,36 m assuming that the NI·I spectrals radiation observed by him came from the core of the leader.

If the current carrying core is 1 m radius, the charge dissi= pated in the example stroke would be about 2 C but if it is of the order of 1 cm or less it would be negligible. A simplified version of equation (15.6) may be obtained by making $V_1 = V_2 = V$ the mean potential of the leader channel whence:

$$q = 2/3(r/2)^{\frac{1}{2}} /\overline{v}.h^{3/2}\ Vx10^{-8}\ C \quad \ldots\ldots\ldots\ldots\ldots\ldots \quad (15.8)$$

The fact that corona losses are less than would be expected is due mostly to the fall in the numerical value of the potential of the leader as it approaches the earth. Also it is certainly dependent on the value to be assumed for the radius of the core of the leader which must be very much smaller than the corona radius.

It must be concluded therefore that whilst there is undoubtedly some corona loss in a lightning leader, the equivalent value of charge dissipated is not large compared to the total charge lowered in the leader. This statement must however be viewed in the context of whether or not Peek's formulae for metalic conductors can indeed be extra-polated to that of the lightning channel.

The position with positive discharges may however ~~by~~ be very different since the corona loss can be expected to increase by a factor of three. In this case the leader is surrounded by a sheath of positive ions which in view of their low mobilities they will not return to the core of the leader as easily as would electrons.

16. The Striking distance of the lightning leader

According to the information provided by the numerical example des= cribed in Section 13, the leader channel proceeds to the earth with slowly decreasing potential gradient, and decreasing velocity ratio, whilst for a linear increasing induced charge the radius of the leader remains constant. For a cloud charge of 71C, the prospective maximum induced charge would appear to be about 1C, and for this value, the potential gradient falls to about $1x10^5$V/m and the velocity ratio to C = 20. This means that the mean velocity of advance of the positive streamers at the top tends to 1/20th of that of the leader tip. The corona radius of the leader remains fairly constant at about 10m and the potential of the tip falls slowly to about $-1,5x10^8$ Volts.

For about 95% of the traverse however, that is 200 m from the earth in this instance, conditions beging to change. In particular the potential of the tip falls rapidly to zero and this in turn leads to a sharp increase in the potential gradient (for constant velocity ratio) and also in the radius of the leader.

80/ .....

In order to examine this phenomena in more detail, Fig. 16.0.1 was first of all drawn up to show the induced charge required for the last 5% of the leader traverse to ground for velocity ratios varying between 20 and 30. The dashed line marked A indicates a linear increase in induced charge with the length of the leader to a prospective maximum of 0,8C, and to achieve this the velocity ratio "C" must be between 28 and 29 (virtually constant).

Next on Fig. 16.0.2 the curves of leader potential gradient were also drawn for the same range, and Curve A then shows the progress for the same value of linear induced charge of 0,8C maximum. This shows that from about 97,5% transverse, the potential gradient would tend to increase.

An increase in potential gradient does not seem to be either realistic or physically possible, particularly as it has been de= creasing steadily up to that point and this has been accompanied by a steady increase in charge deposition and therefore current flow, and these are mutually compatable and correct. Hence the line B was drawn on Fig. 16.0.2 to represent at least a constant value of potential gradient which if it is to be achieved will then necessi= tate a rapid decrease in velocity ratio. Since the velocity of the positive tips in the cloud is not likely to be affected by the lower tip conditions at this stage, it may be expected that the tip speed reduces over the last few percent of its traverse to ground.

Accepting this possibility therefore, the curve B may then also be drawn on Fig. 16.0.1 to show that it must also be accompanied by a sharp increase in the induced charge - something in the order of doubling the prospective charge from 0,8 to 1,6C in a very short dis= tance. This requirement would be accompanied by a sudden increase in electron flow from the top of the channel with an intensification of the positive charge at the tips at that end and a tendency also to increase their velocity - thereby reducing the velocity ratio. This is in any case a consequence of keeping the leader potential gradient constant. Hence there is a physical concept which supports this proposition. It also leads to the conclusion that the electrostatic conditions on the leader are tending towards final breakdown con= ditions upon contact with the earth, where it would be expected that the closer the leader approaches, the higher the charge concentration at the tip will be, accompanied by a rapid increase in current.

The effect of this charge intensification on the potential of the leader tip is illustrated on Fig. 16.0.3. A linear increase in the induced charge to 0,8C would follow the value of C = 28 to C = 29 and is represented by the curve A approximately. A constant leader potential gradient would on the other hand be represented by Curve B which shows that the potential of the tip would tend to remain numerically constant but will be forced to zero eventually. The departure from Curve A is seen to be rather minimal.

Finally the change in leader radius is shown on Fig. 16.0.4, and this was not expected at all since it refers to the whole length of the leader and not just the tip. A uniform leader radius was assumed for the simplification of the model of the discharge, in order to afford a method of calculation which was not too complicated, and there is photographic evidence indicating that this was a reason= able assumption.

81/ .....

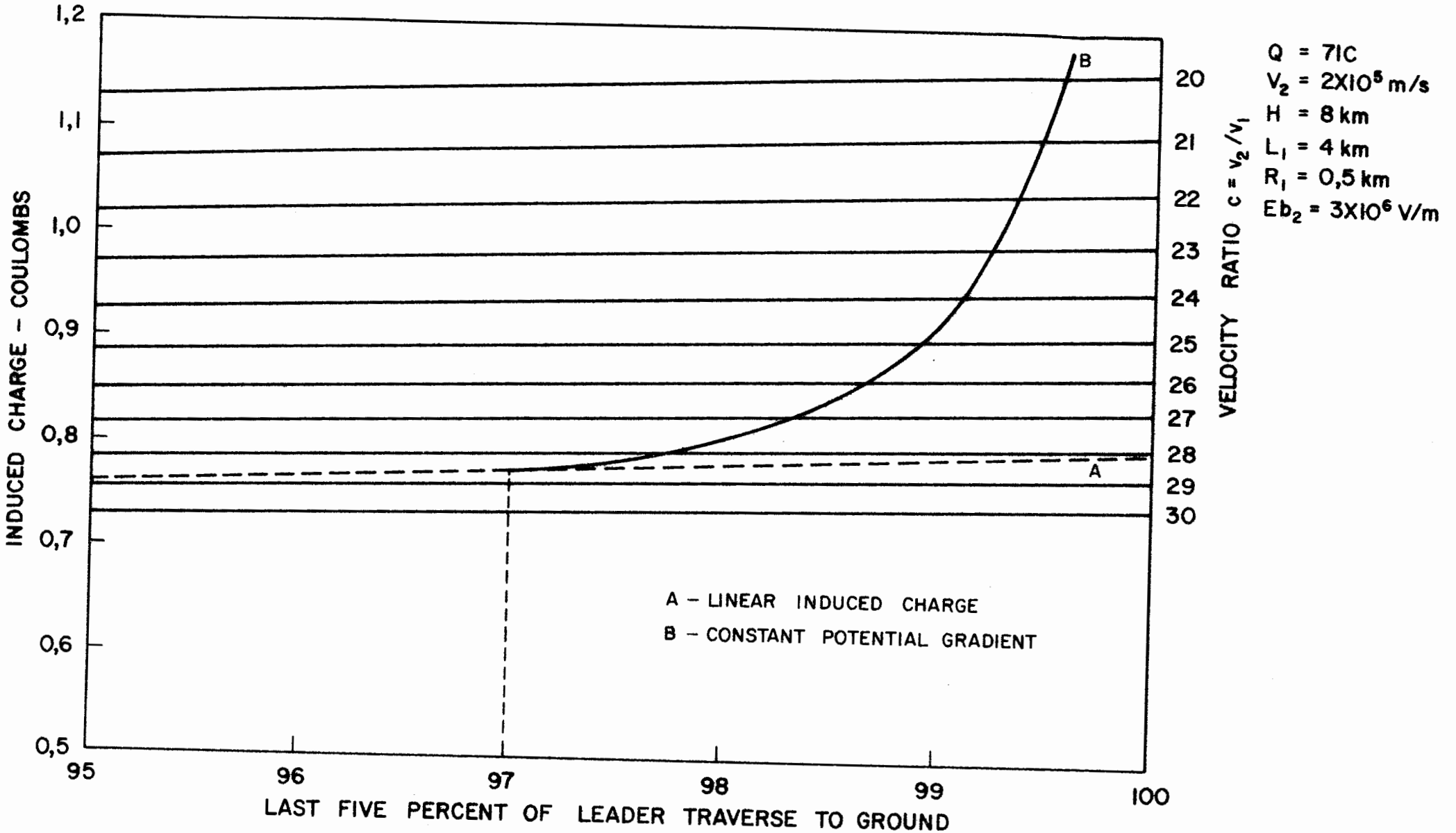

FIGURE 16·0·1

INDUCED CHARGE FOR VARIABLE VELOCITY RATIOS ($Rz_1 = R_1$)

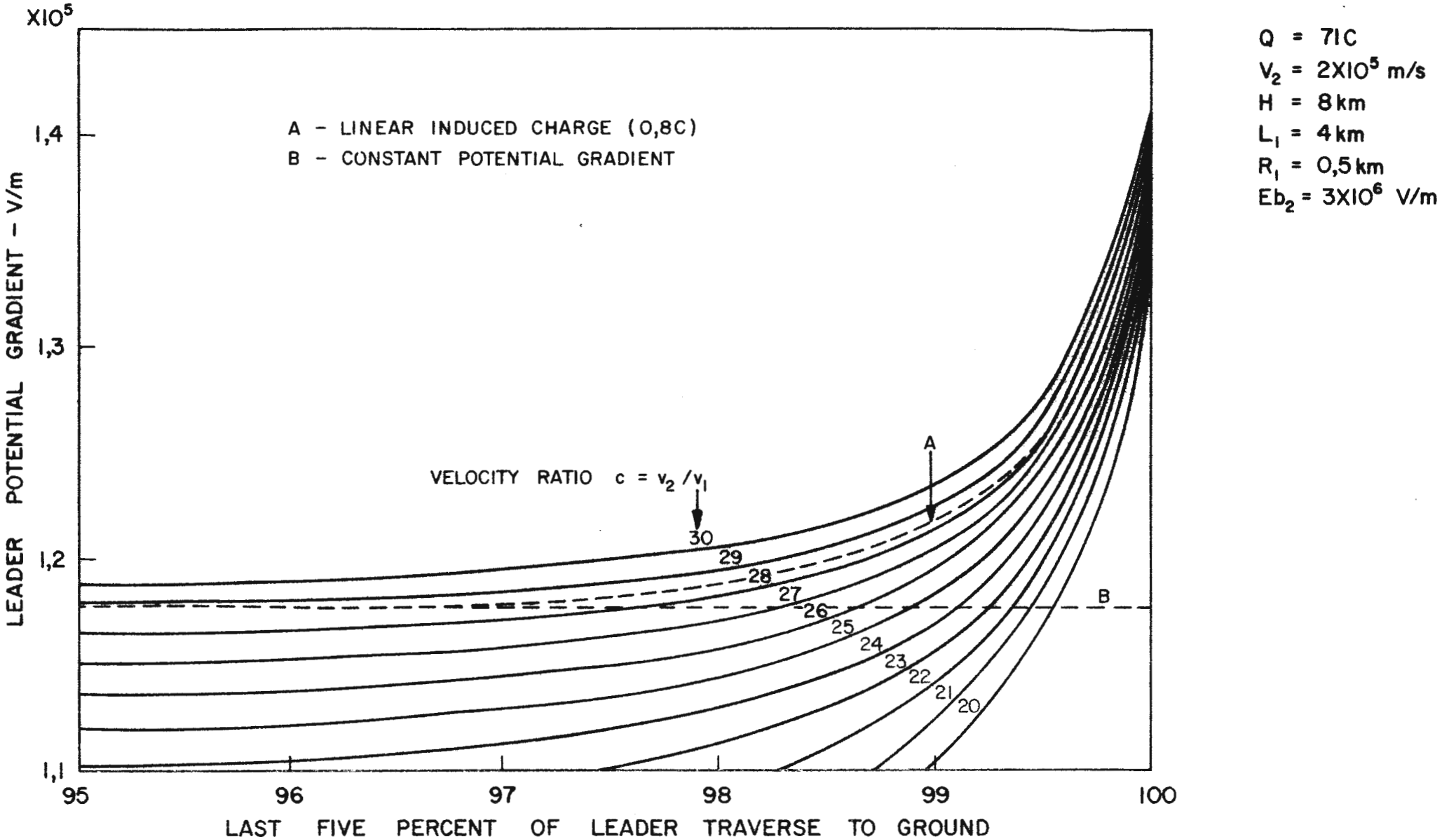

FIGURE 16·0·2

LEADER POTENTIAL GRADIENT FOR VARIABLE VELOCITY RATIO ($Rz_1 = R_1$)

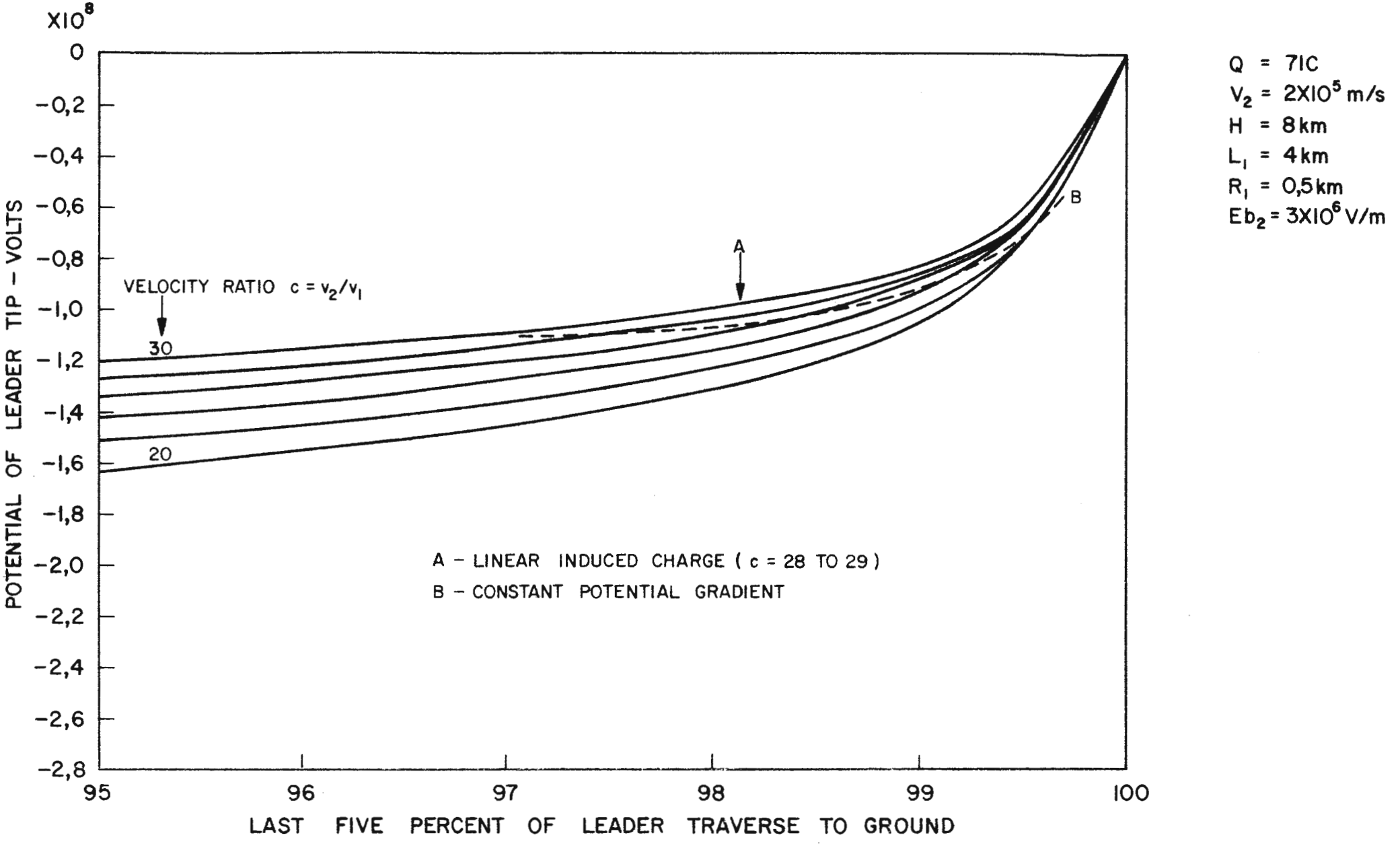

FIGURE 16·0·3

POTENTIAL OF LEADER TIP FOR VARIABLE VELOCITY RATIO ($Rz_1 = R_1$)

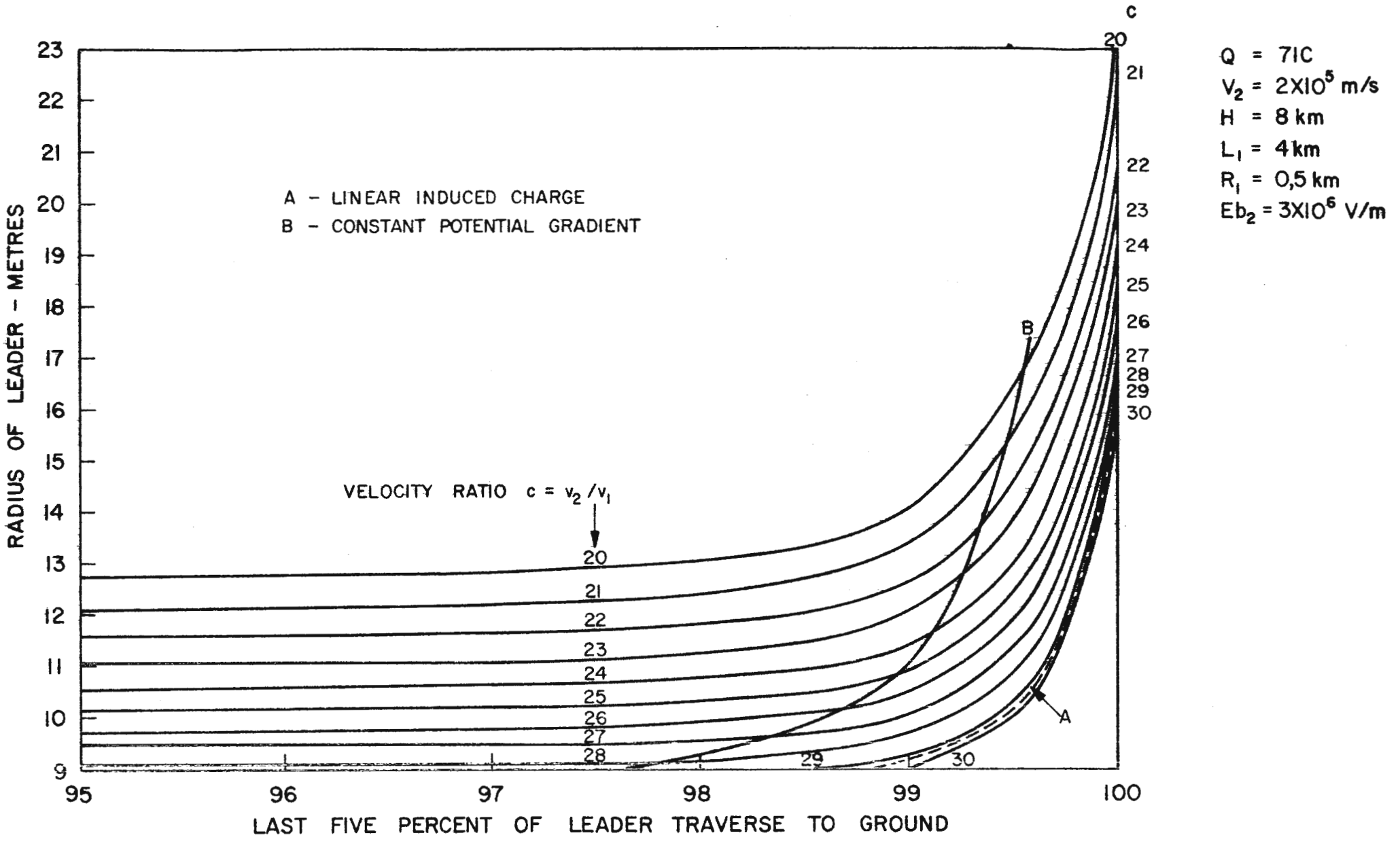

FIGURE 16·0·4

RADIUS OF LEADER FOR VARIABLE VELOCITY RATIO ($Rz_1 = R_1$)

Experience with these calculations however indicates that the shape of the leader channel could be varied since the field intensity at the tip is determined primarily by the charge magnitude and dimensions in the immediate vicinity of the tip. The contribution to the field intensity at the tip due to charge some ten to one hundred metres or so away is small by comparison with that of the more localised charge. Hence an increase in the computed radius could refer equally to the radius near the lower extremity, allowing the rest of the channel to increase a relatively small amount if any.

To assume that the radius of the channel remains constant on approaching ground would mean not only that the ratio between the tip velocities increases, but also that the potential gradient increases even more than shown on Fig. 16.0.2, and as discussed previously there is no physical grounds for this. On the other hand the divergence of a leader tip is common occurence with the long spark, and is more likely to occur when the tip approaches a plane electrode, as was observed by Kritzinger (1962).

Hence the increase in leader radius - or at least the tip radius - is an inescapable conclusion of this excercise and it is shown from Fig. 16.0.4 that when the potential gradient is held constant, the leader radius increases even more as shown on Curve B compared with Curve A.

It is here necessary to consider in more detail the effect of the model adopted for these calculations. The charge has been assumed to be arranged concentrically, and for the purpose of the model the field intensity is calculated at the centre of the annular ring forming the open ended "tube" so to speak. Theoretically this tubular leader may actually contact the earth with the field intensity and potentials calculated, but of course it is a poor physical representation of the leader tip itself which must present a hemispherical shape perhaps in which the electrons are highly concentrated.

However it was shown in Section 10 that the concentric charge distribution assumed produced a field intensity at the centre of the annular ringe of radius R which is the same magnitude as that produced at a distance R from the extremity of a line charge - as illustrated in Fig. 16.0.5 below - provided that the radius of the leader is small compared with its length.

82/ .....

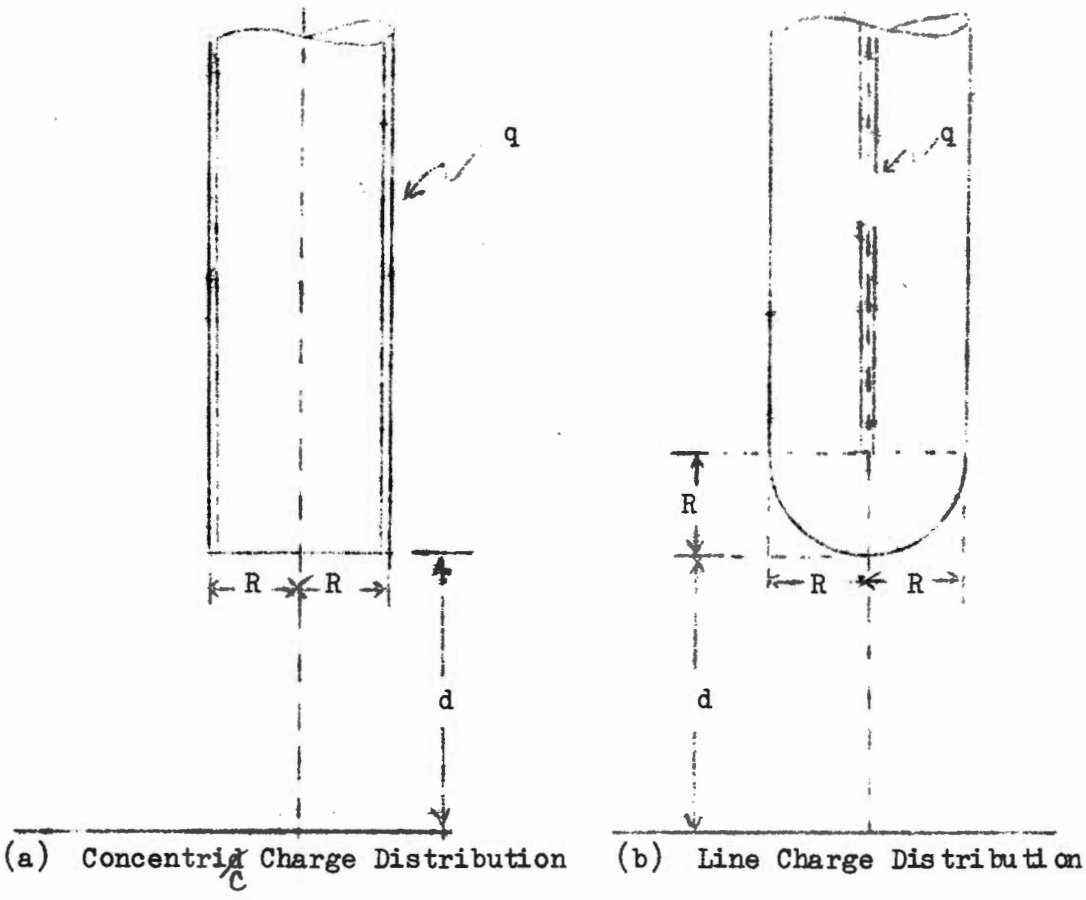

Fig. 16.0.5 Diagram illustrating the line charge equivalent of a concentric charge distribution for the leader tip

This latter model is somewhat similar to that of a charged conducting sphere whereby the field intensity at the surface of the sphere can be calculated by assuming that the charge is concentrated at a point at its centre. Hence when the concentric cylinder of charge reaches the ground it may be assumed that the equivalent line charge is still a distance R from ground, but that the corona radius has in fact made contact and the process breaks down. In this sense the corona radius becomes the so-called striking distance.

From the construction of the model it is obvious that if the field intensity at the leader tip does not exceed the breakdown strength of the air through which the tip is forging, the field intensity at ground level immediately below will always be less, and unless the electric strength of the air at the ground surface is less than that of free air, the leader will proceed until the corona radius reaches the surface. Fig. 16.0.6 shows the field intensity at ground level for the last five percent of the traverse of the leader to ground. According to the computation for this special case, the field intensity at ground level before the leader started out was $3{,}7 \times 10^4$ V/m whereas at 95% of its traverse it has increased to between 3 and 4×10^5 V/m that is nearly ten times. However a further ten fold increase takes place during the last five percent of the traverse and in fact most of this occurs within 3% of the traverse distance to ground, which in this case represents a distance of

83/ .....

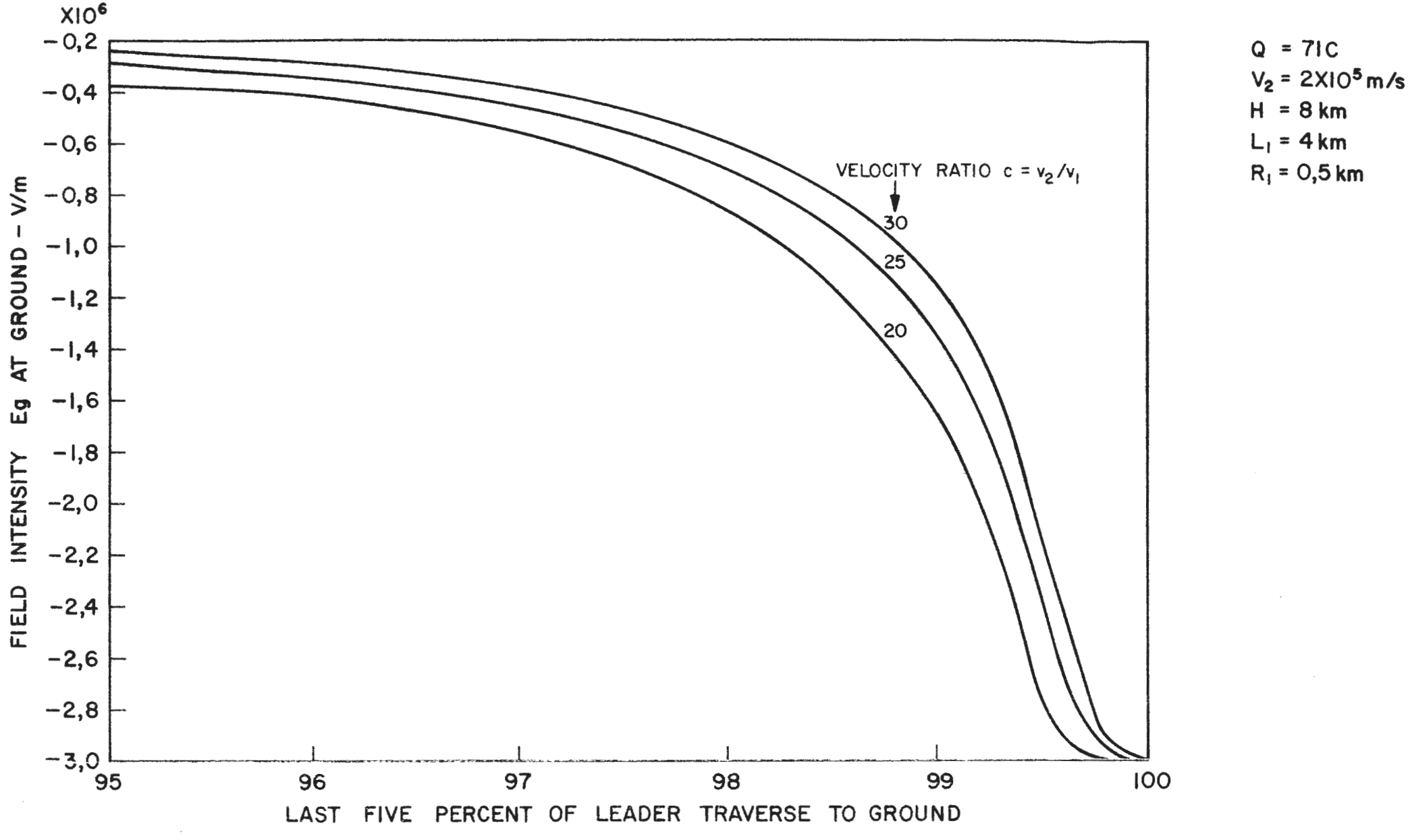

FIGURE 16·0·6

FIELD INTENSITY AT GROUND FOR VARIABLE VELOCITY RATIO ($Rz_1 = R_1$)

120 m. If the breakdown strength of the air at the ground surface is say only 1×10^6 V/m, the tip of the leader would advance to within 2 to 1% of its traverse distance to ground before this occurs, and when it does an upward positive tipped leader should rise from the earth to meet it.

There are however two opposing view points regarding the condition of the air immediately above that of the ground plane. The first is discussed by Loeb (1965) in reviewing the work of Kritzinger (1962) on long sparks. This is to the effect that the image charge in the earth (which is positive in this case) is capable of raising a blanket of negative space charge above the earth and this space charge may be capable of a high enough field intensity to ionise the air at the ground surface thereby raising positive streamers which may then ascend to meet the down coming leader. This mechanism served to explain the phenomena observed when negative streamers cross a point-plane gap, and must be valid if the conductivity of the air in the gap is sufficiently high to muster the requisite quantity of negative ions to do this. On the other hand if the surface is not smooth and contains many sharp corners and points, ionisation of the air at the ground surface may take place at a lower level than normal air breakdown level in which case a positive space charge is created which will tend to form upward streamers as well. Either of these view points will however serve to explain the possibility of an upward leader from level ground. On the other hand, when the corona sheath surrounding the down coming leader tip makes contact with the earth, the resulting breakdown to the conducting core of the channel could be taken for an upward leader of a length equal to the corona radius.

In the particular computed example, the contribution of the charge in the channel to the field intensity at ground level is more than 90% of the total when the leader is within 5% of its traverse to ground, and this must apply to most other cases. Hence calculations may be undertaken neglecting the effect of charges in the cloud as a first approximation, and for this purpose, the leader charge may be assumed to be distributed along the centre line of the leader as illustrated in Fig. 16.0.7.

84/ .....

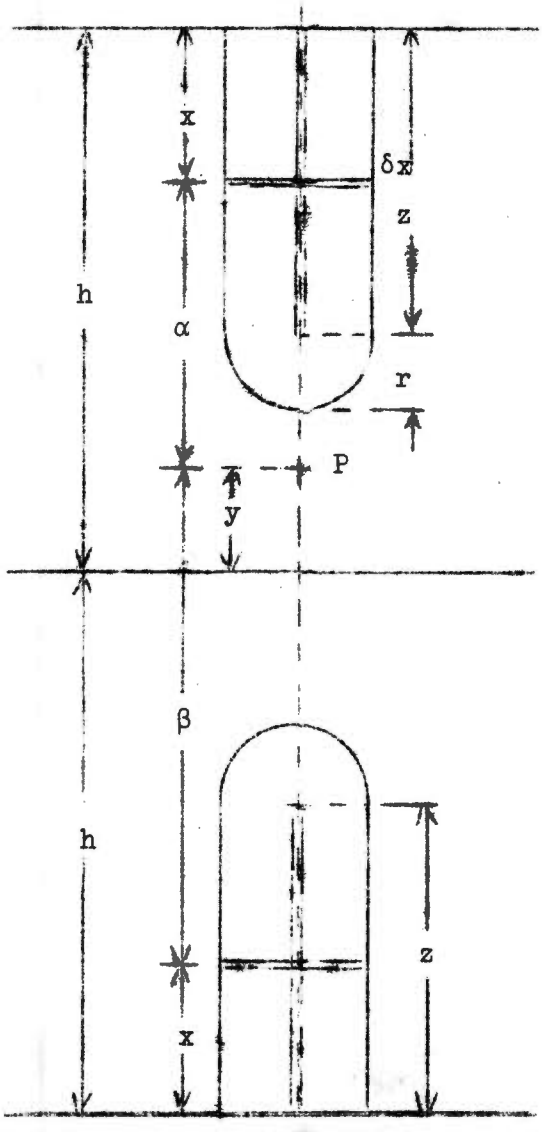

Fig. 16.0.7 Diagrammatic representation of leader stroke with line charge distribution

For a linear charge distribution on the leader, the charge per unit length is $q' = 2qx/h^2$ where $h \gg r$ whence the charge in an element δx is then

$$\delta q = 2qx\delta x/h^2$$

The increment of field intensity at any point P distant y from ground due to the charge in the element δx is then

$$\delta e = \delta q/4\pi\varepsilon \cdot (1/\alpha^2 + 1/\beta^2) \quad \ldots\ldots\ldots\ldots\ldots\ldots \quad (16.1)$$

where $\alpha = a-x \quad \beta = b-x$

$a = h-y \quad b = h+y$

The field intensity at the point P is then the integral given in equation (16.2) namely:

85/ .....

$$E_y = q/2\pi\varepsilon h^2 \cdot \left\{ \int_0^z x(a-x)^{-2}dx + \int_0^z x(b-x)^{-2}dx \right. \quad \ldots\ldots \quad (16.2)$$

$$\text{Hence } E_y = q/2\pi\varepsilon h^2 \left\{ a/(a-z) + \ln (a-z)/a + b/(b-z) \right.$$
$$\left. + \ln (b-z)/b + 2 \right\} \quad \ldots\ldots\ldots\ldots\ldots\ldots \quad (16.3)$$

$$a = h-y \qquad b = h+y$$

When dealing with conditions close to ground h>>y or r and $h \approx z$ whence the logarithmic terms and the constant value of "2" may be neglected compared with the terms a/(a-z) or b/b-z.

Hence as a reasonable approximation equation (16.3) may then be written

$$E_y = q/2\pi\varepsilon h^2 \cdot \left[(h-y)/(h-y-z) + (h+y)/(h+y-z) \right] \ldots \quad (16.4)$$

The field intensity at a distance r ahead of the line charge which is identified as the leader tip, is given by putting y = h-z-r whence

$$E_t = q/2\pi\varepsilon h^2 \cdot \left[(z+r)/r + (2h-z-r)/(2h-2z-r) \right] \ldots. \quad (16.5)$$

Since z>>r the above simplifies to the following:

$$E_t = q/2\pi\varepsilon h^2 \cdot \left[z/r + (2h-z)/(2h-2z-r) \right] \ldots\ldots\ldots \quad (16.6)$$

When the so-called leader tip reaches ground z = h-r and neglecting r compared with h

$$Et_g = q/\pi\varepsilon hr \ldots. \text{ V/m} \quad \ldots\ldots\ldots\ldots\ldots\ldots\ldots \quad (16.7)$$

This familiar expression may be transposed to give the following relationship between r and q namely

$$r/q = 1/\pi\varepsilon Eh \;\ldots \text{ m/C} \quad \ldots\ldots\ldots\ldots\ldots\ldots\ldots \quad (16.8)$$

Hence if the field intensity at the leader tip and at ground level simultaneously can be say $3x10^6$ V/m then for h = 4 km say r/q = 3 m/C and this is the value computed in the numerical model for the case when the leader traverse distance is 100%.

However, if the leader has traversed say 90% of its path, then z = 0,9h say, then the bracket term of equation (16.6) becomes

$$0,9\frac{h}{r} + \frac{h}{r}\left[1,1/(0,2h/r - 1)\right]$$

When h/r is of the order of 400, then 0,2 h/r>>1 which means that the second term resolves to a value of about 5,5 and this is small compared to the first term.

Hence in this case

$$Et(z = 0,9h) \approx q/2\pi\varepsilon hr \quad \ldots\ldots\ldots\ldots\ldots\ldots \quad (16.9)$$

Hence comparing this equation with (16.8) the effect of the proximity of the image charge in the earth introduces a factor of 2 in the field intensity equations over the very short distance of less than 10% of the leader traverse; this is to say that the value of r/q advances from 1,5 m/C to 3 m/C within this distance. In fact Fig. 16.0.4 shows that this effect occurs mainly during the last 2% of the leader traverse in the particular case computed.

Thus the so called striking distance may be calculated from equation (16.8) for the case where the field intensity at ground level can equal that of the tip of the leader before ionisation and breakdown occurs.

On the other hand, if the breakdown field intensity at the surface of the earth is less than that assumed for the leader tip, an upward leader will be forthcoming from the ground before the leader reaches earth and if this instant may now be defined as determining the striking distance it may be obtained by means of the appropriate substitutions in the above equations.

The field intensity of the tip is given by equation (16.6) in which the appropriate value of r can be determined from equation (16.9). The striking distance "d" may then be stated as d = h-z-r where z is still unknown.

The field intensity at ground level is obtained by putting y = 0 in the equation (16.4) for Ey in which case

$$Eg = q/\pi\varepsilon h(h-z) \quad \ldots\ldots\ldots\ldots\ldots\ldots\ldots\ldots \quad (16.10)$$

$$\text{Whence } (h-z)/q = 1/\pi\varepsilon hE_g \quad \ldots\ldots\ldots\ldots\ldots\ldots\ldots \quad (16.11)$$

Dividing by equation (16.9) the following relation is then obtained namely:-

$$(h-z)/r = 2E_t/E_g \quad \ldots\ldots\ldots\ldots\ldots\ldots\ldots\ldots \quad (16.12)$$

Hence if the value of charge q is known, the value of r is obtained and hence the value of z for a known value of h. It should be noted that equation (16.12) is not valid for the case when $E_t = E_g$ since the factor of two referred to previously is assumed to be effective when the leader tip approaches very closely to earth.

87/ .....

The striking distance "d" may therefore be expressed as follows:

$$d = r(2E_t/E_g - 1) \quad \ldots\ldots\ldots\ldots\ldots\ldots\ldots\ldots \quad (16.13)$$

Whence $r = q/2\pi\varepsilon hE_t$ from Equation (16.9)

$$\text{Hence } d/q = (2E_t/E_g - 1)/2\pi\varepsilon hE_t \quad \text{m/C} \qquad (16.14)$$

For example, for $E_t = 3\text{x}10^6$ and $h = 4\text{x}10^3$ m, $r/q = 1{,}5$ m/C. Then if $E_g = 1\text{x}10^6$ V/m for breakdown, $d/r = 5$ whence $d/q = 7{,}5$ m/C.

It is of interest to note here that the striking distance is not only dependent upon the parameters stated namely q, E and h, but it is also dependent upon the charge distribution on the leader.. A uniform distribution of charge for example results in a factor of two decreases in the striking distance compared with the linear dis= tribution assumed. Similarly an exponential distribution of charge which concentrates more charge towards the leader tip than does the linear distribution assumed, would give rise to a longer striking distance This is therefore an important parameters to determine since it directly affects the protection to be afforded by protective conductors such as overhead ground wires or lightning conductors for buildings.

17. The effect of a protuding conductor on the striking distance

Following on the considerations given in Section 16, the effect of a protruding conductor or structure may be qualitatively examined firstly by assuming that the electric field intensity produced by the cloud charges can be neglected compared with that due to the lightning channel. The diagramatic representation of the case is depicted in Fig. 17.0.1.

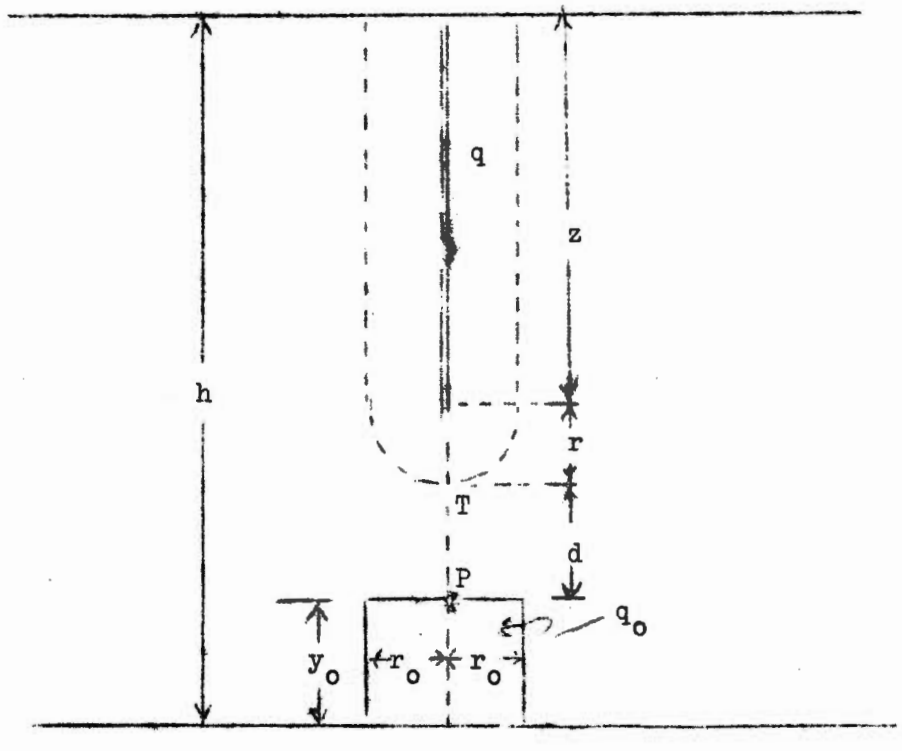

Fig. 17.0.1 Diagramatic representation of a lightning leader approaching a raised structure.

The charge q on the leader is assumed to be distributed linearly along a line, and the field intensity E_t at the tip a distance r from the line charge has been given in Equation (16.6) in the last section.

So also the field intensity at the point P on the top of the structure due to the charge on the leader can also be obtained by putting $y = y_o$ in equation (16.4) whence

$$Ep_1 = q/2\pi\varepsilon h^2 \cdot \left[(h-y_o)/(h-y_o-z) + (h+y_o)/(h+y_o-z) \right] \quad \ldots\ldots\ldots\ldots\ldots\ldots \quad (17.1)$$

Putting $z = h - (r+d+y_o)$ and neglecting y_o compared with h in the numerators Equation 17.1 then simplifies to the following expression:

$$Ep_1 = q/2\pi\varepsilon h \cdot \left[1/(r+d) + 1/(2y_o+r+d) \right] \ldots\ldots\ldots\ldots \quad (17.2)$$

Then if $d' = r+d$ the expression can be written as

$$Ep_1 = q/2\pi\varepsilon h y_o \cdot y_o/d' \cdot \left[1 + 1/(1+2y_o/d') \right]$$

And since the last portion of the expression is purely a function of the ratio (y_o/d') it can be written

$$Ep_1 = q/2\pi\varepsilon h y_o \cdot F_1(y_o/d') \ldots\ldots\ldots\ldots\ldots\ldots\ldots \quad (17.3)$$

Now, referring to Appendix I of Part I dealing with the capacitance of Aerial systems, it would be reasonable to assume that a positive charge is raised in the structure, and that this might be distributed linearly as for a cylindrical cloud charge such that the charge density is a maximum at the top of the structure and zero at ground level. If this charge is say q_o and is contained in a cylinder of radius r_o and height y_o the field intensity at the point P at the top due to this charge is then given by the following expression

$$Ep_2 = - q_o/2\pi\varepsilon y_o^2 \cdot \left[2y_o/r_o - \mathrm{Sinh}^{-1}(2y_o/r_o) \right] \quad \ldots \quad (17.4)$$

Since the bracket term is similarly a function of the ratio (y_o/r_o) the expression can therefore be written

$$Ep_2 = - q_o/2\pi\varepsilon y_o^2 \cdot F_2(y_o/r_o) \quad \ldots\ldots\ldots\ldots\ldots\ldots \quad (17.5)$$

The total field intensity at the top of the structure is the sum $Ep_1 + Ep_2$ and can therefore be written as follows namely:-

$$Ep = q/2\pi\varepsilon h y_o \cdot F_1(y_o/d') - q_o/2\pi\varepsilon y_o^2 \cdot F_2(y_o/r_o) \quad \ldots \quad (17.6)$$

89/ .....

If the charge q in the lightning channel is negative and q_o in the structure positive, E_p is therefore negative and is clearly more intense than in the absence of the structure.

The value of the charge q_o can be related to that of q by making the potential of the structure zero since it is assumed to be conducting and in contact with the earth. Actually of course every part of the structure is at zero potential and the charge in it will distribute itself accordingly, and a close approximation would be to assume that the average potential of the structure due to its own charge should be equal in magnitude but opposite in polarity to the average potential of the structure due to the charge in the lightning channel.

The average potential of the structure due to the charge in the lightning channel would be approximately half the value at the top of the structure since the field gradient is approximately uniform near the earth's surface. The average potential of the structure due to its own charge however will be greater than half the potential at the top because of the fall-off of potential as the top is approached, purely as a consequence of the fact that the assumed linear charge distribution is not ideal as pointed out in Appendix I of Part I. According to that analysis, the charge should actually be more concentrated at the top than assumed. However, no allowance should be made for this in the potential calculation since if the charge is more concentrated at the top of the structure, the field intensity Ep_2 of equation (17.5) is also too low and should also therefore have been adjusted.

Accordingly, since the ratio of q_o/q is to be determined it will be sufficiently accurate to obtain this by equating the potential at the top of the structure only to zero.

The potential at the structure top due to the charge q in the lightning channel is obtained from Fig. 17.0.1 by the expression as follows namely:

$$Vp_1 = q/2\pi\varepsilon h^2 \cdot \int x/(a-x)\cdot dx - \int x/(b-x)\cdot dx \quad .... \quad (17.7)$$

Where $a = h-y_o$ and $b = h+y_o$

This expression resolves after integration to the following namely:

$$Vp_1 = q/2\pi\varepsilon h^2 \cdot \left\{ (h-y_o)\ \ln\cdot\left[(h-y_o)/d'\right] - (h+y_o)\ \ln\cdot\left[(h+y_o)/(2y_o+d')\right]\right\} \quad ..... \quad (17.8)$$

Where d' = r+d as before

Neglecting y_o compared with h where it is appropriate then equation (17.8) simplifies to the following namely:-

90/ .....

$$Vp_1 = q/2\pi\varepsilon h \cdot \ln \cdot 1+2y_o/d' \quad \ldots\ldots\ldots\ldots\ldots\ldots \quad (17.9)$$

$$= q/2\pi\varepsilon h \cdot F_3(y_o/d') \quad \ldots\ldots\ldots\ldots\ldots\ldots \quad (17.10)$$

The potential at the top of the structure due to its own charge q_o is more complicated being given by the derived expression namely:-

$$Vp_2 = q_o/\pi\varepsilon r_o^2 y_o^2 \cdot \left\{ \int_o^{r_o} \int_o^{y_o} (\alpha^2+r^2)^{-\frac{1}{2}} r dr . x dx - \int_o^{r_o} \int_o^{y_o} (\beta^2+r^2)^{-\frac{1}{2}} r dr . x dx \right\}$$

Where $\alpha = y_o - x$ and $\beta = y_o + x$

The integration of the two terms in equation (17.11) finally resolves into the following exact expression namely:

$$Vp_2 = q_o/2\pi\varepsilon y_o \cdot F_4(y_o/r_o) \quad \ldots\ldots\ldots\ldots\ldots\ldots \quad (17.12)$$

$$\text{Where } F_4(y_o/r_o) = 1/a \cdot \left\{ a \operatorname{Sinh}^{-1}(2a) - 2/3 \left[1+(2a)^2 \right]^{3/2} + 2a^2 \left[1+(2a)^2 \right]^{\frac{1}{2}} + 4/3\, a^3 + 2/3 \right\} \quad \ldots\ldots\ldots \quad (17.13)$$

Where $a = y_o/r_o$

It is now possible to equate the total potential at the structure top to zero whence:-

$$V_o = V_{p1} + V_{p2} = 0 \text{ whence from equations (17.10) and (17.12)}$$

$$V_o = q/2\pi\varepsilon h \cdot F_3(y_o/d') + q_o/2\pi\varepsilon y_o \cdot F_4(y_o/r_o) = 0 \quad \ldots \quad (17.14)$$

From this the ratio q_o/q is derived and may be stated therefore as follows namely:

$$q_o/q = - y_o/h \cdot F_3(y_o/d')/F_4(y_o/r_o) \quad \ldots\ldots\ldots\ldots\ldots \quad (17.15)$$

Substituting the value of q_o thereby found in terms of q in equation (17.6) then yields the following relationship namely:-

$$E_p = q/2\pi\varepsilon h y_o \cdot \left[F_1(y_o/d') + F_2(y_o/r_o) \cdot F_3(y_o/d')/F_4(y_o/r_o) \right] \quad \ldots\ldots\ldots\ldots\ldots\ldots \quad (17.16)$$

91/ .....

Hence if E_p is the known value of field intensity required to promote ionisation of the air at the top of the structure, then for a given height h of lightning channel there is a family of curves relating q/y_o with y_o/d' and y_o/r_o since equation (17.16) can be ex= pressed in the following form namely:

$$q/y_o = 2\pi\varepsilon h E_p \cdot \left[F_1(y_o/d') + F_2(y_o/r_o) \cdot F_3(y_o/d')/F_4(y_o/r_o)\right]^{-1} \quad \ldots\ldots\ldots\ldots (17.17)$$

Hence if a range of values of y_o/r_o say from 10 to 100 is chosen and a range of values of y_o/d' say 0,1 to 1,0 and from 1,0 to 10,0 then the corresponding values of q/y_o can be found for $E_p = -1x10^6$ V/m, say, and for $h = 4x10^3$ m say. These values are plotted in Fig. 17.0.2 and Fig. 17.0.3 for the two ranges of y_o/d' respectively.

Then for a particular structure having the height $y_o = 50$ m say and the equivalent radius $r_o = 1$m, values of q/y_o can be established for each value of y_o/d' chosen reading along the line $y_o/r_o = 50$. Since y_o has been chosen this results in a set of values of d' for corresponding values of q, the charge in the lightning leader channel.

Now $d' = d+r$ where r is the corona radius of the lightning leader channel which may be established from the relationship given in equation (16.9) in the previous section, namely as follows:

$$r = q/2\pi\varepsilon h E_t$$

Where E_t is the field intensity for ionisation at the leader tip which may be taken to be say $-3x10^6$ V/m. Hence if $h = 4x10^3$ m, then $r = -1,5\ q$ and the relationship between d and q may therefore be cal= culated for the particular structure. This is illustrated on Fig. 17.0.4 for the various values of y_o/r_o cited above. It is here evident that except for very small values of charge, the relationship between striking distance and leader charge is practically linear, and this could be used to establish a simple empirical set of data for a range of structure heights and radii. The effect of the radius of the structure is seen to be significant, the smaller the radius the greater the striking distance per coulomb of charge. This is to be expected in view of the intensification of the field that occurs as a consequence of the charge raised in the structure needed to keep its potential zero.

This is of course based upon the various assumptions as to charge distribution both in the lightning channel and the structure, and upon the values of breakdown field intensity E_t and E_p, and on the height of the channel. The effect of the standing field due to the cloud charges had also been neglected, because at ground level at least it is less than 10% of that due to the charge in the lightning channel itself. For very tall structures however this may not be valid in view of the field intensification taking place and a correction would have to be applied. Also the charge q_o raised in the structure is assumed not to influence the field intensity at the tip of the leader because it is usually very small compared to the leader charge q but this clearly may not be so with very tall structures.

The charge raised in the structure up to the point where the field intensity at the tip is $1x10^6$ V/m can be calculated from equation

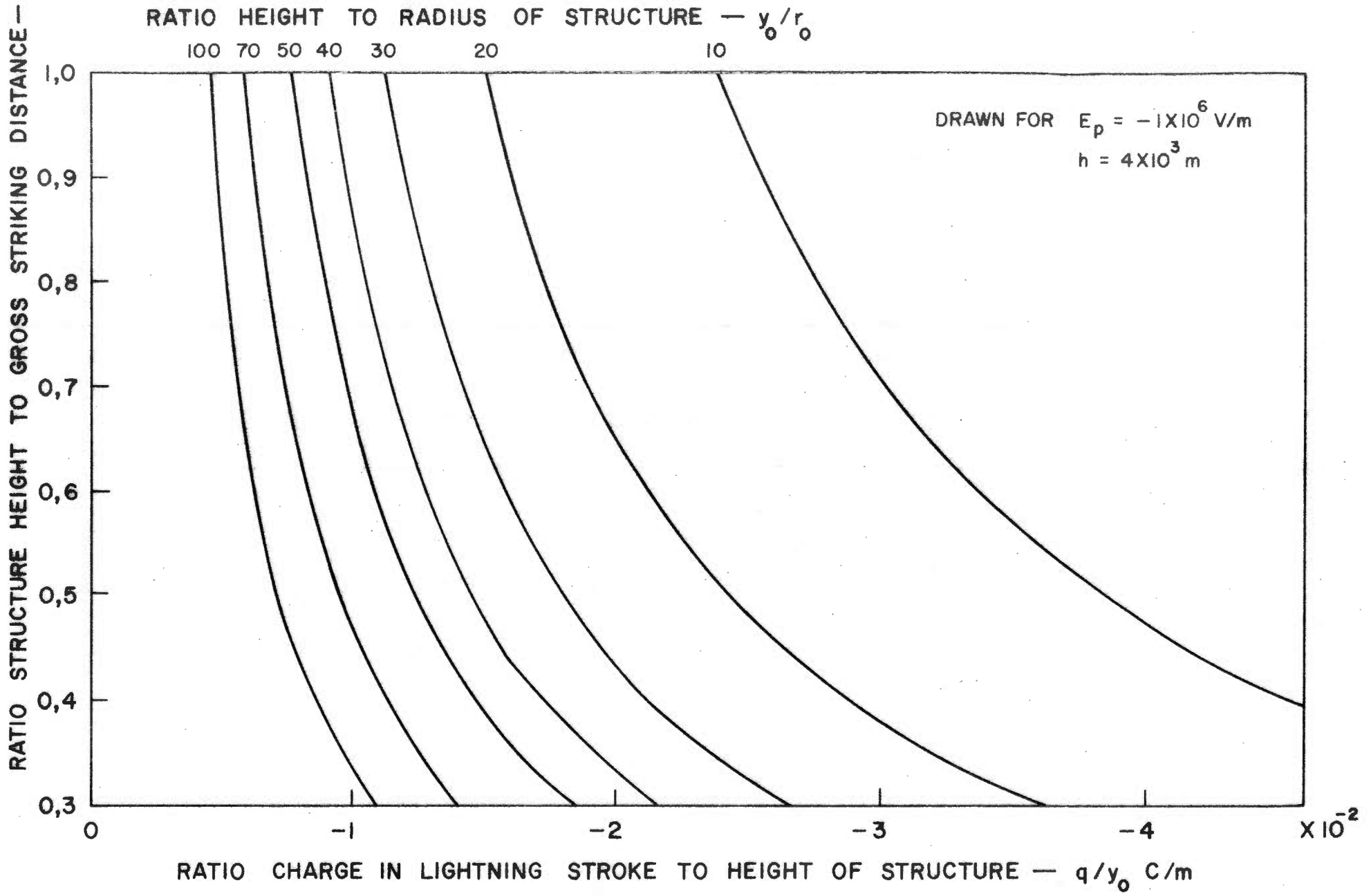

FIGURE 17·0·2

BASIC CURVES FOR STRIKING DISTANCE OF LIGHTNING TO STRUCTURES – SERIES I

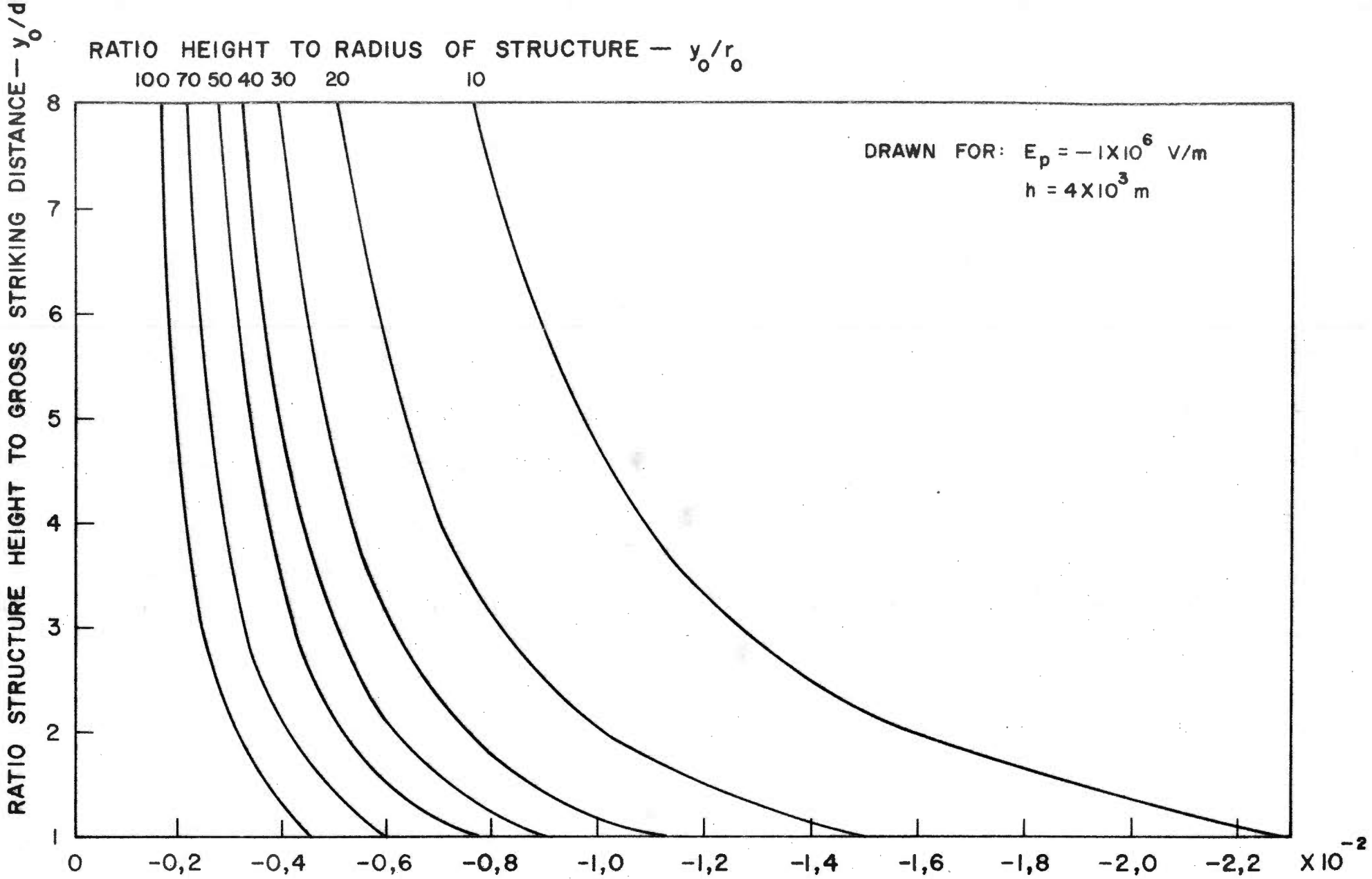

FIGURE 17·0·3

BASIC CURVES FOR STRIKING DISTANCE OF LIGHTNING TO STRUCTURES – SERIES II

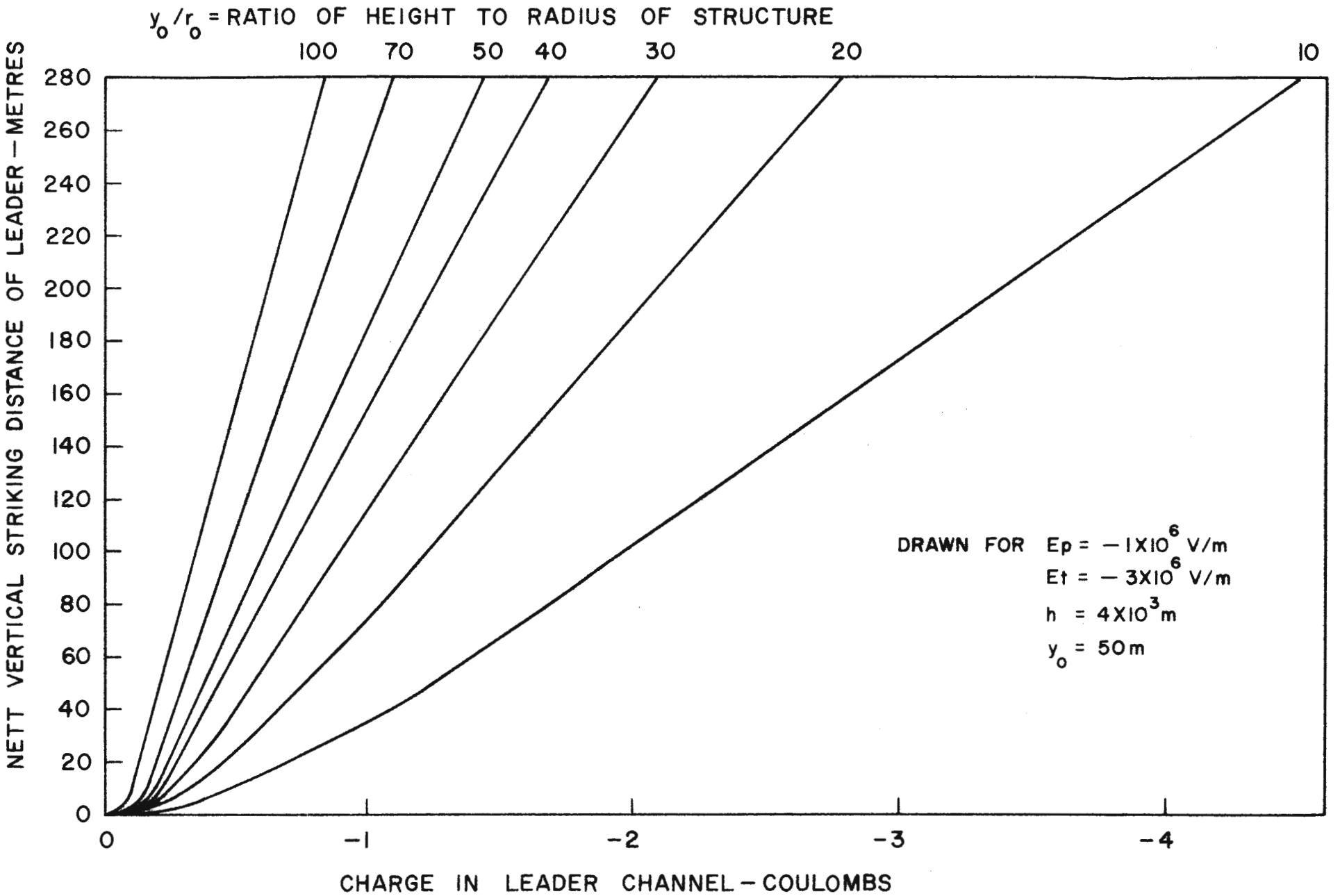

FIGURE 17·0·4

VERTICAL STRIKING DISTANCE VERSUS LIGHTNING LEADER CHARGE FOR A 50m HIGH STRUCTURE

(17.15) and for the two special cases cited it remained remarkably constant over the range of radii chosen. For example, for a structure height of y_o = 50 m and for y_o/r_o = 10 the charge q_o raised was between 7,2 mC to 7,5 mC for a leader charge variation between 1C and 7C. Similarly when y_o/r_o = 50, the charge q_o varied between 1,3 mC to 1,4 mC for the same leader charge variation. Fig. 17.0.5 shows the values of q_o for other values of the ratio y_o/r_o but all are applicable only to a structure height of 50 m. The higher values of charge raised in the structure apply to the lower values of y_o/r_o since to attain the same field intensity at the top, a larger charge would be needed the larger the dimensions (in this case the radius) of the top.

The considerations so far apply to a lightning leader descending directly onto a conducting structure, and merely indicate that an upward streamer could start from the structure before the leader tip reaches it. Inevitably the streamer will contact the leader tip causing final breakdown. Of more importance perhaps is the case of a leader which descends at some distance from the structure in which case it is important to calculate whether an upward streamer could reach the lightning channel before it reaches the earth, since this would direct the discharge to the structure.

Although it is not intended to outline the calculations in full at this stage, the principles of the calculation are exactly similar to those carried out above. Fig. 17.0.6 illustrates a particular case in point.

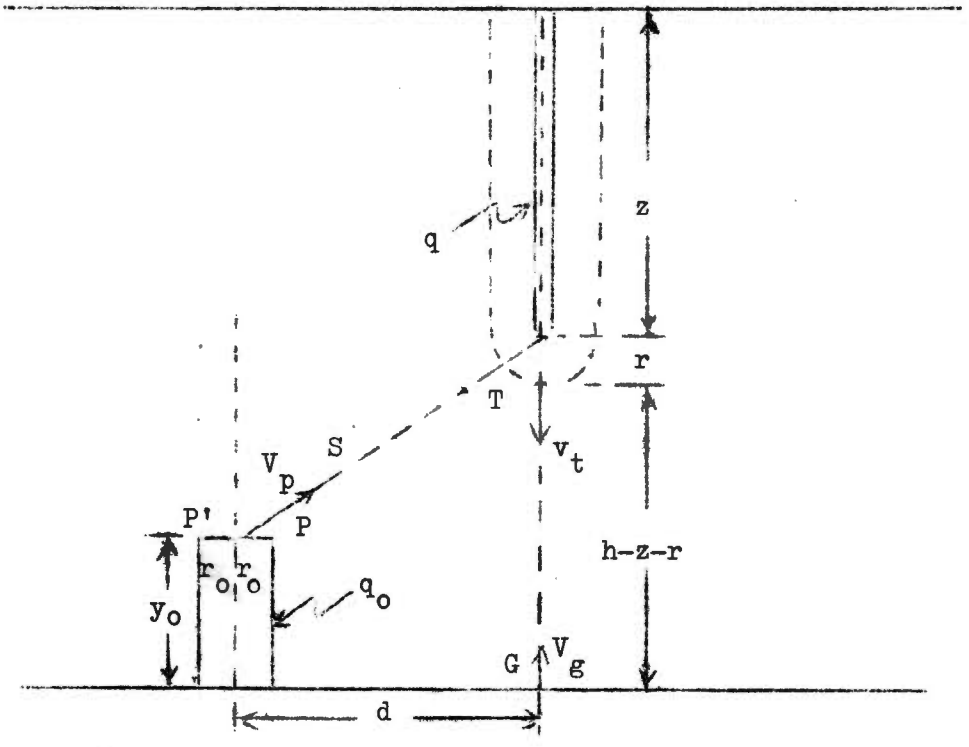

Fig. 17.0.6 Diagram illustrating the possibility of diverting a lightning leader to a structure

Given limiting values of field intensity at P and at G of E_p and E_g respectively which may both be less than that of E_t at the tip of lightning channel, the problem is to calculate the position of the leader tip at the instant when both or either values are reached. From that instant positive streamers advance at velocities of V_p and

93/ .....

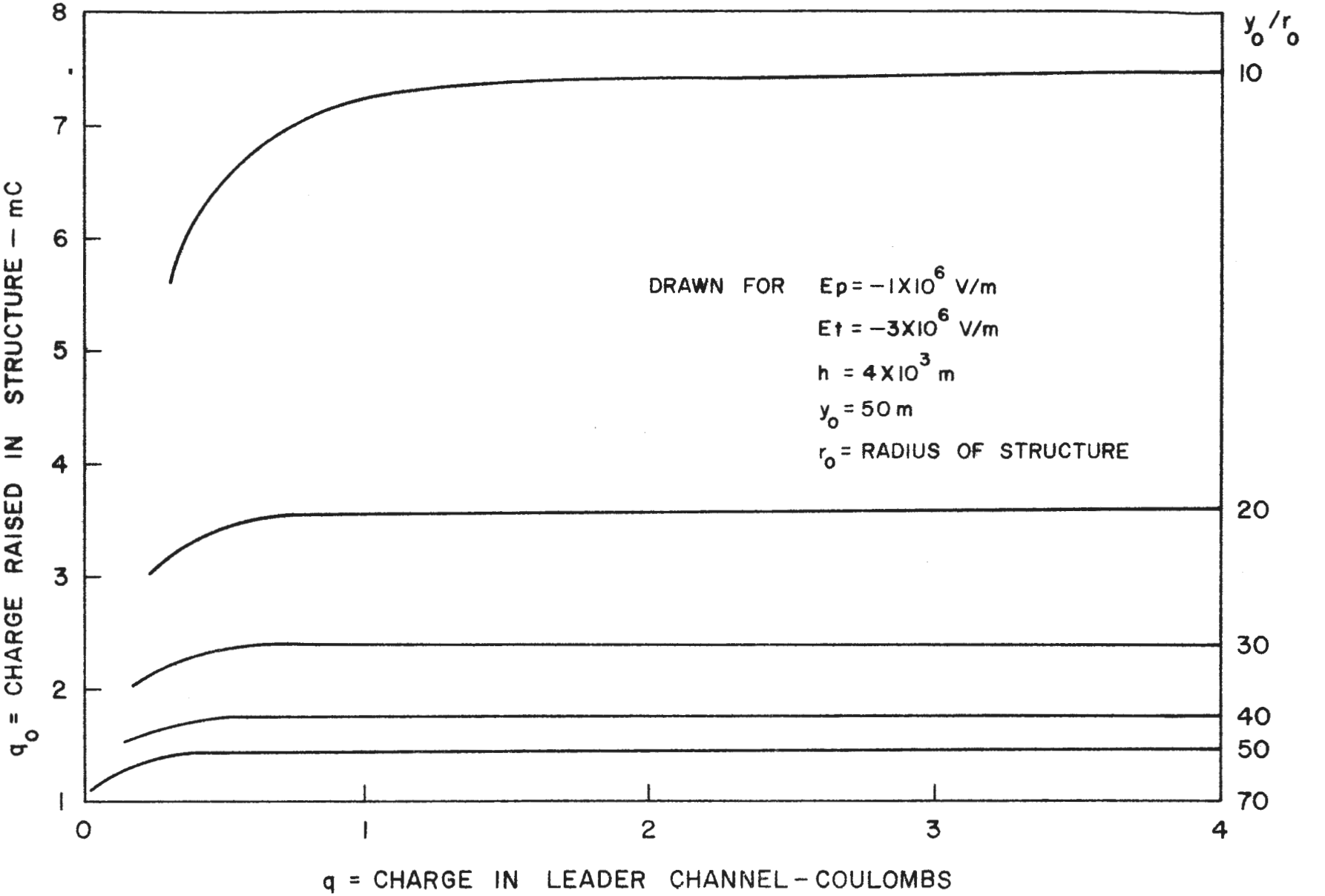

FIGURE 17·0·5

CHARGE RAISED IN A 50 m STRUCTURE VERSUS CHARGE ON LEADER CHANNEL

V_g respectively compared with the leader tip velocity V_t and it is a question as to whether the streamer from P can reach the channel before that from G or before the leader contacts ground if no streamer develops from G.

The field intensity at P due to the charge q in the lightning channel can be resolved into a vertical and horizontal component to which the respective components produced by q_o in the structure must be added, thereby enabling the resultant field intensity E_p to be calculated.

It would be a reasonable approximation to obtain the field intensity at the corner P of the structure by calculating the vertical component as if at the centre point at P' as before, whilst the horizontal component may be found by assuming the charge q_o is distributed along the centre line of the structure and is therefore spaced r_o from the side P. A similar assumption would be necessary for the calculation of the potential at P.

The value of q_o/q is found as before by making the potential at the structure top zero.

The value of z may be expressed in terms of time, if the leader velocity V_t is assumed, whereupon the value of E_p likewise varies with time and the instant it reaches the critical value assumed, if at all, can be established. Thereafter, it can also be established when a streamer developing at a velocity of V_p will reach the channel.

Similarly the field intensity at G may be calculated, and it is likely that the component due to the charge q_o in the structure is negligable compared with that of q in the leader channel. This component however acts in oposition to that of the leader charge so that the position of maximum field intensity on the ground is desplaced in a direction away from the structure, and this may require to be found. Whilst it would be permissable to make the velocities $V_p = V_g$, the time that the leader reaches the point G will be shortened by any upward leader from G.

In concluding this section sight should not be lost of the possibility that in the case of very tall structures, point discharge may occur before the field intensity is sufficiently high to start an upward leader. Such a possibility was cited by Malan (1969) who observed the peculiar behaviour of the 250 m high Hertzhog tower in Johannesburg. Positive ions released as space charge above the tower in very strong electrostatic fields may in fact tend to inhibit streamer development. The opposing view however is that negative ions are attracted from the atmosphere which intensify the field around the top of the structure thereby assisting the development of a discharge. These matters are therefore in need of experimental verification. Certainly during the investigations described in Part I, and later confirmed at the CSIR in Pretoria, there were many occasions on which vertical aerials of only 5 m in height discharged to the atmosphere in field which were high but not sufficiently so to cause breakdown. These discharges lasted 15 to 20 minutes and were finally terminated when a lightning flash occurred in the close vicinity. Although the electric field was intense, it was nevertheless fairly constant, but the discharge from the aerial took place in the form of pulses which increased in frequency as the electric field slowly built up in magnitude. The pulses had a time constant of discharge equal to the time

94/ .....

constant of the aerial circuit.

18. The return stroke

The physical picture of the leader structure deduced from the data discussed so far envisages a channel which essentially consists of a positive ion core surrounded with electrons and negative ions bound in a sheath of some metres in radius as a consequence of the high potential of the leader channel - at least until it approaches close to ground

Substantial changes take place during the last 3% or so of the traverse to ground in that the potential of the leader tip is forced to zero, and there is also a tendency to increase in dimensions - or fanning outwards - to an order of twice the original leader diameter - and these effects are due to the close proximity of the leader image charge - or physically to the concentration of charge in the surface of the earth.

An upward streamer will develop from the earth before the leader corona envelope makes contact with it if the field intensity required to breakdown the air at the surface is less than that of the air ahead of the tip of the leader, or if the leader advances towards a protuding conductor which in consequence intensifies the field at the top of the conductor.

Once the corona envelope of the leader makes contact with the earth the process which began during its approach, intensifies because the whole of the conducting channel now bridges the gap between a very high potential cloud charge and zero potential earth.

The major experimental data available regarding the events which follow are firstly that the current delivered to earth rises rapidly to a maximum of between 2 to 200 kA in the order of from 5 to 20 μs with a mean value of about 10 μs, and then tails off approximately exponentially in a matter of from 100 to 500 μs. However in a large number of cases continuing currents of a few hundred amperes may flow for periods up to one hundred or more milliseconds.

Secondly the luminosity of the channel increases abruptly causing a visible upward moving streamer which proceeds at a velocity of the order of 1/10th of that of light. On meeting a branch in the leader, the streamer follows along the branch with a momentary increase in brightness whilst simultaneously continuing upwards along the main channel with reducing luminosity and velocity.

The process stops when the luminous streamer reaches the cloud or after a period of continuing current: after a quiescent interval of from 10 to 500 ms with a mean value of about 60 ms or a median value of 35 ms, a fast dart leader may occur, only on this occasion the current rise time is less than a microsecond and the current wave tail according to Berger is much more regularly exponential. The peak current delivered can be of the same order of magnitude as that of the first stroke, but the charge deposited is usually less. Other dart leaders may follow, the mean number being three to four and the maximum 30 or more.

Finally from Section 9 comes the suggestion that in order to account for ratios of between 1 and 2 of the leader field change to that observed for the return stroke, whilst still adhering to a charge

distribution which is at least linear and may even be exponential, it is necessary to envisage a discharge of electrons from the leader which exceeds the actual amount deposited - in other words that the leader channel should acquire a positive charge.

Dealing first of all with the question of the velocity of the tip of the luminous return stroke streamer, Loeb (1958) has made a calculation of the velocity which depends upon the concentration of positive ions in the streamer and that of electrons ahead of it and there can be no serious disagreement with this basis. It would be expected that the greater the quantity of charge on the leader, the greater will be the speed of the reaction which neutralises this charge since the field intensity at the upward moving tip will tend to be enhanced.

Since the velocity of positive ions in the tip is very small compared to that of the tip itself, it is clear that electrons must move downward into the tip and that they become the main current carrying media. The upward moving streamer may therefore be regarded as a growing conducting channel of plasma carrying current consisting of free ions of both signs in about equal numbers. The luminosity would therefore be the result of intense collisions and recombinations between the descending electrons and the ions in the streamer. It follows from the above that the velocity of the upward streamer represents the degree to which neutralisation of the charge in the channel is proceeding and a calculation of the velocity can be made starting with the known wave shape of the lightning current delivered to ground.

By way of an example, the current wave form of a lightning discharge proposed by Bruce and Golde (1941) may be assumed namely:

$$i = I \left[\exp(-at) - \exp(-bt) \right] \text{ amperes}$$

Where $a = 4.4 \times 10^4$ and $b = 4.6 \times 10^5$ .... s^{-1} ... (18.1)

The total charge delivered to ground is then

$$q = \int_0^\infty i\,dt = I \left[1/a - 1/b \right] \text{ coulombs} \quad \ldots\ldots\ldots\ldots \quad (18.2)$$

If for the sake of argument the charge q is assumed to have been distributed uniformly along the leader channel of height h_m, the charge per unit length is q/h_m and the neutralisation procedure is illustrated in Fig. 18.0.1.

96/ .....

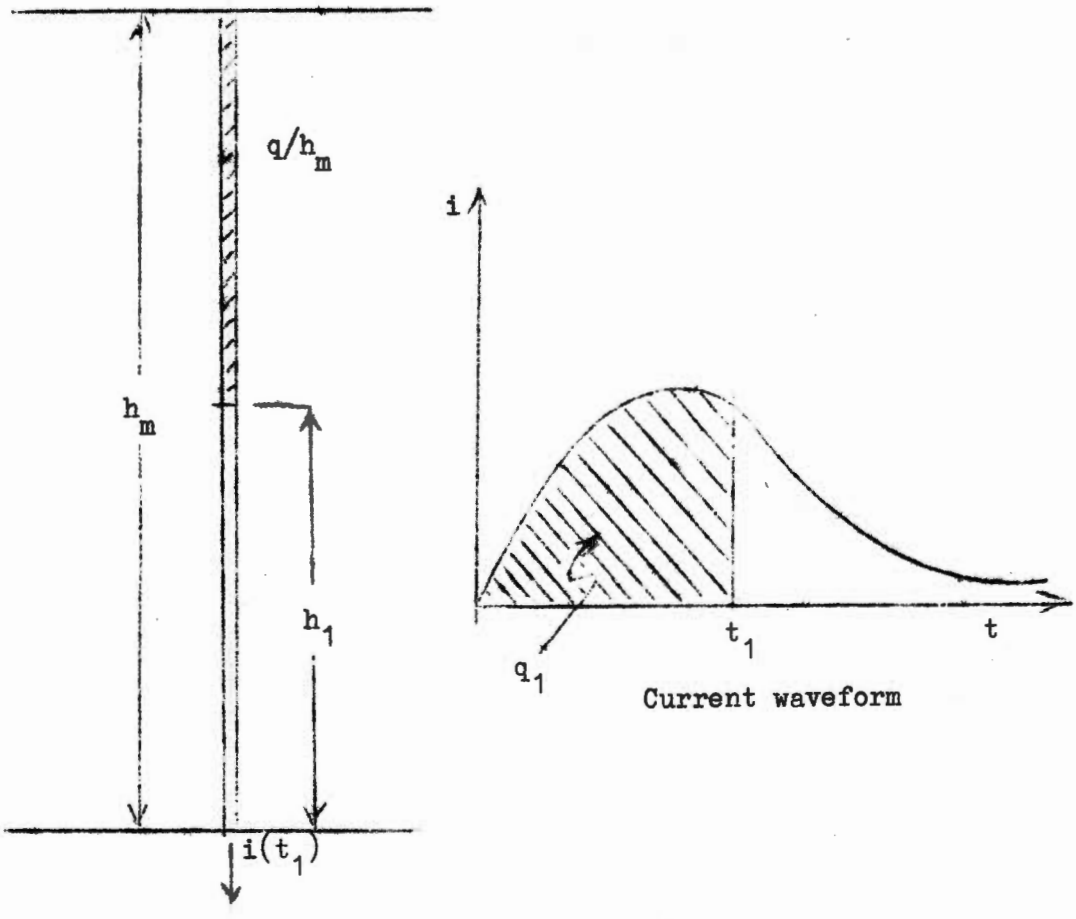

Fig. 18.0.1 Diagram illustrating the part neutralisation of a charge q distributed uniformly over a leader channel.

At any instant t_1 a charge q_1 has been eliminated from the section of channel of height h_1 from the earth; then $q_1 = h_1 q/h$ and also

$$q_1 = \int_0^{t_1} i\,dt.$$

Hence $h_1 = h_m/q \cdot \int_0^{t_1} i\,dt$ ..... (18.3)

The velocity "v" of the tip of the return stroke is therefore

$$v = dh/dt = h_m/q \cdot i(t) \quad \text{.....} \quad (18.4)$$

Substituting for i(t) and q equations (18.1) and (18.2) respectively.

$$v = h_m \left[\exp(-at) - \exp(-bt)\right] \left[1/a - 1/b\right]^{-1} \quad \text{....} \quad (18.5)$$

97/ .....

The maximum velocity occurs at the instant of maximum current, tm, and is given by differentiating equation (18.1) and equating it to zero whance it is found that

$$tm = (b - a)^{-1} \ln (b/a) \text{ seconds} \qquad (18.6)$$

Substituting the values of "a" and "b" and assuming $h_m = 2$ km say it is found that the maximum velocity is approximately 7×10^7 ms compared with the value of 8×10^7 m/s given by Bruce and Golde (1941). Malan (1963) gives extreme values of 2×10^7 up to $1{,}4 \times 10^8$ with $3{,}5 \times 10^7$ m/s as that most frequently occurring. The value calculated above can be varied within a limited range by other assumptions such as the height of the leader, the manner of the charge distribution and the lightning current waveform, but in general the good agreement between calculated and observed velocities merits serious consider= ation of the theory from which it is derived.

In the case of a linear distribution of charge, the charge q' per unit length for a position on the channel at height x above ground is given by the expression

$$q' = 2q/h_m \cdot (1-x/h_m) \text{ C/m} \quad \ldots\ldots\ldots\ldots\ldots\ldots \qquad (18.7)$$

Hence the total charge neutralised in a height h_1 is then

$$q_1 = 2q/h_m \cdot \int_0^{h_1} (1-x/h_m)dx$$

$$\text{Whence } q_1 = 2q(h_1/h_m) \cdot \left[1-1/2(h_1/h_m)\right] \quad \ldots\ldots\ldots\ldots\ldots \qquad (18.8)$$

Equation (18.8) is quadratic in terms of the variable h_1 whence the real solution becomes

$$h_1 = h_m \left[1-(1-q_1/q)^{\frac{1}{2}}\right] \quad \ldots\ldots\ldots\ldots\ldots\ldots\ldots\ldots \qquad (18.9)$$

Now q_1/q is the ratio of the charge neutralised up to a height h_1 and for a time t_1 and may therefore be expressed in terms of the current waveform namely

$$q_1/q = \int_0^{t_1} idt \; / \; \int_0^{\infty} idt = q(t)/q$$

and this must of course vary between 0 and 1 over the time t = 0 to t = respectively. The velocity of the **return** stroke tip is then dh/dt and by differentiating equation (18.9) resolves into the follow= ing expression namely:

$$v = h_m/2q \cdot i(t) \left[1-q(t)/q\right]^{-\frac{1}{2}} \text{ m/s} \quad \ldots\ldots\ldots\ldots \qquad (18.10)$$

98/ .....

Compared with equation (18.4) for a uniform charge distribution the maximum velocity is seen to be reduced by a factor of two, since near the maximum value of i(t) the value of q(t)/q is very small.

Hence in the case of a uniform charge distribution the velocity is proportional to the current and decays rapidly if the current decays. For a linear charge distribution, the initial velocity if half the magnitude and it does not decay so severly as for the uniform charge distribution case. Finally if the charge distribution were to be exponential as suggested by Bruce & Golde (1941) the velocity of the return stroke would be more or less constant on this hypothesis, but its magnitude would be considerably less than that indicated for the other two cases.

According to one example cited by Berger (1967) a charge of 2C coincided with a peak current of about 20 kA. Hence for a leader of 4 km in height, the maximum velocity of the return stroke would be 2×10^7 m/s which is the right order of magnitude.

Wagner et al (1963) derives a relationship showing an approximately linear proportionality between the peak lightning current and the return stroke velocity, which they claim to be supported by observation. As will be clear from above such a relationship could exist if the ratio of peak lightning current to that of the total charge remained sensibly constant - which might reasonably be expected - and provided there is not a very large variation in the height of the leader discharge.

At all events it is clear that there is some fairly close connection between theory and experimental results tending to give support to the basic hypothesis as to the manner in which the lightning channel discharges during the return stroke. However the velocity is relatively slow and the overall duration of the discharge long and not at all commensurate with what would be expected of say a metalic conductor bridging the potential of the cloud charge to earth.

The reasons for this are two-fold. In the first place one source of supply of electrons, namely from the cloud, is inhibited because the electrons are bound upon water droplets or other nuclei and have to be freed by the action of slowly moving positive streamers and this accounts for continuing currents after main strokes. The second source of electrons is in the corona sheath of the lightning channel and since the electrons are mobile this must provide for the main high current discharge.

The known time scale for the discharge is determined by the return stroke streamer which is proceeding at a velocity of say 4×10^7 m/S over 4 km of leader channel could complete the discharge in 100 µs. If on the other hand, the electrons at the top of the channel were able to proceed down the channel at the speed of light, they would complete the traverse in 13,3 µs and allowing for a zero potential wave propagation up the channel at the same velocity to start the reaction, the whole process could not last longer than about 27 µs. On the other hand an analysis carried out on the approximately exponential decay times of the lightning current observed by Berger showed that these had a mean time constant of decay of about 105 µs with a variation of between 50 and 150 µs. From this the mean duration up to 95% of the discharge, was about 300 µs with a maximum of 450 µs.

One explanation that satisfies the conditions stated above is that the discharge process only occurs as the return stroke tip advances up the channel. In this case the total duration of the discharge equals that of the return stroke time, and the velocity to charge and current relations will be in accordance with that described above. However the potential of the advancing tip is not likely to be much in excess of zero because the potential gradient along the channel will be small and when this reaches the top near the cloud charge the field intensity would be so high as to immediately precipitate a rapid discharge of the remainder of the cloud charge, and this does not occur.

On the other hand if the potential gradient along the channel is maintained at least to some extent, the channel may then behave as a short circuited capacitance. Fig. 18.0.2 illustrates the effect of a change in value of potential gradient as a consequence of an increase in the current flowing in the channel.

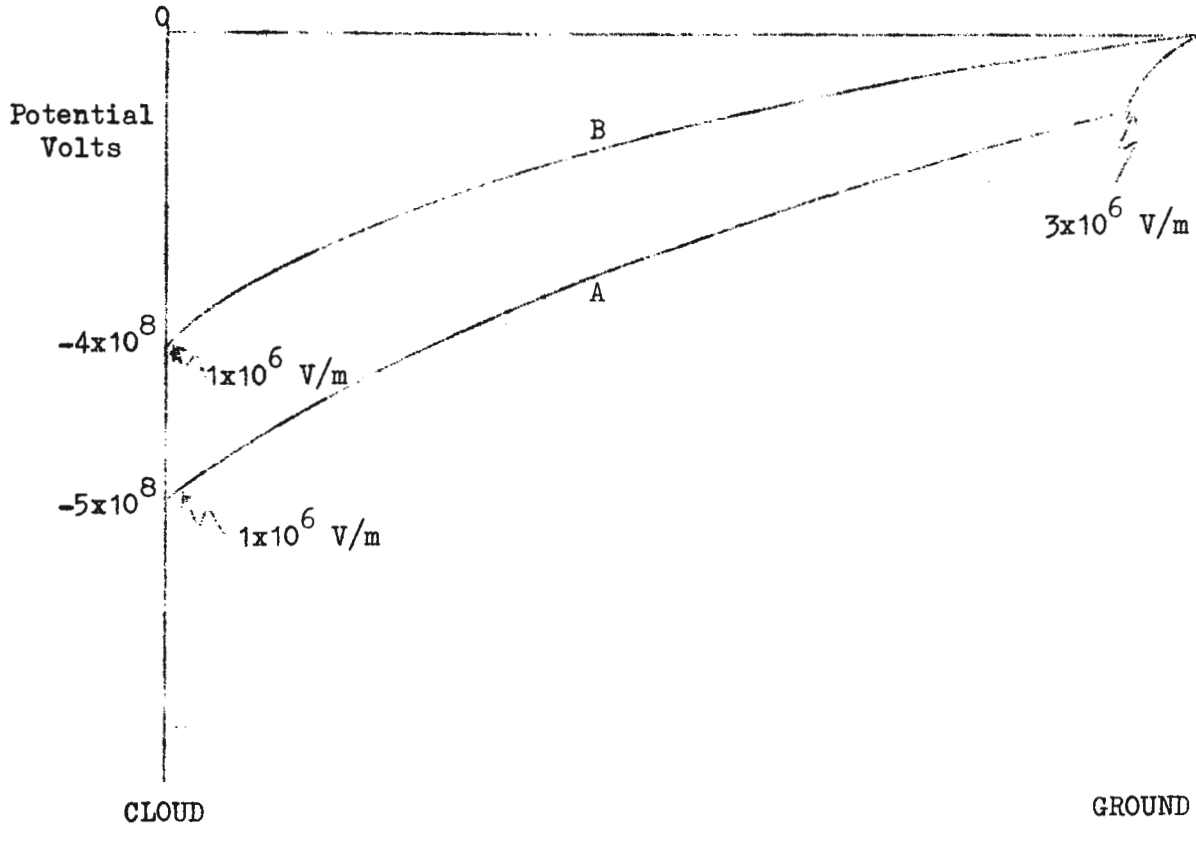

Fig. 18.0.2 Diagram illustrating change in conditions on contact between leader channel and earth
A - Condition just prior to contact
B - Conditions after contact

Fig. 18.0.2 shows that if the potential gradient along the leader is allowed to reduce, the potential at the cloud end of the channel must rise (fall numerically) and in order to do so a large positive charge must be induced in the top end of the channel. This in effect means a transfer of electrons from the top end of the channel leaving an excess of positive ions to make up the positive charge required.

That this process need not proceed at the speed of light is self evident from the fact that it is only the rate of growth of the

100/ .....

return stroke channel which determines the length of channel that requires to have a low value of potential gradient. Hence the transfer of electrons from the corona envelope should proceed at a rate determined by the velocity of the return stroke tip.

This now means that the channel must discharge more electrons than were originally deposited along it as negative charge during the leader process, as had been surmised during earlier discussions; the source of these electrons is assured as a result of the secondary separation of charge which was envisaged within the corona sheath to keep the field intensity equal to the level required for ionisation since this level cannot be exceeded. (See Section 10. Fig. 10.0.3)

It is clear therefore that the current delivered to ground depends not only on the rate of neutralization of charge deposited on the leader channel, but also upon the excess charge delivered from the corona envelope in order to increase the induced positive charge at the top of the channel - which in turn allows the discharge to proceed. This hypothesis also satisfies the requirements that the magnitude of the fast field change during the return stroke can be at least equal to that of the leader at a distance $D \gg H$ despite the fact that the initial charge deposition was not uniform as discussed in Section 9.

The one problem remaining is that of determining the quantity and distribution of positive charge remaining in the channel, after the passage of the return stroke. Firstly it should be noted that positive charge in the form of ions was initially already present in the whole length of the channel by virtue of the secondary corona sheath charge separation, and the distribution of this charge is likely to be proportional to the potential at any point on the channel. This, according to the model described previously, increases from zero on contact with the earth, to the high value existing at the cloud end of the channel.

When the channel discharges a portion if not all the negative counter part of the charge, it will leave positive charge on the return stroke channel which is therefore increasing in quantity per unit length as the tip of the return stroke moves upwards. This view point would also be consistent with the notion that if a vertical conductor is raised from earth in a negative electric field, a positive charge is induced on the conductor in such quantity as to maintain the potential of the conductor at zero, and this too will tend to ensure that there is more positive charge per unit length at the top than there would be at the base.

Suppose the above situation is as shown diagramatically on Fig. 18.0.3.

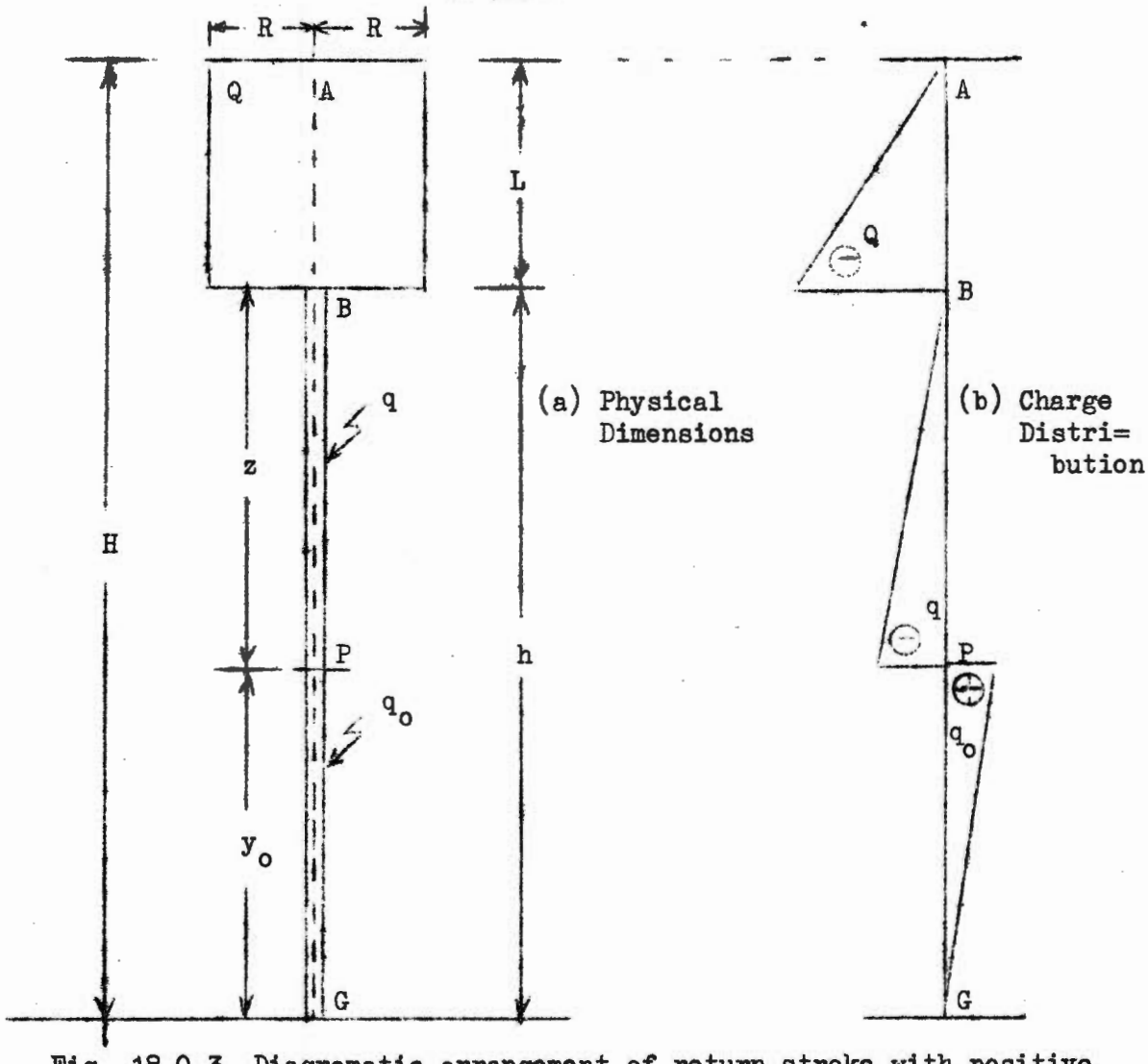

Fig. 18.0.3 Diagramatic arrangement of return stroke with positive charge raised during traverse upwards (Ignoring induced charge on leader)

If Q is the total charge bound in the cloud and distributed linearly as illustrated on Fig. 18.0.3(b) the potential at any point P between B and G due to this charge may be found from the standard formulae given in Section 4 or Appendix I.

Similarly if q is the prospective maximum charge deposited on the channel and it has the length $z = h-y_o$ and a radius r, the po= tential at P due to the charge q may be found either from the formulae given previously for the concentric distribution of charge given in Section 11 or the approximate line charge given in Section 16.

Also if q_o is the prospective charge to be raised by the return stroke - that is by the time it reaches the cloud - and its length and radius are y_o and r_o respectively the potential at the top of the return stroke due to this charge would then be given by equation (17.12) of Section 17 which is repeated as follows namely:

$$V_p = q_o/2\pi\varepsilon y_o \cdot F_4(y_o/r_o)$$

102/ .....

$$\text{Where } F_4(y_o/r_o) = 1/a \left\{ a \, \text{Sinh}^{-1}(2a) - 2/3 \left[1+(2a)^2\right]^{3/2} + 2a^2 \left[1+(2a)^2\right]^{\frac{1}{2}} + 4/3a^3 + 2/3 \right\}$$

And $a = y_o/r_o$

The radius of the return stroke channel is considerably less than that of the leader, reputedly not larger than a few centi= metres, consequently when $y_o \gg r_o$ the above expression simplifies very considerably to the following namely:

$$V_p = q_o/2\pi\varepsilon y_o \cdot \ln(4y_o/r_o) \quad \ldots\ldots\ldots\ldots\ldots\ldots \quad (18.11)$$

When the return stroke reaches the cloud $y_o = h$, and for $h = 4x10^3$ m say and $r_o = 10$ cm say $V_p = q_o x 5{,}4x10^7$ Volts.

Hence it is clear that a positive value of q_o in the order of 10C would be capable of creating a potential at the top of the channel of the same order of magnitude as the negative potential existing as a consequence of the bound charge remaining in the cloud which of course would result in the potential being zero.

The charge required to achieve this would be less if account is taken of the fact previously mentioned that in order to ensure zero potential along the whole length of the channel, the charge would tend to concentrate more severely at the top of the channel than allowed for by a linear distribution. However the field intensity at the channel tip would be given by equation (17.4) of the last section namely

$$E_p = - q_o/2\pi\varepsilon y_o^2 \left[2y_o/r_o - \text{Sinh}^{-1}(2y_o/r_o)\right]$$

When $y_o \gg r_o$ the Sinh^{-1} term can be neglected and at the channel tip $y_o = h$.

$$\text{Whence } E_p = - q_o/\pi\varepsilon h r_o \quad \ldots\ldots\ldots\ldots\ldots\ldots\ldots\ldots \quad (18.12)$$

Hence if $h = 4x10^3$ m $E_p = - q_o/r_o x 9x10^6$ V/m.

If q_o is positive, the field intensity adds to that already present below the cloud charge, and if this is already at an ioni= sation level of say $-1x10^6$ V/m it is quite clear that the effect of increased positive charge at the top of the leader will cause further breakdown for any real value assigned to q_o/r_o.

To illustrate the above by means of a numerical calculation, suppose h = 4km as before, and that the potential of the cloud end of the leader is say $-5x10^8$ Volts - a value which would be quite low

according to the computed examples. The following Table 18.1.1 then shows the calculated values of the charge q_o required to reduce the potential to zero for various assumed values of r_o. It is then possible to calculate the values of field intensity exerted by this charge, by substituting for q_o/r_o so obtained in equation (18.12).

r_o	q_o	q_o/r_o	E_p
1 cm	7,8 C	$7,8 \times 10^2$	$-7,0 \times 10^9$ V/m
10 cm	9,3 C	$9,3 \times 10^1$	$-8,4 \times 10^8$ V/m
1 m	11,5 C	$1,15 \times 10^1$	$-1,0 \times 10^8$ V/m
10 m	15,1 C	1,51	$-1,4 \times 10^7$ V/m

Table 18.1.1 Example of calculation of positive charge q_o raised in return stroke to make cloud potential zero, and resultant field intensities for various values r_o.

$h = 4 \times 10^3$ $V = -5 \times 10^8$ Volts

To recap for a moment, the leader was envisaged as progressing to earth whilst at the same time a positive induced charge at the top end of the leader assisted to maintain the field intensity there at an ionising level of say -1×10^6 V/m. According to the results of computation on this process, a charge of the order of about 1.C. spread out over the whole of the radius of the so called Z_1 area equal to that of the main negative bound-charge radius, was all that was required to do this.

Now the field intensity due to the negative charge in the channel is in such a direction at the top that it tends to lower the field intensity in that region; when it is suddenly removed by the return stroke discharge, therefore, the field intensity at the top of the channel will increase whereupon further breakdown and ionisation will occur, in any case.

If however, in addition to the above, it is now assumed that zero potential is virtually transferred by the tip of the return stroke channel to the cloud area, it is clear from the above calculations that the field intensity in the cloud would be enhanced by a considerable amount as q_o/r_o increases. If q_o/r_o is small, then both the charge which would be needed to make the potential zero, and the radius r_o would need to be very large if the added field intensity has to be small and this does not fit the concept of a small radius for the return stroke channel compared with the leader.

Other difficulties which would result would be that during the upward movement of the return stroke, the charge moved to earth would be the sum of that deposited originally by the leader and that required to balance the positive charge raised by the return stroke. Furthermore the charge deposited by the leader is already to be enhanced by an induced charge which is needed to maintain ionisation

104/ .....

conditions at the cloud end. These charges are mounting up to values well in excess of the 5 C thought to be the mean charge dissipated by a single stroke of lightning. Hence either the whole scale of values, in particular the quantity of accumulated charge in the cloud, would need to be reduced, or the hypothesis of a rising zero potential wave abandoned if it can be satisfactorily replaced.

In order to provide a review of the order of magnitude of the quantities which are being considered a series of data was computed for various values of cloud charge using the model devised in Sections 12 and 13. The examples taken were as follows including the previously described case, and the respective curves drawn up are enumerated in **Table** 18.1.2.

Cloud Charge Q	Height of Separation H	Length of Charge $L_o = L_1$	Height of Leader h	Radius of Charge $R_o = R_1$	Figure Numbers -
Coulombs	km	km	km	km	-
43	8	2	6	0,5	18.0.4-18.0.7
43	6	2	4	0,5	18.0.8-18.0.11
71	8	4	4	0,5	13.0.5-13.0.10
168	8	4	4	1,0	18.0.12-18.0.15

Table 18.1.2 Table indicating details of computed cases of cloud charge arrangements

In each of the curves cited the field intensity for ionisation was assumed to be $-1x10^6$ V/m in the cloud area persisting for 50% of the leader traverse to ground, increasing abruptly to $-2x10^6$ V/m at the cloud-air boundary, and thereafter increasing linearly to $-3x10^6$ V/m at ground level. The program started with a predetermined arbitrary value inserted for the potential gradient along the leader which was maintained until the radius of the positively charged volume RZ1 equalled that of the cloud charge R_1. When this was reached the computer calculated the potential gradient applying thereafter. Calculations proceeded for constant values of "c" which is the ratio of the velocity of the leader tip v_1 to that of the mean value v_2 of the positive streamers at the top of the channel, designated by the symbols $c = v_2/v_1$. As previously, for the purpose of uniformity, the leader tip velocity was kept constant at $v_2 = 2x10^5$ m/s but since all velocities are relative, this substitution is purely for convenience and may be varied at will without affecting the computed results.

Since it is not an easy matter to compare a large set of curves the following tables depict comparative values of charge, potential and potential gradient, for various values of c. Table 18.1.3 first of all shows the value of prospective maximum induced charge needed to maintain the ionisation level at the stipulated figure of $-1x10^6$ V/m. This charge is the value attained when the leader reaches the ground without inducing any intensification due to the proximity of the mirror image near the earth plane. This intensification is achieved by a change in velocity equivalent to a shift to a lower value of c.

105/ .....

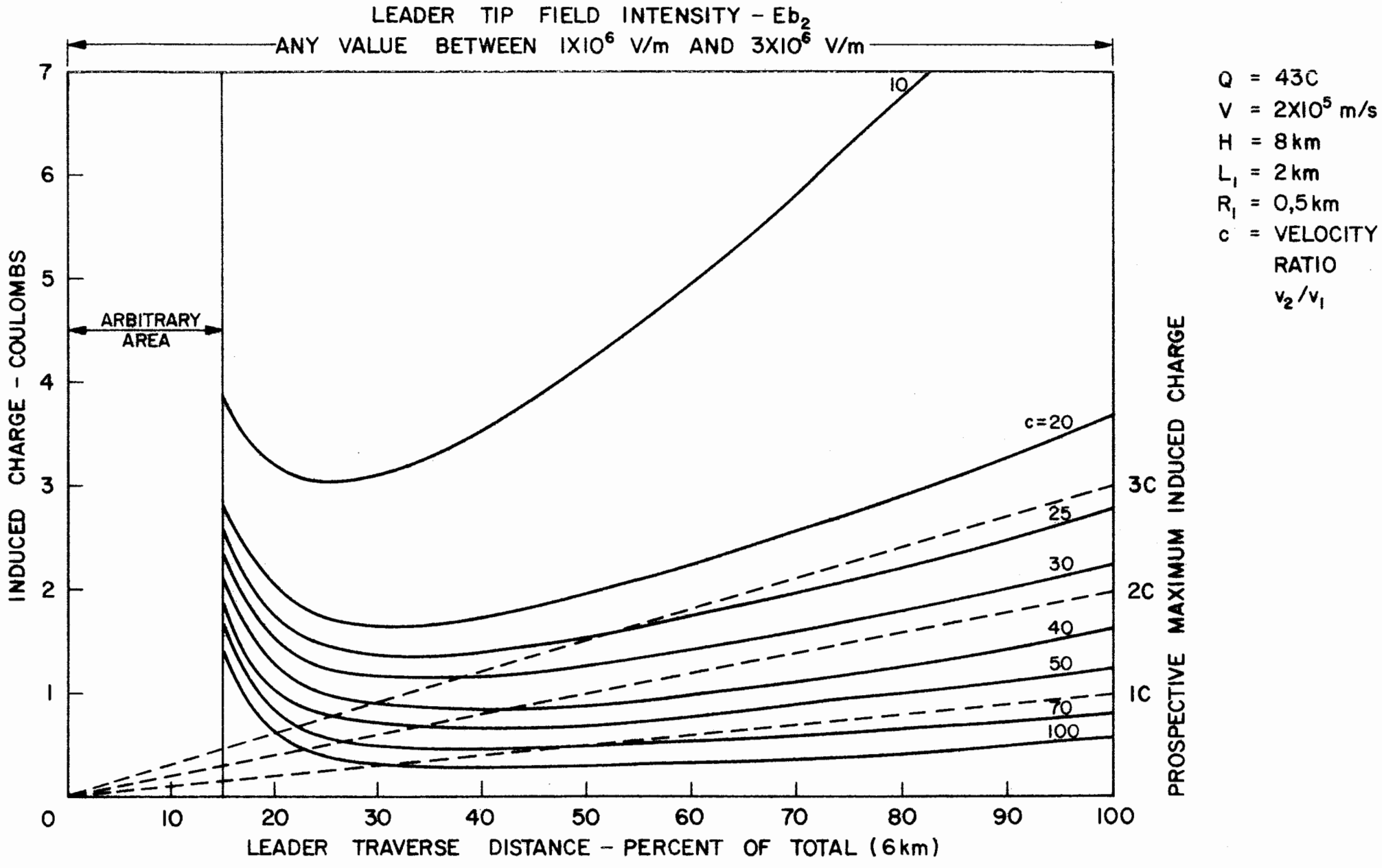

FIGURE 18·0·4

INDUCED CHARGE ON LEADER H=8km ($Rz_1 = R_1$ FROM 15%)

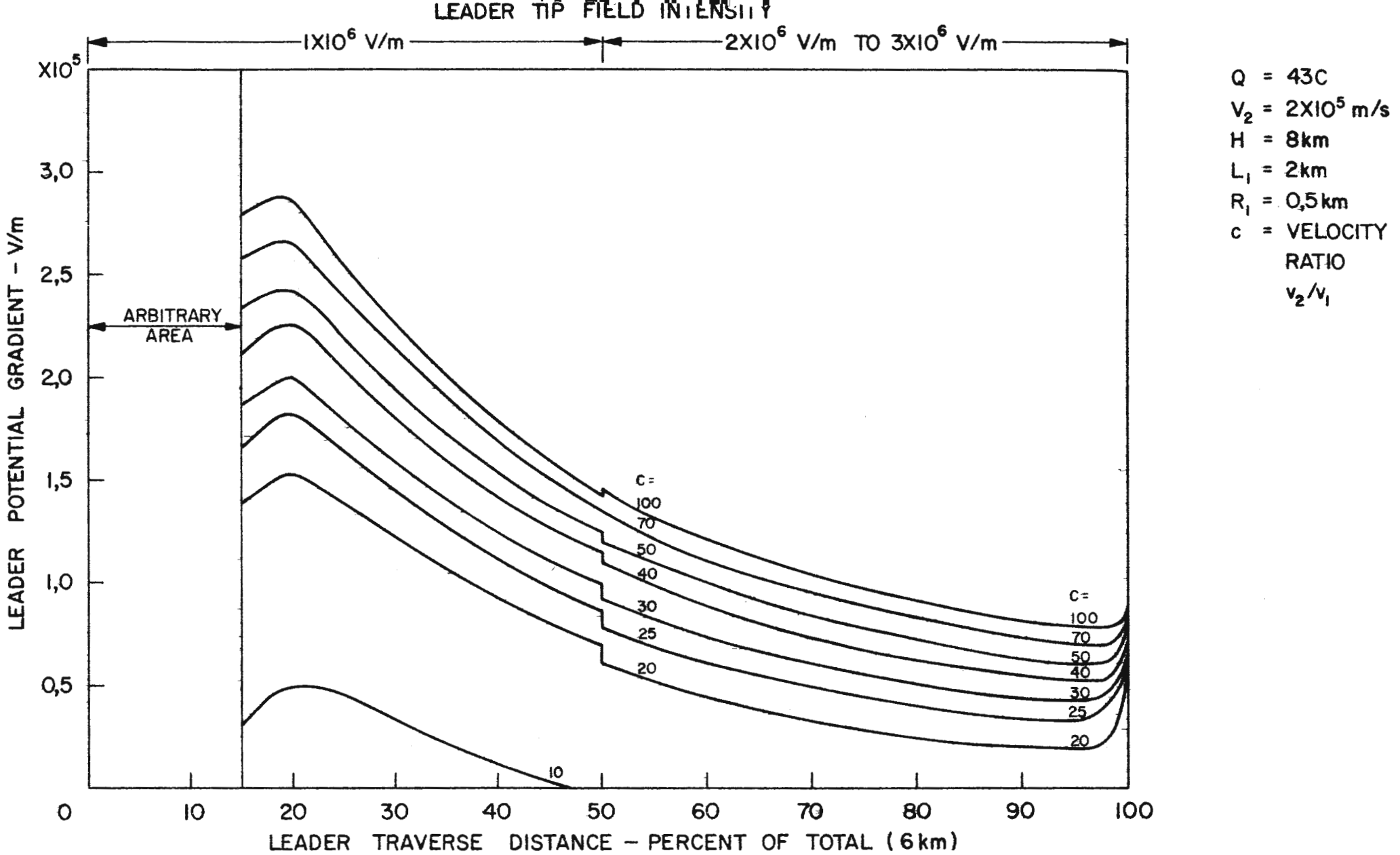

FIGURE 18·0·5

POTENTIAL GRADIENT OF LEADER – H = 8km ($Rz_1 = R_1$ FROM 15 %)

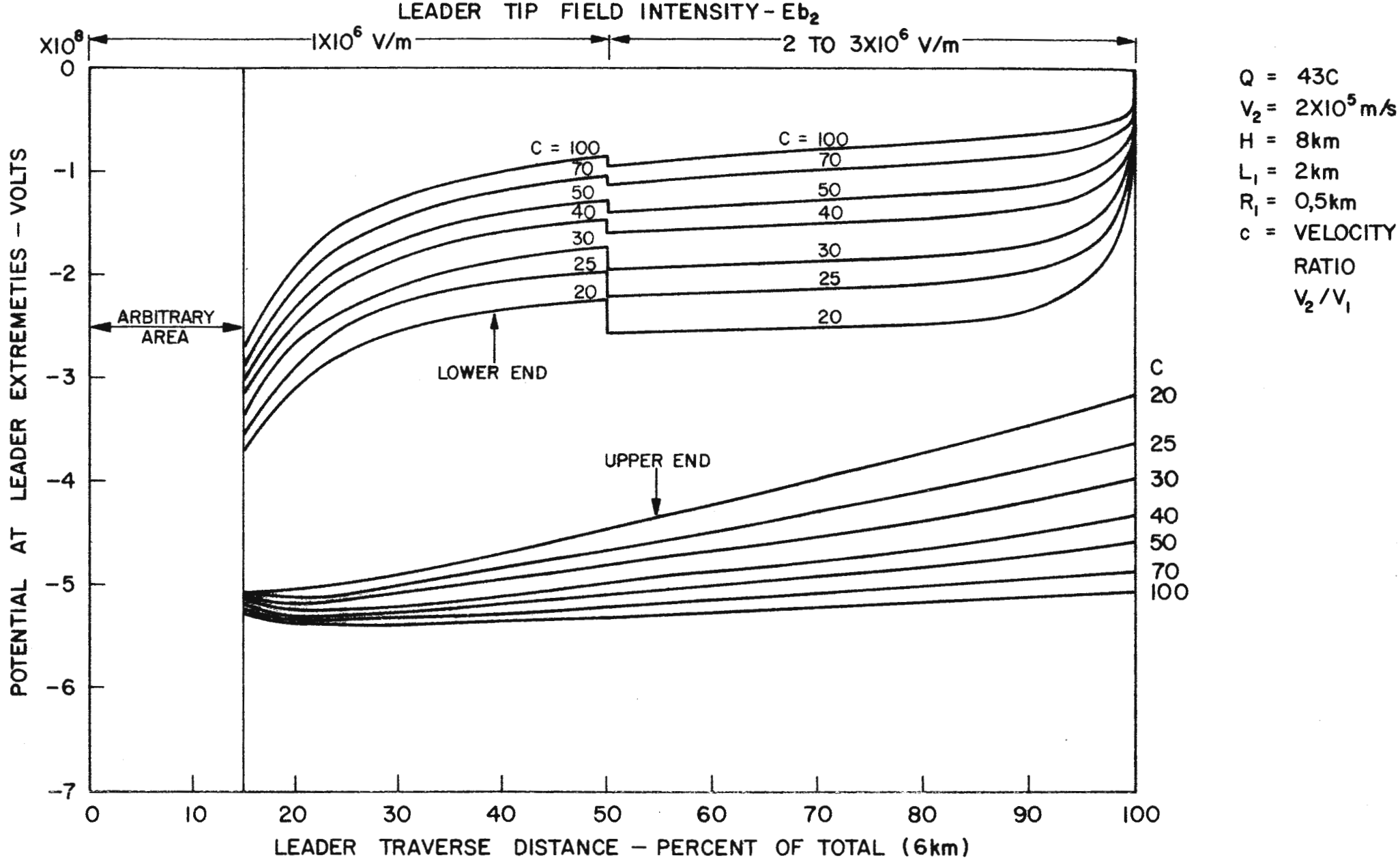

FIGURE 18·0·6

POTENTIAL AT LEADER EXTREMITIES - H = 8km ($Rz_1 = R_1$ FROM 15 %)

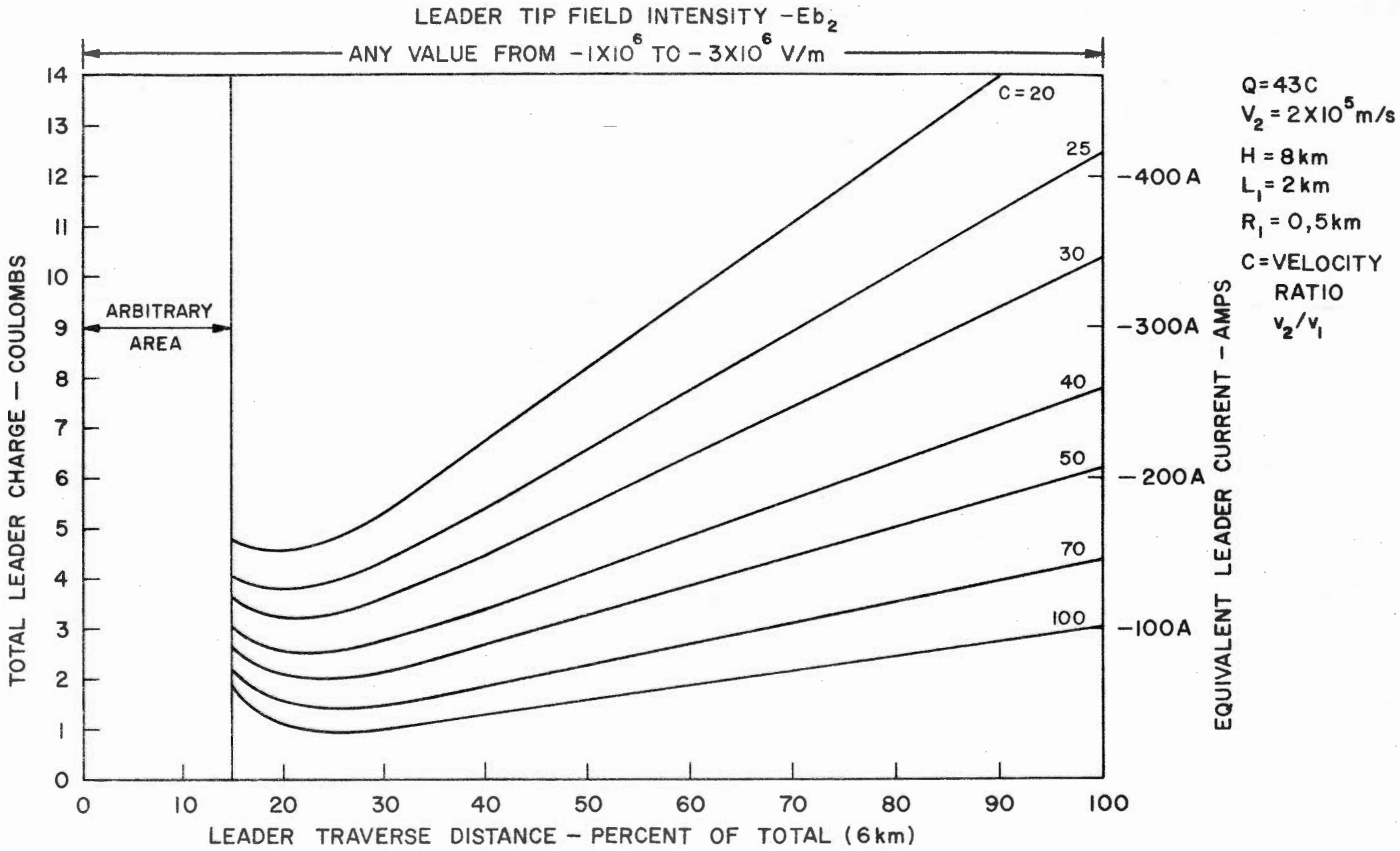

FIGURE 18·0·7

TOTAL CHARGE ON LEADER = 8km ($Rz_1 = R_1$ FROM 15%)

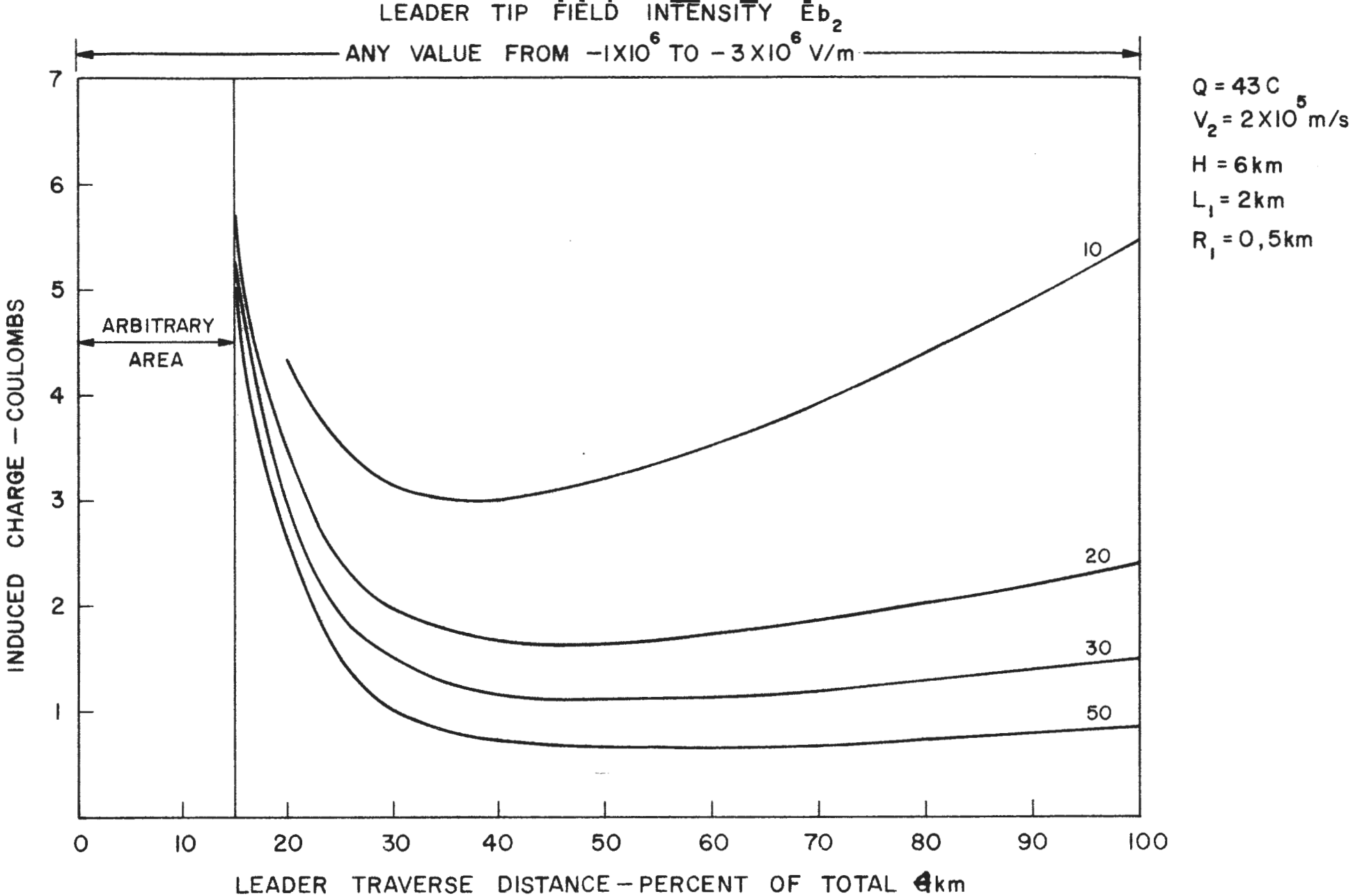

FIGURE 18·0·8

INDUCED CHARGE ON LEADER – H = 6km ($Rz_1 = R_1$ FROM 15 %)

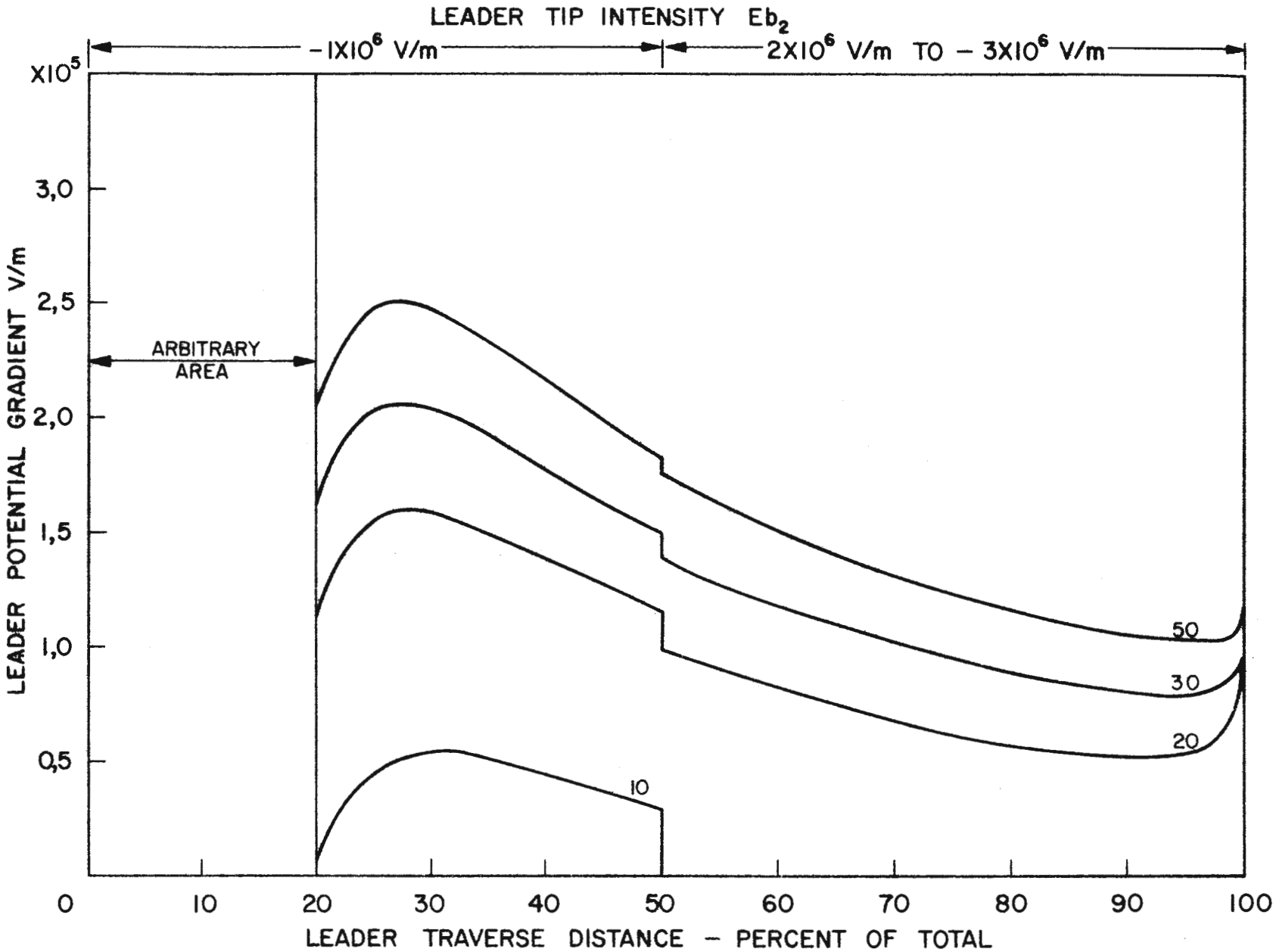

FIGURE 18 · 0 · 9

POTENTIAL GRADIENT OF LEADER H = 6km ($Rz_1 = R_1$ FROM 20%)

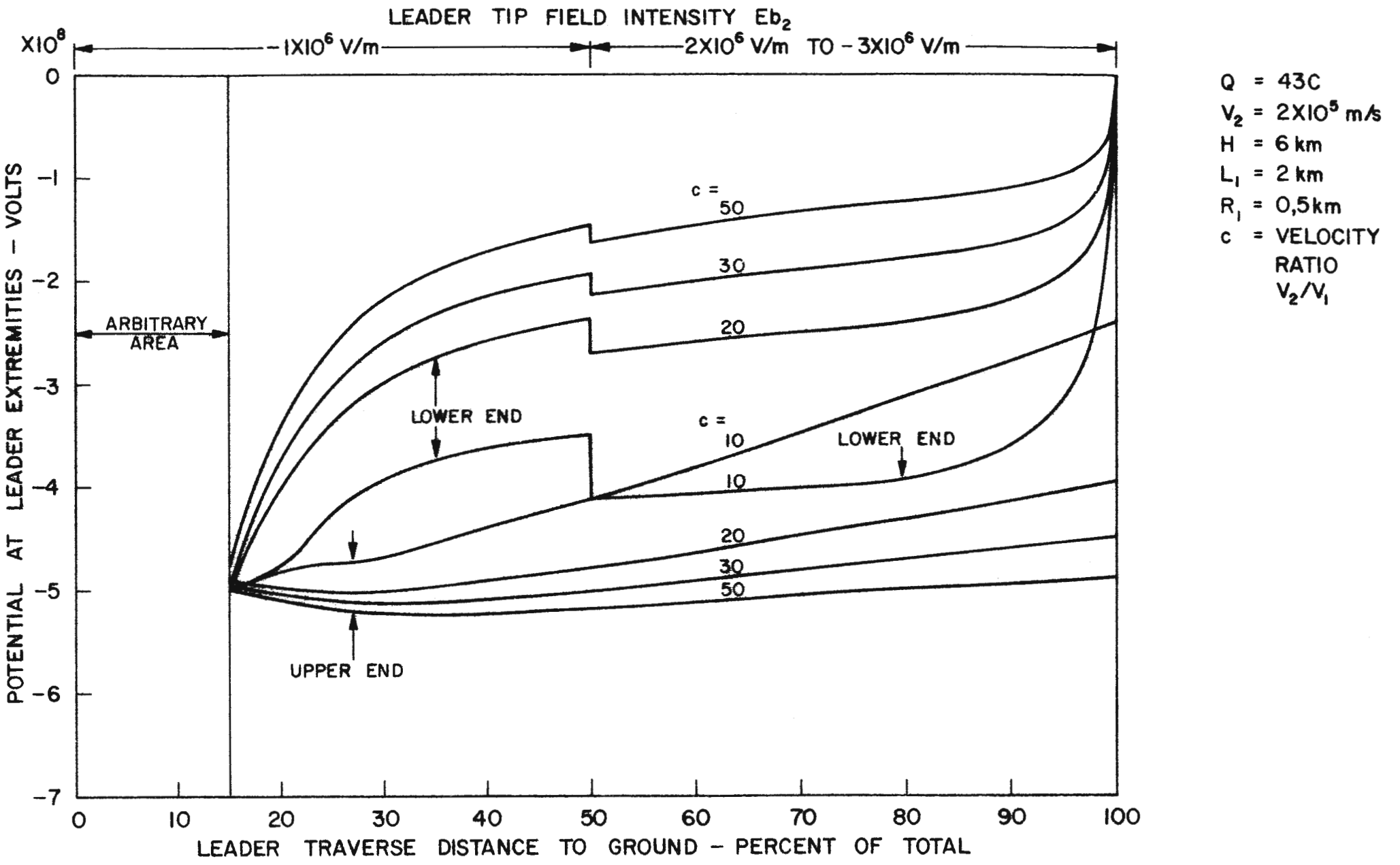

FIGURE 18·0·10

POTENTIAL AT LEADER EXTREMITIES - H = 6km ($Rz_1 = R_1$ FROM 15%)

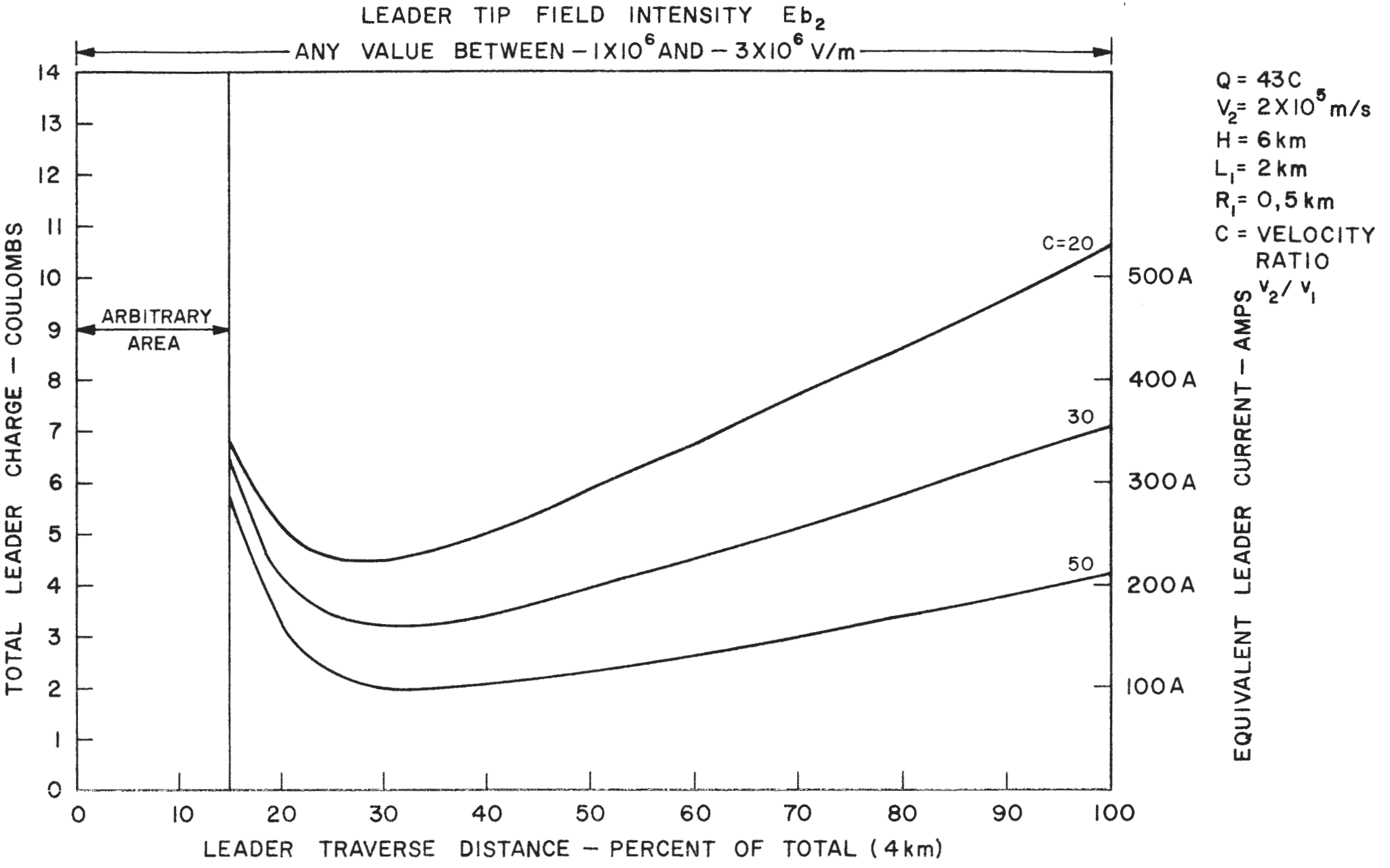

FIGURE 18 · O · 11

TOTAL CHARGE ON LEADER — H = 6km ($Rz_1 = R_1$ FROM 15 %)

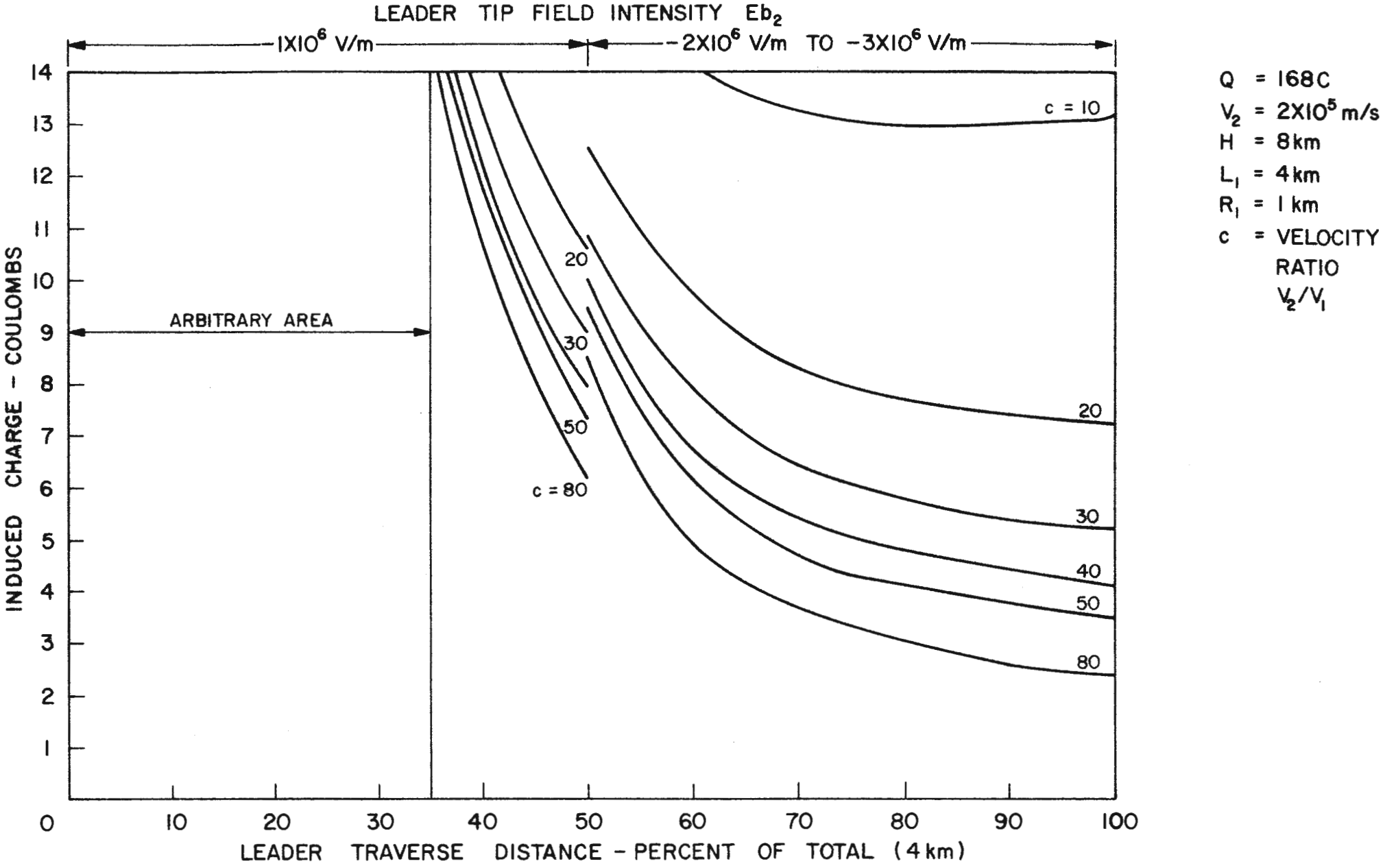

FIGURE 18·0·12

INDUCED CHARGE ON LEADER ($Rz_1 = R_1$ FROM 35 %)

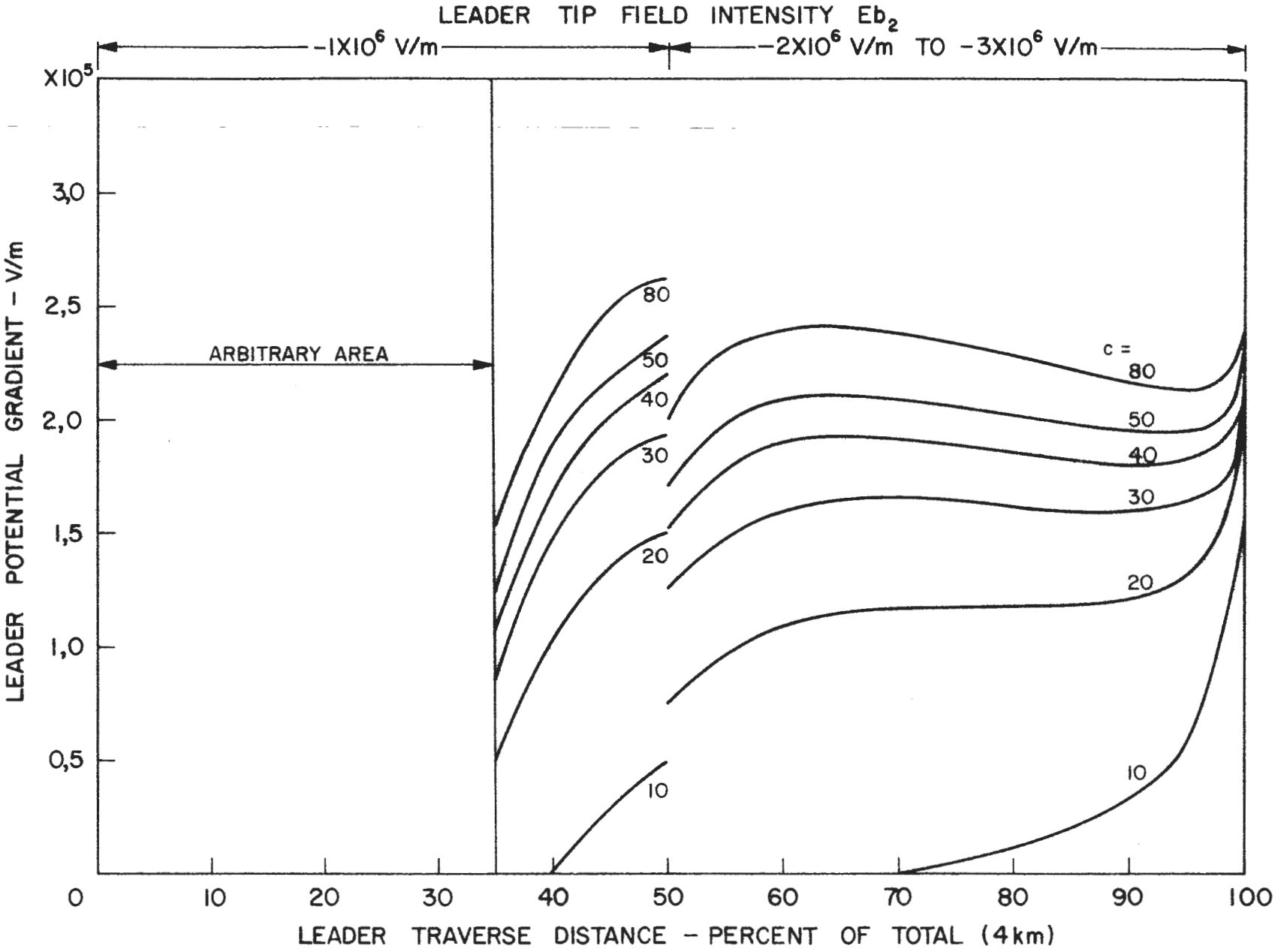

FIGURE 18·0·13

POTENTIAL GRADIENT OF LEADER ($Rz_1 = R_1$ FROM 35%)

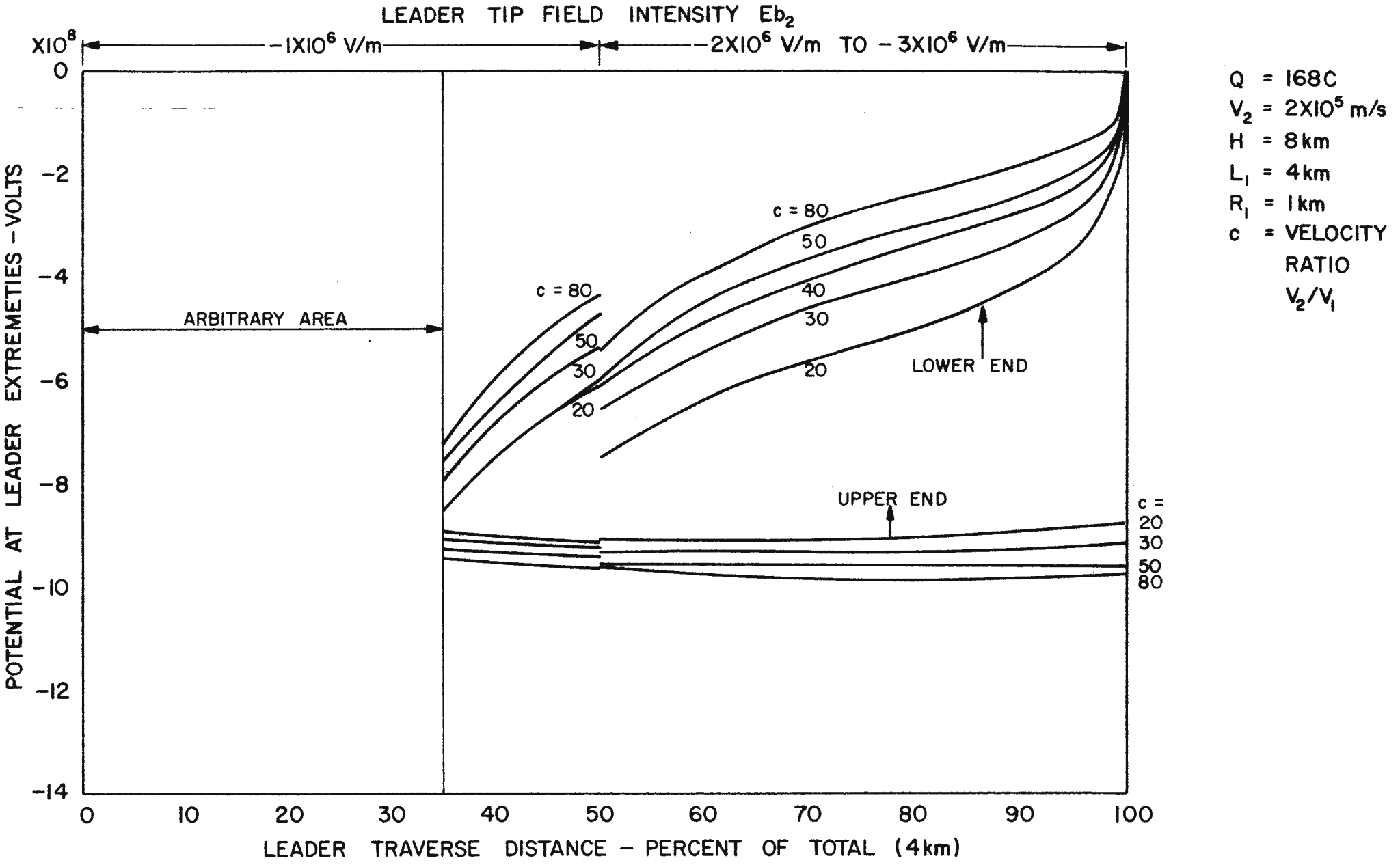

FIGURE 18 · 0 · 14

POTENTIAL AT EXTREMITIES OF LEADER ($Rz_1 = R_1$ FROM 35%)

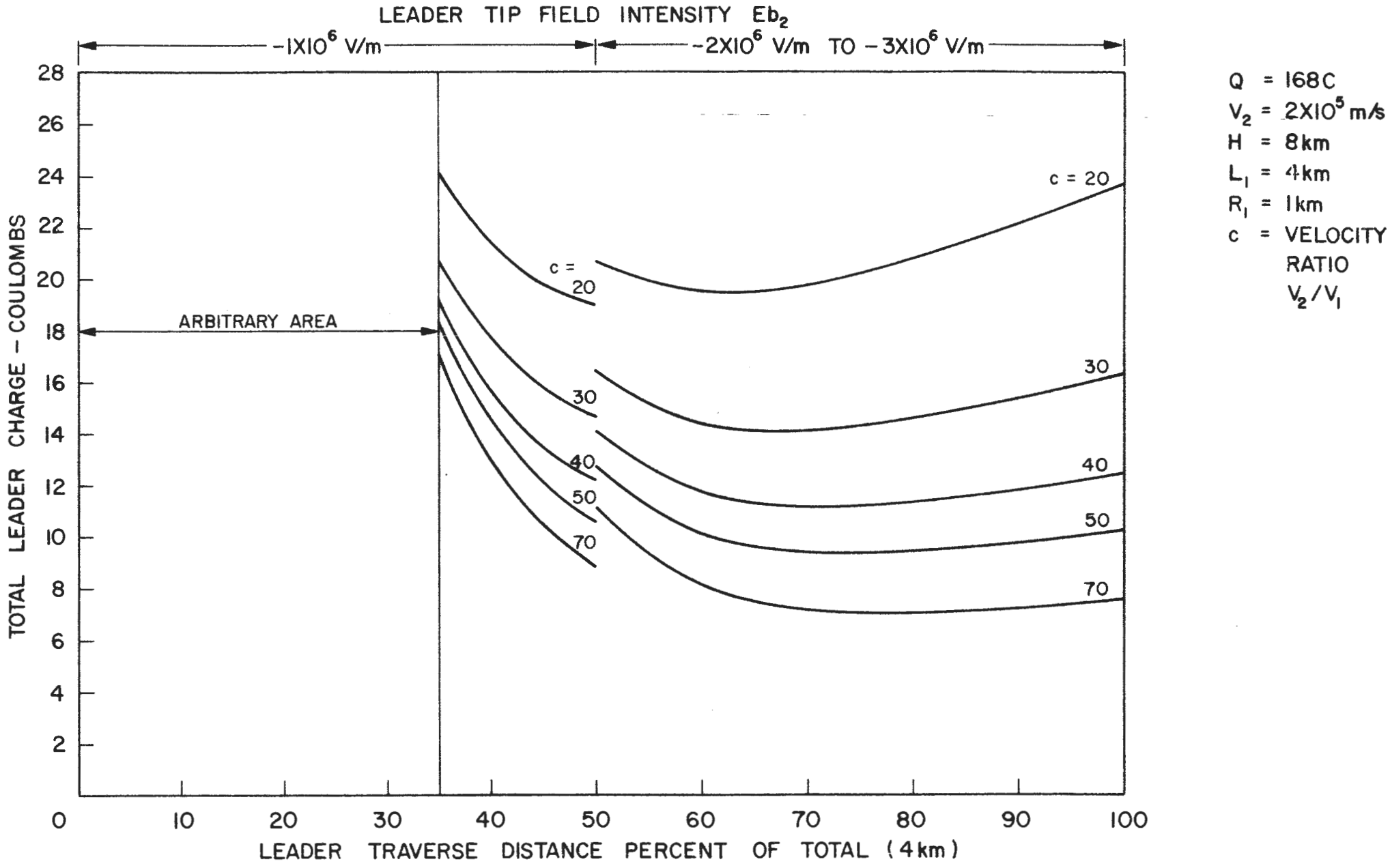

FIGURE 18·0·15

TOTAL CHARGE ON LEADER ($Rz_1 = R_1$ FROM 35%)

Cloud Charge Q	Height of Leaders h	Body of Table shows maximum induced charge - Coulombs					
		Values of velocity ratio $c = v_2/v_1$					
		10	20	30	50	70	100
43	6	9,0	3,7	2,2	1,2	0,8	0,5
43	4	5,5	2,4	1,5	0,8	0,5	0,3
71	4	2,4	1,1	0,7	0,4	-	-
168	4	13,2	7,2	5,2	3,5	2,7	-

Table 18.1.3 Maximum prospective induced charge in leader for various values of velocity ratio $c = v_2/v_1$

The value of induced charge for the 43 C case at 4 km height is approximately 2/3 of the value at 6 km indicating a rough proportionality with the height of the channel other things being equal. The induced charge required for the 71.C case for the same height of leader channel is less than that of the 43C case because of the longer charged cylinder which is 4 km against 2 km, and which means that the influence of the upper positive charge on the field intensity at the top of the channel is less despite the higher value of total charge.

It can also be seen that for the same value of velocity ratio, the induced charge is not proportional to the total charge in the cloud as for instance the comparison between the 168 C and 71 C case. The influence of the radius of the charge is evident since that of the 168 C is 1 km against 0,5 km for the 71 C case.

Hence generally the dependence of the induced charge upon the dimensions and disposition of the main cloud charges is very much in evidence. This would also apply if the lengths of the cylinders enclosing the respective positive and negative charges are not equal.

The total charge lowered by the leader is the sum of the induced charge and that due to penetration of the lower charge by positive streamers at a mean velocity of v_1. If v_2 is held constant therefore, the amount of charge extracted will decrease as the ratio "c" increases as the following Table 18.1.4 indicates.

Cloud Charge Q	Height of Leader h	Body of Table shows total charge on leader - Coulombs					
		Values of velocity ratio $c = v_2/v_1$					
		10	20	30	50	70	100
43	6	30,9	15,6	10,4	6,2	4,4	3,1
43	4	21,0	10,6	7,0	4,2	2,9	2,1
71	4	15,9	8,1	5,4	3,2	-	-
168	4	45,1	23,6	16,2	10,1	7,5	-

Table 18.1.4 Total Charge on Leader Channel for various values of the velocity ratio $c = v_2/v_1$

106/ .....

The common factor which is maintained by the computer program throughout the complete range of data is that the field intensity at the cloud end of the leader should be maintained at -1×10^6 V/m and that at the leader tip extremity should be equal to the breakdown strength of the media through which the leader tip is penetrating at any particular instance. This does not mean however that the velocities of the respective streamers maintain a value proportional to the field intensity, for if they did so, the value of the velocity ratio would be fixed also for the last three cases - and this is clearly not admissable.

The mean velocity v_1 in the cloud is for example primarily dependent upon the rate at which positive charge is induced in the tips and the distance the tips have to cover when the field intensity tends to increase above ionisation - that is it is also dependent upon the field gradient ahead of the tips. If this is very high as would be expected of a charge confined in a small volume such as the 43.C cases, the distances are small and the velocity of the tips also small. The induced charge on the other hand is dependent on the cloud potential as well as the leader dimensions.

The potential of the upper end of the leader at the moment when the leader reaches ground is indicated in Table 18.1.5 which follows:

Cloud Charge	Height of Leader	Body of Table shows negative potential of upper of leader x 10^8 Volts					
		Values of velocity ratio $c = v_2/v_1$					
Q	h	10	20	30	50	70	100
43	6	0,7	3,2	4,0	4,6	4,9	5,1
43	4	2,4	4,0	4,5	4,9	-	-
71	4	4,9	5,6	5,9	6,0	-	-
168	4	7,4	8,8	9,2	9,6	9,7	-

Table 18.1.5 Potential at upper end of leader channel for various values of the velocity ratio $c = v_2/v_1$

The influence of the induced positive charge in lowering the potential is clearly evident in all cases when the value of "c" is low. However the total charge at these values is also high compared with a mean value of say 5 C for the lightning discharge, and it is more probable that the higher values of "c" are the more applicable. The potentials are also seen not to be directly proportional to the charge obviously because they are a function of the dimensions enclosing the charge.

The above potentials are those at the cloud end of the leader at the instant that the leader touches earth so that when divided by the height of the leader the mean potential gradient between cloud and ground is obtained as indicated in the following Table 18.1.6.

107/ .....

Cloud Charge	Height of Leader	Body of Table indicates Mean Potential Gradient of Leader x 10^5 V/m					
		Values of velocity ratio $c = v_2/v_1$					
Q	h	10	20	30	50	70	100
43	6	0,1	0,5	0,6	0,8	0,8	0,8
43	4	0,5	0,9	1,1	1,2	-	-
71	4	1,1	1,3	1,4	1,5	-	-
168	4	1,7	2,1	2,2	2,3	2,4	-

Table 18.1.6 Mean Potential Gradient along leader channel when tip reaches ground for various velocity ratios $c = v_2/v_1$

According to Table 18.1.6 it is an inescapable fact that the initial mean potential gradient along the leader will vary depending upon the cloud potential and will exceed that of the arc voltage drop along the channel. It should of course be appreciated that since the gradient of the positive tip end is $1x10^6$ V/m (or about a factor of ten higher, then an arc gradient) this gradient would exist only over a relatively short distance, so that the mean gradient over the remainder of the channel is not much less than the values stated.

It is clear also that if the gradient is to be reduced, the velocity ratio must change to a smaller value, and this is equivalent to a surge of charge. However as pointed out in a previous section this surge starts to take effect during the last 5% of the traverse or less and the mean potential gradient before this happens is already lower as indicated by the following Table 18.1.7.

Cloud Charge	Height of Leader	Body of Table indicates Mean Potential Gradient at 95% Traverse x 10^5 V/m					
		Values of Velocity Ratio $c = v_2/v_1$					
Q	h	10	20	30	50	70	100
43	6	-0,4	0,2	0,4	0,6	0,7	0,8
43	4	0,1	0,5	0,8	1,0	-	-
71	4	0,6	1,0	1,2	1,3	-	-
168	4	0,5	1,3	1,6	1,9	2,1	-

Table 18.1.7 Mean Potential Gradient along Leader Channel up to 95% of its traverse to ground for varying velocity ratios $c = v_2/v_1$

Comparing Table 18.1.7 with the previous one indicates a considerable change of the potential gradient at the same value of "c". In fact the one case of c = 10 for 43 C at 6 km is negative, indicating that there is a potential rise (numerically) instead of a fall at this value.

108/ .....

It is clear that if the gradient is not permitted, for physical reasons, to increase during the last 5% of traverse, the velocity ratio must be lowered. The following values of ratio change for maintaining a constant potential gradient can be identified from the two above tables and the applicable change in induced charges are also shown.

Cloud Charge Q	Height of Leader h	Mean Potential Gradient $x10^5$ V/m	Value of "c"		Induced Charge Coulombs	
			at 95%	at 100%	95%	100%
43	6	0,6	50	30	1,2	2,2
43	4	1,0	50	25	0,8	2,0
71	4	1,3	50	20	0,4	1,1
168	4	2,1	70	20	2,8	7,2

Table 18.1.8 Table indicating change in velocity ratio to maintain the leader potential gradient constant between 95% and 100% traverse showing also the change in induced charge.

A reduction in the velocity ratio v_2/v_1 would mean of course that if the leader tip velocity v_2 remained constant, the positive tip mean velocity v_1 must increase. Alternatively if v_1 remains unchanged, v_2 must reduce. However the curves have been drawn up on the basis of constant values of velocity ratio which in effect means that the relative extension of the leader channel is accompanied by a proportional extension of the dimension Z_1 or the height of the positive charge area. Hence if the leader extends the last 5% of its traverse, the positive end should extend a relatively larger amount to maintain a constant field gradient.

The sudden increase in charge called for under the above circumstances would be consistant with the probability that the symptoms of a return stroke begin to take effect when the leader tip potential is forced to zero during the last few percent of its traverse to ground - or in other words this signals the start of the breakdown process, and the manner of the change indicates what the return stroke mechanism may consist of. For example an increase in induced charge means a transfer of more electrons to the lower tip thereby creating a larger positive charge at the top end to lower the potential there (numerically) thereby permitting a lower or at least unchanged potential gradient.

That the potential of the leader tip at 95% of its traverse to ground is still quite high is evident from the following Table 18.1.9

109/ .....

Cloud Charge	Height of Leader	Table shows negative potential of leader tip at 95% Traverse $-x10^8$ Volts					
		Values of velocity ratio $c = v_2/v_1$					
Q	h	10	20	30	50	70	100
43	6	3,5	2,1	1,5	1,0	0,8.	0,6
43	4	3,2	1,9	1,4	1,0	-	-
71	4	2,6	1,6	1,2	0,8	-	-
168	4	5,3	3,6	2,8	2,0	1,7	-

Table 18.1.9 The negative value of the potential of the leader tip at 95% traverse for various values of velocity ratio

The above values are of course based upon maintaining a field intensity ahead of the tip of $3x10^6$ V/m and assuming that this could be uniform over the 200 m that represents the last 5% of traverse, the total potential needed over this gap would be $6x10^8$ Volts. None of the above values of course approach near this value except the 168 C case for c = 10 which must therefore by very close to final breakdown.

The Table also illustrates that the magnitude of the cloud charge alone is not necessarily the criterion for breakdown of the last remaining gap to earth for instance the 71 C case compared with the 41 C case.

Having considered the above examples in some detail it would still seem to be an open question as to what are the criteria which determine the total charge lowered by the leader and neutralised by the return stroke, and where the mean level of say 5.C. is to be placed.

In order to explain a multiple stroke flash for example it must be assumed that even if the cloud charge is of unusually high magnitude, the individual stroke charges cannot also be too high, otherwise the number of strokes would be limited, and would tend to be no greater than that of a lesser cloud charge. On the other hand individual stroke charges cannot be regarded as being all of about equal magnitude otherwise there would be no reliable explanation as to the very large divergence in the range of observed peak lightning currents of from 2 to 200 kA.

This argument in itself suggests that there is no direct relationship between the quantity of cloud charge and the charge lowered in the leader and this is further born out by the considerations of the properties of the cylindrical charge dipole whereby there are a large number of variations in cylinder lengths and radii which will produce the same field intensity at the base of the cloud.

However variations in the dimensions of the charge give rise to variations in the initial potential at the base of the cloud even for the same charge magnitude and field intensity, and it is therefore reasonable to suggest that it is this potential which will mainly determine the leader parameters, up to a point at least. Thereafter it should be the limitations imposed upon the leader as to the potential gradient developed along its length and the velocity of the respective streamers at its extremities which will specifically determine the charge.

110/ ....

If for example the mean potential gradient along 95% of the leader traverse was fixed at a value of say $1x10^5$ V/m the following Table 18.1.10 illustrates the conditions that would be applicable to the four examples cited:

Cloud Charge Q	Height of Leader h	Velocity Ratio c	Charge-Coulombs	
			Induced	Total
43	6	> 100	0,5	3,1
43	4	50	0,8	4,2
71	4	20	1,1	8,1
168	4	< 20	7,2	23,6

Table 18.1.10 Values of charge in leader for a mean potential gradient of $1x10^5$ V/m at 95% of its traverse distance

The effect of a lower allowable potential gradient would be to increase the amount of charge delivered and vice-versa, but the approach appears to be generally in accordance with expectation and in conformity with the properties of an arc.

Having completed a review of the effect of lightning leaders originating from differing cloud source charges it is now possible to speculate on what may be a more precise mechanism of the return stroke.

The most significant feature appears to be the change in conditions called for during the last few percent of the traverse to ground. The potential of the leader tip must be forced to zero and this requires abrupt changes in the potential gradient along the leader, or in its velocity and its radius with corresponding changes in the induced charge on the leader, and these effects are primarily due to the proximity of the mirror image of the leader - or physically as a consequence of the concentration of charge on the earth's surface as the leader tip approaches close to it.

If the potential gradient on the leader does not in fact vary over a wide margin, these changes will result in an increase in the induced charge - that is more electrons will concentrate at the lower end thereby allowing positive charge to accumulate at the cloud end in order to raise the potential at that end. This tends to keep the potential of the leader tip high (numerically) but at some instance the remaining gap to earth suddenly breaks down, and the tip potential is forced to zero.

Again if the potential gradient along the leader cannot increase - and this would be expected of an arc channel - more positive charge still is required at the cloud end of the channel to maintain the correct potential, and this is achieved by a sudden drain of electrons from the channel leaving it more positive. This drain of charge must be in excess of that deposited along the channel since the positive charge at the top end must be increased above the level which it was just prior to breakdown.

The source of the excess electron charge required is obviously the corona envelope which virtually collapses at least partially from the

111/ .....

ground up, and it is evident that this discharge proceeds up the channel at the velocity of the return stroke tip and not at the speed of light otherwise the whole channel would radiate light simultaneously. However since the charge is distributed linearly with more charge towards the lower end it would be expected that the extent of collisions and recombinations of electrons with the positive ions of the core would be greatest at the lower end, trailing off towards the top of the channel.

The electron movement during discharge must initially be radially towards the core and the luminosity should therefore increase as the centre is approached when the electron density becomes sufficiently high. This would account for the much smaller radius observed for the return stroke based as it is upon the visible light output. The concentration of electron flow in the core is also probably assisted by the electromagnetic "pinch" effect which intensifies with increasing magnitude of the current.

The potential drop along the return stroke channel is likely to be of the same order as it was during the preceeding leader, but it will be increased by the inductance of the channel coupled with a high rate of change of current magnitude.

Hence the model of the return stroke discharge which envisages an upward moving channel into which electron discharge takes place into the tip as it advances would appear to be tenable with the exception that a nett positive charge must be left on the channel which increases until it reaches the top of the channel. The amount of this charge is of the order of twice the charge induced in the leader prior to contacting ground, and is not the charge that would be needed to carry zero potential to the cloud end of the channel - an eventuality which has been shown to be inadmissable. This positive charge is likely to be distributed such that more charge is left at the top of the channel than at the bottom and this tends to even out the apparent linear distribution of negative change discharged into the return stroke channel.

In other words the original charge deposited on the leader may be distributed linearly say (or even exponentially) with more charge towards the lower end of the leader. When the return stroke occurs, however, this charge is discharged to earth in the reverse manner, but electrons leave the channel in increasing quantity as the tip progresses upwards thereby adding to the diminishing original charge, and tending therefore to simulate a uniform charge distribution.

19. Continuing Current and Subsequent Strokes

Continuing currents following the return stroke have been observed by other investigators to occur in about 50% of the component strokes of a flash although this was not supported by the present investigation reported in Part I. However it is likely that the short time constant used for the measuring circuit in this investigation effectively attenuated the slow field change which would result, and hence it would not be observed except under esceptional circumstances, that is to say when the continuing current was very severe. This is supported by the fact that the leader slow field change was also not observed in the majority of the present records.

Since the above paragraph was written, Berger (1972) has completed an exhaustive analysis of all his downward lightning flashes at Mt. San Salvatore and he has informed the writer that only a few cases of continuing currents were observed by him in contradiction to the belief

that they occur frequently.

This is now understood since all other investigators have assumed continuing current from evidence of the slow field change which fre= quently follows the fast "R" element field change due to the return stroke proper. According to the mechanism proposed herein, the slower neutralisation of the positive charge left at the top of the lightning channel after the fast electron drain comprising the return stroke would give rise to a slow field change but would not give rise to current flow to ground at the root of the channel.

Berger (1972) also measured the field change close to the tower struck by lightning and found that in the case of a negative stroke (i.e. lowering negative charge) the field excursion was negative taking milliseconds as the leader approached. It then rapidly changed in the positive direction in microseconds corresponding to the drain of neg= ative charge of the main return stroke; the field then overshot until it was actually of positive polarity, and then in a matter of milli= seconds it reverted slowly to zero. A change in polarity of the field was also confirmed by the record of a sensitive 7 mA current circuit.

This observation confirms that the channel is left positively charged after the main return stroke and normally delivers no measurable current to the ground when this state is reached, and it therefore is in full support of the hypothesis herein advanced.

However, continuing currents have been observed in some cases and whatever mechanism is proposed must also allow for this to happen.

According to the mechanism described, the return stroke proper ends with an accumulated positive charge on the top end of the leader, and the field intensity there has been maintained. Accordingly the discharge of the cloud must continue at least whilst there is a con= ducting channel still bridging the space between the high potential cloud and ground.

The process is likely to be controlled by the conductivity of the channel, for so long as this remains high, the potential gradient tends to remain low and current flow will continue. If the conductivity diminishes however such as by the action of wind elongating the channel or the lowering of its temperature, with consequent loss of ionisation, it would be expected that the arc could finally extinguish because the potential required to maintain it is higher than that available at the cloud.

Another factor which would tend to maintain the discharge would be the natural rate of charge generation in the cloud as well as the ten= dency to increase the field intensity due to either upward movement of positive charge at the cloud top, or the accumulation of screening layers of negative charge, as described by Brown et al (1971).

The previous history of the channel should also affect its ability to support continuing current - for example a high current discharge would produce a correspondingly high conducting channel more capable of continuing current than a low current discharge. In the latter case also the general level of charge generation would also be at a minimum mitigating against continuing current.

The positive charge left at the top of the channel after the return stroke could not survive a process of continuing current and would of

113/ .....

returning from its positive excursion to a stable field intensity which was only slightly less that it was prior to the stroke. Surprisingly however, the field intensity prior to the second stroke started build=ing up at least 35 ms before the stroke made contact and this is not at all in conformity with the observation of a fast dart leader for subsequent strokes.

On oscillogram No. 141(a) the initial leader took 38 ms whilst the subsequent one took 16 ms and started out from the moment that the field intensity changed polarity from a positive to a negative value. This change in polarity was not so evident in Oscillogram No. 139, but it undoubtedly occured some 5 to 10 ms after the first stroke.

The important point about the above observations is the much slower build up of the field in preparation for a subsequent stroke than would be thought if the charge was lowered by a dart leader, and in view of the discussion in section 14, the conclusion which seems to be emerging is that the dart leader is another phenomena, similar to the step in the first leader, and that it is not responsible for the lowering of the main charge into the channel, in preparation for a subsequent return stroke.

This evidence of a more gradual build up of charge on the channel fits the hypothesis much better for it is then clear that the channel loses conductivity at the base very soon after the return stroke electron avalanche - so to speak - aided by the excess positive ion charge left at the top end. The discharge between the cloud charge and the top of the channel continues until the positive charge is netrualised, but this portion of the channel is still in a conducting state. If the field intensity at the top is brought back to ionisation level a further burst of ionisation takes place which recharges the channel at about the same rate as it did for the first leader, but being partly conducting steps do not occur until, near the base, at least one is needed to break=down the only feintly conducting channel to earth. The well known observation of Berger (1965) that the rise time of the current in sub=sequent strokes is always less than a microsecond compared with 5 to 20 μs for the first stroke adds further confirmation that this is a phenomena dependent upon the breakdown characteristics of the last 100 m or so of the channel path to earth - and it fits the hypothesis of a fast dart leader occuring at the moment of final breakdown of the channel for subsequent strokes.

In view of the above it appears to be highly probable that sub=sequent strokes are entirely dependent upon agencies outside the dis=charge mechanism - for which there is some other considerable support=ing evidence.

Firstly, although the charge separation process has been gauged to be far too slow to produce enough charge in the period required to support a multiple stroke discharge, it does at least act towards doing this. It may well be also that the effect of the generation of opposing screening charges suggested by Brown et al (1971) may mask the rate of charge generation in the cloud as well so that external field measure=ments may produce far too low an estimate of what is happening within the charge separation area.

Secondly the cylindrical model shows that under symmetrical con=ditions at least, if the field intensity at the lower end of the charged cylinder reaches ionisation, that at the upper extremity does so also - or very nearly so. At this altitude the conductivity of the

air is also higher and so the level for ionisation and breakdown lower, so that it is quite probable that ionisation does in fact occur simul= taneously with that of the start of a downward leader at the base. This being so fast positive ions are created which may be expelled up= wards by the electric field of the dipole, and this would tend to en= hance the field intensity at the base of the charge - thus adding to the effect in the same way as additional charge generation. In a similar fashion, fast negative ions drawn in downwards from the upper atmosphere would have an exactly similar enhancing effect upon the field at the base of the charge.

Free positive ions released into the upper atmosphere would of course constitute one source of charge to maintain the fair weather positive field throughout the globe. However the possibility of re= combination of the cloud top charge with free negative ions cannot be overlooked. This would still have the effect of leaving a nett positive charge in the upper atmosphere as if the positive ions had escaped, and it would also still enhance the field intensity below to promote multiple discharges.

Re-combination, unless occuring in a diffusion process would pro= duce light smission which would surely be visible during a lightning-discharge to ground. Procter (1971) has later communicated having ob= served VAF echoes from the top of a cloud which were apparently quite unconnected with those coming from discharges taking place lower down - and this could be due to the effects described above. Proctor in fact should be able to finally confirm or deny much of the phenomena occuring within a cloud which in this thesis has been advanced as hypo= theses only, based upon many observations on lightning.

Finally the effect of free positive ions in the atmosphere below the cloud has also not been taken any account of. Apart from the free ion content of the air, there must be a considerable volume of positive space charge evolved from the earth - particularly from sharp points, protruding structures, mountain ridges and trees to name but a few. The movement of this charge towards the base of the charged dipole must again enhance the field intensity in favour of promoting another dis= charge.

All these factors added together could possibly make up for the short fall evident from the rate of charge generation and promote sub= sequent strokes of a flash - and the time intervals between them would depend upon the collective rate of this activity. Severe charge generation on a large scale would then tend to promote more strokes and short time intervals whereas less active centres would produce less and possibly may not be sufficient to support more than one discharge. This is also a common visual impression of storm activity in the tropics.

An explanation is still needed as to why the charge dissipated to ground in subsequent strokes is less than that during the first stroke. Ulman (1969) quotes various sources as 20% whereas in Part I a value of 70% was deduced from field change measurements. Berger (1972) con= firms that the charge is less for subsequent strokes but the proportion has not yet been evaluated.

One obvious reason is that the first stroke has numerous branches whilst subsequent strokes have not. Also the cloud potential has fallen due to prior discharges. It may well be that the charge on subsequent strokes is due primarily to the induced charge as a consequence of a

116/ .....

final break in the channel at the ground end and this does not constitute more than a coulomb judged from the numerical calculations carried out earlier. This would also tend to explain why in fact there are no branches for subsequent strokes, since charge could only be induced on that part of the channel which has a reasonable conductivity. If the low conductivity at the root of the channel is lost, despite its initial history of very high ionisation, this would apply even more so to the branches which merely dissipated the original charge deposited on them and could not be involved in continuing current to maintain their ionisation.

The explanation for the fast dart leader discussed in section 14 must therefore constitute a secondary breakdown process, similar to that of the stepped dart leader, which occurs just prior to or coincident with the breakdown of the lower portion of the ionised channel to earth.

The sequence of events described herein may now be roughly depicted on Fig. 19.0.1, omitting, however, the intrusion of screening charges. Briefly recapping the process the following is the sequence.

(a) The field intensity at the base C of bound negative charge Q_1 reaches ionisation level and spark streamers start to form having positive and negative tips which advance upwards and downwards along the field direction in general.

(b) By the time the cloud base has been reached some 20 ms or so later, a positive induced charge q_i is firmly established in the network of positive tipped streamers and a negative charge q_1 has been moved from the bound charge and deposited on the leader and branches including the negative counterpart of the induced charge q_i, the total charge deposited being algebriacally (q_1-q_i)

(c) The leader reaches ground with less branching perhaps after about 30 ms and the return stroke begins.

(d) A rapid discharge of the deposited negative charge begins including however an additional negative charge q_r leaving the return stroke streamer more positive towards the top.

(e) After about 100 μs or more all negative charge on the leader and branches is discharged and the luminous streamer reaches the cloud adding a positive charge q_r to the induced charge q_i, and the field intensity between channel and cloud charge is suddenly intensified.

(f) The field intensity between the positive tipped streamers at the top of the channel and the remaining negative charge $Q_2 = Q_1-q_1$ in the cloud has been intensified and further streamer development then occurs releasing more negative charge which dissipates the positive charge (q_1+q_r) left on the channel top. This might take 10-20 ms or more. Meantime if the root of the channel at ground level maintains a high enough conductivity, more charge is dissipated from the cloud in the form of contuing current to ground which may last up to 100 ms or so. If however the conductivity of the base of the channel is reduced to a low value until the current to ground ceases, the discharge only continues at the top of the channel until most of the positive charge is dissipated and the process stops because the field intensity falls below ionisation. The conducting part of the channel will however acquire an induced charge of both signs.

117/ .....

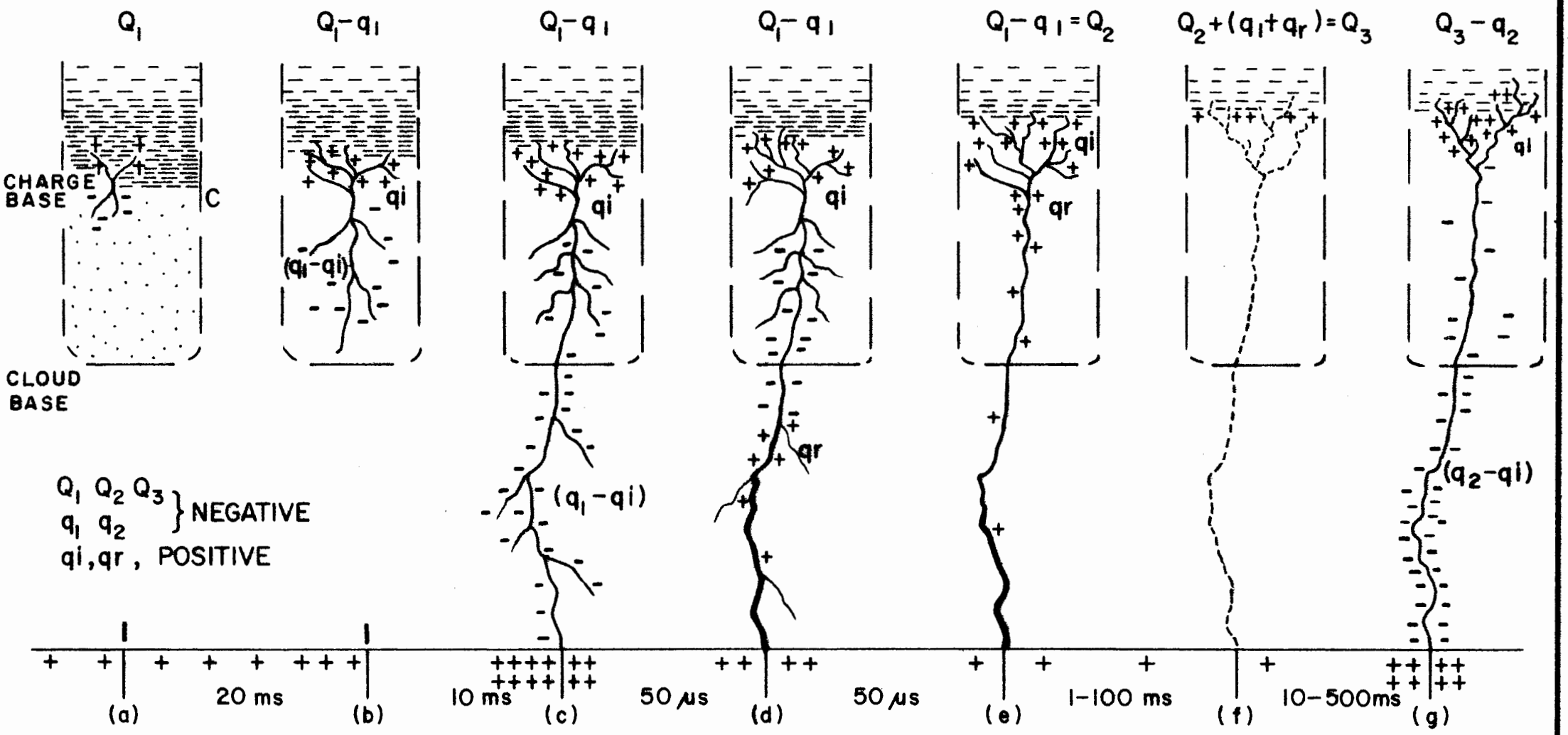

FIGURE 19·0·1

MODIFIED SEQUENCE OF EVENTS OF A GROUND DISCHARGE

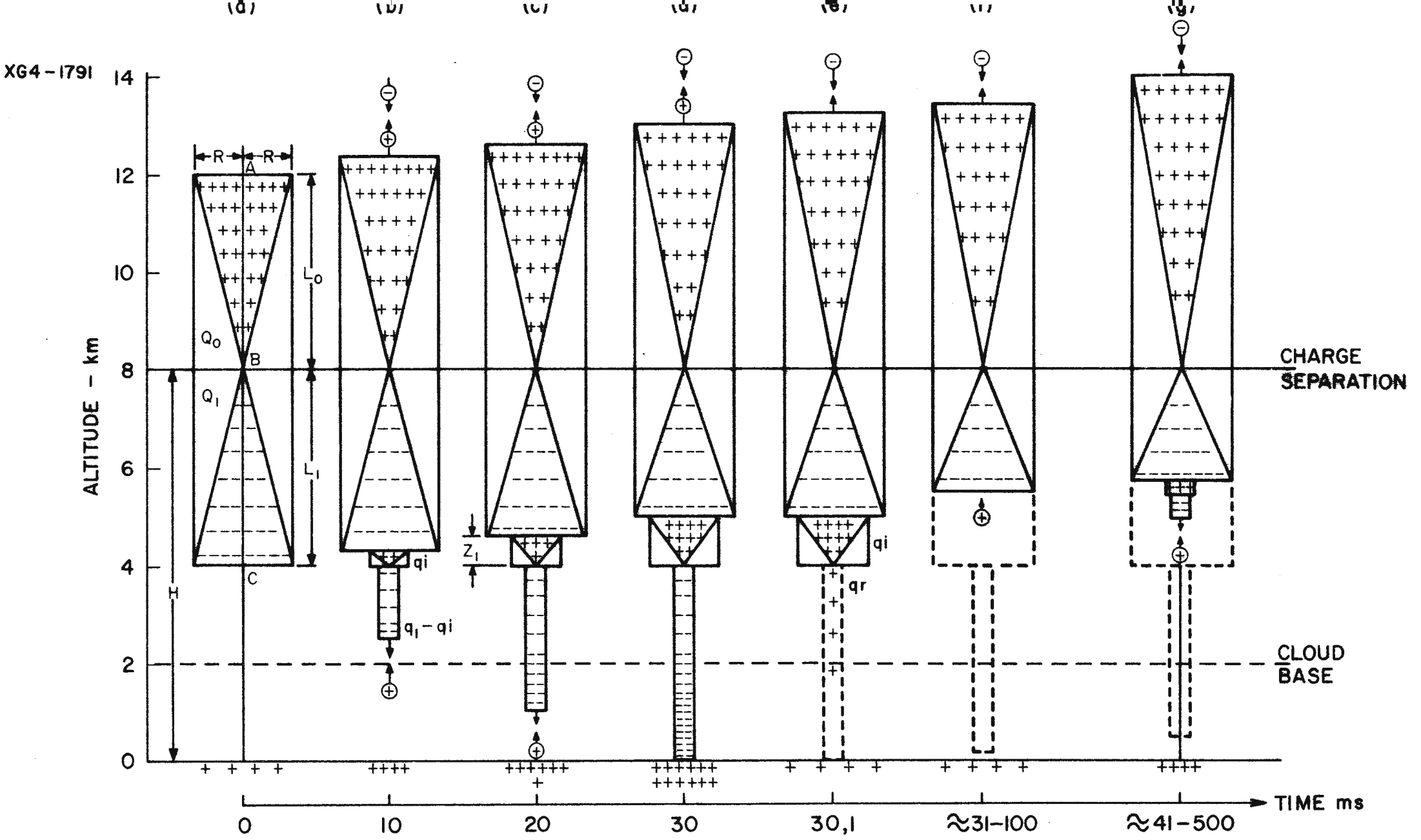

FIGURE 19 · 0 · 2 *DIAGRAMATIC MODEL OF LIGHTNING STROKE TO GROUND*

(g) If the field intensity at the top of the channel is again increased to ionisation a burst of charge resulting in the dart leader will deposit more charge in the channel and once again bridge the gap to earth for a subsequent stroke. This process can continue many times depending upon the rate of charge generation and charge dissipation external to the cloud being sufficiently high to allow the field intensity at the channel top to be repeatedly raised to ionisation level.

A diagramatic representation of the same sequence of events is shown on Fig. 19.0.2 which in this case illustrates the effect of screening charge drawn from the surrounding clear air. It also shows the possibility of the upward movement of the main upper positive charge with possible dissipation in the screening layers at the cloud top. The influence of positive charge in the air below the cloud also is illustrated.

20. The effect of polarity change

Whilst the electrostatic model of the lightning discharge enumerated herein should be unchanged whether the lower cloud charge is negative or positive, distinct differences have been noted by many investigators in the propagation of the spark discharge, and of corona with differing polarities but reasons for this do not appear to have been clearly explained physically.

Positively tipped streamers appear to have considerably less difficulty negotiating spark gaps, as a consequence of which the breakdown potential for positive point-negative plane gaps is very much less than when the point is negative. Also positive corona streamers are long and continuous whereas negative corona is confined and pulsating.

Berger (1967) on the other hand noted that streamers leaving the top of negative towers were able to propagate amazingly long distances towards the cloud compared with the short streamers from positive towers in contradiction to experience with long spark gaps. He also found that no case of multiple positive discharge of lightning took place in his investigation over 18 years or so. In this investigation, reported in Part I, there was conclusive evidence that the probability of a positive multiple stroke discharge was considerably less than for the negative strokes which were by far the more frequent.

In the proposed mechanism for negative discharges propounded in this thesis, the affected portions would be as follows:

When the cloud charge is negative the propagation of positive streamers into it is by means of ionisation by field intensification as the tip ions get closer to the charged water drops. At the other end, namely the downward leader, propagation proceeds as a consequence of ionisation both by field intensification as well as collision, and there is no charge ahead of the tip. If this process is reversed it follows that the velocity of negatively tipped streamers advancing into a positively charged cloud will be faster and the velocity of the positive leader slower since the latter must rely upon a sufficient charge concentration to ionise the air ahead of it and thereby advance. Hence the velocity ratio $c = v_2/v_1$ (i.e. leader to cloud streamer velocity) will be considerably reduced, and according to the model developed this will result in more charge being deposited on the positive leader compared with the negative case. This was indeed observed by Berger (1967)

and confirmed by his 1972 analysis - in fact the median charge de= posited was seven to ten times greater for positive leaders. This would also be one good reason why positive discharges do not produce many multiple strokes, since there would simply not be enough charge to support too many consecutive strokes.

On the other hand a negative cloud top is likely to be more ammenable to ionisation and dissipation of the charge, but in all likelihood the usual bipolar cloud structure does not exist in this case of a positive discharge to earth. It is more probable that either the positive charge is isolated or the negative charge origi= nally beneath it has been dissipated by previous ground strokes.

At ground level, on the other hand, a concentration of negative charge as opposed to positive would facilitate ionisation of the air above the surface and particularly at the top of a tall tower, and it is not difficult to understand how a self propegating upward leader can develop having in mind the powerful ionisation capability of nega= tive streamers once started. Why the reverse should be true for the laboratory point-plane gap is probably due to the relative proximity of the plane whereby the image charge is able to exert influence upon the field intensity at both anode and cathode.

Then looking at the make up of the leader channel itself, the position of ions and electrons is reversed in the corona sheath, positive ions being in the outer shell. Firstly the corona losses should be at least twice as high as the negative case - as observed for conductors, presumably because positive ions tend to propagate into the surrounding space, whereas electrons tend to attach themselves to heavy molecules and do not escape beyond the ionisation field boundary. In the case of the positive leader therefore the charge lowered to meet corona losses should not be negligible as assumed for the negative leader in Section 15.

The propagation of a positive leader, should follow the same pattern as that proposed, except of course that electrons move up the channel towards the cloud. The charge distribution should also be the same - namely more positive ions towards the lower tip than the top. However in the case of the negative tip reaching ground, the electrons were dislodged from the collapsing corona sheath to discharge to ground - in fact over-discharge-to provide a nett positive charge on the return stroke channel.

In the case of the positive discharge however, the electrons are freely available both in the channel core and in the ground and the positive charge is lodged as relatively immobile ions in the outer corona sheath and bound on water drops in the cloud. The resulting recombination process must therefore differ substantially from the negative discharge case in that the electrons may now flow unimpeded to neutralise the positive ion charge without any stopping mechanism. It is most probable therefore that the return stroke takes place at a much higher velocity - though this has never been observed - and that a continuing current is inevitable until all positive charge in the cloud is neutralised. This latter statement is confirmed by every observation of Berger (1972) although the number of cases was only twenty-seven. Fifty percent of these cases had impulse charge ex= ceeding 15 C with 8% exceeding 170 C but the total charge dissipated, that is including continuing current had a median value of 85 C with 5% exceeding 400 C. It was hardly surprising therefore that no multi= ple strokes occurred.

119/ .....

The field changes of the positive discharges reported in Part I did not however exhibit observable continuing current but as previously stated the time constant of the measuring circuit was less than 9 ms and this could therefore have gone undetected. Secondly whilst about 50% of these discharges were single stroke discharges, the remainder were in fact multiple stroke flashes.

21. Field Changes due to lightning

Some aspects of the electrostatic field change which occurs during leaders and return strokes of lightning have already been fully dis= cussed in Section 9 in relation to their respective magnitudes for differing assumptions as to the charge distribution on the leader.

This discussion finally resolved into the present hypothesis whereby the ratio of the two field changes could approach unity for a non-uniform charge distribution on the leader only if a positive charge was virtually raised on the leader during the return stroke - reverting once again to the most common negative leader. This argument applied only to the overall field change at a distance "D" from the stroke which very much exceeded "H" the stroke height.

This present section is therefore now to be limited to a short and perhaps incomplete discourse on the field change occuring during the return stroke only - incomplete because there has been very little experimental work done on the subject of the time resolved field change during the 100 μs or so that this occurs. Secondly since the mechanism of the discharge is somewhat hypothetical and may require further experimental proof, it is desirable at this stage to consider mainly the principles involved.

For this purpose the simplest of cases is first of all outlined and extensions to this are considered afterwards in discussion.

In order to calculate the field change during the return stroke, a model representing the approximate conditions is essential, and the one chosen is in accordance with that set out in Section 18. It is assumed that during the leader process, charge is distributed uniformly over a vertical channel with no branches. Immediately contact is made with the earth, a current "i" begins to flow, and this signals the start of the return stroke. The current channel elongates upwards with a velocity of the order of 10^7 to 10^8 m/s and during this process the charge along the leader is dissipated until on reaching the top of the channel the process stops, continuing currents thereafter being neglected. The surrent carrying portion of the channel is assumed to have no nett quantity of charge, and the calculation of the field change proceeds on this basis. See Fig. 21.0.1

120/ .....

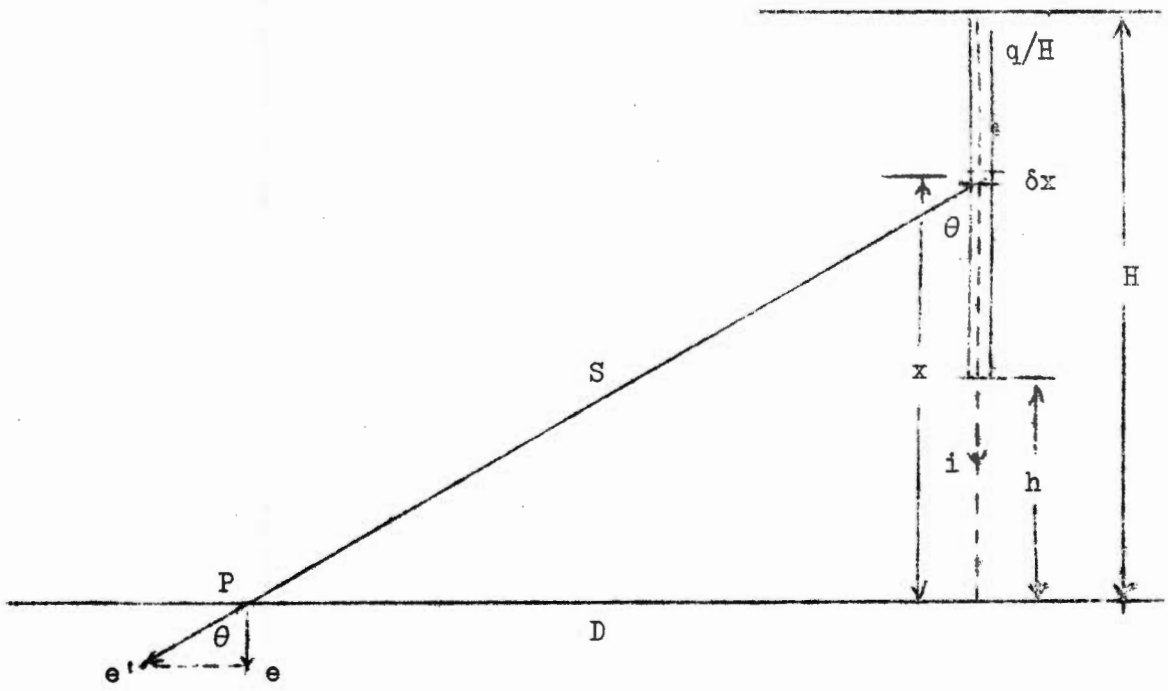

Fig. 21.0.1 Diagram illustrating calculation of the electrostatic field change during the return stroke

The vertical components of the electrostatic field intensity at the point "P" due to the charge in a small element δx is given by $e = e' \cos\theta$, where $\cos\theta = x/S$, $S = (x^2+D^2)^{\frac{1}{2}}$, and $e' = 2q'/4\pi\varepsilon S^2$ and $q' = q/H.\delta x$. Whence the field intensity at P due to all elements between x = h and x = H is

$$E_s = q/2\pi\varepsilon H \cdot \int_h^H x.(x^2+D^2)^{-3/2}.dx \quad \ldots\ldots\ldots\ldots \quad (21.1)$$

This integral resolves into the following:

$$E_s = -q/2\pi\varepsilon H \cdot \quad [1/D - (h^2+D^2)^{-\frac{1}{2}}] \quad V/m \quad \ldots\ldots\ldots \quad (21.1)$$

Now if the lightning current "i" to ground is expressed as a function of time t the charge delivered to ground in a time "t" is:

$$q(t) = \int_0^t i.dt \quad \ldots\ldots\ldots\ldots\ldots\ldots\ldots\ldots\ldots \quad (21.3)$$

and the total charge "q" on the leader is obtained from the same ex= pression putting the limit of "t" at infinity. Hence the height "h" which has been neutralised up to a time t is therefore

$$h(t) = H \cdot \int_0^t \frac{i.dt}{q} = H.F(q,t) \quad \ldots\ldots\ldots\ldots\ldots \quad (21.4)$$

Substituting for "h" in equation (21.2) and re-arranging the terms to indicate the value D/H, the electrostatic field change with respect to time is therefore

121/ .....

$$E_s(t) = -q/2\pi\varepsilon H^2 \cdot \left\{ (D/H)^{-1} - [\, F^2(q,t) + (D/H)^2 \,]^{-\frac{1}{2}} \right\} \text{ V/m} \quad \ldots\ldots\ldots\ldots\ldots\ldots \quad (21.5)$$

It can be shown that when $D/H >> 1$ equation (21.5) reduces to

$$E_s(t) = -qH/4\pi\varepsilon D^3 \cdot F^2(q,t) \quad \text{V/m} \quad \ldots\ldots\ldots\ldots\ldots\ldots \quad (21.6)$$

When t is infinite, $F(q,t) = 1$ whence it is seen that when D is large compared with H the electrostatic field change during the return stroke is half the total field change.

The electromagnetic field changes are, according to Le Jay (1926), related to the electrostatic field change by the following classical statement namely:-

$$E = E_s + E_i + E_r = 1/D^3 \cdot M + 1/cD^2 \cdot dM/dt + 1/c^2 D \cdot d^2M/dt^2 \text{ esu} \quad \ldots\ldots\ldots\ldots\ldots\ldots \quad (21.7)$$

Where M is the charge moment 2QH, and $c = 3 \times 10^8$ m/s.

The analysis in elemental form as calculated by Jordan (1953) gives the following results of the solution of the appropriate Max= well equations for an alternating current element $I \cdot \delta l \cdot \cos\omega t$ located at the origin of a spherical co-ordinate system namely

$$E(\theta) = I\delta l \cdot \sin\theta/4\pi\varepsilon \; [\, \sin \omega t'/\omega r^3 + \cos \omega t'/cr^2 - \omega \sin \omega t'/c^2 r] \quad \ldots\ldots\ldots\ldots\ldots\ldots \quad (21.8)$$

$$\text{and} \quad E_{(r)} = 2I\delta l \cos\theta/4\pi\varepsilon \; [\sin \omega t'/\omega r^3 + \cos \omega t'/cr^2\,] \quad \ldots\ldots\ldots\ldots\ldots\ldots \quad (21.9)$$

$$\text{and} \quad H_{(\phi)} = I\delta l \sin\theta/4\pi[\, \cos \omega t'/r^2 - \omega \sin \omega t'/cr] \quad .. \quad (21.10)$$

Where $t' = t - r/c$ and $c = 3 \times 10^5$ m/s

Hence the three terms of the electric field are identified, with the Le Jay statement, the electrostatic field being proportional to $1/r^3$, the induction field to $1/cr^2$ and the radiation field to $1/c^2 r$; also the induction field is the first derivative of the electrostatic field multiplied by r/c, and the radiation field is likewise obtained from the induction field.

In the case under consideration, namely at the surface of the zero potential plane, the component vector of the electric field is in the vertical direction, and if the electrostatic field change is expressed as a function of time then

122/ .....

$$E_i = S/c.d(E_s)/dt' \text{ and } E_r = S/c.d(E_i)/dt' \quad ..... \quad (21.11)$$

Neglecting for the present the retarded time t'

$$d(E_s) = -q/2\pi\varepsilon H.\ h.dh.\ (h^2+D^2)^{-3/2} \quad ..... \quad (21.12)$$

Whence $d.(E_s)/dt = -q/2\pi\varepsilon H.\ h.\ (h^2+D^2)^{-3/2}\ .dh/dt$ ... (21.13)

From (21.4) $dh/dt = H/q.\ i(t)$ and $S = (h^2+D^2)^{\frac{1}{2}}$

Whence the following statement can be derived namely

$$E_i = S/c.d(E_s)/dt = -1/2\pi\varepsilon cH.F(q,t)i(t).[\ F^2(q,t)+(D/H)^2]^{-1} \quad ..... \quad (21.14)$$

And when $D/H \gg F(q,t) \rightarrow 1$

$$E_i = -H/2\pi\varepsilon cD^2\ [\ F(q,t)i(t)\ ] \quad ..... \quad (21.15)$$

Hence it is seen that the induction field E_i is proportional to the current in the channel and to $1/D^2$ as expected.

In an exactly similar manner the radiation field E_r is determined by differentiating the expression for $E_i(t)$

$$\text{Hence } E_r(t) = -1/2\pi\varepsilon c^2.\ [F^2(q,t)+(D/H)^2\ ]^{-\frac{1}{2}}\left\{ F(q,t)di/dt + i^2(t)/q.\left[[1-2F^2(q,t)\ [F^2(q,t)+(D/H)^2\ ]^{-1}\right]\right\} \quad ..... \quad (21.16)$$

And when $D/H \gg F(q,t) \rightarrow 1$

$$E_r(t) = -H/2\pi\varepsilon c^2 D.\left\{F(q,t)di/dt + i^2(t)/q.\right\} \quad .... \quad (21.17)$$

Whilst the radiation field conforms in all respects to the accepted requirement that it is proportional to di/dt and to 1/D it also contains an unusual term proportional to the square of the current. In the event therefore of very high rates of rise of current, coincident with the peak value as observed by Berger (1967) for the first stroke of a lightning flash, the radiation field intensity could be a more predominant factor than previously thought possible.

To take account of the retarded time for propagation between the lightning channel and the point of observation it is evident that if an incident occurs at a time t, then a small increment of time represented by (S-D)/c passes before any change takes place at a position

123/ .....

which is distant D away from the base of the channel and S away from the location of the change.

Hence $t' = t + (S-D)/c$ Where $S = H[F^2(q,t)+(D/H)^2]^{\frac{1}{2}}$

So $\delta t' = \delta t + \delta S/c$

Where $\delta S/c$ can be shown to be $4h.\delta h/c(D^2+h^2)^{\frac{1}{2}}$

Hence $\delta t/\delta t' = \left\{1+4H/qc.F(q,t)i(t).[F^2(q,t)+(D/H)^2]^{-\frac{1}{2}}\right\}^{-1}$ ..... (21.18)

The fact that $\delta t/\delta t'$ is shown as a function of the current in the stroke is merely incidental to the geometry for the calculation of "h".

Hence if on a computation program the value of $d(E_s)/dt$ is calculated for a small increment of time δt, it is multiplied by the above fraction to obtain the value $d(E_s)/dt'$ and the function representing the particular field change can be computed in terms of the time at the point of observation

As a check on the above results the electromagnetic field may be calculated directly referring to Fig. 21.0.2 as follows:

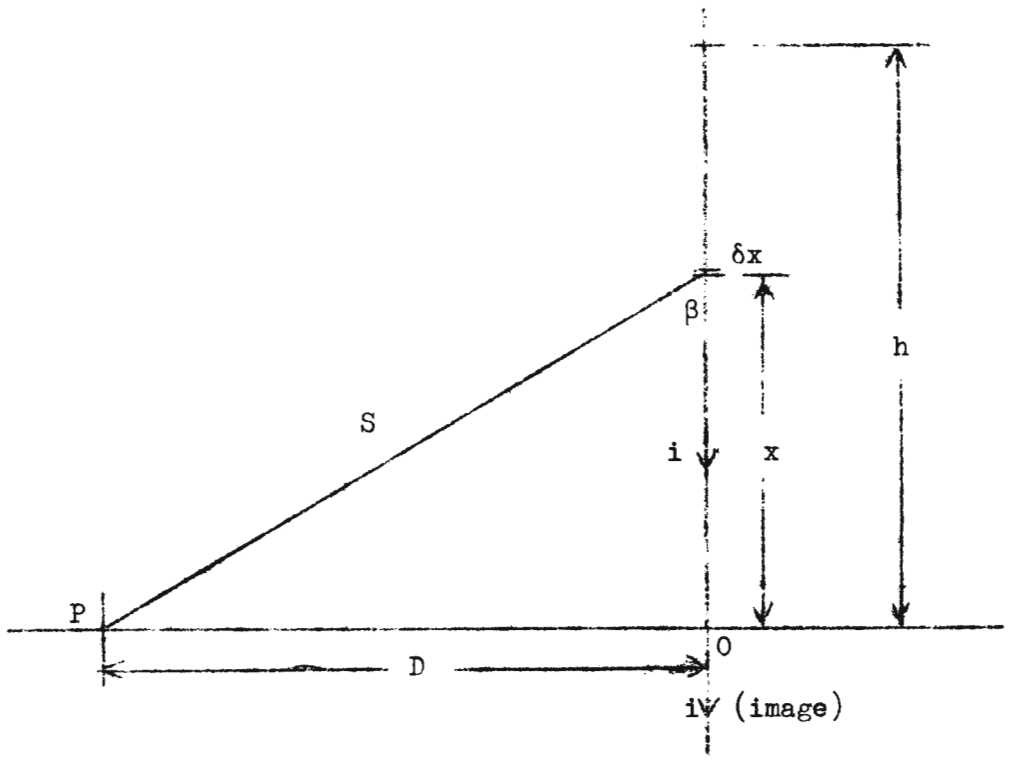

Fig. 21.0.2 Diagrammatic representation of lightning current flowing in a section of lightning channel of length h.

The increment of the magnetic field intensity at P due to the current "i" flowing in the small element δx of the channel, is then

$$\delta \mathcal{H} = 2i(h)\delta x.\mathrm{Sin}\beta/4\pi S^2 \quad \ldots\ldots\ldots\ldots\ldots\ldots \quad (21.19)$$

Where $\mathrm{Sin}\beta = D/S$ and $S = (x^2+D^2)^{\frac{1}{2}}$

Hence the field intensity at P due to current in the whole length of channel of height "h" is the

$$\mathcal{H}(h) = i(h)D/2\pi \cdot \int_0^h (x^2+D^2)^{-3/2}\, dx \quad \ldots\ldots\ldots \quad (21.20)$$

Hence $\mathcal{H}(h) = i(h)/2\pi D \cdot h(h^2+D^2)^{-\frac{1}{2}}$ $\ldots\ldots\ldots\ldots\ldots$ (21.21)

Now according to the assumptions made for Fig. 21.0.1 "h" is a function of time and from (21.4) $h(t) = H.F(q,t)$ as defined, and substituting this in (21.21) the following expression is derived namely:

$$\mathcal{H}(t) = 1/2\pi D \cdot F(q,t).i(t)\ [\ F^2(q,t) + (D/H)^2\ ]^{-\frac{1}{2}}$$

$\ldots\ldots\ldots\ldots\ldots$ (21.22)

The flux density as a function of time at the point P is then $B = \mu_o \mathcal{H}$ and the vertical electromagnetic field intensity is - Bc V/m where "c" is the velocity of light. Hence making these subsitutions in (21.22), the induction field intensity as a function of time is then given by the expression namely:-

$$E_i(t) = -\ \mu_o c/2\pi D \cdot F(q,t).i(t).\ [F^2(q,t) + (D/H)^2]^{-\frac{1}{2}}$$

$\ldots\ldots\ldots\ldots\ldots$ (21.23)

Putting $\mu_o c = 1/\varepsilon c$

$$E_i(t) = -1/2\pi\varepsilon c D \cdot F(q,t).i(t).[\ F^2(q,t) + (D/H)^2\ ]^{-\frac{1}{2}}\ \mathrm{V/m}$$

$\ldots\ldots\ldots\ldots\ldots$ (21.24)

It is of more than passing interest to note that the above con= version from electromagnetic units to electric units of V/m is equi= valent to the assumption that the electromagnetic field radiates from the lightning channel at the velocity of light, and that the electric field intensity at any given point is found by assuming that the flux cuts a vertical conductor at that point producing a potential gradient along this conductor numerically equal to the field intensity.

Whilst equation (21.24) is not identical in form to equation (21.14) derived from the differentiation of the electrostatic field intensity, both expressions converge to the same value when $D/H \gg F(q,t) \rightarrow 1$. This is because neither expression takes account of

125/ .....

the retardation in time due to propagation at the velocity of light which becomes more prominant at points close to the lightning channel.

If now the radiation field is derived by differentiating equation (21.24) as was the previous procedure the following expression results namely:-

$$E_r(t) = -H/2\pi\varepsilon c^2 D \cdot \left\{ F(q,t) \cdot di/dt + i^2(t)/q \cdot (D/H)^2 \cdot [F^2(q,t)+(D/H)^2]^{-1} \right\} V/m \quad \ldots\ldots\ldots\ldots\ldots \quad (21.25)$$

And when $D/H \gg F(q,t) \rightarrow 1$ this resolves to

$$E_r(t) = H/2\pi\varepsilon c^2 D \cdot [F(q,t).di/dt + i^2(t)/q] \ V/m \ .. \ (21.26)$$

Once again the expression (21.25) is not quite identical to equation (21.16) but (21.26) is the same as (21.17). Both approaches include the term $i^2(t)/q$ which adds a component of field intensity directly to the di/dt term.

It may be concluded from the above comparisons that the two approaches to the problem of the calculations of the three components of the total electric field are compatable and should lead to the same result if the retardation time is taken into account.

Now for a distribution of charge which is linear instead of be= ing uniform the charge distribution per unit length is given by the expression namely:

$$q' = 2q/H \cdot (1-x/H) \text{ coulombs/m} \quad \ldots\ldots\ldots\ldots\ldots \quad (21.27)$$

For a given lightning current wave form i(t) the height of channel neutralised at any instant of time is then given by

$$h(t) = H \left\{ 1- [1-F(q,t)]^{\frac{1}{2}} \right\} = H\, G(q,t) \quad (21.28)$$

Whence $F(q,t) = 1/q \int_0^t idt$ as given by equation (21.4)

The electrostatic field change with time is then calculated in an exactly similar manner as outlined in detail for the uniform charge distribution case given above with the results which follow namely

$$E_s(t) = -q/\pi\varepsilon H^2 \cdot \left\{ (D/H)^{-1} - [1-G(q,t)] \, [G^2(q,t)+(D/H)^2]^{-\frac{1}{2}} - \text{Sinh}^{-1} [G(q,t).(D/H)^{-1}] \right\} \quad \ldots\ldots\ldots\ldots\ldots \quad (21.29)$$

And when $D/H \gg G'(q,t) \rightarrow 1$

126/ .....

$$E_s(t) = -qH/2\pi\varepsilon D^3 \cdot G^2(q,t)\ [1-2/3\ G(q,t)] \ldots\ldots \quad (21.30)$$

Comparing (21.30) with the uniform charge distribution case (21.6) it is seen that the overall field change when $t = \infty$ and $F(q,t)$ and $G(q,t)$ are unity, the linear field change is 2/3rd that of the uniform field change for the same value of charge q, H ε D. This fits in with previous calculations that showed that when the charge distribution was uniform, the return stroke field change was one half of the total field change, that is including that during the leader, whereas when the charge was distributed linearly, the return stroke field change was only 1/3rd that of the total.

Then continuing with the derivation of the electromagnetic field change as before the expression obtained is as follows namely:

$$E_i(t) = -1/2\pi\varepsilon cH \cdot G(q,t)\cdot i(t).\left[\ G^2(q,t) + (D/H)^2\ \right]^{-1}$$

$$\ldots\ldots\ldots\ldots\ldots \quad (21.31)$$

And when $D/H \gg G(q,t) \rightarrow 1$

$$E_i(t) = -H/2\pi\varepsilon cD^2 \cdot G(q,t)i(t) \quad \ldots\ldots\ldots\ldots\ldots \quad (21.32)$$

This expression is exactly analogous to the uniform distribution case equation (21.15) with $G(q,t)$ replacing $F(q,t)$.

Similarly the radiation field component is derived as before giving the result as follows namely:-

$$E_r(t) = -1/2\pi\varepsilon c^2 \cdot \left[G^2(q,t) + (D/H)^2\right]^{-\frac{1}{2}} \Bigg\{ G(q,t).di/dt$$

$$+1/2\ .i^2(t)/q.\ [\ 1-F(q,t)\ ]^{-\frac{1}{2}} \left[1-3G^2(q,t)\cdot\right.$$

$$\left.\left[\left[G^2(q,t) + (D/H)^2\ \right]^{-1}\ \right]\right\} \ldots\ldots\ldots\ldots\ldots \quad (21.33)$$

Again when $D/H \gg G(q,t) \rightarrow 1$

$$E_r(t) = -H/2\pi\varepsilon c^2 D \cdot \left\{ G(q,t)\cdot di/dt + 1/2\cdot i^2(t)/q.\ [1-F(q,t)]^{-\frac{1}{2}} \right\}$$

$$\ldots\ldots\ldots\ldots\ldots \quad (21.34)$$

The radiation field in this case differs slightly from the uni= form change case in that it contains the term

$$[1-F(q,t)]^{-\frac{1}{2}}$$

which approaches infinity when $F(q,t) \rightarrow 1$. However this is counter

balanced by $i^2(t) \rightarrow 0$.

Finally the case for an exponential charge distribution can be handled by a computer incremental program in the following manner.

If the charge distribution per unit length is expressed in the form

$$q' = q/kH \cdot [\exp.(-x/H)] \quad C/m \quad \ldots\ldots\ldots\ldots\ldots\ldots \quad (21.35)$$

Where $k = (e-1)/e$, "e" being the base of the Naperian logarithm.

Then the charge $q(h)$ dissipated from a length h of channel is

$$q(h) = q/k \cdot [1-\exp(-h/H)] = q(t) \quad \ldots\ldots\ldots\ldots \quad (21.36)$$

Where $q(t)$ is the charge dissipated in a time "t" corresponding to the height "h"

Then from (21.36)

$$1-\exp(-h/H) = kq(t)/q = kF(q,t) \quad \ldots\ldots\ldots\ldots\ldots\ldots \quad (21.37)$$

Hence by taking logarithms the relationship connecting the value of h with time is derived namely that:

$$h(t) = -H \ln. [1-kF(q,t)] \quad \ldots\ldots\ldots\ldots\ldots\ldots\ldots \quad (21.38)$$

Whence $dh/dt = Hk\, i(t)/q\, [1-kF(q,t)]$ $\ldots\ldots\ldots\ldots\ldots\ldots$ (21.39)

For a small change in h of δh, the change in charge δq is given by

$\delta q = \delta h \cdot q'$ and from (21.35) with $x = h$

$$\delta q = q\delta h/kH \cdot \exp(-h/H) \quad \ldots\ldots\ldots\ldots\ldots\ldots\ldots \quad (21.40)$$

The resulting change in electrostatic field (referring to Fig. 21.0.1) is then

$$\delta(E_s) = -\delta q.h/2\pi\varepsilon S^3 \quad \text{Where } S = (h^2+D^2)^{\frac{1}{2}} \quad \ldots\ldots\ldots \quad (21.41)$$

and substituting for δq. and dividing both sides by δt.

128/ .....

$$\delta(E_s)/dt = -q/2\pi\varepsilon H.h \exp(-h/H)/kS^3 \cdot dh/dt \quad ..... \quad (21.42)$$

The electromagnetic induction field is then given by $E_i(t) = S/C.d(E_s)/dt$ whence

$$E_i(t) = -1/2\pi\varepsilon c \cdot h.\exp(-h/H\ i(t)/(h^2+D^2)\,[1-kF(q,t)]$$

$$..... \quad (21.43)$$

Where h(t) is given by equation (21.38)

Now to account for the retardation time for propagation as before

$$\delta t' = \delta t + \delta S/c \text{ where } \delta S = 4h.\delta h.(h^2+D^2)^{-\frac{1}{2}}$$

and δh is found from (21.39) whence substituting these values

$$\delta t/\delta t' = \left\{ 1+4Hk/cq \cdot h.i(t)/(h^2+D^2)^{\frac{1}{2}} \ [1-kF(q,t)] \right\}^{-1}$$

$$..... \quad (21.44)$$

Hence given a current wave form i(t), the charge q is calculated by integration and then starting with a small interval of time δt, the increments δq and δh can be found, and the increment $\delta t'$ for a chosen value of D and H.

A numerical calculation was carried out of the total electric field assuming a current wave approximating to the observations of Berger, a typical example of which is illustrated in Fig. 21.0.3.

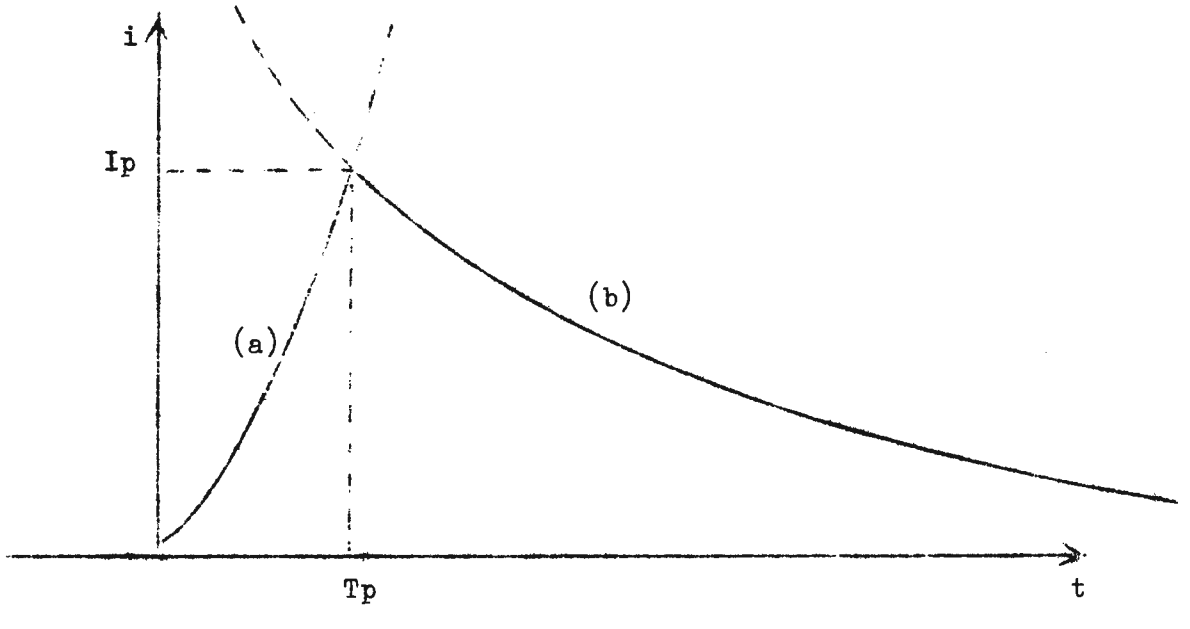

Fig. 21.0.3 Typical current waveform for first strokes approximating those observed by Berger

129/ .....

Disregarding pulsations which were observed at the wave peak, the waveforms consisted of two parts namely:

(a) For $t = 0$ to $t = T_p$ $\quad i = I_p \alpha \exp(\beta t/T_p)$ .... (21.45)

and (b) For $t = T_p$ to $t = \infty$ $\quad i = I_p \exp\left[-(t-T_p)/T\right]$ ... (21.46)

Mean values derived for the constants were $\alpha = 4 \times 10^{-2}$ and $\beta = 3{,}22$ and $\alpha e^{\beta} = 1$. Typical values of T_p lay between 8 and 25 µs with a mean value of 13 µs and for T between 50 and 150 µs with a mean value of 105 µs.

For the purpose of calculation of the electric fields the following values were assumed:-

$H = 4$ km

$T_p = 10$ µs

$T = 100$ µs

$I_p = -20$ kA

$q = -2{,}06$ C

The computer program was written by Miss A. van Wyk de Vries of the Numerical Analysis Division and allowed for the computation and plotting of the total electric field change for the three cases of assumed uniform, linear and exponential charge distributions, including the effect of propagation time, and these are shown in the three pairs of curves from Fig. 21.0.4 to Fig. 21.0.9.

The curves were plotted against a normalised value of E which must be multiplied by the scale factor shown on the right hand side of the graph. This provided a simple means to compare the actual wave form and from which it is clear that the electromagnetic field starts to exert influence at fairly close ranges and overtakes the effect of the electrostatic field at the following distances from the lightning stroke.

Uniform Charge Distribution < 20 km

Linear Charge Distribution < 20 km

Exponential Charge Distribution < 40 km

According to Malan (1963) the two field intensities were observed to be about equal at about 25 km, and on the above evidence this would again suggest that the distribution of charge was at least linear.

However the above data does not include the effect of a positive charge being induced on the return stroke channel as it progresses upwards as proposed in Section 18. This would have the effect of evening out the charge distribution towards a more uniform distribution if it was linear in the first place, and hence the tendency would be for an earlier intrusion of the electromagnetic field.

130/ .....

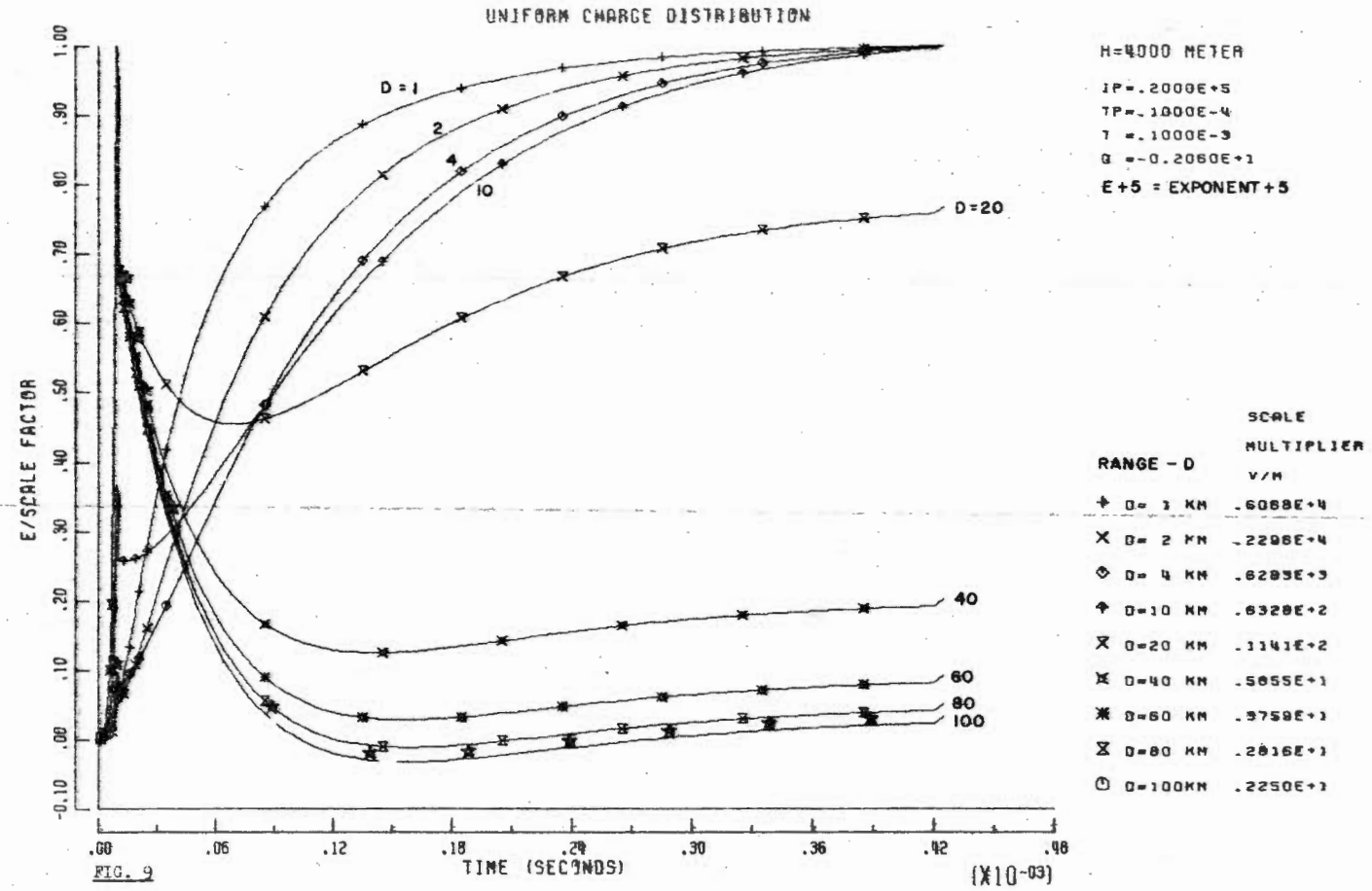

FIG. 9

FIGURE 21·0·4

TOTAL ELECTRIC FIELD DURING RETURN STROKE (480 μs)

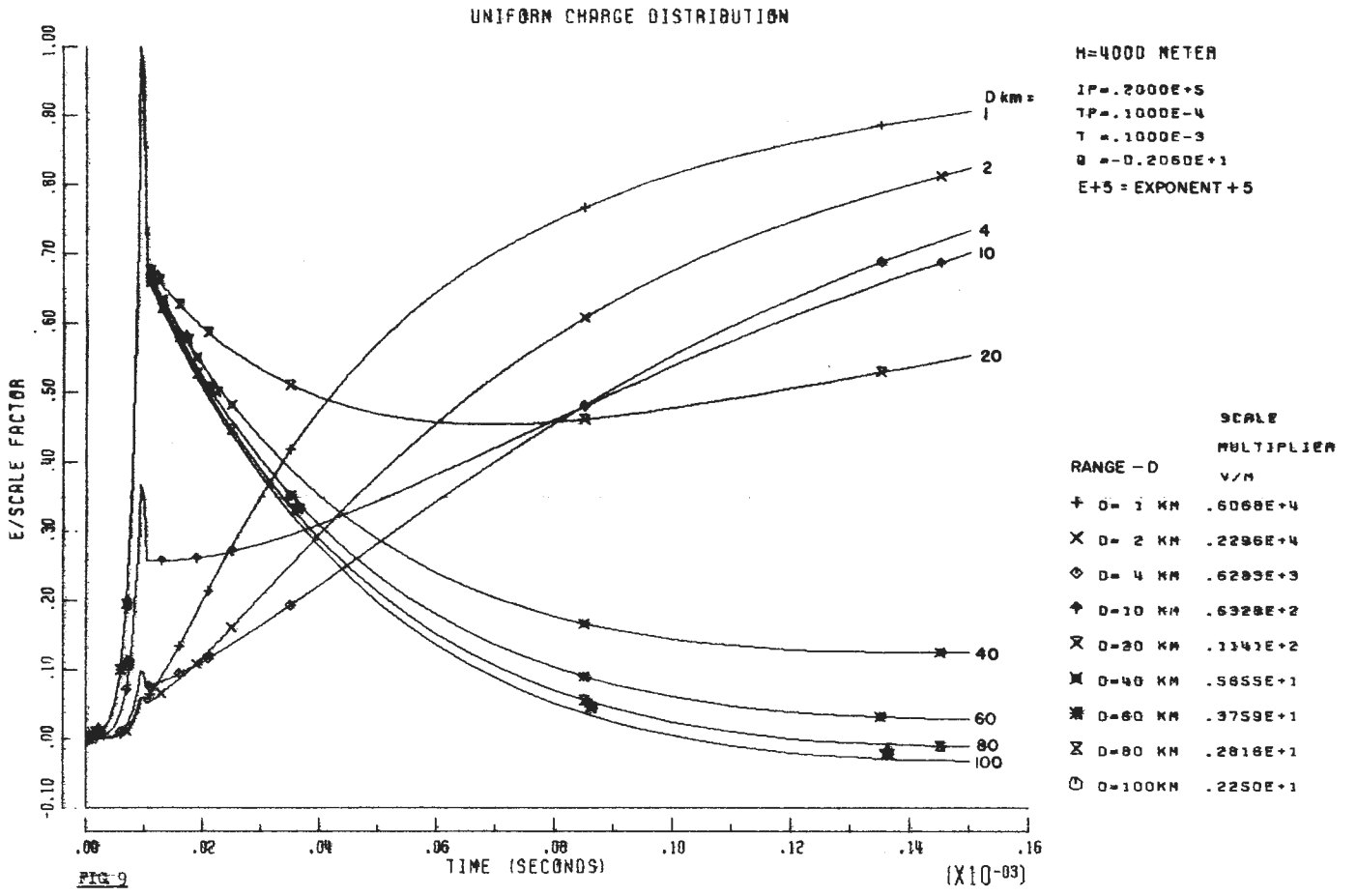

FIGURE 21·0·5

TOTAL ELECTRIC FIELD CHARGE DURING RETURN STROKE (160 μs)

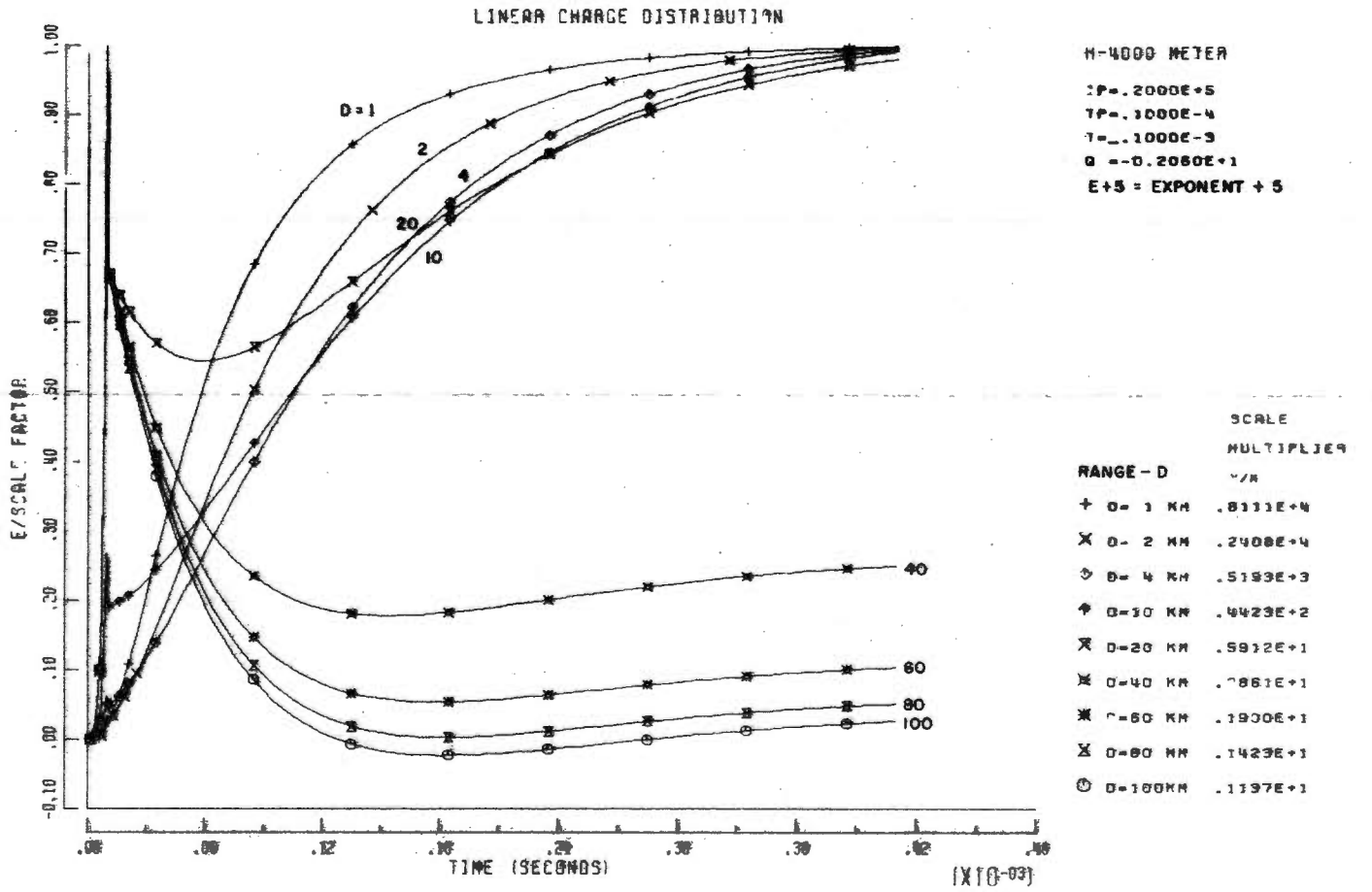

FIGURE 21·0·6

TOTAL ELECTRIC FIELD CHARGE DURING RETURN STROKE (480 μs)

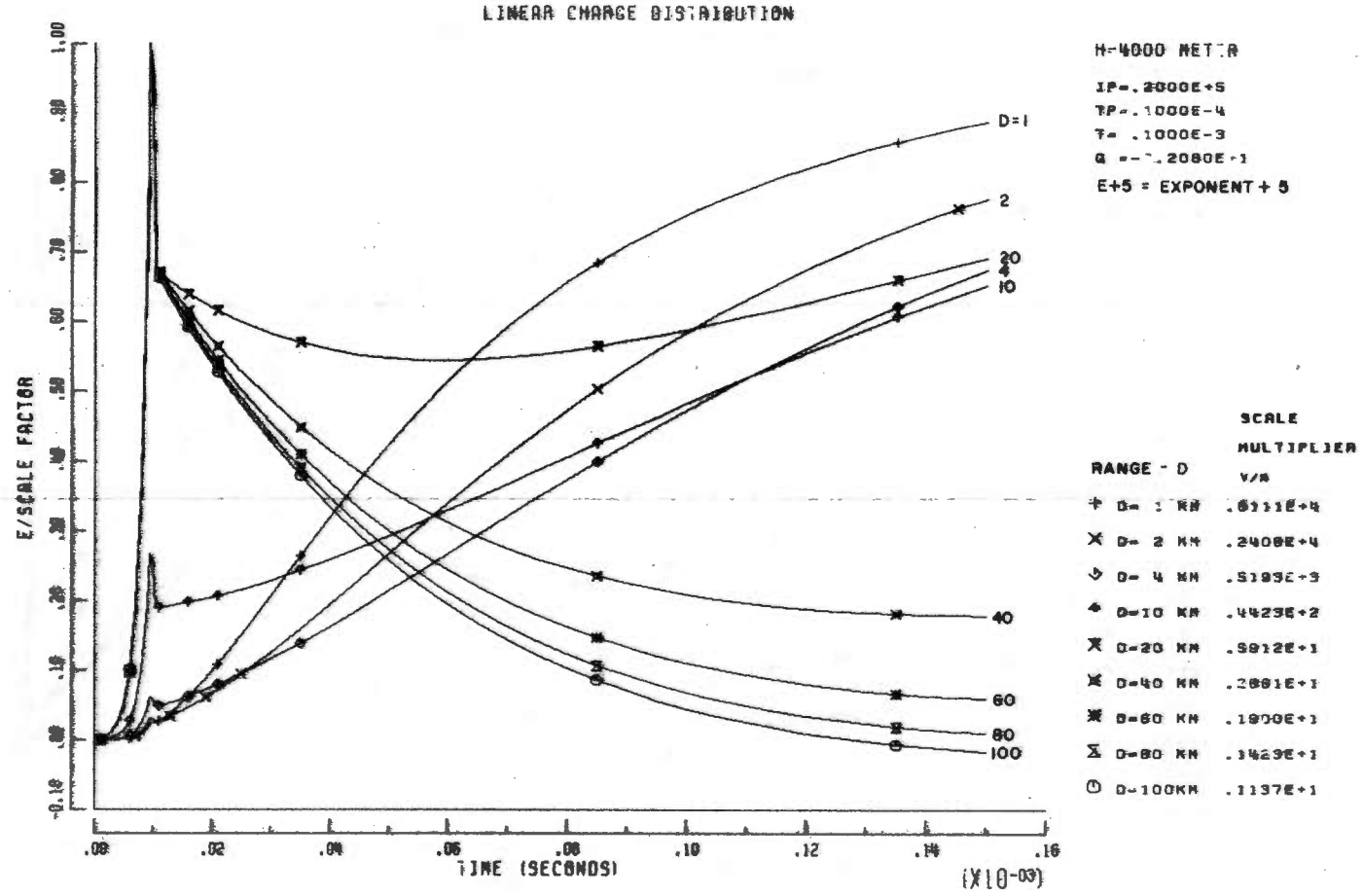

FIGURE 21·0·7

TOTAL ELECTRIC FIELD CHARGE DURING RETURN STROKE (160 μs)

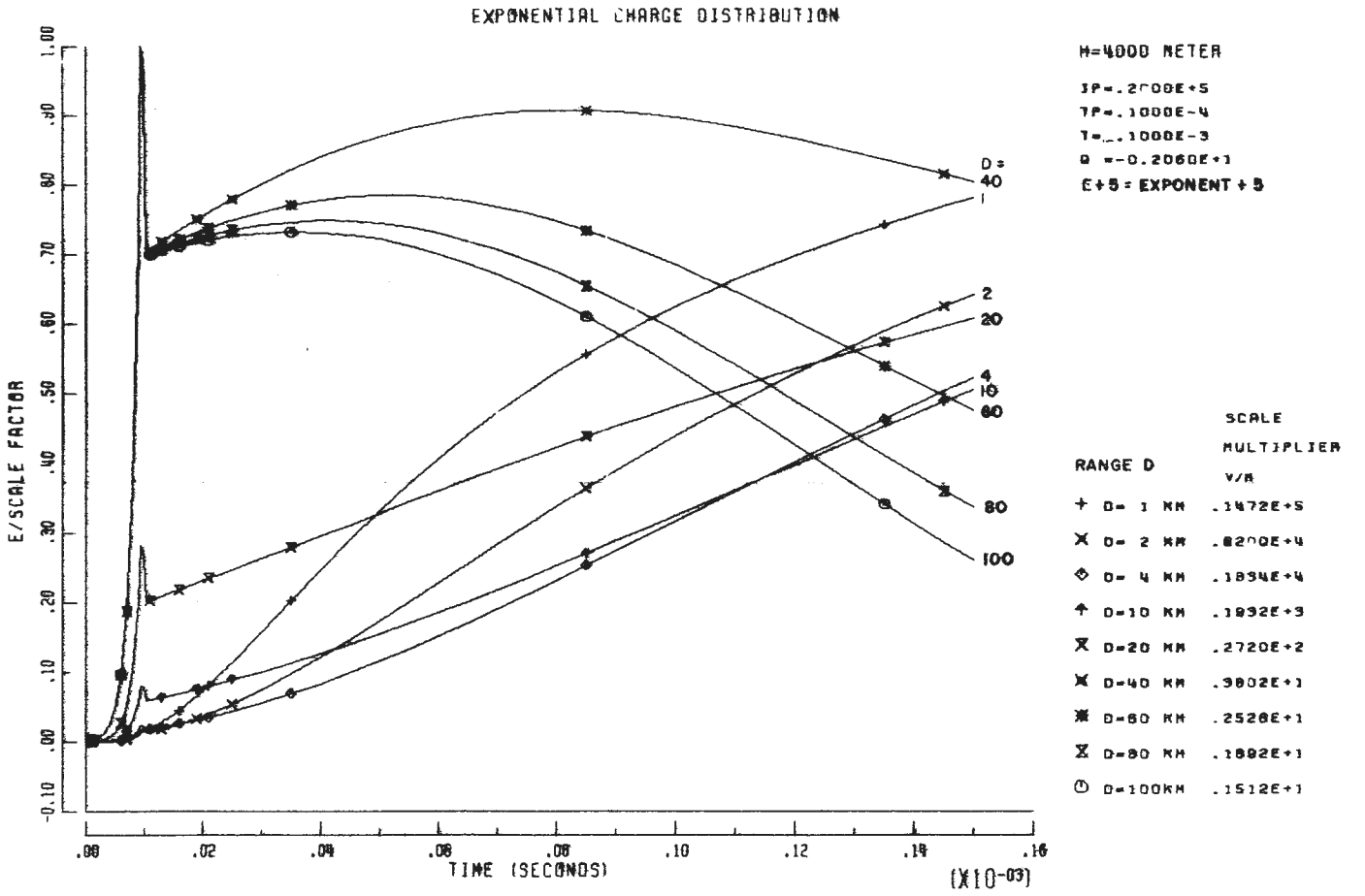

FIGURE 21·0·9

TOTAL ELECTRIC FIELD CHARGE DURING RETURN STROKE (160 μs)

It is furthermore clear that if the rate of change of current is less than the values assumed - for example for subsequent strokes, Berger observed that the time to peak T_p was less than 1 μs - then the electromagnetic field will intrude even sooner than the curves indicate.

Hence these factors provide a possible explanation as to why the observed field change magnitudes reported in Part I did not appear to be decreasing with range according to a D^{-3} relationship. On the other hand the data excluded the effect of very near flashes since the recorded field change would have been invariably off-scale, and this would have tended to slant the data to show a slower rate of field attenuation than may have actually taken place.

It is obvious however that the relationship can only be checked by observation of the wave front of the field change, in which case it would be possible to discern when the electromagnetic field starts to overtake the electrostatic field charge.

22. Acknowledgements

The author is indebted to so many people for assistance that it would not be possible to name all personally. However first and foremost he pays tribute to his wife and family who have born with him the rigours of work over a period of ten years, involving many evenings which have filled over ten volumes and more than 2 000 pages of detailed calculation and argument. It would be difficult to decide whether in fact the outcome of the thesis justifies the sacrifice of some aspects of family life, but he would hope that his family would join him in the thought that something useful might have been achieved. The author can therefore only express sincere thanks that he has been able to complete the task without irreparable family disharmony.

Secondly the author wishes to thank the Council for Scientific and Industrial Research of South Africa for allowing him to proceed with his work during the course of his duties since 1965 to date, and for the very substantial support received through the facilities of the various National Research Institutes. These include Dr. A.P. Burger, the Director of the National Research Institute for Mathematical Sciences and in particular the Numerical Analysis Division headed by Prof. C. Jacobsz who permitted the untiring support of Miss A van Wyk de Vries and Mrs. Louisa Stander. Miss De Vries undertook the programming and plotting of the field change calculations over several months in 1970 whilst Mrs. Stander bore the brunt of the development of the program for simulating the leader progression which took a year to complete to the present stage. Much was learnt, not only about the factors controlling the leader progression itself, but also about the iterative processes needed to obtain satisfactory results.

The National Electrical Engineering Research Institute was formally constituted in January 1971 under the Directorship of Mr. J.D.N. van Wyk and the author is very appreciative of the encouragement and advice received from him to complete the work and this includes his authorisation of the costs involved which were not inconsiderable. The author acknowledges helpful advice received in discussion with Divisional Heads of the Institute and with his own Divisional Staff and for undertaking extra burdens of administrative duties and in recent months, Mr. D.V. Meal for organising the reproduction of drawings and final copy through the sturdy efforts of the Technical Services Drawing office staff and Graphic Arts, and of

131/ .....

course the painstaking typing of Mrs. Lynette Lochtenbergh for first draft and then the final wax sheets.

The author is beholden also to the members of CIGRE Study Committee No. 33 Working Group Lightning for discussion on his tentative proposals during the evolvement of the thesis, and for active encouragement and advice from Dr. R.H. Golde, Prof. Dr. K. Berger and Dr. T.E. Allibone and many others including Prof. S.A. Prentice and Dr. D. Mackerras who have freely offered advice and encouragement over many years of association. Prominent amongst those who were ever ready to assist with detailed data and constructive suggestions was the late Prof. D.J. Malan to whom the author owes a considerable debt of gratitude. Without his guidance and inspiration in the earlier years, this thesis would not have progressed at all.

Finally the author sincerely thanks his supervisors at the University of Cape Town - Dr. H.D. Einhorn and Col. G.H. Webster. Despite the distance which seperated him from them, they were always ready to help and assist in difficult periods - more than they probably realised. Many serious barriers were negotiated with their help and guidance and their encouragement to the author to finally conclude the work - despite some questions which inevitably must go unanswered at this stage.

The author has attempted in the course of this Part II of his thesis, to follow up every avenue of approach to the subject of a clear physical explanation of the lightning discharge from its inception in the clouds, to the leader and finally to the return stroke and subsequent strokes. Difficulties of one kind or another have been encountered almost at every stage. Either there has been uncertainty regarding the absolute parameters that should be applied, or there has been difficulty in explaining a mechanism in view of conflicting experimental data. However in general it is believed that at least it has been shown where data is still lacking. All in all, hypotheses have been advanced which, though possibly needing further experimental proof in some instances, at least serves to explain many of the observations, and it is believed casts some further light on the possible truth of the matter.

If the thesis stimulates further work to fully explaining the lightning discharge, the author feels that his efforts in this direction will have been justified.

R.B. Anderson,
National Electrical Engineering Research Institute,
Council for Scientific and Industrial Research of South Africa,
P.O. Box 395,
PRETORIA.

27 September 1972

23. References

ALSTON et al (1968) High Voltage Technology edited by L.L. Alston Harwell post-graduate series, Oxford University Press 1968 p 48.

ALLIBONE T.E. and MEEK J.M. (1938) The development of the spark discharge. Proc. Roy. Soc. A. (166) p 97 1938

ANDERSON R.B. (1969) The measurement of lightning ground flash density. Trans. S.A. Inst. Elect. Engrs. Vol. 60. Pt. II Paper 7 P. 247

ANDERSON R.B. (1969a) The waveform of the field change during lightning strokes to ground. Electrical Engineering Research Department, Internal Report 11/1969 submitted to CIGRE WG 33.01 (Lightning)

BROOK M and KITAGAWA N. (1960) Some aspects of lightning activity and related meteorological conditions Jour. Geophys. Res. 65 (4) pp 1203-1210, 1960a.

BROWN K.A. and KREIHBIEL P.R., MOORE C.B. and SARGENT G.N. (1971) Electrical Screening Layers around Charged Clouds. Jour. Geophys. Res. Vol. 76 No. 12 April 20, 1971, pp 2825-2835.

BRUCE C.E.R. and GOLDE R.H. (1941) The lightning discharge Jour. Instn. Elect. Eng. (London) Vol. 88 Pt. II pp 487-520, 1941.

BROOK M., KITAGAWA N. and WORKMAN E.J. (1962) Quantitative study of strokes and continuing currents in lightning discharges to ground. Jour. Geophys. Res. 67 (2) pp 649-659, 1962.

BERGER K. (1971) Preliminary results of the evaluation of downward lightning strokes to Mt. San Salvatore Report to CIGRE Working Group 33.01 (Lightning) not for publication.

BRUCE C.E.R. (1944) The initiation of long electrical discharges Proc. Roy. Soc. Series A 183 p 228, 1944.

BERGER K. (1967) Novel observation on Lightning Discharges Jour. Franklin Inst. Vol. 283, No. 6, June 1967, pp 478-525.

BERGER K. (1972) Analysis of all downward strokes to Mt. San Sal= vatore - Report to CIGRE Working Group 33.01 Lightning to be published in Swiss Bulletin SEV.

GOLDE R.H. (1970) Thunder and Lightning The Rhodesian Engineer Paper 112, July 1970, p 903.

HEWITT F.J. (1957) Radar echoes from inter-stroke processes in lightning Proc. Phys. Soc. London, B.70. pp 961-979, 1957.

JORDAN E.C. (1953) "Electromagnetic waves and radiating systems" Constable Company Ltd., 1953, pp 303-306

KRITZINGER J.J. Doctoral Dissertation in Electrical Engineering, University of Witwatersrand, Johannesburg (1962) reported in Nature 197, 1165 (1963) and discussed by LOEB L.B. (1965) Appendix I.

LE JAY P. (1962) L'Onde Electrique (1926) 5 p 493

133/ .....

LOEB L.B. (1965) Electrical Coronas, their basic physical mechanisms. University of California Press, Berkeley, California, 1965.

LOEB L.B. (1966) The mechanism of stepped and dart leaders in cloud-to-ground lightning strokes. Jour. Geophys. Res. 71 (20) pp 4711-4721, 1966.

LOEB L.B. (1958) The positive streamer spark in air in relation to the lightning stroke H.G. Houghton (ed) "Atmospheric Explorations" pp 46-75 John Wiley ε Sons Inc. New York (1958).

MACKY W.A. (1931) Some investigations on the deformation and break= ing of water drops in strong electric fields. Proc. Roy. Soc. London A133 p 565-587, 1931.

MASON B.J. (1961) Generation of Electricity in Thunderclouds. Dis= covery April 1961, pp 147-150

MACKERRAS D. (1968) A comparison of discharge processes in cloud and ground lightning flashes. Jour. Geophys. Res. 73 (4) 1175-1183, 1968.

MALAN D.J. (1967) Physics of the Thunderstorm Electric Circuit, Jour. Franklin Inst. 283 (6) June, 1967.

MALAN D.J. and SCHONLAND B.F.J. (1951) The electrical processes in the intervals between the strokes of a lightning discharge. Proc. Roy. Soc. A. Vol. 206, pp 145-163, 1951.

MALAN D.J. (1963) Physics of Lightning, English Universities Press Ltd., London, p 49.

MEEK J.M. and CRAGGS J.D. Electrical Breakdown in gasses Oxford University Press, 1954

MALAN D.J. (1969) "Lightning and its effects on high structures" Trans. South African Inst. Elect. Engnrs. Vol. 60, Part II, Paper No. 6, pp 241-242, November 1969.

ORVILLE R.E. (1968) The spectrum of the Lightning Stepped-Leader Jour. Geophys. Res. submitted, June 1968.

PEEK J.W. (1929) Dielectric Phenomena in High Voltage Engineering, Third Edition, New York and London, McGraw Hill Book Company, 1929.

PIERCE E.T. (1955) "Electrostatic field changes due to lightning discharges" Quart. Jour. Roy. Met. Soc., 81 (348) pp 211-228, 1955.

PRENTICE S.A. (1960) Thunderstorms in the Brisbane Area Jour. Inst. Engnrs. Australia 32 (3) March, 1960.

SCHONLAND B.F.J. (1938) Progressive lightning IV - The discharge mechanism. Proc. Roy. Soc. Series A No. 916 Vol. 164, pp 132-150 January 1938.

SCHONLAND B.F.J. (1953) The pilot streamer in Lightning and the Long Spark. Proc. Roy. Soc. (London) A220 : 25-38 (1953).

UMAN M.A. (1969) Lightning, McGraw Hill, New York, 1969.

134/ .....

VONEGUT B. (1965) Thundercloud electricity Discovery March 1965 pp 12-17

WORKMAN E.J. (1967) The production of thunderstorm electricity. Jour. Franklin Inst. 283 (6) p 540-557, 1967.

WAGNER C.F. (1963) Relation between stroke current and velocity of the return stroke IEEE Trans. on Power Apparatus and Systems pp 609-617, 1963.

Appendix I/ .....

THE CYLINDRICAL MODEL OF CLOUD CHARGES

PART II APPENDIX I

Summary The classical model of cloud charges contained on spheres or in sperical space charge volumes, does not explain how cloud-ground lightning flashes may be initiated as opposed to intra-cloud flashes, since the field intensity on the centre line between say two charged spheres of opposing polarity is invariably greater than that on the centre line below the charges - particularly when sepe= ration distances are relatively small. The model representing charge seperation taking place within a cylindrical form, with zero charge density at or near the centre and a maximum at the extre= mities does, on the other hand, provide a basis for the calculation of critical conditions when intra-cloud or cloud-ground discharges have an equal or greater probability of occurence.

This appendix describes the detailed derivation of the cylin= drical model and indicates the significance of the various numerical results computed.

Contents

List of attached figures/(ii)

THE CYLINDRICAL MODEL OF CLOUD CHARGES

PART II APPENDIX I

1. Basic Concepts

The physical explanation of charge seperation in clouds is not as yet fully determined as may be gathered from a recent review by Stow (1969) in which all current models are critically examined against the requirements enumerated originally by Mason (1953) and which are requoted below:

"1. The average duration of precipitation and lightning from a single-cell thunderstorm is of the order of 30 min.

2. The average electric moment destroyed in a lightning flash is about 110 Coulomb-km, the corresponding charge being about 20-30 Coulombs.

3. The magnitude of the charge that is being seperated immediately after a flash, by virtue of the fall speed v of the precipitation elements, is of the order 8000/v Coulombs, where v is measured in metres per second.

4. In a large, extensive thundercloud this charge is generated and seperated in a volume bounded by the - 5 and - 40°C levels and having an average radius of perhaps 2 km.

5. The negative charge is centred near the - 5°C isotherm while the main positive charge is situated some kilometres higher up, usually above or near the - 20°C level.

6. The charge generation and seperation processes are closely associated with the development of precipitation in the ice phase - probably in the form of soft hail. These precipitation particles must be capable of falling through upcurrents of several metres per second.

7. Sufficient charge must be generated and seperated to supply the first lightning flash within 12-20 min of the appearance of precipitation particles of radar-detectable size.

2/...

an invoronment in which water can be frozen.

In storms having cloud bases from 1 km to 3 or 4 kms elevation the position of the negative charge center is the same with respect to temperature. Lightning strokes to ground start at this center regardless of the depth of cloud below this level. They never start in lower levels of the cloud nor do they originate in the rain below the cloud.

The cloud must contain an ample supply of liquid water supercooled. A 0°C isotherm must be above the cloud base. A relatively tall, nearly vertical, cloud tower must exist above the freezing level. Evidence is overwhelming that this cloud tower contains ice forms as well as liquid water.

The vertical cloud must be strongly convective during the electricity producing stage. The circulation must be strong enough to handle a very critical trans= portation job - electrical charges, once made free, must be separated rapidly over distances of 3 to 5 or more km. The carriers of free charge, both positive and negative, must be differentiated in such a way that they may be separated vertically by gravity versus updraft while in the same vertical air stream,

The charge transportation mechanism must be such as to provide a recovery time sufficiently short to allow for lightning flashes seperated in time by as little as 10 or 20 seconds. At the same time, as will be seen later, the cloud must be able to contain the charges being transported without developing such high potential gradients as to cause breakdown through the sides of the cloud. Considerations relative to recovery time and charge containment during transport are crucial and provide the most exacting acceptance criteria for the selection of an electrification process.

Although it may not be necessary in all cases, the charge structure should develop in such a way that the first lightning discharge takes place between the two centers within the cloud, as is usually observed.

4/...

The delivery of negative charge to the lower center must continue for a variable time of approximately 12 minutes after the top of the radar cloud begins to descend."

Workmen, later in the same publication, envisages charge seperation taking place in a vertical direction with a gradual concentration of charge of one sign at the upper and lower extremities and with charges of both signs present near the midway mark but the nett charge being zero at about -18°C or at approximately 8 km altitude.

Hence the concept of the cylindrical model is again not at variance with even this explanation of the charge seperation process along a vertical plane.

The unknown factors are of course the manner in which the charge is concentrated and the actual dimensions of the phenomenon. The charge density may be assumed to increase in a linear manner, or more steeply at a parabolic or even exponential rate, or it may assume some other more complicated form. Certainly no single assumption will be completely right, and most likely, in practice, it is continuously varying in any case. However in the absence of any real evidence to the contrary, a uniformly increasing charge density, namely a linear form, is assumed as a first approximation because this leads to more simple mathematical expressions for the field intensity and potentials which have to be calculated.

2. <u>The electrical characteristics of the cylindrical charge model</u>.

Figure 2.1.1 illustrates a single cylinder of charge of length L and radius R with the charge density zero at one end and increasing uniformly to a maximum at the other, and the total charge being say Q

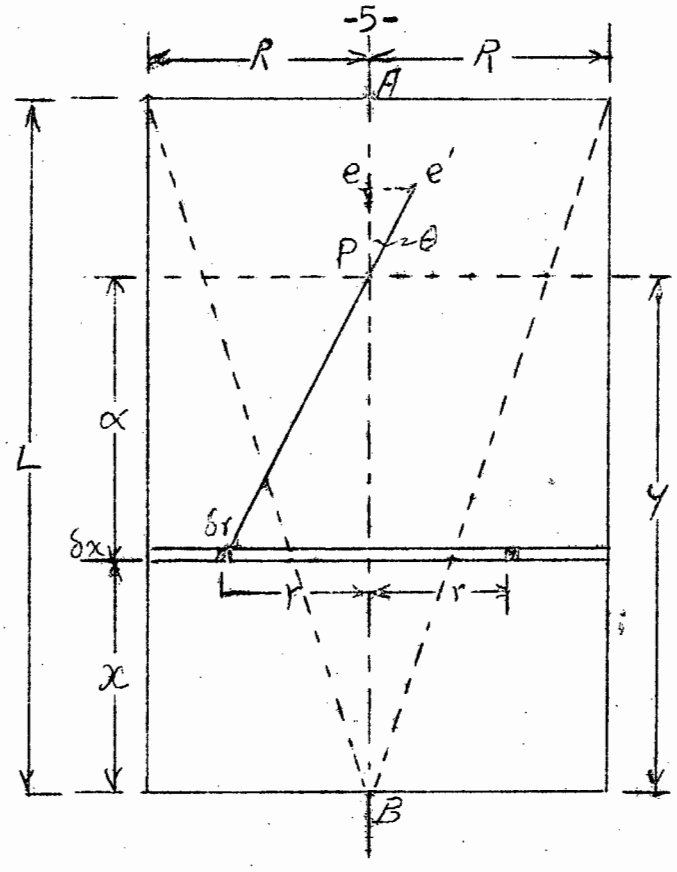

Figure 2.1.1 Diagram showing a unit cylindrical charge model. The dotted triangle illustrates the charge distribution pattern.

If it is further assumed that the charge density throughout a thin disc of δx in thickness is uniform, the charge density can then be expressed in the form

$$q' = \frac{2\,Q\,x}{\Pi R^2 L^2} \quad \text{clbs/m}^3 \tag{2.1}$$

The charge on the thin disc is then:-

$$\delta q = \Pi R^2\, q' \delta x = \frac{2Q\,x\,\delta x}{L^2} \tag{2.2}$$

$$\text{And the total charge} = \frac{2Q}{L^2} \int_0^L x\,dx = Q \tag{2.3}$$

Now the vertical field intensity at any point P along the axis AB of the cylinder distant y from B can be calcu= lated in the following manner: assume first of all an annular ring of radius r and width δr situated in the aforementioned

6/...

disc of thickness δx distant x from B then the volume of this ring is $2\Pi r.\delta r.\delta x$ and its charge δq is therefore:-

$$\delta q = 2\Pi r.\delta r.\delta x.q' = \frac{4Q}{R^2L^2} r.\delta r.x.\delta x \qquad (2.4)$$

The convention used throughout these calculations is to assume all charges are positive and that the direction of the electric field is positive at a point if unit positive charge placed at that point would trend to more downwards - that is assuming that eventually the calculation will be referred to the earth at a lower level.

In this case the charge in the cylinder lying below the point P will produce a negative vertical field at P, whilst that above P will produce a positive field. The field intensity $\delta e'$ at P due to the charge δq in the annular ring is therefore given by

$$\delta e' = -\delta q/4\Pi\epsilon_o\epsilon_r S^2 \qquad (2.5)$$

Where $\epsilon_o = \epsilon = 10^{-9}/36\Pi$ and $\epsilon_r = 1$ for air.

And $S = [\alpha^2+r^2]^{\frac{1}{2}}$ and $\alpha = y-x$.

However the vertical component of the field is

$$\delta e = \delta e.'\cos\theta \qquad (2.6)$$

Where $\cos\theta = x/s$

And hence

$$\delta e = -\delta q\alpha/4\Pi\epsilon S^3 \qquad (2.7)$$

The horizontal component of the field at the point P is zero since it is radial and each vector component is cancelled by an equal and opposite component due to the charge situated diametrically opposed to it.

The total electric field intensity at P due to the charge situated below P is therefore given by the integral:-

7/...

$$E_1 = \frac{-Q}{\Pi \epsilon R^2 L^2} \int_o^R \int_o^y \frac{r dr . x dx}{S^3} \qquad (2.8)$$

First treating x as constant, the integral is of the standard form

$$A \int_o^R \frac{rdr}{[r^2+\alpha^2]^{3/2}}$$

and has the solution $-A \left\{[r^2+\alpha^2]^{-\frac{1}{2}}\right\}_o^R$ and this over the limits of r = o to r = R is $- A \left[[\alpha^2+R^2]^{-\frac{1}{2}} - 1/\alpha\right]$

Where $\alpha = y-x$.

$$\text{Hence } E_1 = \frac{Q}{\Pi \epsilon R^2 L^2} \left\{ \underbrace{\int_o^y \frac{\alpha x dx}{[\alpha^2+R^2]^{\frac{1}{2}}}}_{(I)} - \underbrace{\int_o^y x\, dx}_{(II)} \right\} \qquad (2.9)$$

If $X = y - x$, $dX = -dx$ and $x = y - X$

$$I = \int \frac{\alpha x dx}{[\alpha^2+R^2]^{\frac{1}{2}}} = - \int \frac{(y-X)X dX}{[X^2+R^2]^{\frac{1}{2}}} = - y \int \frac{X dX}{[X^2+R^2]^{\frac{1}{2}}} + \int \frac{X^2 dX}{[X^2+R^2]^{\frac{1}{2}}}$$

Both the R.H.S. integrals are now standard forms and the solution is therefore

$$I = -y\,[X^2+R^2]^{\frac{1}{2}} + \frac{X}{2}\,[X^2+R^2]^{\frac{1}{2}} - \frac{R^2}{2} \ln\left| X + \sqrt{X^2+R^2} \right| \qquad (2.10)$$

Resubstituting for X = y-x and applying the limits of integration between x=o and x=y then

$$I = \left\{ -y[(y-x)^2+R^2]^{\frac{1}{2}} + \frac{(y-x)[(y-x)^2+R^2]^{\frac{1}{2}}}{2} - \frac{R^2}{2} \ln\left|(y-x) + \sqrt{(y-x)^2+R^2}\right| \right\}_o^y$$

Whence $I = -yR - \frac{R^2}{2} \text{Ln}.R + y\,(y^2+R^2)^{\frac{1}{2}} - y/2(y^2+R^2)^{\frac{1}{2}}$

$$+ \frac{R^2}{2} \ln\left|y + \sqrt{y^2+R^2}\right|$$

$$I = \frac{R^2}{2} \sinh^{-1}\left(\frac{y}{R}\right) + y/2\,(y^2+R^2)^{\frac{1}{2}} - yR \qquad (2.11)$$

And $\quad II = -\int_o^y x dx = -y^2/2 \qquad (2.12)$

8/...

If the factor $R^2/2$ is taken out of the brackets of (2.11) and (2.12)

$$E_1 = \frac{Q}{2\Pi\epsilon L^2}\left\{\sinh^{-1}(y/R) + y/R\,[1+(y/R)^2]^{\frac{1}{2}} - 2\,y/R - (y/R)^2\right\} \qquad (2.13)$$

The field intensity at Point A is then given by putting y = L in (2.13)

$$\text{Whence } E_A = \frac{Q}{2\Pi\epsilon L^2}\left\{\sinh^{-1}(L/R) + L/R[1+(L/R^2]^{\frac{1}{2}} - 2\,L/R - (L/R)^2\right\} \qquad (2.14)$$

Similarly Figure 2.1.2 indicates the position for the calculation of the field intensity at P due to the charge located above P.

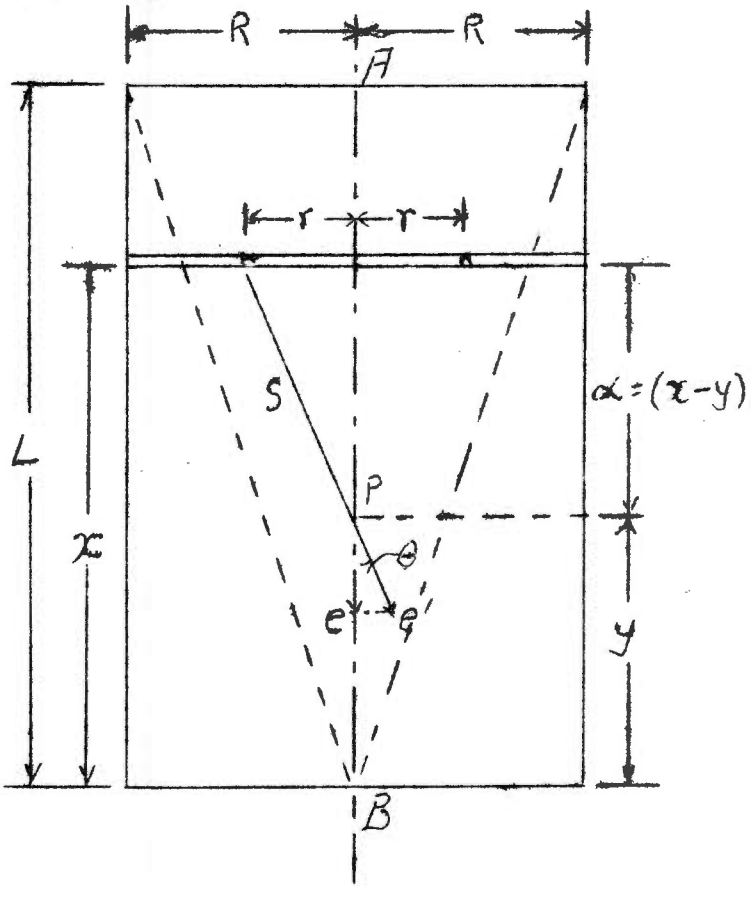

Figure 2.1.2 The cylindrical charge model for calculation of the field intensity at P due to the portion of charge Q lying above point P.

9/...

The direction of the electric field at P is in this case positive, by definition, and all equations are otherwise identical up to (2.9) which can be restated as follows:-

$$E_2 = \frac{\theta}{\Pi\epsilon R^2 L^2}\left\{ -\int_y^L \frac{\alpha\, x dx}{[\alpha^2+R^2]^{\frac{1}{2}}} + \int_y^L x dx \right\} \qquad (2.15)$$

Where $\alpha = (x-y)$

Putting $X = x-y$ $dx = dX$ and $x = y+X$ and substituting these in the first integral:-

$$I = -\int_y^L \frac{\alpha x dx}{[\alpha^2+R^2]^{\frac{1}{2}}} == -\int \frac{(y+X)X dX}{[X^2+R^2]^{\frac{1}{2}}} = -y\int \frac{X dX}{[X^2+R^2]^{\frac{1}{2}}} - \int \frac{X^2 dX}{[X^2+R^2]^{\frac{1}{2}}}$$

Hence $I = -y\,[X^2+R^2]^{\frac{1}{2}} - \frac{X}{2}[X^2+R^2]^{\frac{1}{2}} + \frac{R^2}{2}\mathrm{Ln}\left|X+\sqrt{X^2+R^2}\right|$

Putting $X = x-y$ and applying the limits of $x = y$ to $x = L$

$$I = \left\{ -y[(x-y)^2+R^2]^{\frac{1}{2}} - \frac{(x-y)}{2}[(x-y)^2+R^2]^{\frac{1}{2}} + \frac{R^2}{2}\mathrm{Ln}\left|(x-y)+\sqrt{(x-y)^2+R^2}\right| \right\}_y^L$$

$$I = -y[(L-y)^2+R^2]^{\frac{1}{2}} - \frac{(L-y)}{2}[(L-y)^2+R^2]^{\frac{1}{2}} + \frac{R^2}{2}\mathrm{Ln}\left|(L-y)+\sqrt{(L-y)^2+R^2}\right| + yR - \frac{R^2}{2}\mathrm{Ln}|R|$$

So $$I = \frac{R^2}{2}\sinh^{-1}\frac{(L-y)}{R} - \frac{(L+y)}{2}[(L-y)^2+R^2]^{\frac{1}{2}} + yR \qquad (2.16)$$

And $$II = \int_y^L x\, dx = \frac{L^2}{2} - \frac{y^2}{2} \qquad (2.17)$$

Taking out $R^2/2$ the field intensity is therefore

$$E_2 = \frac{Q}{2\pi\epsilon L^2}\left\{ \sinh^{-1}\frac{(L-y)}{R} - \frac{(L+y)}{R}\left[1+\frac{(L-y)^2}{R}\right]^{\frac{1}{2}} + \frac{2y}{R} + \frac{(L)^2}{R} - \frac{(y)^2}{R} \right\} \qquad (2.18)$$

10/...

Hence the field intensity at point B is given by putting y = o in (2.18)

$$\text{So} \quad E_B = \frac{Q}{2\pi\epsilon L^2}\left\{\sinh^{-1}(L/R) - L/R[1+(L/R)^2]^{\frac{1}{2}}+(L/R)^2\right\} \tag{2.19}$$

Since the field intensities at A and B are in opposing directions, the algebraic sum of the two expressions for E_A and E_B will result in the numerical difference in magnitudes and from inspection of (2.14) and (2.19).

$$E_A + E_B = \frac{Q}{\pi\epsilon L^2}\left[\sinh^{-1}\left(\frac{L}{R}\right) - \frac{L}{R}\right] \tag{2.20}$$

The field intensity at any point P is given by E_1+E_2 from (2.13) and (2.18) as follows:-

$$E_y = \frac{Q}{2\pi\epsilon L^2}\left\{\sinh^{-1}\left(\frac{L-y}{R}\right) + \sinh^{-1}\left(\frac{y}{R}\right) - \left(\frac{L+y}{R}\right)[1+\left(\frac{L-y}{R}\right)^2]^{\frac{1}{2}}\right.$$
$$\left. + (y/R)[1 + (y/R)^2]^{\frac{1}{2}}+\left(\frac{L}{R}\right)^2 - 2\left(\frac{y}{R}\right)^2\right. \tag{2.21}$$

It is noted that the primary equations for the field intensity have the general form:-

$$E = \pm \frac{Q}{2\pi\epsilon L^2}\left\{\sinh^{-1}\left(\frac{a-b}{R}\right) - \sinh^{-1}\left(\frac{a-c}{R}\right) + \left(\frac{a+b}{R}\right)[1+\left(\frac{a-b}{R}\right)^2]^{\frac{1}{2}}\right.$$
$$\left. - \left(\frac{a+c}{R}\right)[1 + \left(\frac{a-c}{R}\right)^2]^{\frac{1}{2}} + \left(\frac{b}{R}\right)^2 - \left(\frac{c}{R}\right)^2\right\} \tag{2.22}$$

Hence it is convenient to summarise the above by means of a diagram and a statement of the value of the constants as indicated below:-

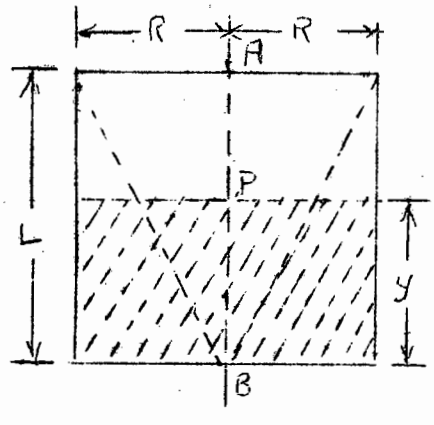

1. Field Intensity at P due to charge in cylinder lying below P.

For Equation (2.13) substitute a = y b = y c = o in General Equation (2.22)

For the field intensity at A Equation (2.14) Put y = L.

11/...

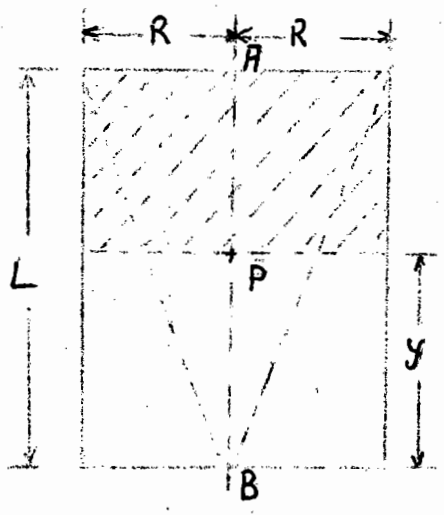

2. Field Intensity at P due to charge in cylinder lying above P

For Equation (2.18) substitute $a = -y \quad b = -L \quad c = -y$ in general equation (2.22)

For the field intensity at B, Equation (2.19) Put $y = 0$.

The above rule only applies to discrete calculations for a particular configuration and not to their sum or difference. For example (2.20) and (2.21) do not conform to the general equation. However having demonstrated the manner of derivation of this type of equation it is proposed hereafter merely to quote the values of the constants for convenience whereever possible.

3. Field Intensity of a bi-polar model of cylindrical charges

Having considered a single charged cylinder, the next step to a bi-polar model can be constructed; this is done with a view to the arrangement which may be later applied to a bi-polar thunder cloud and is illustrated in Figure 3.1.1.

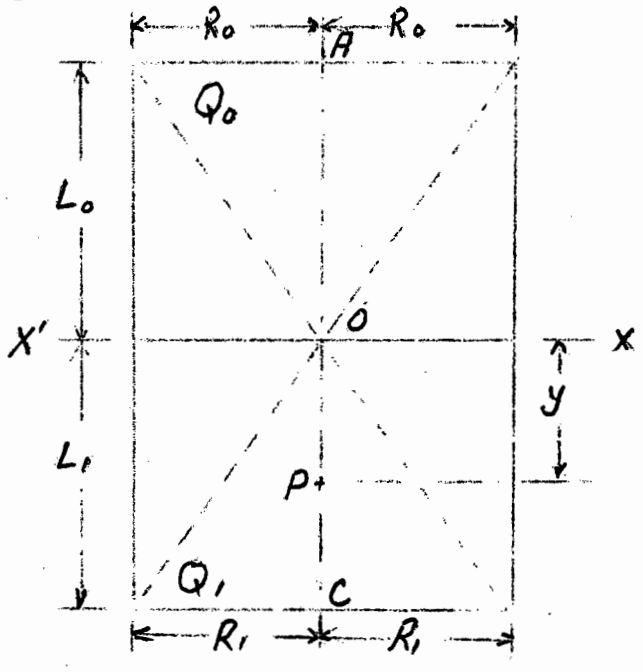

Figure 3.1.1. Diagram illustrating a bi-polar cylindrical charge. Dotted lines indicate form of charge distribution.

12/...

It can be seen that the field intensity pattern (neglecting the effect of earth) is symmetrical around the horizontal plane XBX' and hence the field intensity at a point P distant y from the axis need only be considered. Conventionally the two charges Q_o and Q_1 are both considered positive, but a numerical negative value may be given to one of them at a later stage.

There are three sections of charge involved in calculating the field intensity at the point P, and as shown in the previous section the values may be expressed in the general form of equation (2.22) and the constants for each case are given below:-

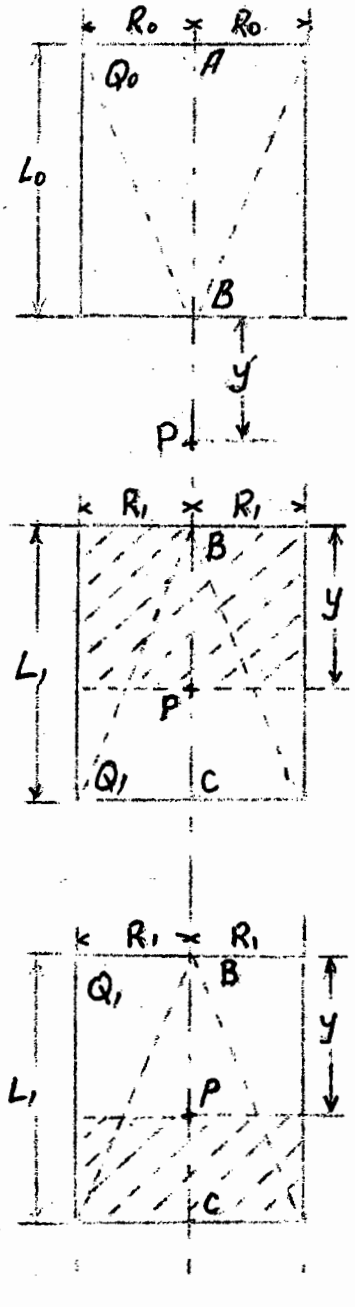

1. <u>Field Intensity at P due to charge Q_o</u>

$$E_o = \frac{Q_o}{2\pi\epsilon L_o^2} \quad [+ \text{ General Equation}] \qquad (2.22)$$

$$a = y \quad b = -L_o \quad c = o$$
$$R = R_o. \qquad (3.1)$$

2. <u>Field Intensity at P due to portion of charge Q_1 lying above point P</u>

$$E_{11} = \frac{Q_1}{2\pi\epsilon L_1^2} \quad [+ \text{ General Equation}] \qquad (2.22)$$

$$a = y \quad b = y \quad c = o$$
$$R = R_1 \qquad (3.2)$$

3. <u>Field Intensity at P due to portion of charge Q_1 lying below point P.</u>

$$E_{12} = \frac{Q_1}{2\pi\epsilon L_1^2} \quad [- \text{ General Equation}] \qquad (2.22)$$

$$a = -y \quad b = -L_1 \quad c = -y$$
$$R = R_1 \qquad (3.3)$$

13/...

Hence the resultant vertical field intensity at the point P is

$$Ey = E_o + E_{11} + E_{12} \qquad (3.4)$$

For the special case of equal and opposite charges, $Q_o=+Q$ and $Q_1=-Q$ and for $L_o=L_1=L$ and $R_o=R_1=R$ Equation (3.4) resolves into the following:-

$$E_y = \frac{Q}{2\pi\epsilon L^2}\left\{\sinh^{-1}\left(\frac{L+y}{R}\right) + \sinh^{-1}\left(\frac{L-y}{R}\right) - \left(\frac{L-y}{R}\right)\left[1+\left(\frac{L+y}{R}\right)^2\right]^{\frac{1}{2}} - \left(\frac{L+y}{R}\right)\left[1+\left(\frac{L-y}{R}\right)^2\right]^{\frac{1}{2}} + 2\left(\frac{L}{R}\right)^2 - 2\left(\frac{y}{R}\right)^2\right\} \qquad (3.5)$$

In this special case the field intensity at B is given by putting y = o whence:-

$$E_B = \frac{Q}{\pi\epsilon L^2}\left\{\sinh^{-1}\left(\frac{L}{R}\right) - \frac{L}{R}\left[1 + \left(\frac{L}{R}\right)^2\right]^{\frac{1}{2}} + \left(\frac{L}{R}\right)^2\right\} \qquad (3.6)$$

and the field intensity at A or C is given by putting y = L whence

$$E_A = E_C = \frac{Q}{2\pi\epsilon L^2}\left\{\sinh^{-1}\left(\frac{2L}{R}\right) - \left(\frac{2L}{R}\right)\right\} \qquad (3.7)$$

An inspection of (3.6) and (3.7) indicates that the ratio E_B/E_C for example, is dependent only on the ratio L/R, and this means that it is the geometric dimensions of the charges which will determine whether or not a discharge will start in the centre between the charges - namely an intra-cloud discharge, or at say the lower extremity to indicate a discharge towards ground.

In order to find the critical dimensions, Figure 3.1.2 (attached) has been computed to indicate the ratio E_p/E_c using equations (3.5) and (3.7) respectively. In the case of this diagram the length L is the cylinder length for one of the charges in conformity with the equations from which the information is derived.

14/...

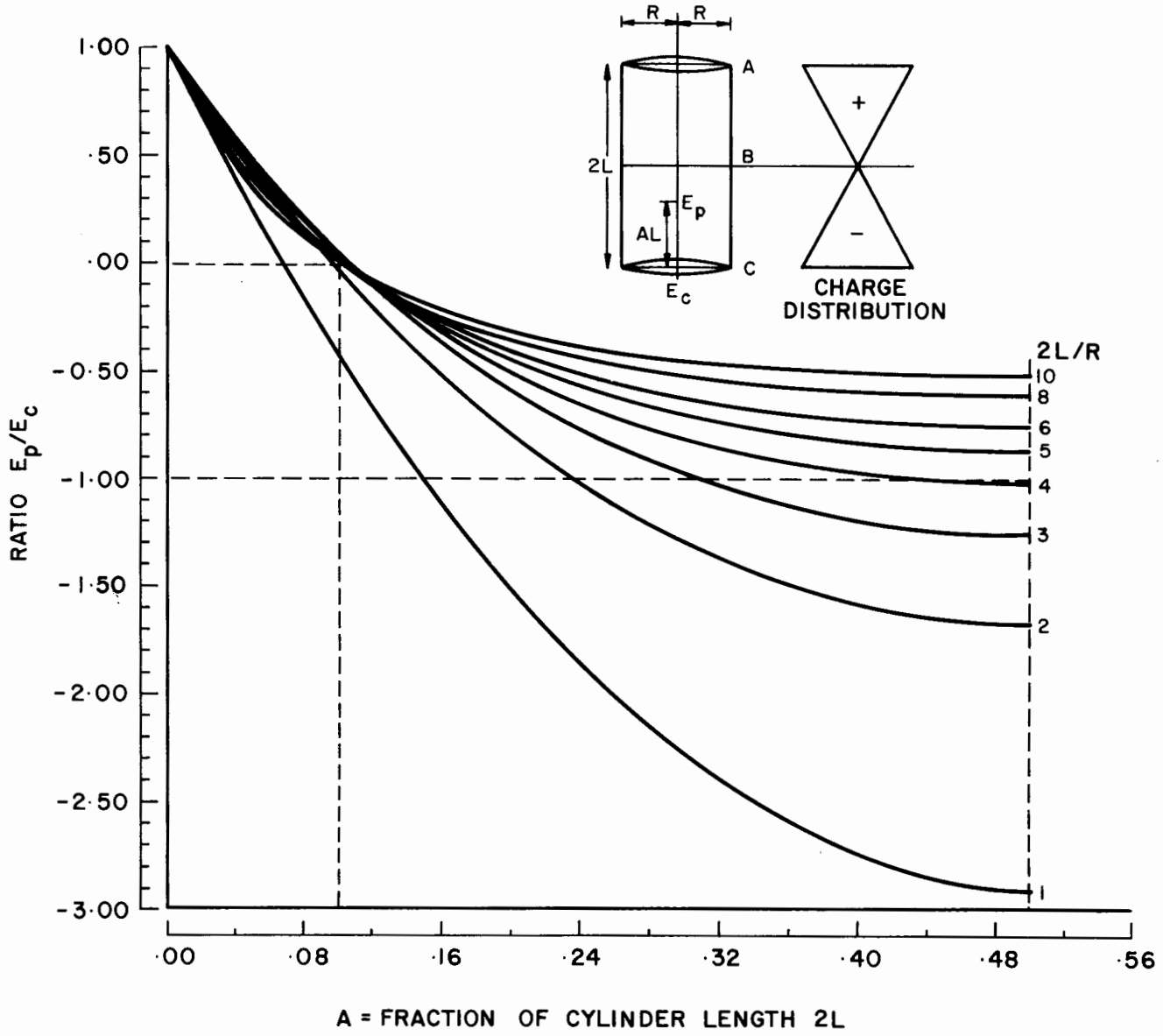

FIGURE 3·1·2

RATIO OF FIELD INTENSITY E_p/E_c FOR VARIOUS VALUES OF RATIO 2L/R

When the ratio $E_p/E_c = 1$ or -1 it of course means that the field intensities at P and at C are equal, and it can be seen that at the centre of the cylinder (A = 0,5) the ratio $E_p/E_c = 1$ when 2L/R = 4 approximately. For larger ratios of 2L/R the field intensity E_c exceeds that at the centre, or any where else in the region between the centre and the extremity.

Hence when 2L/R = 4, conditions are critical, and intra-cloud or cloud-ground discharges are equally probable. When the ratio exceeds this value however, a discharge to ground is more probable.

In terms of the aerodynamic situation within a thunder= storm therefore, it is clear that if charge separation takes place over a given area, say circular of radius R, then in the initial separation process the ratio of L/R is inevitably small and an intra-cloud discharge would be favoured if the amount of charge generated is sufficient to produce breakdown conditions. Once the separation process has proceeded beyond the critical dimensions, a discharge towards ground could be initiated. Hence the rate of charge separation, in terms of quantity of charge, is also an important factor; if for example under severe conditions charge separation areas are extensive and the rate of charge build up is also high, intra-cloud flashes would be favoured. If on the other hand the quantity of of charge separated proceeded at a relatively slow rate compared with the rate at which the cylinder elongated, the critical dimensions for ground flashes to occur would be reached before an intra-cloud discharge could take place. Hence small areas of charge separation coupled with a low rate of charge build up, together with high velocities of separation are most likely to lead to ground flashes whereas large active charge separation areas with low velocities of separation would create conditions more favourable for intra-cloud flashes.

Another important feature which is evident from Figure 3.1.2 (attached) is that except for 2L/R ratios of less than 2,0 the position of zero field intensity is relatively close

15/...

to the extremity, namely about 2L/10. If breakdown and ionisation occurs at the extremity therefore, it will be confined to small dimensions, since the field intensity falls away very rapidly towards the charge separation area.

The same is not true of the conditions around the charge separation area. For example when 2L/R = 4 the field intensity could reach ionisation level over a comparitively large distance, and this distance increases with increasing 2L/R ratios.

The initiation of arcs in the cloud separation area therefore, if it occurs, is likely to be over a widespread area compared to an arc at the extremities where the field gradients change rapidly with distance by comparison.

So far the effect of earth has been neglected, and in general this is a valid assumption during the initial separation process, that is when the separation distances are small, and when charge separation is taking place at very high altitudes, for example 8 km above ground. However the effect of earth increases in prominence when the separation distances have become large, and the lower charge is appreciably closer to earth than the charge separation area or the upper extremity. Hence the critical L/R ratios will be lowered and also there will be a greater tendency for a discharge to be initiated from the lower extremity than from the upper, assuming that breakdown conditions are homogeneous throughout the cell.

The equations for the effect of the mirror images of charges are of the standard form equation (2.22) and the applicable constants are given below. However it is convenient first of all to introduce a standard dimension for the height above ground H, and in order to maintain a uniform presentation, and this value is taken to be that to the charge separation area - or region of zero charge density as shown in figure 3.1.3.

16/...

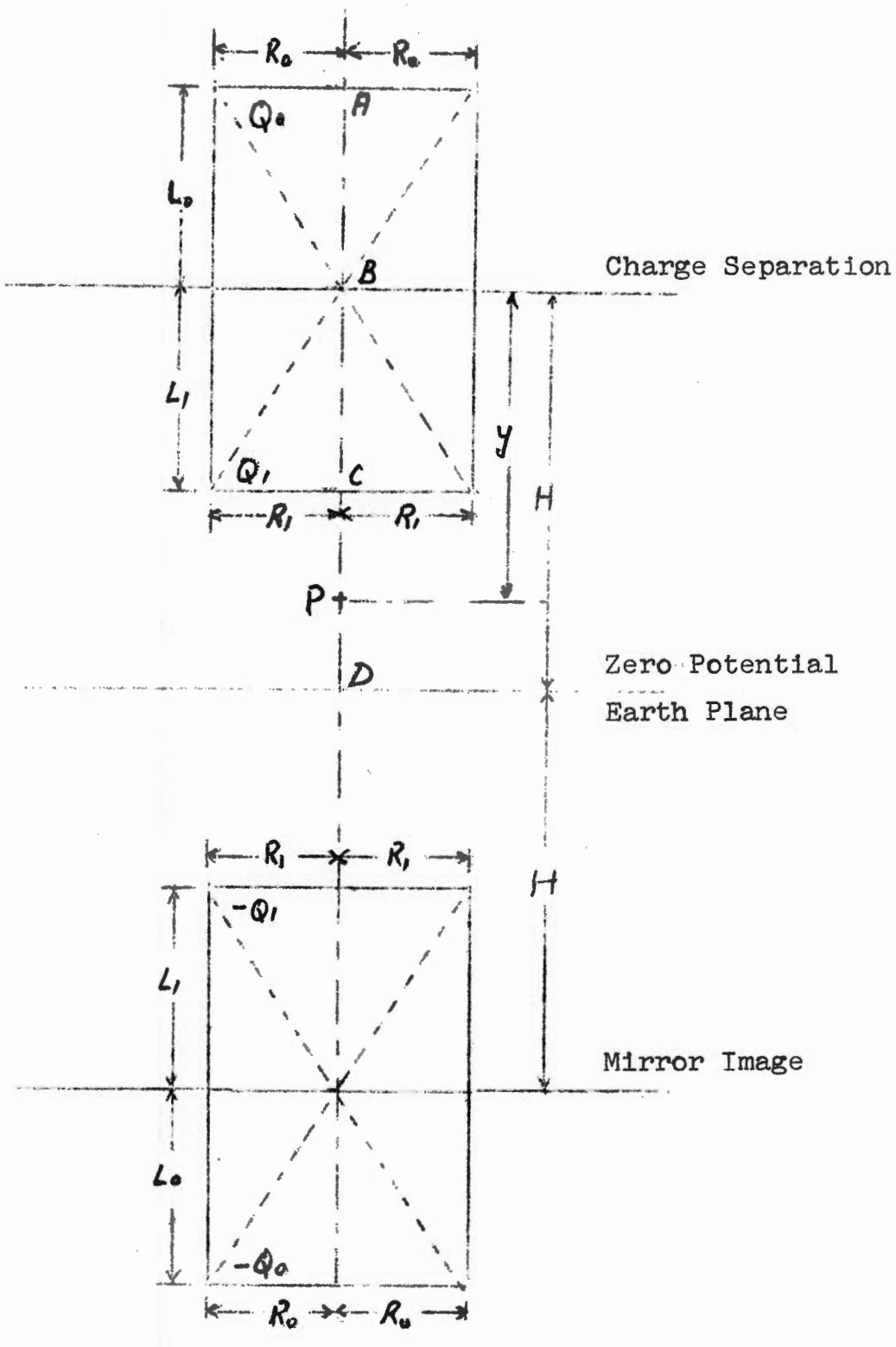

Figure 3.1.3. Standard Bi-polar Cylindrical Charge arrangement indicating zero potential earth plane and mirror image of charges.

The equations for the vertical field intensity at any point P lying between the charge separation area at B and the earth at D, can then be generally stated as follows:-

17/...

$$Ep = \frac{Q}{2\pi\epsilon L^2} \left\{ \pm \text{Part I} \pm \text{Part II} \right\} \qquad (3.8)$$

Where Part I refers to the real charges and Part II to the imaginary or mirror image charges respectively, and are of the form previously given in (2.22) and repeated hereunder for convenience.

Part I or Part II

$$= \left\{ \sinh^{-1} \left(\frac{a-b}{R}\right) - \sinh^{-1} \left(\frac{a-c}{R}\right) + \left(\frac{a+b}{R}\right) \left[1 + \left(\frac{a-b}{R}\right)^2\right]^{\frac{1}{2}} \right.$$
$$\left. - \left(\frac{a+c}{R}\right) \left[1 + \left(\frac{a-c}{R}\right)^2\right]^{\frac{1}{2}} + \left(\frac{b}{R}\right)^2 - \left(\frac{c}{R}\right)^2 \right\} \qquad (2.22)$$

In order to determine the relative effects at the points A, B, and C in Figure 3.1.3. a computer program was devised to calculate the values of charge which would be required to produce a breakdown field intensity of $1{,}0 \times 10^6$ V/m at each of the points in turn, assuming that $Q_o = +Q$ $Q_1 = -Q$ and $L_o = L_1 = L$ and $R_o = R_1 = R$. A range of values of R and L applicable to values of $H = 4 \times 10^3$ m and 8×10^3 were selected. The respective equations of field intensity are as follows referring to the general equation (3.8) and (2.22) above:-

$E_A = E_{AO} + E_{A1}$ Where EA_o = Field Intensity at A due to the upper charge Q_o, L_o, R_o.
And E_{A1} = Field Intensity at A due to the lower charge Q_1 L_1 R_1, in both cases including their images.

$$\text{And } E_{Ao} = \frac{Q}{2\pi\epsilon L^2} \left\{ - \underset{\substack{a=L \\ b=L \\ c=o}}{\text{Part I}} + \underset{\substack{a=2H+L \\ b=-L \\ c=o}}{\text{Part II}} \right\} \qquad (3.9)$$

$$\text{Also } E_{A1} = \frac{-Q}{2\pi\epsilon L^2} \left\{ - \underset{\substack{a=L \\ b=-L \\ c=o}}{\text{Part I}} + \underset{\substack{a=2H+L \\ b=L \\ c=o}}{\text{Part II}} \right\} \qquad (3.10)$$

18/...

Similarly for the point B, $E_B = E_{Bo} + E_{B1}$

Where $E_{Bo} = \frac{Q}{2\pi\epsilon L^2} \left\{ + \underset{\substack{a=o \\ b=-L \\ c=o}}{\text{Part I}} + \underset{\substack{a=2H \\ b=-L \\ c=o}}{\text{Part II}} \right\}$ (3.11)

And $E_{B1} = \frac{-Q}{2\pi\epsilon L^2} \left\{ - \underset{\substack{a=o \\ b=-L \\ c=o}}{\text{Part I}} + \underset{\substack{a=2H \\ b=L \\ c=\infty}}{\text{Part II}} \right\}$ (3.12)

Also for the point C, $E_C = E_{Co} + E_{C1}$

Where $E_{Co} = \frac{Q}{2\pi\epsilon L^2} \left\{ + \underset{\substack{a=L \\ b=-L \\ c=o}}{\text{Part I}} + \underset{\substack{a=2H-L \\ b=-L \\ c=o}}{\text{Part II}} \right\}$ (3.13)

And $E_{C1} = \frac{-Q}{2\pi\epsilon L^2} \left\{ + \underset{\substack{a=L \\ b=L \\ c=o}}{\text{Part I}} + \underset{\substack{a=2H-L \\ b=L \\ c=o}}{\text{Part II}} \right\}$ (3.14)

The computed results indicated the following:

Maximum values of charge Q_A for vertical field intensity at A
" " " " Q_B " " " " " B
" " " " Q_C " " " " " C

Ratio of maximum charges Q_A/Q_C
" " " " Q_B/Q_C

The purpose of the program was to illustrate that starting with a given value of R for the radius of the charge separation area, the charge must build up to the values computed for each extended value of L to achieve a critical breakdown level at the respective points A, B, or C. (figure 3.1.3). If the actual charge separated does not surpass the least value indicated, no discharge will start anywhere. However if the actual charge build up does exceed the least value, ionisation and breakdown would occur at that point.

Furthermore if the ratios Q_A/Q_C or Q_B/Q_C exceed unity breakdown would occur first at C in preferance to A or B respectively, that is to indicate a discharge to earth. On the other hand if these ratios are less than unity a discharge is most likely to start from points A or B.

19/...

cloud flashes are probable up to cylinder length L of 0,5 km namely L/R = 4 where 2L is the total length of the charged cylinder. Beyond this point, discharges from either the top or the lower extremity may take place.

In the case of a larger value of R = 1,0 km say, intra-cloud discharges will take place first, if the charge builds up to at least the values stated for Q_B, up to L = 1,75 km. From L = 2 km onwards however discharges from the lower extre= mity to earth are certain if the charge magnitude is suffi= cient.

The effect of the earth on the lower extremity compared with the upper is more clearly in evidence in this case, and so long as the electric strength of the air is the same for the two, a discharge from the lower end will be favoured.

Other cases of the value R are illustrated in Fig. 3.1.4 and 3.1.5 attached which show the charge required for a given value of L and R for H = 4 and H = 8 km respectively. Only the lowest values of Q are plotted, excluding Q_A and the dividing line between the probability of intra-cloud and cloud-ground discharges is shown and this follows the 2L/R ratio of 4 using the total length, or L/R = 2 if only the dimensions of the one of the charges is considered.

Of course the position differs if the values for L for the two charges differ, as they most probably do in practise, and also if the charges differ in magnitude say as a result of previous discharges to earth which deplete the lower charge. This is considered in more detail in the following section, but the principle remains the same namely that the tendency to one or other type of discharge depends on the geometric arrangement of the charges and the rate of increase in charge build-up compared with that of the elongation of the cylinder.

It is also of interest to note that the quantity of charge required for intra-cloud discharge will be in general less than that for discharges to ground simply on account of the fact that intra-cloud discharges will take place during the initial process of charge separation when the

21/...

XG4-1779

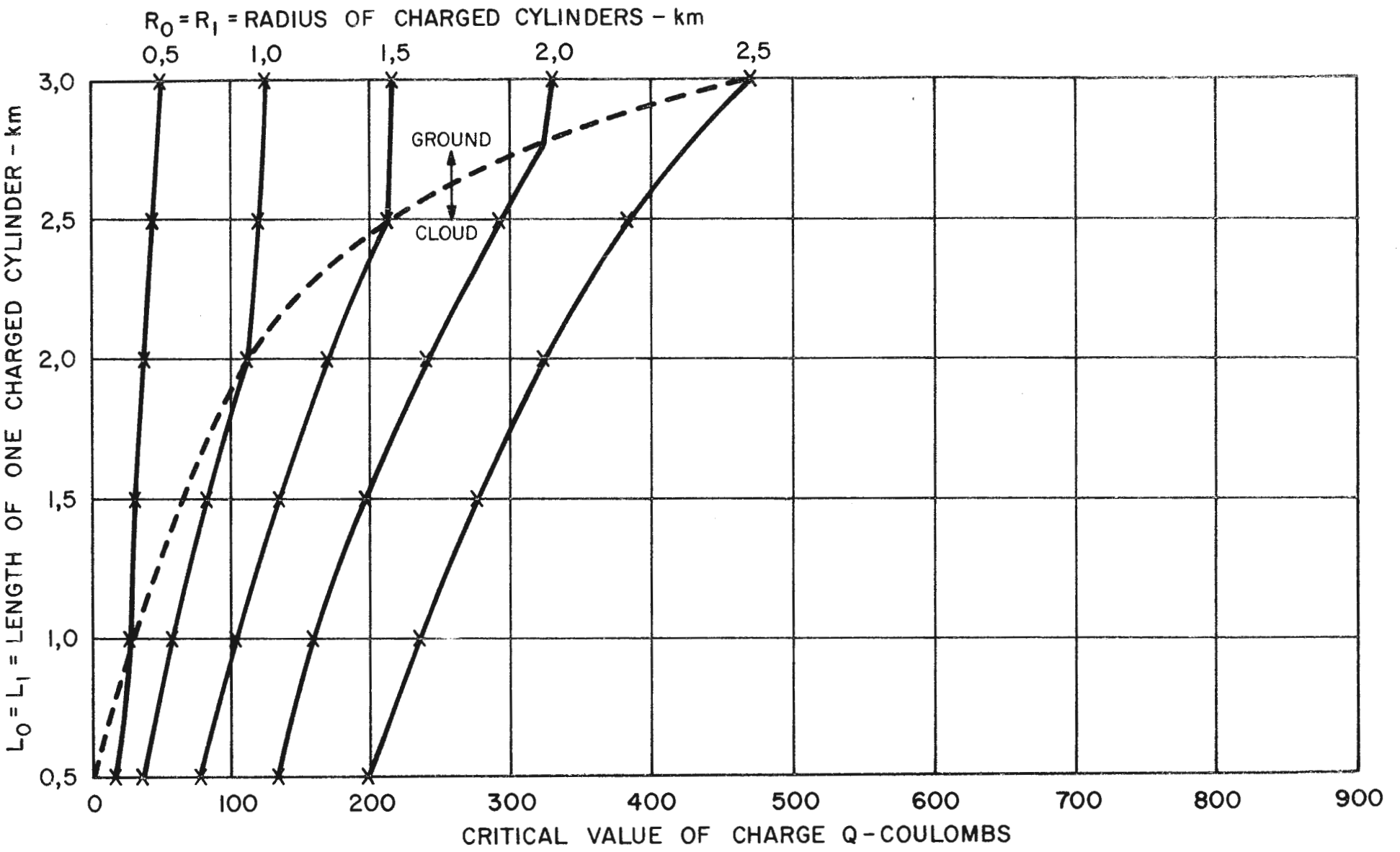

FIGURE 3.1.4 PART II APPENDIX I

$H = 4\,km \quad Q_0 = +Q \quad Q_1 = -Q \quad R_0 = R_1 \quad L_0 = L_1 \quad E = 1 \times 10^6\ V/m$

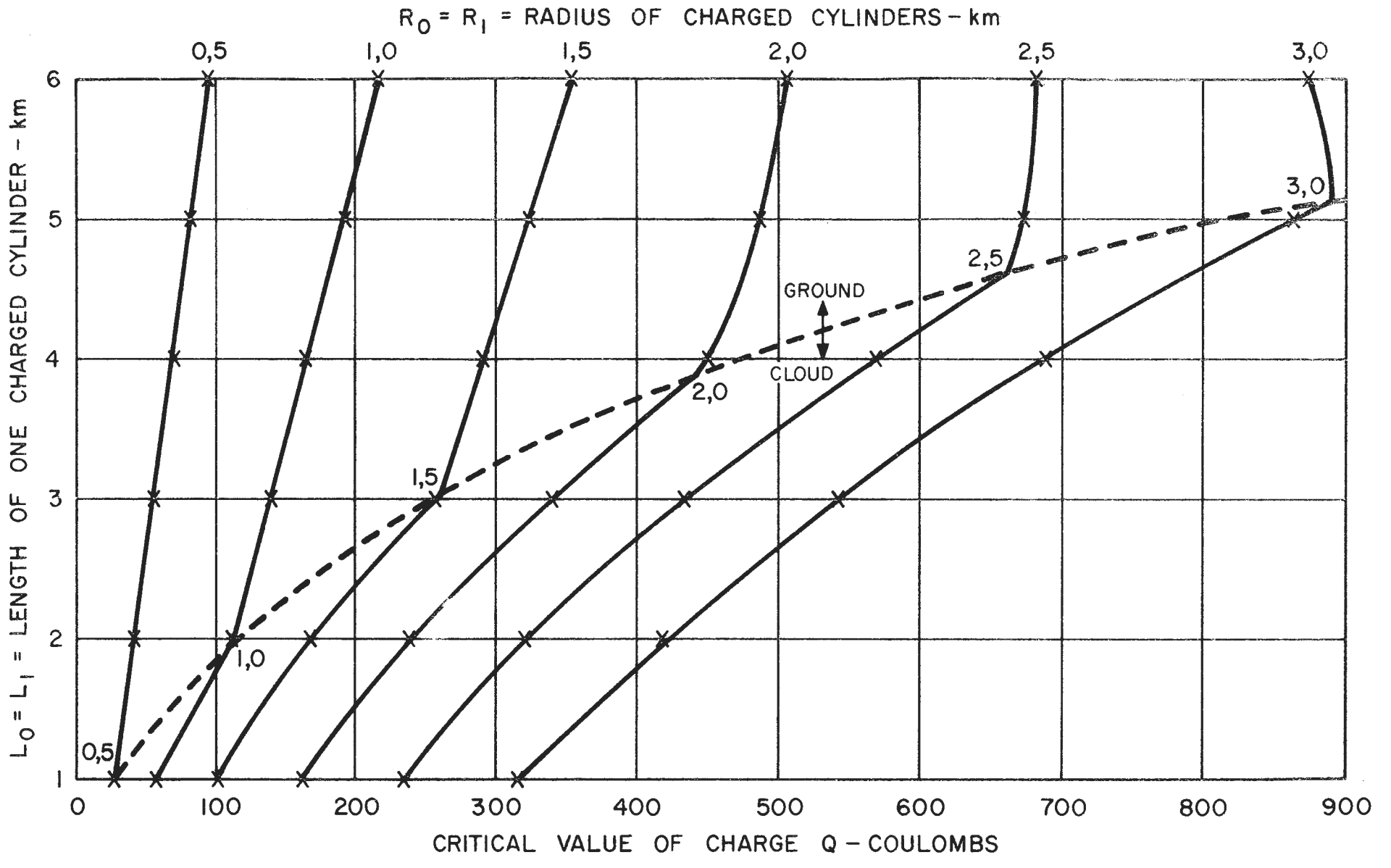

FIGURE 3.1.5 PART II APPENDIX I

H = 8 km $Q_0 = +Q$ $Q_1 = -Q$ $R_0 = R_1$ $L_0 = L_1$ $E = 1 \times 10^6$ V/m

charge build up is least.

Furthermore the quantity of charge involved in the more active and extensive charge separation process when the value of R is large, is very much greater for discharges to ground than for small values of R. It follows that the more active thunderstorms, whilst tending to produce intra-cloud discharges more frequently, would also tend to produce ground discharges involving the larger quantities of charge. From this it may be inferred that in terms of high thunder= storm activity, ground flashes of lightning, although in the minority would nevertheless be more severe than in times when the thunderstorm activity is less intense.

4. Critical parameters of the bi-polar cylindrical charge model

In order to determine the critical values of charge, cylinder radius for any given conditions of the respective lengths of the positive and negative charge cylinders, a further computor program was devised. The lengths of cylinder namely L_o and L_1 were varied over a range accor= ding to whether H was taken as 4 or 8 km. It was also assumed that the charges may not be equal, and that ratio of the negative charge quantity to that of the upper positive charge was varied from 0,5 to unity.

The program was then arranged to calculate the critical value of R, assuming that this was the same for both charges, which would produce an equal value of field intensity at the points B and C Fig. 3.1.3 - that is at the charge separation area and the lower extremity respectively.

Having calculated the critical value of R, the corres= ponding critical value of the positive charge Q was calcu= lated which would give rise to an equal field intensity of $1.x10^6 V/m$ at the two points, and also the maximum charge density all on the assumption of a linear charge distribu= tion of course.

The position of zero intensity was also interpolated in terms of the fraction of the length of the lower negative charged cylinder, in order that its relative movement could

22/...

be studied. It was also needed for the calculation of the maximum potential existing within the charged negative cylinder as a second part of the program.

The volume of data so produced in the form of tables is so large that it is doubtful if it would serve any useful purpose reproducing it here in full. Accordingly it is proposed to indicate only some pertinent results as evidence of a cross section of the data by means of tables and curves as follows:-

Length L_1 Lower Charge Cylinder	Body of Table indicates Critical Values of Radius R - km					
	Length of upper positive charge cylinder - L_o km					
km	1	2	3	4	5	6
0,5	0,42	0,64	0,83	0,98	1,14	1,28
1,0	0,49	0,84	1,10	1,33	1,56	1,79
1,5	0,49	0,95	1,30	1,62	1,94	2,29
2,0	0,45	1,03	1,49	1,93	2,41	2,97
2,5	0,41	1,11	1,74	2,42	3,23	4,25
3,0	0,36	1,28	2,33	3,48	4,73	6,01

Table 4.2.1 Critical Values of the Radius R of charged cylinders for $Q_o = +Q$; $Q_1 = -Q$; H = 4 km.

Length L_1 Lower Charge Cylinder	Body of Table indicates Critical Values of R - km					
	Length of upper positive charge Cylinder - L_o - km					
km	1	2	3	4	5	6
0,5	0,27	0,45	0,59	0,71	0,82	0,92
1,0	0,27	0,53	0,74	0,90	1,06	1,21
1,5	0,22	0,55	0,81	1,02	1,22	1,40
2,0	0,18	0,53	0,84	1,10	1,35	1,59
2,5	0,14	0,50	0,85	1,18	1,49	1,81
3,0	0,12	0,47	0,89	1,32	1,75	2,20

Table 4.2.2 Critical values of the radius R of charged cylinders $Q_o = +Q$; $Q_1 = -0,5\ Q$; H = 4 km.

23/...

A comparison between tables 4.2.1 and table 4.2.2 indicates generally that if the lower negative charge is less than the upper charge, the critical radius for any configuration of the respective length of the charged cylinders is also less. This means, as would be expected, that the critical ratios of L/R are increased in consequence of which it would be more difficult to initiate discharge from the lower end of the cylinder. However a discharge could be initiated under these conditions but there would be a limiting point beyond which this could not happen, for example when the quantity of negative charge tends to zero.

The table 4.2.3 indicates the values of the critical radius R for H = 8 km and these are in general less than the values for H = 4 km.

Length L_1 Lower Cylinder km	Body of Table indicates Critical Values of Radius R - km					
	Length of upper positive charge cylinder - L_o - km					
	1	2	3	4	5	6
1	0,48	0,83	1,07	1,28	1,47	1,65
2	0,44	0,98	1,35	1,67	1,94	2,19
3	0,33	0,98	1,49	1,90	2,26	2,60
4	0,24	0,91	1,54	2,06	2,53	2,97
5	0,18	0,81	1,54	2,22	2,86	3,48
6	0,14	0,71	1,59	2,56	3,58	4,65

Table 4.2.3 Critical Values of the Radius R of charged cylinders $Q_o = +Q$; $Q_1 = -Q$; H = 8 km.

Figures 4.1.1 and 4.1.2 attached indicates the results of the above tables graphically for the case of $Q_o = -Q$, and H = 4 km and H = 8 km respectively.

Comparing the effect of differing heights namely Table 4.2.1 and Table 4.2.3 for H = 4 and H = 8 km respectively, the differences between the critical radius are small when the lengths of the charges are small. However at the limits, for example when L_1 = 3 km and L_o = 6 km. The critical radius is much larger for the 4 km case,

24/...

XG4-1781

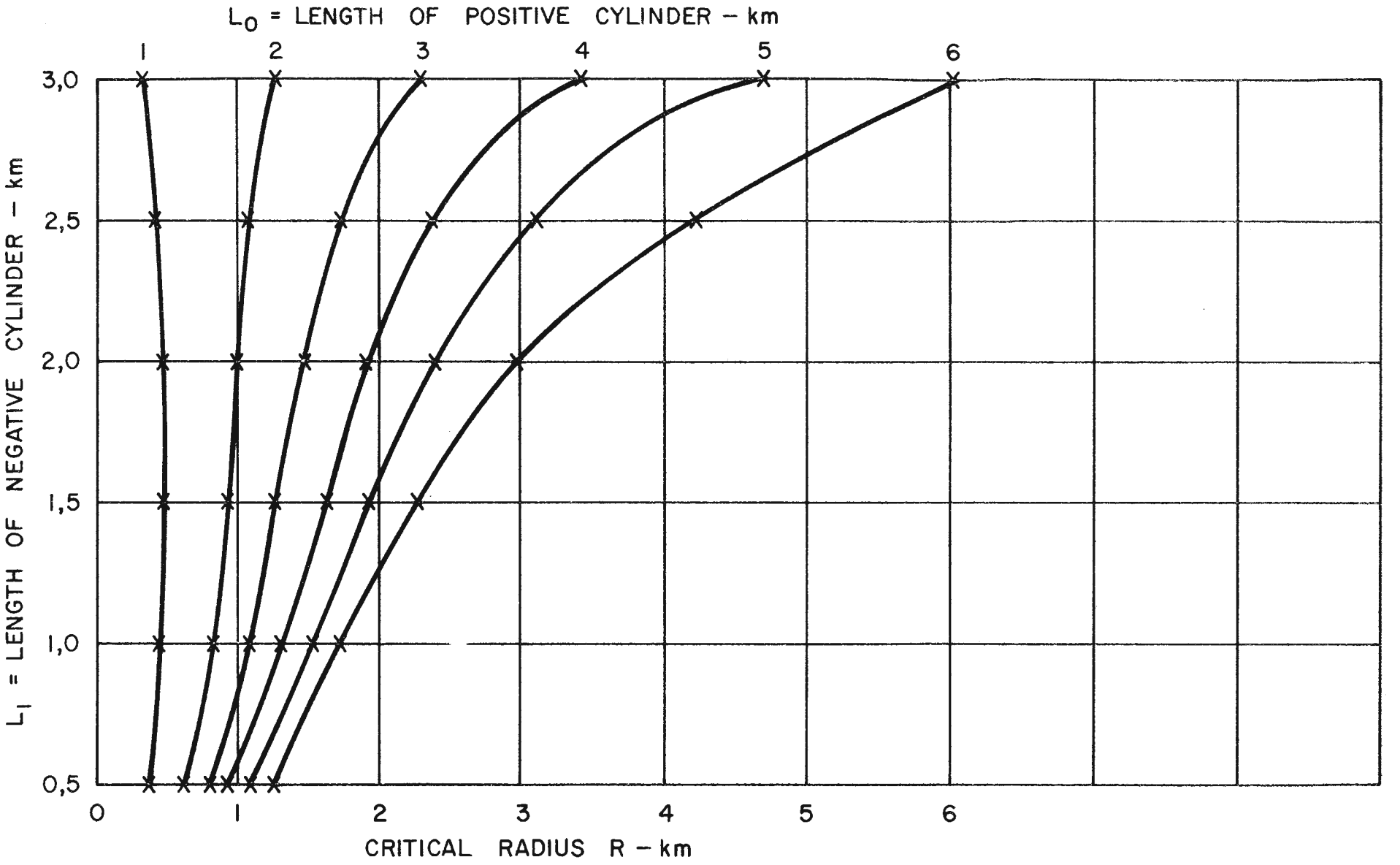

FIGURE 4.1.1 PART II APPENDIX I

$H = 4\,km \quad Q_0 = -Q_1 \quad R_0 = R_1 \quad E = 1 \times 10^6\ V/m$

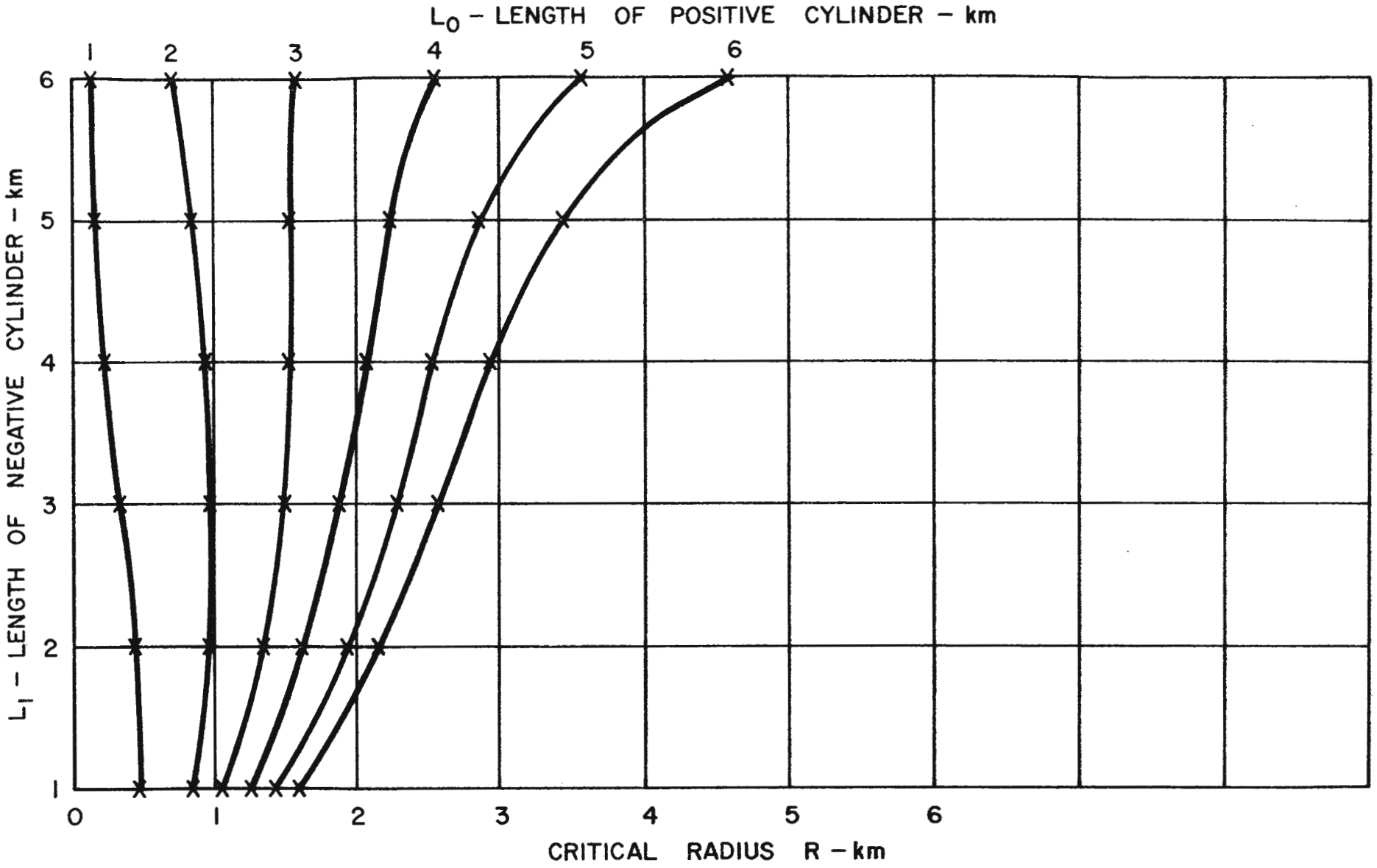

FIGURE 4.1.2 PART II APPENDIX I

$H = 8\,km \quad Q_0 = -Q_1 \quad R_0 = R_1 \quad E = 1 \times 10^6\ V/m$

resulting in much smaller values of the ratio L/R. Conse= quently the effect of ground in this case has become more evident towards the end of the separation process, but it would have little influence during the initial stages. Hence intra-cloud discharges can occur equally readily whether charge separation takes place at 4 or 8 km altitude, but discharges towards ground are more probable at the later stage when H = 4 km than they are when H = 8 km.

The following Table 4.2.4 shows the value of the ratio 2L/R, assuming $L_o=L_1=L$ and for equal charges.

(a) Length L km	Value of 2L/R for $Q_o=Q_1$		(b) Ratio 2L/H	Ratio 2L/R
	H = 4 km	H = 8 km		
1	4,06	4,14	0,25	4,14
2	3,88	4,08	0,50	4,07
3	2,58	4,03	0,75	4,03
4	-	3,89	1,00	3,88
5	-	3,50	1,25	3,50
6	-	2,58	1,50	2,58

Table 4.2.4 (a) Value of Critical Ratio 2L/R for two altitudes and for equal charges $L_o=L_1=L$ and $Q_1=-Q_o$
(b) Normalised values per unit H.

The values of 2L/R shown on table 4.2.4 are obviously equal for unit value of L/H indicating the equivalence of the two cases by means of their gemoetric configuration. Hence one value of the critical ratio 2L/R can be found for each value of 2L/H, and this simplifies the understanding of the data. For example for 2L/H = 1,5 then 2L/R = 2,58 and so on, and it is therefore clear that the effect of earth starts to become significant when 2L/H is 1,0 or greater, since the critical ratio when remote from earth is approxi= mately 4,0 as previously derived from Fig. 3.1.2 attached.

By definition, the critical values of R calculated for each case are those for which the field intensity in the region of charge separation equals that at the lower extre= mity, that is to say the probability of a discharge starting

25/...

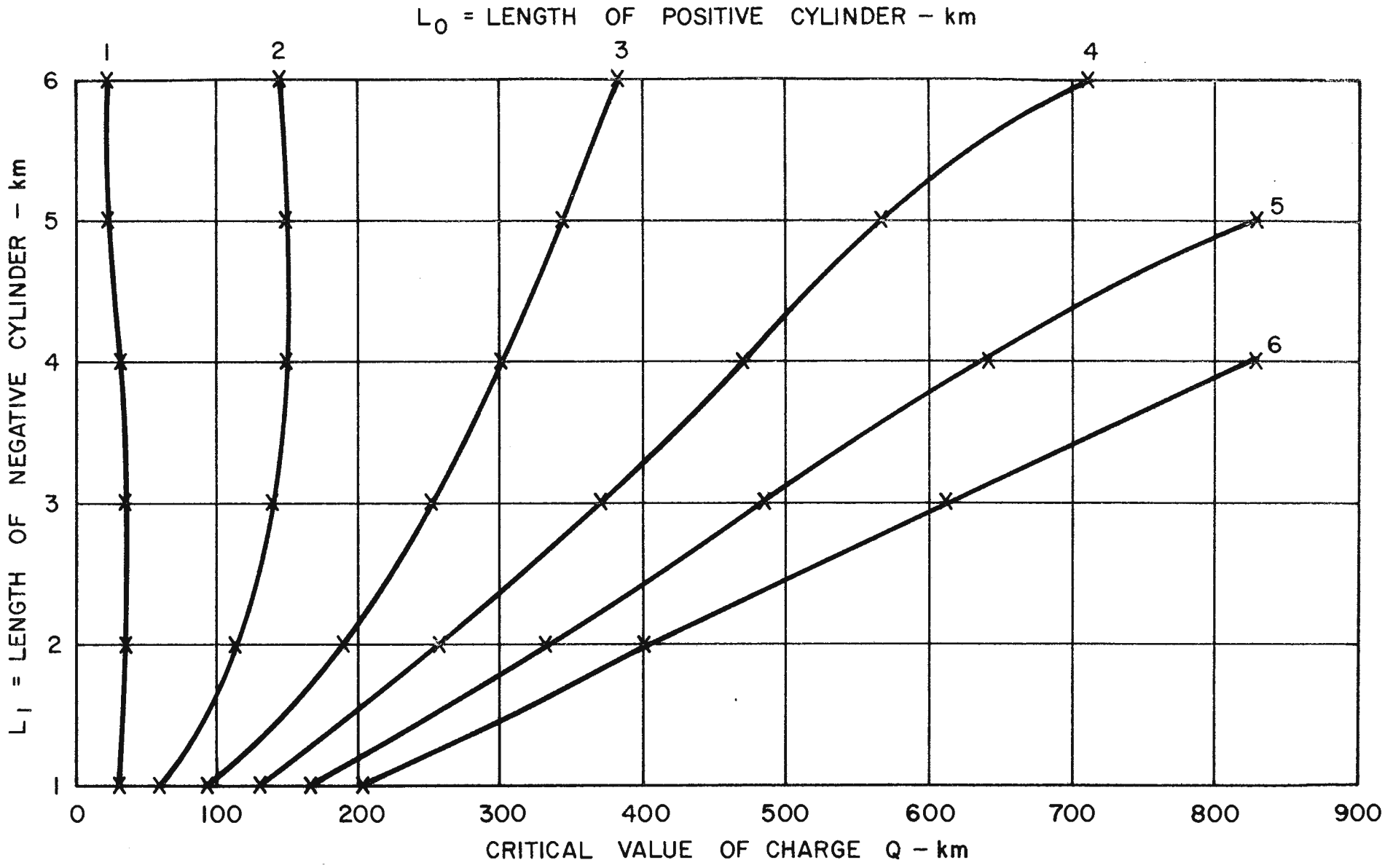

FIGURE 4.1.4 PART II APPENDIX I

$H = 8\,km \quad Q_0 = +Q \quad Q_1 = -Q \quad R_0 = R_1 \quad E = 1 \times 10^6\ V/m$

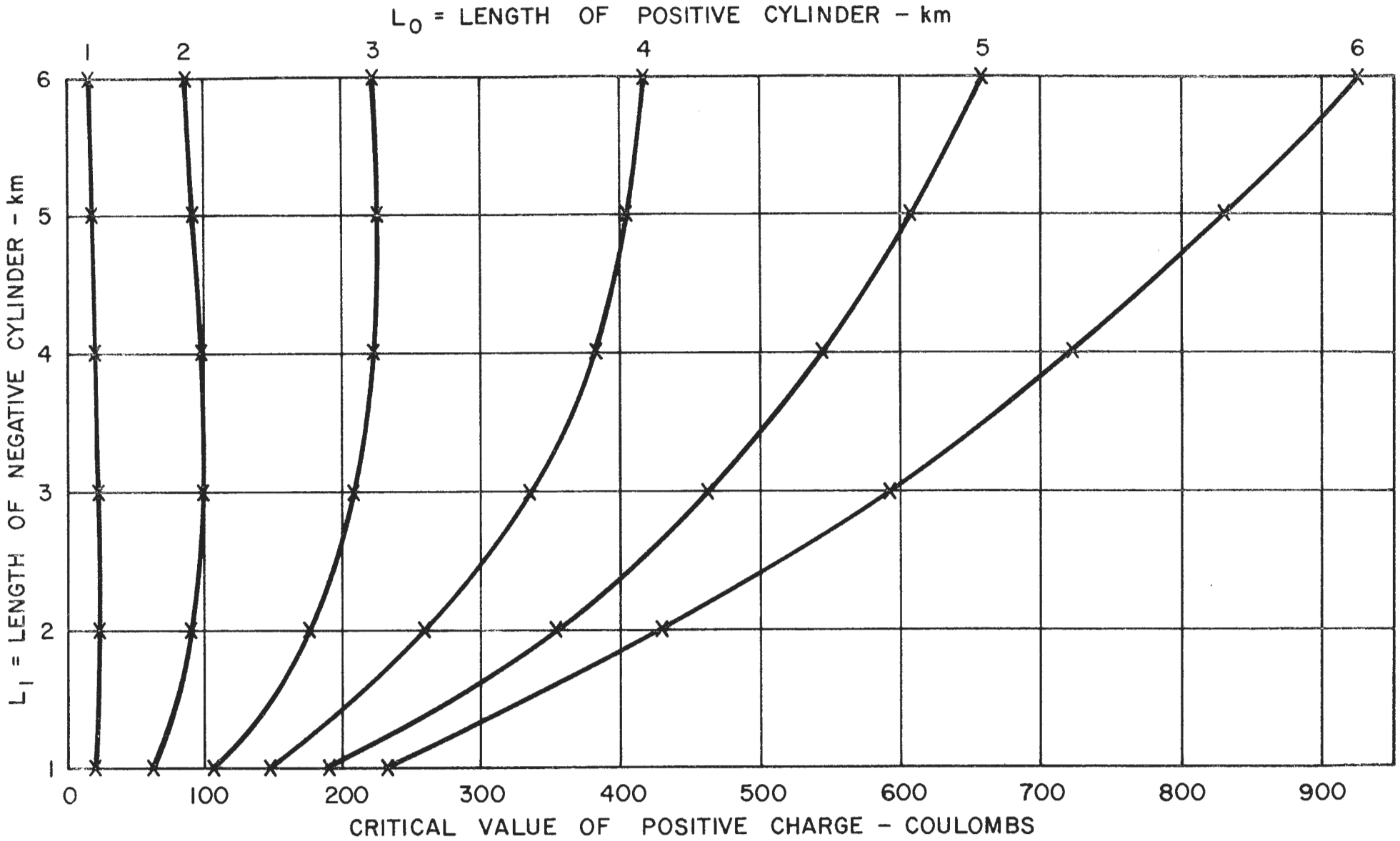

FIGURE 4.1.5 PART II APPENDIX I

$H = 8\,km \quad Q_0 = +Q \quad Q_1 = -0{,}5Q \quad R_0 = R_1 \quad E = 1 \times 10^6\ V/m$

of $1/H^2$ as indicated in the last column. This relationship, as with that of the critical radius R, follows from the geometry of the arrangement if normalised to the basis of per unit H, and the inverse square proportion arises from the fact that the field intensity at differing altitudes is inversely proportional to the square of the distance between the charge and its image. However, once again it is demonstrated that the effect of earth is small during the initial stages of separation; for example up to a cylinder length of 2 km the critical charge is practically the same whether the charge separation zone is at 4 km or 8 km hence the probability of a discharge to ground during this period is remote in either case, but the probability of an intra-cloud discharge is about equal if the rate of charge separation is equal. If the critical values of charge are not reached during the early stages of separation, then the effect of earth becomes more prominent thereafter, and this affects discharges to ground. According to table 4.2.5 more charge has to be accumulated at L = 3 km for H = 4 compared with H = 8 km, thus apparently favouring ground discharges at H = 8 km. This result is misleading however, because the critical ratio 2L/R has to be in excess of 4 for H = 8 km compared with 2,58 for H = 4km before a ground discharge can take place; hence the results of Table 4.2.5 must be viewed in conjunction with those of Table 4.2.4.

5. <u>The Potential of a cylindrical charge model</u>

The calculation of the potential at any point along the centre line of a cylindrical charge is effected in a similar manner to that of the calculation of field intensity described is Section 2; this also results in a standard form of equation the derivation of which will be demonstrated in the two examples which follow. Thereafter it is merely necessary to state the value of the constants to be used for any other variation.

27/...

The following Figure 5.1.1 illustrates the case of a charge distributed in a cylinder of length L and radius R, situated for convenience beneath the charge separation area which is at an altitude of H above ground. The charge dis= tribution is assumed to be linear, that is zero at the altitude H and increasing uniformly to a maximum at the lower end of the cylinder.

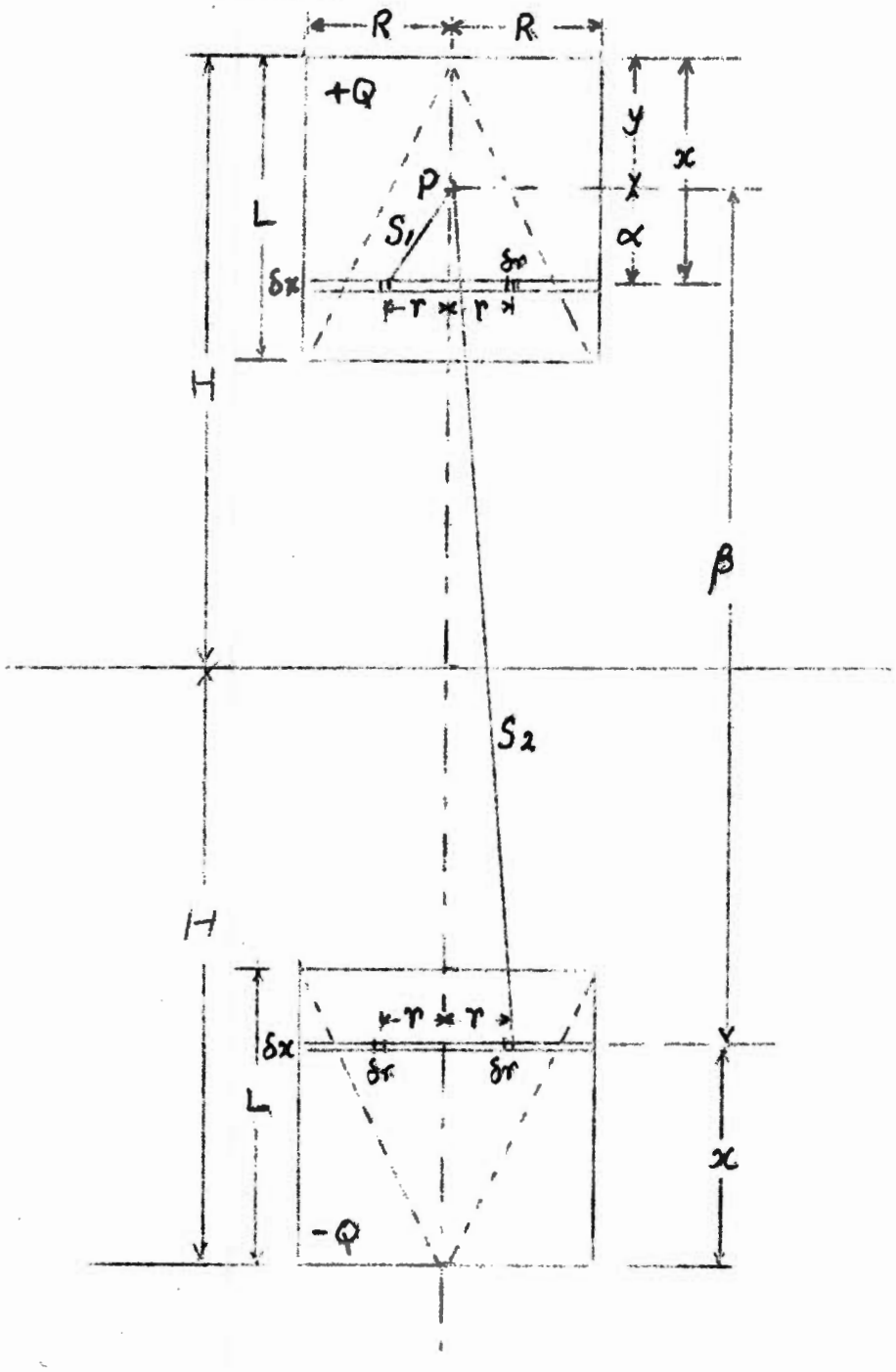

Figure 5.1.1 Diagram illustrating the calculation of the potential at the point P due to portion of charge lying below P.

28/...

As in Section 2 the charge density is expressed as follows:-

$$q' = 2Qx/\pi R^2L^2 \text{ clbs/m}^3 \qquad (5.1)$$

The charge on an annular ring of radius r, width δr and thickness δx situated at x from the one end is also as previously derived namely

$$\delta q = 4Qr.\delta r.x.\delta x/R^2L^2 \qquad \text{clbs} \qquad (5.2)$$

The potential at P due to the increment of charge δq is then:-

$$\delta V = \delta q/4\pi\epsilon.[1/S_1 - 1/S_2] \qquad (5.3)$$

Where $S_1 = (\alpha^2+R^2)^{\frac{1}{2}}$ $\alpha = x - a$ $a = y$

and $S_2 = (\beta^2+r^2)^{\frac{1}{2}}$ $\beta = b - x$ $x = 2H-y$

(The reason for putting y = a will become clear below) Thus the potential at P due to all charge in the cylindrical region lying below P is therefore as follows:-

$$V_1 = Q/\Pi R^2L^2.\left\{\int_o^R\int_y^L (\alpha^2+r^2)^{-\frac{1}{2}}\, r.dr.x.dx \quad \ldots \right.$$
$$\left. -\int_o^R\int_y^L (\beta^2+r^2)^{-\frac{1}{2}} r.dr.x.dx\right\} \qquad (5.4)$$

First treating x as constant and integrating with respect to r between the limits r = o and r = R.

$$V = Q/\pi R^2L^2.\left\{\int_y^L [(x - a)^2+R^2]^{\frac{1}{2}}x\, dx \right.$$
$$- \int_y^L (x-a)\, x\, dx - \int_y^L [(b-x)^2+R^2]^{\frac{1}{2}}\, x\, dx$$
$$\left. + \int_y^L (b-x)x\, dx \right\} \qquad (5.5)$$

29/...

Rewriting (5.5) as follows for easier handling:-

$$V = Q/\pi R^2 L^2 \left\{ I(a) + I(b) + II(a) + II(b) \right\} \qquad (5.6)$$

Where I(a), I(b), II(a) II(b) are the above integrals in sequence:-

Each part is then integrated with respect to x between the limits x = y and x = L with the following results:-

$$I(a) = R^3/2 \left\{ a/R \sinh^{-1} [(L-a)/R] - a/R \sinh^{-1}[(y-a)/R] \right.$$
$$+ 2/3 \left[1 + (L-a)/R]^2\right]^{3/2} - 2/3 \left[1 +[(y-a)/R]^2\right]^{3/2}$$
$$+ a/R[(L-a)/R][1+[(L-a)/R]^2]^{\frac{1}{2}}$$
$$\left. - a/R [(y-a)/R] \left[1+[(y-a)/R]^2\right]^{\frac{1}{2}} \right. \qquad (5.7)$$

When a = y equation (5.7) simplifies to the following:-

$$\text{Hence } I(a) = R^3/2 \left\{ y/R \sinh^{-1}[(L-y)/R] + 2/3 \left[1+[(L-y)/R]^2\right]^{3/2} \right.$$
$$\left. - 2/3 + y/R[(L-y)/R] \left[1+ (L-y)/R]^2\right]^{\frac{1}{2}} \right\} \qquad (5.8)$$

$$\text{Also } I(b) = R^3/2 \left\{ (a/R)(L/R)^2 - 2/3(L/R)^3 - (a/R)(y/R)^2 \right.$$
$$\left. + 2/3 (y/R)^3 \right\} \qquad (5.9)$$

Similarly when a = y, equation (5.9) simplifies to the following:-

$$I(b) = R^3/2 \left\{ (y/R)(L/R)^2 - 2/3(L/R)^3 - 1/3(y/R)^3 \right\} \qquad (5.10)$$

Continuing with the integration of II(a) and II(b) as follows:-

30/...

$$II(a) = R^3/2\Big\{b/R \sinh^{-1}[(b-L)/R] - b/R \sinh^{-1}[(b-y)/R] - 2/3\Big[1+[(b-L)/R]^2\Big]^{3/2} + 2/3\Big[1+[(b-y)/R]^2\Big]^{3/2} + b/R[(b-L)/R]\Big[1+[(b-L)/R]^2\Big]^{\frac{1}{2}} - b/R[(b-y)/R]\Big[1+[(b-y)/R]^2\Big]^{\frac{1}{2}} \qquad (5.11)$$

Where $b = 2H-y$

and $$II(b) = R^3/2\Big\{(b/R)(L/R)^2 - 2/3(L/R)^3 - (b/R)(y/R)^2 + 2/3(y/R)^3\Big\} \qquad (5.12)$$

At this stage attention is drawn to the similarity between the above integrations whether they refer to the upper positive charge involving a = y or whether to the image in which b = 2H-y. Both parts may in fact, and as previously stated, be expressed in a general form as follows:-

$$\text{Part I or Part II} = \Big\{a/r \sinh^{-1}[(a-b)/R] - a/R \sinh^{-1}[(a-c)/R] - 2/3\Big[1+[(a-b)/R]^2\Big]^{3}/2 + 2/3\Big[1+[(a-c)/R]^2\Big]^{3/2} + a/R[(a-b)/R]\Big[1+[(a-b)/R]^2\Big]^{\frac{1}{2}} - a/R[(a-c)/R]\Big[1+[(a-c)/R]^2\Big]^{\frac{1}{2}} + a/R(b/R)^2 - 2/3(b/R)^3 - a/R(c/R)^2 + 2/3(c/R)^3\Big\} \qquad (5.13)$$

Hence the general form of the equation for potential can be written

$$V = QR/2\pi\epsilon L^2.\Big\{\pm \text{Part I} \pm \text{Part II}\Big\} \qquad (5.14)$$

In this particular case the sign of the Part and the constants a,b,c in (5.13) would be assigned the following values.

31/...

$$V_1 = QR/2\pi\epsilon L^2 \cdot \left\{ -\text{Part I}[a=-y,\ b=-L,\ c=-y] + \text{Part II}\ [a=2H-y,\ b=L,\ c=y] \right\} \qquad (5.15)$$

Hence it will be most convenient for future similar statements of potential to use the above general form

Proceeding therefore to the remainder of the calculation for the potential at P this time due to the portion of charge situated in the cylinder above point P, it is convenient to express the equation as follows with an illustration.

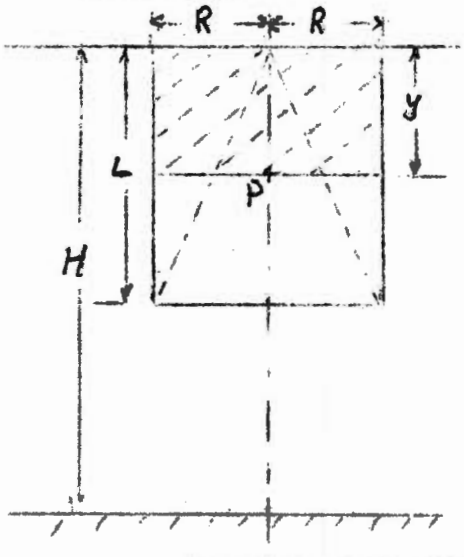

Potential at P due to charge situated above P:-

$$= V_2 = QR/2\pi\epsilon L^2 \cdot \left\{ \begin{array}{cc} -\underline{\text{Part I}} & + \underline{\text{Part II}} \\ a = y & a = 2H-y \\ b = y & b = y \\ c = o & c = o \end{array} \right\} \qquad (5.16)$$

Hence the potential at P due to all charge in the cylinder is simply V_1+V_2.

Dealing now with the potential at P due to the upper positive charge, the equation of potential is as given below:

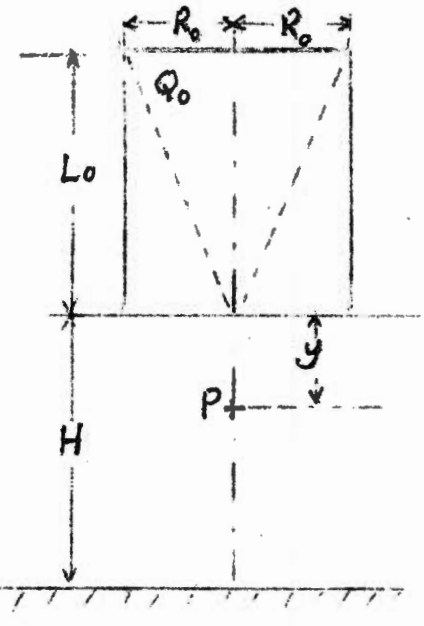

Potentital at P due to the upper positive charge

$$V_o = Q_o R_o/2\pi\epsilon L_o^2 \cdot \left\{ \begin{array}{cc} -\underline{\text{Part I}} & + \underline{\text{Part II}} \\ a = y & a = 2H-y \\ b = -L_o & b = -L_o \\ \underline{c = o} & \underline{c = o} \end{array} \right\} \qquad (5.17)$$

32/...

In order to calculate the potential at P due to the effect of both the upper positive and the lower negative charge, the basic dimensions being Q_o, L_o R_o and H and Q_1, L_1, R_1 and H, respectively, and assuming that the quantity of charge in the lower cylinder is perhaps less than that of the upper by a fraction p say, then by putting $Q_o = +Q$ and $Q_1 = -pQ$, the above expressions are calculated and the resultant potentials added.

6. Potentials of a bi-polar model

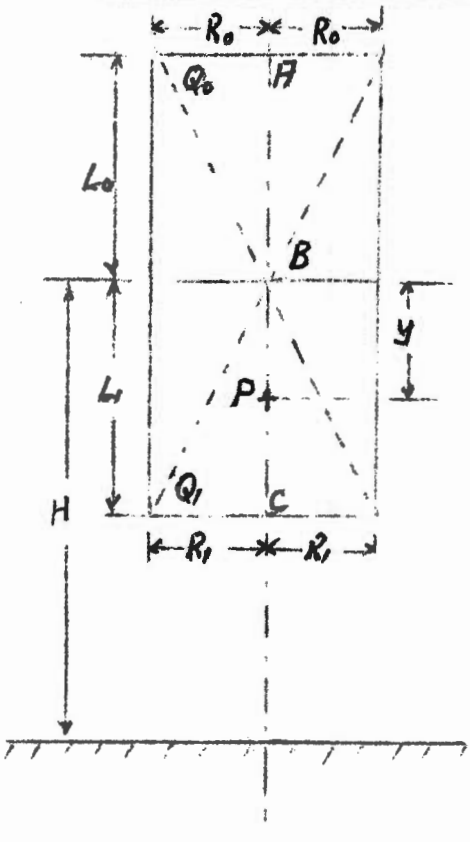

Referring to the diagram, the potential at P at any distance y from the charge separation level at B is given by the sum of the potentials due to the various portions of charge described in section 5.

The portion of the cylinder between B and C is of most interest in view of the possibility of a lightning discharge originating in this region and in this regard it is of interest to note that the potential at B must be close to zero and that maximum positive potentail must exist at some point between A and B closer to A (in view of the charge distribution assumed) whereas maximum negative potential must exist on the line between B and C and closer to C. The position of maximum potential must necessarily coincide with that of zero field intensity and this in fact leads to the method of its its calculation.

The computor program was first arranged to solve for the value of y lying between B and C which resulted in zero field intensity, and this was done for a number of conditions of differing lengths of L_o and L_1 and of charges Q_o aand Q_1 but it was assumed for the purpose of calculation that $R_o = R_1$.

33/...

This turned out to be an iterative process of some complexity in view of the type of expressions which had to be employed, and the programming was undertaken by a member of the Numerical Analysis Division of the CSIR as duly acknowledged at the conclusion of this appendix. Some of the results are indicated in figures 6.1.1 and 6.1.2 indicating the value of "K_o" in the relation $y_o = K_o L_1$ when the field intensity is zero for conditions of equal charges and for H = 4 and 8 km respectively.

These figures show that the range of the factor K_o varies between about 0,71 to about 0,81 for the conditions assumed for H = 4 km, and from 0,75 to 0,85 for the 8 km case, indicating the fact that zero intensity is located fairly close to the lower extremity, and hence also the maximum negative potential. Hence when considering a discharge starting towards ground from the lower end, the position of zero field intensity lies within a relatively short distance. At the same time the potential at the start of the discharge is likely to be very high as will be further discussed later.

The following Table 6.2.1 gives some values of K_o for the case when $Q_1 = -Q_o$ and $L_o = L_1$, namely the condition which exists at the start of a discharge when H = 4 km and 8 km.

(a) Length L of cylinder	Factor K_o for Zero Field Intensity		(b) Ratio 2L/H	K_o
km	H = 4 km	H = 8 km		
1,0	0,781	0,782	0,25	0,782
2,0	0,775	0,781	0,50	0,781
3,0	0,738	0,779	0,75	0,779
4,0	-	0,775	1,00	0,775
5,0	-	0,764	1,25	0,764
6,0	-	0,738	1,50	0,738

Table 6.2.1 (a) Values of the factor K_o as a fraction of L indicating the position of zero field intensity and maximum potential within the lower negative charged cylinder. $Q_1 = -Q_o$ $L_o = L_1$

(b) Normalised Values per unit H.

34/...

XG4 - 1786

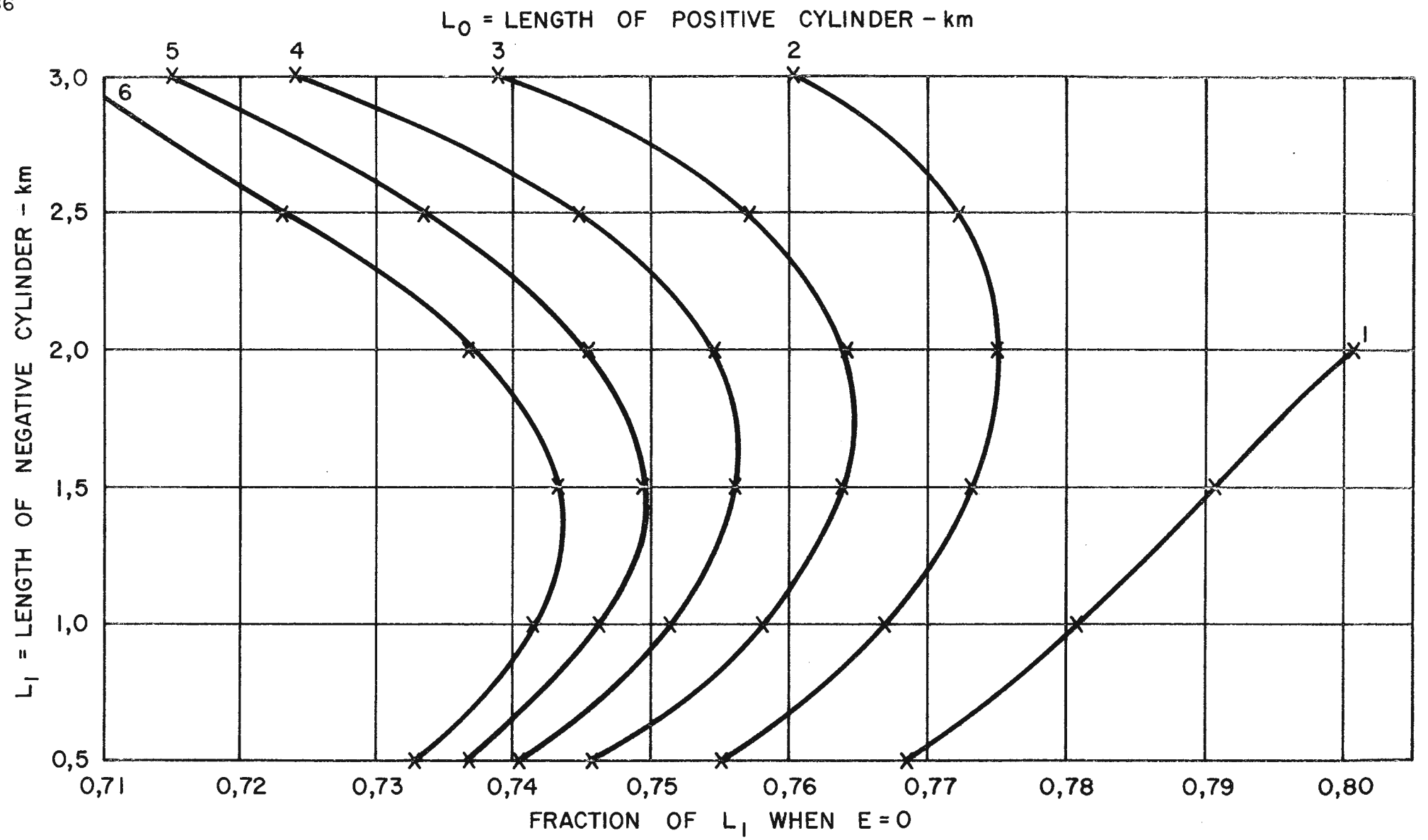

FIGURE 6.1.1 PART II APPENDIX I

$H = 4km \quad Q_0 = +Q \quad Q_1 = -Q \quad R_0 = R_1$

XG4-1787

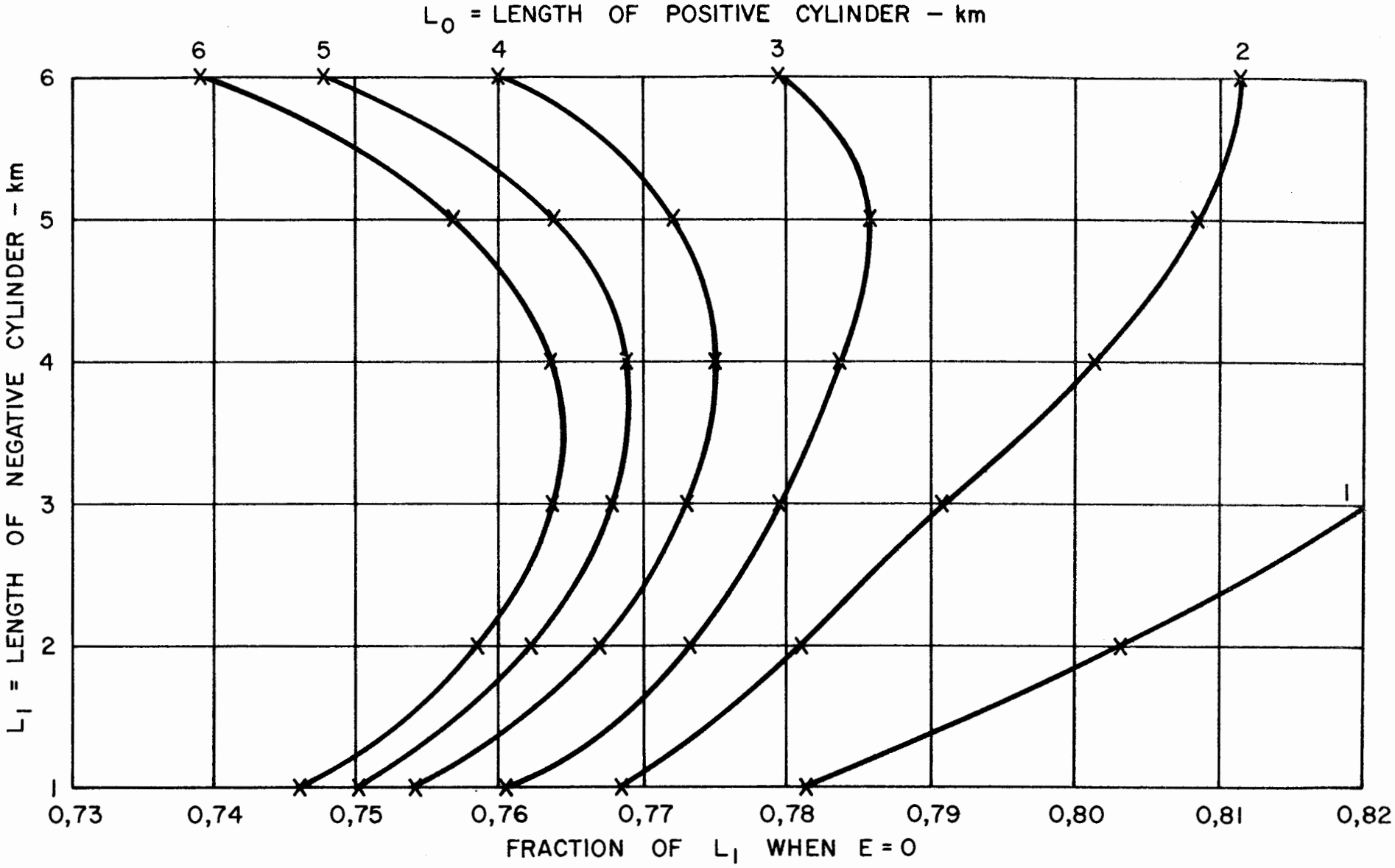

FIGURE 6.1.2 PART II APPENDIX I

H = 8km $Q_0 = +Q$ $Q_1 = -Q$ $R_0 = R_1$

The above table also shows the values of K_o for the corresponding ratio of 2L/H and this again indicates the dependance upon the geometric symmetry of the arrangement whether at H = 4 or H = 8 km.

Having once found the value of K_o for any particular case, by putting $y = K_o L_1$ in the respective equations listed in section 5 and the critical values of Q and R as calculated before, the potentials existing at any point can be calculated for these critical conditions.

Since they refer to the critical conditions they are termed critical potentials and would therefore be defined as the potentials which would occur if breakdown conditions of $E = 1 \times 10^6$ V/m occur simultaneously at both the charge separation area B or the lower extremity C. They are therefore representative values of the potential for these conditions.

The following Table 6.2.2 gives values of the maximum critical potentials which occur for the conditions when $Q_1 = -Q_o$ and $L_o = L_1$ and for H = 4 km and 8 km showing also the dependence upon the geometry of the arrangement.

Length L of Cylinder Km	(a) Maximum Critical Potential		(b) Ratio 2L/H	VMax/H
	H = 4 km	H = 8 km		
1	$-0,55 \times 10^9$	$-0,55 \times 10^9$	0,25	$-0,69 \times 10^5$
2	-1,04 "	-1,10 "	0,50	-1,38 "
3	-1,27 "	-1,63 "	0,75	-2,03 "
4	-	-2,10 "	1,00	-2,62 "
5	-	-2,47 "	1,25	-3,09 "
6	-	-2,53 "	1,50	-3,16 "

Table 6.2.2 (a) Maximum Potentials in negative charge cylinder model of bi-polar charges. $Q_1 = -Q_o$ $L_o = L_1$ $R_o = R_1$ (b) Normalised Values per unit H.

The critical potentials indicated in Table 6.2.2 follow the geometric proportionality to 1/H in view of the fact that the potentials are inversely proportional to the distance between the charges and their images, and this is to be compared with Table 4.2.5 where the critical charges

35/...

approximately half the height of the separation area. This effect is not so prominent when H = 8 km, but it is nevertheless present particularly when L_o = 6 km as indicated in Fig. 6.1.5 attached.

36/...

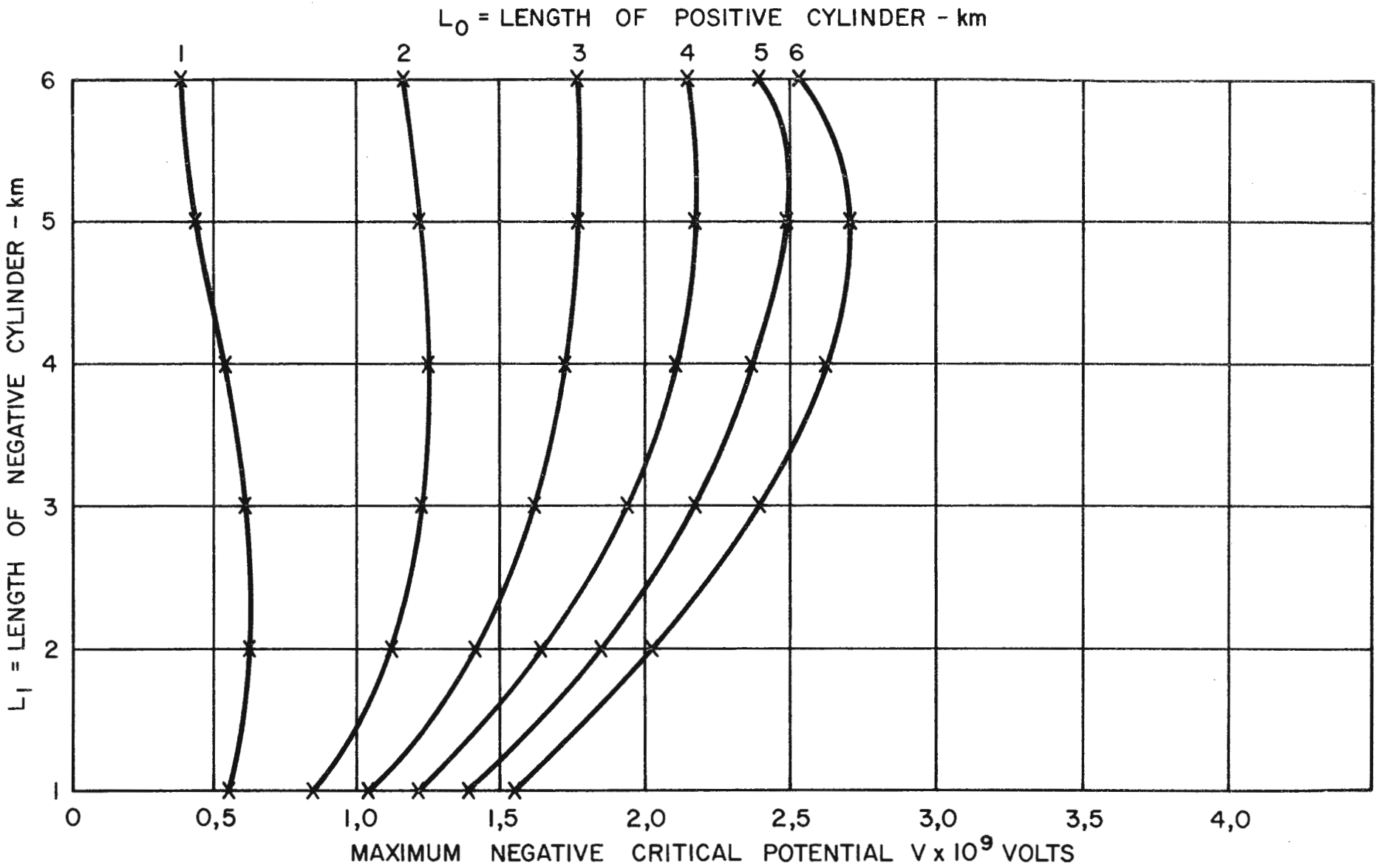

FIGURE 6.1.3 PART II APPENDIX I

$H = 8\,km \quad Q_0 = +Q \quad Q_1 = -Q \quad R_0 = R_1 \quad E = 1 \times 10^6\ V/m$

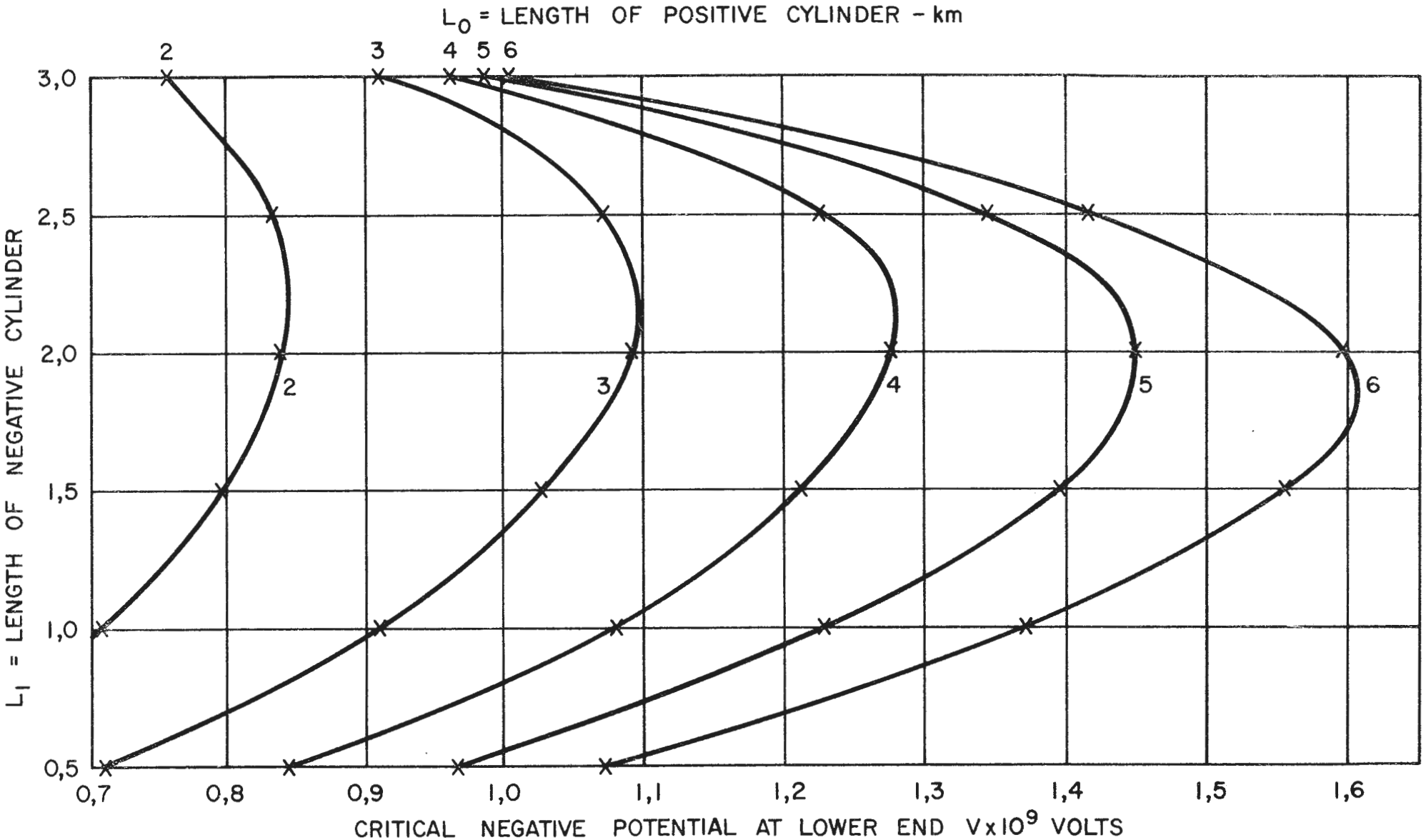

FIGURE 6.1.4 PART II APPENDIX I

$H = 4\,km \quad Q_0 = +Q \quad Q_1 = -Q \quad R_0 = R_1 \quad E = 1 \times 10^6\ V/m$

XG4 - 1790

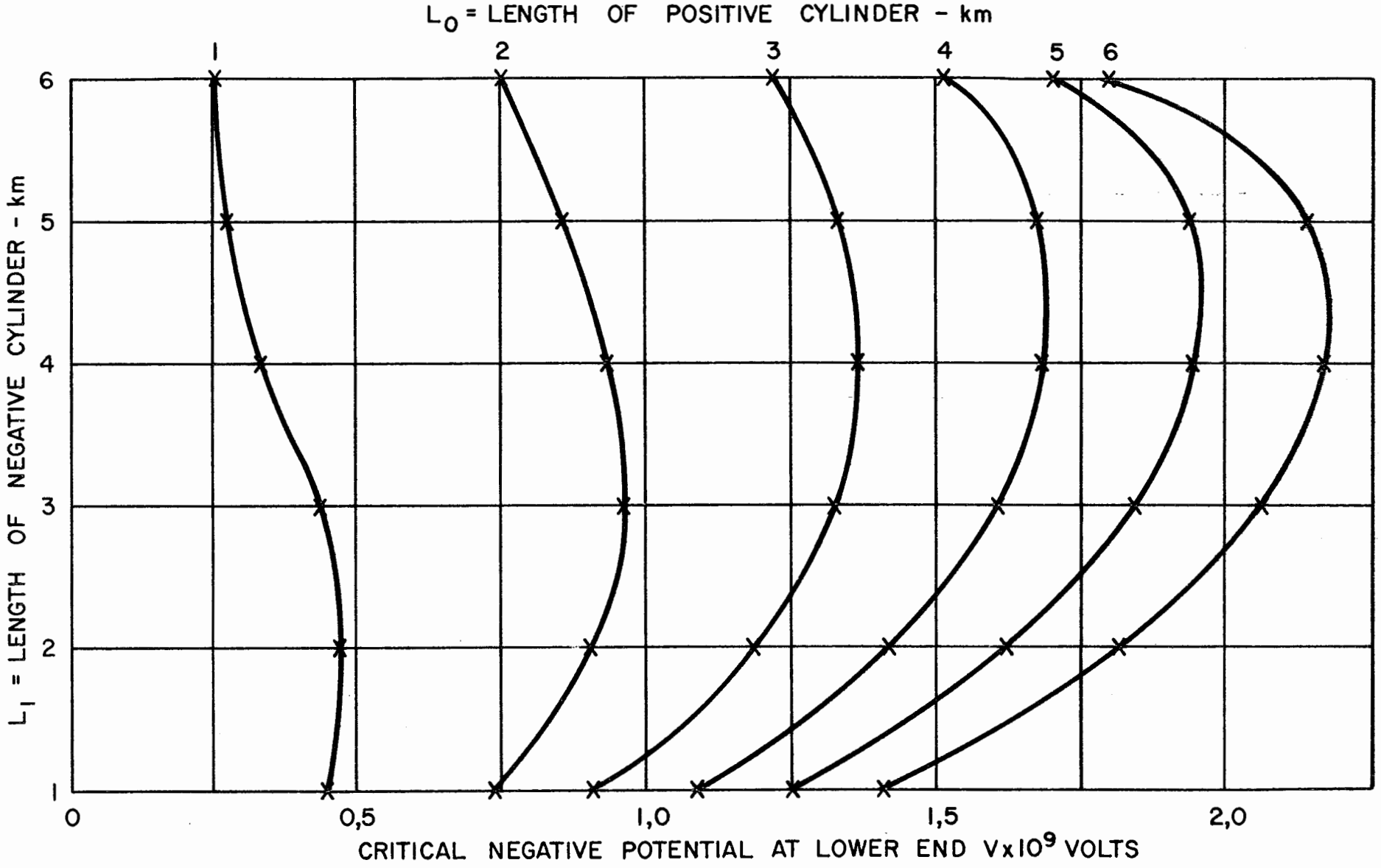

FIGURE 6.1.5 PART II APPENDIX I

$H = 8km \quad Q_0 = +Q \quad Q_1 = -Q \quad R_0 = R_1 \quad E = 1 \times 10^6 V/m$

7. Acknowledgements

The writer acknowledges the great assistance received from Prof. Jacobsz, Head of the Numerical Analysis Division of the National Research Institute for Mathematical Sciences, and the members of his staff. Mr. J.v.R.Stander programmed the data in connection with the multi-parameters of the cylindrical model and Mrs. L.D. Stander undertook further programming and the computer plotting of the figures from his data, thereby enabling the characteristics to be reviewed in great detail.

8. References

Mason B.J. 1953 Tellus pp 446-60.

Stow C.D. " Atmospheric Electricity" Rep. Prog. Phys. Vol. 32 Pt. I (1969) pp 31-42

Workman E.J."The production of Thunderstorm Electricity" Jour. Franklin Inst. Vol. 283 No. 6 June 1967 pp. 544-545.

Part II Appendix II

Description and Flow Chart of Computer Programme for Lightning Discharge Model

by L.O. Stander, Computer Science Division, National Institute for Mathematical Sciences

The programme computes electric field intensities and potentials generated at different positions for each of a number of successive time intervals during a discharge from a cylindrical cloud. Figure 3 is a general flow chart of the programme, in which the field intensities and potentials are referred to by symbol. A description of the model and definitions of the main symbols are to be found in section 12 of Part II.

The total duration of the flash is divided into a number of equal time intervals, and the calculations are made using the appropriate value for time elapsed for each interval. The size of each time interval is calculated as a percentage of the total duration of the flash, and the percentage increase of time at each step is controlled by parameters read in at execution time.

R_2 and R_{z1} are controlled at each step by feedback to the start of calculation as in Figure 1.

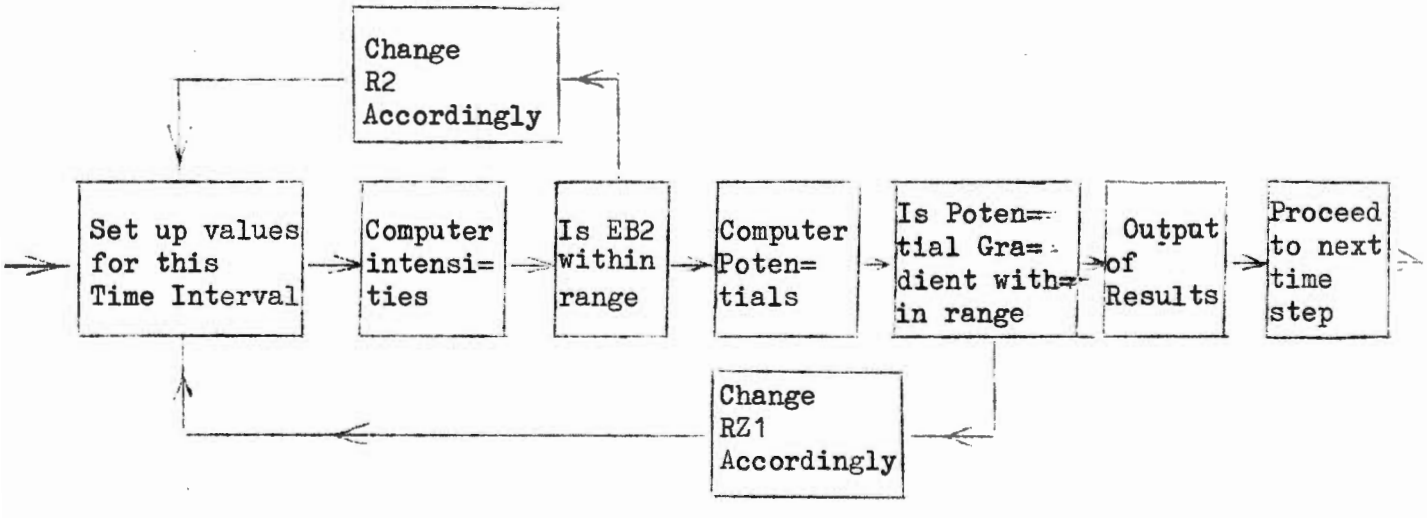

FIGURE 1

In the case of R_2 feedback and recalculation occurs only when EB_2 differs by more than one percent from a control value supplied via data card. Inspection of the potential gradient between positions B_1 and B_2 determines whether R_{z1} needs to be adjusted and the computations repeated or not.

Once both R_2 and R_{z1} are satisfactory, the intensities at ground level and at the top of the cloud are found for the current time step.

If/ .....

If time elapsed is not equal to the duration of the flash, the time is incremented and all calculations are repeated for the next time step.

An option exists to sub-divide the last time interval into 10 smaller, equal steps, and the complete set of calculations is done for each of the smaller steps. To exercise the option an input parameter is set to one of three meaningful values:

0 - terminate normally at the end of the flash without sub-division of the last time step.

1 - subdivide the last time interval into 10 smaller, equal intervals and print out the complete set of results

2 - as for (1), but print out only the last time interval, sub-divided into 10 smaller intervals.

A complete printout, with the option set to 1, is attached to this appendix.

Subroutines called to compute field strengths and potentials

On inspection the formulae used to compute the field intensities and potentials were found to consist of two similar parts, called PART (1) and PART (2) in the programme, differing only in the values assigned to certain of the variables.

As an example, the formula used by the subroutine FIELD to compute electric field intensities due to the upper charge is as follows:

$$E_y = \frac{Q}{2\pi\varepsilon L^2}\left\{\sinh^{-1}\left(\frac{L+y}{R}\right) - \sinh^{-1}\left(\frac{y}{R}\right) - \left(\frac{L-y}{R}\right)\left[1+\left(\frac{L+y}{R}\right)^2\right]^{\frac{1}{2}} - \frac{y}{R}\left[1+\left(\frac{y}{R}\right)^2\right]^{\frac{1}{2}} + \left(\frac{L}{R}\right)^2\right.$$

$$+ \sinh^{-1}\left(\frac{2H+L-y}{R}\right) - \sinh^{-1}\left(\frac{2H-y}{R}\right) + \left(\frac{2H-L-y}{R}\right)\left[1+\left(\frac{2H+L-y}{R}\right)^2\right]^{\frac{1}{2}}$$

$$\left. - \left(\frac{2H-y}{R}\right)\left[1+\left(\frac{2H-y}{R}\right)^2\right]^{\frac{1}{2}} + \left(\frac{L}{R}\right)^2\right\}$$

Inspection shows that it is a linear combination of two parts, where each part is found by computing:

PART (1)/ .....

$$PART(1) = -\sinh^{-1}\left(\frac{A(I)+Z(I)}{R}\right)+\sinh^{-1}\left(\frac{A(I)}{R}\right)-\left(\frac{A(I)-Z(I)}{R}\right)\left[\left(1+\frac{A(I)+Z(I)}{R}\right)^2\right]^{\frac{1}{2}}$$

$$+\left(\frac{A(I)}{R}\right)\left[1+\left(\frac{A(I)}{R}\right)^2\right]^{\frac{1}{2}}-\left(\frac{Z(I)}{R}\right)^2, \qquad I = 1,2$$

The values assigned to R, A(1) and Z(1) are used to compute PART(1), and for PART(2) the appropriate values are assigned to A(2) and Z(2), while R remains the same.

On returning to the main programme, PS = p.PART(1) + q.PART(2), $p = \pm 1$; $q = \pm 1$ is found, and finally the field intensity

$$E = \frac{Q.1.8\times10^8}{B^2} \; . \; PS$$

where Q, an electrical charge, and B a distance are variables.

In the above case the values would be

A(1) = y A(2) = 2H-y

Z(1) = L Z(2) = L

and PS = -PART(1) - PART(2)

Subroutine FLDZ2 uses a modified version of the same formula, and subroutine POT computes the two parts of the formula used for potentials, so that

$$P = \frac{Q.1.8\;\;10^8}{B^2} \quad (p.PART(1) + q.PART(2))$$

with B, p ε q as for field intensities and Q = product of R and a charge, both variable.

Subroutines called in connection with R_2 and R_{z1}

The flow chart shows that acceptable values for R_2 and R_{z1} must be found by iterative processes. In each case the programme stops if the number of iterations exceeds a predetermined limit.

Subroutine ADJUST for R_2

The absolute value of EB_2 and corresponding values of R_2 obtained from preliminary runs suggest a relation as shown in Figure 2.

Graph/ .....

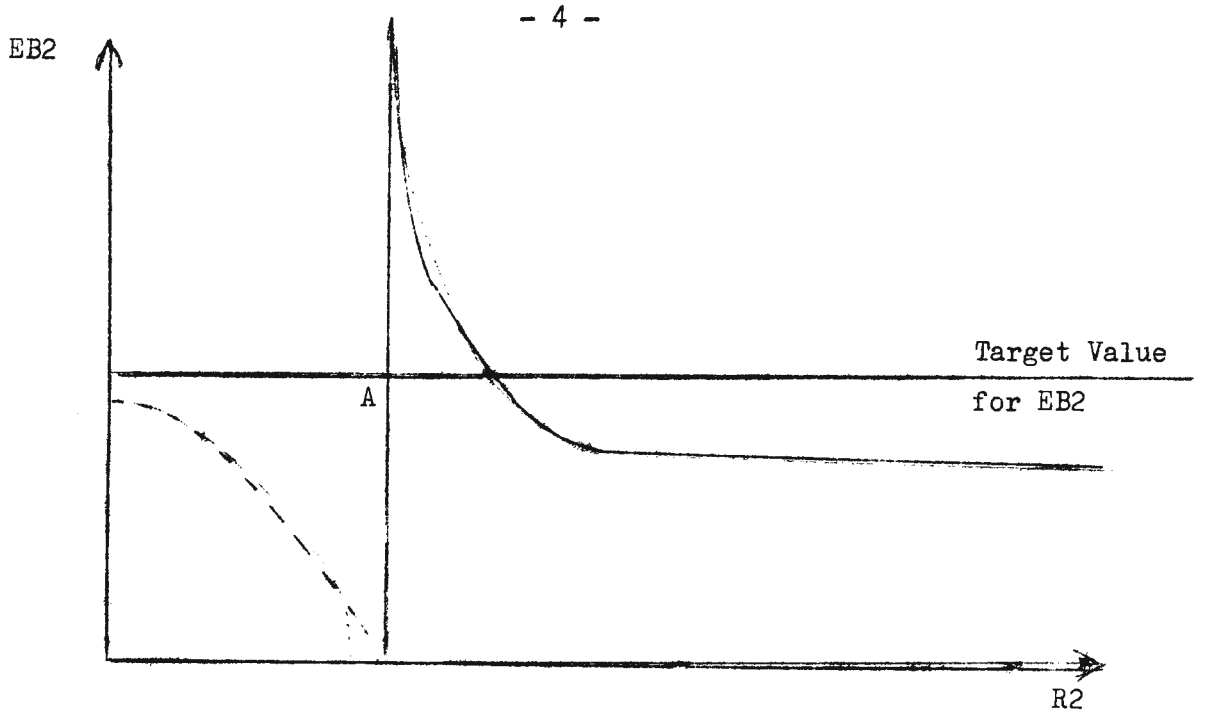

FIGURE 2

Graph of Field Intensity EB_2 versus values of leader R_2 showing location of target value for iterative process

In this paragraph, EB_2 refers to the absolute value of EB_2. As long as EB2 remains less than the target value (read in from a data card), R_2 is decreased by successive bi-section until EB_2 becomes larger than the target value, than averages are used. This method fails if the starting value of R_2 is to the left of A, where the relation is partly guesswork at any rate. If a decrease in R_2 results in a decrease of EB_2, a shift across A is assumed and a larger fraction of the previous R_2 is tried. In some cases, solu= tions could not be found.

Subroutine ADJSTR

This subroutine is called to test the ratio (VB2-VB1)/(ZD1+ZD2). RTFLTR and fit RZ1 accordingly. (RTFCTR supplied via data card).

If the ratio lies between 0.9 and 1.1, no adjustment of RZ1 is required.

When the ratio is less than 0.9, RZ1 is reduced by 20% and if the ratio exceeds 1.1, RZ1 is increased by 20%. Averages are used once values of RZ1 resulting in ratios on either side of the range are available.

This subroutine is called only while RZ1 is still smaller than RZ1STP, a parameter read in from a data card. Once RZ1 reaches or exceeds this value, RZ1 is set equal to RZ1STP and the subroutine is bypassed thereafter.

Parameters

The programme allows for a choice of values for the following para= meters which must be provided on data cards.

Q_o, Q_1, L_o, L_1, R_1, H, V_2, C, R_2 see section 12 for a description

D, G

RZ1/ .....

RZ1	F for Z1 cases
RZ1STP	once RZ1 reaches this value, it is kept constant at RZ1 = RZ1STP
TMAX	duration of the flash in seconds x 10^{-2}
ISTART, ISTOP, ISTEP	allows for a choice of time increment size from 0% to 100% of duration of the flash
CEB1	used to control EB1
RTFCTR	used with ratio of potentials which in turn is used to control RZ1. Once RZ1 reaches the value RZ1STP, RTFCTR is set to 1.0
TARGET	an array of values which EB2 must take on (see subroutine ADJUST)
IDTAIL	used to provide an optional breakup of the last time increment into 10 smaller increments

Error Stops

The programme has the following error stops:

(1) excessive number of iterations for RZ1
(2) excessive number of iterations for R2
(3) field intensity at ground level exceeds the maximum value of EB2 (i.e. the highest value in the array TARGET)
(4) Z2 = V2 x time elapsed exceeds (H-L1)

In the case of error stops (2) and (3) the programme will make one attempt to revert to the conditions at the beginning of the last time interval and repeat the interval in ten smaller steps. After that, the occurrence of either (2) or (3) will cause the programme to stop.

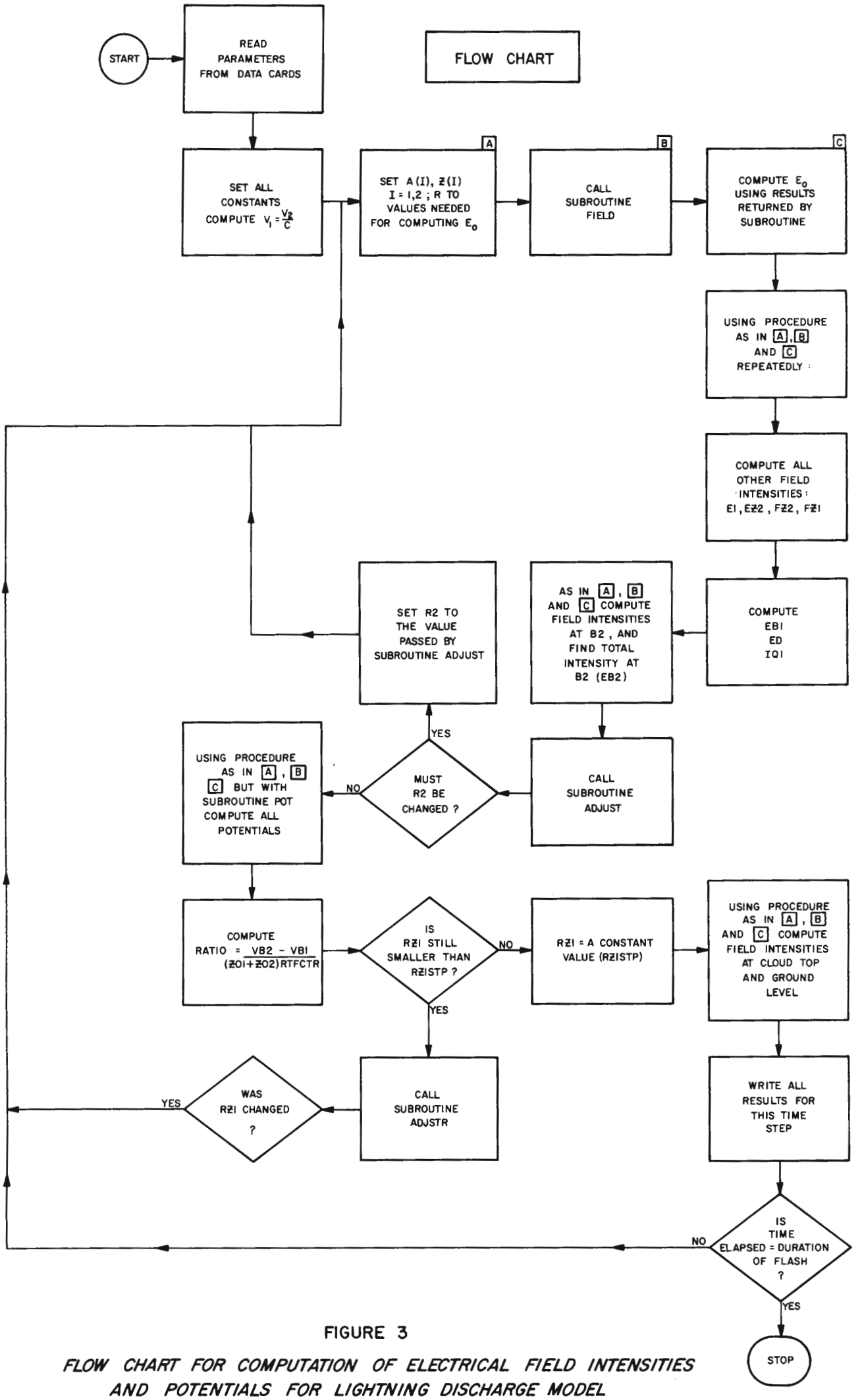

FIGURE 3

FLOW CHART FOR COMPUTATION OF ELECTRICAL FIELD INTENSITIES AND POTENTIALS FOR LIGHTNING DISCHARGE MODEL

C= 20.0 R2= 0.1000000D 03 D 1.00G 1.00 C0= 0.200D 06

Z2 CONCENTRIC RATIO FACTOR IS 0.20000 04

Q0= 0.71000000000 02 Q1=-0.71000000000 02 SL0= 0.40000000000 04 SL1= 0.40000000000 04

R1= 0.50000000000 03 H= 0.80000000000 04 V1= 0.10000000000 05 V0= 0.10000000000 01

R FOR Z1 CASES= 0.200 03

%TIME	TIME	Q	IQ1	-Q1+Q	EB2	R2	VB1	VB0	VB2
0.0	0.0	0.0	0.0	0.0	-0.10056D 07	0.10000D 03	0.0	0.0	0.0
5.0	0.100D-02	-0.35456D 00	0.17904D 01	-0.21450D 01	-0.99451D 06	0.98255D 02	-0.62981D 09	-0.63061D 09	-0.62936D 09
10.0	0.200D-02	-0.70822D 00	0.38365D 01	-0.45448D 01	-0.99604D 06	0.12102D 03	-0.60302D 09	-0.59986D 09	-0.60215D 09
15.0	0.300D-02	-0.10610D 01	0.51693D 01	-0.62303D 01	-0.10058D 07	0.12300D 03	-0.58610D 09	-0.57590D 09	-0.58773D 09
20.0	0.400D-02	-0.14129D 01	0.28551D 01	-0.42680D 01	-0.10070D 07	0.80716D 02	-0.59718D 09	-0.57196D 09	-0.44120D 09
25.0	0.500D-02	-0.17639D 01	0.18699D 01	-0.36338D 01	-0.99551D 06	0.60537D 02	-0.60471D 09	-0.56787D 09	-0.36863D 09
30.0	0.600D-02	-0.21140D 01	0.14351D 01	-0.35491D 01	-0.10074D 07	0.57132D 02	-0.60736D 09	-0.56073D 09	-0.32543D 09
35.0	0.700D-02	-0.24633D 01	0.12112D 01	-0.36745D 01	-0.99769D 06	0.45433D 02	-0.60757D 09	-0.55200D 09	-0.29452D 09
40.0	0.800D-02	-0.28116D 01	0.10895D 01	-0.39011D 01	-0.99356D 06	0.42593D 02	-0.60634D 09	-0.54240D 09	-0.27158D 09
45.0	0.900D-02	-0.31591D 01	0.10214D 01	-0.41804D 01	-0.99568D 06	0.40596D 02	-0.60428D 09	-0.53237D 09	-0.25364D 09
50.0	0.1000-01	-0.35056D 01	0.98458D 00	-0.44902D 01	-0.99544D 06	0.39328D 02	-0.60168D 09	-0.52214D 09	-0.23870D 09
50.0	0.100D-01	-0.35056D 01	0.99390D 00	-0.44995D 01	-0.19972D 07	0.19818D 02	-0.60146D 09	-0.52218D 09	-0.26649D 09
55.0	0.110D-01	-0.38513D 01	0.97471D 00	-0.48260D 01	-0.20994D 07	0.18424D 02	-0.59854D 09	-0.51190D 09	-0.25490D 09
60.0	0.120D-01	-0.41961D 01	0.97031D 00	-0.51664D 01	-0.22020D 07	0.17273D 02	-0.59532D 09	-0.50158D 09	-0.24482D 09
65.0	0.130D-01	-0.45400D 01	0.97641D 00	-0.55164D 01	-0.23002D 07	0.16328D 02	-0.59187D 09	-0.49129D 09	-0.23565D 09
70.0	0.140D-01	-0.48830D 01	0.99032D 00	-0.58733D 01	-0.23903D 07	0.15563D 02	-0.58824D 09	-0.48105D 09	-0.22687D 09
75.0	0.150D-01	-0.52252D 01	0.10102D 01	-0.62354D 01	-0.24903D 07	0.14833D 02	-0.58445D 09	-0.47089D 09	-0.21832D 09
80.0	0.160D-01	-0.55664D 01	0.10349D 01	-0.66013D 01	-0.25990D 07	0.14138D 02	-0.58054D 09	-0.46082D 09	-0.20941D 09
85.0	0.170D-01	-0.59068D 01	0.10633D 01	-0.69701D 01	-0.26962D 07	0.13586D 02	-0.57651D 09	-0.45084D 09	-0.19897D 09
90.0	0.180D-01	-0.62462D 01	0.10949D 01	-0.73412D 01	-0.28058D 07	0.13055D 02	-0.57238D 09	-0.44096D 09	-0.18550D 09
95.0	0.190D-01	-0.65848D 01	0.11291D 01	-0.77139D 01	-0.29025D 07	0.12749D 02	-0.56816D 09	-0.43118D 09	-0.16270D 09
100.0	0.200D-01	-0.69225D 01	0.11651D 01	-0.80876D 01	-0.29932D 07	0.23705D 02	-0.56386D 09	-0.42143D 09	-0.15815D-04
95.0	0.190D-01	-0.65848D 01	0.11291D 01	-0.77139D 01	-0.28997D 07	0.12761D 02	-0.56816D 09	-0.43118D 09	-0.16266D 09
95.5	0.191D-01	-0.66185D 01	0.11326D 01	-0.77513D 01	-0.29197D 07	0.12743D 02	-0.56773D 09	-0.43021D 09	-0.15916D 09
96.0	0.192D-01	-0.66524D 01	0.11362D 01	-0.77886D 01	-0.29201D 07	0.12755D 02	-0.56731D 09	-0.42923D 09	-0.15520D 09
96.5	0.193D-01	-0.66862D 01	0.11398D 01	-0.78260D 01	-0.29301D 07	0.12774D 02	-0.56688D 09	-0.42826D 09	-0.15066D 09
97.0	0.194D-01	-0.67200D 01	0.11434D 01	-0.78634D 01	-0.29398D 07	0.12817D 02	-0.56645D 09	-0.42729D 09	-0.14535D 09
97.5	0.195D-01	-0.67538D 01	0.11470D 01	-0.79008D 01	-0.29496D 07	0.12899D 02	-0.56602D 09	-0.42632D 09	-0.13897D 09
98.0	0.196D-01	-0.67875D 01	0.11507D 01	-0.79382D 01	-0.29594D 07	0.13059D 02	-0.56558D 09	-0.42535D 09	-0.13098D 09
98.5	0.197D-01	-0.68213D 01	0.11543D 01	-0.79756D 01	-0.29697D 07	0.13343D 02	-0.56515D 09	-0.42438D 09	-0.12036D 09
99.0	0.198D-01	-0.68550D 01	0.11580D 01	-0.80130D 01	-0.29806D 07	0.14021D 02	-0.56472D 09	-0.42341D 09	-0.10464D 09
99.5	0.199D-01	-0.68888D 01	0.11616D 01	-0.80504D 01	-0.29901D 07	0.16417D 02	-0.56429D 09	-0.42244D 09	-0.75216D 08

VALUES AT B1(CONTINUED)

%TIME	TIME	FZ1	FZ2	E0	E1	EZ2
0.0	0.0	0.0	0.0	0.18357D 05	-0.10240D 07	0.0
5.0	0.100D-02	-0.28910D 06	-0.24248D 06	0.18403D 05	-0.10209D 07	0.85974D 05
10.0	0.200D-02	-0.11697D 06	-0.98614D 05	0.18448D 05	-0.10179D 07	0.69841D 05
15.0	0.300D-02	-0.70422D 05	-0.57836D 05	0.18494D 05	-0.10148D 07	0.61365D 05
20.0	0.400D-02	-0.69944D 05	-0.45196D 05	0.18540D 05	-0.10117D 07	0.63857D 05
25.0	0.500D-02	-0.69466D 05	-0.33020D 05	0.18587D 05	-0.10087D 07	0.58245D 05
30.0	0.600D-02	-0.68989D 05	-0.24231D 05	0.18633D 05	-0.10056D 07	0.51224D 05
35.0	0.700D-02	-0.68514D 05	-0.18200D 05	0.18680D 05	-0.10026D 07	0.44830D 05
40.0	0.800D-02	-0.68039D 05	-0.14077D 05	0.18727D 05	-0.99951D 06	0.39578D 05
45.0	0.900D-02	-0.67566D 05	-0.11170D 05	0.18775D 05	-0.99646D 06	0.35287D 05
50.0	0.100D-01	-0.67094D 05	-0.90518D 04	0.18823D 05	-0.99341D 06	0.31732D 05
50.0	0.100D-01	-0.67094D 05	-0.91721D 04	0.18823D 05	-0.99341D 06	0.32154D 05
55.0	0.110D-01	-0.66624D 05	-0.75475D 04	0.18871D 05	-0.99036D 06	0.29068D 05
60.0	0.120D-01	-0.66155D 05	-0.63057D 04	0.18919D 05	-0.98731D 06	0.26459D 05
65.0	0.130D-01	-0.65689D 05	-0.53347D 04	0.18967D 05	-0.98426D 06	0.24219D 05
70.0	0.140D-01	-0.65224D 05	-0.45604D 04	0.19016D 05	-0.98121D 06	0.22269D 05
75.0	0.150D-01	-0.64762D 05	-0.39324D 04	0.19065D 05	-0.97816D 06	0.20548D 05
80.0	0.160D-01	-0.64303D 05	-0.34152D 04	0.19115D 05	-0.97511D 06	0.19011D 05
85.0	0.170D-01	-0.63845D 05	-0.29832D 04	0.19164D 05	-0.97207D 06	0.17621D 05
90.0	0.180D-01	-0.63390D 05	-0.26178D 04	0.19214D 05	-0.96902D 06	0.16351D 05
95.0	0.190D-01	-0.62938D 05	-0.23049D 04	0.19264D 05	-0.96598D 06	0.15177D 05
100.0	0.200D-01	-0.62489D 05	-0.20310D 04	0.19315D 05	-0.96294D 06	0.14060D 05
95.0	0.190D-01	-0.62938D 05	-0.23049D 04	0.19264D 05	-0.96598D 06	0.15177D 05
95.5	0.191D-01	-0.62893D 05	-0.22760D 04	0.19270D 05	-0.96568D 06	0.15064D 05
96.0	0.192D-01	-0.62848D 05	-0.22476D 04	0.19275D 05	-0.96537D 06	0.14952D 05
96.5	0.193D-01	-0.62803D 05	-0.22195D 04	0.19280D 05	-0.96507D 06	0.14840D 05
97.0	0.194D-01	-0.62758D 05	-0.21919D 04	0.19285D 05	-0.96476D 06	0.14729D 05
97.5	0.195D-01	-0.62713D 05	-0.21646D 04	0.19290D 05	-0.96446D 06	0.14619D 05
98.0	0.196D-01	-0.62668D 05	-0.21377D 04	0.19295D 05	-0.96415D 06	0.14510D 05
98.5	0.197D-01	-0.62623D 05	-0.21111D 04	0.19300D 05	-0.96385D 06	0.14401D 05
99.0	0.198D-01	-0.62579D 05	-0.20848D 04	0.19305D 05	-0.96355D 06	0.14292D 05
99.5	0.199D-01	-0.62534D 05	-0.20585D 04	0.19310D 05	-0.96324D 06	0.14181D 05

%TIME	TIME	VD1	VD2	VD1/VD2	RZ1
0.0	0.0	0.15567D-81	0.73515D-50	0.0	0.20000D 03
5.0	0.100D-02	0.44900D 06	0.42000D 06	0.10690D 01	0.24778D 03
10.0	0.200D-02	0.87939D 06	0.84000D 06	0.10469D 01	0.38867D 03
15.0	0.300D-02	0.18368D 08	0.63000D 03	0.29155D 05	0.50000D 03
20.0	0.400D-02	0.15616D 09	0.84000D 03	0.18591D 06	0.50000D 03
25.0	0.500D-02	0.23608D 09	0.10500D 04	0.22484D 06	0.50000D 03
30.0	0.600D-02	0.28193D 09	0.12600D 04	0.22375D 06	0.50000D 03
35.0	0.700D-02	0.31305D 09	0.14700D 04	0.21296D 06	0.50000D 03
40.0	0.800D-02	0.33476D 09	0.16800D 04	0.19926D 06	0.50000D 03
45.0	0.900D-02	0.35064D 09	0.18900D 04	0.18552D 06	0.50000D 03
50.0	0.100D-01	0.36298D 09	0.21000D 04	0.17285D 06	0.50000D 03
50.0	0.100D-01	0.33496D 09	0.21000D 04	0.15951D 06	0.50000D 03
55.0	0.110D-01	0.34364D 09	0.23100D 04	0.14876D 06	0.50000D 03
60.0	0.120D-01	0.35049D 09	0.25200D 04	0.13909D 06	0.50000D 03
65.0	0.130D-01	0.35622D 09	0.27300D 04	0.13048D 06	0.50000D 03
70.0	0.140D-01	0.36137D 09	0.29400D 04	0.12291D 06	0.50000D 03
75.0	0.150D-01	0.36613D 09	0.31500D 04	0.11623D 06	0.50000D 03
80.0	0.160D-01	0.37113D 09	0.33600D 04	0.11045D 06	0.50000D 03
85.0	0.170D-01	0.37754D 09	0.35700D 04	0.10575D 06	0.50000D 03
90.0	0.180D-01	0.38688D 09	0.37800D 04	0.10235D 06	0.50000D 03
95.0	0.190D-01	0.40546D 09	0.39900D 04	0.10162D 06	0.50000D 03
100.0	0.200D-01	0.56386D 09	0.42000D 04	0.13425D 06	0.50000D 03
95.0	0.190D-01	0.40550D 09	0.39900D 04	0.10163D 06	0.50000D 03
95.5	0.191D-01	0.40857D 09	0.40110D 04	0.10186D 06	0.50000D 03
96.0	0.192D-01	0.41211D 09	0.40320D 04	0.10221D 06	0.50000D 03
96.5	0.193D-01	0.41622D 09	0.40530D 04	0.10269D 06	0.50000D 03
97.0	0.194D-01	0.42109D 09	0.40740D 04	0.10336D 06	0.50000D 03
97.5	0.195D-01	0.42705D 09	0.40950D 04	0.10428D 06	0.50000D 03
98.0	0.196D-01	0.43460D 09	0.41160D 04	0.10559D 06	0.50000D 03
98.5	0.197D-01	0.44479D 09	0.41370D 04	0.10751D 06	0.50000D 03
99.0	0.198D-01	0.46008D 09	0.41580D 04	0.11065D 06	0.50000D 03
99.5	0.199D-01	0.48907D 09	0.41790D 04	0.11703D 06	0.50000D 03

VALUES AT B1 (CONTINUED)

%TIME	TIME	EQ1	EZ2(-Q1+Q	EB1	ED	EB1(1)
0.0	0.0	0.0	0.0	-0.10056D 07	0.56230D 04	-0.10056D 07
5.0	0.100D-02	-0.51760D 06	0.52012D 06	-0.10000D 07	-0.83458D 05	-0.91654D 06
10.0	0.200D-02	-0.44877D 06	0.44818D 06	-0.10000D 07	-0.70432D 05	-0.92957D 06
15.0	0.300D-02	-0.36404D 06	0.36034D 06	-0.10000D 07	-0.65061D 05	-0.93494D 06
20.0	0.400D-02	-0.19970D 06	0.19290D 06	-0.10000D 07	-0.70659D 05	-0.92934D 06
25.0	0.500D-02	-0.12990D 06	0.11999D 06	-0.10000D 07	-0.68150D 05	-0.93185D 06
30.0	0.600D-02	-0.99006D 05	0.85997D 05	-0.10000D 07	-0.64233D 05	-0.93577D 06
35.0	0.700D-02	-0.82986D 05	0.66874D 05	-0.10000D 07	-0.60942D 05	-0.93906D 06
40.0	0.800D-02	-0.74128D 05	0.54915D 05	-0.10000D 07	-0.58792D 05	-0.94121D 06
45.0	0.900D-02	-0.69010D 05	0.46696D 05	-0.10000D 07	-0.57601D 05	-0.94240D 06
50.0	0.100D-01	-0.66059D 05	0.40644D 05	-0.10000D 07	-0.57147D 05	-0.94285D 06
50.0	0.100D-01	-0.66685D 05	0.41270D 05	-0.10000D 07	-0.57569D 05	-0.94243D 06
55.0	0.110D-01	-0.64939D 05	0.36425D 05	-0.10000D 07	-0.57582D 05	-0.94242D 06
60.0	0.120D-01	-0.64191D 05	0.32578D 05	-0.10000D 07	-0.58072D 05	-0.94193D 06
65.0	0.130D-01	-0.64139D 05	0.29428D 05	-0.10000D 07	-0.58931D 05	-0.94107D 06
70.0	0.140D-01	-0.64593D 05	0.26785D 05	-0.10000D 07	-0.60077D 05	-0.93992D 06
75.0	0.150D-01	-0.65425D 05	0.24520D 05	-0.10000D 07	-0.61453D 05	-0.93855D 06
80.0	0.160D-01	-0.66546D 05	0.22545D 05	-0.10000D 07	-0.63012D 05	-0.93699D 06
85.0	0.170D-01	-0.67890D 05	0.20793D 05	-0.10000D 07	-0.64717D 05	-0.93528D 06
90.0	0.180D-01	-0.69408D 05	0.19218D 05	-0.10000D 07	-0.66542D 05	-0.93346D 06
95.0	0.190D-01	-0.71064D 05	0.17779D 05	-0.10000D 07	-0.68461D 05	-0.93154D 06
100.0	0.200D-01	-0.72803D 05	0.16426D 05	-0.10000D 07	-0.70437D 05	-0.92956D 06
95.0	0.190D-01	-0.71064D 05	0.17779D 05	-0.10000D 07	-0.68461D 05	-0.93154D 06
95.5	0.191D-01	-0.71236D 05	0.17642D 05	-0.10000D 07	-0.68658D 05	-0.93134D 06
96.0	0.192D-01	-0.71408D 05	0.17506D 05	-0.10000D 07	-0.68855D 05	-0.93115D 06
96.5	0.193D-01	-0.71582D 05	0.17370D 05	-0.10000D 07	-0.69053D 05	-0.93095D 06
97.0	0.194D-01	-0.71757D 05	0.17236D 05	-0.10000D 07	-0.69251D 05	-0.93075D 06
97.5	0.195D-01	-0.71933D 05	0.17102D 05	-0.10000D 07	-0.69450D 05	-0.93055D 06
98.0	0.196D-01	-0.72110D 05	0.16969D 05	-0.10000D 07	-0.69650D 05	-0.93035D 06
98.5	0.197D-01	-0.72287D 05	0.16837D 05	-0.10000D 07	-0.69850D 05	-0.93015D 06
99.0	0.198D-01	-0.72464D 05	0.16706D 05	-0.10000D 07	-0.70050D 05	-0.92995D 06
99.5	0.199D-01	-0.72640D 05	0.16572D 05	-0.10000D 07	-0.70248D 05	-0.92975D 06

VALUES AT B2

%TIME	TIME	E0	EZ1(2)	E1	E72
0.0	0.0	0.18357D 05	0.0	-0.10240D 07	0.0
5.0	0.100D-02	0.17501D 05	0.18898D 06	-0.64458D 06	-0.55642D 06
10.0	0.200D-02	0.16735D 05	0.12472D 06	-0.42380D 06	-0.71370D 06
15.0	0.300D-02	0.16047D 05	0.83328D 05	-0.29721D 06	-0.80795D 06
20.0	0.400D-02	0.15431D 05	0.30169D 05	-0.22081D 06	-0.83176D 06
25.0	0.500D-02	0.14878D 05	0.13785D 05	-0.17173D 06	-0.85245D 06
30.0	0.600D-02	0.14382D 05	0.77745D 04	-0.13843D 06	-0.89117D 06
35.0	0.700D-02	0.13939D 05	0.50314D 04	-0.11484D 06	-0.90182D 06
40.0	0.800D-02	0.13543D 05	0.35940D 04	-0.97536D 05	-0.91316D 06
45.0	0.900D-02	0.13190D 05	0.27556D 04	-0.84499D 05	-0.92712D 06
50.0	0.100D-01	0.12877D 05	0.22281D 04	-0.74471D 05	-0.93608D 06
50.0	0.100D-01	0.12877D 05	0.22492D 04	-0.74471D 05	-0.19379D 07
55.0	0.110D-01	0.12602D 05	0.18918D 04	-0.66636D 05	-0.20473D 07
60.0	0.120D-01	0.12361D 05	0.16476D 04	-0.60445D 05	-0.21555D 07
65.0	0.130D-01	0.12154D 05	0.14773D 04	-0.55521D 05	-0.22583D 07
70.0	0.140D-01	0.11977D 05	0.13578D 04	-0.51598D 05	-0.23521D 07
75.0	0.150D-01	0.11830D 05	0.12755D 04	-0.48483D 05	-0.24546D 07
80.0	0.160D-01	0.11711D 05	0.12218D 04	-0.46037D 05	-0.25659D 07
85.0	0.170D-01	0.11619D 05	0.11913D 04	-0.44159D 05	-0.26649D 07
90.0	0.180D-01	0.11554D 05	0.11809D 04	-0.42774D 05	-0.27758D 07
95.0	0.190D-01	0.11516D 05	0.11890D 04	-0.41831D 05	-0.28733D 07
100.0	0.200D-01	0.11503D 05	0.12146D 04	-0.41295D 05	-0.29646D 07
95.0	0.190D-01	0.11516D 05	0.11890D 04	-0.41831D 05	-0.28706D 07
95.5	0.191D-01	0.11513D 05	0.11908D 04	-0.41760D 05	-0.28817D 07
96.0	0.192D-01	0.11511D 05	0.11928D 04	-0.41692D 05	-0.28911D 07
96.5	0.193D-01	0.11509D 05	0.11949D 04	-0.41629D 05	-0.29012D 07
97.0	0.194D-01	0.11508D 05	0.11973D 04	-0.41569D 05	-0.29109D 07
97.5	0.195D-01	0.11506D 05	0.11998D 04	-0.41514D 05	-0.29208D 07
98.0	0.196D-01	0.11505D 05	0.12025D 04	-0.41462D 05	-0.29306D 07
98.5	0.197D-01	0.11504D 05	0.12053D 04	-0.41415D 05	-0.29410D 07
99.0	0.198D-01	0.11503D 05	0.12084D 04	-0.41371D 05	-0.29528D 07
99.5	0.199D-01	0.11503D 05	0.12115D 04	-0.41331D 05	-0.29614D 07

POTENTIALS AT B1

%TIME	TIME	VC1	V11	V711	VZ21	VB1
5.0	0.100D-02	0.54324D 08	-0.68087D 09	0.12632D 09	-0.12959D 09	-0.62981D 09
10.0	0.200D-02	0.54508D 08	-0.67872D 09	0.17037D 09	-0.14918D 09	-0.60302D 09
15.0	0.300D-02	0.54693D 08	-0.67658D 09	0.17666D 09	-0.14086D 09	-0.58610D 09
20.0	0.400D-02	0.54878D 08	-0.67444D 09	0.96916D 08	-0.74537D 08	-0.59718D 09
25.0	0.500D-02	0.55064D 08	-0.67229D 09	0.63049D 08	-0.50530D 08	-0.60471D 09
30.0	0.600D-02	0.55250D 08	-0.67015D 09	0.48066D 08	-0.40527D 08	-0.60736D 09
35.0	0.700D-02	0.55436D 08	-0.66800D 09	0.40299D 08	-0.35299D 08	-0.60757D 09
40.0	0.800D-02	0.55623D 08	-0.66586D 09	0.36009D 08	-0.32117D 08	-0.60634D 09
45.0	0.900D-02	0.55811D 08	-0.66371D 09	0.33535D 08	-0.29912D 08	-0.60428D 09
50.0	0.100D-01	0.55999D 08	-0.66157D 09	0.32115D 08	-0.28225D 08	-0.60168D 09
50.0	0.100D-01	0.55999D 08	-0.66157D 09	0.32420D 08	-0.28309D 08	-0.60146D 09
55.0	0.110D-01	0.56187D 08	-0.65942D 09	0.31586D 08	-0.26892D 08	-0.59854D 09
60.0	0.120D-01	0.56376D 08	-0.65727D 09	0.31239D 08	-0.25662D 08	-0.59532D 09
65.0	0.130D-01	0.56566D 08	-0.65512D 09	0.31233D 08	-0.24543D 08	-0.59187D 09
70.0	0.140D-01	0.56756D 08	-0.65297D 09	0.31474D 08	-0.23491D 08	-0.58824D 09
75.0	0.150D-01	0.56946D 08	-0.65083D 09	0.31901D 08	-0.22474D 08	-0.58445D 09
80.0	0.160D-01	0.57137D 08	-0.64868D 09	0.32471D 08	-0.21471D 08	-0.58054D 09
85.0	0.170D-01	0.57328D 08	-0.64653D 09	0.33152D 08	-0.20467D 08	-0.57651D 09
90.0	0.180D-01	0.57520D 08	-0.64438D 09	0.33922D 08	-0.19449D 08	-0.57238D 09
95.0	0.190D-01	0.57713D 08	-0.64223D 09	0.34760D 08	-0.18407D 08	-0.56816D 09
100.0	0.200D-01	0.57906D 08	-0.64008D 09	0.35643D 08	-0.17329D 08	-0.56386D 09
95.0	0.190D-01	0.57713D 08	-0.64223D 09	0.34760D 08	-0.18407D 08	-0.56816D 09
95.5	0.191D-01	0.57732D 08	-0.64201D 09	0.34848D 08	-0.18301D 08	-0.56773D 09
96.0	0.192D-01	0.57751D 08	-0.64180D 09	0.34935D 08	-0.18195D 08	-0.56731D 09
96.5	0.193D-01	0.57770D 08	-0.64158D 09	0.35023D 08	-0.18088D 08	-0.56688D 09
97.0	0.194D-01	0.57790D 08	-0.64137D 09	0.35112D 08	-0.17981D 08	-0.56645D 09
97.5	0.195D-01	0.57809D 08	-0.64115D 09	0.35201D 08	-0.17874D 08	-0.56602D 09
98.0	0.196D-01	0.57828D 08	-0.64094D 09	0.35291D 08	-0.17766D 08	-0.56558D 09
98.5	0.197D-01	0.57848D 08	-0.64072D 09	0.35381D 08	-0.17658D 08	-0.56515D 09
99.0	0.198D-01	0.57867D 08	-0.64051D 09	0.35471D 08	-0.17550D 08	-0.56472D 09
99.5	0.199D-01	0.57886D 08	-0.64029D 09	0.35560D 08	-0.17440D 08	-0.56429D 09

POTENTIALS AT BO

%TIME	TIME	V00	V10	V710	V720	VB0
5.0	0.100D-02	0.54140D 08	-0.67077D 09	0.12460D 09	-0.13858D 09	-0.63061D 09
10.0	0.200D-02	0.54140D 08	-0.65881D 09	0.16739D 09	-0.16258D 09	-0.59986D 09
15.0	0.300D-02	0.54140D 08	-0.64712D 09	0.17302D 09	-0.15594D 09	-0.57590D 09
20.0	0.400D-02	0.54140D 08	-0.63570D 09	0.94269D 08	-0.84668D 08	-0.57196D 09
25.0	0.500D-02	0.54140D 08	-0.62455D 09	0.60904D 08	-0.58365D 08	-0.56787D 09
30.0	0.600D-02	0.54140D 08	-0.61364D 09	0.46111D 08	-0.47334D 08	-0.56073D 09
35.0	0.700D-02	0.54140D 08	-0.60299D 09	0.38394D 08	-0.41544D 08	-0.55200D 09
40.0	0.800D-02	0.54140D 08	-0.59258D 09	0.34072D 08	-0.38038D 08	-0.54240D 09
45.0	0.900D-02	0.54140D 08	-0.58240D 09	0.31514D 08	-0.35627D 08	-0.53237D 09
50.0	0.100D-01	0.54140D 08	-0.57246D 09	0.29973D 08	-0.33795D 08	-0.52214D 09
50.0	0.100D-01	0.54140D 08	-0.57246D 09	0.30257D 08	-0.34125D 08	-0.52218D 09
55.0	0.110D-01	0.54140D 08	-0.56274D 09	0.29279D 08	-0.32577D 08	-0.51190D 09
60.0	0.120D-01	0.54140D 08	-0.55324D 09	0.28761D 08	-0.31242D 08	-0.50158D 09
65.0	0.130D-01	0.54140D 08	-0.54395D 09	0.28560D 08	-0.30035D 08	-0.49129D 09
70.0	0.140D-01	0.54140D 08	-0.53487D 09	0.28586D 08	-0.28903D 08	-0.48105D 09
75.0	0.150D-01	0.54140D 08	-0.52600D 09	0.28780D 08	-0.27811D 08	-0.47089D 09
80.0	0.160D-01	0.54140D 08	-0.51732D 09	0.29098D 08	-0.26735D 08	-0.46082D 09
85.0	0.170D-01	0.54140D 08	-0.50884D 09	0.29511D 08	-0.25655D 08	-0.45084D 09
90.0	0.180D-01	0.54140D 08	-0.50054D 09	0.29996D 08	-0.24558D 08	-0.44096D 09
95.0	0.190D-01	0.54140D 08	-0.49242D 09	0.30535D 08	-0.23430D 08	-0.43118D 09
100.0	0.200D-01	0.54140D 08	-0.48449D 09	0.31105D 08	-0.22192D 08	-0.42143D 09
95.0	0.190D-01	0.54140D 08	-0.49242D 09	0.30535D 08	-0.23430D 08	-0.43118D 09
95.5	0.191D-01	0.54140D 08	-0.49162D 09	0.30591D 08	-0.23315D 08	-0.43021D 09
96.0	0.192D-01	0.54140D 08	-0.49082D 09	0.30648D 08	-0.23199D 08	-0.42923D 09
96.5	0.193D-01	0.54140D 08	-0.49002D 09	0.30705D 08	-0.23083D 08	-0.42826D 09
97.0	0.194D-01	0.54140D 08	-0.48923D 09	0.30762D 08	-0.22967D 08	-0.42729D 09
97.5	0.195D-01	0.54140D 08	-0.48843D 09	0.30820D 08	-0.22849D 08	-0.42632D 09
98.0	0.196D-01	0.54140D 08	-0.48764D 09	0.30878D 08	-0.22731D 08	-0.42535D 09
98.5	0.197D-01	0.54140D 08	-0.48685D 09	0.30937D 08	-0.22612D 08	-0.42438D 09
99.0	0.198D-01	0.54140D 08	-0.48606D 09	0.30995D 08	-0.22489D 08	-0.42341D 09
99.5	0.199D-01	0.54140D 08	-0.48527D 09	0.31053D 08	-0.22356D 08	-0.42244D 09

POTENTIALS AT B2

%TIME	TIME	V02	V12	VZ12	VZ22	VB2
5.0	0.100D-02	0.50556D 08	-0.50925D 09	0.58823D 08	-0.22949D 09	-0.62936D 09
10.0	0.200D-02	0.47134D 08	-0.39782D 09	0.65889D 08	-0.31735D 09	-0.60215D 09
15.0	0.300D-02	0.43857D 08	-0.32215D 09	0.59431D 08	-0.34886D 09	-0.56773D 09
20.0	0.400D-02	0.40710D 08	-0.26746D 09	0.25117D 08	-0.23938D 09	-0.44102D 09
25.0	0.500D-02	0.37680D 08	-0.22584D 09	0.13042D 08	-0.19351D 09	-0.36863D 09
30.0	0.600D-02	0.34755D 08	-0.19286D 09	0.81392D 07	-0.17547D 09	-0.32543D 09
35.0	0.700D-02	0.31924D 08	-0.16589D 09	0.56858D 07	-0.16624D 09	-0.29452D 09
40.0	0.800D-02	0.29177D 08	-0.14327D 09	0.42845D 07	-0.16178D 09	-0.27158D 09
45.0	0.900D-02	0.26504D 08	-0.12389D 09	0.33904D 07	-0.15964D 09	-0.25364D 09
50.0	0.100D-01	0.23898D 08	-0.10700D 09	0.27690D 07	-0.15837D 09	-0.23870D 09
50.0	0.100D-01	0.23898D 08	-0.10700D 09	0.27953D 07	-0.18619D 09	-0.26649D 09
55.0	0.110D-01	0.21351D 08	-0.92044D 08	0.23228D 07	-0.18653D 09	-0.25490D 09
60.0	0.120D-01	0.18855D 08	-0.78620D 08	0.19521D 07	-0.18701D 09	-0.24482D 09
65.0	0.130D-01	0.16404D 08	-0.66422D 08	0.16450D 07	-0.18727D 09	-0.23565D 09
70.0	0.140D-01	0.13991D 08	-0.55211D 08	0.13781D 07	-0.18703D 09	-0.22687D 09
75.0	0.150D-01	0.11611D 08	-0.44796D 08	0.11359D 07	-0.18627D 09	-0.21832D 09
80.0	0.160D-01	0.92575D 07	-0.35022D 08	0.90773D 06	-0.18456D 09	-0.20941D 09
85.0	0.170D-01	0.69249D 07	-0.25759D 08	0.68573D 06	-0.18083D 09	-0.19897D 09
90.0	0.180D-01	0.46080D 07	-0.16898D 08	0.46377D 06	-0.17367D 09	-0.18550D 09
95.0	0.190D-01	0.23014D 07	-0.83403D 07	0.23672D 06	-0.15690D 09	-0.16270D 09
100.0	0.200D-01	0.43133D-04	-0.22702D-05	-0.64609D-05	-0.50217D-04	-0.15815D-04
95.0	0.190D-01	0.23014D 07	-0.83403D 07	0.23672D 06	-0.15686D 09	-0.16266D 09
95.5	0.191D-01	0.20711D 07	-0.74979D 07	0.21356D 06	-0.15395D 09	-0.15916D 09
96.0	0.192D-01	0.18409D 07	-0.66576D 07	0.19029D 06	-0.15057D 09	-0.15520D 09
96.5	0.193D-01	0.16107D 07	-0.58192D 07	0.16692D 06	-0.14662D 09	-0.15066D 09
97.0	0.194D-01	0.13805D 07	-0.49828D 07	0.14344D 06	-0.14189D 09	-0.14535D 09
97.5	0.195D-01	0.11504D 07	-0.41482D 07	0.11984D 06	-0.13609D 09	-0.13897D 09
98.0	0.196D-01	0.92028D 06	-0.33154D 07	0.96127D 05	-0.12868D 09	-0.13098D 09
98.5	0.197D-01	0.69019D 06	-0.24842D 07	0.72290D 05	-0.11864D 09	-0.12036D 09
99.0	0.198D-01	0.46012D 06	-0.16546D 07	0.48325D 05	-0.10350D 09	-0.10464D 09
99.5	0.199D-01	0.23006D 06	-0.82660D 06	0.24229D 05	-0.74644D 08	-0.75216D 08

%TIME	TIME	EG0	EG1	EGZ1	EGZ2	EG
0.0	0.0	0.11503D 05	-0.48633D 05	0.0	0.0	-0.37131D 05
5.0	0.100D-02	0.11503D 05	-0.48240D 05	0.20018D 04	-0.25810D 04	-0.37316D 05
10.0	0.200D-02	0.11503D 05	-0.47850D 05	0.42576D 04	-0.58711D 04	-0.37960D 05
15.0	0.300D-02	0.11503D 05	-0.47462D 05	0.56919D 04	-0.86770D 04	-0.38945D 05
20.0	0.400D-02	0.11503D 05	-0.47078D 05	0.31335D 04	-0.64423D 04	-0.38884D 05
25.0	0.500D-02	0.11503D 05	-0.46696D 05	0.20455D 04	-0.59689D 04	-0.39116D 05
30.0	0.600D-02	0.11503D 05	-0.46317D 05	0.15648D 04	-0.63768D 04	-0.39626D 05
35.0	0.700D-02	0.11503D 05	-0.45941D 05	0.13164D 04	-0.72647D 04	-0.40386D 05
40.0	0.800D-02	0.11503D 05	-0.45567D 05	0.11803D 04	-0.85463D 04	-0.41431D 05
45.0	0.900D-02	0.11503D 05	-0.45197D 05	0.11029D 04	-0.10231D 05	-0.42822D 05
50.0	0.100D-01	0.11503D 05	-0.44829D 05	0.10597D 04	-0.12396D 05	-0.44662D 05
50.0	0.100D-01	0.11503D 05	-0.44829D 05	0.10698D 04	-0.12425D 05	-0.44681D 05
55.0	0.110D-01	0.11503D 05	-0.44464D 05	0.10457D 04	-0.15208D 05	-0.47123D 05
60.0	0.120D-01	0.11503D 05	-0.44101D 05	0.10377D 04	-0.18846D 05	-0.50407D 05
65.0	0.130D-01	0.11503D 05	-0.43741D 05	0.10409D 04	-0.23714D 05	-0.54912D 05
70.0	0.140D-01	0.11503D 05	-0.43384D 05	0.10523D 04	-0.30454D 05	-0.61283D 05
75.0	0.150D-01	0.11503D 05	-0.43030D 05	0.10701D 04	-0.40241D 05	-0.70698D 05
80.0	0.160D-01	0.11503D 05	-0.42678D 05	0.10927D 04	-0.55467D 05	-0.85549D 05
85.0	0.170D-01	0.11503D 05	-0.42328D 05	0.11192D 04	-0.81794D 05	-0.11150D 06
90.0	0.180D-01	0.11503D 05	-0.41981D 05	0.11488D 04	-0.13648D 06	-0.16581D 06
95.0	0.190D-01	0.11503D 05	-0.41637D 05	0.11809D 04	-0.30706D 06	-0.33602D 06
100.0	0.200D-01	0.11503D 05	-0.41295D 05	0.12146D 04	-0.29646D 07	-0.29932D 07
95.0	0.190D-01	0.11503D 05	-0.41637D 05	0.11809D 04	-0.30706D 06	-0.33601D 06
95.5	0.191D-01	0.11503D 05	-0.41603D 05	0.11842D 04	-0.34553D 06	-0.37445D 06
96.0	0.192D-01	0.11503D 05	-0.41568D 05	0.11876D 04	-0.39374D 06	-0.42262D 06
96.5	0.193D-01	0.11503D 05	-0.41534D 05	0.11909D 04	-0.45584D 06	-0.48468D 06
97.0	0.194D-01	0.11503D 05	-0.41500D 05	0.11943D 04	-0.53867D 06	-0.56747D 06
97.5	0.195D-01	0.11503D 05	-0.41466D 05	0.11977D 04	-0.65441D 06	-0.68317D 06
98.0	0.196D-01	0.11503D 05	-0.41432D 05	0.12011D 04	-0.82675D 06	-0.85548D 06
98.5	0.197D-01	0.11503D 05	-0.41398D 05	0.12046D 04	-0.11081D 07	-0.11368D 07
99.0	0.198D-01	0.11503D 05	-0.41363D 05	0.12080D 04	-0.16344D 07	-0.16631D 07
99.5	0.199D-01	0.11503D 05	-0.41329D 05	0.12114D 04	-0.27198D 07	-0.27484D 07

%TIME	TIME	EA0	EA1	EAZ1	EAZ2	EA
0.0	0.0	-0.10152D 07	0.13206D 05	0.0	0.0	-0.10020D 07
5.0	0.100D-02	-0.10152D 07	0.13169D 05	-0.18913D 03	0.21511D 03	-0.10020D 07
10.0	0.200D-02	-0.10152D 07	0.13132D 05	-0.40576D 03	0.43334D 03	-0.10020D 07
15.0	0.300D-02	-0.10152D 07	0.13094D 05	-0.54729D 03	0.56467D 03	-0.10021D 07
20.0	0.400D-02	-0.10152D 07	0.13057D 05	-0.30304D 03	0.36759D 03	-0.10021D 07
25.0	0.500D-02	-0.10152D 07	0.13019D 05	-0.19896D 03	0.29717D 03	-0.10021D 07
30.0	0.600D-02	-0.10152D 07	0.12982D 05	-0.15308D 03	0.27538D 03	-0.10021D 07
35.0	0.700D-02	-0.10152D 07	0.12944D 05	-0.12952D 03	0.27024D 03	-0.10021D 07
40.0	0.800D-02	-0.10152D 07	0.12906D 05	-0.11680D 03	0.27166D 03	-0.10021D 07
45.0	0.900D-02	-0.10152D 07	0.12869D 05	-0.10977D 03	0.27528D 03	-0.10022D 07
50.0	0.100D-01	-0.10152D 07	0.12831D 05	-0.10608D 03	0.27919D 03	-0.10022D 07
50.0	0.100D-01	-0.10152D 07	0.12831D 05	-0.10708D 03	0.27978D 03	-0.10022D 07
55.0	0.110D-01	-0.10152D 07	0.12793D 05	-0.10527D 03	0.28285D 03	-0.10022D 07
60.0	0.120D-01	-0.10152D 07	0.12755D 05	-0.10506D 03	0.28485D 03	-0.10023D 07
65.0	0.130D-01	-0.10152D 07	0.12717D 05	-0.10599D 03	0.28545D 03	-0.10023D 07
70.0	0.140D-01	-0.10152D 07	0.12680D 05	-0.10776D 03	0.28447D 03	-0.10023D 07
75.0	0.150D-01	-0.10152D 07	0.12642D 05	-0.11020D 03	0.28179D 03	-0.10024D 07
80.0	0.160D-01	-0.10152D 07	0.12604D 05	-0.11318D 03	0.27735D 03	-0.10024D 07
85.0	0.170D-01	-0.10152D 07	0.12566D 05	-0.11658D 03	0.27107D 03	-0.10025D 07
90.0	0.180D-01	-0.10152D 07	0.12527D 05	-0.12034D 03	0.26294D 03	-0.10025D 07
95.0	0.190D-01	-0.10152D 07	0.12489D 05	-0.12440D 03	0.25290D 03	-0.10026D 07
100.0	0.200D-01	-0.10152D 07	0.12451D 05	-0.12869D 03	0.24093D 03	-0.10026D 07
95.0	0.190D-01	-0.10152D 07	0.12489D 05	-0.12440D 03	0.25290D 03	-0.10026D 07
95.5	0.191D-01	-0.10152D 07	0.12486D 05	-0.12483D 03	0.25180D 03	-0.10026D 07
96.0	0.192D-01	-0.10152D 07	0.12482D 05	-0.12525D 03	0.25067D 03	-0.10026D 07
96.5	0.193D-01	-0.10152D 07	0.12478D 05	-0.12568D 03	0.24952D 03	-0.10026D 07
97.0	0.194D-01	-0.10152D 07	0.12474D 05	-0.12610D 03	0.24835D 03	-0.10026D 07
97.5	0.195D-01	-0.10152D 07	0.12470D 05	-0.12654D 03	0.24717D 03	-0.10026D 07
98.0	0.196D-01	-0.10152D 07	0.12466D 05	-0.12697D 03	0.24596D 03	-0.10026D 07
98.5	0.197D-01	-0.10152D 07	0.12463D 05	-0.12740D 03	0.24473D 03	-0.10026D 07
99.0	0.198D-01	-0.10152D 07	0.12459D 05	-0.12784D 03	0.24349D 03	-0.10026D 07
99.5	0.199D-01	-0.10152D 07	0.12455D 05	-0.12827D 03	0.24222D 03	-0.10026D 07